STREAMING INFLAMMATION: FROM DAMAGE TO HEALING AND RESILIENCE

EDITED BY: Pallavi R. Devchand, Eric Schadt and Garret A. FitzGerald
PUBLISHED IN: Frontiers in Pharmacology

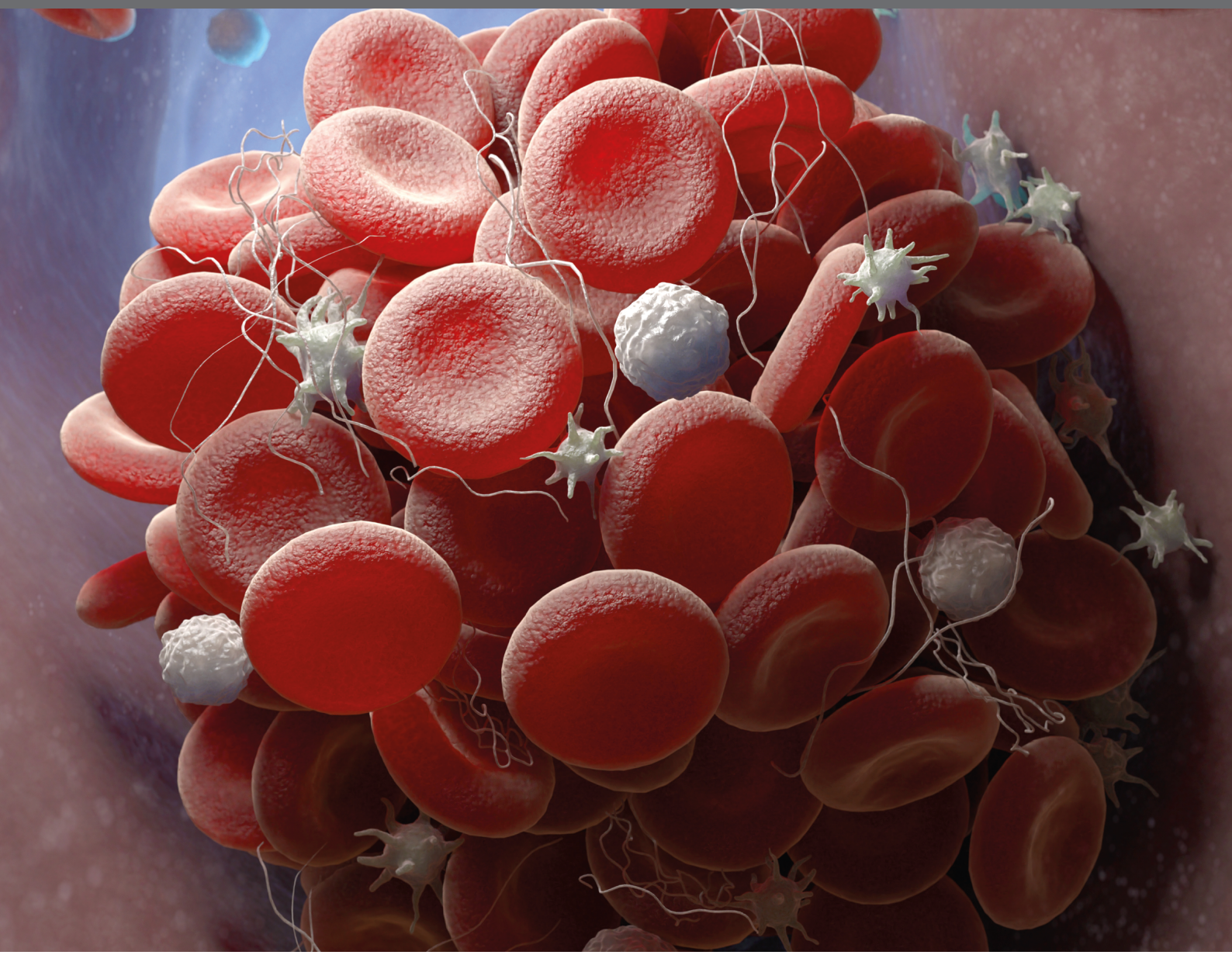

frontiers Research Topics

ISSN 1664-8714
ISBN 978-2-88976-417-4
DOI 10.3389/978-2-88976-417-4

About Frontiers

Frontiers is more than just an open-access publisher of scholarly articles: it is a pioneering approach to the world of academia, radically improving the way scholarly research is managed. The grand vision of Frontiers is a world where all people have an equal opportunity to seek, share and generate knowledge. Frontiers provides immediate and permanent online open access to all its publications, but this alone is not enough to realize our grand goals.

Frontiers Journal Series

The Frontiers Journal Series is a multi-tier and interdisciplinary set of open-access, online journals, promising a paradigm shift from the current review, selection and dissemination processes in academic publishing. All Frontiers journals are driven by researchers for researchers; therefore, they constitute a service to the scholarly community. At the same time, the Frontiers Journal Series operates on a revolutionary invention, the tiered publishing system, initially addressing specific communities of scholars, and gradually climbing up to broader public understanding, thus serving the interests of the lay society, too.

Dedication to Quality

Each Frontiers article is a landmark of the highest quality, thanks to genuinely collaborative interactions between authors and review editors, who include some of the world's best academicians. Research must be certified by peers before entering a stream of knowledge that may eventually reach the public - and shape society; therefore, Frontiers only applies the most rigorous and unbiased reviews.
Frontiers revolutionizes research publishing by freely delivering the most outstanding research, evaluated with no bias from both the academic and social point of view. By applying the most advanced information technologies, Frontiers is catapulting scholarly publishing into a new generation.

What are Frontiers Research Topics?

Frontiers Research Topics are very popular trademarks of the Frontiers Journals Series: they are collections of at least ten articles, all centered on a particular subject. With their unique mix of varied contributions from Original Research to Review Articles, Frontiers Research Topics unify the most influential researchers, the latest key findings and historical advances in a hot research area! Find out more on how to host your own Frontiers Research Topic or contribute to one as an author by contacting the Frontiers Editorial Office: frontiersin.org/about/contact

STREAMING INFLAMMATION: FROM DAMAGE TO HEALING AND RESILIENCE

Topic Editors:
Pallavi R. Devchand, University of Calgary, Canada
Eric Schadt, Icahn School of Medicine at Mount Sinai, United States
Garret A. FitzGerald, University of Pennsylvania, United States

Citation: Devchand, P. R., Schadt, E., FitzGerald, G. A., eds. (2022). Streaming Inflammation: From Damage to Healing and Resilience. Lausanne: Frontiers Media SA. doi: 10.3389/978-2-88976-417-4

Table of Contents

frontiers | Frontiers in Pharmacology

EDITORIAL
published: 12 July 2022
doi: 10.3389/fphar.2022.969453

Editorial: Streaming Inflammation: From Damage to Healing and Resilience

Pallavi R. Devchand[1]*, *Eric E. Schadt*[2] and *Garret A. FitzGerald*[3]

[1]Department of Physiology and Pharmacology, University of Calgary, Calgary, AB, Canada, [2]SEMA4, Stamford, CT, United States, [3]Department of Systems Pharmacology and Translational Therapeutics, Perelman School of Medicine, University of Pennsylvania, Philadelphia, PA, United States

Keywords: resilience, disease states, drug target, healing, identity, trafficking

Editorial on the Research Topic

Streaming Inflammation: From Damage to Healing and Resilience

" We were born before the wind
Also younger than the sun... "

-*Van Morrison* in *Into the Mystic (1970)*.

Every human is a multiplex of ecosystems. The balance of symbiosis and competition from within is as critical as maintenance and defense systems, like inflammation. To achieve homeostasis, these adaptive processes occur at different stages in different scenarios - all over the body - at the same time, and often unnoticed. How are the streams of molecular and cellular players coordinated in systemic responses that maintain integrity of the whole? This collection of articles aims to spotlight three dynamic relationships: damage, healing and resilience.

In a pilot study on Sjogren's Syndrome, Das et al. profile human saliva and tears using a proteomics workflow to create a proof-of-concept working model for examining altered protease activity associated with the damage inflicted in this rare disease.

Three articles target catabolism of bioactive lipids and impact on responsiveness to high fat diet. In LPS-induced human phagocytes, Tang et el didactically examine leukotriene biosynthesis pathways to arrive at a fitting model of the ATP-binding domain of p38 to KIRA6, a widely-used inhibitor of the IRE1alpha component of the unfolding protein response with p38. Using knock-out mice of soluble epoxide hydrolase, Wagner et al. associated metabolism of high fat diet and diet-induced obesity to organ-selective observations of sex-specific responsiveness. Along this same vein, Ulu et al. opted to modulate endogenous polyunsaturated fatty acid levels by using a fatty-acyl transferase transgenic mouse, and evaluated impact on lung inflammation triggered by repetitive exposure to liquid dust.

In the healing process, Cen et al. focused on lipopolysaccharide-induced migration and proliferation of human dermal fibroblasts to identify a role for strathmin via p38 mitogen-activated protein kinase. With a novel twist of local scar formation and liver function, Lyu et al. measured effects of combinatorial drug treatments (anisodamine and neostigmine) on local and chronic inflammation in a rat model of biliary obstruction.

Several articles argue for fresh perspective in dynamic disease scenarios. After framing recent advances in the complex and fluid roles of macrophages in different stages of atherosclerosis pathogenesis, Farahi et al. propose provocative macrophage-based therapies

OPEN ACCESS

Edited and reviewed by:
Paola Patrignani,
University of Studies G d'Annunzio Chieti and Pescara, Italy

***Correspondence:**
Pallavi R. Devchand
Pallavi.Devchand@ucalgary.ca

Specialty section:
This article was submitted to Inflammation Pharmacology, a section of the journal Frontiers in Pharmacology

Received: *15 June 2022*
Accepted: *22 June 2022*
Published: *12 July 2022*

Citation:
Devchand PR, Schadt EE and FitzGerald GA (2022) Editorial: Streaming Inflammation: From Damage to Healing and Resilience. Front. Pharmacol. 13:969453. doi: 10.3389/fphar.2022.969453

FIGURE 1 | Islands in The Sea. A series of Monuments and Rituals by Amanda Phingbodhipakkiya at the Paul Milstein Reflecting Pool, New York. Photo by Pallavi R. Devchand.

for disease management. From an alternate perspective on atherosclerosis, Botts et al. focus on vascular endothelial cells as drivers of disease, and postulate on molecular approaches to re-routing inflammation away from disease progression. Ballerini et al. weave us through chronic inflammation in select cancers and liver diseases to hone in on the roles of platelets, and the potential of platelets as target cell types for biomarkers and drug therapy. In their white paper, Zhu et al. take a step out of the fray of activated immune traffic and argue for the relevance of dynamics in the ecosystems of somatic cells, particularly in the subtle context of personalized health and medicine over a lifetime.

On earth, Devchand noted the scientific and artistic drivers of human complexity in personal expressions of resilience, susceptibility and passion (**Figure 1**). And out of this world, the brave Millie Elizabeth Hughes-Fulford (1945–2021) lived her mantra of an astronaut-scientist:

"To dream and to explore is the nature of humankind.
And to find new knowledge is key."

AUTHOR CONTRIBUTIONS

PD wrote the manuscript, ES and GF contributed to final edits.

FUNDING

PD and ES were funded in part by The Leducq Foundation. All authors belong to the PENTACON consortium (funded by the National Institutes of Health HL117798).

ACKNOWLEDGMENTS

The editors appreciate the enlightening chapter contributions of the authors and the valuable critiques of the reviewers.

Conflict of Interest: ES is employed by SEMA4.

The remaining authors declare that the research was conducted in the absence of any commercial or financial relationships that could be construed as a potential conflict of interest.

Publisher's Note: All claims expressed in this article are solely those of the authors and do not necessarily represent those of their affiliated organizations, or those of the publisher, the editors and the reviewers. Any product that may be evaluated in this article, or claim that may be made by its manufacturer, is not guaranteed or endorsed by the publisher.

frontiers in Pharmacology

PERSPECTIVE
published: 26 May 2021
doi: 10.3389/fphar.2021.698567

Scientific and Artful Voices of Resilience

*Pallavi R. Devchand**

Department of Physiology and Pharmacology, Cumming School of Medicine, University of Calgary, Calgary, AB, Canada

Resilience is a fluid trait that is triggered by personal experience. It is, arguably, a necessity for a scientist. What is it? You know it, when you see it. One thing is for certain: resilience reflects the dynamic toggle between change and an individual's identity.

Keywords: systems biology, inflammation, AI, resilience, rare disease

"Nobody knows me, but I'm always there.
A statistic, a reminder of a world that doesn't care"
- UB40 *in* One in Ten, 1981

In the early 1990s, young Alan Wolffe would regularly hop on a flight from DC to the Canadian Rockies. He was test-driving his research: touting the delicate roles of nucleosome positioning in the fine-tune regulation of transcription. In those days of yore, the topic was debatable. And frankly, students in Calgary were perplexed by his energy. Here was a witty Englishman who reveled in facing a critical Calgarian crowd, knowing that the last question to him would always be the same riddle. Even when he was armed with beautiful data using the estrogen receptor activity on the vitellogenin gene of *Xenopus laevis* (Schild et al., 1993), the riddle was still asked and remained unanswered. Alan had more than data in his arsenal. He was a prolific, competitive and effective communicator – obsessed with a mission. Today, Alan's spirit reflects in the casual acceptance of his science – I imagine he would have quipped at the business of histone regulation. How did the man fuel simple "beads-on-a-string" into a science fad that rocketed to potential of clinical relevance?

We call it customary – the passage of habits and food from one generation to another. Fascinating! to follow documented trails from the Egyptians Papyrus (Ebbell, 1937) to Guido Majno's Healing Hand (Majno, 1975); or from a monk's letter (Stone, 1763) to Nobel prizes (Bergstrom et al., 1982). Have you heard the English gentleman (Flower, 2013) challenge Shakespeare's potions? Not everyone is a foodie. Louis Thomas spun biological tales of *Medusa and the Snail* (Thomas, 1974). And Gerry Weissman - oh my! – he will essay you deep into science of the humanities (Weissmann, 2006-2016). Wanna get out some? Steven J. Gould pairs well with a 22 km hike to a soft quarry in the Canadian Rockies (Gould, 1990). And if you are up for a laugh, Uncle Syd will tickle you sarcastic with his seven deadly sins (Brenner, 2019). Of course, you could simply bide time with Alan Lightman (2004). Why is it that despite Nobel prizes and landmark discoveries, these men created bandwidth for communicating their (lesser) passions?

Precious insights come from personal journeys. Paul Allen (2012) and Max Perutz (2002) remind us that even the most famous scientists are fated by human interactions. Oliver Sacks (2015) and Peter Bach (2011) went to a newspaper and won the hearts of so many suffering in silence. Mesmerizing blockbuster movies limelight our global responsibilities and gaping loopholes in our system. Constant Gardener (2005), *Ex Machina* (2014), Side Effect (2013), Eye in the Sky (2015), Little Boy and Fat Man (1989) rightfully message, "Kudos for inventing something, but - "

You bet! There are many vested interests in the businesses of health (Devchand, 2019a). Who can ignore the bloody unicorns (Carreyrou, 2018) or the painful ones (Keefe, 2021)? There is an art to

OPEN ACCESS

Edited by:
Paola Patrignani,
University of Studies G. d'Annunzio Chieti and Pescara, Italy

Reviewed by:
Patrizia Ballerini,
University of Studies G. d'Annunzio Chieti and Pescara, Italy
Pietro Minuz,
University of Verona, Italy

***Correspondence:**
Pallavi R. Devchand
Pallavi.Devchand@ucalgary.ca

Specialty section:
This article was submitted to Inflammation Pharmacology, a section of the journal Frontiers in Pharmacology

Received: *21 April 2021*
Accepted: *06 May 2021*
Published: *26 May 2021*

Citation:
Devchand PR (2021) Scientific and Artful Voices of Resilience. Front. Pharmacol. 12:698567. doi: 10.3389/fphar.2021.698567

busting open a new field and influencing the culture and direction of medicine (FitzGerald, 2005; Schadt, 2005; Devchand et al., 1999). Luckily, we have a narrative of the beginning of Biotech (Hughes, 2013), an award-winning movie that institutionalized multi-scale biology as (The New Biology, 2011), and a vision for artificial intelligence to increase empathy in medicine (Topol, 2019; Devchand, 2019b). Increasingly, patient advocates seed and sustain their missions. What do you do when you are statistically disadvantaged because your disease is rare rather than common? One man's trip with Castleman disease cracks open a cytokine storm of research with a global reach (Fajgenbaum, 2019).

In all tales, change comes with a resilient voice of awareness:

"And I'll tell it and think it and speak it and breathe it
And reflect it from the mountains
So all souls can see it"
- Bob Dylan *in* The Freewheelin', 1963

DATA AVAILABILITY STATEMENT

The original contributions presented in the study are included in the article/Supplementary Material, further inquiries can be directed to the corresponding author.

AUTHOR CONTRIBUTIONS

The author confirms being the sole contributor of this work and has approved it for publication.

FUNDING

PRD was funded in part as K.A.S.H. Research Scientist in Preventative Medicine, with support from NIH (AR002218), the CADgenomics consortium (Leducq Foundation) and the PENTACON consortium (NIH HL117798).

REFERENCES

Allen, P. (2012). *Idea Man: A Memoir by the Cofounder of Microsoft*. New York City: Penguin Books.

Bach, P. (2011). *Well Blog*. New York: New York Times.

Bergstrom, S. K., Samuelsson, B. I., and Vane, J. R. (1982). Nobel Prize in Medicine. Available at: https://www.nobelprize.org/prizes/medicine/1982/summary/ (Accessed April 20, 2021).

Brenner, S. (2019). *Loose ends. . .False Starts*. Singapore: World Scientific.

Carreyrou, J. (2018). *Bad Blood: Secrets and Lies in a Silicon Valley Startup*. New York City: Knopf.

Constant Gardener (2005). *(based on Novel by John Le Carré) Potboiler Productions*, London.

Devchand, P. R., Hihi, A. K., Perroud, M., Schleuning, W. D., Spiegelman, B. M., and Wahli, W. (1999). Chemical Probes that Differentially Regulate Peroxisome Proliferator-Activated Receptor Alpha and BLTR, Nuclear and Cell Suface Receptors for Leukotriene B4. *J. Biol. Chem.* 274 (13), 23341–23348. doi:10.1074/jbc.274.33.23341

Devchand, P. R. (2019a). It Is Personal - or Not!. *Egypt. J. Basic Clin. Pharmacol.* 9, 101416–101417. doi:10.32527/2019/101416

Devchand, P. R. (2019b). Well. From Artificial Intelligence to Empathy? *Nucl. Receptor Res.* 6, 101436. doi:10.32527/2019/101436

Ebbell, B. (1937). *The Papyrus Ebers: The Greatest Egyptian Medical Document*. Copenhagen: Levin and Munksgaard.

Ex Machina (2014). *Film4 DNA Films*, London.

Eye in the Sky (2015). *Eye in the Sky*. London: Entertainment One.

Fajgenbaum, D. (2019). *Chasing My Cure: A Doctor's Race to Turn hope into Action*. New York: Ballantine Books.

FitzGerald, G. A. (2005). Anticipating Change in Drug Development: the Emerging Era of Translational Medicine and Therapeutics. *Nat. Rev. Drug Discov.* 4 (10), 815–818. doi:10.1038/nrd1849

Flower, R. (2013). *Shakespeare's Medicine Cabinet*. IGMB Personal Highlights Series @ Mount Sinai. Available at: https://www.frontiersin.org/events/Shakespeare_s_Medicine_Cabinet/2139 (Accessed April 20, 2021).

Gould, S. J. (1990). *Wonderful Life: The Burgess Shale and the Nature of History*. New York: W.W. Norton and Company.

Hughes, S. S. (2013). *Genentech: The Beginnings of Biotech (Synthesis)*. Chicago: University of Chicago Press.

Keefe, P. R. (2021). *Empire of Pain: The Secret History of the Sackler Dynasty*. New York City: Doubleday.

Lightman, A. (2004). *Einstein's Dreams*. New York City: Vintage Books.

Little Boy and Fat Man (1989). *Little Boy and Fat Man*. Los Angeles: Paramount Pictures.

Majno, G. (1975). *The Healing Hand: Man and Wound in the Ancient World*. Boston: Harvard University Press.

Perutz, M. (2002). *I Wish I Had Made You Angry Earlier (Essays on Science, Scientists and Humanity)*. Long Island, NY: Cold Spring Harbour Laboratory Press.

Sacks, O. (2015). *My Periodic Table*. New York: New York Times Opinion.

Schadt, E. E. (2005). Exploiting naturally occurring DNA variation and molecular profiling data to dissect disease and drug response traits. *Curr. Opin. Biotechnol.* 16 (6), 647–54. doi:10.1016/j.copbio.2005.10.005

Schild, C., Claret, F. X., Wahli, W., and Wolffe, A. P. (1993). A Nucleosome-dependent Static Loop Potentiates Estrogen-Regulated Transcription from the Xenopus Vitellogenin B1 Promoter *In Vitro*. *EMBO J.* 12 (2), 423–433. doi:10.1002/j.1460-2075.1993.tb05674.x

Side Effect (2013). *Endgame Entertainment*, Northbrook.

Stone, E. (1763). An Account of the success of the Bark of Willow in the Cure of Agues. *Philos. Trans. R. Soc.* 53, 195–200.

The New Biology (2011). (directors: John Rubin, Eric Schadt, Glenn Farrell) PacBio. Available at: https://www.youtube.com/watch?v=sjTQD6E3lH4 (Accessed April 20, 2021).

Thomas, L. (1974). *Medusa and the Snail: More Notes of a Biology Watcher*. New York: Penguin Books.

Topol, E. J. (2019). *Deep Medicine: How Artificial Intelligence Can Make Healthcare Human Again*. New York: Hachette Book Group Inc.

Weissmann, G. (2006-2016). *Editorials in FASEB Journal*, Hoboken.

Conflict of Interest: The author declares that the research was conducted in the absence of any commercial or financial relationships that could be construed as a potential conflict of interest.

frontiers in Pharmacology

ORIGINAL RESEARCH
published: 29 September 2021
doi: 10.3389/fphar.2021.700050

Therapeutic Effect of Combining Anisodamine With Neostigmine on Local Scar Formation Following Roux-en-Y Choledochojejunostomy in a Novel Rat Model

*Shao-cheng Lyu†, Jing Wang†, Wen-li Xu†, Han-xuan Wang, Fei Pan, Tao Jiang, Qiang He and Ren Lang**

Department of Hepatobiliary and Pancreaticosplenic Surgery, Beijing Chaoyang Hospital, Capital Medical University, Beijing, China

OPEN ACCESS

Edited by:
Pallavi R. Devchand, University of Calgary, Canada

Reviewed by:
Yuanli Chen, Hefei University of Technology, China
Ling-shiang Felix Chuang, Icahn School of Medicine at Mount Sinai, United States

***Correspondence:**
Ren Lang
langren@bjcyh.com

†These authors have contributed equally to this work

Specialty section:
This article was submitted to Inflammation Pharmacology, a section of the journal Frontiers in Pharmacology

Received: *25 April 2021*
Accepted: *14 June 2021*
Published: *29 September 2021*

Citation:
Lyu S, Wang J, Xu W, Wang H, Pan F, Jiang T, He Q and Lang R (2021) Therapeutic Effect of Combining Anisodamine With Neostigmine on Local Scar Formation Following Roux-en-Y Choledochojejunostomy in a Novel Rat Model. Front. Pharmacol. 12:700050. doi: 10.3389/fphar.2021.700050

Background: The present study aimed to explore the potential effect of combining anisodamine with neostigmine on local scar formation following Roux-en-Y choledochojejunostomy (RCJS) in a novel rat model.

Methods: The biliary obstruction model of Sprague Dawley (SD) rats was established in advance, and 54 rats were divided into nine groups randomly (sham operation group, anisodamine group, neostigmine group, combination group, and control group). Anisodamine (25 mg/kg) and neostigmine (50 μg/kg) were injected to the abdominal cavity separately or simultaneously for 1 week since the first day after surgery according to their allocated intervention, while the same amount of saline (0.5 ml) was injected intraperitoneally in the control group. Indexes including body weight, the diameter of the common bile duct, liver function, inflammatory indexes, and the condition of scar formation in different groups at certain time were evaluated in our study.

Results: Recovery of liver function (ALT, AST, TB, DB, and GGT) and systematic inflammation indexes (CRP, TNF-α, and IL-1β) in the combination group was prior to that in the control group ($p < 0.05$), while no statistical difference in the serum level of IL-10 was observed among groups. Rats in the combination group represented a wider anastomotic diameter and lower expression of α-SMA and TGF-β1 at anastomotic stoma compared to the control group ($p < 0.05$). Histopathological staining showed slighter proliferation of collagen and smooth muscle fibers in rats' bile duct wall and less local scar formation at anastomotic stoma compared to the control group.

Conclusion: The combination of anisodamine and neostigmine can alleviate local and systemic inflammatory response, promote the recovery of liver function, and reduce scar formation in rats after the RCJS procedure.

Keywords: Roux-en-Y choledochojejunostomy, scar formation, anisodamine, neostigmine, inflammatory response

INTRODUCTION

While a variety of techniques are available to restore biliary-enteric continuity, the biliary tree is most commonly anastomosed to the jejunum; choledochojejunostomy (CJS) has been widely adopted to biliary surgeries and represents a routine method of biliary reconstruction after surgical resection of pancreatic head carcinoma, cholangiocarcinoma, ampullary carcinoma, duodenal papillary carcinoma, and other tumors (Hirano et al., 2012; Singh and Arora, 2014). Meanwhile, as the morbidity of cancer and radical resection rate increased in recent years, CJS is gaining more and more popularity in clinical settings, among which Roux-en-Y choledochojejunostomy (RCJS) is the most commonly used surgical procedure in clinical practice.

However, intestinal contents and bile reflux secondary to RCJS are inevitable since the valve function of Oddi's sphincter is no longer available after reconstruction. Continuous stimulation of refluxing fluid can lead to cholangitis and local scar tissue hyperplasia, eventually causing CJS stenosis and even cancer (Kadaba et al., 2017; Bettschart et al., 2002). According to research studies, the incidence rate of CJS stenosis is as high as 13–58% 1 year after CJS (Booij et al., 2018; Yang et al., 2019; Birgin et al., 2020), indicating that inhibiting anastomotic scar formation remains a tough clinical problem. Our previous research studies concluded that the root cause of anastomotic scar formation is the early inflammatory stimulation caused by intestinal content reflux which leads to the activation of fibroblasts and the proliferation of collagen and smooth muscle fibers, ultimately forming a scar (Lyu et al., 2021).

The cholinergic anti-inflammatory pathway has been reported to have modulating effect on inflammatory response in recent years (Ke et al., 2017; Gatta et al., 2020). It transmits anti-inflammatory signals to the reticuloendothelial system (RES) and activates the vagus nerve to release acetylcholine (ACh). The interaction between ACh and α7 nicotinic acetylcholine receptor (α7nAChR) plays a key role in inhibiting inflammatory response and relieving tissue damage. Anisodamine, a widely used belladonna alkaloid that antagonizes mAChR non-selectively, can reinforce the binding force between endogenous ACh and α7nAChR, while neostigmine, a widely used inhibitor against acetylcholinesterase (AChE), can suppress the activity of AChE and prolong the action time of ACh effectively. Their different mechanisms enable them to modulate the cholinergic system in different ways and have synergistic effect when applied simultaneously, increasing inhibition effects on inflammatory reflex effectively (Qian et al., 2015).

Our study aims to figure out the potential effect of combining anisodamine with neostigmine on local scar formation at anastomotic stoma in the novel rat model following RCJS.

METHODS

Ethics Approval

The study was performed under a project license (No. 2019-D.-304) granted by the Ethics Committee of Beijing Chaoyang Hospital and complied with the institutional guidelines for the care and use of animals.

Experimental Animals

Specific pathogen free (SPF)-grade male Sprague Dawley (SD) rats aged 6–8 weeks and weighing about 250 g were selected for the present study. The experimental animals were purchased from Beijing Weitong Lihua Animal Experimental (Beijing, China) and were housed at the Medical Research Center of Beijing Chaoyang Hospital (Beijing, China) at normal room temperature with standard chow. The circadian rhythm of the rats was monitored for 12 h.

Perioperative Management

The rats were fasted (including no access to water) for 6 h before surgery. Surgical anesthesia was performed by an intraperitoneal injection of chloral hydrate (0.5 ml/100 g). After completing the operation, the rats were put into a 37° rewarming table to recover from anesthesia. The rats were not given water for another 12 h after the operation, and normal feeding was resumed after 12 h. All the rats were sacrificed by inferior vena cava bloodletting after the tissue was obtained by laparotomy. All operations were in line with the ethical principles of laboratory animal welfare and approved by the Ethical Member Association of Beijing Chaoyang Hospital affiliated to Capital Medical University.

Grouping and Intervention

A total of 54 SD rats were randomly divided into nine groups with six rats in each group, which are the sham operation group, anisodamine group (observed for 1 week and 1 month), neostigmine group (observed for 1 week and 1 month), combination group (observed for 1 week and 1 month), and control group (observed for 1 week and 1 month). Rats in the sham operation group received abdominal incision and suture only, while rats in other groups underwent surgery based on the RCJS procedure established in our previous study (Lyu et al., 2021). Anisodamine (25 mg/kg) and neostigmine (50 μg/kg), which had been diluted to 0.5 ml, were injected to the abdominal cavity separately or simultaneously according to their allocated intervention (Li et al., 2014), while the same amount of saline (0.5 ml) was injected to the rats' abdominal cavity in the control group. The intervention lasted for 1 week since the first day after surgery.

Measurement and Laboratory Examination

The rats in the sham operation group were sacrificed on the first day after the operation, while other rats were sacrificed at the corresponding time point and reweighed at the time of death, and the diameter of the common bile duct was measured with a vernier caliper. In total, 4 ml blood was collected from the inferior vena cava, and the tissue of RCJS anastomosis was obtained for follow-up examination after the rats were sacrificed. Rats in the sham operation group received same postoperative dispositions as rats in other groups. All blood samples acquired from rats were placed at room temperature for 30 min and then separated by centrifugation (3500 g/min for 10 min; German Sigma Company) to obtain serum. The enzyme-linked immunosorbent assay (ELISA) was applied to measure serum levels of alanine

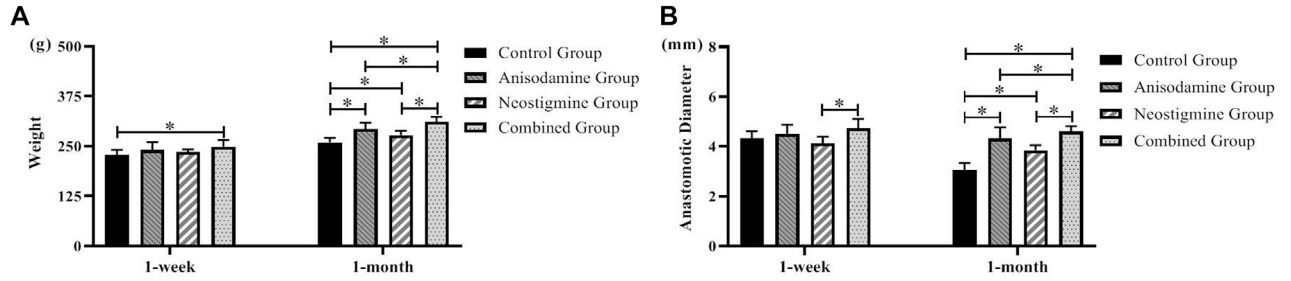

FIGURE 1 | Changes of weight and anastomotic diameter in rats at different time points after the RCJS procedure (* refers to the comparison between the two groups, $p < 0.05$). Comparison of **(A)** weight (g) and **(B)** anastomotic diameter (mm) of rats in different groups at different time points.

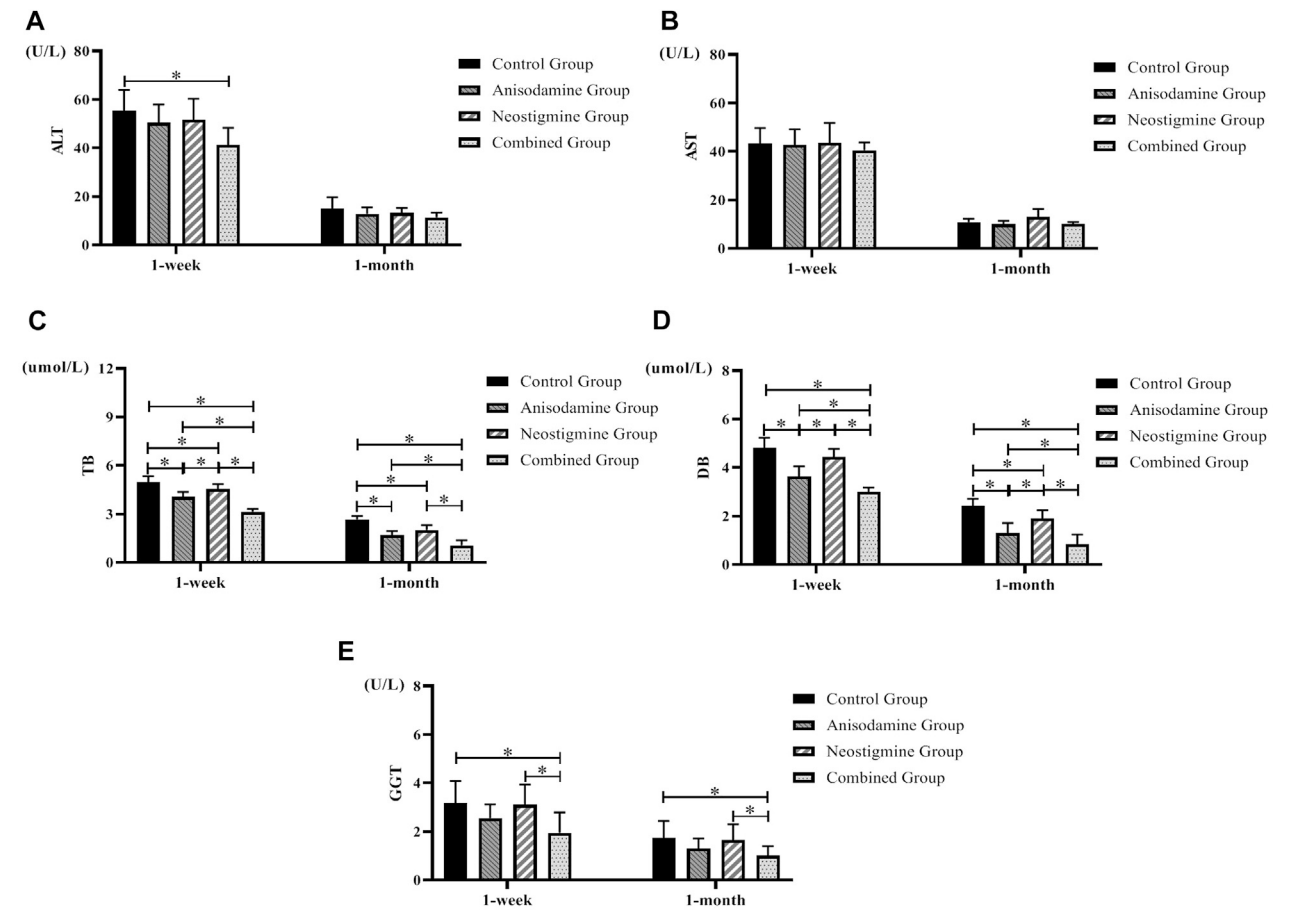

FIGURE 2 | Changes of liver function in rats at different time points after the RCJS procedure (* refers to the comparison between the two groups, $p < 0.05$). Comparison of **(A)** ALT (U/L), **(B)** AST (U/L), **(C)** TB (μmol/L), **(D)** DB (μmol/L), and **(E)** GGT (U/L) at different time points in rats of each group.

aminotransferase (ALT; Jiancheng, China), aspartate aminotransferase (AST; Jiancheng, China), total bilirubin (TB; Jiancheng, China), direct bilirubin (DB; Jiancheng, China), gamma-glutamyltransferase (GGT; Jiancheng, China), C-reactive protein (CRP; Jianglai Bio, China), tumor necrosis factor-α (TNF-α; Jianglai Bio), interleukin-10 (IL-10; Jianglai Bio, China), and interleukin-1β (IL-1β; Jianglai Bio, China).

Histological Examination

The tissue of RCJS anastomosis obtained from rats was divided into two pieces averagely. One piece (4-μm section) was fixed in 10% formalin for 48 h, and the tissue specimen was embedded in wax after dehydration, followed by hematoxylin–eosin (HE) staining, Masson's staining, α-smooth muscle actin (α-SMA) immunohistochemical staining (Abcam, United Kingdom),

transforming growth factor-β1 (TGF-β1) immunohistochemical staining (Abcam, United Kingdom), and observation. The mean optical density (MOD) values of Masson's staining and immunohistochemical staining sections were calculated by Image-Pro Plus 6.0 software; three areas were randomly selected to measure the MOD value of each pathological section under the 200X field of vision, and their average value was taken as the MOD value of the section. The other piece was immediately transferred to liquid nitrogen for preservation and the relative quantitative detection of α-SMA and TGF-β1 by reverse transcription–polymerase chain reaction (RT-PCR). Total RNA was extracted by the TRIzol method (Invitrogen, United States), and cDNA synthesis was carried out by using the SuperScript First Chain Synthesis System (Thermo, United States). The primers were synthesized by raw engineering, and real-time PCR was carried out using SYBR Green PCR Master Mix (Roche, Switzerland).

Primer information was as follows:

GAPDH primer: Forward：5′-GGCAAGTTCAACGGCACAG-3′

Reverse：5′-CGCCAGTAGACTCCACGACA-3′

α-SMA primer: Forward：5′-ATGCTTCTGGACGTACAACTG-3′

Reverse：5′-GGAATAGCCACGCTCAGTCAG-3′

TGF-β1 primer: Forward：5′-ATAGCAACAATTCCTG GCGTTACCTT-3′

Reverse：5′-CCTGTATTCCGTCTCCTTGGTTCAG-3′

Statistical Analysis

Measurement data are expressed as mean ± standard deviation, following a normal distribution, and median (quartile spacing) in non-normal distribution. For the comparison of measurement data between multiple groups, analysis of variance was used for the normal distribution, while the rank-sum test was used for the non-normal distribution. Comparing the measurement data between the two groups, the *t*-test was used for the normal distribution and the rank-sum test was used for the non-normal distribution. The error diagram was used to describe the observation index. Differences were considered statistically significant when $p < 0.05$. All data were analyzed by SPSS version 22.0 software (IBM, Armonk, NY, United States).

RESULTS

Changes of Postoperative Weight and RCJS Anastomotic Diameter in Different Groups

The rats' weight in one-month groups was significantly higher than that in one-week groups ($p < 0.05$), indicating that rats were able to regain their weight gradually after the RCJS procedure. After a week of recovery, only the weight of rats in the combination group exceeded that in the control group ($p < 0.05$). However, after a month of recovery, the weight of rats in all intervention groups including the anisodamine group, neostigmine group, and combination group exceeded that in the control group ($p < 0.05$), and the change was more significant in the combination group. In the control group, the anastomotic diameter of rats in the one-month group was significantly narrower than that in the one-week group, indicating a descent tendency of it as time goes by. Only the diameter of anastomosis in the combination group was wider than that in the neostigmine group after a week of recovery ($p < 0.05$). After a month of recovery, the anastomotic diameter in all intervention groups was greater than that in the control group ($p < 0.05$), and the outcome was much better in the combination group compared to the anisodamine group and neostigmine group ($p < 0.05$) (**Figure 1**).

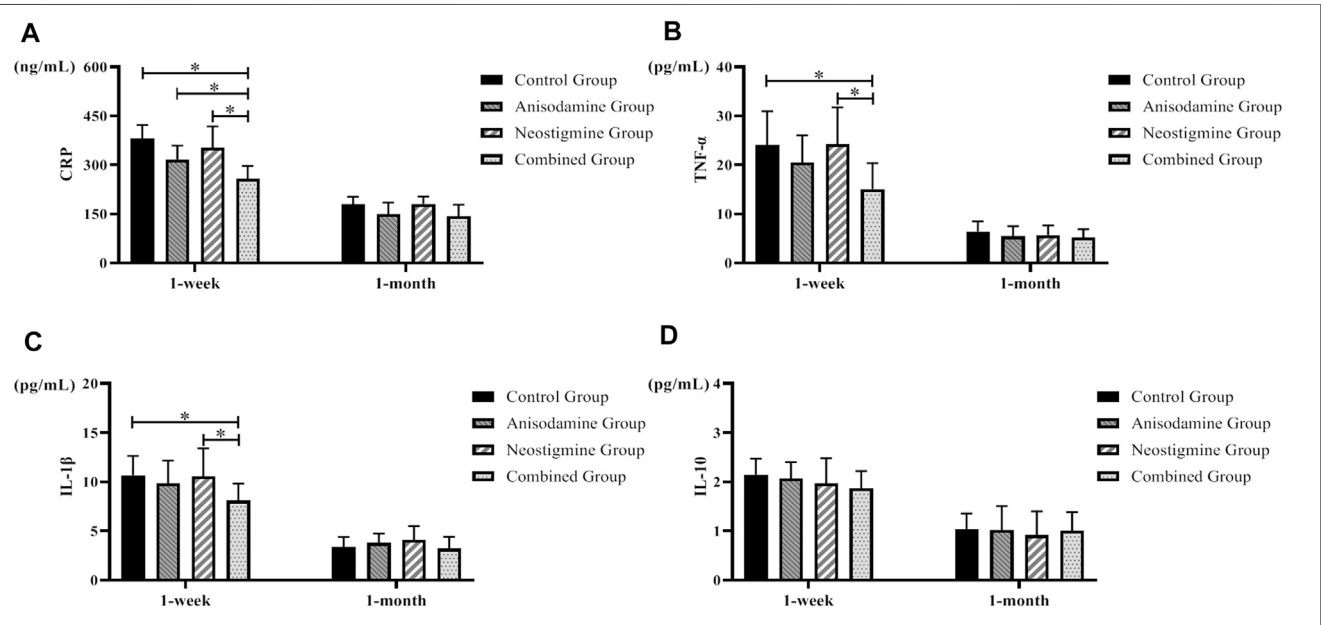

FIGURE 3 | Changes of inflammatory indexes in rats at different time points after the RCJS procedure (* refers to the comparison between the two groups, $p < 0.05$). Comparison of **(A)** CRP (ng/ml), **(B)** TNF-α (pg/ml), **(C)** IL-1β (pg/ml), and **(D)** IL-10 (pg/ml) at different time points in rats of each group.

Changes of Liver Function in Different Groups After Surgery

Our study indicated that rats were able to gradually regain their liver function over time after the RCJS procedure. In terms of alanine transaminase (ALT), only the rats in the combination group were lower than those in the control group at 1 week after operation ($p < 0.05$); 1 month after operation, there was no significant difference between the experimental groups and the control group. As for aspartate transaminase (AST), there was no significant difference between the experimental groups and the control group at 1 week and 1 month after surgery. At 1 week and 1 month after operation, the level of total bilirubin (TB) and direct bilirubin (DB) in each experimental group was significantly lower than that in the control group ($p < 0.05$); meanwhile, the level in the combination group was lower than that in the anisodamine group and neostigmine group ($p < 0.05$). As for gamma-glutamyl transpeptidase (GGT), only the rats in the combination group were lower than those in the control group at 1 week and 1 month after operation ($p < 0.05$), and the level in the combination group was also lower than that in the neostigmine group ($p < 0.05$). In sum, indexes of liver function recovered more quickly in the combination group than in other groups (**Figure 2**).

Changes of Postoperative Inflammatory Indexes in Different Groups

We observed a gradual recovery in the level of inflammatory indexes in rats after the RCJS procedure. Rats have a lower level of proinflammatory cytokines (CRP, TNF-α, and IL-1β) at 1 week after surgery in the combination group than in the control group and neostigmine group ($p < 0.05$), while no statistical differences were observed in these indexes after 1 month of recovery. As for the level of IL-10, there was no statistical difference between intervention groups and the control group, neither at 1 week after surgery nor at 1 month after surgery. In conclusion, the level of proinflammatory cytokines decreased more rapidly in the combination group, while the level of IL-10 had no statistical difference within different groups at any time points (**Figure 3**).

The Pathological Condition of RCJS Anastomotic Stoma After Surgery

The results of HE staining, Masson's staining, α-SMA immunohistochemical staining, and TGF-β1 immunohistochemical staining at RCJS anastomotic stoma in

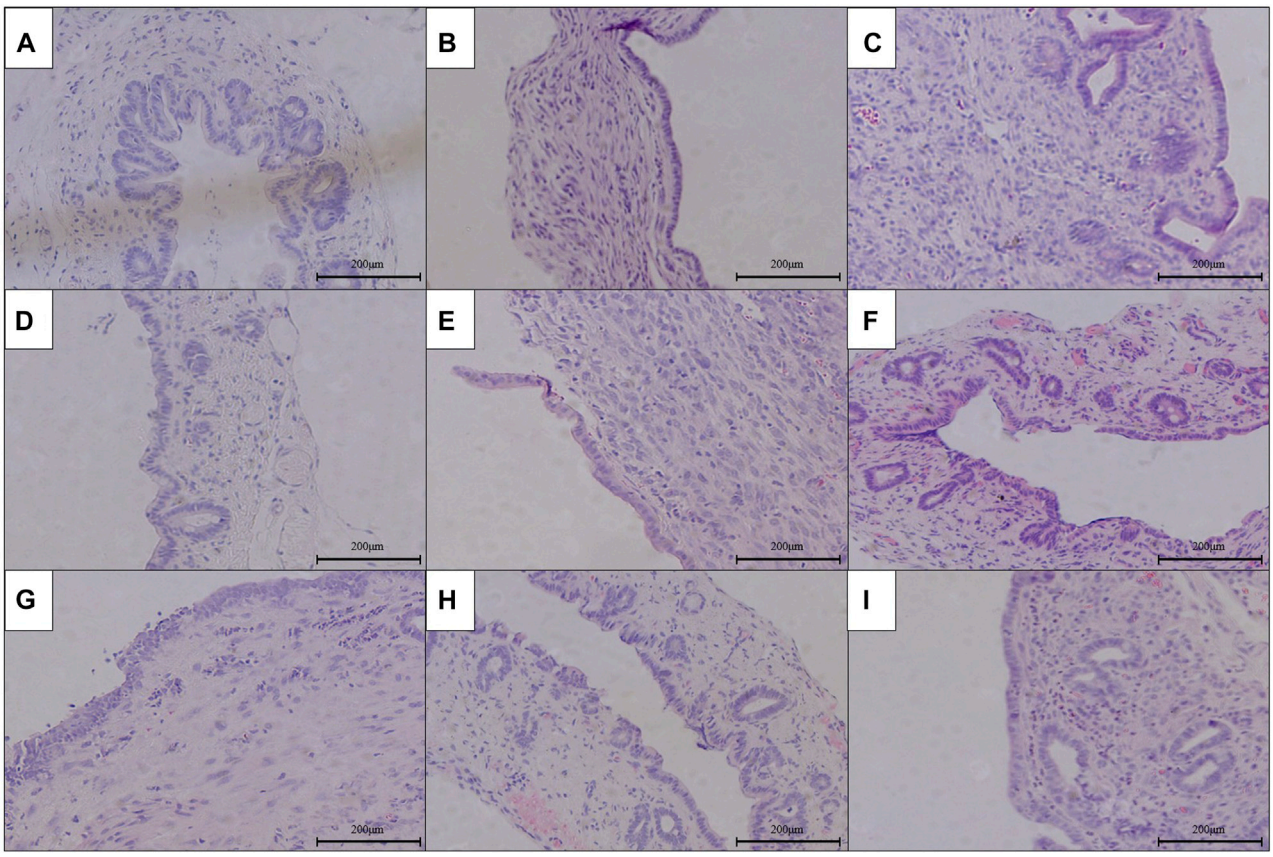

FIGURE 4 | HE staining of anastomotic stoma in different groups after the RCJS procedure (×200). **(A)** Sham operation group. **(B)** Control group at 1 week after the RCJS procedure. **(C)** Control group at 1 month after the RCJS procedure. **(D)** Anisodamine intervention group at 1 week after the RCJS procedure. **(E)** Anisodamine intervention group at 1 month after the RCJS procedure. **(F)** Neostigmine intervention group at 1 week after the RCJS procedure. **(G)** Neostigmine intervention group at 1 month after the RCJS procedure. **(H)** Combination group at 1 week after the RCJS procedure. **(I)** Combination group at 1 month after the RCJS procedure.

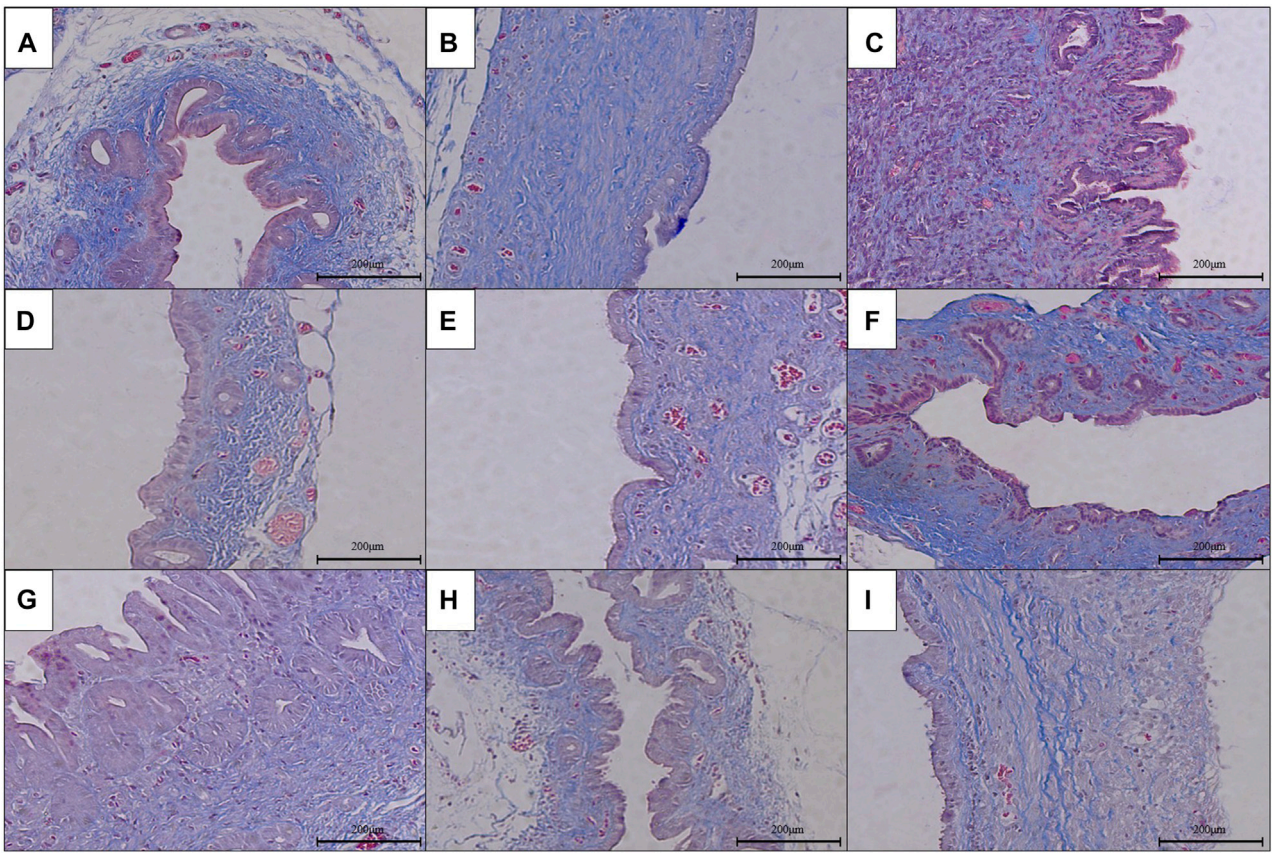

FIGURE 5 | Masson's staining of anastomotic stoma in different groups after the RCJS procedure (×200). **(A)** Sham operation group. **(B)** Control group at 1 week after the RCJS procedure. **(C)** Control group at 1 month after the RCJS procedure. **(D)** Anisodamine intervention group at 1 week after the RCJS procedure. **(E)** Anisodamine intervention group at 1 month after the RCJS procedure. **(F)** Neostigmine intervention group at 1 week after the RCJS procedure. **(G)** Neostigmine intervention group at 1 month after the RCJS procedure. **(H)** Combination group at 1 week after the RCJS procedure. **(I)** Combination group at 1 month after the RCJS procedure.

different groups are shown in **Figures 4–8**. In the sham operation group, we observed the condition of normal bile duct walls which can be divided into three layers: mucosa layer, muscle layer, and adventitia, which were covered with a monolayer columnar epithelium; normal bile duct walls showed no sign of inflammatory cell infiltration in HE staining. In addition, uniform light blue staining and neatly arranged collagen fibers could be seen in Masson's staining, while yellow staining of smooth muscle cells along with yellow particles could rarely be found in bile duct walls in α-SMA and TGF-β1 immunohistochemical staining.

However, after the RCJS procedure, inflammatory cell infiltration and incrassation of the bile duct wall were observed at anastomotic stoma and kept deteriorating as time increased. The obvious proliferation and irregular arrangement of collagen and smooth muscle fibers as well as a large amount of yellow-stained smooth muscle cells and yellow particles in the bile duct wall were seen in Masson's staining and α-SMA and TGF-β1 immunohistochemical staining. Moreover, the proliferation of collagen and smooth muscle fibers along with the expression of yellow particles was at a lower level in the combination group compared to other groups. The results of pathological staining also showed that the MOD values of Masson's staining and α-SMA and TGF-β1 immunohistochemical staining in the combination group were lower than those in other groups at 1 week and 1 month after operation ($p < 0.05$).

Relative Quantitative Detection of PCR at RCJS Anastomotic Stoma in Different Groups

By comparing the expression level of α-SMA and TGF-β1 at 1 week and 1 month after surgery, we found that, after a week of recovery, the level of TGF-β1 in all intervention groups was lower than that in the control group ($p < 0.05$), while the level of α-SMA showed no statistical difference among the groups. At a month after surgery, only the rats in the combination group had a lower expression level of α-SMA and TGF-β1 compared to those in the other groups ($p < 0.05$) (**Figure 9**).

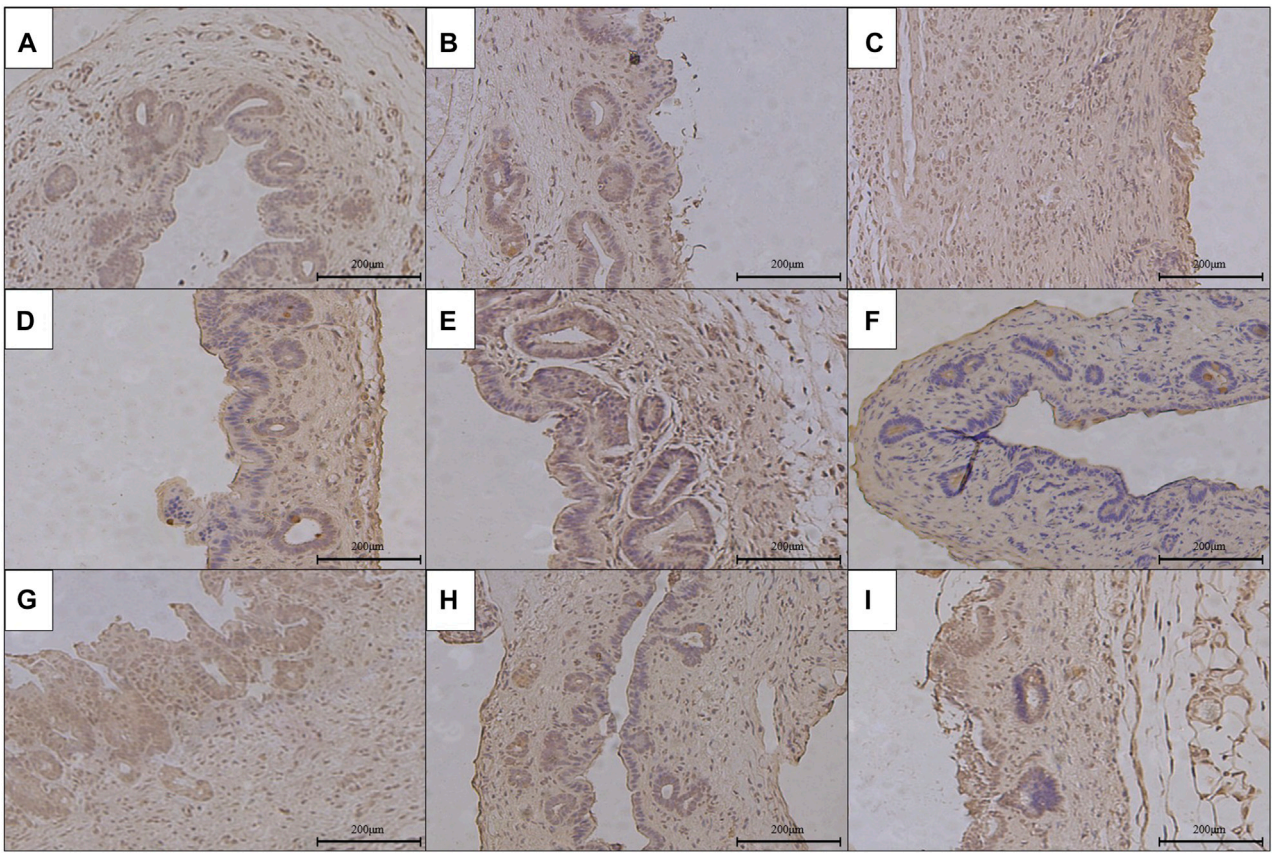

FIGURE 6 | Immunohistochemical staining of α-SMA in the anastomotic stoma after RCJS in different groups (×200). **(A)** IHC staining of α-SMA in the sham operation group. **(B)** IHC staining of α-SMA in the control group at 1 week after the RCJS procedure. **(C)** IHC staining of α-SMA in the control group at 1 month after the RCJS procedure. **(D)** IHC staining of α-SMA in the anisodamine intervention group at 1 week after the RCJS procedure. **(E)** IHC staining of α-SMA in the anisodamine intervention group at 1 month after the RCJS procedure. **(F)** IHC staining of α-SMA in the neostigmine intervention group at 1 week after the RCJS procedure. **(G)** IHC staining of α-SMA in the neostigmine intervention group at 1 month after the RCJS procedure. **(H)** IHC staining of α-SMA in the combination group at 1 week after the RCJS procedure. **(I)** IHC staining of α-SMA in the combination group at 1 month after the RCJS procedure.

DISCUSSION

The RCJS procedure is widely adopted to biliary reconstruction in clinical practice (Xu et al., 2014). However, since the procedure inevitably brings destruction to the function of Oddi's sphincter, intestinal content and bile reflux have always been a huge problem in spite of the great progress we have made in medical techniques, and recurring cholangitis caused by intestinal fluid reflux will cause scar hyperplasia, eventually resulting in CJS stenosis and even canceration (Asano et al., 2016; Dimou et al., 2016). Therefore, effective methods to prevent and control local scar formation are still badly needed and have great significance in clinical practice.

Scar formation is a complicated pathophysiological process in which many cells, tissues, and cytokines are involved and can divided into three overlapping phases, inflammatory phase, cell proliferation phase, and tissue remodeling phase. At the initial stage of scar formation (Kerwin et al., 2014; Yen et al., 2018), inflammation plays a key role in this pathophysiological process and may be a potential target where we can modulate this process effectively. In addition, the effects of inflammation on regeneration and repair have also been studied in various mammalian model systems. During postnatal life, the reparative response of most mammalian organisms does not result in tissue regeneration but in the formation of scars with partial loss of organ function. In contrast, the repair response during the early fetal period is regenerative and scar-less (Colwell et al., 2003). The hallmark of fetal repair is the lack of a typical inflammatory response, suggesting that the absence of inflammation is a prerequisite of regenerative and scar-less repair (Redd et al., 2004). In recent years, numerous genetically modified mouse models have advanced our understanding of how the immune response in postnatal life impacts on regeneration and scar formation. Recently, several review articles were published on this topic (Martin and Leibovich, 2005; Mescher and Neff, 2005; Eming et al., 2007). Taken together, gene-modified mouse models highlight the complex and crucial role of inflammation in controlling the quality of repair; however, further studies are necessary to better understand which processes are positive and which are harmful.

Meanwhile, some reports have pointed out that inflammation reaction has run through the whole process of tissue repair and

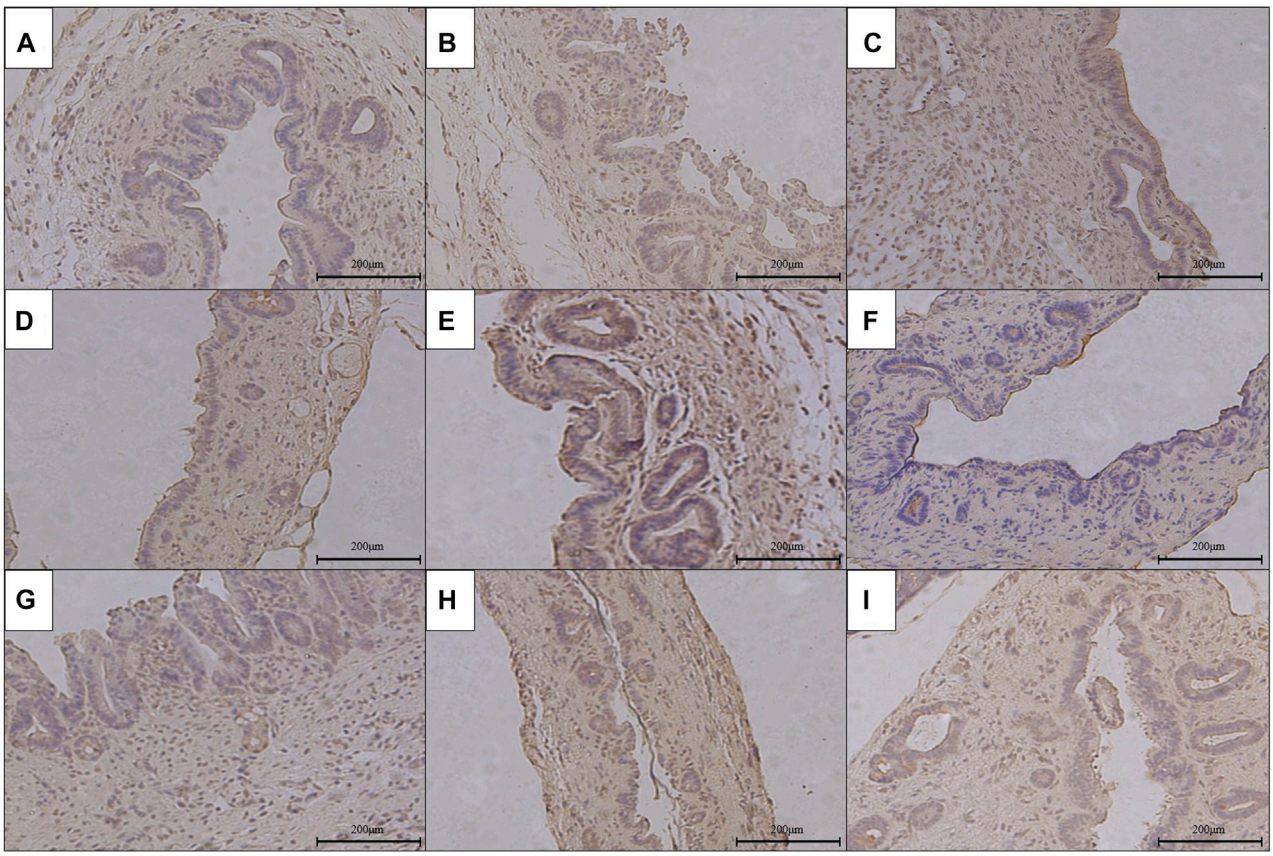

FIGURE 7 | Immunohistochemical staining of TGF-β1 in the anastomotic stoma after RCJS in different groups (×200). **(A)** IHC staining of TGF-β1 in the sham operation group. **(B)** IHC staining of TGF-β1 in the control group at 1 week after the RCJS procedure. **(C)** IHC staining of TGF-β1 in the control group at 1 month after the RCJS procedure. **(D)** IHC staining of TGF-β1 in the anisodamine intervention group at 1 week after the RCJS procedure. **(E)** IHC staining of TGF-β1 in the anisodamine intervention group at 1 month after the RCJS procedure. **(F)** IHC staining of TGF-β1 in the neostigmine intervention group at 1 week after the RCJS procedure. **(G)** IHC staining of TGF-β1 in the neostigmine intervention group at 1 month after the RCJS procedure. **(H)** IHC staining of TGF-β1 in the combination group at 1 week after the RCJS procedure. **(I)** IHC staining of TGF-β1 in the combination group at 1 month after the RCJS procedure.

has played the role like a double sword (Eming et al., 2009; Wang et al., 2019). On the one hand, inflammation can induce wound healing and closing through fibrosis and scar formation and prevent wound infection; on the other hand, inflammation-induced scar healing can hamper tissue regeneration and further may reduce the function of tissue or organ. To sum up, inflammatory cell infiltration can inhibit wound repair and regeneration, resulting in excessive scar formation. Therefore, based on the pathophysiology of scar formation and the negative role of early inflammation in scar formation, we believe that controlling early inflammation is the key step to inhibit scar formation.

It is the recurring inflammatory after the RCJS procedure at anastomotic stoma secondary to intestinal fluid reflux that causes local scar formation and leads to aggravation of anastomotic stenosis after surgery as time goes by, showing proliferation of fibroblasts and myofibroblasts in the bile duct wall as their main performance pathologically (Zhang et al., 2011). Siqueira et al. (2017) asserted that, after receiving end-to-end anastomosis, the proportion of collagen and TGF-β1 in the pig's common bile duct wall in the operation group was significantly higher than that in the sham operation group while showing active proliferation of fibroblasts in the operation group. Our previous research studies (Lyu et al., 2021) also confirmed that the expression of α-SMA and TGF-β1 increased significantly at an early stage after RCJS; subsequently, the fibroblasts proliferated and transformed to myofibroblasts gradually at anastomotic stoma, finally leading to local scar formation. Due to the lack of effective therapeutic targets and drugs to reverse the proliferation of fibroblasts, it will be impossible to modulate and inhibit local scar formation if fibroblasts proliferate extensively or reach the remodeling stage (Block et al., 2015). Through Masson's staining, we observed a large amount of irregularly arranged collagen and smooth muscle fibers as well as local scar formation in the bile duct wall 1 month after the RCJS procedure in rats. These findings indicated that it may be possible to prevent local scar formation at anastomotic stoma if we can reduce local inflammatory response and inhibit the activation of fibroblasts at an early stage.

Numerous studies (Ren et al., 2017; Shao et al., 2019) have shown that the cholinergic pathway can promote the release of

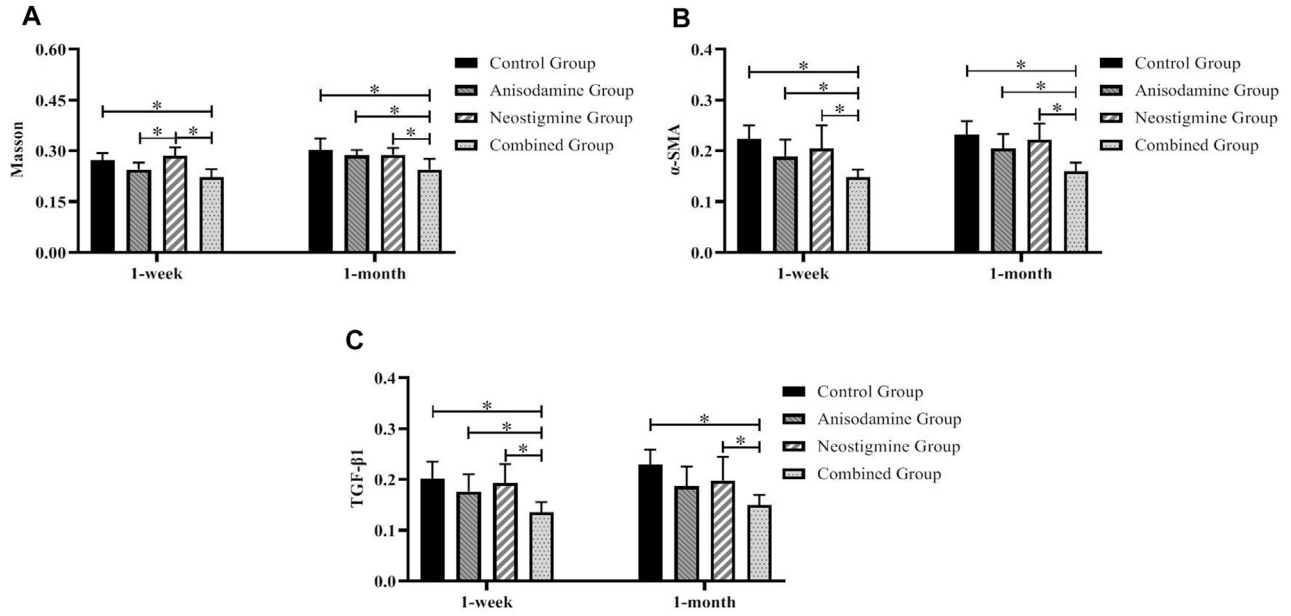

FIGURE 8 | Comparison of the pathological staining MOD of anastomotic stoma in rats at different time points after the RCJS procedure (* refers to the comparison between the two groups, $p < 0.05$). Comparison of MOD values of **(A)** Masson's staining, **(B)** α-SMA immunohistochemical staining, and **(C)** TGF-β1 immunohistochemical staining at different time points in rats of each group.

ACh through modulating the efferent vagus nerve. By interacting with α7nAChR distributed on the surface of macrophages, neutrophils, T-cells, and dendritic cells, increasing ACh can act on nucleus and mitochondria through a variety of signal pathways including JAK2-STAT3 and P13K-Akt and subsequently interfere with the expression and synthesis of proinflammatory cytokines including TNF-α, IL-1β, and IL-6, eventually reducing local inflammatory response.

Ulleryd et al. (2019) reported that the serum level of TNF-α, IL-1β, and IL-6 in rats under stress decreased significantly after activating α7nAChR with its agonist. Xu et al. (2016) observed a dramatic increase in the level of TNF-α and IL-6 in muscular tissue of rats with acute crush syndrome and found that activating α7nAChR could not only decrease the level of TNF-α and IL-6 but also prolong the survival period of rats. Further research studies confirmed that these protective effects against inflammatory response were highly dependent on the JAK2-STAT3 pathway.

Anisodamine, a widely used belladonna alkaloid in clinical practice that antagonizes mAChR non-selectively (Eisenkraft and Falk, 2016), is mainly adopted to relieve abdominal pain caused by gastrointestinal spasm and treat septic shock. Neostigmine (Luo et al., 2018), a widely used inhibitor against AChE that can suppress the activity of AChE and prolong the action time of ACh effectively, is clinically applied to antagonize muscle relaxation effect after surgery and treat patients with myasthenia gravis (MG). When applied jointly, anisodamine can reinforce the binding force between endogenous ACh and α7nAChR, while neostigmine can suppress the activity of AChE. Their different mechanisms enable them to modulate the cholinergic system in different ways and have synergistic effect when applied simultaneously, increasing inhibition effects on inflammatory reflex effectively (Zhou et al., 2014). Sun et al. (2012) discovered that, after injecting anisodamine and neostigmine into endotoxic shock mice, they had a lower level of TNF-α and IL-1β and a higher survival rate compared to those in the control group. However, similar results were not observed in α7nAChR-knockout mice with endotoxic shock after same intervention. Li et al. (2014) focused on therapeutic effects of anisodamine combined with neostigmine in rats after partial hepatectomy and found not only a significant decline in serum levels of TNF-α and IL-1β and mRNA levels of TNF-α, IL-1β, and IL-6 in remnant liver but also a significant improvement in the regeneration rate in the combination group compared to the control group. They concluded that the combination of anisodamine and neostigmine was able to reduce inflammatory response and improve remnant liver regeneration after partial hepatectomy through the cholinergic system.

In the present study, we discovered that applying anisodamine and neostigmine jointly at an early stage after the RCJS procedure is able to decrease the serum level of proinflammatory cytokines, relieving the postoperative inflammation and promoting the recovery of liver function in rats. We also found a significant decline in expression levels of α-SMA and TGF-β1 in anastomotic tissue at an early stage after surgery and detected a milder inflammation at anastomotic stoma in the combination group compared to other groups after a month of recovery. We attributed it to the inhibition effect of the cholinergic system on proinflammatory cytokines instead of influencing expression levels of α-SMA and TGF-β1 in anastomotic tissues directly. By inhibiting the synthesis of proinflammatory cytokines, the

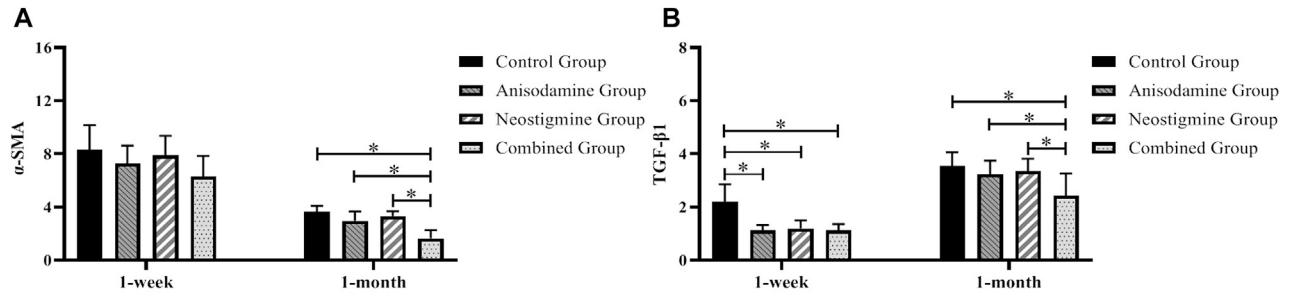

FIGURE 9 | Changes of the expression levels of α-SMA and TGF-β1 in rats at different time points after the RCJS procedure (* refers to the comparison between the two groups, $p < 0.05$). Comparison of **(A)** α-SMA gene expression and **(B)** TGF-β1 gene expression among different groups of rats at different time points.

cholinergic system reduces the inflammatory reaction and infiltration of inflammatory cells at anastomotic stoma, therefore decreasing the secretion of TGF-β1. Without the stimulation of increasing TGF-β1, the activation, proliferation, and differentiation of fibroblasts will be inhibited effectively, ultimately reducing the formation of anastomotic scar tissue. Through the calculation of the MOD value of pathological staining, we also found that Masson's staining and α-SMA and TGF-β1 immunohistochemical staining of anastomotic tissue in the combination group were better than those in other groups, and the expression of α-SMA and TGF-β1 genes in the combination group was significantly lower than that in the other groups. Meanwhile, at the same time, our study also found that there was no significant change in postoperative ALT and AST among different groups, but the levels of TB and DB in the combination group were significantly lower than those in other groups; we considered that this was due to the fact that the diameter of the anastomotic stoma was relatively wider in the combination group, which was more conducive to bile excretion after biliary obstruction, so the decrease in bilirubin was more significant.

CONCLUSION

In conclusion, our study confirmed that the combination of anisodamine and neostigmine can reduce local and systemic inflammatory response, promote the recovery of liver function, and reduce scar formation at anastomotic stoma in rats after the RCJS procedure. Our conclusion brings forward a new idea for preventing and reducing local scar formation after the RCJS procedure, but much more research studies have to be done to verify its clinical value.

DATA AVAILABILITY STATEMENT

The raw data supporting the conclusions of this article will be made available by the authors, without undue reservation.

ETHICS STATEMENT

The animal study was reviewed and approved by the Ethics Committee of Beijing Chaoyang Hospital.

AUTHOR CONTRIBUTIONS

S-cL and JW conceptualized the idea, designed the study, established the rat model, and analyzed and interpreted data. QH and RL provided administrative support and contributed to provision of study materials. JW, W-lX, H-xW, FP, and TJ collected and assembled data. All authors wrote the manuscript and approved the final manuscript.

FUNDING

The present study was supported by the Beijing Natural Science Foundation (Grant No. 7194274).

REFERENCES

Asano, T., Natsume, S., Senda, Y., Sano, T., Matsuo, K., Kodera, Y., et al. (2016). Incidence and Risk Factors for Anastomotic Stenosis of Continuous Hepaticojejunostomy After Pancreaticoduodenectomy. *J. Hepatobiliary Pancreat. Sci.* 23 (10), 628–635. doi:10.1002/jhbp.385

Bettschart, V., Clayton, R. A. E., Parks, R. W., Garden, O. J., and Bellamy, C. O. C. (2002). Cholangiocarcinoma Arising After Biliary-Enteric Drainage Procedures for Benign Disease. *Gut* 51 (1), 128–129. doi:10.1136/gut.51.1.128

Birgin, E., Téoule, P., Galata, C., Rahbari, N. N., and Reissfelder, C. (2020). Cholangitis Following Biliary-Enteric Anastomosis: A Systematic Review and Meta-Analysis. *Pancreatology* 20 (4), 736–745. doi:10.1016/j.pan.2020.04.017

Block, L., Gosain, A., and King, T. W. (2015). Emerging Therapies for Scar Prevention. *Adv. Wound Care* 4 (10), 607–614. doi:10.1089/wound.2015.0646

Booij, K. A. C., Coelen, R. J., de Reuver, P. R., Besselink, M. G., van Delden, O. M., Rauws, E. A., et al. (2018). Long-term Follow-Up and Risk Factors for Strictures after Hepaticojejunostomy for Bile Duct Injury: An Analysis of Surgical and Percutaneous Treatment in a Tertiary center. *Surgery* 163 (5), 1121–1127. doi:10.1016/j.surg.2018.01.003

Colwell, A. S., Longaker, M. T., and Lorenz, H. P. (2003). Fetal Wound Healing. *Front. Biosci.* 8, s1240–s1248. doi:10.2741/1183

Dimou, F. M., Adhikari, D., Mehta, H. B., Olino, K., Riall, T. S., and Brown, K. M. (2016). Incidence of Hepaticojejunostomy Stricture After Hepaticojejunostomy. *Surgery* 160 (3), 691–698. doi:10.1016/j.surg.2016.05.021

Eisenkraft, A., and Falk, A. (2016). Possible Role for Anisodamine in Organophosphate Poisoning. *Br. J. Pharmacol.* 173 (11), 1719–1727. doi:10.1111/bph.13486

Eming, S. A., Hammerschmidt, M., Krieg, T., and Roers, A. (2009). Interrelation of Immunity and Tissue Repair or Regeneration. *Semin. Cel Develop. Biol.* 20, 517–527. doi:10.1016/j.semcdb.2009.04.009

Eming, S. A., Krieg, T., and Davidson, J. M. (2007). Inflammation in Wound Repair: Molecular and Cellular Mechanisms. *J. Invest. Dermatol.* 127 (3), 514–525. doi:10.1038/sj.jid.5700701

Gatta, V., Mengod, G., Reale, M., and Tata, A. M. (2020). Possible Correlation between Cholinergic System Alterations and Neuro/Inflammation in Multiple Sclerosis. *Biomedicines* 8 (6), 153. doi:10.3390/biomedicines8060153

Hirano, S., Tanaka, E., Tsuchikawa, T., Matsumoto, J., Shichinohe, T., and Kato, K. (2012). Techniques of Biliary Reconstruction Following Bile Duct Resection (With Video). *J. Hepato-Biliary-Pancreatic Sci.* 19 (3), 203–209. doi:10.1007/s00534-011-0475-5

Kadaba, R., Bowers, K., Khorsandi, S., Hutchins, R., Abraham, A., Sarker, S.-J., et al. (2017). Complications of Biliary-Enteric Anastomoses. *annals* 99 (3), 210–215. doi:10.1308/rcsann.2016.0293

Ke, P., Shao, B.-Z., Xu, Z.-Q., Chen, X.-W., Wei, W., and Liu, C. (2017). Activating α7 Nicotinic Acetylcholine Receptor Inhibits NLRP3 Inflammasome through Regulation of β-arrestin-1. *CNS Neurosci. Ther.* 23 (11), 875–884. doi:10.1111/cns.12758

Kerwin, L. Y., El Tal, A. K., Stiff, M. A., and Fakhouri, T. M. (2014). Scar Prevention and Remodeling: A Review of the Medical, Surgical, Topical and Light Treatment Approaches. *Int. J. Dermatol.* 53 (8), 922–936. doi:10.1111/ijd.12436

Li, C. H., Zhang, X., Ge, X. L., Huang, X, Zhang, AQ, Gu, WQ, et al. (2014). Effects of Combined Anisodamine and Neostigmine Treatment on the Inflammatory Response and Liver Regeneration of Obstructive Jaundice Rats After Hepatectomy. *Biomed. Res. Int.* 2014, 362024. doi:10.1155/2014/362024

Luo, J., Chen, S., Min, S., and Peng, L. (2018). Reevaluation and Update on Efficacy and Safety of Neostigmine for Reversal of Neuromuscular Blockade. *Tcrm* 14, 2397–2406. doi:10.2147/tcrm.s179420

Lyu, S.-C., Wang, J., Zhou, L., Zhu, J.-Q., Pan, F., Jiang, T., et al. (2021). Mechanism of Scar Formation Following Roux-En-Y Choledochojejunostomy in a Novel Rat Model of Obstructive Jaundice. *Ann. Transl Med.* 9 (6), 456. doi:10.21037/atm-20-5135

Martin, P., and Leibovich, S. J. (2005). Inflammatory Cells During Wound Repair: The Good, the Bad and the Ugly. *Trends Cel Biol.* 15 (11), 599–607. doi:10.1016/j.tcb.2005.09.002

Mescher, A. L., and Neff, A. W. (2005). Regenerative Capacity and the Developing Immune System. *Adv. Biochem. Eng. Biotechnol.* 93, 39–66. doi:10.1007/b99966

Qian, J., Zhang, J.-M., Lin, L.-L., Dong, W.-Z., Cheng, Y.-Q., Su, D.-F., et al. (2015). A Combination of Neostigmine and Anisodamine Protects Against Ischemic Stroke by Activating α7nAChR. *Int. J. Stroke* 10 (5), 737–744. doi:10.1111/ijs.12458

Redd, M. J., Cooper, L., Wood, W., Stramer, B., and Martin, P. (2004). Wound Healing and Inflammation: Embryos Reveal the Way to Perfect Repair. *Phil. Trans. R. Soc. Lond. B* 359 (1445), 777–784. doi:10.1098/rstb.2004.1466

Ren, C., Tong, Y.-I., Li, J.-C., Lu, Z.-Q., and Yao, Y.-M. (2017). The Protective Effect of Alpha 7 Nicotinic Acetylcholine Receptor Activation on Critical Illness and its Mechanism. *Int. J. Biol. Sci.* 13 (1), 46–56. doi:10.7150/ijbs.16404

Shao, B.-Z., Wang, S.-L., Fang, J., Li, Z.-S., Bai, Y., and Wu, K. (2019). Alpha7 Nicotinic Acetylcholine Receptor Alleviates Inflammatory Bowel Disease through Induction of AMPK-mTOR-p70S6K-Mediated Autophagy. *Inflammation* 42 (5), 1666–1679. doi:10.1007/s10753-019-01027-9

Singh, D. P., and Arora, S. (2014). Evaluation of Biliary Enteric Anastomosis in Benign Biliary Disorders. *Indian J. Surg.* 76 (3), 199–203. doi:10.1007/s12262-012-0648-8

Siqueira, O. H. K., Oliveira, K. J., Carvalho, A. C. G., da Nóbrega, A. C. L., Medeiros, R. F., Felix-Patrício, B., et al. (2017). Effect of Tamoxifen on Fibrosis, Collagen Content and Transforming Growth Factor-B1, -β2 and -β3 Expression in Common Bile Duct Anastomosis of Pigs. *Int. J. Exp. Path.* 98 (5), 269–277. doi:10.1111/iep.12250

Sun, L., Zhang, G.-f., Zhang, X., Liu, Q., Liu, J.-g., Su, D.-f., et al. (2012). Combined Administration of Anisodamine and Neostigmine Produces Anti-shock Effects: Involvement of α7 Nicotinic Acetylcholine Receptors. *Acta Pharmacol. Sin* 33 (6), 761–766. doi:10.1038/aps.2012.26

Ulleryd, M. A., Mjörnstedt, F., Panagaki, D., Yang, L. J., Engevall, K., Gutiérrez, S., et al. (2019). Stimulation of Alpha 7 Nicotinic Acetylcholine Receptor (α7nAChR) Inhibits Atherosclerosis Via Immunomodulatory Effects on Myeloid Cells. *Atherosclerosis* 287, 122–133. doi:10.1016/j.atherosclerosis.2019.06.903

Wang, Y., He, G., Tang, H., Shi, Y, Kang, X, Lyu, J, et al. (2019). Aspirin Inhibits Inflammation and Scar Formation in the Injury Tendon Healing Through Regulating JNK/STAT-3 Signalling Pathway. *Cell Prolif* 52 (4), e12650. doi:10.1111/cpr.12650

Xu, M., Wang, M., Zhu, F., Tian, R., Shi, C.-J., Wang, X., et al. (2014). A New Approach for Roux-En-Y Reconstruction After Pancreaticoduodenectomy. *Hepatobiliary Pancreat. Dis. Int.* 13 (6), 649–653. doi:10.1016/s1499-3872(14)60047-3

Xu, Z. Q., Shao, B. Z., Ke, P., Liu, JG, Liu, GK, Chen, XW, et al. (2016). Combined Administration of Anisodamine and Neostigmine Rescued Acute Lethal Crush Syndrome Through α7nAChR-dependent JAK2-STAT3 Signaling. *Sci. Rep.* 6, 37709. doi:10.1038/srep37709

Yang, J.-r., Zhou, J., Wang, L., Wang, Z.-f., Ren, J.-j., and Xiao, R. (2019). A Modified Technique of Biliary-Enteric Anastomosis with Two-point Interrupted Eversion Suture on the Posterior Wall: A Surgeon's Experience. *Asian J. Surg.* 42 (4), 580–581. doi:10.1016/j.asjsur.2018.12.003

Yen, Y.-H., Pu, C.-M., Liu, C.-W., Chen, Y.-C., Chen, Y.-C., Liang, C.-J., et al. (2018). Curcumin Accelerates Cutaneous Wound Healing Via Multiple Biological Actions: The Involvement of TNF-α, MMP-9, α-SMA, and Collagen. *Int. Wound J.* 15 (4), 605–617. doi:10.1111/iwj.12904

Zhang, X., Tian, Y., Xu, Z., Wang, L., Hou, C., and Ling, X. (2011). Healing Process of the Guinea Pig Common Bile Duct After End-To-End Anastomosis: Pathological Evaluation After 6 Months. *Eur. Surg. Res.* 46 (4), 194–206. doi:10.1159/000325451

Zhou, J. X., Ke, P., Huan, G., Shao, B. Z., and Liu, C. (2014). Combined Treatment with Anisodamine and Neostigmine Inhibits Joint Inflammation in Collagen-Induced Arthritis Mice. *CNS Neurosci. Ther.* 20 (2), 186–187. doi:10.1111/cns.12213

Conflict of Interest: The authors declare that the research was conducted in the absence of any commercial or financial relationships that could be construed as a potential conflict of interest.

Publisher's Note: All claims expressed in this article are solely those of the authors and do not necessarily represent those of their affiliated organizations, or those of the publisher, the editors and the reviewers. Any product that may be evaluated in this article, or claim that may be made by its manufacturer, is not guaranteed or endorsed by the publisher.

frontiers in Pharmacology

REVIEW
published: 26 November 2021
doi: 10.3389/fphar.2021.785220

Roles of Macrophages in Atherogenesis

Lia Farahi[1], *Satyesh K. Sinha*[2] *and Aldons J. Lusis*[2]*

[1]Monoclonal Antibody Research Center, Avicenna Research Institute, Tehran, Iran, [2]Department of Medicine, David Geffen School of Medicine, University of California, Los Angeles, Los Angeles, CA, United States

Atherosclerosis is a chronic inflammatory disease that may ultimately lead to local proteolysis, plaque rupture, and thrombotic vascular disease, resulting in myocardial infarction, stroke, and sudden cardiac death. Circulating monocytes are recruited to the arterial wall in response to inflammatory insults and differentiate into macrophages which make a critical contribution to tissue damage, wound healing, and also regression of atherosclerotic lesions. Within plaques, macrophages take up aggregated lipoproteins which have entered the vessel wall to give rise to cholesterol-engorged foam cells. Also, the macrophage phenotype is influenced by various stimuli which affect their polarization, efferocytosis, proliferation, and apoptosis. The heterogeneity of macrophages in lesions has recently been addressed by single-cell sequencing techniques. This article reviews recent advances regarding the roles of macrophages in different stages of disease pathogenesis from initiation to advanced atherosclerosis. Macrophage-based therapies for atherosclerosis management are also described.

Keywords: atherosclerosis, inflammation, macrophages, lipid, plaque, biomarker

OPEN ACCESS

Edited by:
Pallavi R. Devchand,
University of Calgary, Canada

Reviewed by:
Thomas A. Angelovich,
RMIT University, Australia
Jiansheng Huang,
Vanderbilt University Medical Center, United States

***Correspondence:**
Aldons J. Lusis
jlusis@mednet.ucla.edu

Specialty section:
This article was submitted to Inflammation Pharmacology, a section of the journal Frontiers in Pharmacology

Received: *28 September 2021*
Accepted: *04 November 2021*
Published: *26 November 2021*

Citation:
Farahi L, Sinha SK and Lusis AJ (2021) Roles of Macrophages in Atherogenesis. Front. Pharmacol. 12:785220. doi: 10.3389/fphar.2021.785220

1 INTRODUCTION

Atherosclerosis (AS) is associated with both metabolic dysfunction and chronic inflammatory processes. AS is initiated by endothelial dysfunction caused by factors such as high plasma cholesterol, hypertension, diabetes, leukocytosis, cigarette smoking, and low shear stress (Xu et al., 2019). A particularly central event is the subendothelial accumulation of low-density lipoproteins (LDL) and very-low-density lipoproteins (VLDL), which are then subjected to aggregation, oxidation, and enzymatic modifications. The resulting oxidized phospholipids (OxPLs), then contribute to inflammatory processes that promote the activation of endothelial cells (ECs) to express several types of leukocyte adhesion molecules (Marchio et al., 2019). This, in turn, results in leukocyte recruitment, including blood monocytes, neutrophils, lymphocytes, and also platelets to the vessel wall. The monocytes differentiate into macrophages (Mφs) which then proliferate in response to Mφ colony-stimulating factor (M-CSF) and other factors (Robbins et al., 2013b; Sinha et al., 2021). Local proliferation dominates lesional Mφ accumulation in AS. Monocyte recruitment can not fully account for lesional Mφ accumulation in established AS and lesional Mφ can replenish either through the continuous recruitment of circulating monocytes or through some other processes. Mφ self-renewal was identified as a therapeutic target for cardiovascular diseases (Robbins et al., 2013a). Mφs can polarize and reprogram their functional phenotypes in response to different stimuli, and thus display distinct functions related to tissue homeostasis and inflammation (Park, 2021). Mφs take up the aggregated and oxidized LDL (Ox-LDL) leading to their transformation into cholesterol engorged foam cells. Such uptake of modified lipoproteins is mediated primarily by scavenger receptors (SRs) expressed on Mφs. Besides Mφs, vascular

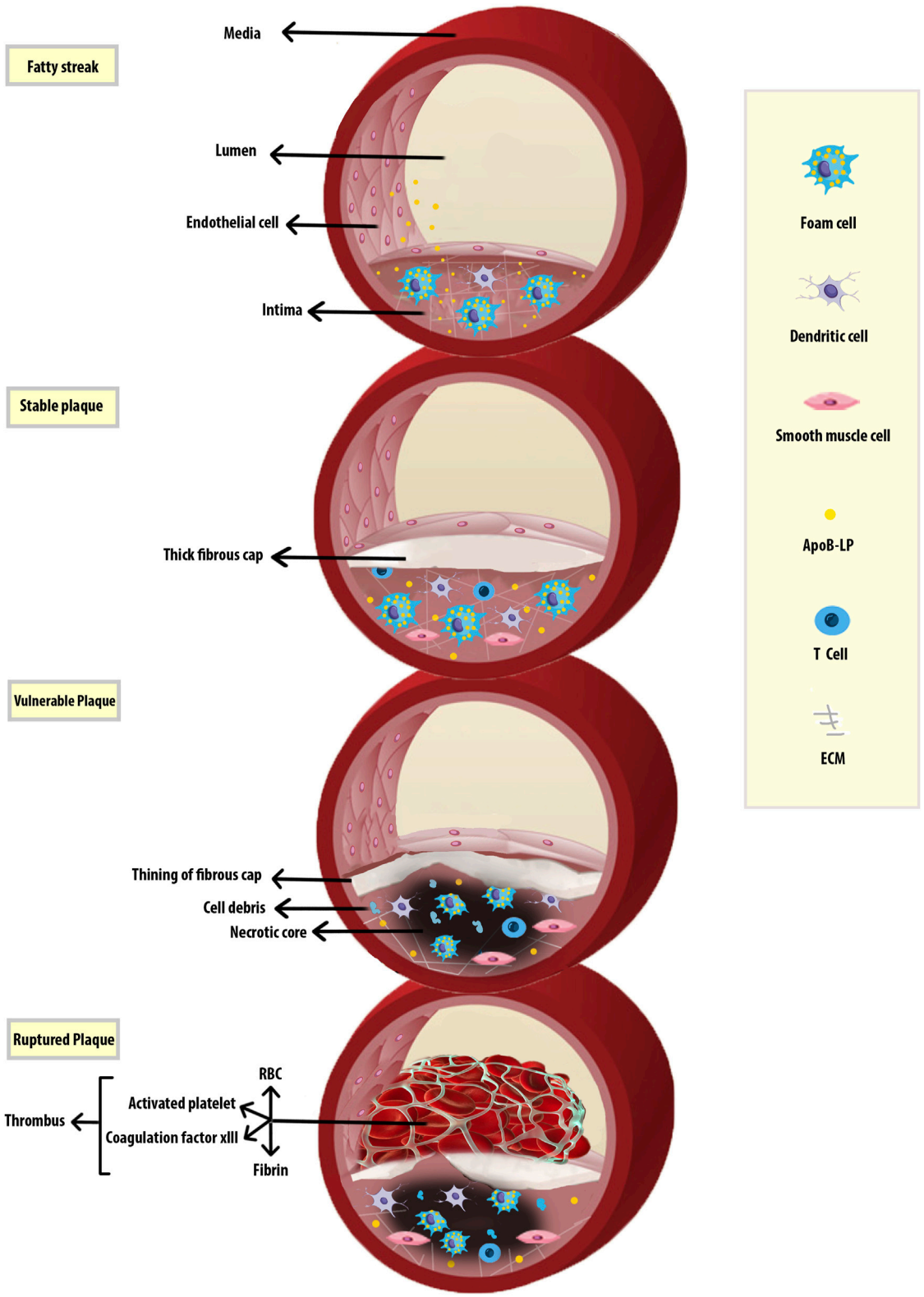

FIGURE 1 | Progression of Atherosclerosis. Early fatty streak lesions are characterized by subendothelial accumulation of ApoB-LPs, the main protein constituent of lipoproteins such as VLDL and LDL which promote the recruitment of Mφs. As the atherosclerotic lesion progresses, ApoB-LP retention is amplified. Vulnerable plaques are characterized by the accumulation of ACs and defective efferocytosis, resulting in the lipid-filled necrotic core. A thinning fibrous cap reduces plaque stability and makes them susceptible to rupture and thrombus formation. Apolipoprotein B-containing lipoproteins (ApoB-LPs).

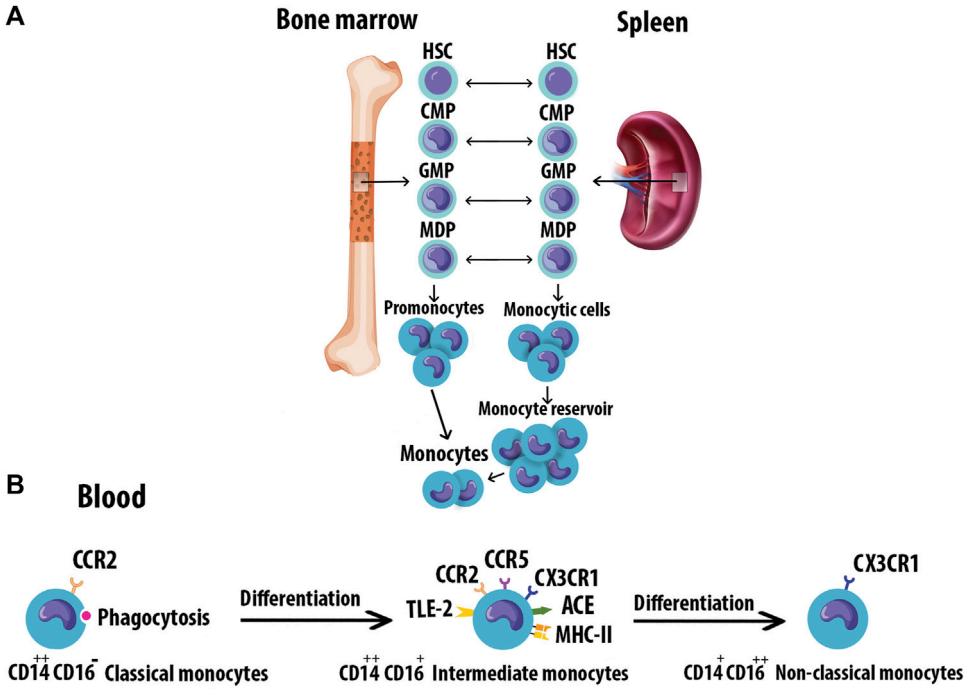

FIGURE 2 | Monocyte origin and heterogeneity. **(A)** Blood monocytes originate from HSC-derived progenitors with myeloid restricted differentiation potential. Successive commitment steps in the bone marrow include CMPs, GMPs, and MDPs. MDPs give rise to monocytes. **(B)** Human monocytes are classified into three subtypes based on the differential expression of CD14 and CD16. Monocytes mature in the bone marrow and are subsequently released into the circulation. Progressively, classical monocytes $CD14^{++}CD16$ give rise to non-classical monocytes $CD14^{+}CD16^{++}$ through an intermediate step of $CD14^{++}CD16^{+}$ monocytes. Hematopoietic stem cell (HSC), Common myeloid progenitors (CMPs), Granulocyte-Mφ precursors (GMPs), Mφ/Dendritic cell progenitor cells (MDPs).

smooth muscle cells (VSMCs) can also transdifferentiate into lesional Mφ-like cells through cholesterol loading (Rong et al., 2003). Advanced plaques are characterized by subendothelial deposition of lipids, necrotic cell debris, calcium phosphate crystals, fibrosis, and inflammatory immune cells including Mφs, T and B lymphocytes, neutrophils, dendritic cells (Canet-Soulas et al., 2021). Lesional T cells can recognize local antigens, leading to activation, clonal expansion, and cytokine production (Robertson and Hansson, 2006). Leukocytosis, an increase in the numbers of circulating leukocytes, is associated with cardiovascular (CV) diseases. Some leukocytes are atherogenic and sustain oxidative stress (OS) and inflammation after myocardial infarction (MI) while others are atheroprotective and help it resolve (Swirski and Nahrendorf, 2013b). For example, $CD4^{+}$ T cell deficiency results in a delay in the switch of $Ly6C^{hi}$ into $Ly6C^{Low}$ monocytes and impaired healing. The inflammatory $Ly\text{-}6C^{hi}$ phenotypes are required during the early response to ischemic injury, but if they persist in the infarct too long, the reparative functions of $Ly\text{-}6C^{low}$ monocytes are impaired (Nahrendorf et al., 2007; Leuschner et al., 2012). The progression of an atherosclerotic lesion including the formation of early fatty streak lesions, fibrous cap, necrotic core, and thrombus have been displayed in **Figure 1** (Virmani et al., 2002; Chinetti-Gbaguidi et al., 2015). In this review, we provide an overview of the critical role of Mφs in the pathogenesis of AS, including recent findings relating to clonal hematopoiesis, single-cell sequencing, and senescence. Mφ-based therapies for the management of AS are also discussed.

MONOCYTE ADHESION TO THE ENDOTHELIUM AND ENTRY INTO THE SUBENDOTHELIAL SPACE

Monocytes originate from hematopoietic stem cell progenitors in the bone marrow. They have also been found to reside in the spleen as a secondary reservoir. **Figure 2A** depicts the differentiation of blood monocytes from bone marrow progenitors (Teh et al., 2019). The heterogeneous population of monocytes is classified into classical, intermediate, and non-classical subtypes based on the differential expression of CD14 and CD16 (**Figure 2B**). The characteristics of monocyte subsets are summarized in **Table 1** (Kapellos et al., 2019). Evidence supports a causal role of atherogenic lipoproteins, especially LDL, in the pathogenesis of AS.

The subendothelial deposition of LDL is likely a key driver of monocyte-ECs adhesion, an early event of AS by activating the overlying EC (Alderson et al., 1986). Factors such as high-fat diets, smoking, and radiation exposure may increase the risk of long-term OS which manifests itself in excessive reactive oxygen species (ROS) generation and LDL oxidation (Poznyak et al., 2021). In lesions, LDL is oxidized to form Ox-LDL which is pro-inflammatory and appears to contribute to AS initiation and

TABLE 1 | Characterization of monocyte subsets.

	Classical	Intermediate	Non-Classical
Surface marker	CCR2, CD62L, CD11b, TLR4, CD36, CD64	CCR2, CX3CR1, HLA-DR, CD74, CD163, CLEC10A, GFRA2, CD86, CCR5	CX3CR1, CX3CR4, HLA-DR, LFA-1
Chemotaxis	CCR2/CCL2	CCR2/CCL2, CX3CR1/CX3CL1	CX3CR1/CX3CL1
Cytokine	IL-1, IL-10	TNF-α, IL-10	TNF-α, IL-1β
Distribution	~85%	~5%	~10%
Function	Phagocytosis, adhesion, migration, anti-inflammatory responses, anti-microbial responses, scavenger activity	Antigen presentation, regulation of apoptosis, transendothelial migration, pro- and anti-inflammatory responses	Complement and FcR mediated phagocytosis, transendothelial migration, adhesion, healing, pro-inflammatory responses, anti-viral responses (Kapellos et al., 2019)

LFA-1, Lymphocyte function-associated antigen 1.

progression (Que et al., 2018). For example, Ox-LDL promotes the expression of vascular cell adhesion molecule-1 (VCAM-1) and intercellular adhesion molecules (ICAM-1) by the ECs which attract the leukocytes into the vessel wall (Milioti et al., 2008). Others have suggested that native or aggregated LDL particles are the key drivers of atherogenesis (Boyle, 2005; Libby, 2021).

Activated lesional ECs and platelets express P- and E-selectin while L-selectin is expressed on leukocytes. The major ligand for selectin is P-selectinglycoprotein ligand 1 (PSGL1) which is expressed on leukocytes and binds to all three selectins. The interaction between selectins and PSGL-1 decelerates fast-flowing leukocytes from the central bloodstream and enables circulating leukocytes to adhere to the activated endothelium. Differential expression or glycosylation of PSGL-1 in leukocytes may result in selective recruitment of monocytes or lymphocytes to atherosclerotic lesions (Huo and Xia, 2009). In addition to inflammatory cells, pro-inflammatory mediators such as cytokines and interleukins are also known to contribute to atherogenesis (Kaperonis et al., 2006).

The adhesion molecules, VCAM1 and ICAM1, are overexpressed on activated ECs (Thayse et al., 2020). Integrins mediate firm leukocyte adhesion on ECs through ligation of monocytes or lymphocytes with VCAM1 or ICAM1 by engaging integrin (Ley et al., 2007). PSGL-1 also interacts with chemokine ligand CCL 21 or CCL19 and enhances chemotactic $CD4^+$ T cells to the vulnerable plaques. Activated $CD4^+$ T lymphocytes secrete interferon-γ (IFN-γ), tumor necrosis factor-α (TNF-α), pro-inflammatory cytokines enhancing immune responses during atherogenesis (Veerman et al., 2007). IFN-β also increases Mφ accumulation in the plaques and accelerates lesion formation (Goossens et al., 2010). Furthermore, activated platelets, a major component of inflammatory lesions, are phagocytosed by monocytes, inducing secretion of pro-inflammatory chemokines such as CCL5. Thus, the presence of activated platelets on the inflamed endothelium may exacerbate pro-inflammatory Mφ activation (Scull et al., 2010). Human IgG1 against a specific Ox-LDL antigenic epitope promoted the regression of atherosclerotic lesions by inhibiting Mφ recruitment and increasing lipid efflux (Schiopu et al., 2007). Monocyte recruitment is also mediated in part by C-C chemokine receptors (CCR)2, CCR5, and CX3C chemokine receptor 1 (CX3CR1) (Tacke et al., 2007).

Macrophage Lipid Uptake and Foam Cells

Monocytes migrate into the intima by chemotactic activity and differentiate into Mφs. Mφs can bind to the circulating lipids through several SRs, such as SR-A1, CD36 (SR-B2), and the lectin-type oxidized LDL receptor 1 (LOX1/SR-E1) that mediate uptake of modified LDL (Syväranta et al., 2014).

SR-A1 is mostly on Mφs but also present on VSMCs and ECs experiencing OS. SR-A1 binds to the modified LDL and is involved in the subendothelial translocation of LDL (Apostolov et al., 2009). The c-Jun N-terminal kinase 2 (JNK2)-dependent phosphorylation of SR-A promotes the uptake of lipids in Mφs and thus mediates foam cell formation (Ricci et al., 2004). Deletion of SR-A reduces plaque inflammation and progression toward more advanced necrotic lesions, but it does not abrogate lipid uptake and Mφ foam cell formation in $ApoE^{-/-}$ mice (Manning-Tobin et al., 2009). SR-A1 expression in aortic VSMCs also leads to foam cell formation and enhanced apoptosis in transfected VSMCs (Lehtolainen et al., 2000). SR-A1 triggers endocytosis through two clathrin- and caveolae-dependent routes. Uptake of modified LDL by SR-A primarily goes through clathrin-dependent pathway. SR-A-induced apoptosis needs endocytosis by the caveola route, which activates p38 MAPK and JNK2 signaling (Zhu et al., 2011). NF-κB also regulates the expression of SR-A1 which can be stimulated by pro-inflammatory cytokines (Chistiakov et al., 2017).

CD36 has a high affinity for Ox-LDL, and Ox-LDL/CD36 interactions inhibit cell polarization and Mφ migration (Park et al., 2012). CD36 is upregulated in Mφ-derived foam cells in plaques. Advanced glycation end products (AGEs) are also recognized by CD36 as overexpression of this receptor facilitated AGE uptake in CHO cells (Ohgami et al., 2001). CD36 is also involved in inflammatory processes, including AS, negative regulation of microvascular angiogenesis, lipid metabolism, and clearance of ACs (Febbraio et al., 2001). CD36 showed a conserved role in lipid sensorial recognition. Ox-LDL binds CD36 and triggers TLR4/TLR6 complex to promote pro-inflammatory signaling (Hoebe et al., 2005). Myricetin, a natural flavonoid, contributes to decreased accumulation of cholesterol in Mφ foam cells by inhibition of CD36-mediated Ox-LDL uptake in $Ldlr^{-/-}$ mice, resulting in a reduction of atherosclerotic lesions (Meng et al., 2019).

LOX-1 augments the uptake of Ox-LDL by Mφs and ECs. Thus, LOX-1 is implicated in atherogenic deposition of lipids and foam cell formation. The expression of LOX-1 is low under

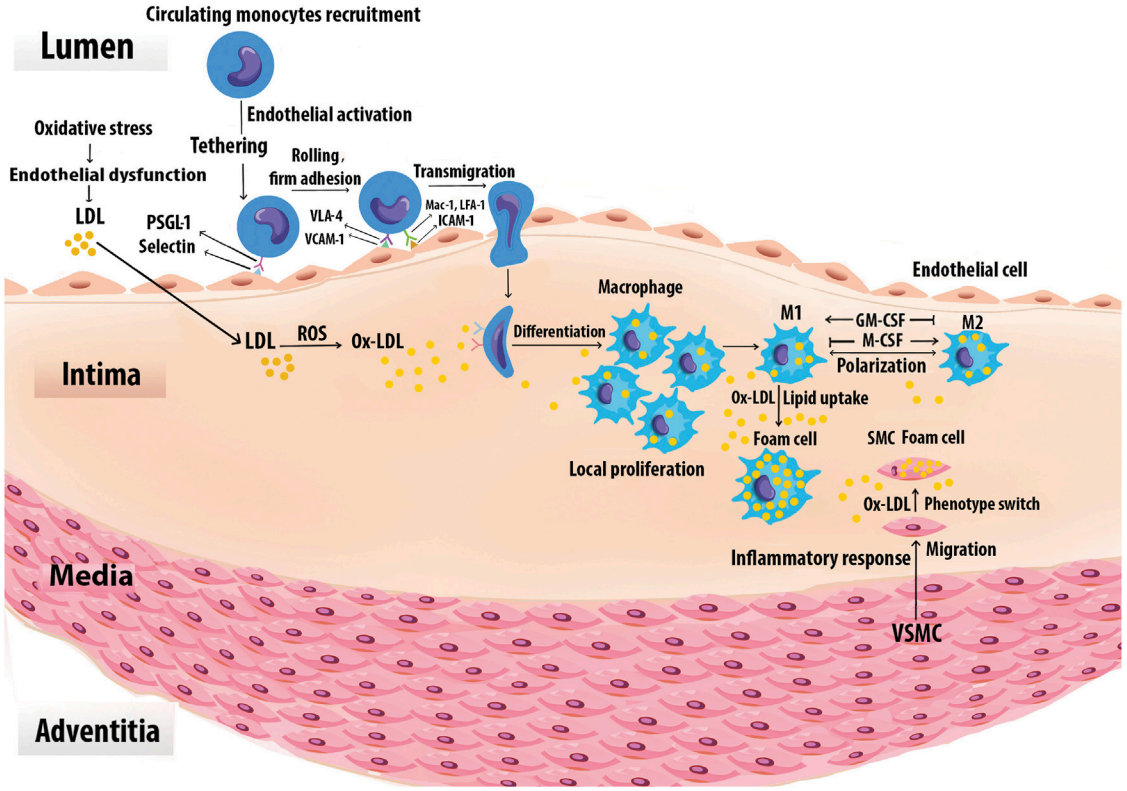

FIGURE 3 | Foam cell formation. Monocytes are recruited to the vascular arginase wall in response to Ox-LDL. Specific adhesion molecules such as the selectins, VCAM-1, and ICAM-1 are expressed on the surface of activated vascular ECs, mediate monocyte adhesion. Once adherent, the monocytes enter the intima and differentiate into Mφs. The differentiation process may be mediated by GM-CSF and M-CSF. Local Mφ proliferation contributes to lesion growth. Upon extensive uptake of Ox-LDL via SRs, Mφs are ultimately turned into foam cells. Chemoattractants, growth factors, and cytokines also promote SMC proliferation, uptake of Ox-LDL, and eventually conversion to foam cells. Foam cells derived from SMCs together with those derived from Mφs generate the fatty lesion.

normal physiological conditions, but inflammatory modulators, including Ox-LDL, LPS, mitochondrial ROS, angiotensin II, sheer stress, pro-inflammatory cytokines, AGEs, and conditions such as high blood pressure, dyslipidemia, and diabetes mellitus, upregulate LOX-1 in AS (Kattoor et al., 2019). In addition, Ox-LDL and pro-inflammatory molecules like TNF-α upregulate the LOX-1 expression in VSMCs and facilitate VSMCs transformation to foam cells, a major source of plaque foam cells in human atherogenesis (Kattoor et al., 2019). LOX-1 also contributes to endothelial dysfunction, Mφ differentiation, apoptosis, the proliferation and migration of VSMCs, foam cell formation, platelet activation, as well as plaque instability, and subsequent plaque rupture (Xu et al., 2013).

The uptake of lipids by Mφs in lesions leads to the formation of cholesterol engorged foam cells (**Figure 3**). Foam cells are the first sign of initial atherogenesis, although they also play an important role in lesion development and advanced plaques (Chistiakov et al., 2017). The endothelin-1 receptor antagonist directly reduced Mφ lipid accumulation and AS in *Ldlr*$^{-/-}$ mice, indicating the role of endothelin-1 in foam-cell formation (Babaei et al., 2000). The cholesteryl esters in modified lipoproteins are hydrolyzed in lysosomes to free cholesteryl, which is then re-esterified by acetyl-CoA acetyltransferase (Chang et al., 2009) and the accumulating cholesteryl esters are stored as cytoplasmic lipid droplets. Increased cholesterol ester accumulation promotes the development of atherosclerotic lesions, unstable plaque with cap rupture, and thrombosis (Yu et al., 2013). Neutral cholesteryl ester hydrolases are responsible for the removal of the ester group from cholesteryl esters to liberate FC which is then effluxed from cells to HDL through ABCA1, ABCG1, and SR-B1 (Chistiakov et al., 2016). Mφ cholesterol uptake and efflux have been shown in **Figure 4**.

ABCA1 activity in arterial Mφs plays a major role in the prevention of foam cell formation by mediating the active transfer of cellular phospholipid and FC to apolipoprotein A-1 (ApoA-1), the major apoprotein in HDL (Phillips, 2018). Multiple factors can affect the expression of ABCA1. Extra-virgin olive oil, cineole, quercetin, apelin-13, S-allylcysteine, and TLR2, increase ABCA1 expression, whereas unsaturated FA, miR-26, and IL-12 in synergy with IL-18 inhibit ABCA1 expression.

ABCG1 exports FC or cellular phospholipid to HDL but not to lipid-free ApoA-1. ABCG1 localizes in the plasma membrane, late endosomes, and ER network (Neufeld et al., 2014). Fucosterol, resveratrol, extra-virgin olive oil, and cineole increase ABCG1 expression and significantly reduce cholesterol deposits in the arteries.

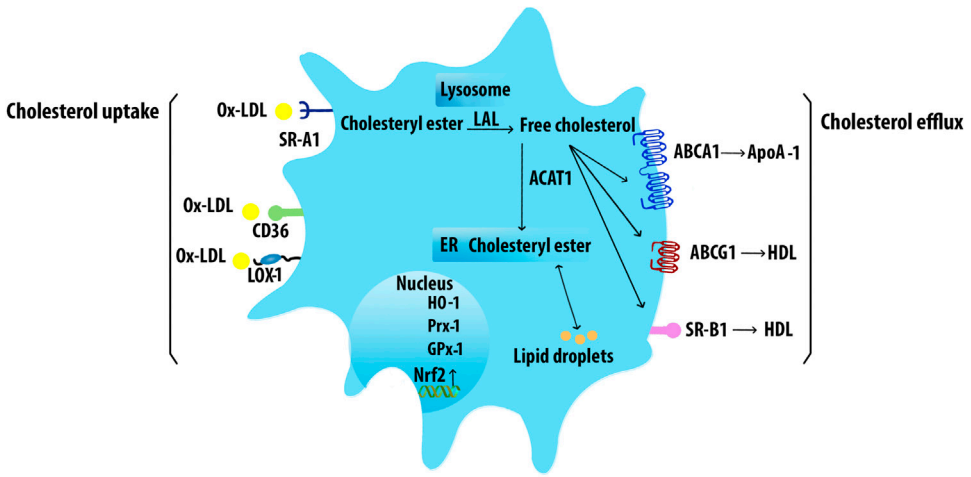

FIGURE 4 | Macrophage cholesterol uptake and efflux. Mφs uptake VLDL and Ox-LDL via SRs including SR-A1, CD36, and LOX-1. The internalized LDL is esterified by acetyl-coenzyme A acetyltransferases and stored in lipid droplets. The ester group is removed from cholesteryl by neutral cholesteryl ester hydrolase through lysosomal acid lipase (LAL) to release FC. ABCA1 transporter mediates the FC efflux from Mφs with ApoA-1. ABCG1 and SR-B1 also efflux FC to mature HDL. Acetyl-CoA acetyltransferase 1 (ACAT1).

SR-B1 promotes FC efflux to mature HDL particles via passive diffusion. The conserved function of SR-B1 across species indicates the importance of its regulation for cholesterol efflux. SR-B1-deficient mice exhibit an increase in accumulation of cholesterol-rich HDL that is accompanied by reduced cholesterol in secreted bile and increased susceptibility to AS (Van Eck et al., 2003). In contradistinction, overexpression of SR-B1 in mice accelerates the metabolism of HDL (Kozarsky et al., 1997). SR-B1 also mediates efferocytosis and reduces atherosclerotic necrosis and inflammation. Deficiency of Mφ SR-BI promoted defective efferocytosis signaling via the Src/PI3K/Rac1 signaling, leading to increased plaque size, necrosis, and inflammation (Tao et al., 2015). Multiple factors were identified to regulate SR-B1 expression. Resveratrol and 13-hydroxy linoleic acid increase the expression of SR-B1, ABCA1, and ABCG1. Caffeic acid and ferulic acid appear to have an antiatherogenic effect by increasing the expression of SR-B1 and ABCG1. Omega-3 fatty acids also induce the activation of SR-B1, ABCA1, and ABCG5, enhancing cholesterol efflux from Mφs (Yu et al., 2013). Risk factors such as infections and fatty diets can change the gut microbiota habitat and increase the levels of circulating LPS which reduces ABCA1/ABCG1 and SR-B1 expression and cholesterol efflux from Mφs (Yu et al., 2013).

Macrophage Phenotypes in Atherosclerosis

Monocytes/Mφs play a central role in innate immune responses, expressing a variety of receptors that modulate their activation. The expression of monocyte and Mφ markers has been shown in **Figure 5A**. Mφ polarization refers to a process by which Mφs can differentiate into distinct functional phenotypes in response to microenvironmental stimuli, such as cytokines, chemokines, growth factors, and pathogen-derived molecules (Murray, 2017). M-CSF in early lesions induces anti-inflammatory M2 (M2a, M2b, M2c, and M2d) Mφs, whereas granulocyte M-CSF (GM-CSF) expression upon AS development promotes polarization of pro-inflammatory M1 phenotypes (Colin et al., 2014). Mφ activation states and markers associated with distinct activation phenotypes have been shown in **Figure 5B**. The dynamic plasticity of Mφs is achieved by transcriptional regulation and thus, specific genes are associated with each type of Mφs (Gerrick et al., 2018). The most abundant T cells in atherosclerotic plaques are Th1 cells and memory $CD4^+$ T cells. The Mφ-directed immune response includes both M1/Th1 and M2/Th2 responses. Th1 and Th2 cells in lesions release Mφ-polarizing factors that affect the balancing of M1 and M2 Mφ phenotypes (Bartlett et al., 2019). Both M1 and M2 Mφs contribute to plaque establishment, while M1 and Th1 cells promote plaque destabilization (Bartlett et al., 2019). M2 Mφs were reported to be found at early stages of AS but showed a switch to M1 phenotypes in advanced lesions of $ApoE^{-/-}$ mice (Khallou-Laschet et al., 2010). The mixture of Mφ subsets likely exists simultaneously within atherosclerotic aortas *in vivo*, contributing to the progression and persistence of atherosclerotic lesions (Butcher and Galkina, 2012). Gene signatures of Mφ activation are highly robust in predicting inflammation, disease susceptibility, and outcomes, suggesting that immune diversity is a valuable parameter in translational research (Buscher et al., 2017). M1/M2 Mφ subpopulations fail to reflect the full complexity of microenvironments in the plaque. A wide range of cytokines and growth factors are present in AS that could affect the phenotype and polarisation state of Mφs. Atherosclerotic plaques contain other Mφ phenotypes include metabolically activated (MMe) Mφs, oxidized (Mox) Mφs, hemoglobin-related (HA-mac, M(Hb), and Mhem) Mφs, M4 Mφs, lipid metabolism-related trigger receptor expressed on myeloid cells 2 (TREM2, also called lipid-associated Mφs), and

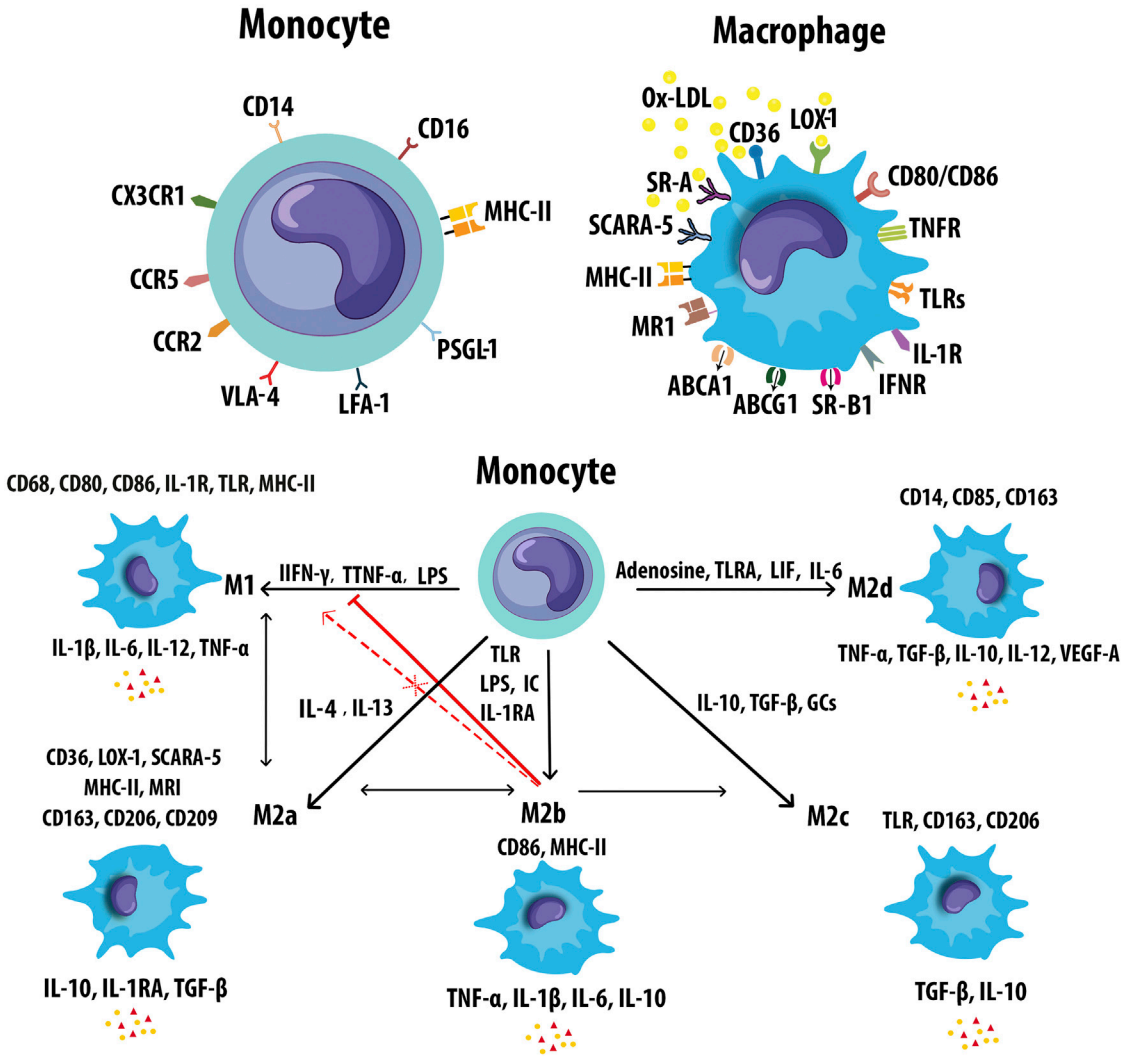

FIGURE 5 | Markers of monocyte and macrophages. **(A)** Monocytes and macrophages express an ample variety of receptors that modulate monocyte and Mφ activation. **(B)** Mφs can polarize to M1 or M2 (M2a, M2b, M2c, and M2d) in response to different inducers and secrete pro- and anti-inflammatory cytokines respectively. M2b Mφs can convert to the other M2 subtypes in response to activated factors. M2b Mφs inhibit the conversion from monocyte to M1 Mφs. M2b also cannot repolarize to M1 during exposure to M1 inducer. Leukemia inhibitory factor (LIF), mannose receptor (MR).

neuroimmunological Mφs including nerve-associated Mφs (NAM), and sympathetic neuron-associated Mφs (SAM) (Nagenborg et al., 2017; Kolter et al., 2020b; Porsch et al., 2020). The main properties and functions of polarized Mφ subtypes are summarized in **Table 2**.

M1 Macrophages

Th1 cytokines including IFN-γ, TNF-α, GM-CSF, and also bacterial stimuli such as LPS polarize Mφs toward the M1 phenotype (Nikonova et al., 2020). M1 cells secrete high levels of pro-inflammatory factors including interleukin-1β (IL-1β), IL-6, IL-12, IL-23, low levels of IL-10, and chemokines such as CXCL-9, CXCL-10, and CXCL-11. M1 Mφ polarization is a tightly controlled process including a set of signaling pathways. Toll-like receptor 4 (TLR4) can be stimulated by LPS or other microbial ligands. This, in turn, promotes activation of interferon regulatory factor-3, activator protein 1 (AP-1), and NF-κB. Myeloid differentiation factor 88 (MyD88), one of the adaptors in responding to TLR4 activation, triggers NF-κB pathway (p65 and p50). This pathway regulates inflammatory genes including pro-inflammatory cytokines such as TNF-α, IL-6, and IL-12. MyD88 activates AP-1 via MAPK signaling. Enhanced AP-1 expression is also mediated by cytokine receptors. Signal transducer and activator of transcription 1 (STAT1) is activated by IFN-γ receptor which regulates the expression of specific genes such as MHC-II, IL-12, nitric oxide synthase 2, and the suppressor of cytokine signaling to promote the M1 Mφ polarization (**Figure 6**) (Wang et al., 2014b). Mφs express Akt1, Akt2, and Akt3 isoforms which are vital for cell proliferation, migration, and survival (Babaev et al., 2014). Akt1 and Akt2 play opposing roles in Mφ polarization. Akt1 deficiency inducing M1 and

TABLE 2 | Activating stimuli, properties, and functions of polarized macrophage subtypes.

Subtypes		Inducers	Secreted factors and related genes	Functions
M1		GM-CSF, TNF-α, IFN-γ, endogenous signals (e.g., Ox-LDL, HSP, HMGB1), bacterial stimuli (e.g., LPS, lipoproteins, dsRNA, LTA)	IL-1, IL-6, IL-12, IL-23, TNF, CXCL8, CXCL9, CXL10, CXCL11, CXCL16, CCL2, CCL3, CCL5	Pro-inflammatory responses
M2	M2a	IL-4, IL-13	IL-1R, IL-10, TGF-β, CCL17, CCL18, CCL22, CCL24	Tissue repair
	M2b	LPS, Immune complexes + TLR, IL-RA	IL-1, IL-6, IL-10, TNF, CCL1	Immunoregulation
	M2c	TGFβ, IL-10, Glucocorticoids	TGF-β, IL-10, CCL16, CCL18, CXCL13	Efferocytosis
	M2d	TLR Agonists + Adenosine, IL-6, LIF	IL-6, IL-10, IL-12, TNF-α, TGF-β, CCL5, CXCL10, CXCL16, CCL18	Wound healing, Angiogenesis, Development of tumors (Cheng et al., 2019)
MMe		NOX2, OxPLs, Glucose, Insulin, FFAs	IL-6 (NOX2-dependent) (Li et al., 2020b)	Pro-inflammatory effect, Chronic inflammation, Dead adipocyte clearance
Mox		OxPL	IL-1β, IL-10, VEGF, CX3CR1^{-} (mouse)	Phagocytosis^{L}, Anti-inflammatory action, Pro-inflammatory effect, AS development, Chronic inflammation, Anti-oxidant
M(Hb)		Hb/Hp complex	ABCA1, ABCG1, LXR-α, IL-10	Cholesterol efflux^{H}, Formation of foam cell, iron content and ROS product^{L}, HB clearance, Atheroprotective (Chistiakov et al., 2015)
HA-mac		Hb/Hp complex	IL-10 (Boyle et al., 2009)	HB clearance, Reduction of OS, Atheroprotective
Mhem		Heme	LXR-β, ABCA1, ABCG1 (Medbury et al., 2014)	Erytrophagocytosis, Atheroprotective
M4		CXCL4	TNF-α, IL-6, CCL18, CCL22	Weak phagocytosis, Minimal foam cell formation Fibrous cap degradation, Proatherogenic action (Chistiakov et al., 2015)
TREM2		LDL, ApoE, (Deczkowska et al., 2020), Nucleotides released from damaged cells (Kober and Brett, 2017)	SPP1, RNASE1, MT1G, SEPP1, FOLR2, NUPR1, KLHDC8B, CCL18, MMP12, ApoC2, and complement system genes (C3, C1QA, C1QB, C1QC) (Xiong et al., 2020)	Lipid metabolism, OS, Lesion calcification, Marker of TAMs, Immunosuppressive activity, Regulation of phagocytosis, proliferation, survival (Porsch et al., 2020; Xiong et al., 2020)
SAM		NI	NI	Pro-inflammatory effect, Thermogenesis, Obesity, NE homeostasis
NAM		NI	NI	Weak energy metabolism with age and obesity, NE homeostasis (Kolter et al., 2020a)

HMGB1, High-mobility group box 1tbox1 protein; LTA, lipoteichoic acid; NOX2, NADPH-oxidase-2; VEGF, vascular endothelial growth factor; Hb/Hp complex, Hemoglobin–haptoglobin complex; LXR, Liver X receptor; SPP1, Secreted Phosphoprotein 1; RNASE1, Ribonuclease A Family Member 1; MT1G, Metallothionein-1G; SEPP1, selenoprotein P plasma 1; FOLR2, Folate receptor 2; NUPR1, Nuclear Protein 1; KLHDC8B, Kelch Domain Containing 8B; C3, Complement component 3; C1QA, C1QB, C1QC, Complement C1q A, B, C Chains; TAMs, Tumor-associated Mφs; NE, norepinephrine; H, high; L, low; NI, not identified.

Akt2 ablation resulting in M2 phenotype (Arranz et al., 2012). Deficiency of Akt2 suppressed the ability of Mφ to undergo M1 polarization reducing the formation of both early and advanced AS in *Ldlr*$^{-/-}$ mice (Babaev et al., 2014). While deletion of Akt1 resulted in enhanced AS and occlusive coronary artery disease in *ApoE*$^{-/-}$ mice (Fernández-Hernando et al., 2007). Mice with reduced mitochondrial oxidative phosphorylation (OxPhos), showed increased M1-like Mφ polarization and decreased Th2 cytokine responsiveness (Jung et al., 2018). Activated M1 Mφs also produce ROS and nitric oxide (NO) through NADPH oxidase system, which may regulate the phagocytosis process of Mφ, disrupting normal cell metabolism, inducing apoptosis, and ultimately causing chronic tissue damage and plaque formation (Xu et al., 2019). M1 Mφs are enriched in lipids and implicated in initiating and sustaining inflammation, atherosclerotic lesion enlargement, and promoting unstable plaques. M1 Mφs are also the most abundant cells in the lesions of infarction and coronary artery disease (CAD) patients (Barrett, 2020).

M2 Macrophages

Alternatively, activated M2 Mφs accumulate at the site of injury and release mediators that suppress inflammation in plaques, clear apoptotic cells (ACs), promote allergy, angiogenesis, tissue repair, fibrosis, and plaque stability (Wynn and Vannella, 2016; Barrett, 2020; Miki et al., 2021). M2 phenotypes are stimulated by the Th2 cytokines including IL-4 and IL-13 which bind to the receptor IL-4Rα and promote the M2 polarization through several pathways such as JAK1 and JAK3 signaling which further result in the activation of STAT6, IRF4, and peroxisome proliferator-activated receptor γ (PPAR-γ). STAT6, IRF4, and PPARγ regulate many of the genes such as *Arg1*, *Fizz1*, and *Ym1* associated with mouse M2 Mφs. The fatty acid receptor also activates PPARγ. Inhibition of PPARγ with its antagonist blocked convallatoxin-induced M2 Mφ polarization and enhanced inflammatory responses (Wang et al., 2014a; Zhang et al., 2021). Convallatoxin is a natural cardiac glycoside that protects against AS. Intracellular glucocorticoids bind the glucocorticoid receptor resulting in the nuclear translocation of the complex. The complex binds DNA, promoting the transcription of anti-inflammatory genes such as IL-10 and IL1R2. Alternatively, the complex can also interact with other transcription factors such as NF-κB or AP-1. IL-10 can be produced by all leukocytes, and IL-10 receptor ligation leads to activation of the transcription factor STAT3 that upregulates the expression of SOCS3 which in turn mediates the suppression of pro-inflammatory cytokine signaling (**Figure 6**)

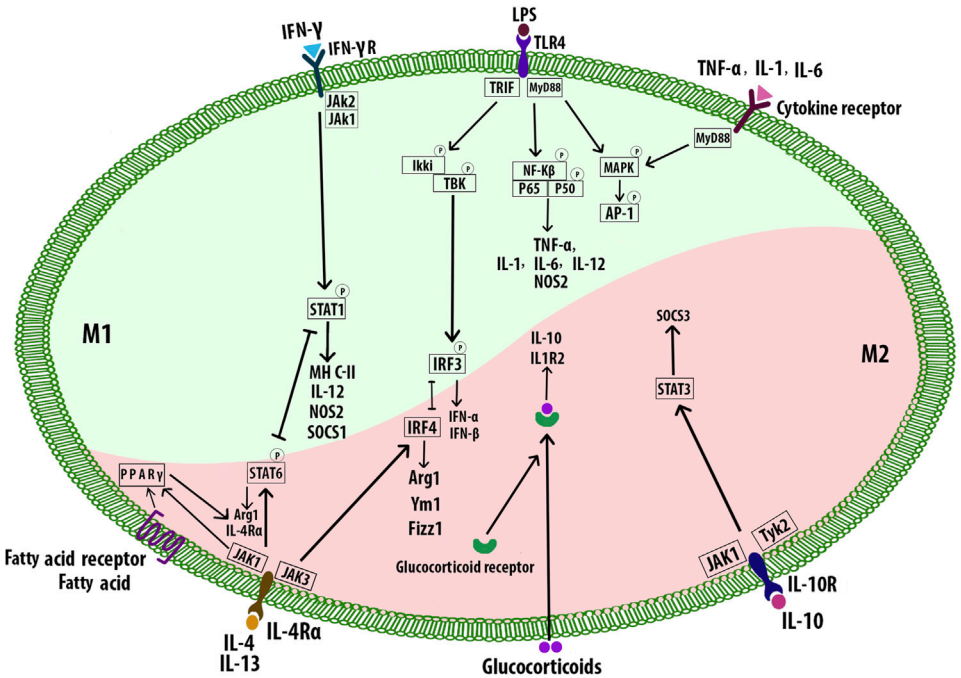

FIGURE 6 | Macrophage polarization signaling pathways. M1 phenotypes express transcription factors such as NF-κB, STAT1, AP-1, and IRF3. M2 subtypes are stimulated by the Th2 cytokines IL-4 and IL-13 which bind to the receptor IL-4Rα and cause the activation of STAT6, IRF4, and PPAR-γ. The intracellular glucocorticoids also promote the transcription of anti-inflammatory genes. IL-10 activates STAT3 and subsequent upregulation of SOCS3. Signal transducer and activator of transcription 1 (STAT1), interferon regulatory factor -3 (IRF3), nitric oxide synthase 2 (NOS2), suppressor of cytokine signaling 3 (SOCS3), arginase 1 (Arg1).

(Wang et al., 2014a). Akt activation is required for M2 activation (Covarrubias et al., 2015). Several signals such as IL-10, and TGF-β promote M2 polarization via PI3K/Akt signaling (Park et al., 2011; Gong et al., 2012). Akt2$^{-/-}$ Mφs attributed to the reduced level of miR-155, which targets C/EBPβ, a key regulator of Arg1 expression and M2 polarization (Arranz et al., 2012). Different stimuli have been associated with the differentiation of M2 subtypes. IL-4, IL-13, and also high levels of CD206 and IL-1 receptor antagonist induce M2a which has anti-inflammatory and tissue remodeling properties. M2b is affected by immune complexes in combination with IL-1β and LPS, and it is involved in immunoregulation. IL-10 and TGFβ or glucocorticoids drive M2c, which has a role in efferocytosis and tissue remodeling. M2b and M2c share regulatory functions, characterized by the secretion of IL-10, and suppression of pro-inflammatory cytokines. IL-6, leukemia inhibitory factor adenosine, and TLR signals induce M2d with angiogenesis, and tumor growth effects (De Paoli et al., 2014; Liberale et al., 2017; Raggi et al., 2017; Abdelaziz et al., 2020). M2 cells also induce the expression of specific chemokines CCL24, CCL17, and CCL22 (M2a), CCL1 (M2b), CCL16, and CCL18 (M2c) (Mantovani et al., 2004). Overall, M2-derived chemokines and cytokines recruit tissue repair cells. Reducing Mφ-inflammation by modulating inflammatory cytokine secretion can promote plaque regression (Lin et al., 2021). M2 Mφs can affect plaque regression via anti-inflammatory effects (Moore et al., 2013) and promote wound healing and tissue repair through collagen formation (Spiller et al., 2014) and removal of dead cells by efferocytosis (Chang et al., 2015). Thus, regulating Mφ polarization to the M2 phenotype could be a therapeutic strategy to prevent the progression of AS or even hasten regression of plaques (Bi et al., 2019). In mouse models of AS regression, the plaque content of M2 markers increased, while M1 markers decreased. Lesions enriched in M2 Mφ are characterized by less inflammation and more stabilizing material, increased content of collagen, and a reduction in the cholesterol content in the plaques (Feig et al., 2011). Administration of IL-13, which is an M2 polarizing factor, protected from AS by increasing lesional collagen content and reducing VCAM-1-dependent monocyte recruitment in *Ldlr*$^{-/-}$ mice (Cardilo-Reis et al., 2012). AS regression after lipid-lowering is dependent on the recruitment of Ly6C^{hi} inflammatory monocytes and their STAT6-dependent polarization to the M2 subtype in mice. The local accumulation of Mφs are highly efficient in clearing ACS. M2 subtype Mφ localized in areas of neovascularization, outside the lipid core, and can phagocytose apoptotic M1 phenotype Mφ, contributing to the resolution of inflammation and inhibition of necrotic core formation within lesions (Chinetti-Gbaguidi et al., 2015).

Other Macrophage Phenotypes

Mφ differentiation into MMe and Mox phenotypes in adipose tissue (AT) is induced by cytokines and OxPLs derived from Ox-LDL which play important roles in the development of chronic inflammation (Haka et al., 2016). NADPH-oxidase-2 is the main driver of MMe Mφs functions (Coats et al., 2017). The Mox

phenotype is associated with the expression of surface markers including *Srnx-1* and *Txnrd-1* and it is abundant in advanced plaques comprising $CD68^+$ cells (Kadl et al., 2010; Leitinger and Schulman, 2013).

HA-mac and M(Hb) are atheroprotective phenotypes that are induced by a hemoglobin-haptoglobin complex, implicated in hemoglobin clearance in hemorrhagic sites. M(Hb) Mφs regulate intracellular lipid balance by increasing cholesterol efflux mediators, thereby preventing the formation of foam cells (Chistiakov et al., 2015). Since Mφ intracellular iron levels may drive cholesterol efflux in M(Hb) cells, the manipulation of Mφ iron levels can be useful to retard AS development by upregulation of Mφ cholesterol efflux (Habib and Finn, 2014). Following endocytosis of hemoglobin-haptoglobin complex, heme is released from RBCs which stimulates Mφ polarization to human atheroprotective Mhem subtype implicated in erythrophagocytosis. The Mhem Mφ suppressed OS, lipid accumulation, and foam cell formation, sharing properties with M (Hb) (Skuratovskaia et al., 2020).

M4 Mφs are induced by CXCL-4 in human atherosclerotic plaques. M4 Mφs have pro-inflammatory and proatherogenic properties which may develop in arterial thrombosis (Skuratovskaia et al., 2020). M4 Mφs are unable to efficiently phagocytose Ox-LDL, with minimal formation of foam cells, and also may not function as efferocytes within plaques (Butcher and Galkina, 2012). They can be involved in fibrous cap degradation, and plaque rupture by producing the enzyme MMP12. M4 Mφ also seems to be irreversible and can not switch like M1, M2, or hemorrhage-associated phenotypes (Skuratovskaia et al., 2020).

TREM2 is a main determinant of adipose tissue homeostasis and a modulatory receptor involved in the regulation of phagocytosis, proliferation, and cell survival. TREM2 Mφs correspond to foamy lipid-laden Mφs accumulating in atherosclerotic plaques. Hematopoietic TREM2 is overexpressed on a subset of AS-associated aortic Mφs and is associated with lipid metabolic processes, OS, and lesion calcification while downregulating pro-inflammatory genes (Porsch et al., 2020).

Neuroimmunological Mφs have been reported in different tissues such as the sciatic nerve, adipose tissue, intestine, skin, and microglia which are implicated in thermogenesis, norepinephrine homeostasis, and obesity (Kolter et al., 2020a). Obesity may increase the risk of OS, and subsequent oxidation of LDL particles and atherogenesis (Poznyak et al., 2021). Neuroimmunological Mφs may have therapeutic potential for individuals with obesity (Skuratovskaia et al., 2020).

BACTERIAL AND VIRAL MEDIATORS OF MACROPHAGE FUNCTION

Bacterial and viral mediators are modulators of Mφ lipid metabolism and AS. ECs and Mφs in atherosclerotic plaques upregulate the expression of TLR in response to microbial antigens followed by inflammatory signals leading to AS. There is evidence that TLR3/4 ligands inhibit cholesterol efflux from Mφs leading to increased susceptibility to AS (Castrillo et al., 2003). *Porphyromonas gingivalis* induces its uptake by Mφs and stimulates the formation of foam cells, the hallmark of early atherogenesis (Giacona et al., 2004). Similar mechanisms have been observed for Chlamydophila pneumoniae infection where surface antigens such as LPS and heat shock protein (HSP) participate in this process. LPS has been shown to promote Mφs development into foam cells and chlamydial HSP60 may induce LDL oxidation on the lesion site (Milioti et al., 2008). The role of *H. pylori*, in Mφs differentiation into foam cells in a TLR-2- and TLR-4-dependent way has also been reported (Li B. et al., 2020). During *H. pylori* infection, Mφs are typically polarized to M1 phenotype which induces pro-inflammatory cytokines and promotes AS (Quiding-Järbrink et al., 2010; Vijayvergiya and Vadivelu, 2015).

Transcriptome analysis suggests that human cytomegalovirus reprograms monocyte differentiation toward pro-inflammatory M1 Mφs following infection. The upregulation of monocyte migration is necessary for the hematogenous spread of the virus and as a consequence, could promote AS associated with human cytomegalovirus infection (Smith et al., 2004; Chan et al., 2008). The enterovirus receptor CXADR is upregulated in Mφs in atherosclerotic plaques. CXADR expression was associated with M1 Mφ polarization and foam cells formation, suggesting a mechanism by which enterovirus may infect the cells in atherosclerotic lesions (Nilchian et al., 2020).

MACROPHAGE-RELATED CYTOKINES IN ATHEROSCLEROSIS

Pro-Inflammatory Cytokines

Mφs release cytokines such as IL-1, IL-6, IL-8, IL-12, IL-18, soluble CD40L (sCD40L), and, TNF in response to various inflammatory stimuli. These factors exhibit a variety of effects, discussed below, and appear to induce inflammation-mediated increases in vascular permeability (Arango Duque and Descoteaux, 2014; Jansen et al., 2016).

IL-1 signaling is proatherogenic and implicated in atherothrombosis. The isoforms IL-1α and IL-1β use a shared IL-1R1. Mice deficient in IL-1β show reduced atherosclerotic disease severity (Arango Duque and Descoteaux, 2014). Canakinumab Anti-inflammatory Thrombosis Outcomes Study (CANTOS) measured the efficacy of IL-1β inhibition in reducing CV event rates (Ridker et al., 2011). Targeting IL-1β by monoclonal antibodies inhibited atherosclerotic plaque formation and the progression of AS (Bhaskar et al., 2011). IL-1β induces angiogenesis by recruitment of myeloid and endothelial lineage cells (Carmi et al., 2009). Deficiency of IL-1α inhibited early lesion formation and inflammation in the $ApoE^{-/-}$ mice (Kamari et al., 2011).

IL-6 is associated with multiple inflammatory disorders. IL-6 can bind to the membrane-bound IL-6R or soluble IL-6R. The CANTOS trial showed that modulation of the IL-6 signaling after taking canakinumab, a human anti-IL-1β monoclonal antibody, is associated with decreased CV events independent of lipid-lowering (Ridker et al., 2018). Senescence-associated IL-6 is upregulated in several tissues and may accelerate atherogenesis

due to aging-related alterations. Thus, the blockade of IL-6 might be an effective strategy to reduce AS in old people (Tyrrell and Goldstein, 2020). The MIRACL study showed that the levels of high-sensitivity C-reactive protein (hs-CRP), serum amyloid A protein (SAA), and IL-6 inflammatory markers were related to the risk of stroke (Kinlay et al., 2008). A phase II clinical trial demonstrating ziltivekimab, a fully human monoclonal antibody targeting the IL-6 ligand, markedly reduced multiple biomarkers of systemic inflammation and thrombosis including hsCRP, fibrinogen, SAA, sPLA2, and Lp(a). Thus, the direct inhibition of IL-6 might have the potential to maximize anti-inflammatory atherosclerotic benefits (Ridker et al., 2021). Since IL-6 is a pleiotropic cytokine, depending on the target cell type, it can exhibit both pro- and anti-inflammatory properties. IL-6 contributes to pro-inflammatory responses such as Mφ and neutrophil chemotaxis, induction of chemokine, adhesion molecule production, and promotes vascular endothelial growth factor production and conversely anti-inflammatory functions such as inhibition of IL-1 production, and induction of IL-1R antagonist indicating that IL-6 can act to reduce inflammation and protect the CV system. IL-6 promotes the development of CV disease through activation of ECs, induction of VSMC proliferation, pro-thrombotic effects on platelets, and accumulation of Mφ lipid (Reiss et al., 2017). A high serum level of IL-6 in intermediate CV risk patients referred for coronary angiography is predictive of CAD (Wainstein et al., 2017).

IL-8 is a proatherogenic cytokine produced by Mφs. Upregulation of IL-8 in atherosclerotic plaques promotes recruitment of monocytes by mediating the rolling of monocytes to adhere firmly to the vascular EC (Apostolopoulos et al., 1996; Gerszten et al., 1999). In addition, elevated serum levels of IL-8 are increased in patients with unstable angina (Romuk et al., 2002). High serum levels of IL-8 are related to an increased risk of all-cause mortality independent of the underlying cause (Velásquez et al., 2019).

IL-12 is formed mainly by plaque Mφs and stimulates the differentiation of $CD4^+$ T cells into Th1 cells through the IL-12Rβ2 chain. Th1 cells can further activate Mφs and subsequently the inflammatory cascade (Kleemann et al., 2008). The administration of IL-12 resulted in enhanced lesion size in $ApoE^{-/-}$ mice (Davenport and Tipping, 2003). $ApoE^{-/-}$ mice lacking TLR4 or MyD88 showed a decrease in AS that was associated with a significant reduction in the circulating levels of IL-12 (Michelsen et al., 2004). Exposure of non-stimulated $CD4^+CD28^-$ T cells to IL-12 induced recruitment of T cells into the atherosclerotic plaque in human atheroma-SCID mouse chimeras (Zhang et al., 2006). These results suggest that IL-12 is a proatherogenic and pro-inflammatory cytokine.

IL-18 acts as a pro-inflammatory cytokine by mediating the production of IL-1β, IL-8, and the expression of ICAM-1 and VCAM-1 (Dinarello et al., 2013). IL-18 accelerated AS by upregulation of CD36 and MMP-9 expression via NF-κB pathway in $ApoE^{-/-}$ mice. NF-κB blockade inhibited IL-18 signaling through downregulation of IL-18, IL-18Rα, CD36, and MMP-9, and upregulation of LXR-α resulted in protection against IL-18-induced AS (Bhat et al., 2015). The proatherogenic effect of IL-18 in the absence of T cells is accompanied by elevation of IFN-γ and CXCL16 expression (Tenger et al., 2005). High serum concentrations of IL-18 increase the risk of future coronary heart disease (Jefferis et al., 2011).

CD40 is expressed mostly on the M1 phenotype (Jansen et al., 2016). Plasma CD40 levels are associated with the severity of carotid AS and an increased risk for future CV events. Intra-plaque levels of sCD40 and sCD40L are also associated with vulnerability and remodeling (Shami et al., 2020). The co-stimulatory CD40 and CD40L are implicated in the regulation of the inflammatory response during AS development. Targeting non-classical CD40L-Mac1 interactions and the inflammatory CD40-TRAF6 signaling may have the potential to reduce the residual inflammatory risk that drives AS (Bosmans et al., 2020).

TNF activates ECs to induce the expression of multiple adhesion molecules and promotes secretion of a variety of inflammatory cytokines and chemokines to enhance the recruitment of activated leukocytes into the lesions (McKellar et al., 2009). TNF-α is a pleiotropic cytokine and functions through its two main receptors including TNF receptors 1 and 2 (TNFR1 and TNFR2). Pro-inflammatory signaling, apoptosis, and degenerative cascades are reported to mediate through TNFR1 while TNF-α signaling through TNFR2 activation is anti-inflammatory and cytoprotective, leading to cell proliferation, differentiation, angiogenesis, and tissue repair (Subedi et al., 2020). TNF-α is implicated in vascular dysfunction. The increase of TNF-α expression by AGEs, their receptors, LOX-1, and NF-κB signaling may induce ROS production leading to endothelial dysfunction in CV disease (Zhang et al., 2009). TNF-α enhances the progression of lesions towards an advanced phenotype by stimulating necrosis and decreasing the incidence of apoptosis in transgenic mice (Boesten et al., 2005). Anti-TNF-α therapy and drugs like thalidomide that inhibit TNF-α production may reduce CV events and inhibit the early development of AS (Chew et al., 2003).

Anti-Inflammatory Cytokines

IL-10 exhibits anti-inflammatory properties that may be protective against AS (Mallat et al., 1999). IL-10 appears to impair HIV-related $CD4^+$ T cells and might be a potential target for the treatment of AS in HIV (Fourman et al., 2020). An inverse correlation between AS severity and $IL\text{-}10^+$ B cells was found in $Ldlr^{-/-}$ mice, while increased cholesterol may mask the protective effects of $IL\text{-}10^+$ B cells (Douna et al., 2019). AS was attenuated through increased expression of IL-10 in programmed cell death protein 4 (PDCD4)-deficient mice. Thus, PDCD4 could affect AS development by regulating the expression of IL-10 (Jiang et al., 2016).

TGF-β is a pleiotropic cytokine that can be both atheroprotective and atherogenic. Deficiency of growth differentiation factor 15 (GDF15), a member of TGF-β family, attenuated lesion formation in $Ldlr^{-/-}$ mice in a TGFβRII-dependent manner that reduced Mφ chemotaxis (de Jager et al., 2011). Suppression of endothelial TGF-β signaling reduced inflammation and vascular permeability in hyperlipidemic mice and attenuated disease progression (Chen

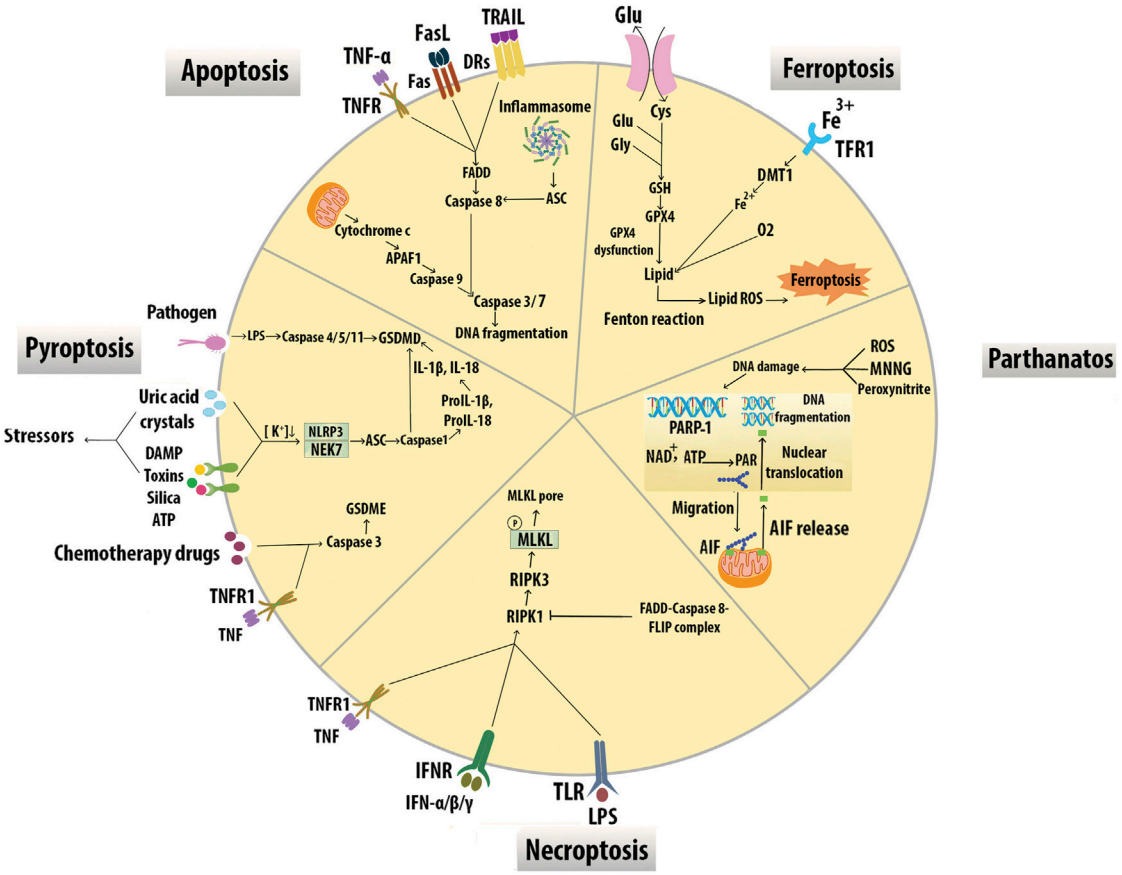

FIGURE 7 | Modes of macrophage death. Different modes of cell death including apoptosis, pyroptosis, necroptosis, parthanatos, and ferroptosis have unique activating stimuli and present different signaling pathways and distinct physiological outcomes. Inhibitors of the divalent metal transporter 1 (DMT1).

et al., 2019). TGF-β can also elicit atherogenic effects through its actions on VSMCs in early plaque lesions (Low et al., 2019). An inverse relationship between serum TGF-β1 levels and advanced AS has been observed (Grainger et al., 1995). Inhibition of TGF-β signaling promoted the development of atherosclerotic lesions with unstable plaque phenotype, increased inflammatory cells, and decreased collagen content in ApoE$^{-/-}$ mice (Mallat et al., 2001). TGF-β1 increased cholesterol efflux and attenuated Mφ foam cell formation in ApoE$^{-/-}$ mice (Panousis et al., 2001). Deletion of Tgfb1 resulted in reduced VSMC differentiation, accelerated lesion formation, and increased inflammation in heterozygous mice, indicating that TGF-β can protect against AS (Low et al., 2019).

Programmed Cell Death of Macrophages and Interactions of Efferocytosis Signaling

Mφ apoptosis, impaired Mφ efferocytosis, and secondary Mφ necrosis have been implicated in necrotic core and vulnerable plaque formation (Gonzalez and Trigatti, 2017). While the most common form of Mφ death is apoptosis, other programmed cell death modalities in Mφ include immune-reactive cell death (pyroptosis), necroptosis, mitochondrial-dependent cell death (parthanatos), and iron-dependent cell death (ferroptosis) (Yan et al., 2020) (**Figure 7**).

Apoptosis can be triggered by the activation of a mitochondrial pathway by cellular stress or through the activation of death receptors (DRs) at the cell surface. The mitochondrial intermembrane protein, cytochrome c, is released into the cytosol and triggers apoptotic protease-activating factor 1 (APAF1), which in turn activates the serine protease caspase 9. Active caspase 9 stimulates the executioner caspases caspase 3 and caspase 7, leading to DNA fragmentation. Death receptors include TNFR1, FAS receptor, and TNF-related apoptosis-inducing ligand (TRAIL). Receptor ligation promotes the recruitment of adaptor proteins, including FAS-associated death domain protein (FADD), which bind and activate caspase 8. Caspase 8 activates the executioner caspases results in cell death. Inflammasomes can also trigger caspase 8 via apoptosis-associated protein (ASC) leading to DNA damage-induced apoptosis (Boada-Romero et al., 2020). Mφ SR-A has a protective effect in early lesions but proatherosclerotic roles in advanced plaques for induction of Mφ apoptosis and efferocytosis. (Devries-Seimon et al., 2005). STAT1 appears to be an essential component of ER stress/SRA-induced Mφ apoptosis in advanced atheromata (Lim et al., 2008).

Overexpression of IL-10 by T cells was reported to suppress STAT1 activity and protect from excessive cell death and plaque necrosis (Pinderski et al., 2002). Transcription factor *Zhx2* deficiency promoted Mφ apoptosis and exhibited a reduction in lesion size and resistance to AS in mice. Evidence including BM transplantation studies also supports this effect of *Zhx2* which is mediated in part by monocytes/Mφs (Erbilgin et al., 2018). A prolonged increase of CHOP levels induces apoptosis through cytoplasmic Ca^{2+} metabolism and suppression of prosurvival molecules like Bcl-2 (Tabas, 2010). In early lesions, efferocytosis prevents cellular necrosis and induces anti-inflammatory pathways through TGF-β and the activation of NF-κB signaling to promote cell survival (Henson et al., 2001). In contrast, ER stress in foam cells induces inflammatory pathways within the lesion by suppressing NF-κB signaling and activating JNK, activator protein-1, ROS, and spliced X-box binding protein 1, which promote apoptosis (Xu et al., 2019).

Pyroptosis results in the death of Mφs in response to bacterial infection, accompanied by activation of inflammasomes and maturation of pro-inflammatory cytokines IL-1β and IL-18. Gasdermin D (GSDMD) pores are the effectors of pyroptosis. Cytosolic LPS binds caspase 4/5/11 to trigger their cleavage of GSDMD and subsequent plasma membrane permeabilization leading to pyroptosis. Inflammasome sensor proteins, such as NLRP3, recognize cellular stressors, including those from bacteria, viruses, toxins, ATP, uric acid crystals, silica, and damage-associated molecular pattern (DAMPs). These stressors activate NLRP3 indirectly through potassium efflux, which leads to NEK7 binding NLRP3 to trigger its oligomerization. NLRP3 subsequently activates caspase-1 via the adaptor protein ASC and cleaves GSDMD resulting in pyroptotic cell death. Active caspase 1 also proteolytically processes IL-1β and IL-18 into their active forms, which are subsequently released from pyroptotic cells (Frank and Vince, 2019). Chemotherapy drugs induce pyroptosis through caspase 3 cleavage of Gasdermin E (GSDME) (Wang et al., 2017). Cleavage of GSDME by caspase 3 may also switch TNF-induced apoptosis to pyroptosis (Rogers et al., 2017). AS risk factors could activate NLRP3 inflammasomes in ECs and Mφs. NLRP3 inflammasome-mediated pyroptosis in the atherosclerotic plaques is correlated with plaque rupture and vascular inflammation, suggesting that NLRP3 inflammasome and related pyroptosis play an important role in the pathogenesis of AS (Zeng et al., 2019).

Necroptosis is activated by death receptors including TNFR1, IFNR, and TLR3/4. Necroptosis is initiated through the activation of RIPK1, which binds and activates RIPK3. RIPK3-mediated phosphorylation of the mixed-lineage kinase domain-like protein (MLKL) results in membrane lysis. This process is inhibited by the activation of caspase 8 and its apoptotic inhibitor FLIP which cleaves RIPK1 to prevent necroptosis (Boada-Romero et al., 2020). The expression of necroptosis mediators RIPK3 and MLKL is upregulated in atherosclerotic plaques, especially in vulnerable plaques supporting the role of RIPK3-mediated Mφ necroptosis in the development of AS (Karunakaran et al., 2016; Tian et al., 2016).

Parthanatos in plaque Mφs is triggered by DNA damaging stimuli such as N-methyl-N′-nitro-N-nitrosoguanidine (MNNG), peroxynitrite, and ROS-dependent activation of poly ADP-ribose polymerase (PARP)1. The PAR polymer is synthesized by PARP1 in response to DNA breaks, migrates to the mitochondria, and releases apoptosis-inducing factor (AIF) which interacts with Mφ migration inhibitory factor and degrades DNA (Robinson et al., 2019). PARP1 inhibition may affect endothelial function, lipid metabolism, foam cell formation, switch from necrosis to apoptosis, and thus play a major role in atherogenesis (Xu et al., 2014).

Ferroptosis is associated with iron-dependent accumulation of lipid hydroperoxides during cell death. Cysteine (Cys_2) can enter the cytoplasm via xCT and synthesizes glutathione (GSH) with glutamate (Glu), and glycine (Gly). Glutathione peroxidase 4 (GPX4) is an antioxidant enzyme that removes oxidative modifications from lipids. When GPX4 dysfunction, lipid transforms into lipid ROS with O2 and Fe^{2+} via the Fenton reaction (Zuo et al., 2020). Lipid peroxidation, intraplaque hemorrhages, and iron deposition are hallmarks of advanced human plaques, which is indirect evidence for the initiation of Mφ ferroptosis and plaque destabilization. Overexpression of GPX4 decreased lipid peroxidation and inhibited plaque development in $ApoE^{-/-}$ mice indicating the possible role of ferroptosis in CV disease (Guo et al., 2008).

Efferocytosis is the process by which cells undergoing apoptosis are cleared by Mφs, thereby reducing inflammation and maintaining tissue homeostasis (Yan et al., 2020). Disposal of the dying cells requires a variety of signal molecules through which phagocytes recognize and engulf ACs. Find-me signals, such as lysophosphatidylcholine (LPC), ATP/UTP, CX3CL1, and sphingosine-1-phosphate (S1P) are released by ACs, which promote attracting phagocytes to the sites of death. Phagocytes sense these signals via receptors including G2A, P2Y2, CX3CLR, and S1PRs respectively. (**Figure 8A**). Bridging molecules such as apoE and MFGE8 connect phagocytes to ACs. Afterward, ACs exposed to a variety of signals on their surfaces, interacting with receptors on the phagocytic membrane through Eat-me signals, and efficiently process the AC constituents to maintain homeostasis. The most common Eat-me signal, phosphatidylserine (PS), can interact with a variety of receptors on the surface of phagocytes, such as BAI1 and αvβ3 integrin. Other Eat-me signals, such as calreticulin and ICAM3 modulate the identification and engulfment of ACS via the receptors LRP1 and CD14 respectively (**Figure 8B**). Healthy cells display don't-eat-me signals such as CD47, CD31, and CD24, on their surface which binds to receptors SIRP a, CD31, and Siglec-10, respectively expressed on phagocytes to avoid efferocytosis (**Figure 8C**). Programmed cell removal can be countermanded by anti-phagocytic don't-eat-me signals such as cell surface expression of CD47. Mouse model studies showed that administration of CD47-blocking antibodies increased intraplaque efferocytosis efficiency and inhibited AS (Kojima et al., 2016). Defective phagocytosis of apoptotic foam cells has several consequences that promote the progression of chronic and non-resolving inflammatory diseases such as advanced AS (**Figure 8D**)

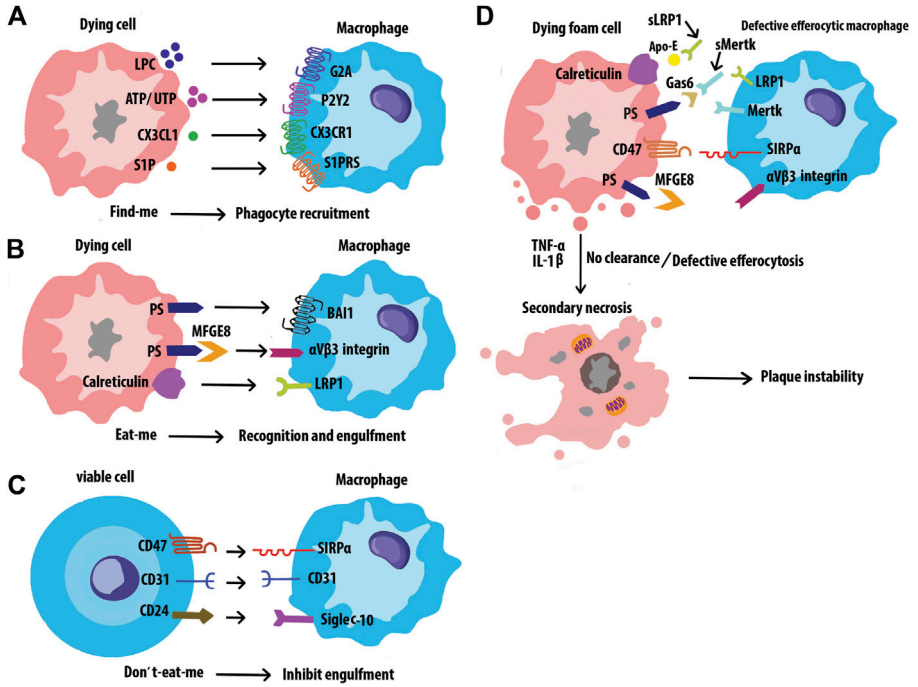

FIGURE 8 | Interactions of efferocytosis signaling. Find-me signals recruit phagocytes to the sites of cell death. The dying cells will express Eat-me signals to facilitate interactions with phagocytes. Non-ACs send a Don't-eat-me signal to avoid efferocytosis when exposed to phagocytes. Defective efferocytosis leading to inefficient clearance of ACs and subsequent necrosis and inflammation in plaques.

TABLE 3 | Efferocytosis signaling molecules.

Role	Molecule	Expression	Receptor
Find-me signals	CX3CL1	Dying cell	CX3CR1
	LPC	Dying cell	G2A
	S1P	Dying cell	S1PRs
	ATP/UTP	Dying cell	P2Y2
Eat-me signals	PS	Dying cell	BAI1/MFGE8-aVβ3 integrin
	Calreticulin	Dying cell	LRP1
	ICAM3	Dying cell	CD14
Bridging molecules	MFGE8	Dying cell	avβ5 integrin/avβ3 integrin
	C1q	Macrophage	SCARF1/aMβ2 integrin
	GAS6	Dying cell/Macrophage	AXL/Mertk
	TSP-1	Dying cell	CD36/avβ3 integrin
Don't-eat-me signals	CD47	Viable cell	SIRPα
	CD31	Viable cell	CD31
	CD24	Viable cell	Siglec-10 (Wang et al., 2020)

CX3CL1, CX3C chemokine ligand 1; LPC, lysophosphatidylcholine; S1P, Sphingosine-1-phosphate; ATP/UTP, Adenosine Triphosphate/Uridine Triphosphate; CX3CR1, CX3C chemokine receptor 1; G2A, G-protein-coupled receptor; S1PRs, Sphingosine-1 phosphate receptors; P2Y2, Purinergic receptor P2Y2; PS, phosphatidylserine; BAI1, Brain-specific angiogenesis inhibitor 1; MFGE8, Milk fat globule-EGF, factor 8; LRP1, Low-density lipoprotein receptor-related protein 1; C1q, Complement component 1q; GAS6, Growth arrest-specific gene 6 product; TSP-1, Thrombospondin-1; SCARF1, Scavenger receptor F1; AXL, anexelekto receptor tyrosine kinase; Mertk, Mer tyrosine kinase; SIRPa, Signal regulatory protein a; Siglec-10, Sialic acid binding ig like lectin 10.

(Wang et al., 2020). Angiotensin II is a multifunctional hormone that plays a major role in the development of AS. Angiotensin II promotes MerTK shedding via AT_1R/ROS/p38 MAPK/ADAM17 pathway in Mφs, which leads to defective efferocytosis, accumulation of ACs, and progression of AS (Zhang et al., 2019). Mφs in atherosclerotic plaques express angiotensin II type 1 receptor. This receptor of bone marrow-derived Mφs worsens the renal injury-induced AS by shifting the Mφ phenotype to M1 and decreasing the M2 phenotype which leads to impaired efferocytosis and enhanced necrosis (Yamamoto et al., 2011) Efferocytosis signaling molecules have been shown in **Table 3**.

MACROPHAGES IN ADVANCED ATHEROSCLEROSIS

Atherosclerotic lesions typically consist of a lipid core which is covered by a fibrous cap. Matrix composition, thickness, cellularity, the collagen content of fibrous caps, and chronic inflammatory infiltrate are important factors in plaque stability. Vulnerable plaques are associated with active inflammation and a thin fibrous cap (Sodhi and Brown, 2018). Mφs secrete proteolytic enzymes, especially matrix metalloproteinase (MMP)-2 and MMP-9, causing degradation of ECM proteins such as collagen and elastin leading, to fibrous cap thinning and destabilization of advanced plaques. Thus, MMP-9 inhibitors have the potential to stabilize vulnerable plaques (Gough et al., 2006). Lesional Mφs induced apoptosis of VSMCs by TNF-α, the Fas apoptotic pathway, and NO production and appear to promote rupture-prone plaques (Boyle et al., 2003).

A key feature of unstable plaques is the formation of necrotic cores. If efferocytosis is insufficient, dead M1 Mφs accumulate and undergo postapoptotic necrosis, leading to the formation of a necrotic core. The thin fibrous cap and large necrotic core make lesions susceptible to rupture, leading to thrombosis, heart attack, or stroke (Virmani et al., 2002; Chinetti-Gbaguidi et al., 2015).

CLONAL HEMATOPOIESIS AND LEUKOCYTOSIS IN ATHEROSCLEROSIS

Normal circulating blood cells consist of a polyclonal mixture descended from thousands of hematopoietic stem cells (HSC). During aging, or in blood cell cancers, individual HSC clones can become relatively abundant. In 2017–2018, several groups reported that clonal hematopoiesis (CH), defined as expanded somatic blood cell clones in the absence of hematologic abnormalities, dramatically accelerates AS and increases the risk of MI (Fuster et al., 2017; Jaiswal et al., 2017; Sano et al., 2018). These clones were associated with various driver gene mutations such as the epigenetic modifiers TET2 and DNMT3A, suggesting that the mutations not only enhanced cell proliferation but also conferred pro-inflammatory or other properties to the leukocytes. Several subsequent studies on CH and AS have now been reported and they generally support the pro-inflammatory effects of certain driver mutations (Bick et al., 2020; Fidler et al., 2021).

The possibility that these observations with clonal hematopoiesis are due in part to increased hematopoiesis rather than pro-inflammatory clones was raised by Heyde et al. (Heyde et al., 2021). It has long been known that elevated levels of blood leukocytes, a phenomenon termed leukocytosis, predicts CV events, and certain studies have suggested that the presence of a vicious cycle in which events such as MI and AS risk factors promote leukocytosis (Swirski and Nahrendorf, 2013a). Previous studies had shown that the hematopoietic system is activated in AS in a variety of species including mice and humans. The authors showed, using fundamental evolutional dynamics, that this would predict the expansion of clones harboring both advantageous (in terms of increased proliferation) and neutral mutations. The authors quantitatively examined HSC proliferation in atherosclerotic mouse models as well as human subjects using incorporation of bromodeoxyuridine into DNA or the expression of the proliferation marker Ki67. In both atherosclerotic mice and patients with AS, HSC proliferation was markedly increased, roughly 2-fold, as compared to controls. It is noteworthy that smoking, a strong risk factor for AS, promotes CH and leukocytosis. A particularly exciting connection with HSC proliferation and clonal hematopoiesis in AS relates to the role of chronic stress. Sleep modulates hematopoiesis and protects against AS. Previously, McAlpine et al. (McAlpine et al., 2019) showed that sleep fragmentation in mice suppressed hypothalamic secretion of the wake-promoting peptide hypocretin, resulting in elevated M-CSF expression by pre-neutrophils in bone marrow that, in turn, increased blood monocytes and AS. The authors confirm in the present study that sleep fragmentation increases HSC proliferation. Thus, the relative importance in AS of driver mutations such as TET2, as compared to increased hematopoiesis and leukocytosis, is uncertain. Since both are potential therapeutic targets, the answer is of considerable interest.

SINGLE-CELL TECHNIQUES AND MACROPHAGE HETEROGENEITY IN ATHEROSCLEROSIS

Single-cell sequencing technologies can be applied to sequence DNA, RNA, open chromatin, or methylated DNA in single-cells in the context of normal or diseased tissues (Williams et al., 2020). The single-cell sequencing studies reported thus far have relied primarily on RNA sequencing (scRNAseq). In some cases, the studies have been complemented by time of flight mass cytometry analyses. Over the past 3 years, several groups have used scRNAseq to examine leukocyte heterogeneity in various mouse models of AS (Cochain et al., 2018; Kim et al., 2018; Winkels et al., 2018; Lin et al., 2019; Zernecke et al., 2020) and in human carotid AS (Fernandez et al., 2019) and these studies have been recently reviewed (Willemsen and de Winther, 2020; Fernandez and Giannarelli, 2021). ScRNAseq analyses of mouse atherosclerotic lesions identified three main clusters of the Mφs in AS, resident-like, inflammatory, and TREM2hi (Willemsen and de Winther, 2020). The resident-like Mφs, some of which are found in the adventitia, can proliferate and resemble an M2-like phenotype. The inflammatory Mφs are the major component of the Mφ population within the intima of the plaque. They appear to be the main cellular drivers of lesional inflammation and are enriched in both M1-associated genes and Mox-associated transcription factor NRF2. They are mainly non-foamy (Kim et al., 2018). The third subtype, TREM2hi Mφs, are foamy lipid-laden Mφs enriched for lipid metabolic processes, regulation of cholesterol efflux, OS and cellular catabolic processes and. have an M2-like phenotype. In a comprehensive meta-analysis of mouse studies, Ley's group (Zernecke et al., 2020) confirmed these known Mφ subsets

and identified a new Mφ subset resembling peritoneal cavity Mφs. Thus far only one study has examined human lesion (Fernandez et al., 2019). In that study, carotid plaques of clinically symptomatic disease (stroke) were compared to asymptomatic disease and scRNAseq was complemented with mass cytometry. Mφs from the plaques exhibited alternatively activated phenotypes, some of which were associated with plaque vulnerability.

MACROPHAGE SENESCENCE IN ATHEROSCLEROSIS

Accumulating evidence from both human and mouse studies suggests that cellular senescence contributes to the pathogenesis of AS. The senescent cells can be recognized by the irreversible loss of proliferative capacity, resistance to cell death, and the production of a bioactive secretome, known as the senescence-associated secretory phenotype (SASP). The main components of SASP include inflammatory cytokines, immune modulators, growth factors, and proteases (Childs et al., 2017). Recent findings in mouse models show that among cells with elevated p16INK4a and senescence-associated beta-galactosidase (SA-β-Gal) expression (common biomarkers of senescence) are Mφs (Prattichizzo et al., 2016; Liu et al., 2019). In mouse models of AS foamy senescent Mφs expressing inflammatory cytokines/chemokines accumulate in the subendothelial space in the early stages of disease while in advanced lesions there is evidence senescent Mφs promote plaque instability (Childs et al., 2016). Yang et al. found that microRNA-216a (miR-216a) promotes Mφ senescence as characterized by increased SA-β-GAL activity and p53 and p16 expression, and it has been reported that patients with vulnerable coronary plaques have elevated levels of plasma miR-216a (Yang et al., 2019). A recent study demonstrated that the senescent cells promote thinning of the fibrous cap, and the clearance of these cells by a synolitic agent (ABT263) helped maintain the fibrous caps in mice with advanced lesions. The senescent cells antagonize insulin-like growth factor (IGF)-1 through the secretion of IGF-binding protein-3, thereby inhibiting innate smooth muscle cell repair (Childs et al., 2021). Acting through the phosphatidylinositide 3 kinase-AKT-mTOR-p53 signal pathway, CD9 upregulation initiates cellular senescence while knocking it down in senescent cells reduces senescence (Brosseau et al., 2018; Cho et al., 2020). In human atherosclerotic lesions, most Mφs in plaques exhibited CD9 immunoreactivity (Nishida et al., 2000). In hyperlipidemic ApoE$^{-/-}$ mice, selective delivery of the anti-senescence drug rosuvastatin to the atherosclerotic plaques using nanoparticles alleviated the progression of AS (Kim et al., 2021). Recent studies indicate that certain immune cells, in particular iNKT cells, can function to remove senescent cells (Kale et al., 2020; Arora et al., 2021).

MACROPHAGE-BASED THERAPEUTIC STRATEGIES

Mφ dynamics play a role in all stages of AS and represent potential drug targets. A Mφ-biomimetic drug delivery system, in which ROS responsive nanoparticles were coated with Mφ membrane was developed. The Mφ membrane may sequester key pro-inflammatory cytokines to decrease local inflammation. The combination of pharmacotherapy and inflammatory cytokines sequestration offered by this platform led to improved therapeutic efficacy in AS (Gao et al., 2020).

Mφ death is an important feature of advanced plaques and is used as a therapeutic target in AS. Ox-LDL within advanced atherosclerotic plaque is directly responsible for the upregulation of RIP3, which is required to induce necroptosis in Mφs and lesion progression. Mφ necroptosis can be inhibited by necrostatin-1 to reduce lesion size and necrotic core formation for diagnostic and therapeutic interventions in AS (Karunakaran et al., 2016). Mφ pyroptosis is associated with the activation of NLRP3 inflammasome which has been linked to CV risk factors such as obesity and is an important regulator of CV inflammation. Thus, the therapeutic approaches targeting the activation of NLRP3 inflammasome and pyroptosis offer good prospects for the treatment of AS (Zeng et al., 2019). PARP inhibition attenuated plaque development and promoted plaque stability, likely through a reduction in the expression of inflammatory factors in ApoE$^{-/-}$ mice. Thus, PARP1 inhibitors such as 3-aminobenzamide, INO-1001, methoxyflavones, PJ34, and DPQ may prove beneficial for the treatment of AS (Oumouna-Benachour et al., 2007; Martinet et al., 2019). Ferrostatin, an inhibitor of Mφ ferroptosis, suffers from inherent stability but anti-ferroptosis analog drugs with improved potency such as liproxstatins and anti-oxidants can inhibit ferroptotic cell death (Hofmans et al., 2016; Martinet et al., 2019).

Lipid deposition in the arterial wall is an initial step in AS, which promotes an inflammatory response. However, it was recently reported that the SR-B1 in ECs binds plasma LDL and mediates the delivery of LDL into arteries and its engulfment by artery wall Mφs to form foam cells. Thus, inhibition of SR-B1 in ECs might reduce lipid deposition with the potential of anti-inflammatory therapy in AS (Huang et al., 2019).

Photobiomodulation therapy has a protective role on AS through promoting the ABCA1-medicated cholesterol efflux in Mφ to inhibit foam cells formation (Yin et al., 2021). Proefferocytic therapy which specifically targets the necrotic core can potentially be used for the treatment of advanced AS (Kojima et al., 2017). 2-hydroxybenzylamine treatment reduced inflammation and plaque apoptotic cells but promoted efferocytosis and features of stable plaques in hypercholesterolemic *Ldlr*$^{-/-}$ mice supporting its potential as a therapeutic approach for atherosclerotic cardiovascular disease (Tao et al., 2020). An atheroprotective strategy that uses plaque targeting to deliver a proresolving mediator may stabilize advanced atherosclerotic lesions. Thus, defective inflammation resolution may have a role in advanced AS (Fredman et al., 2015).

Inhibition of local proliferation of Mφs is key in plaque regression in response to cholesterol-lowering. Thus, Mφ proliferation was identified as the predominant turnover determinant and a target for induction of plaque regression (Härdtner et al., 2020). HDL nanoparticles are used to target

atherosclerotic Mφs. Nanoparticle-based delivery of simvastatin was used to inhibit plaque Mφ proliferation. This resulted in the rapid reduction of plaque inflammation when it was combined with oral statin treatment. Thus, pharmacologically inhibiting plaque Mφ proliferation by nanotherapy can effectively suppress plaque inflammation and reduce AS (Tang et al., 2015).

Defective autophagy in Mφs contributes to impaired cholesterol metabolism and defective efferocytosis leading. Mφs treated with anti-miR-33 showed increased autophagy, lipid droplet catabolism, and enhanced efferocytosis to reduce plaque necrosis (Ouimet et al., 2017).

CONCLUSION AND FUTURE PERSPECTIVE

AS is an inflammation-driven disease and Mφs play a central role in the pathogenesis of AS and controlling inflammation in all stages. Understanding monocytes differentiation into either pro- or anti-inflammatory Mφs within lesions and how Mφs affect plaque initiation and progression is of potential importance for the treatment of AS. Several strategies including anti-inflammatory approaches, depolarizing Mφs, modulation of Mφs, survival, and enhancing efferocytosis have been proposed as possible therapies. Targeting inflammation may be a promising therapeutic option for reducing AS. However, anti-inflammatory strategies may elicit undesirable effects such as infection (Moriya, 2019). Since the complex environmental stimuli within atherosclerotic plaques *in vivo* affects monocyte-derived Mφs, studying the effects of signaling crosstalk on inflammatory responses can be helpful to understand Mφ activation in the lesion and the development of therapeutic interventions. Another aspect that complicates therapeutic inhibition of Mφ death in atherosclerotic plaques is the crosstalk between cell death mechanisms (Nikoletopoulou et al., 2013). There is a balanced interaction between different types of cell death so that blocking one type of death may stimulate cells to initiate another death pathway. For instance, inhibition of caspases by the pan-caspase inhibitor zVAD promotes apoptosis but may facilitate the necroptosis program downstream of TNFR. Several main mediators of different types of cell death have been identified but more investigation is still needed (Chen et al., 2018). Cholesterol homeostasis in Mφs involves a dynamic balance between cholesterol uptake and efflux (Remmerie and Scott, 2018). These processes are regulated by signaling systems that are also affected by the events such as Mφ pro-inflammatory activation, phagocytosis stimulation, and autophagy induction. The signaling networks regulating these events in Mφs involve specific proteins that might be used as potential therapeutic targets in AS management. The divergent functions of Mφs, including contributions to inflammation, healing, regeneration, and remodeling arise due to the numerous types of Mφs, which can quickly adapt their phenotype in response to the microenvironment changes. Insufficient understanding of Mφ functions represents a major obstacle in Mφ targeting. For instance, M1 Mφs impair wound healing in some situations (Mirza et al., 2014) while promoting regeneration in others (Novak et al., 2014). M2 Mφs have also been associated with both tissue regeneration (Godwin et al., 2013) and fibrosis (Furukawa et al., 2015). In addition, data from cultured Mφs and animal models may not completely reflect the process in human atherosclerotic lesions. In this regard, Useful mouse models of plaque instability have been developed (Chen et al., 2013) Of course, translational studies are needed to confirm the observations made in preclinical murine models.

AUTHOR CONTRIBUTIONS

LF prepared the draft and designed the figures. SS edited and contributed to the manuscript. AJL reviewed, revised, and overall supervised the whole work.

FUNDING

This work was supported in part by NIH grants HL144651, DK117850, HL147883, HL148577, HL148110, HL152176, and DA-Army Medical Research Grant W81XWH2110115.

REFERENCES

Abdelaziz, M. H., Abdelwahab, S. F., Wan, J., Cai, W., Huixuan, W., Jianjun, C., et al. (2020). Alternatively Activated Macrophages; a Double-Edged Sword in Allergic Asthma. *J. Transl Med.* 18 (1), 58. doi:10.1186/s12967-020-02251-w

Alderson, L. M., Endemann, G., Lindsey, S., Pronczuk, A., Hoover, R. L., and Hayes, K. C. (1986). LDL Enhances Monocyte Adhesion to Endothelial Cells *In Vitro*. *Am. J. Pathol.* 123 (2), 334–342.

Apostolopoulos, J., Davenport, P., and Tipping, P. G. (1996). Interleukin-8 Production by Macrophages from Atheromatous Plaques. *Arterioscler Thromb. Vasc. Biol.* 16 (8), 1007–1012. doi:10.1161/01.atv.16.8.1007

Apostolov, E. O., Shah, S. V., Ray, D., and Basnakian, A. G. (2009). Scavenger Receptors of Endothelial Cells Mediate the Uptake and Cellular Proatherogenic Effects of Carbamylated LDL. *Arterioscler Thromb. Vasc. Biol.* 29 (10), 1622–1630. doi:10.1161/atvbaha.109.189795

Arango Duque, G., and Descoteaux, A. (2014). Macrophage Cytokines: Involvement in Immunity and Infectious Diseases. *Front. Immunol.* 5, 491. doi:10.3389/fimmu.2014.00491

Arora, S., Thompson, P. J., Wang, Y., Bhattacharyya, A., Apostolopoulou, H., Hatano, R., et al. (2021). Invariant Natural Killer T Cells Coordinate Removal of Senescent Cells. *Med* 2 (8), 938–950.e8. doi:10.1016/j.medj.2021.04.014

Arranz, A., Doxaki, C., Vergadi, E., Martinez de la Torre, Y., Vaporidi, K., Lagoudaki, E. D., et al. (2012). Akt1 and Akt2 Protein Kinases Differentially Contribute to Macrophage Polarization. *Proc. Natl. Acad. Sci. U S A.* 109 (24), 9517–9522. doi:10.1073/pnas.1119038109

Babaei, S., Picard, P., Ravandi, A., Monge, J. C., Lee, T. C., Cernacek, P., et al. (2000). Blockade of Endothelin Receptors Markedly Reduces Atherosclerosis in LDL Receptor Deficient Mice: Role of Endothelin in Macrophage Foam Cell Formation. *Cardiovasc. Res.* 48 (1), 158–167. doi:10.1016/s0008-6363(00)00169-3

Babaev, V. R., Hebron, K. E., Wiese, C. B., Toth, C. L., Ding, L., Zhang, Y., et al. (2014). Macrophage Deficiency of Akt2 Reduces Atherosclerosis in Ldlr Null Mice. *J. Lipid Res.* 55 (11), 2296–2308. doi:10.1194/jlr.M050633

Barrett, T. J. (2020). Macrophages in Atherosclerosis Regression. *Atvb* 40 (1), 20–33. doi:10.1161/atvbaha.119.312802

Bartlett, B., Ludewick, H. P., Misra, A., Lee, S., and Dwivedi, G. (2019). Macrophages and T Cells in Atherosclerosis: a Translational Perspective. *Am. J. Physiol. Heart Circ. Physiol.* 317 (2), H375–H386. doi:10.1152/ajpheart.00206.2019

Bhaskar, V., Yin, J., Mirza, A. M., Phan, D., Vanegas, S., Issafras, H., et al. (2011). Monoclonal Antibodies Targeting IL-1 Beta Reduce Biomarkers of Atherosclerosis *In Vitro* and Inhibit Atherosclerotic Plaque Formation in Apolipoprotein E-Deficient Mice. *Atherosclerosis* 216 (2), 313–320. doi:10.1016/j.atherosclerosis.2011.02.026

Bhat, O. M., Kumar, P. U., Giridharan, N. V., Kaul, D., Kumar, M. J., and Dhawan, V. (2015). Interleukin-18-induced Atherosclerosis Involves CD36 and NF-Kb Crosstalk in Apo E-/- Mice. *J. Cardiol.* 66 (1), 28–35. doi:10.1016/j.jjcc.2014.10.012

Bi, Y., Chen, J., Hu, F., Liu, J., Li, M., and Zhao, L. (2019). M2 Macrophages as a Potential Target for Antiatherosclerosis Treatment. *Neural Plast.* 2019, 6724903. doi:10.1155/2019/6724903

Bick, A. G., Pirruccello, J. P., Griffin, G. K., Gupta, N., Gabriel, S., Saleheen, D., et al. (2020). Genetic Interleukin 6 Signaling Deficiency Attenuates Cardiovascular Risk in Clonal Hematopoiesis. *Circulation* 141 (2), 124–131. doi:10.1161/CIRCULATIONAHA.119.044362

Boada-Romero, E., Martinez, J., Heckmann, B. L., and Green, D. R. (2020). The Clearance of Dead Cells by Efferocytosis. *Nat. Rev. Mol. Cel Biol* 21 (7), 398–414. doi:10.1038/s41580-020-0232-1

Boesten, L. S., Zadelaar, A. S., van Nieuwkoop, A., Gijbels, M. J., de Winther, M. P., Havekes, L. M., et al. (2005). Tumor Necrosis Factor-Alpha Promotes Atherosclerotic Lesion Progression in APOE*3-Leiden Transgenic Mice. *Cardiovasc. Res.* 66 (1), 179–185. doi:10.1016/j.cardiores.2005.01.001

Bosmans, L. A., Bosch, L., Kusters, P. J. H., Lutgens, E., and Seijkens, T. T. P. (2020). The CD40-Cd40l Dyad as Immunotherapeutic Target in Cardiovascular Disease. *J. Cardiovasc. Transl Res.* 14 (1), 1–10. doi:10.1007/s12265-020-09994-3

Boyle, J. J., Harrington, H. A., Piper, E., Elderfield, K., Stark, J., Landis, R. C., et al. (2009). Coronary Intraplaque Hemorrhage Evokes a Novel Atheroprotective Macrophage Phenotype. *Am. J. Pathol.* 174 (3), 1097–1108. doi:10.2353/ajpath.2009.080431

Boyle, J. J. (2005). Macrophage Activation in Atherosclerosis: Pathogenesis and Pharmacology of Plaque Rupture. *Curr. Vasc. Pharmacol.* 3 (1), 63–68. doi:10.2174/1570161052773861

Boyle, J. J., Weissberg, P. L., and Bennett, M. R. (2003). Tumor Necrosis Factor-Alpha Promotes Macrophage-Induced Vascular Smooth Muscle Cell Apoptosis by Direct and Autocrine Mechanisms. *Arterioscler Thromb. Vasc. Biol.* 23 (9), 1553–1558. doi:10.1161/01.atv.0000086961.44581.b7

Brosseau, C., Colas, L., Magnan, A., and Brouard, S. (2018). CD9 Tetraspanin: a New Pathway for the Regulation of Inflammation? *Front. Immunol.* 9, 2316. doi:10.3389/fimmu.2018.02316

Buscher, K., Ehinger, E., Gupta, P., Pramod, A. B., Wolf, D., Tweet, G., et al. (2017). Natural Variation of Macrophage Activation as Disease-Relevant Phenotype Predictive of Inflammation and Cancer Survival. *Nat. Commun.* 8 (1), 16041–16110. doi:10.1038/ncomms16041

Butcher, M. J., and Galkina, E. V. (2012). Phenotypic and Functional Heterogeneity of Macrophages and Dendritic Cell Subsets in the Healthy and Atherosclerosis-Prone Aorta. *Front. Physiol.* 3, 44. doi:10.3389/fphys.2012.00044

Canet-Soulas, E., Bessueille, L., Mechtouff, L., and Magne, D. (2021). The Elusive Origin of Atherosclerotic Plaque Calcification. *Front Cel Dev Biol* 9, 622736. doi:10.3389/fcell.2021.622736

Cardilo-Reis, L., Gruber, S., Schreier, S. M., Drechsler, M., Papac-Milicevic, N., Weber, C., et al. (2012). Interleukin-13 Protects from Atherosclerosis and Modulates Plaque Composition by Skewing the Macrophage Phenotype. *EMBO Mol. Med.* 4 (10), 1072–1086. doi:10.1002/emmm.201201374

Carmi, Y., Voronov, E., Dotan, S., Lahat, N., Rahat, M. A., Fogel, M., et al. (2009). The Role of Macrophage-Derived IL-1 in Induction and Maintenance of Angiogenesis. *J. Immunol.* 183 (7), 4705–4714. doi:10.4049/jimmunol.0901511

Castrillo, A., Joseph, S. B., Vaidya, S. A., Haberland, M., Fogelman, A. M., Cheng, G., et al. (2003). Crosstalk between LXR and Toll-like Receptor Signaling Mediates Bacterial and Viral Antagonism of Cholesterol Metabolism. *Mol. Cel* 12 (4), 805–816. doi:10.1016/s1097-2765(03)00384-8

Chan, G., Bivins-Smith, E. R., Smith, M. S., Smith, P. M., and Yurochko, A. D. (2008). Transcriptome Analysis Reveals Human Cytomegalovirus Reprograms Monocyte Differentiation toward an M1 Macrophage. *J. Immunol.* 181 (1), 698–711. doi:10.4049/jimmunol.181.1.698

Chang, H. Y., Lee, H. N., Kim, W., and Surh, Y. J. (2015). Docosahexaenoic Acid Induces M2 Macrophage Polarization through Peroxisome Proliferator-Activated Receptor γ Activation. *Life Sci.* 120, 39–47. doi:10.1016/j.lfs.2014.10.014

Chang, T. Y., Li, B. L., Chang, C. C., and Urano, Y. (2009). Acyl-coenzyme A: cholesterol Acyltransferases. *Am. J. Physiol. Endocrinol. Metab.* 297 (1), E1–E9. doi:10.1152/ajpendo.90926.2008

Chen, P. Y., Qin, L., Li, G., Wang, Z., Dahlman, J. E., Malagon-Lopez, J., et al. (2019). Endothelial TGF-β Signalling Drives Vascular Inflammation and Atherosclerosis. *Nat. Metab.* 1 (9), 912–926. doi:10.1038/s42255-019-0102-3

Chen, Q., Kang, J., and Fu, C. (2018). The independence of and Associations Among Apoptosis, Autophagy, and Necrosis. *Signal. Transduct Target. Ther.* 3 (1), 18–11. doi:10.1038/s41392-018-0018-5

Chen, Y. C., Bui, A. V., Diesch, J., Manasseh, R., Hausding, C., Rivera, J., et al. (2013). A Novel Mouse Model of Atherosclerotic Plaque Instability for Drug Testing and Mechanistic/therapeutic Discoveries Using Gene and microRNA Expression Profiling. *Circ. Res.* 113 (3), 252–265. doi:10.1161/CIRCRESAHA.113.301562

Cheng, H., Wang, Z., Fu, L., and Xu, T. (2019). Macrophage Polarization in the Development and Progression of Ovarian Cancers: An Overview. *Front. Oncol.* 9, 421. doi:10.3389/fonc.2019.00421

Chew, M., Zhou, J., Daugherty, A., Eriksson, T., Ellermann-Eriksen, S., Hansen, P. R., et al. (2003). Thalidomide Inhibits Early Atherogenesis in apoE-Deficient Mice. *APMIS Suppl.* Suppl (109), 113–116.

Childs, B. G., Baker, D. J., Wijshake, T., Conover, C. A., Campisi, J., and Van Deursen, J. M. (2016). Senescent Intimal Foam Cells Are Deleterious at All Stages of Atherosclerosis. *Science* 354 (6311), 472–477. doi:10.1126/science.aaf6659

Childs, B. G., Gluscevic, M., Baker, D. J., Laberge, R. M., Marquess, D., Dananberg, J., et al. (2017). Senescent Cells: an Emerging Target for Diseases of Ageing. *Nat. Rev. Drug Discov.* 16 (10), 718–735. doi:10.1038/nrd.2017.116

Childs, B. G., Zhang, C., Shuja, F., Sturmlechner, I., Trewartha, S., Velasco, R. F., et al. (2021). Senescent Cells Suppress Innate Smooth Muscle Cell Repair Functions in Atherosclerosis. *Nat. Aging* 1 (8), 1–17. doi:10.1038/s43587-021-00089-5

Chinetti-Gbaguidi, G., Colin, S., and Staels, B. (2015). Macrophage Subsets in Atherosclerosis. *Nat. Rev. Cardiol.* 12 (1), 10–17. doi:10.1038/nrcardio.2014.173

Chistiakov, D. A., Bobryshev, Y. V., and Orekhov, A. N. (2015). Changes in Transcriptome of Macrophages in Atherosclerosis. *J. Cel Mol Med* 19 (6), 1163–1173. doi:10.1111/jcmm.12591

Chistiakov, D. A., Bobryshev, Y. V., and Orekhov, A. N. (2016). Macrophage-mediated Cholesterol Handling in Atherosclerosis. *J. Cel Mol Med* 20 (1), 17–28. doi:10.1111/jcmm.12689

Chistiakov, D. A., Melnichenko, A. A., Myasoedova, V. A., Grechko, A. V., and Orekhov, A. N. (2017). Mechanisms of Foam Cell Formation in Atherosclerosis. *J. Mol. Med. (Berl)* 95 (11), 1153–1165. doi:10.1007/s00109-017-1575-8

Cho, J. H., Kim, E. C., Son, Y., Lee, D. W., Park, Y. S., Choi, J. H., et al. (2020). CD9 Induces Cellular Senescence and Aggravates Atherosclerotic Plaque Formation. *Cell Death Differ* 27 (9), 2681–2696. doi:10.1038/s41418-020-0537-9

Coats, B. R., Schoenfelt, K. Q., Barbosa-Lorenzi, V. C., Peris, E., Cui, C., Hoffman, A., et al. (2017). Metabolically Activated Adipose Tissue Macrophages Perform Detrimental and Beneficial Functions during Diet-Induced Obesity. *Cell Rep* 20 (13), 3149–3161. doi:10.1016/j.celrep.2017.08.096

Cochain, C., Vafadarnejad, E., Arampatzi, P., Pelisek, J., Winkels, H., Ley, K., et al. (2018). Single-cell RNA-Seq Reveals the Transcriptional Landscape and Heterogeneity of Aortic Macrophages in Murine Atherosclerosis. *Circ. Res.* 122 (12), 1661–1674. doi:10.1161/CIRCRESAHA.117.312509

Colin, S., Chinetti-Gbaguidi, G., and Staels, B. (2014). Macrophage Phenotypes in Atherosclerosis. *Immunol. Rev.* 262 (1), 153–166. doi:10.1111/imr.12218

Covarrubias, A. J., Aksoylar, H. I., and Horng, T. (2015). "Control of Macrophage Metabolism and Activation by mTOR and Akt Signaling," in *Seminars in Immunology* (Elsevier), 286–296.

Davenport, P., and Tipping, P. G. (2003). The Role of Interleukin-4 and Interleukin-12 in the Progression of Atherosclerosis in Apolipoprotein E-Deficient Mice. *Am. J. Pathol.* 163 (3), 1117–1125. doi:10.1016/s0002-9440(10)63471-2

de Jager, S. C., Bermúdez, B., Bot, I., Koenen, R. R., Bot, M., Kavelaars, A., et al. (2011). Growth Differentiation Factor 15 Deficiency Protects against Atherosclerosis by Attenuating CCR2-Mediated Macrophage Chemotaxis. *J. Exp. Med.* 208 (2), 217–225. doi:10.1084/jem.20100370

De Paoli, F., Staels, B., and Chinetti-Gbaguidi, G. (2014). Macrophage Phenotypes and Their Modulation in Atherosclerosis. *Circ. J.* 78 (8), 1775–1781. doi:10.1253/circj.cj-14-0621

Deczkowska, A., Weiner, A., and Amit, I. (2020). The Physiology, Pathology, and Potential Therapeutic Applications of the TREM2 Signaling Pathway. *Cell* 181 (6), 1207–1217. doi:10.1016/j.cell.2020.05.003

Devries-Seimon, T., Li, Y., Yao, P. M., Stone, E., Wang, Y., Davis, R. J., et al. (2005). Cholesterol-induced Macrophage Apoptosis Requires ER Stress Pathways and Engagement of the Type A Scavenger Receptor. *J. Cel Biol* 171 (1), 61–73. doi:10.1083/jcb.200502078

Dinarello, C. A., Novick, D., Kim, S., and Kaplanski, G. (2013). Interleukin-18 and IL-18 Binding Protein. *Front. Immunol.* 4, 289. doi:10.3389/fimmu.2013.00289

Douna, H., Amersfoort, J., Schaftenaar, F. H., Kroon, S., van Puijvelde, G. H. M., Kuiper, J., et al. (2019). Bidirectional Effects of IL-10+ Regulatory B Cells in Ldlr-/- Mice. *Atherosclerosis* 280, 118–125. doi:10.1016/j.atherosclerosis.2018.11.019

Erbilgin, A., Seldin, M. M., Wu, X., Mehrabian, M., Zhou, Z., Qi, H., et al. (2018). Transcription Factor Zhx2 Deficiency Reduces Atherosclerosis and Promotes Macrophage Apoptosis in Mice. *Arterioscler Thromb. Vasc. Biol.* 38 (9), 2016–2027. doi:10.1161/ATVBAHA.118.311266

Febbraio, M., Hajjar, D. P., and Silverstein, R. L. (2001). CD36: a Class B Scavenger Receptor Involved in Angiogenesis, Atherosclerosis, Inflammation, and Lipid Metabolism. *J. Clin. Invest.* 108 (6), 785–791. doi:10.1172/jci14006

Feig, J. E., Parathath, S., Rong, J. X., Mick, S. L., Vengrenyuk, Y., Grauer, L., et al. (2011). Reversal of Hyperlipidemia with a Genetic Switch Favorably Affects the Content and Inflammatory State of Macrophages in Atherosclerotic Plaques. *Circulation* 123 (9), 989–998. doi:10.1161/circulationaha.110.984146

Fernández-Hernando, C., Ackah, E., Yu, J., Suárez, Y., Murata, T., Iwakiri, Y., et al. (2007). Loss of Akt1 Leads to Severe Atherosclerosis and Occlusive Coronary Artery Disease. *Cell Metab* 6 (6), 446–457. doi:10.1016/j.cmet.2007.10.007

Fernandez, D. M., Rahman, A. H., Fernandez, N. F., Chudnovskiy, A., Amir, E. D., Amadori, L., et al. (2019). Single-cell Immune Landscape of Human Atherosclerotic Plaques. *Nat. Med.* 25 (10), 1576–1588. doi:10.1038/s41591-019-0590-4

Fernandez, D. M., and Giannarelli, C. (2021). Immune Cell Profiling in Atherosclerosis: Role in Research and Precision Medicine. *Nat. Rev. Cardiol.*, 1–16. doi:10.1038/s41569-021-00589-2

Fidler, T. P., Xue, C., Yalcinkaya, M., Hardaway, B., Abramowicz, S., Xiao, T., et al. (2021). The AIM2 Inflammasome Exacerbates Atherosclerosis in Clonal Haematopoiesis. *Nature* 592 (7853), 296–301. doi:10.1038/s41586-021-03341-5

Fourman, L. T., Saylor, C. F., Cheru, L., Fitch, K., Looby, S., Keller, K., et al. (2020). Anti-Inflammatory Interleukin 10 Inversely Relates to Coronary Atherosclerosis in Persons with Human Immunodeficiency Virus. *J. Infect. Dis.* 221 (4), 510–515. doi:10.1093/infdis/jiz254

Frank, D., and Vince, J. E. (2019). Pyroptosis versus Necroptosis: Similarities, Differences, and Crosstalk. *Cel Death Differ* 26 (1), 99–114. doi:10.1038/s41418-018-0212-6

Fredman, G., Kamaly, N., Spolitu, S., Milton, J., Ghorpade, D., Chiasson, R., et al. (2015). Erratum for the Research Article: "Targeted Nanoparticles Containing the Proresolving Peptide Ac2-26 Protect against Advanced Atherosclerosis in Hypercholesterolemic Mice" by G. Fredman, N. Kamaly, S. Spolitu, J. Milton, D. Ghorpade, R. Chiasson, G. Kuriakose, M. Perretti, O. Farokzhad, I. Tabas. *Sci. Transl Med.* 7 (275), 277er2-275ra220. doi:10.1126/scitranslmed.aaa106510.1126/scitranslmed.aaa9877

Furukawa, S., Moriyama, M., Tanaka, A., Maehara, T., Tsuboi, H., Iizuka, M., et al. (2015). Preferential M2 Macrophages Contribute to Fibrosis in IgG4-Related Dacryoadenitis and Sialoadenitis, So-Called Mikulicz's Disease. *Clin. Immunol.* 156 (1), 9–18. doi:10.1016/j.clim.2014.10.008

Fuster, J. J., MacLauchlan, S., Zuriaga, M. A., Polackal, M. N., Ostriker, A. C., Chakraborty, R., et al. (2017). Clonal Hematopoiesis Associated with TET2 Deficiency Accelerates Atherosclerosis Development in Mice. *Science* 355 (6327), 842–847. doi:10.1126/science.aag1381

Gao, C., Huang, Q., Liu, C., Kwong, C. H. T., Yue, L., Wan, J. B., et al. (2020). Treatment of Atherosclerosis by Macrophage-Biomimetic Nanoparticles via Targeted Pharmacotherapy and Sequestration of Proinflammatory Cytokines. *Nat. Commun.* 11 (1), 2622–2714. doi:10.1038/s41467-020-16439-7

Gerrick, K. Y., Gerrick, E. R., Gupta, A., Wheelan, S. J., Yegnasubramanian, S., and Jaffee, E. M. (2018). Transcriptional Profiling Identifies Novel Regulators of Macrophage Polarization. *PLoS One* 13 (12), e0208602. doi:10.1371/journal.pone.0208602

Gerszten, R. E., Garcia-Zepeda, E. A., Lim, Y. C., Yoshida, M., Ding, H. A., Gimbrone, M. A., et al. (1999). MCP-1 and IL-8 Trigger Firm Adhesion of Monocytes to Vascular Endothelium under Flow Conditions. *Nature* 398 (6729), 718–723. doi:10.1038/19546

Giacona, M. B., Papapanou, P. N., Lamster, I. B., Rong, L. L., D'Agati, V. D., Schmidt, A. M., et al. (2004). Porphyromonas Gingivalis Induces its Uptake by Human Macrophages and Promotes Foam Cell Formation *In Vitro*. *FEMS Microbiol. Lett.* 241 (1), 95–101. doi:10.1016/j.femsle.2004.10.009

Godwin, J. W., Pinto, A. R., and Rosenthal, N. A. (2013). Macrophages Are Required for Adult Salamander Limb Regeneration. *Proc. Natl. Acad. Sci. U S A.* 110 (23), 9415–9420. doi:10.1073/pnas.1300290110

Gong, D., Shi, W., Yi, S. J., Chen, H., Groffen, J., and Heisterkamp, N. (2012). TGFβ Signaling Plays a Critical Role in Promoting Alternative Macrophage Activation. *BMC Immunol.* 13 (1), 31–10. doi:10.1186/1471-2172-13-31

Gonzalez, L., and Trigatti, B. L. (2017). Macrophage Apoptosis and Necrotic Core Development in Atherosclerosis: a Rapidly Advancing Field with Clinical Relevance to Imaging and Therapy. *Can. J. Cardiol.* 33 (3), 303–312. doi:10.1016/j.cjca.2016.12.010

Goossens, P., Gijbels, M. J., Zernecke, A., Eijgelaar, W., Vergouwe, M. N., van der Made, I., et al. (2010). Myeloid Type I Interferon Signaling Promotes Atherosclerosis by Stimulating Macrophage Recruitment to Lesions. *Cel Metab* 12 (2), 142–153. doi:10.1016/j.cmet.2010.06.008

Gough, P. J., Gomez, I. G., Wille, P. T., and Raines, E. W. (2006). Macrophage Expression of Active MMP-9 Induces Acute Plaque Disruption in apoE-Deficient Mice. *J. Clin. Invest.* 116 (1), 59–69. doi:10.1172/JCI25074

Grainger, D. J., Kemp, P. R., Metcalfe, J. C., Liu, A. C., Lawn, R. M., Williams, N. R., et al. (1995). The Serum Concentration of Active Transforming Growth Factor-Beta Is Severely Depressed in Advanced Atherosclerosis. *Nat. Med.* 1 (1), 74–79. doi:10.1038/nm0195-74

Guo, Z., Ran, Q., Roberts, L. J., II, Zhou, L., Richardson, A., Sharan, C., et al. (2008). Suppression of Atherogenesis by Overexpression of Glutathione Peroxidase-4 in Apolipoprotein E-Deficient Mice. *Free Radic. Biol. Med.* 44 (3), 343–352. doi:10.1016/j.freeradbiomed.2007.09.009

Härdtner, C., Kornemann, J., Krebs, K., Ehlert, C. A., Jander, A., Zou, J., et al. (2020). Inhibition of Macrophage Proliferation Dominates Plaque Regression in Response to Cholesterol Lowering. *Basic Res. Cardiol.* 115 (6), 78–19. doi:10.1007/s00395-020-00838-4

Habib, A., and Finn, A. V. (2014). The Role of Iron Metabolism as a Mediator of Macrophage Inflammation and Lipid Handling in Atherosclerosis. *Front. Pharmacol.* 5, 195. doi:10.3389/fphar.2014.00195

Haka, A. S., Barbosa-Lorenzi, V. C., Lee, H. J., Falcone, D. J., Hudis, C. A., Dannenberg, A. J., et al. (2016). Exocytosis of Macrophage Lysosomes Leads to Digestion of Apoptotic Adipocytes and Foam Cell Formation. *J. Lipid Res.* 57 (6), 980–992. doi:10.1194/jlr.M064089

Henson, P. M., Bratton, D. L., and Fadok, V. A. (2001). Apoptotic Cell Removal. *Curr. Biol.* 11 (19), R795–R805. doi:10.1016/s0960-9822(01)00474-2

Heyde, A., Rohde, D., McAlpine, C. S., Zhang, S., Hoyer, F. F., Gerold, J. M., et al. (2021). Increased Stem Cell Proliferation in Atherosclerosis Accelerates Clonal Hematopoiesis. *Cell* 184 (5), 1348–e22. e1322. doi:10.1016/j.cell.2021.01.049

Hoebe, K., Georgel, P., Rutschmann, S., Du, X., Mudd, S., Crozat, K., et al. (2005). CD36 Is a Sensor of Diacylglycerides. *Nature* 433 (7025), 523–527. doi:10.1038/nature03253

Hofmans, S., Vanden Berghe, T., Devisscher, L., Hassannia, B., Lyssens, S., Joossens, J., et al. (2016). Novel Ferroptosis Inhibitors with Improved Potency and ADME Properties. *J. Med. Chem.* 59 (5), 2041–2053. doi:10.1021/acs.jmedchem.5b01641

Huang, L., Chambliss, K. L., Gao, X., Yuhanna, I. S., Behling-Kelly, E., Bergaya, S., et al. (2019). SR-B1 Drives Endothelial Cell LDL Transcytosis via DOCK4 to Promote Atherosclerosis. *Nature* 569 (7757), 565–569. doi:10.1038/s41586-019-1140-4

Huo, Y., and Xia, L. (2009). P-selectin Glycoprotein Ligand-1 Plays a Crucial Role in the Selective Recruitment of Leukocytes into the Atherosclerotic Arterial wall. *Trends Cardiovasc. Med.* 19 (4), 140–145. doi:10.1016/j.tcm.2009.07.006

Jaiswal, S., Natarajan, P., Silver, A. J., Gibson, C. J., Bick, A. G., Shvartz, E., et al. (2017). Clonal Hematopoiesis and Risk of Atherosclerotic Cardiovascular Disease. *N. Engl. J. Med.* 377 (2), 111–121. doi:10.1056/NEJMoa1701719

Jansen, M. F., Hollander, M. R., van Royen, N., Horrevoets, A. J., and Lutgens, E. (2016). CD40 in Coronary Artery Disease: a Matter of Macrophages? *Basic Res. Cardiol.* 111 (4), 38. doi:10.1007/s00395-016-0554-5

Jefferis, B. J., Papacosta, O., Owen, C. G., Wannamethee, S. G., Humphries, S. E., Woodward, M., et al. (2011). Interleukin 18 and Coronary Heart Disease: Prospective Study and Systematic Review. *Atherosclerosis* 217 (1), 227–233. doi:10.1016/j.atherosclerosis.2011.03.015

Jiang, Y., Gao, Q., Wang, L., Guo, C., Zhu, F., Wang, B., et al. (2016). Deficiency of Programmed Cell Death 4 Results in Increased IL-10 Expression by Macrophages and Thereby Attenuates Atherosclerosis in Hyperlipidemic Mice. *Cell Mol Immunol* 13 (4), 524–534. doi:10.1038/cmi.2015.47

Jung, S. B., Choi, M. J., Ryu, D., Yi, H. S., Lee, S. E., Chang, J. Y., et al. (2018). Reduced Oxidative Capacity in Macrophages Results in Systemic Insulin Resistance. *Nat. Commun.* 9 (1), 1551–1615. doi:10.1038/s41467-018-03998-z

Kadl, A., Meher, A. K., Sharma, P. R., Lee, M. Y., Doran, A. C., Johnstone, S. R., et al. (2010). Identification of a Novel Macrophage Phenotype that Develops in Response to Atherogenic Phospholipids via Nrf2. *Circ. Res.* 107 (6), 737–746. doi:10.1161/circresaha.109.215715

Kale, A., Sharma, A., Stolzing, A., Desprez, P. Y., and Campisi, J. (2020). Role of Immune Cells in the Removal of Deleterious Senescent Cells. *Immun. Ageing* 17 (1), 16–19. doi:10.1186/s12979-020-00187-9

Kamari, Y., Shaish, A., Shemesh, S., Vax, E., Grosskopf, I., Dotan, S., et al. (2011). Reduced Atherosclerosis and Inflammatory Cytokines in Apolipoprotein-E-Deficient Mice Lacking Bone Marrow-Derived Interleukin-1α. *Biochem. Biophys. Res. Commun.* 405 (2), 197–203. doi:10.1016/j.bbrc.2011.01.008

Kapellos, T. S., Bonaguro, L., Gemünd, I., Reusch, N., Saglam, A., Hinkley, E. R., et al. (2019). Human Monocyte Subsets and Phenotypes in Major Chronic Inflammatory Diseases. *Front. Immunol.* 10, 2035. doi:10.3389/fimmu.2019.02035

Kaperonis, E. A., Liapis, C. D., Kakisis, J. D., Dimitroulis, D., and Papavassiliou, V. G. (2006). Inflammation and Atherosclerosis. *Eur. J. Vasc. Endovasc Surg.* 31 (4), 386–393. doi:10.1016/j.ejvs.2005.11.001

Karunakaran, D., Geoffrion, M., Wei, L., Gan, W., Richards, L., Shangari, P., et al. (2016). Targeting Macrophage Necroptosis for Therapeutic and Diagnostic Interventions in Atherosclerosis. *Sci. Adv.* 2 (7), e1600224. doi:10.1126/sciadv.1600224

Kattoor, A. J., Goel, A., and Mehta, J. L. (2019). LOX-1: Regulation, Signaling and its Role in Atherosclerosis. *Antioxidants (Basel)* 8 (7), 218. doi:10.3390/antiox8070218

Khallou-Laschet, J., Varthaman, A., Fornasa, G., Compain, C., Gaston, A. T., Clement, M., et al. (2010). Macrophage Plasticity in Experimental Atherosclerosis. *PLoS One* 5 (1), e8852. doi:10.1371/journal.pone.0008852

Kim, K., Shim, D., Lee, J. S., Zaitsev, K., Williams, J. W., Kim, K. W., et al. (2018). Transcriptome Analysis Reveals Nonfoamy rather Than Foamy Plaque Macrophages Are Proinflammatory in Atherosclerotic Murine Models. *Circ. Res.* 123 (10), 1127–1142. doi:10.1161/CIRCRESAHA.118.312804

Kinlay, S., Schwartz, G. G., Olsson, A. G., Rifai, N., Szarek, M., Waters, D. D., et al. (2008). Inflammation, Statin Therapy, and Risk of Stroke after an Acute Coronary Syndrome in the MIRACL Study. *Arterioscler Thromb. Vasc. Biol.* 28 (1), 142–147. doi:10.1161/ATVBAHA.107.151787

Kleemann, R., Zadelaar, S., and Kooistra, T. (2008). Cytokines and Atherosclerosis: a Comprehensive Review of Studies in Mice. *Cardiovasc. Res.* 79 (3), 360–376. doi:10.1093/cvr/cvn120

Kober, D. L., and Brett, T. J. (2017). TREM2-Ligand Interactions in Health and Disease. *J. Mol. Biol.* 429 (11), 1607–1629. doi:10.1016/j.jmb.2017.04.004

Kojima, Y., Volkmer, J. P., McKenna, K., Civelek, M., Lusis, A. J., Miller, C. L., et al. (2016). CD47-blocking Antibodies Restore Phagocytosis and Prevent Atherosclerosis. *Nature* 536 (7614), 86–90. doi:10.1038/nature18935

Kojima, Y., Weissman, I. L., and Leeper, N. J. (2017). The Role of Efferocytosis in Atherosclerosis. *Circulation* 135 (5), 476–489. doi:10.1161/circulationaha.116.025684

Kolter, J., Kierdorf, K., and Henneke, P. (2020a). Origin and Differentiation of Nerve-Associated Macrophages. *J. Immunol.* 204 (2), 271–279. doi:10.4049/jimmunol.1901077

Kolter, J., Kierdorf, K., and Henneke, P. (2020b). Origin and Differentiation of Nerve-Associated Macrophages. *J. Immunol.* 204 (2), 271–279. doi:10.4049/jimmunol.1901077

Kozarsky, K. F., Donahee, M. H., Rigotti, A., Iqbal, S. N., Edelman, E. R., and Krieger, M. (1997). Overexpression of the HDL Receptor SR-BI Alters Plasma HDL and Bile Cholesterol Levels. *Nature* 387 (6631), 414–417. doi:10.1038/387414a0

Lehtolainen, P., Takeya, M., and Ylä-Herttuala, S. (2000). Retrovirus-mediated, Stable Scavenger-Receptor Gene Transfer Leads to Functional Endocytotic Receptor Expression, Foam Cell Formation, and Increased Susceptibility to Apoptosis in Rabbit Aortic Smooth Muscle Cells. *Arterioscler Thromb. Vasc. Biol.* 20 (1), 52–60. doi:10.1161/01.atv.20.1.52

Leitinger, N., and Schulman, I. G. (2013). Phenotypic Polarization of Macrophages in Atherosclerosis. *Arterioscler Thromb. Vasc. Biol.* 33 (6), 1120–1126. doi:10.1161/ATVBAHA.112.300173

Leuschner, F., Rauch, P. J., Ueno, T., Gorbatov, R., Marinelli, B., Lee, W. W., et al. (2012). Rapid Monocyte Kinetics in Acute Myocardial Infarction Are Sustained by Extramedullary Monocytopoiesis. *J. Exp. Med.* 209 (1), 123–137. doi:10.1084/jem.20111009

Ley, K., Laudanna, C., Cybulsky, M. I., and Nourshargh, S. (2007). Getting to the Site of Inflammation: the Leukocyte Adhesion cascade Updated. *Nat. Rev. Immunol.* 7 (9), 678–689. doi:10.1038/nri2156

Li, B., Xia, Y., and Hu, B. (2020a). Infection and Atherosclerosis: TLR-dependent Pathways. *Cell Mol Life Sci* 77 (14), 2751–2769. doi:10.1007/s00018-020-03453-7

Li, Y., Yun, K., and Mu, R. (2020b). A Review on the Biology and Properties of Adipose Tissue Macrophages Involved in Adipose Tissue Physiological and Pathophysiological Processes. *Lipids Health Dis.* 19 (1), 164–169. doi:10.1186/s12944-020-01342-3

Libby, P. (2021). The Changing Landscape of Atherosclerosis. *Nature* 592 (7855), 524–533. doi:10.1038/s41586-021-03392-8

Liberale, L., Dallegri, F., Montecucco, F., and Carbone, F. (2017). Pathophysiological Relevance of Macrophage Subsets in Atherogenesis. *Thromb. Haemost.* 117 (01), 7–18. doi:10.1160/TH16-08-0593

Lim, W. S., Timmins, J. M., Seimon, T. A., Sadler, A., Kolodgie, F. D., Virmani, R., et al. (2008). Signal Transducer and Activator of Transcription-1 Is Critical for Apoptosis in Macrophages Subjected to Endoplasmic Reticulum Stress *In Vitro* and in Advanced Atherosclerotic Lesions *In Vivo*. *Circulation* 117 (7), 940–951. doi:10.1161/circulationaha.107.711275

Lin, J. D., Nishi, H., Poles, J., Niu, X., Mccauley, C., Rahman, K., et al. (2019). Single-cell Analysis of Fate-Mapped Macrophages Reveals Heterogeneity, Including Stem-like Properties, during Atherosclerosis Progression and Regression. *JCI insight* 4 (4). doi:10.1172/jci.insight.124574

Lin, P., Ji, H.-H., Li, Y.-J., and Guo, S.-D. (2021). Macrophage Plasticity and Atherosclerosis Therapy. *Front. Mol. Biosciences* 8, 324. doi:10.3389/fmolb.2021.679797

Liu, J. Y., Souroullas, G. P., Diekman, B. O., Krishnamurthy, J., Hall, B. M., Sorrentino, J. A., et al. (2019). Cells Exhibiting strong P16 INK4a Promoter Activation *In Vivo* Display Features of Senescence. *Proc. Natl. Acad. Sci. U S A.* 116 (7), 2603–2611. doi:10.1073/pnas.1818313116

Low, E. L., Baker, A. H., and Bradshaw, A. C. (2019). TGFβ, Smooth Muscle Cells and Coronary Artery Disease: a Review. *Cell Signal* 53, 90–101. doi:10.1016/j.cellsig.2018.09.004

Mallat, Z., Gojova, A., Marchiol-Fournigault, C., Esposito, B., Kamaté, C., Merval, R., et al. (2001). Inhibition of Transforming Growth Factor-Beta Signaling Accelerates Atherosclerosis and Induces an Unstable Plaque Phenotype in Mice. *Circ. Res.* 89 (10), 930–934. doi:10.1161/hh2201.099415

Mallat, Z., Heymes, C., Ohan, J., Faggin, E., Lesèche, G., and Tedgui, A. (1999). Expression of Interleukin-10 in Advanced Human Atherosclerotic Plaques: Relation to Inducible Nitric Oxide Synthase Expression and Cell Death. *Arterioscler Thromb. Vasc. Biol.* 19 (3), 611–616. doi:10.1161/01.atv.19.3.611

Manning-Tobin, J. J., Moore, K. J., Seimon, T. A., Bell, S. A., Sharuk, M., Alvarez-Leite, J. I., et al. (2009). Loss of SR-A and CD36 Activity Reduces Atherosclerotic Lesion Complexity without Abrogating Foam Cell Formation in Hyperlipidemic Mice. *Arterioscler Thromb. Vasc. Biol.* 29 (1), 19–26. doi:10.1161/atvbaha.108.176644

Mantovani, A., Sica, A., Sozzani, S., Allavena, P., Vecchi, A., and Locati, M. (2004). The Chemokine System in Diverse Forms of Macrophage Activation and Polarization. *Trends Immunol.* 25 (12), 677–686. doi:10.1016/j.it.2004.09.015

Marchio, P., Guerra-Ojeda, S., Vila, J. M., Aldasoro, M., Victor, V. M., and Mauricio, M. D. (2019). *Targeting Early Atherosclerosis: A Focus on Oxidative Stress and Inflammation.* Oxidative Medicine and Cellular Longevity *2019*.

Martinet, W., Coornaert, I., Puylaert, P., and De Meyer, G. R. Y. (2019). Macrophage Death as a Pharmacological Target in Atherosclerosis. *Front. Pharmacol.* 10, 306. doi:10.3389/fphar.2019.00306

McAlpine, C. S., Kiss, M. G., Rattik, S., He, S., Vassalli, A., Valet, C., et al. (2019). Sleep Modulates Haematopoiesis and Protects against Atherosclerosis. *Nature* 566 (7744), 383–387. doi:10.1038/s41586-019-0948-2

McKellar, G. E., McCarey, D. W., Sattar, N., and McInnes, I. B. (2009). Role for TNF in Atherosclerosis? Lessons from Autoimmune Disease. *Nat. Rev. Cardiol.* 6 (6), 410–7. doi:10.1038/nrcardio.2009.57

Medbury, H. J., Williams, H., and Fletcher, J. P. (2014). Clinical Significance of Macrophage Phenotypes in Cardiovascular Disease. *Clin. Transl Med.* 3 (1), 63–10. doi:10.1186/s40169-014-0042-1

Meng, Z., Wang, M., Xing, J., Liu, Y., and Li, H. (2019). Myricetin Ameliorates Atherosclerosis in the Low-Density-Lipoprotein Receptor Knockout Mice by Suppression of Cholesterol Accumulation in Macrophage Foam Cells. *Nutr. Metab. (Lond)* 16 (1), 25–29. doi:10.1186/s12986-019-0354-7

Michelsen, K. S., Wong, M. H., Shah, P. K., Zhang, W., Yano, J., Doherty, T. M., et al. (2004). Lack of Toll-like Receptor 4 or Myeloid Differentiation Factor 88 Reduces Atherosclerosis and Alters Plaque Phenotype in Mice Deficient in Apolipoprotein E. *Proc. Natl. Acad. Sci. U S A.* 101 (29), 10679–10684. doi:10.1073/pnas.0403249101

Miki, H., Pei, H., Gracias, D. T., Linden, J., and Croft, M. (2021). Clearance of Apoptotic Cells by Lung Alveolar Macrophages Prevents Development of House Dust Mite-Induced Asthmatic Lung Inflammation. *J. Allergy Clin. Immunol.* 147 (3), 1087–1092. doi:10.1016/j.jaci.2020.10.005

Milioti, N., Bermudez-Fajardo, A., Penichet, M. L., and Oviedo-Orta, E. (2008). Antigen-induced Immunomodulation in the Pathogenesis of Atherosclerosis. *Clin. Dev. Immunol.* 2008, 723539. doi:10.1155/2008/723539

Mirza, R. E., Fang, M. M., Weinheimer-Haus, E. M., Ennis, W. J., and Koh, T. J. (2014). Sustained Inflammasome Activity in Macrophages Impairs Wound Healing in Type 2 Diabetic Humans and Mice. *Diabetes* 63 (3), 1103–1114. doi:10.2337/db13-0927

Moore, K. J., Sheedy, F. J., and Fisher, E. A. (2013). Macrophages in Atherosclerosis: a Dynamic Balance. *Nat. Rev. Immunol.* 13 (10), 709–721. doi:10.1038/nri3520

Moreno Velásquez, I., Gajulapuri, A., Leander, K., Berglund, A., de Faire, U., and Gigante, B. (2019). Serum IL8 Is Not Associated with Cardiovascular Events but with All-Cause Mortality. *BMC Cardiovasc. Disord.* 19 (1), 34–38. doi:10.1186/s12872-019-1014-6

Moriya, J. (2019). Critical Roles of Inflammation in Atherosclerosis. *J. Cardiol.* 73 (1), 22–27. doi:10.1016/j.jjcc.2018.05.010

Murray, P. J. (2017). Macrophage Polarization. *Annu. Rev. Physiol.* 79, 541–566. doi:10.1146/annurev-physiol-022516-034339

Nagenborg, J., Goossens, P., Biessen, E. A. L., and Donners, M. M. P. C. (2017). Heterogeneity of Atherosclerotic Plaque Macrophage Origin, Phenotype and Functions: Implications for Treatment. *Eur. J. Pharmacol.* 816, 14–24. doi:10.1016/j.ejphar.2017.10.005

Nahrendorf, M., Swirski, F. K., Aikawa, E., Stangenberg, L., Wurdinger, T., Figueiredo, J. L., et al. (2007). The Healing Myocardium Sequentially Mobilizes Two Monocyte Subsets with Divergent and Complementary Functions. *J. Exp. Med.* 204 (12), 3037–3047. doi:10.1084/jem.20070885

Neufeld, E. B., O'Brien, K., Walts, A. D., Stonik, J. A., Demosky, S. J., Malide, D., et al. (2014). Cellular Localization and Trafficking of the Human ABCG1 Transporter. *Biology (Basel)* 3 (4), 781–800. doi:10.3390/biology3040781

Nikoletopoulou, V., Markaki, M., Palikaras, K., and Tavernarakis, N. (2013). Crosstalk between Apoptosis, Necrosis and Autophagy. *Biochim. Biophys. Acta* 1833 (12), 3448–3459. doi:10.1016/j.bbamcr.2013.06.001

Nikonova, A., Khaitov, M., Jackson, D. J., Traub, S., Trujillo-Torralbo, M. B., Kudlay, D. A., et al. (2020). M1-like Macrophages Are Potent Producers of Anti-viral Interferons and M1-Associated Marker-Positive Lung Macrophages Are Decreased during Rhinovirus-Induced Asthma Exacerbations. *EBioMedicine* 54, 102734. doi:10.1016/j.ebiom.2020.102734

Nilchian, A., Plant, E., Parniewska, M. M., Santiago, A., Rossignoli, A., Skogsberg, J., et al. (2020). Induction of the Coxsackievirus and Adenovirus Receptor in Macrophages during the Formation of Atherosclerotic Plaques. *J. Infect. Dis.* 222 (12), 2041–2051. doi:10.1093/infdis/jiaa418

Nishida, M., Miyagawa, J., Yamashita, S., Higashiyama, S., Nakata, A., Ouchi, N., et al. (2000). Localization of CD9, an Enhancer Protein for Proheparin-Binding Epidermal Growth Factor-like Growth Factor, in Human Atherosclerotic Plaques: Possible Involvement of Juxtacrine Growth Mechanism on Smooth Muscle Cell Proliferation. *Arterioscler Thromb. Vasc. Biol.* 20 (5), 1236–1243. doi:10.1161/01.atv.20.5.1236

Novak, M. L., Weinheimer-Haus, E. M., and Koh, T. J. (2014). Macrophage Activation and Skeletal Muscle Healing Following Traumatic Injury. *J. Pathol.* 232 (3), 344–355. doi:10.1002/path.4301

Ohgami, N., Nagai, R., Ikemoto, M., Arai, H., Kuniyasu, A., Horiuchi, S., et al. (2001). Cd36, a Member of the Class B Scavenger Receptor Family, as a Receptor for Advanced Glycation End Products. *J. Biol. Chem.* 276 (5), 3195–3202. doi:10.1074/jbc.M006545200

Ouimet, M., Ediriweera, H., Afonso, M. S., Ramkhelawon, B., Singaravelu, R., Liao, X., et al. (2017). microRNA-33 Regulates Macrophage Autophagy in Atherosclerosis. *Arterioscler Thromb. Vasc. Biol.* 37 (6), 1058–1067. doi:10.1161/atvbaha.116.308916

Oumouna-Benachour, K., Hans, C. P., Suzuki, Y., Naura, A., Datta, R., Belmadani, S., et al. (2007). Poly(ADP-ribose) Polymerase Inhibition Reduces Atherosclerotic Plaque Size and Promotes Factors of Plaque Stability in Apolipoprotein E-Deficient Mice: Effects on Macrophage Recruitment, Nuclear Factor-kappaB Nuclear Translocation, and Foam Cell Death. *Circulation* 115 (18), 2442–2450. doi:10.1161/circulationaha.106.668756

Panousis, C. G., Evans, G., and Zuckerman, S. H. (2001). TGF-beta Increases Cholesterol Efflux and ABC-1 Expression in Macrophage-Derived Foam Cells: Opposing the Effects of IFN-Gamma. *J. Lipid Res.* 42 (5), 856–863. doi:10.1016/s0022-2275(20)31648-5

Park, H. J., Lee, S. J., Kim, S. H., Han, J., Bae, J., Kim, S. J., et al. (2011). IL-10 Inhibits the Starvation Induced Autophagy in Macrophages via Class I Phosphatidylinositol 3-kinase (PI3K) Pathway. *Mol. Immunol.* 48 (4), 720–727. doi:10.1016/j.molimm.2010.10.020

Park, S. H. (2021). Regulation of Macrophage Activation and Differentiation in Atherosclerosis. *J. Lipid Atheroscler.* 10, 251–267. doi:10.12997/jla.2021.10.3.251

Park, Y. M., Drazba, J. A., Vasanji, A., Egelhoff, T., Febbraio, M., and Silverstein, R. L. (2012). Oxidized LDL/CD36 Interaction Induces Loss of Cell Polarity and Inhibits Macrophage Locomotion. *Mol. Biol. Cel* 23 (16), 3057–3068. doi:10.1091/mbc.E11-12-1051

Pham, L. M., Kim, E. C., Ou, W., Phung, C. D., Nguyen, T. T., Pham, T. T., et al. (2021). Targeting and Clearance of Senescent Foamy Macrophages and Senescent Endothelial Cells by Antibody-Functionalized Mesoporous Silica Nanoparticles for Alleviating Aorta Atherosclerosis. *Biomaterials* 269, 120677. doi:10.1016/j.biomaterials.2021.120677

Phillips, M. C. (2018). Is ABCA1 a Lipid Transfer Protein? *J. Lipid Res.* 59 (5), 749–763. doi:10.1194/jlr.R082313

Pinderski, L. J., Fischbein, M. P., Subbanagounder, G., Fishbein, M. C., Kubo, N., Cheroutre, H., et al. (2002). Overexpression of Interleukin-10 by Activated T Lymphocytes Inhibits Atherosclerosis in LDL Receptor-Deficient Mice by Altering Lymphocyte and Macrophage Phenotypes. *Circ. Res.* 90 (10), 1064–1071. doi:10.1161/01.res.0000018941.10726.fa

Porsch, F., Kiss, M. G., Goederle, L., Hendrikx, T., Hladik, A., Knapp, S., et al. (2020). Haematopoetic TREM2 Deficiency Modulates Atherosclerosis and Lipid Metabolism. *Atherosclerosis* 315, e58–e59. doi:10.1016/j.atherosclerosis.2020.10.180

Poznyak, A. V., Nikiforov, N. G., Markin, A. M., Kashirskikh, D. A., Myasoedova, V. A., Gerasimova, E. V., et al. (2021). Overview of OxLDL and its Impact on Cardiovascular Health: Focus on Atherosclerosis. *Front. Pharmacol.* 11, 2248. doi:10.3389/fphar.2020.613780

Prattichizzo, F., Bonafè, M., Olivieri, F., and Franceschi, C. (2016). Senescence Associated Macrophages and "Macroph-Aging": Are They Pieces of the Same Puzzle? *Aging (Albany NY)* 8 (12), 3159–3160. doi:10.18632/aging.101133

Que, X., Hung, M. Y., Yeang, C., Gonen, A., Prohaska, T. A., Sun, X., et al. (2018). Oxidized Phospholipids Are Proinflammatory and Proatherogenic in Hypercholesterolaemic Mice. *Nature* 558 (7709), 301–306. doi:10.1038/s41586-018-0198-8

Quiding-Järbrink, M., Raghavan, S., and Sundquist, M. (2010). Enhanced M1 Macrophage Polarization in Human helicobacter Pylori-Associated Atrophic Gastritis and in Vaccinated Mice. *PLoS One* 5 (11), e15018. doi:10.1371/journal.pone.0015018

Raggi, F., Pelassa, S., Pierobon, D., Penco, F., Gattorno, M., Novelli, F., et al. (2017). Regulation of Human Macrophage M1-M2 Polarization Balance by Hypoxia and the Triggering Receptor Expressed on Myeloid Cells-1. *Front. Immunol.* 8, 1097. doi:10.3389/fimmu.2017.01097

Reiss, A. B., Siegart, N. M., and De Leon, J. (2017). Interleukin-6 in Atherosclerosis: Atherogenic or Atheroprotective? *Clin. Lipidol.* 12 (1), 14–23.

Remmerie, A., and Scott, C. L. (2018). Macrophages and Lipid Metabolism. *Cell Immunol* 330, 27–42. doi:10.1016/j.cellimm.2018.01.020

Ricci, R., Sumara, G., Sumara, I., Rozenberg, I., Kurrer, M., Akhmedov, A., et al. (2004). Requirement of JNK2 for Scavenger Receptor A-Mediated Foam Cell Formation in Atherogenesis. *Science* 306 (5701), 1558–1561. doi:10.1126/science.1101909

Ridker, P. M., Libby, P., MacFadyen, J. G., Thuren, T., Ballantyne, C., Fonseca, F., et al. (2018). Modulation of the Interleukin-6 Signalling Pathway and Incidence Rates of Atherosclerotic Events and All-Cause Mortality: Analyses from the Canakinumab Anti-inflammatory Thrombosis Outcomes Study (CANTOS). *Eur. Heart J.* 39 (38), 3499–3507. doi:10.1093/eurheartj/ehy310

Ridker, P. M., Thuren, T., Zalewski, A., and Libby, P. (2011). Interleukin-1β Inhibition and the Prevention of Recurrent Cardiovascular Events: Rationale and Design of the Canakinumab Anti-inflammatory Thrombosis Outcomes Study (CANTOS). *Am. Heart J.* 162 (4), 597–605. doi:10.1016/j.ahj.2011.06.012

Ridker, P. M., Devalaraja, M., Baeres, F. M. M., Engelmann, M. D. M., Hovingh, G. K., Ivkovic, M., et al. (2021). IL-6 Inhibition with Ziltivekimab in Patients at High Atherosclerotic Risk (RESCUE): a Double-Blind, Randomised, Placebo-Controlled, Phase 2 Trial. *The Lancet* 397 (10289), 2060–2069. doi:10.1016/s0140-6736(21)00520-1

Robbins, C. S., Hilgendorf, I., Weber, G. F., Theurl, I., Iwamoto, Y., Figueiredo, J. L., et al. (2013a). Local Proliferation Dominates Lesional Macrophage Accumulation in Atherosclerosis. *Nat. Med.* 19 (9), 1166–1172. doi:10.1038/nm.3258

Robbins, C. S., Hilgendorf, I., Weber, G. F., Theurl, I., Iwamoto, Y., Figueiredo, J. L., et al. (2013b). Local Proliferation Dominates Lesional Macrophage Accumulation in Atherosclerosis. *Nat. Med.* 19 (9), 1166–72. doi:10.1038/nm.3258

Robertson, A. K., and Hansson, G. K. (2006). T Cells in Atherogenesis: for Better or for Worse? *Arterioscler Thromb. Vasc. Biol.* 26 (11), 2421–2432. doi:10.1161/01.ATV.0000245830.29764.84

Robinson, N., Ganesan, R., Hegedűs, C., Kovács, K., Kufer, T. A., and Virág, L. (2019). Programmed Necrotic Cell Death of Macrophages: Focus on Pyroptosis, Necroptosis, and Parthanatos. *Redox Biol.* 26, 101239. doi:10.1016/j.redox.2019.101239

Rogers, C., Fernandes-Alnemri, T., Mayes, L., Alnemri, D., Cingolani, G., and Alnemri, E. S. (2017). Cleavage of DFNA5 by Caspase-3 during Apoptosis Mediates Progression to Secondary Necrotic/pyroptotic Cell Death. *Nat. Commun.* 8, 14128. doi:10.1038/ncomms14128

Romuk, E., Skrzep-Poloczek, B., Wojciechowska, C., Tomasik, A., Birkner, E., Wodniecki, J., et al. (2002). Selectin-P and Interleukin-8 Plasma Levels in Coronary Heart Disease Patients. *Eur. J. Clin. Invest.* 32 (9), 657–661. doi:10.1046/j.1365-2362.2002.01053.x

Rong, J. X., Shapiro, M., Trogan, E., and Fisher, E. A. (2003). Transdifferentiation of Mouse Aortic Smooth Muscle Cells to a Macrophage-like State after Cholesterol Loading. *Proc. Natl. Acad. Sci. U S A.* 100 (23), 13531–13536. doi:10.1073/pnas.1735526100

Sano, S., Oshima, K., Wang, Y., Katanasaka, Y., Sano, M., and Walsh, K. (2018). CRISPR-mediated Gene Editing to Assess the Roles of Tet2 and Dnmt3a in Clonal Hematopoiesis and Cardiovascular Disease. *Circ. Res.* 123 (3), 335–341. doi:10.1161/CIRCRESAHA.118.313225

Schiopu, A., Frendéus, B., Jansson, B., Söderberg, I., Ljungcrantz, I., Araya, Z., et al. (2007). Recombinant Antibodies to an Oxidized Low-Density Lipoprotein Epitope Induce Rapid Regression of Atherosclerosis in Apobec-1(-/-)/low-Density Lipoprotein Receptor(-/-) Mice. *J. Am. Coll. Cardiol.* 50 (24), 2313–2318. doi:10.1016/j.jacc.2007.07.081

Scull, C. M., Hays, W. D., and Fischer, T. H. (2010). Macrophage Pro-inflammatory Cytokine Secretion Is Enhanced Following Interaction with Autologous Platelets. *J. Inflamm. (Lond)* 7, 53. doi:10.1186/1476-9255-7-53

Shami, A., Edsfeldt, A., Shore, A. C., Natali, A., Khan, F., Nilsson, J., et al. (2020). CD40 Levels in Plasma Are Associated with Cardiovascular Disease and in Carotid Plaques with a Vulnerable Plaque Phenotype and Remodelling. *Eur. Heart J.* 41 (Suppl. ment_2), ehaa946–3782. doi:10.1093/ehjci/ehaa946.3782

Sinha, S. K., Miikeda, A., Fouladian, Z., Mehrabian, M., Edillor, C., Shih, D., et al. (2021). Local M-CSF (Macrophage colony-stimulating Factor) Expression Regulates Macrophage Proliferation and Apoptosis in Atherosclerosis. *Arteriosclerosis, Thromb. Vasc. Biol.* 41 (1), 220–233.

Skuratovskaia, D., Vulf, M., Khaziakhmatova, O., Malashchenko, V., Komar, A., Shunkin, E., et al. (2020). Tissue-Specific Role of Macrophages in Noninfectious Inflammatory Disorders. *Biomedicines* 8 (10), 400. doi:10.3390/biomedicines8100400

Smith, M. S., Bentz, G. L., Smith, P. M., Bivins, E. R., and Yurochko, A. D. (2004). HCMV Activates PI(3)K in Monocytes and Promotes Monocyte Motility and Transendothelial Migration in a PI(3)K-dependent Manner. *J. Leukoc. Biol.* 76 (1), 65–76. doi:10.1189/jlb.1203621

Sodhi, N., and Brown, D. L. (2018). *Pathophysiology of Acute Coronary Syndromes: Plaque Rupture and Atherothrombosis*. Philadelphia: Cardiac Intensive Care-E-Book, 68.

Spiller, K. L., Anfang, R. R., Spiller, K. J., Ng, J., Nakazawa, K. R., Daulton, J. W., et al. (2014). The Role of Macrophage Phenotype in Vascularization of Tissue Engineering Scaffolds. *Biomaterials* 35 (15), 4477–4488. doi:10.1016/j.biomaterials.2014.02.012

Subedi, L., Lee, S. E., Madiha, S., Gaire, B. P., Jin, M., Yumnam, S., et al. (2020). Phytochemicals against TNFα-Mediated Neuroinflammatory Diseases. *Int. J. Mol. Sci.* 21 (3), 764. doi:10.3390/ijms21030764

Swirski, F. K., and Nahrendorf, M. (2013a). Leukocyte Behavior in Atherosclerosis, Myocardial Infarction, and Heart Failure. *Science* 339 (6116), 161–166. doi:10.1126/science.1230719

Syväranta, S., Alanne-Kinnunen, M., Oörni, K., Oksjoki, R., Kupari, M., Kovanen, P. T., et al. (2014). Potential Pathological Roles for Oxidized Low-Density Lipoprotein and Scavenger Receptors SR-AI, CD36, and LOX-1 in Aortic Valve Stenosis. *Atherosclerosis* 235 (2), 398–407. doi:10.1016/j.atherosclerosis.2014.05.933

Tabas, I. (2010). The Role of Endoplasmic Reticulum Stress in the Progression of Atherosclerosis. *Circ. Res.* 107 (7), 839–850. doi:10.1161/circresaha.110.224766

Tacke, F., Alvarez, D., Kaplan, T. J., Jakubzick, C., Spanbroek, R., Llodra, J., et al. (2007). Monocyte Subsets Differentially Employ CCR2, CCR5, and CX3CR1 to Accumulate within Atherosclerotic Plaques. *J. Clin. Invest.* 117 (1), 185–194. doi:10.1172/JCI28549

Tang, J., Lobatto, M. E., Hassing, L., Van Der Staay, S., Van Rijs, S. M., Calcagno, C., et al. (2015). Inhibiting Macrophage Proliferation Suppresses Atherosclerotic Plaque Inflammation. *Sci. Adv.* 1 (3), e1400223. doi:10.1126/sciadv.1400223

Tao, H., Huang, J., Yancey, P. G., Yermalitsky, V., Blakemore, J. L., Zhang, Y., et al. (2020). Scavenging of Reactive Dicarbonyls with 2-hydroxybenzylamine Reduces Atherosclerosis in Hypercholesterolemic Ldlr-/- Mice. *Nat. Commun.* 11 (1), 4084–4115. doi:10.1038/s41467-020-17915-w

Tao, H., Yancey, P. G., Babaev, V. R., Blakemore, J. L., Zhang, Y., Ding, L., et al. (2015). Macrophage SR-BI Mediates Efferocytosis via Src/PI3K/Rac1 Signaling and Reduces Atherosclerotic Lesion Necrosis. *J. Lipid Res.* 56 (8), 1449–1460. doi:10.1194/jlr.M056689

Teh, Y. C., Ding, J. L., Ng, L. G., and Chong, S. Z. (2019). Capturing the Fantastic Voyage of Monocytes through Time and Space. *Front. Immunol.* 10, 834. doi:10.3389/fimmu.2019.00834

Tenger, C., Sundborger, A., Jawien, J., and Zhou, X. (2005). IL-18 Accelerates Atherosclerosis Accompanied by Elevation of IFN-Gamma and CXCL16 Expression Independently of T Cells. *Arterioscler Thromb. Vasc. Biol.* 25 (4), 791–796. doi:10.1161/01.atv.0000153516.02782.65

Thayse, K., Kindt, N., Laurent, S., and Carlier, S. (2020). VCAM-1 Target in Non-invasive Imaging for the Detection of Atherosclerotic Plaques. *Biology (Basel)* 9 (11), 368. doi:10.3390/biology9110368

Tian, F., Yao, J., Yan, M., Sun, X., Wang, W., Gao, W., et al. (2016). 5-Aminolevulinic Acid-Mediated Sonodynamic Therapy Inhibits RIPK1/RIPK3-dependent Necroptosis in THP-1-Derived Foam Cells. *Sci. Rep.* 6 (1), 21992–22013. doi:10.1038/srep21992

Tyrrell, D. J., and Goldstein, D. R. (2020). Ageing and Atherosclerosis: Vascular Intrinsic and Extrinsic Factors and Potential Role of IL-6. *Nat. Rev. Cardiol.* 18, 1–11. doi:10.1038/s41569-020-0431-7

Van Eck, M., Twisk, J., Hoekstra, M., Van Rij, B. T., Van der Lans, C. A., Bos, I. S., et al. (2003). Differential Effects of Scavenger Receptor BI Deficiency on Lipid Metabolism in Cells of the Arterial wall and in the Liver. *J. Biol. Chem.* 278 (26), 23699–23705. doi:10.1074/jbc.M211233200

Veerman, K. M., Williams, M. J., Uchimura, K., Singer, M. S., Merzaban, J. S., Naus, S., et al. (2007). Interaction of the Selectin Ligand PSGL-1 with Chemokines CCL21 and CCL19 Facilitates Efficient Homing of T Cells to Secondary Lymphoid Organs. *Nat. Immunol.* 8 (5), 532–539. doi:10.1038/ni1456

Vijayvergiya, R., and Vadivelu, R. (2015). Role of *Helicobacter pylori* Infection in Pathogenesis of Atherosclerosis. *World J. Cardiol.* 7 (3), 134–143. doi:10.4330/wjc.v7.i3.134

Virmani, R., Burke, A. P., Kolodgie, F. D., and Farb, A. (2002). Vulnerable Plaque: the Pathology of Unstable Coronary Lesions. *J. Interv. Cardiol.* 15 (6), 439–446. doi:10.1111/j.1540-8183.2002.tb01087.x

Wainstein, M. V., Mossmann, M., Araujo, G. N., Gonçalves, S. C., Gravina, G. L., Sangalli, M., et al. (2017). Elevated Serum Interleukin-6 Is Predictive of Coronary Artery Disease in Intermediate Risk Overweight Patients Referred for Coronary Angiography. *Diabetol. Metab. Syndr.* 9, 67. doi:10.1186/s13098-017-0266-5

Wang, L., Li, H., Tang, Y., and Yao, P. (2020). Potential Mechanisms and Effects of Efferocytosis in Atherosclerosis. *Front. Endocrinol. (Lausanne)* 11, 585285. doi:10.3389/fendo.2020.585285

Wang, N., Liang, H., and Zen, K. (2014a). Molecular Mechanisms that Influence the Macrophage M1-M2 Polarization Balance. *Front. Immunol.* 5, 614. doi:10.3389/fimmu.2014.00614

Wang, Y., Gao, W., Shi, X., Ding, J., Liu, W., He, H., et al. (2017). Chemotherapy Drugs Induce Pyroptosis through Caspase-3 Cleavage of a Gasdermin. *Nature* 547 (7661), 99–103. doi:10.1038/nature22393

Willemsen, L., and de Winther, M. P. (2020). Macrophage Subsets in Atherosclerosis as Defined by Single-Cell Technologies. *J. Pathol.* 250 (5), 705–714. doi:10.1002/path.5392

Williams, J. W., Winkels, H., Durant, C. P., Zaitsev, K., Ghosheh, Y., and Ley, K. (2020). Single Cell RNA Sequencing in Atherosclerosis Research. *Circ. Res.* 126 (9), 1112–1126. doi:10.1161/CIRCRESAHA.119.315940

Winkels, H., Ehinger, E., Vassallo, M., Buscher, K., Dinh, H. Q., Kobiyama, K., et al. (2018). Atlas of the Immune Cell Repertoire in Mouse Atherosclerosis Defined by Single-Cell RNA-Sequencing and Mass Cytometry. *Circ. Res.* 122 (12), 1675–1688. doi:10.1161/CIRCRESAHA.117.312513

Wynn, T. A., and Vannella, K. M. (2016). Macrophages in Tissue Repair, Regeneration, and Fibrosis. *Immunity* 44 (3), 450–462. doi:10.1016/j.immuni.2016.02.015

Xiong, D., Wang, Y., and You, M. (2020). A Gene Expression Signature of TREM2hi Macrophages and γδ T Cells Predicts Immunotherapy Response. *Nat. Commun.* 11 (1), 5084–5112. doi:10.1038/s41467-020-18546-x

Xu, H., Jiang, J., Chen, W., Li, W., and Chen, Z. (2019). Vascular Macrophages in Atherosclerosis. *J. Immunol. Res.* 2019, 4354786. doi:10.1155/2019/4354786

Xu, S., Bai, P., Little, P. J., and Liu, P. (2014). Poly(ADP-ribose) Polymerase 1 (PARP1) in Atherosclerosis: from Molecular Mechanisms to Therapeutic Implications. *Med. Res. Rev.* 34 (3), 644–675. doi:10.1002/med.21300

Xu, S., Ogura, S., Chen, J., Little, P. J., Moss, J., and Liu, P. (2013). LOX-1 in Atherosclerosis: Biological Functions and Pharmacological Modifiers. *Cel Mol Life Sci* 70 (16), 2859–2872. doi:10.1007/s00018-012-1194-z

Yamamoto, S., Yancey, P. G., Zuo, Y., Ma, L. J., Kaseda, R., Fogo, A. B., et al. (2011). Macrophage Polarization by Angiotensin II-type 1 Receptor Aggravates Renal Injury-Acceleration of Atherosclerosis. *Arterioscler Thromb. Vasc. Biol.* 31 (12), 2856–2864. doi:10.1161/atvbaha.111.237198

Yan, G., Elbadawi, M., and Efferth, T. (2020). Multiple Cell Death Modalities and Their Key Features. *World Acad. Sci. J.* 2 (2), 39–48.

Yang, S., Li, J., Chen, Y., Zhang, S., Feng, C., Hou, Z., et al. (2019). MicroRNA-216a Promotes M1 Macrophages Polarization and Atherosclerosis Progression by Activating Telomerase via the Smad3/NF-Kb Pathway. *Biochim. Biophys. Acta Mol. Basis Dis.* 1865 (7), 1772–1781. doi:10.1016/j.bbadis.2018.06.016

Yin, Q., Chang, H., Shen, Q., and Xing, D. (2021). Photobiomodulation Therapy Promotes the ATP-Binding Cassette Transporter A1-dependent Cholesterol Efflux in Macrophage to Ameliorate Atherosclerosis. *J. Cel Mol Med* 25 (11), 5238–5249. doi:10.1111/jcmm.16531

Yu, X. H., Fu, Y. C., Zhang, D. W., Yin, K., and Tang, C. K. (2013). Foam Cells in Atherosclerosis. *Clin. Chim. Acta* 424, 245–252. doi:10.1016/j.cca.2013.06.006

Zeng, C., Wang, R., and Tan, H. (2019). Role of Pyroptosis in Cardiovascular Diseases and its Therapeutic Implications. *Int. J. Biol. Sci.* 15 (7), 1345–1357. doi:10.7150/ijbs.33568

Zernecke, A., Winkels, H., Cochain, C., Williams, J. W., Wolf, D., Soehnlein, O., et al. (2020). Meta-analysis of Leukocyte Diversity in Atherosclerotic Mouse Aortas. *Circ. Res.* 127 (3), 402–426. doi:10.1161/CIRCRESAHA.120.316903

Zhang, H., Park, Y., Wu, J., Chen, Xp., Lee, S., Yang, J., et al. (2009). Role of TNF-Alpha in Vascular Dysfunction. *Clin. Sci. (Lond)* 116 (3), 219–230. doi:10.1042/cs20080196

Zhang, X., Niessner, A., Nakajima, T., Ma-Krupa, W., Kopecky, S. L., Frye, R. L., et al. (2006). Interleukin 12 Induces T-Cell Recruitment into the Atherosclerotic Plaque. *Circ. Res.* 98 (4), 524–531. doi:10.1161/01.RES.0000204452.46568.57

Zhang, Y., Wang, Y., Zhou, D., Zhang, L. S., Deng, F. X., Shu, S., et al. (2019). Angiotensin II Deteriorates Advanced Atherosclerosis by Promoting MerTK Cleavage and Impairing Efferocytosis through the AT1R/ROS/p38 MAPK/ADAM17 Pathway. *Am. J. Physiol. Cel Physiol* 317 (4), C776–C787. doi:10.1152/ajpcell.00145.2019

Zhang, Y., Shi, X., Han, J., Peng, W., Fang, Z., Zhou, Y., et al. (2021). Convallatoxin Promotes M2 Macrophage Polarization to Attenuate Atherosclerosis through PPARγ-Integrin αvβ5 Signaling Pathway. *Dddt* 15, 803–812. doi:10.2147/dddt.s288728

Zhu, X. D., Zhuang, Y., Ben, J. J., Qian, L. L., Huang, H. P., Bai, H., et al. (2011). Caveolae-dependent Endocytosis Is Required for Class A Macrophage Scavenger Receptor-Mediated Apoptosis in Macrophages. *J. Biol. Chem.* 286 (10), 8231–8239. doi:10.1074/jbc.M110.145888

Zuo, S., Yu, J., Pan, H., and Lu, L. (2020). Novel Insights on Targeting Ferroptosis in Cancer Therapy. *Biomark Res.* 8 (1), 50–11. doi:10.1186/s40364-020-00229-w

Conflict of Interest: The authors declare that the research was conducted in the absence of any commercial or financial relationships that could be construed as a potential conflict of interest.

frontiers in Pharmacology

ORIGINAL RESEARCH
published: 07 December 2021
doi: 10.3389/fphar.2021.787193

Proteomics Analysis of Tears and Saliva From Sjogren's Syndrome Patients

Nabangshu Das[1,2†], Nikhil G. Menon[3†], Luiz G. N. de Almeida[1,2], Paige S. Woods[4], Miriam L. Heynen[5], Gregory D. Jay[4], Barbara Caffery[6], Lyndon Jones[5], Roman Krawetz[2,7], Tannin A. Schmidt[2,3] and Antoine Dufour[1,2,8]**

[1]Departments of Physiology and Pharmacology and Kinesiology, University of Calgary, Calgary, AB, Canada, [2]McCaig Institute, University of Calgary, Calgary, AB, Canada, [3]Department of Biomedical Engineering, School of Dental Medicine, UConn Health, Farmington, CT, United States, [4]Department of Emergency Medicine, Warren Alpert Medical School and School of Engineering, Brown University, Providence, RI, United States, [5]Centre for Ocular Research and Education (CORE), School of Optometry and Vision Science, University of Waterloo, Waterloo, ON, Canada, [6]Toronto Eye Care, Toronto, ON, Canada, [7]Department of Cell Biology and Anatomy, University of Calgary, Calgary, AB, Canada, [8]Hotchkiss Brain Institute, University of Calgary, Calgary, AB, Canada

Sjogren's syndrome (SS) is characterized by dysfunctional mucous membranes and dysregulated moisture-secreting glands resulting in various symptoms, including dry mouth and dry eyes. Here, we wanted to profile and compare the tear and saliva proteomes of SS patients to healthy controls. Tear and saliva samples were collected and subjected to an isotopic dimethylation labeling shotgun proteomics workflow to identify alterations in protein levels. In tear samples, we identified 83 upregulated and 112 downregulated proteins. Pathway enrichment analysis of the changing proteins by Metascape identified leukocyte transendothelial migration, neutrophil degranulation, and post-translation protein phosphorylation in tears of SS patients. In healthy controls' tears, an enrichment for proteins related to glycolysis, amino acid metabolism and apoptotic signaling pathway were identified. In saliva, we identified 108 upregulated and 45 downregulated proteins. Altered pathways in SS patients' saliva included cornification, sensory perception to taste and neutrophil degranulation. In healthy controls' saliva, an enrichment for proteins related to JAK-STAT signaling after interleukin-12 stimulation, phagocytosis and glycolysis in senescence were identified. Dysregulated protease activity is implicated in the initiation of inflammation and immune cell recruitment in SS. We identified 20 proteases and protease inhibitors in tears and 18 in saliva which are differentially expressed between SS patients and healthy controls. Next, we quantified endogenous proteoglycan 4 (PRG4), a mucin-like glycoprotein, in tear wash and saliva samples via a bead-based immune assay. We identified decreased levels of PRG4 in SS patients' tear wash compared to normal samples. Conversely, in saliva, we found elevated levels of PRG4 concentration and visualized PRG4 expression in human parotid gland *via* immunohistological staining. These findings will improve our mechanistic understanding of the disease and changes in SS patients' protein expression will help identify new potential drug targets. PRG4 is among the promising targets, which we identified here, in saliva, for the first time.

Keywords: lubricin, PRG4, protease, protease inhibitor, proteomics, saliva, tears, Sjogren's Syndrome

OPEN ACCESS

Edited by:
Pallavi R. Devchand, University of Calgary, Canada

Reviewed by:
Maurizio Ronci, University "G. d'Annunzio" of Chieti-Pescara, Italy
Sigrun Lange, University of Westminster, United Kingdom

***Correspondence:**
Tannin A. Schmidt
tschmidt@uchc.edu
Antoine Dufour
antoine.dufour@ucalgary.ca

[†]These authors have contributed equally to this work

Specialty section:
This article was submitted to Inflammation Pharmacology, a section of the journal Frontiers in Pharmacology

Received: *30 September 2021*
Accepted: *02 November 2021*
Published: *07 December 2021*

Citation:
Das N, Menon NG, de Almeida LGN, Woods PS, Heynen ML, Jay GD, Caffery B, Jones L, Krawetz R, Schmidt TA and Dufour A (2021) Proteomics Analysis of Tears and Saliva From Sjogren's Syndrome Patients. Front. Pharmacol. 12:787193. doi: 10.3389/fphar.2021.787193

INTRODUCTION

Sjogren's syndrome (SS) is a chronic autoimmune disease that predominantly affects middle-aged women, with a high female to male ratio (9:1), and is characterized by both local and systemic inflammations, with exocrine glands (i.e., salivary, parotid and lacrimal glands) being the primary site of disease manifestation (Virdee et al., 2017; Vivino, 2017; Mavragani and Moutsopoulos, 2020). Lymphocyte infiltration and inflammation in salivary and lacrimal glands result in dryness of the mucosal surfaces, including the mouth (xerostomia) and eye (xerophthalmia), which are the key symptoms that lead to clinical suspicion of the disease occurring in more than 95% of the patients (Ramos-Casals et al., 2012; Brito-Zerón et al., 2016). Dry mouth and eye can progress into further complications, including accelerated caries, loss of dentition, corneal ulcer, vision loss, in addition to internal organ inflammation and morbidity (Vivino, 2017). SS is further defined as primary Sjogren's syndrome (pSS) when it presents alone and as secondary Sjogren's syndrome (sSS) when accompanied by other diseases, such as systemic lupus erythematosus (SLE), rheumatoid arthritis (RA) or systemic sclerosis (Mavragani and Moutsopoulos, 2020). Although the exact etiology of SS is not clear, previous research indicates that it is a multifactorial disease with involvement of both genetic and environmental factors activating innate and adaptive immune pathways (Ramos-Casals et al., 2012; Both et al., 2017; Mavragani, 2017). Around 75% of infiltrating lymphocytes in the salivary glands of SS constitute T cells, which are mostly composed of $CD4^+$ T cells (Fox et al., 1983; Verstappen et al., 2017). These cells can produce both Th1 and Th2 cytokines but are characterized by a shift in the favor of Th1 in the salivary gland in patients with SS (Mitsias et al., 2002). Moreover, an overexpression of the cytokines IL4, IL17, and IFNγ have been associated with the pathogenesis of SS (Verstappen et al., 2017; López-Villalobos et al., 2021).

Annual healthcare costs for SS patients were found to be over twice those for a community control group and comparable to those for patients with RA (Callaghan et al., 2007). Unfortunately, diagnosis of SS is often delayed or incorrect due to our limited understanding of disease pathogenesis; therefore, a better characterization of disease mechanisms and pathways altered in SS will be beneficial. Salivary gland biopsy, which is often considered to be the gold standard test for SS, is invasive and can be associated with serious post-operative complications including excessive bleeding, swelling and numbness in the lower lip (Richards et al., 1992). Hallmarks of SS-associated markers include autoantibodies, such as anti-SSA and anti-SSB, IFNγ and other cytokines; however, these markers are also associated with other autoimmune diseases such as RA, SLE, or polymyositis and are therefore not specific to SS (Burbelo et al., 2009; Dufour et al., 2018; Seror et al., 2021). Furthermore, drugs previously implemented in other autoimmune diseases including RA and SLE failed to reach primary outcomes in randomized double-blind controlled trials for the treatment of SS (Mavragani and Moutsopoulos, 2020; Seror et al., 2021). Failure in therapeutic approaches targeting Cathepsin S, an inducible costimulator of T cell ligand and lymphotoxin beta receptor indicated lack of appropriate drug targets/specific biomarker in SS (Mavragani and Moutsopoulos, 2020). Therefore, a specific, sensitive, and non-invasive biomarker for SS diagnosis is urgently needed to reduce morbidity and improve patients' quality of life.

Mass spectrometry (MS) is widely utilized as an effective proteomics tool for biomarker discovery owing to its ability to provide sensitive and selective detection, multi-analyte analysis, and information about post-translational modifications of proteins or peptides (Addona et al., 2009; Aebersold and Mann, 2016; Geyer et al., 2017). Advantages of MS and proteomics analyses is the capacity for a comprehensive characterization of proteomes using a small volume of tears (Zhou et al., 2009; Li et al., 2015) and saliva samples (Ryu et al., 2006; Al-Tarawneh et al., 2011). Importantly, collection of both tear and saliva samples is non-invasive and relatively simple to undertake; therefore, a routine collection could be done that could help in early diagnosis, monitoring disease progression, or treatment response. However, the precise mechanism and altered proteins have not been extensively characterized in SS patients.

Proteoglycan 4 (PRG4), also known as lubricin, is a mucin-like glycoprotein with an important role in maintaining homeostasis through its ability to provide boundary lubrication and regulate inflammatory signaling (Das et al., 2019). PRG4 expression in the eye is found to be critical for ocular surface composition (Schmidt et al., 2013; Samsom et al., 2015) and maintaining tear film integrity (Rabiah et al., 2020), as evidenced by the $Prg4^{-/-}$ mice that displayed significantly higher red corneal fluorescein staining (representing damage of the ocular surface) compared to wild type counterparts (Schmidt et al., 2013). A recent clinical trial showed that recombinant human PRG4 (rhPRG4) was effective at reducing signs and symptoms of dry eye disease, where ~38% of the people enrolled were SS patients (Lambiase et al., 2017). *In vitro,* the expression of PRG4 by human corneal epithelial cells was found to be altered by the proinflammatory cytokines TNFα and IL1β (Menon et al., 2021). Furthermore, PRG4 was shown to be reduced on the corneal epithelium and in the lacrimal gland in an animal model of experimental dry eye disease (Menon et al., 2021). Despite some studies that have characterized certain protein changes in tears (Zhou et al., 2009; Li et al., 2015), it is still unclear what are the normal levels of PRG4 found in SS tears. Similar analyses have been performed in saliva, but PRG4 has never been detected (Ryu et al., 2006; Al-Tarawneh et al., 2011). Previously, we demonstrated that Cathepsin S, whose activity is upregulated in SS tear (Hamm-Alvarez et al., 2014; Hargreaves et al., 2019), is capable of proteolytic processing of endogenous PRG4 in tear samples as well as purified rhPRG4, that latter of which resulted in reduced ocular surface boundary lubricating properties (Regmi et al., 2017). Therefore, we wanted to conduct an unbiased investigation to identify what other proteases and proteases inhibitors could be implicated in the pathogenesis of SS. We also wanted to measure the levels of PRG4 in SS tears and saliva as a SS is characterized by dryness of mucosal surfaces like eyes and mouth. Here, using quantitative proteomics and bioinformatics analyses, we characterize tears and saliva biopsies in SS and healthy controls. Additionally, for

TABLE 1 | Patient's information.

		Healthy controls	Sjogren's syndrome
Tears	Number	20	17
	Age	31.2 ± 11.4 years old	56.2 ± 16.7 years old
	Sex	13 females 7 males	15 females 2 males
Tear Washes	Number	29	14
	Age	34.1 ± 14.2 years old	59.5 ± 12.0 years old
	Sex	17 females 12 males	13 females 1 male
Saliva	Number	10	30
	Age	46.8 ± 14.5 years old	45.2 ± 14.6 years old
	Sex	5 females 5 males	22 females 8 males

the first time, we present evidence that PRG4 is downregulated in SS tear washes but upregulated in SS saliva as measured by quantitative proteomics and our custom PRG4 AlphALISA. We present new unbiased and quantitative proteomics data to improve our understanding of the mechanisms and altered proteins in SS patients.

MATERIALS AND METHODS

Patient Information and Sample Collection

We were exempt from ethics for the analysis done as all samples were commercially purchased or from de-identified patients and from biobank indicated below. Tears and washes were collected from Sjogren's syndrome (SS) patients and healthy controls (**Table 1**). All collection procedures were performed at the Centre for Ocular Research and Education, University of Waterloo, Ontario, Canada. SS patients were identified using the following criteria: Ocular Surface disease Index (OSDI) ≥ 23, non-invasive tear breakup time (NIBUT) < 10 s, and diagnosis of primary SS using the American European Consensus Criterion (Vitali et al., 2002). Healthy controls were identified using the following criteria: OSDI score <13, NIBUT ≥10 s, and has not been diagnosed with dry eye and does not use artificial tears, gels, or rewetting drops to relieve ocular symptoms. To collect tear, up to 5 µl of tears were collected from the inferior temporal tear meniscus, without corneal anesthesia, using a glass microcapillary tube. A maximum of 5 min of tear collection was allowed per eye. Tears were collected from both eyes and stored at −80°C. In total, tears were collected from 22 SS patients (20 female, 2 male, 60.0 ± 16.5 years old, mean ± SD) and 20 healthy patients (13 female, 7 male, 31.2 ± 11.4 years old, mean ± SD) (**Table 1** and **Supplementary Material**).

The same criteria were used to select SS patients and healthy controls for collecting tear washes. Tears were collected from both eyes and stored at −80°C. To collect tear washes, 40 µl of sterile 0.9% saline was instilled onto the superior bulbar region of the eyes. The patients then rotated their eyes, and the washes were collected from the inferior fornix regions and stored separately at −80°C for each eye. In total, tear washes were collected from 14 SS patients (13 female, 1 male, 59.5 ± 12.0 years old, mean ± SD) and 29 healthy patients (17 female, 12 male, 34.1 ± 14.2 years old, mean ± SD) (**Table 1** and **Supplementary Material**).

Unstimulated whole saliva samples from SS patients were obtained from the Sjogren's International Collaborative Clinical Alliance (SICCA) biorepository (**Table 1**). SS patients were identified using the new American College of Rheumatology Classification Criteria for Sjogren's syndrome (Shiboski et al., 2012). Patients had to be above 18 years old and recruited in the United States, as well as have at least two of the following criteria: positive serology for anti-SSA and/or anti-SSB antibodies (or positive rheumatoid factor and antinuclear antibodies (ANA) titer ≥1:320), ocular staining ≥3, and presence of focal lymphocytic sialadentis with a focus score ≥1 focus/4 mm^2. Saliva samples from healthy controls were purchased from BioIVT (Westbury, NY). In total, 30 SS samples (22 female, 8 male, 45.2 ± 14.6, mean ± SD) and 10 healthy (5 female, 5 male, 46.8 ± 14.5, mean ± SD) were obtained (**Table 1** and **Supplementary Material**). For the proteomics experiment, the closest age matched groups were selected: SS 37.8 ± 5.8 years old and healthy controls 42.2 ± 17.9 years old. We analyzed 5 female samples for SS and 2 females/3 males for healthy controls.

Parotid gland samples were obtained from the University of Connecticut Health Center's Research Tissue Biorepository Core Facility, which were flash frozen in liquid nitrogen, embedded in optimal cutting temperature (OCT), and cryopreserved. In total, 5 samples were analyzed from four patients: two men, age 69- and 70- years old and two women, age 73- and 93-year-old. All patients all free of any cancer diagnosis at time of sample collection.

Shotgun Proteomics Analysis

Tears and saliva were used for shotgun proteomics analysis. Protein samples were lysed with 1% SDS, 0.1 M EDTA in 200 nM HEPES (pH 8), protease cOmplete™ inhibitor tablets (Sigma-Aldrich, ON, Canada). Proteins were denatured with the addition of a final concentration of 10 mM dithiothreitol (DTT). Samples were alkylated by incubation with a final concentration of 15 mM iodoacetamide (IAA) in the dark for 25 min at room temperature. Samples were next digested with Trypsin (Promega, Madison, WI, United States). With HCl the pH adjusted to 6.5. Next, to label peptide α- and ε-amines, samples were incubated for 18 h at 37°C with isotopically heavy (40 mM $^{13}CD_2O$+20 mM $NaBH_3CN$ (sodium cyanoborohydride)) or light labels (40 mM light formaldehyde (CH_2O) + 20 mM $NaBH_3CN$), all final concentrations. Samples were subjected to C18 chromatography using Pierce™ C18 columns (Thermo Scientific™, ON, Canada) before being subjected to liquid chromatography and tandem mass spectrometry (LC-MS/MS).

High Performance Liquid Chromatography (HPLC) and Mass Spectrometry (MS)

All liquid chromatography and mass spectrometry experiments were carried out by the Southern Alberta Mass Spectrometry (SAMS) core facility at the University of Calgary, Canada. Analysis was performed on an Orbitrap Fusion Lumos Tribrid mass spectrometer (Thermo Scientific, ON, Canada) operated with Xcalibur (version 4.0.21.10) and coupled to a Thermo Scientific Easy-nLC (nanoflow Liquid Chromatography) 1,200 system. Tryptic peptides (2 µg) were loaded onto a C18 trap (75 um x 2 cm; Acclaim PepMap 100, P/N 164,946; Thermo Scientific, ON, Canada) at a flow rate of 2 µl/min of solvent A

(0.1% formic acid and 3% acetonitrile in LC-MS grade water). Peptides were eluted using a 120 min gradient from 5 to 40% (5–28% in 105 min followed by an increase to 40% B in 15 min) of solvent B (0.1% formic acid in 80% LC-MS grade acetonitrile) at a flow rate of 0.3 µl/min and separated on a C18 analytical column (75 um x 50 cm; PepMap RSLC C18; P/N ES803; Thermo Scientific). Peptides were then electrosprayed using 2.3 kV voltage into the ion transfer tube (300°C) of the Orbitrap Lumos operating in positive mode. The Orbitrap first performed a full MS scan at a resolution of 120,000 FWHM to detect the precursor ion having an m/z between 375 and 1,575 and a +2 to +7 charge. The Orbitrap AGC (Auto Gain Control) and the maximum injection time were set at 4×10^5 and 50 ms, respectively. The Orbitrap was operated using the top speed mode with a 3 s cycle time for precursor selection. The most intense precursor ions presenting a peptidic isotopic profile and having an intensity threshold of at least 5,000 were isolated using the quadrupole and fragmented with HCD (30% collision energy) in the ion routing multipole. The fragment ions (MS^2) were analyzed in the ion trap at a rapid scan rate. The AGC and the maximum injection time were set at 1×10^4 and 35 ms, respectively, for the ion trap. Dynamic exclusion was enabled for 45 s to avoid the acquisition of the same precursor ion having a similar m/z (±10 ppm).

Proteomic Data Analysis

Spectral data were matched to peptide sequences in the human UniProt protein database using the Andromeda algorithm (Cox et al., 2011) as implemented in the MaxQuant (Cox and Mann, 2008) software package v.1.6.10.23, at a peptide-spectrum match FDR of < 0.01. Search parameters included a mass tolerance of 20 p.p.m. for the parent ion, 0.5 Da for the fragment ion, carbamidomethylation of cysteine residues (+57.021464 Da), variable N-terminal modification by acetylation (+42.010565 Da), and variable methionine oxidation (+15.994915 Da). N-terminal and lysine heavy (+34.063116 Da) and light (+28.031300 Da) dimethylation were defined as labels for relative quantification. The cleavage site specificity was set to Trypsin/p for the proteomics data, with up to two missed cleavages allowed. Significant outlier cutoff values were determined after log (2) transformation by boxplot-and-whiskers analysis using the BoxPlotR tool (Spitzer et al., 2014). The data were deposited into ProteomeXchange via the PRIDE database and are freely available (PXD028922).

Bioinformatics Analysis

To identify protein–protein interactions, the STRING (Search Tool for the Retrieval of Interacting Genes) database was used to illustrate interconnectivity among proteins (Szklarczyk et al., 2019). Protein-protein interactions relationship were encoded into networks in the STRING v11 database (https://string-db.org). Data were analyzed using the *homo sapiens* as the organism at a false discovery rate of 5% and the reactome pathways were analyzed. Metascape analysis was also used to identify enriched pathways (Zhou et al., 2019). Protein-protein interactions relationship were encoded into networks using the metascape website (https://metascape.org/), and the enriched pathways were plotted as heatmaps. The Circos graphs were generated with Metascape. On the outside, each arc represents the identity of each gene list (Sjogren's syndrome in magenta and Healthy control in grey). On the inside, each cyan arc represents a gene list, where each gene has a spot on the arc. Black lines link the different genes where they connect to the same ontology term. A large number of black lines indicates higher amount of functional overlap among the input gene lists.

Histology

Five different OCT blocks from four different patients were sectioned onto slides and probed for immunoreactivity to anti-PRG4 mAb 4D6 (Abubacker et al., 2016) (Regmi et al., 2017) using an anti-mAb-HRP conjugate developed with DAB and counter stained with light hematoxylin. Negative control samples received no primary mAb (University of Connecticut Health Center Research Histology Core).

PRG4 Quantification in Tear Wash and Saliva

PRG4 levels in saliva and tear washes were quantified using a bead-based immunoassay using the AlphaLISA® (Perkin-Elmer, ON, Canada) platform technology. Full-length rhPRG4 (Lubris BioPharma) was biotinylated (brhPRG4) using a commercially available kit (EZ-Link Sulfo-NHS-LC-Biotinylation Kit, Thermo Scientific 21,435), as per the manufacturer's instructions. Anti-PRG4 mAb 4D6 (Regmi et al., 2017) was bound to AlphaScreen unconjugated acceptor beads (Perkin-Elmer 6,762,003), following manufacturer guidelines. Then, 5 µl of brhPRG4 per well (at 8 ng/ml) was mixed with 5 µl per well of 4D6-conjugated AlphaLISA acceptor beads at a final concentration of 80 µg/ml and 5 µl per well of streptavidin coated AlphaScreen donor beads (Perkin-Elmer 6760002S) at a final concentration of 80 µg/ml. Next, 15 µl of the resulting solution was transferred to each well of an opaque 96-well half-plate under low light. Finally, 5 µl of rhPRG4 (at concentrations of 0.8, 8, 80, 240, 800, 8,000, 80,000 µg/ml) or 5 µl of tear/saliva sample at multiple serial dilutions were added to the wells and allowed to incubate for 2 h protected from light. The total reaction volume summed to 20 µl, including 5 µl of sample, with final concentrations of 1 ng/ml, 20 µg/ml, and 20 µg/ml for the brhPRG4, 4D6-conjugated acceptor beads, and streptavidin coated donor beads, respectively. Plates were then read on a SpectraMax i3 microplate reader (Molecular Devices) using an excitation wavelength of 680 nm and an emission wavelength of 625 nm. All reagents were prepared and/or diluted in PBS with 0.05% Tween 20, and all incubations were done at room temperature, with gentle nutation, and a plate sealer to prevent evaporation. All samples were run in duplicate. Calculated PRG4 levels were also normalized to total protein concentrations measured using a BCA assay (Thermo Scientific 23,227).

PIGNON Analysis

For PIGNON analysis, the normalized protein ratios were used as calculated by Maxquant and available in the proteingroups. txt file. PIGNON was set to use the "physical link" network (v11)

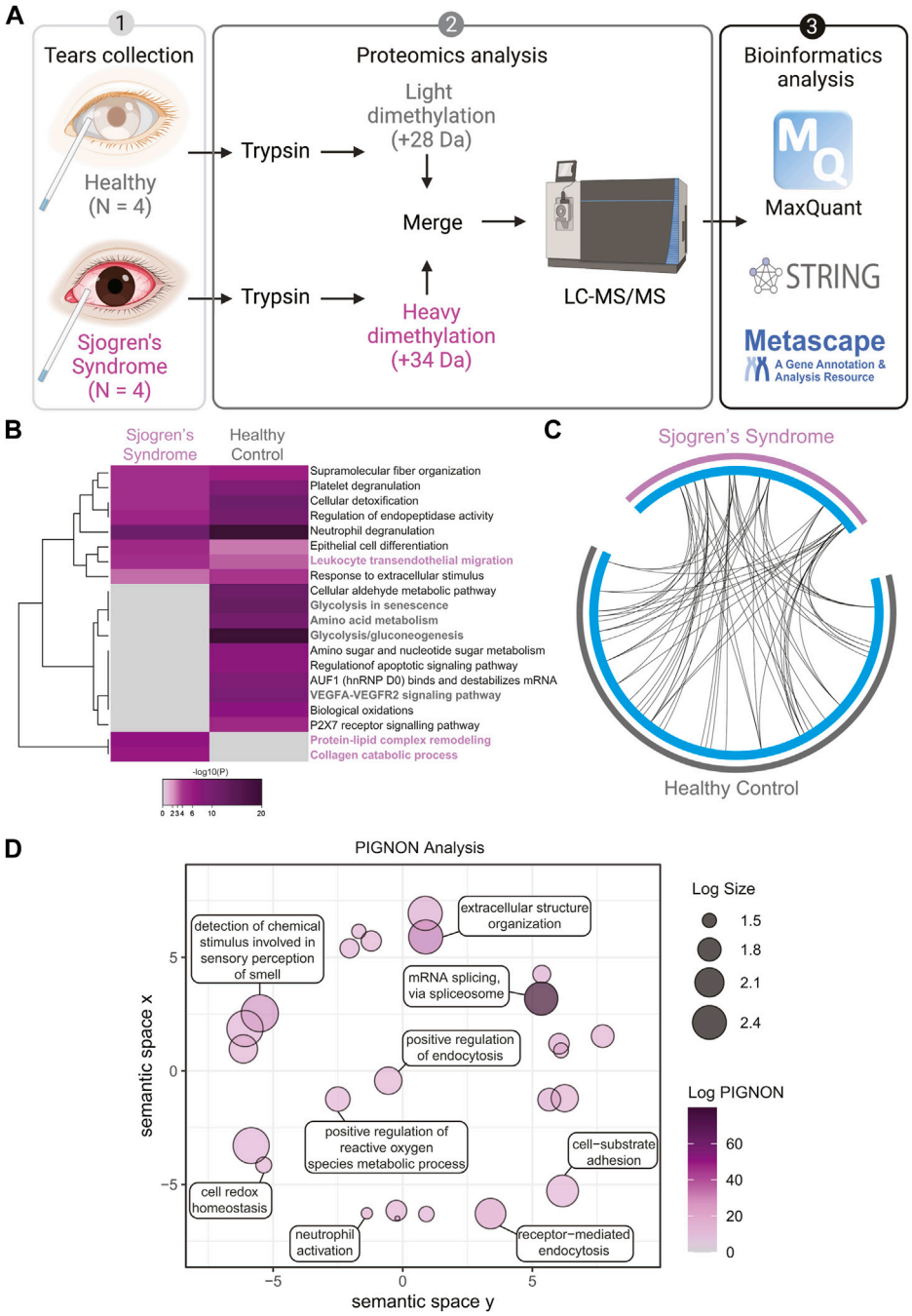

FIGURE 1 | Quantitative Proteomics of Human Sjogren's Syndrome Tears Washes. **(A)** Proteomics workflow and analysis (N = 4, Sjogren's syndrome (SS) and N = 4 healthy controls). STRINGdb and Metascape software were used to identify pathway enrichment and protein-protein interactions. A list of all detected proteins is provided in **Supplementary Table S1**. **(B)** Metascape analysis of different pathways between SS and healthy control tear washes. Magenta marked are upregulated in SS and grey marked are upregulated pathways in healthy controls. Accumulative hypergeometric *p*-values and enrichment factors were calculated and used for filtering. Remaining significant terms were then hierarchically clustered into a tree based on Kappa-statistical similarities among their genes memberships. Then, 0.3 kappa score was applied as the threshold to cast the tree into term clusters. **(C)** Circos plot shows how significant proteins from the input lists overlap and were generated with Metascape. On the outside, each arc represents the identity of each gene list (Sjogren's syndrome in magenta and Healthy control in grey). On the inside, each cyan arc represents a gene list, where each gene has a spot on the arc. Black lines link the different genes where they fall into the same ontology term. **(D)** Visualization of PIGNON results using Revigo. The x- and *y*-axis have no intrinsic meaning. In the plot, semantically similar GO terms remain close together. LogSize equals to the Log_{10}(Number or annotations for GO Term ID in *Homo sapiens* in the EBI GOA database). Log PIGNON equals to the -Log_{10}(FDR-adjusted *p* value as

(*Continued*)

FIGURE 1 | generated by PIGNON). The PIGNON analysis was performed using the normalized protein ratios as calculated by Maxquant. PIGNON was set to use the "physical link" network (v11) from the STRING database, due to the small size of our dataset. The Monte Carlo sampling was set to 3 and 500 for the lower and upper bound, respectively. The results included mapped pathways that were trimmed according to a false discovery rate (FDR) of 1%. The lists of enriched gene ontology (GO) terms, along with the *p*-values, were submitted to Revigo to summarize the biological functions and provide visualization of enriched terms.

from the STRING database due to the small size of our dataset. The mapping file was obtained from the input_file.zip available at PIGNON's Github (https://github.com/LavalleeAdamLab/PIGNON). The inferred Gene Ontology (GO) terms were obtained from www.git.dhimmel.com/gene-ontology. The STRING accepted combined score was set to 400. The tear and saliva datasets were analyzed with weighted and unweighted networks. The number of samplings was set to 100,000. The sampling type was set to weighted. The Monte Carlo sampling was set to 3 and 500 for the lower and upper bound, respectively. The results included mapped pathways that were trimmed according to an FDR of 1%. Next, only the GO terms unique to the weighted network were considered true positives, which were obtained by subtracting the GO terms that were also present in the unweighted network. The lists of enriched GO terms, along with the *p*-values, were submitted to Revigo (Supek et al., 2011) to summarize the biological functions and provide visualization of enriched terms. The scatterplot and table generated by Revigo was modified using R (v4.0.3) (R Development Core Team, 2011) to substitute the color scale with a magenta-based color palette.

Statistical Analysis

The differences in PRG4 concentration, volume, and mass in tear washes were analyzed, using the Prism software, using Welch's unpaired 2-way *t*-tests if the data were heteroscedastic or unpaired 2-way t-tests otherwise. The difference in PRG4 concentration in saliva was analyzed using a Welch's unpaired 2-way *t*-test. All data reported as mean ± standard deviation (SD).

RESULTS

Quantitative Proteomics of Human Sjogren's Syndrome Tear

To assess the global proteome changes in Sjogren's syndrome (SS) patients, we collected tears of 4 SS patients and 4 healthy controls using glass microcapillary tube, and we performed a quantitative shotgun proteomics analysis (**Figure 1A**). Tear lysates were digested with trypsin and isotopically labeled. Healthy control tears were tagged with light formaldehyde (+28 Da) and SS patients' tears with heavy formaldehyde (+34 Da; **Figure 1A**). Data were analyzed using MaxQuant (Cox and Mann, 2008) (Cox et al., 2011) at a 1% false discovery rate (FDR), and data integration for pathway and gene ontology (GO) enrichment was performed with Metascape (Zhou et al., 2019), STRING-db (Szklarczyk et al., 2019) and PIGNON (Nadeau et al., 2021). For the data interpretation, we describe changes in abundance of proteins as log2 fold change (SS tears over healthy controls), which means log2 values > 0 represent proteins that were upregulated in SS tears, <0 represents downregulation. In the proteomics analysis (**Supplementary Figure S1** and **Supplementary Table S1**), we identified 83 unique proteins that were upregulated in SS tears and 112 unique downregulated proteins. By using the online meta-analysis tool Metascape (https://metascape.org/), we identified several enriched pathways between SS and healthy control tears (**Figure 1B**, **Supplementary Figure S2A,B**). Some enriched pathways in SS tears include leukocyte transendothelial migration (CTSB, ITGB2, MMP9), protein-lipid complex remodeling (PSAP, PLTP, APOE, MPO) and collagen catabolic process (CST3, VIM, MMP8, TGM2, ITGB2, MMP9, CTSB) (**Figure 1B**, **Supplementary Table S1**). Conversely, some enriched pathways in the healthy control tears include glycolysis/gluconeogenesis and glycolysis in senescence (ENO1, ENO2, ALDOA, PGD, PGK1, PGAM1), amino acid metabolism (MDH2, IDH1, ALDH1A1, GLO1, PKM) and VEGFA-VEGFR2 signaling pathway (HSP90AA1, PRDX2, PRDX6, RAN) (**Figure 1B**, **Supplementary Table S1**). Although we identified key differences in pathway enrichment and GO terms, there was some overlap between the SS and healthy control tears (**Figure 1C**).

To better understand and visualize our data, we used two additional bioinformatics tools, PIGNON (Nadeau et al., 2021) and STRING-db (Szklarczyk et al., 2019), to add a more comprehensive characterization of our tear washes dataset. PIGNON was used to identify enriched biological processes via GO terms, while STRING-db was used to identity reactome pathways. Using PIGNON, we identified mRNA splicing (via spliceosome), cell-substrate adhesion and detection of chemical organization stimulus involved in sensory perception of smell (**Figure 1D**, **Supplementary Figure S2C**). Using STRING-db v11 (https://string-db.org), we observed that the majority of the upregulated proteins in SS tears were proteins clustered with neutrophil degranulation as red nodes (CTSB, ITGB2, MMP8, MMP9), post-translation protein phosphorylation as blue nodes (APOE, CALU, CP, CST3) and immune system as green nodes (CTSB, ITGB2, LCP1, MMP8, MMP9) (**Figure 2A**). In healthy control tears, enriched reactome pathways include metabolic pathways as purple nodes (ENO1, ENO2, ALDOA, PGD, PGK1, PGAM1), regulation of actin cytoskeleton as cyan nodes (ACTB, ACTN4, CFL1, EZR, VCL) and glycolysis/gluconeogenesis as yellow nodes (ALDH3A1, ALDOC, ENO1, FBP1, PKM) (**Figure 2B**). Overall, it seems that there is a loss of glycolysis and metabolism but an elevation of immune processes in SS tears samples. Additionally, we identified multiple proteases (Cathepsin B, MMP8, MMP9, Leukotriene A-4 hydrolase, and Prostasin) and protease

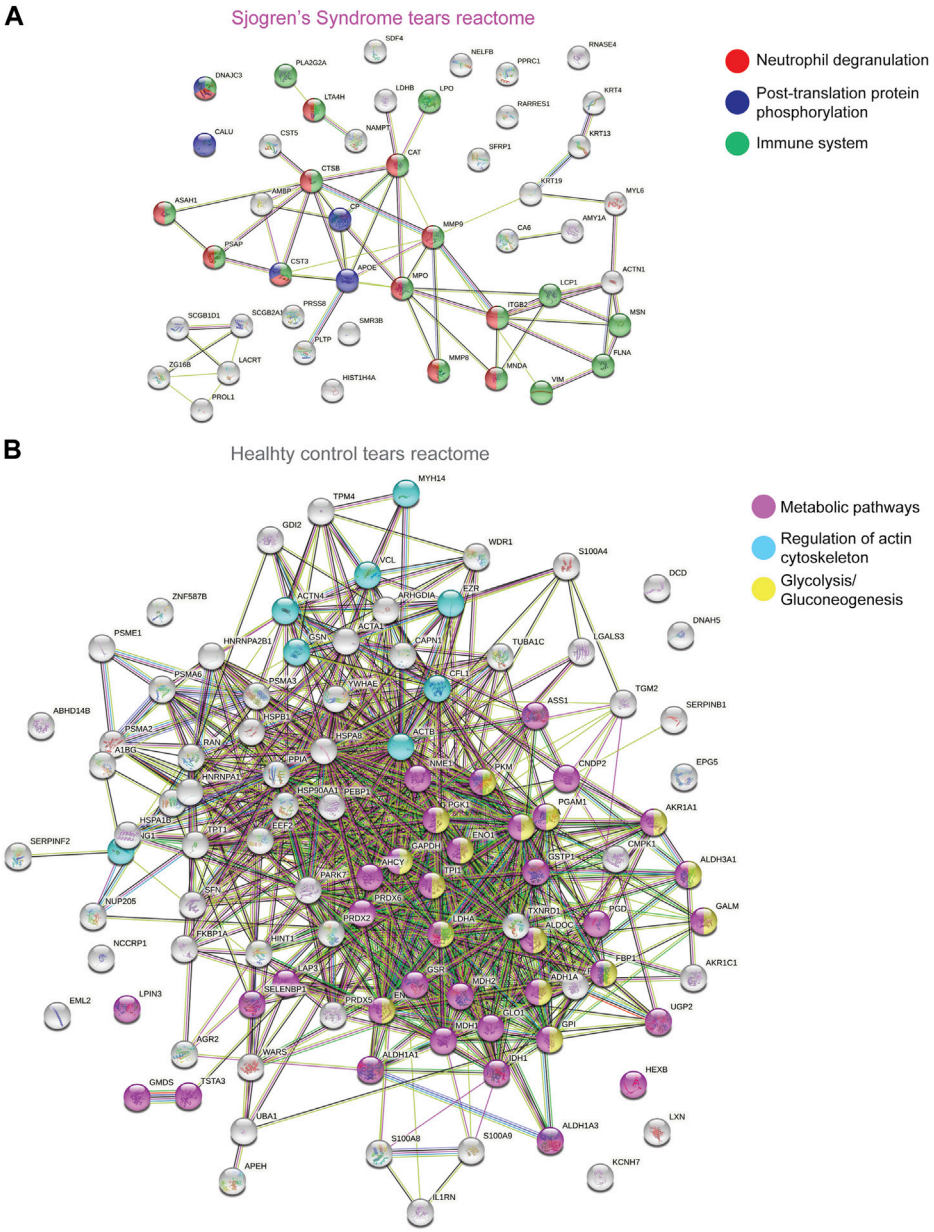

FIGURE 2 | STRING Analysis of Quantitative Proteomics Data of Human Sjogren's Syndrome Tears Washes. Analysis of protein–protein interaction network by STRING v11. Elevated proteins from **(A)** SS or **(B)** healthy control tears identified from the quantitative proteomics analysis were mapped by searching the STRING v11 software with a confidence level of 1% false discovery rate. Colored lines between the proteins indicate different types of interaction evidence: known interactions (teal), experimentally determined (pink), predicted interactions gene neighborhood (green), gene fusions (red), gene co-occurrence (blue), text-mining (yellow), coexpression (black), protein homology (purple).

inhibitors (Cystatin-C and -D) that were elevated SS tears compared to healthy controls (**Table 2**).

Decrease of PRG4 in Tear Wash

As we demonstrated previously, increased proteolytic activity of cathepsin S in SS tears resulted in decreased lubrication (Regmi et al., 2017) (Menon et al., 2021). Therefore, we wanted to test if the levels of PRG4, also known as lubricin, are changed between SS and healthy control tear washes. Using an AlphaLISA (**Figure 3A**), we measured the concentration of PRG4 in tear wash of 39 patients (healthy, N = 29 and SS, N = 10) and we found that it was significantly decreased in SS patients compared to healthy controls (**Figure 3B**, $^{**}p < 0.01$). The collected volume of tear washes was also decreased in SS tears (**Figure 3C**, $^{**}p < 0.01$). Therefore, the total PRG4 mass was also found to be significantly decreased in SS tears compared to

TABLE 2 | Proteases and protease inhibitors significantly elevated in Sjogren's Syndrome (SS) tear wash over healthy controls.

Uniprot ID	Gene name	Protein name	Fold difference SS/healthy
		Elevated in Sjogren's Syndrome	
P14780	*MMP9*	Matrix metalloproteinase-9	88.4
P28325	*CST5*	Cystatin-D	12.5
P22894	*MMP8*	Neutrophil collagenase	9.4
P01034	*CST3*	Cystatin-C	8.5
P07858	*CTSB*	Cathepsin B	6.2
P09960	*LTA4H*	Leukotriene A-4 hydrolase	5.3
Q16651	*PRSS8*	Prostasin	5.1
		Elevated in healthy	
P07384	*CAPN1*	Calpain-1	−21.8
Q96KP4	*CNDP2*	Cytosolic non-specific dipeptidase	−17.7
P01042	*KNG1*	Kininogen-1	−12.4
P08697	*SERPINF2*	Alpha-2-antiplasmin	−11.9
Q99497	*PARK7*	DJ-1/Parkinson disease protein 7	−11.6
P60900	*PSMA6*	Proteasome subunit alpha type-6	−10.6
P25788	*PSMA3*	Proteasome subunit alpha type-3	−10.6
P13798	*APEH*	Acylamino-acid-releasing enzyme	−9.3
P25787	*PSMA2*	Proteasome subunit alpha type-2	−9.0
P28838	*LAP3*	Cytosol aminopeptidase	−8.5
P30086	*PEBP1*	Phosphatidylethanolamine-binding protein	−7.6
Q5JNW7	*PSMB8*	Proteasome subunit beta type-8	−6.1
P30740	*SERPINB1*	Leukocyte elastase inhibitor	−5.6

healthy controls (**Figure 3D**, $*p < 0.05$). In summary, we identified a significant decrease in PRG4 levels in SS tear washes.

Quantitative Proteomics of Sjogren's Syndrome Saliva

SS patients suffer from dry mouth (Brito-Zerón et al., 2016); therefore, we wanted to assess the global proteome changes in SS saliva compared to healthy controls (**Figure 4A**). Saliva lysates of 5 healthy controls and 5 SS patients were digested with trypsin and isotopically labeled with light formaldehyde (+28 Da) and heavy formaldehyde (+34 Da; **Figure 4A**), respectively. Data were analyzed using MaxQuant (Cox and Mann, 2008) (Cox et al., 2011) at a 1% false discovery rate (FDR), and data integration for pathway enrichment was performed with STRING-db (Szklarczyk et al., 2019), PIGNON (Nadeau et al., 2021), and Metascape (Zhou et al., 2019), which are based on reactome, GO terms (biological process), and a combination of multiple databases, respectively. For the interpretation, we describe changes in abundance of proteins as log2 fold change (SS saliva over healthy controls), which means log2 values > 0 represent proteins that were upregulated in SS tears, <0 represent downregulation. In the proteomics analysis (**Supplementary Figure S3** and **Supplementary Table S2**), we identified 104 unique proteins that were upregulated in SS saliva and 42 unique downregulated proteins. By using Metascape, we identified several enriched pathways between SS and healthy control saliva (**Figure 4B**, **Supplementary Figure S4A,B**). Some enriched pathways in SS saliva include JAK-STAT signaling after interleukin-12 stimulation (CTSG, ITGB2, ITGAM, LCP1, TALDO1), superoxide metabolic process (CBR1, MPO, ARG1, RYR2, ITGAM) and phagocytosis (CTSG, ELANE, ITGAM, ITGB2, PRG4, PRTN3, MPO, PARK7) (**Figure 4B**, **Supplementary Table S2**). Conversely, some enriched pathways in the healthy control saliva include neutrophil degranulation (CD14, MMP8, S100A11, SLPI), negative regulation of peptidase activity (ECM1, CST1, CST4, CST5, SLPI, SERPINB3, TIMP1) and NABA matrisome associated (FLG, FLG2, MMP8, MUC5B, MUC7, RPTN, TIMP1) (**Figure 4B**, **Supplementary Table S2**). Although we identified key differences in pathway enrichment and GO terms, there was some overlap between the SS and healthy control saliva (**Figure 4C**).

To better understand and visualize our data, we used two additional bioinformatics tools, PIGNON (Nadeau et al., 2021) and STRING-db (Szklarczyk et al., 2019), to add a more comprehensive characterization of our tear datasets. Using PIGNON, we identified mRNA splicing (*via* spliceosome), cell adhesion mediated by integrin and detection of chemical organization stimulus involved in sensory perception of smell (**Figure 4D**, **Supplementary Figure S4C**). Using STRING-db v11 to analyze the reactome pathways, we observed that the majority of the upregulated proteins in SS saliva were innate immune system as yellow nodes (AZU1, LRG1, MPO, STOM, VAT1), biosynthesis of amino acids as green nodes (ALDOC, ARG1, IDH2, PKM, TKT), pentose phosphate pathway as purple nodes (ALDOC, TALDO1, TKT) and leukocyte transendothelial migration as cyan nodes (ACTN1, ITGAM, ITGB2, RHOA) reactome pathways (**Figure 5A**). In healthy control saliva, enriched reactome pathways included proteins clustered with salivary secretion as red nodes (CST1, CST4, CST5, MUC5B, MUC7) and innate immune system as blue nodes (BPIFA2, BPIFB1, BPIFB2,

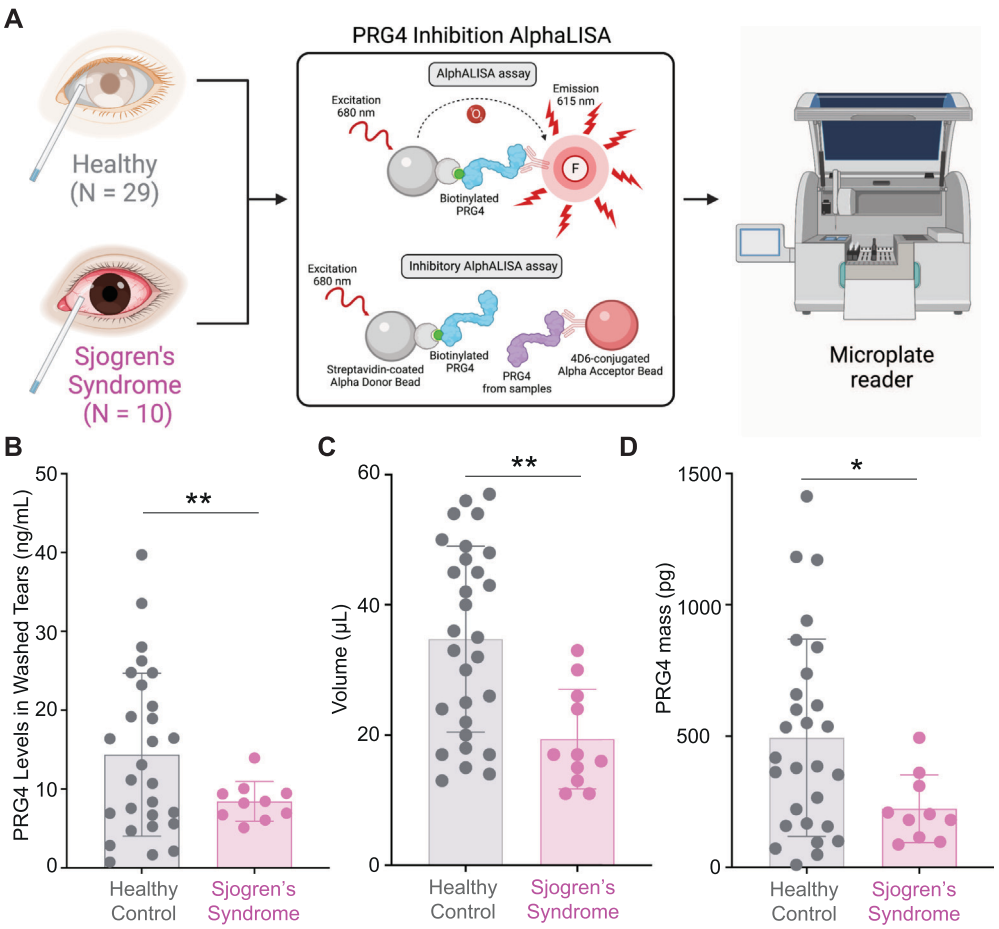

FIGURE 3 | Measurements of PRG4 in Tear Washes. **(A)** AlphALISA workflow using a designed PRG4 antibody 4D6-based assay. **(B)** PRG4 levels, **(C)** volume and **(D)** PRG4 mass were measured. Data are represented as bar graphs with ±standard deviation (SD) and analyzed by a Welch's two-tailed paired *t* test: $*p > 0.05$, $**p > 0.01$.

DCD, S100A11, SERPINB3, SLPI) (**Figure 5B**). Interestingly, using quantitative proteomics, we identified a 2.4-fold increase of PRG4 in SS saliva. Additionally, we identified multiple proteases and protease inhibitors that had various expression levels between SS and healthy control saliva (**Table 3**). As expected, our analysis of tears and saliva samples resulted in the identification of different proteins that are likely contributing in distinct ways to the pathogenesis of SS in a fluid/tissue-dependent manner (**Supplementary Figure S5**).

Increase of PRG4 in Saliva and Parotid Gland

As we identified a 2.4-fold increase of PRG4 in SS saliva (**Supplementary Table S2**), we wanted to validate our finding using an AlphALISA (**Figure 6A**). We measured the concentration of PRG4 in saliva of 39 patients (healthy, N = 10 and SS, N = 29) and we found a significant difference of PRG4, corresponding to a 2.3-fold increase in SS patients compared to healthy controls (**Figure 6B**, $*p < 0.05$). Another commons symptom of SS is salivary glands swelling, as the parotid glands are commonly involved in SS (Rischmueller et al., 2016); therefore, we wanted to verify the PRG4 expression level. By analyzing five different blocks from 4 different patients, PRG4 signal was found in both the serous acinii and the striated duct (**Figure 6C**), indicating that PRG4 is produced and secreted by the parotid gland. This signal was specific, as shown by the lack of signal in the secondary only control (**Figure 6C**).

DISCUSSION

To improve current diagnosis and therapeutic responses in SS patients, better characterization and understanding of the disease is urgently needed. With a coherent pipeline connecting potential biomarker identification with well-established methods for validation, mass spectrometry-based approaches are an effective way to discover novel biomarkers (Rifai et al., 2006; Aebersold and Mann, 2016; Nakayasu et al., 2021). Identifying protein biomarkers in tear washes and saliva offers several advantages as it is manageable for sampling/repeated sampling in addition to being inexpensive and non-invasive (Chen et al., 2015; Nakayasu et al., 2021). Here, we performed an unbiased investigation using quantitative proteomics of SS saliva and tear washes compared to healthy controls. In tear washes, we

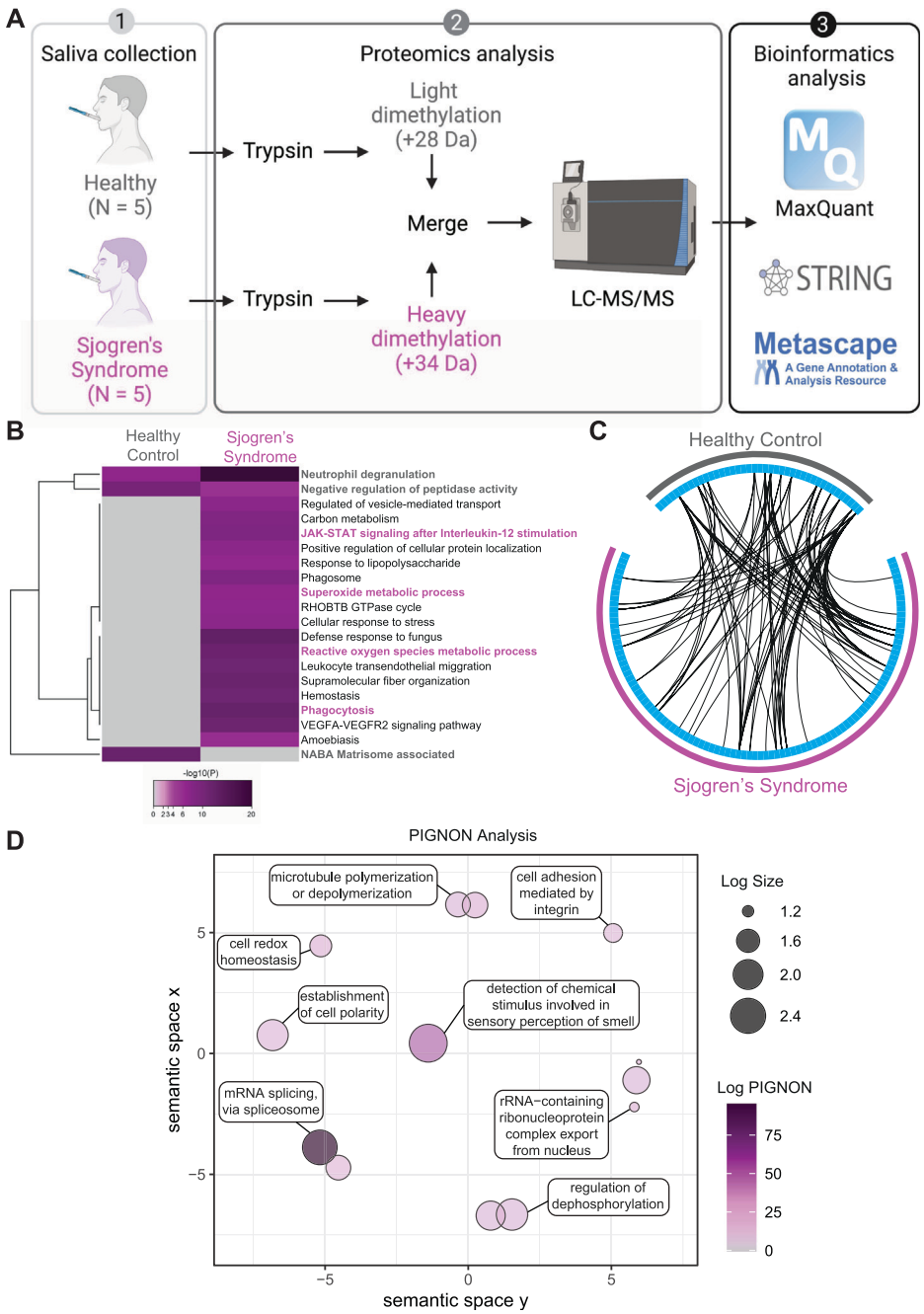

FIGURE 4 | Quantitative Proteomics of Sjogren's Syndrome Saliva. **(A)** Proteomics workflow and analysis (N = 5, Sjogren's syndrome (SS) and N = 5 healthy controls). STRINGdb and Metascape software were used to identify pathway enrichment and protein-protein interactions. A list of all detected proteins is provided in **Supplementary Table S2**. **(B)** Metascape analysis of different pathways between SS and healthy control saliva samples. Magenta marked are upregulated in SS and grey marked are upregulated pathways in healthy controls. Accumulative hypergeometric *p*-values and enrichment factors were calculated and used for filtering. Remaining significant terms were then hierarchically clustered into a tree based on Kappa-statistical similarities among their genes memberships. Then, 0.3 kappa score was applied as the threshold to cast the tree into term clusters. **(C)** Circos plot shows how significant proteins from the input lists overlap and were generated with Metascape. On the outside, each arc represents the identity of each gene list (Sjogren's syndrome in magenta and Healthy control in grey). On the inside, each cyan arc represents a gene list, where each gene has a spot on the arc. Black lines link the different genes where they fall into the same ontology term. **(D)** Visualization of PIGNON results using Revigo. The x- and *y*-axis have no intrinsic meaning. In the plot, semantically similar GO terms remain close together. LogSize equals to the Log_{10}(Number or annotations for GO Term ID in *Homo sapiens* in the EBI GOA database). Log PIGNON equals to the -Log_{10}(FDR-adjusted *p* value as generated by PIGNON). The PIGNON analysis was performed using the normalized protein ratios as calculated by Maxquant. PIGNON was set to use the "physical link" network (v11) from the STRING database due to the small size of our dataset. The results included mapped pathways that were trimmed according to a false discovery rate (FDR) of 1%. The lists of enriched gene ontology (GO) terms, along with the *p*-values, were submitted to Revigo to summarize the biological functions and provide visualization of enriched terms.

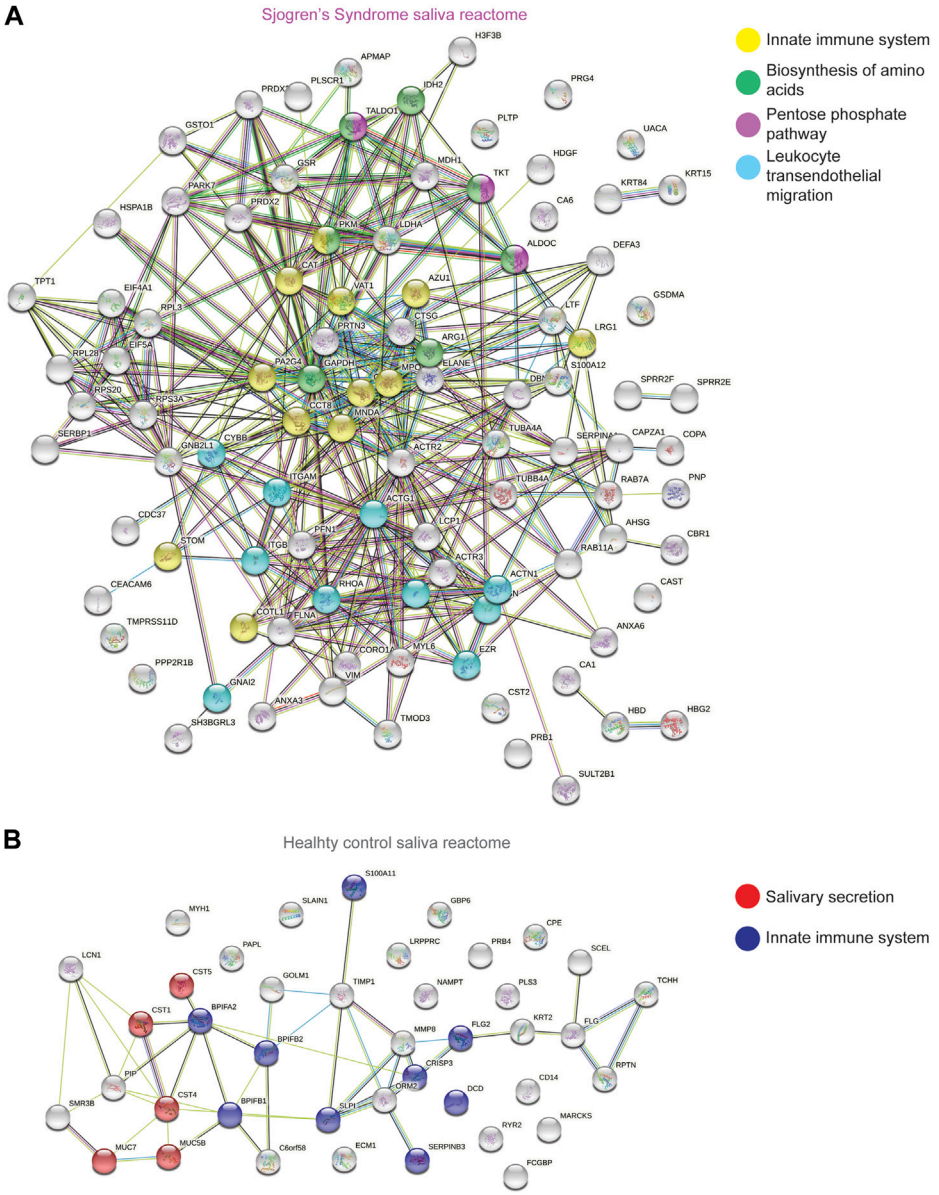

FIGURE 5 | STRING Analysis of Quantitative Proteomics Data of Human Sjogren's Syndrome Saliva Samples. Analysis of protein–protein interaction network by STRING v11. Elevated proteins from **(A)** SS or **(B)** healthy control saliva samples identified from the quantitative proteomics analysis were mapped by searching the STRING v11 software with a confidence level of 1% false discovery rate. Colored lines between the proteins indicate different types of interaction evidence: known interactions (teal), experimentally determined (pink), predicted interactions gene neighborhood (green), gene fusions (red), gene co-occurrence (blue), text-mining (yellow), coexpression (black), protein homology (purple).

identified significant changes in proteins expression associated with leukocyte transendothelial migration, which is an early inflammatory event occurring before the differentiation and activation of leukocytes and a subsequent downstream cascade of immune and inflammatory signaling (Muller, 2011). Changes in the transendothelial migration of leukocyte pathway is a feature of other inflammatory diseases like SLE (Marshall, 2003) or atherosclerosis (Shang et al., 2014). In the MRL/lpr autoimmune model in mouse that resembles human SLE, intercellular adhesion molecule 1 (ICAM-1) dependent exaggerated leukocyte-endothelial interactions was found to be associated with disease onset and severity (Marshall, 2003). Previous studies had characterized the transendothelial migration of leukocytes, as per the analysis of gene expression profiles of mRNA from parotid glands of SS patients (Wei et al., 2018). Using quantitative proteomics, we also identified an enrichment of proteins associated with transendothelial migration of leukocyte associated with an elevation of cathepsin B (CTSB), integrin beta 2 (ITGB2) and matrix metalloproteinase-9 (MMP9) in SS tear wash. Higher

TABLE 3 | Proteases and protease inhibitors significantly elevated in Sjogren's Syndrome (SS) saliva over healthy controls.

Uniprot ID	Gene name	Protein name	Fold difference SS/healthy
		Elevated in Sjogren's Syndrome	
Q99497	*PARK7*	DJ-1/Parkinson disease protein 7	3.9
P08311	*CTSG*	Cathepsin G	3.8
P08246	*ELANE*	Neutrophil elastase	3.6
P02788	*LTF*	Lactransferrin	3.6
P20160	*AZU1*	Azurocidin	3.3
P09228	*CST2*	Cystatin-SA	3.1
P20810	*CAST*	Calpastatin	3.1
P24158	*PRTN3*	Proteinase 3/Myeloblastin	3.0
P01009	*SERPINA1*	Alpha-1-antitrypsin	2.9
O60235	*TMPRSS11D*	Transmembrane protease serine 11D	2.5
		Elevated in healthy	
P16870	*CPE*	Carboxypeptidase We	-4.0
Q9HC84	*MUC5B*	Mucin-5B	–3.4
P01037	*CST1*	Cystatin-SN	–3.2
P28325	*CST5*	Cystatin-D	–2.8
P01036	*CST4*	Cystatin-S	–2.6
P22894	*MMP8*	Neutrophil collagenase	–2.5
P29508	*SERPINB3*	Serpin B3	–2.5
P03973	*SLPI*	Antileukoproteinase	–2.0

expression of MMP9 in tears aligns with previous findings which reported that an increase expression of MMP9 in tears was correlated with increased disease severity in patients with dry eye disease (Luo et al., 2004; Pinto-Fraga et al., 2018) and also in SS patients' saliva (Garreto et al., 2021). Cathepsin S has been previously demonstrated to be elevated in SS tears (Hamm-Alvarez et al., 2014; Regmi et al., 2017; Hargreaves et al., 2019). In our study, we identified an elevation of cathepsin B in SS tears, which was previously demonstrated in the first 5 years of SS diagnosis (Sohar et al., 2005). Pharmacological inhibition of cathepsin B was shown to reverse ICAM-1 dependent leukocyte endothelial adhesion in neurovascular inflammation (Wang et al., 2019). A better characterization of the role of cathepsin B in SS could reveal a potential approach to reduce vascular inflammation in the eye. Proteins regulating leukocyte functions, several integrins, have been drug targets for autoimmune diseases such as psoriasis and multiple sclerosis; however, a better understanding of their individual functions could result in better treatment strategies and avoid side effects associated with integrin inhibitions such as progressive multifocal leukoenphalopathy (Mitroulis et al., 2015) (Chopra et al., 2021). We also identified an elevation of the protein-lipid complex remodeling pathway associated with apolipoprotein E (APOE) in SS tears. APOE was associated with preventing disease progression in the experimental autoimmune encephalomyelitis (EAE) mouse model by regulating Th1 and Th17 responses (Wei et al., 2013). Interestingly, in SS, APOE polymorphisms were significantly associated with the early onset of disease (Pertovaara, 2004). Additionally, although the patients we evaluated here did not have cancer, SS patients are more susceptible to cancer development (Brito-Zerón et al., 2016; Igoe et al., 2020); yet, the specific reason is not known but sustained and increased inflammation observed in SS patients could be associated with increased cancer risk. The expression of cystatin S (CTS3) was reported to be significantly elevated in saliva from SS patients (van der Reijden et al., 1996) and here we found a potential association of cystatin S with collagen catabolic process, neutrophils and immune system enrichment pathways. MMP8 levels were elevated in SS tear wash and were previously found to be associated with ocular inflammation, as its expression in tears was significantly higher in patients with ocular rosacea compared to healthy controls (Määttä et al., 2006).

Downregulation of glycolysis in SS tear wash compared to healthy controls indicated a dysregulation of metabolism in SS. We identified other dysregulated pathways associated with metabolism between healthy and SS saliva; specifically, the biosynthesis of amino acids and pentose phosphate pathways were upregulated in SS saliva compared to healthy controls. In inflammation, pentose phosphate pathway was demonstrated to act as a key gatekeeper by supplying ribose-5-phophate to increase cell proliferation and NADPH for antioxidative defense (Perl, 2017). Metabolic profiling of saliva demonstrated differential expression of metabolites in SS compared to healthy controls (Mikkonen, 2012). Analysis of blood serum revealed that SS patients tend to have a higher prevalence of metabolic disorders, such as dyslipidemia, diabetes mellitus and hyperuricemia, in comparison with an age and sex-matched control group (Ramos-Casals et al., 2007). Therapeutic approaches targeting metabolic pathways, such as the mTOR pathway, have been suggested as a way to treat SLE (Perl, 2017). However, no unbiased metabolomics profiling has yet been performed on SS tear or saliva samples and relatively little is known about what metabolites are implicated in SS pathogenesis.

In vivo pre-clinical animal studies and *ex vivo* studies on human tissues have demonstrated that altered expression and function of PRG4 (i.e. diminished lubrication and increased inflammation) has been associated with joint damage and pain in osteoarthritis (OA) and RA (Ludwig et al., 2012; Iqbal et al.,

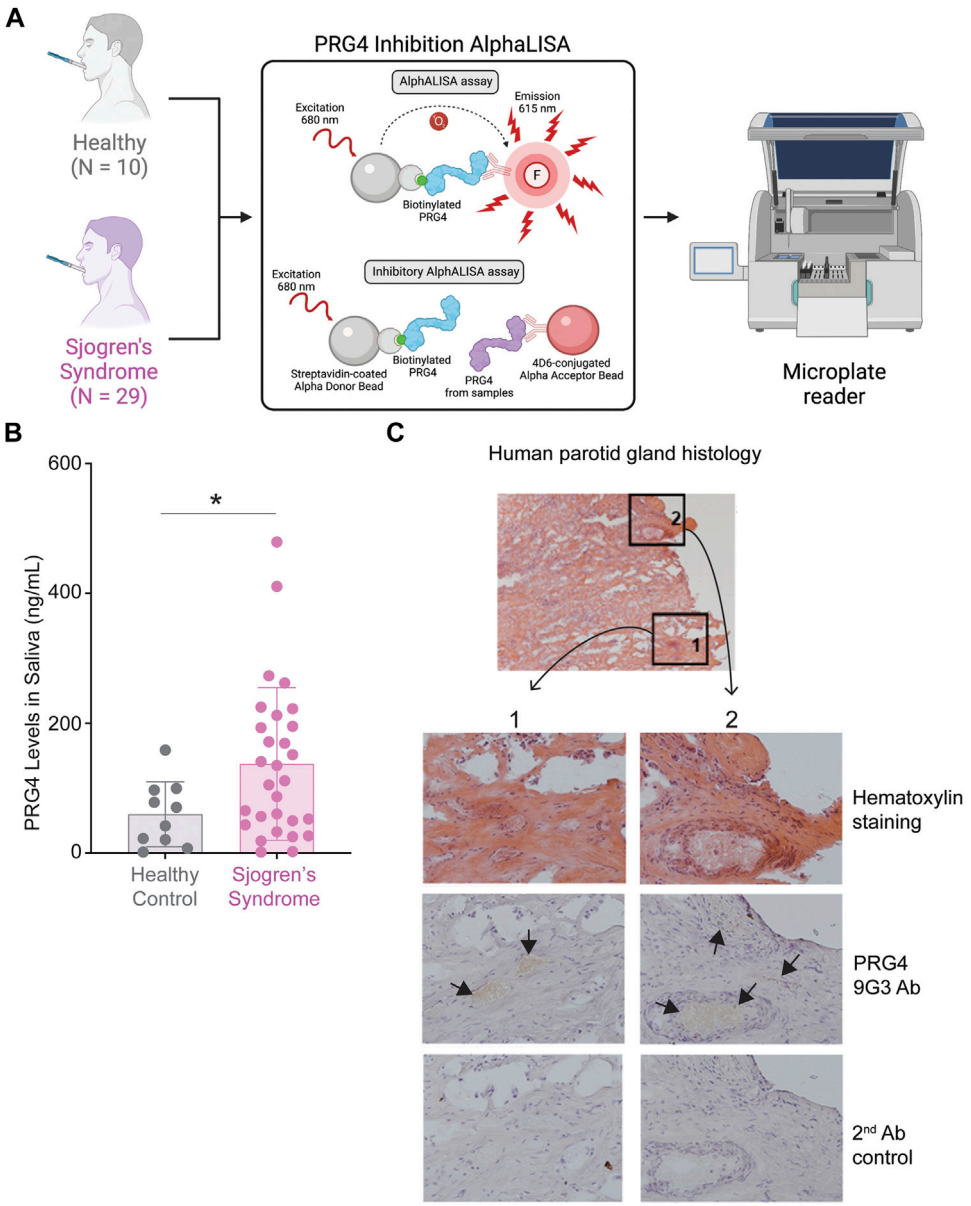

FIGURE 6 | increase of PRG4 in Saliva and Parotid Gland. **(A)** AlphALISA workflow using a designed PRG4 antibody 4D6-based assay. **(B)** PRG4 levels were measured. Data are represented as bar graphs with ±standard deviation (SD) and analyzed by a Welch's two-tailed paired *t* test: $^{*}p > 0.05$, $^{**}p > 0.01$. **(C)** Parotid gland histology using hematoxylin staining and a PRG4 antibody (9G3). As a control, secondary antibody control was used without the addition of a primary PRG4 antibody.

2016; Das et al., 2019). We previously demonstrated that *ex vivo* proteolytic processing of PRG4 in tears reduced boundary lubricating ability compared to unprocessed controls (Regmi et al., 2017) and that proinflammatory cytokines altered the expression of PRG4 by corneal epithelium cells *in vitro* (Menon et al., 2021). Here, we show, for the first time, that PRG4 has different levels in SS tear wash and saliva compared to healthy controls. In SS tear washes, we found reduced concentration, tear volume, and total mass of PRG4 compared to healthy controls. This could be due to increased degradation from CTSS (Regmi et al., 2017) or CTSB (Elsaid et al., 2007) which was upregulated in our quantitative proteomics data. Although a previous study on PRG4 levels in the SS tears had found no significant changes between the SS and healthy controls (Schmidt et al., 2018), the AlphaLISA used in that study was based on an anti-PRG4 mAb 9G3-coated Protein G bead, which had previously been shown to be effective in measuring PRG4 levels *ex vivo* in pericardial and synovial fluid (Park et al., 2018). However, the protein-G beads were later found to interact with immunoglobulin G (IgG) molecules present in tears and as IgGs have been shown to be elevated in SS, it made the interpretation difficult (Domingo et al., 1998). Thus, the 9G3-based AlphaLISA

can still be an effective tool for measuring biological samples where the concentration of IgG is low; however, an optimized experimental setup was required to measure PRG4 in tears and saliva. Thus, our newly designed 4D6-based assay did not react with sample IgGs, making our PRG4 measurements accurate. One limitation of our study was that our proteomics analysis was performed on neat tears while our PRG4 analysis was performed on tear washes. The samples analyzed by quantitative proteomics (**Figure 1A**) were previously analyzed using the 9G3-based AlphaLISA (Schmidt et al., 2018) but there was not enough sample volume to re-analyze them using the newly developed 4D6-based AlphaLISA. Since SS patients typically produce a significantly lower volume of tear fluid than healthy controls, analyzing tear washes allows for a greater variety of testing methods while still preserving the qualities of the original tear fluid. Future work could explore if the trends found in tear washes also apply to basal tears. The presence of PRG4 staining in both the serous acini, where proteins are typically secreted, and the striated duct, which directly leads to the interlobular ducts where saliva is secreted, indicates that PRG4 is produced and secreted into the oral cavity. Interestingly, a 2.3- and 2.4-fold increase of PRG4 in SS saliva concentration was found, as measured by AlphALISA and quantitative proteomics, respectively. However, we identified a decrease of PRG4 in tear samples. A possible explanation could be that the body responds to normalize salivary homeostasis. Another explanation could be that endogenous PRG4 is more concentrated in a lower volume since less saliva is produced by SS patients. Future studies could examine how PRG4 production and secretion in the salivary gland is influenced by SS.

Our metascape analysis identified that the JAK-STAT signaling after interleukin-12 stimulation was enriched in SS saliva compared to healthy controls. In a cell culture system using the human salivary gland (HSG) cell line, treatment with JAK inhibitors (AG490 and ruxolitinib) resulted in suppression of the innate epigenetic reprogramming observed when these cells were treated with interferon-α (IFNα), IFNγ and H_2O_2 to re-create a cellular model of proinflammation (Charras et al., 2020). In preclinical models of RA and EAE, JAK-STAT inhibition was demonstrated to be effective by suppressing proinflammatory cytokines and chemokines (Stump et al., 2011) (Liu et al., 2014). We detected an enrichment in pathways associated with polymorphonuclear leukocytes as indicated by myeloperoxidase (MPO) in SS tear and saliva. While the potential role of oxidative stress in ocular surface inflammation and dry eye disease has been investigated (Dogru et al., 2018), our study suggests an upregulation of superoxide metabolic processes in the saliva of patients with SS. Aberrant phagocytosis in the peripheral blood of patients with primary SS has also been reported (Fragoulis et al., 2015). Our analyses have also identified an upregulation of phagocytosis in SS saliva compared to healthy controls.

There are a few limitations of our current study. Collecting enough proteins from tears and saliva to run quantitative proteomics can be a challenge. Therefore, additional samples would need to be run in the future to assess additional factors such as sex differences (as SS is more prevalent in women than men), age and drugs that the patients are taking and see if they impact certain significant proteins that we have detected in addition to proteases, protease inhibitors and PRG4. Our current proteomic analysis has revealed enrichment of several newly associated but also previously reported proteases and protease inhibitors in SS. The activity of cysteine proteases (cathepsins) and serine proteases (neutrophil elastase, prostasin, proteinase-3/myeloblastin) could be further investigated using activity-based probes in SS (Edgington-Mitchell et al., 2017; Anderson et al., 2019, 2020; Mainoli et al., 2020; Mountford et al., 2020; Tu et al., 2021). The upregulation of cathepsin G in the saliva of patients with SS is likely associated with an increase in neutrophils and corresponds to an elevation in synovial fluid of RA patients (Gao, 2018). Calpain-1 was upregulated in healthy control tears and was previously found to play an important role in cerebellar plasticity and eye-blink conditioning, as evidenced by impairment in both of these measures in *Capn1*$^{-/-}$ mice (Heysieattalab et al., 2020). Interestingly, upregulation of several cysteine protease inhibitors in the saliva of healthy controls included cystatin-D, cystatin-S and cystatin-SN, indicating a possible regulation and inhibition of cathepsin activity (Balbín et al., 1994). Further studies to characterize these proteases enriched in SS tears and saliva using N-terminomics could identify their potential substrates, which could help find new drug targets in SS (Dufour, 2015; Mainoli et al., 2020; Longxiang Wang, Kimberly Main, Henry; Wang, Olivier Julien, 2021). Our data present new proteases, metabolic and cellular signaling pathways that are elevated in SS and could lead to unbiased investigations of new regulators of SS pathogenesis.

DATA AVAILABILITY STATEMENT

The original contributions presented in the study are publicly available. This data can be found here *via* the PRIDE database and are freely available: PXD028922.

AUTHOR CONTRIBUTIONS

ND and NM performed the experiments, data analysis and wrote the manuscript. LD and AD performed proteomics and bioinformatics data analysis. PW, MH, GJ, and BC contributed to samples collection and data analysis. LJ, RK, TS, and AD reviewed and wrote the manuscript.

FUNDING

AD was supported by an NSERC Discovery Grant (DGECR-2019- 00112), Alberta Innovates AICE concepts (202102341) and Canadian Institutes of Health Research (449589). AD and RK are funded by The Arthritis Society (Canada) stars career development award. TS is supported through the Department of Biomedical Engineering at the University of Connecticut

Health Center, and was supported through a Canada Research Chair (CRC) Tier II at the University of Calgary.

ACKNOWLEDGMENTS

We would like to thank Dr. Mathieu Lavallée-Adam and Rachel Nadeau for their help and guidance using PIGNON. We would like to acknowledge Sjogren's International Collaborative Clinical Alliance (SICCA) Biorepository for the saliva samples. Some data and specimens used in this manuscript were obtained from the Sjögren's International Collaborative Clinical Alliance (SICCA) Biorepository, funded under contracts N01 DE32636 and HHSN26S201300057C, and grant U01DE028891 by the National Institute of Dental and Craniofacial Research. This manuscript was prepared using a publicly available SICCA data set and does not necessarily reflect the opinions or views of all SICCA investigators or NIDCR. We would like to thank Lubris BioPharma for providing the tear collection and the rhPRG4 in kind. We would also like to thank Dr. Sruthi Srinivasan and Dr. Lakshman N Subbaraman for their aid in collecting tears at CORE.

SUPPLEMENTARY MATERIAL

The Supplementary Material for this article can be found online at: https://www.frontiersin.org/articles/10.3389/fphar.2021.787193/full#supplementary-material

REFERENCES

Abubacker, S., Ponjevic, D., Ham, H. O., Messersmith, P. B., Matyas, J. R., and Schmidt, T. A. (2016). Effect of Disulfide Bonding and Multimerization on Proteoglycan 4's Cartilage Boundary Lubricating Ability and Adsorption. *Connect. Tissue Res.* 57, 113–123. doi:10.3109/03008207.2015.1113271

Addona, T. A., Abbatiello, S. E., Schilling, B., Skates, S. J., Mani, D. R., Bunk, D. M., et al. (2009). Multi-site Assessment of the Precision and Reproducibility of Multiple Reaction Monitoring-Based Measurements of Proteins in Plasma. *Nat. Biotechnol.* 27, 633–641. doi:10.1038/nbt.1546

Aebersold, R., and Mann, M. (2016). Mass-Spectrometric Exploration of Proteome Structure and Function. *Nature* 537, 347–355. doi:10.1038/nature19949

Al-Tarawneh, S. K., Border, M. B., Dibble, C. F., and Bencharit, S. (2011). Defining Salivary Biomarkers Using Mass Spectrometry-Based Proteomics: A Systematic Review. *OMICS* 15, 353–361. doi:10.1089/omi.2010.0134

Anderson, B. M., Poole, D. P., Aurelio, L., Ng, G. Z., Fleischmann, M., Kasperkiewicz, P., et al. (2019). Application of a Chemical Probe to Detect Neutrophil Elastase Activation during Inflammatory Bowel Disease. *Sci. Rep.* 9, 13295. doi:10.1038/s41598-019-49840-4

Anderson, B. M., De Almeida, L. G. N., Sekhon, H., Young, D., Dufour, A., and Edgington-Mitchell, L. E. (2020). N-Terminomics/TAILS Profiling of Macrophages after Chemical Inhibition of Legumain. *Biochemistry* 59, 329–340. doi:10.1021/acs.biochem.9b00821

Balbín, M., Hall, A., Grubb, A., Mason, R. W., López-Otín, C., and Abrahamson, M. (1994). Structural and Functional Characterization of Two Allelic Variants of Human Cystatin D Sharing a Characteristic Inhibition Spectrum against Mammalian Cysteine Proteinases. *J. Biol. Chem.* 269, 23156–23162. doi:10.1016/S0021-9258(17)31633-2

Both, T., Dalm, V. A., van Hagen, P. M., and van Daele, P. L. (2017). Reviewing Primary Sjögren's Syndrome: Beyond the Dryness - from Pathophysiology to Diagnosis and Treatment. *Int. J. Med. Sci.* 14, 191–200. doi:10.7150/ijms.17718

Brito-Zerón, P., Baldini, C., Bootsma, H., Bowman, S. J., Jonsson, R., Mariette, X., et al. (2016). Sjögren Syndrome. *Nat. Rev. Dis. Primers* 2, 16047. doi:10.1038/nrdp.2016.47

Burbelo, P. D., Ching, K. H., Issa, A. T., Loftus, C. M., Li, Y., Satoh, M., et al. (2009). Rapid Serological Detection of Autoantibodies Associated with Sjögren's Syndrome. *J. Transl. Med.* 7, 83. doi:10.1186/1479-5876-7-83

Callaghan, R., Prabu, A., Allan, R. B., Clarke, A. E., Sutcliffe, N., Pierre, Y. S., et al. (2007). Direct Healthcare Costs and Predictors of Costs in Patients with Primary Sjogren's Syndrome. *Rheumatology (Oxford)* 46, 105–111. doi:10.1093/rheumatology/kel155

Charras, A., Arvaniti, P., Le Dantec, C., Arleevskaya, M. I., Zachou, K., Dalekos, G. N., et al. (2020). JAK Inhibitors Suppress Innate Epigenetic Reprogramming: a Promise for Patients with Sjögren's Syndrome. *Clin. Rev. Allergy Immunol.* 58, 182–193. doi:10.1007/s12016-019-08743-y

Chen, W., Cao, H., Lin, J., Olsen, N., and Zheng, S. G. (2015). Biomarkers for Primary Sjögren's Syndrome. *Genomics. Proteomics Bioinf.* 13, 219–223. doi:10.1016/j.gpb.2015.06.002

Chopra, S., Myers, Z., Sekhon, H., and Dufour, A. (2021). The Nerves to Conduct a Multiple Sclerosis Crime Investigation. *Int. J. Mol. Sci.* 22, 2498. doi:10.3390/ijms22052498

Cox, J., and Mann, M. (2008). MaxQuant Enables High Peptide Identification Rates, Individualized p.p.b.-Range Mass Accuracies and Proteome-Wide Protein Quantification. *Nat. Biotechnol.* 26, 1367–1372. doi:10.1038/nbt.1511

Cox, J., Neuhauser, N., Michalski, A., Scheltema, R. A., Olsen, J. V., and Mann, M. (2011). Andromeda: A Peptide Search Engine Integrated into the MaxQuant Environment. *J. Proteome Res.* 10, 1794–1805. doi:10.1021/pr101065j

Das, N., Schmidt, T. A., Krawetz, R. J., and Dufour, A. (2019). Proteoglycan 4: From Mere Lubricant to Regulator of Tissue Homeostasis and Inflammation: Does Proteoglycan 4 Have the Ability to Buffer the Inflammatory Response? *BioEssays* 41, e1800166. doi:10.1002/bies.201800166

Dogru, M., Kojima, T., Simsek, C., and Tsubota, K. (2018). Potential Role of Oxidative Stress in Ocular Surface Inflammation and Dry Eye Disease. *Invest. Ophthalmol. Vis. Sci.* 59, DES163. doi:10.1167/iovs.17-23402

Domingo, I., Coll, J., Ribas-Montobio, J., Marrugat, J., and Rubiés-Prat, J. (1998). Lacrimal Immunoglobulins in Rheumatoid Arthritis Patients with or without Sjögren's Syndrome. *Ophthalmologica* 212, 30–33. doi:10.1159/000027255

Dufour, A., Bellac, C. L., Eckhard, U., Solis, N., Klein, T., Kappelhoff, R., et al. (2018). C-terminal Truncation of IFN-γ Inhibits Proinflammatory Macrophage Responses and Is Deficient in Autoimmune Disease. *Nat. Commun.* 9, 2416. doi:10.1038/s41467-018-04717-4

Dufour, A. (2015). Degradomics of Matrix Metalloproteinases in Inflammatory Diseases. *Front. Biosci. (Schol Ed.)* 7, 150–167. doi:10.2741/s430

Edgington-Mitchell, L. E., Barlow, N., Aurelio, L., Samha, A., Szabo, M., Graham, B., et al. (2017). Fluorescent Diphenylphosphonate-Based Probes for Detection of Serine Protease Activity during Inflammation. *Bioorg. Med. Chem. Lett.* 27, 254–260. doi:10.1016/j.bmcl.2016.11.064

Elsaid, K. A., Jay, G. D., and Chichester, C. O. (2007). Reduced Expression and Proteolytic Susceptibility of Lubricin/superficial Zone Protein May Explain Early Elevation in the Coefficient of Friction in the Joints of Rats with Antigen-Induced Arthritis. *Arthritis Rheum.* 56, 108–116. doi:10.1002/art.22321

Fox, R. I., Adamson, T. C., Fong, S., Young, C., and Howell, F. V. (1983). Characterization of the Phenotype and Function of Lymphocytes Infiltrating the Salivary Gland in Patients with Primary Sjogren Syndrome. *Diagn. Immunol.* 1, 233–239.

Fragoulis, G. E., Vakrakou, A. G., Papadopoulou, A., Germenis, A., Kanavakis, E., Moutsopoulos, H. M., et al. (2015). Impaired Degradation and Aberrant Phagocytosis of Necrotic Cell Debris in the Peripheral Blood of Patients with Primary Sjögren's Syndrome. *J. Autoimmun.* 56, 12–22. doi:10.1016/j.jaut.2014.08.004

Gao, S., Zhu, H., Zuo, X., and Luo, H. (2018). Cathepsin G and its Role in Inflammation and Autoimmune Diseases. *Arch. Rheumatol.* 33, 498–504. doi:10.5606/ArchRheumatol.2018.6595

Garreto, L., Charneau, S., Mandacaru, S. C., Nóbrega, O. T., Motta, F. N., de Araújo, C. N., et al. (2021). Mapping Salivary Proteases in Sjögren's Syndrome Patients Reveals Overexpression of Dipeptidyl Peptidase-4/CD26. *Front. Immunol.* 12, 686480. doi:10.3389/fimmu.2021.686480

Geyer, P. E., Holdt, L. M., Teupser, D., and Mann, M. (2017). Revisiting Biomarker Discovery by Plasma Proteomics. *Mol. Syst. Biol.* 13, 942. doi:10.15252/msb.20156297

Hamm-Alvarez, S. F., Janga, S. R., Edman, M. C., Madrigal, S., Shah, M., Frousiakis, S. E., et al. (2014). Tear Cathepsin S as a Candidate Biomarker for Sjögren's Syndrome. *Arthritis Rheumatol.* 66, 1872–1881. doi:10.1002/art.38633

Hargreaves, P., Daoudlarian, D., Theron, M., Kolb, F. A., Manchester Young, M., Reis, B., et al. (2019). Differential Effects of Specific Cathepsin S Inhibition in Biocompartments from Patients with Primary Sjögren Syndrome. *Arthritis Res. Ther.* 21, 175. doi:10.1186/s13075-019-1955-2

Heysieattalab, S., Lee, K. H., Liu, Y., Wang, Y., Foy, M. R., Bi, X., et al. (2020). Impaired Cerebellar Plasticity and Eye-Blink Conditioning in Calpain-1 Knock-Out Mice. *Neurobiol. Learn. Mem.* 170, 106995. doi:10.1016/j.nlm.2019.02.005

Igoe, A., Merjanah, S., and Scofield, R. H. (2020). Sjögren Syndrome and Cancer. *Rheum. Dis. Clin. North. Am.* 46, 513–532. doi:10.1016/j.rdc.2020.05.004

Iqbal, S. M., Leonard, C., Regmi, S. C. S., De Rantere, D., Tailor, P., Ren, G., et al. (2016). Lubricin/Proteoglycan 4 Binds to and Regulates the Activity of Toll-like Receptors *In Vitro*. *Sci. Rep.* 6, 18910. doi:10.1038/srep18910

Lambiase, A., Sullivan, B. D., Schmidt, T. A., Sullivan, D. A., Jay, G. D., Truitt, E. R., et al. (2017). A Two-Week, Randomized, Double-Masked Study to Evaluate Safety and Efficacy of Lubricin (150 µg/mL) Eye Drops versus Sodium Hyaluronate (HA) 0.18% Eye Drops (Vismed®) in Patients with Moderate Dry Eye Disease. *Ocul. Surf.* 15, 77–87. doi:10.1016/j.jtos.2016.08.004

Li, B., Sheng, M., Li, J., Yan, G., Lin, A., Li, M., et al. (2015). Tear Proteomic Analysis of Sjögren Syndrome Patients with Dry Eye Syndrome by Two-Dimensional-Nano-Liquid Chromatography Coupled with Tandem Mass Spectrometry. *Sci. Rep.* 4, 5772. doi:10.1038/srep05772

Liu, Y., Holdbrooks, A. T., De Sarno, P., Rowse, A. L., Yanagisawa, L. L., McFarland, B. C., et al. (2014). Therapeutic Efficacy of Suppressing the JAK/STAT Pathway in Multiple Models of Experimental Autoimmune Encephalomyelitis. *J. Immunol.* 192, 59–72. doi:10.4049/jimmunol.1301513

López-Villalobos, E. F., Muñoz-Valle, J. F., Palafox-Sánchez, C. A., García-Arellano, S., Martínez-Fernández, D. E., Orozco-Barocio, G., et al. (2021). Cytokine Profiles and Clinical Characteristics in Primary Sjögren´s Syndrome Patient Groups. *J. Clin. Lab. Anal.* 35, e23629. doi:10.1002/jcla.23629

Ludwig, T. E., McAllister, J. R., Lun, V., Wiley, J. P., and Schmidt, T. A. (2012). Diminished Cartilage-Lubricating Ability of Human Osteoarthritic Synovial Fluid Deficient in Proteoglycan 4: Restoration through Proteoglycan 4 Supplementation. *Arthritis Rheum.* 64, 3963–3971. doi:10.1002/art.34674

Luo, L., Li, D. Q., Doshi, A., Farley, W., Corrales, R. M., and Pflugfelder, S. C. (2004). Experimental Dry Eye Stimulates Production of Inflammatory Cytokines and MMP-9 and Activates MAPK Signaling Pathways on the Ocular Surface. *Invest. Ophthalmol. Vis. Sci.* 45, 4293–4301. doi:10.1167/iovs.03-1145

Määttä, M., Kari, O., Tervahartiala, T., Peltonen, S., Kari, M., Saari, M., et al. (2006). Tear Fluid Levels of MMP-8 Are Elevated in Ocular Rosacea-Ttreatment Effect of Oral Doxycycline. *Graefes Arch. Clin. Exp. Ophthalmol.* 244, 957–962. doi:10.1007/s00417-005-0212-3

Mainoli, B., Hirota, S., Edgington-Mitchell, L. E., Lu, C., and Dufour, A. (2020). Proteomics and Imaging in Crohn's Disease: TAILS of Unlikely Allies. *Trends Pharmacol. Sci.* 41, 74–84. doi:10.1016/j.tips.2019.11.008

Marshall, D., Dangerfield, J. P., Bhatia, V. K., Larbi, K. Y., Nourshargh, S., and Haskard, D. O. (2003). MRL/lpr Lupus-Prone Mice Show Exaggerated ICAM-1-dependent Leucocyte Adhesion and Transendothelial Migration in Response to TNF-Alpha. *Rheumatology (Oxford)* 42, 929–934. doi:10.1093/rheumatology/keg251

Mavragani, C. P., and Moutsopoulos, H. M. (2020). Sjögren's Syndrome: Old and New Therapeutic Targets. *J. Autoimmun.* 110, 102364. doi:10.1016/j.jaut.2019.102364

Mavragani, C. P. (2017). Mechanisms and New Strategies for Primary Sjögren's Syndrome. *Annu. Rev. Med.* 68, 331–343. doi:10.1146/annurev-med-043015-123313

Menon, N. G., Goyal, R., Lema, C., Woods, P. S., Tanguay, A. P., Morin, A. A., et al. (2021). Proteoglycan 4 (PRG4) Expression and Function in Dry Eye Associated Inflammation. *Exp. Eye Res.* 208, 108628. doi:10.1016/j.exer.2021.108628

Mikkonen, J. J. (2012). Metabolic Profiling of Saliva in Patients with Primary Sjogren's Syndrome. *Metabolomics* 03, 1–6. doi:10.4172/2153-0769.1000128

Mitroulis, I., Alexaki, V. I., Kourtzelis, I., Ziogas, A., Hajishengallis, G., and Chavakis, T. (2015). Leukocyte Integrins: Role in Leukocyte Recruitment and as Therapeutic Targets in Inflammatory Disease. *Pharmacol. Ther.* 147, 123–135. doi:10.1016/j.pharmthera.2014.11.008

Mitsias, D. I., Tzioufas, A. G., Veiopoulou, C., Zintzaras, E., Tassios, I. K., Kogopoulou, O., et al. (2002). The Th1/Th2 Cytokine Balance Changes with the Progress of the Immunopathological Lesion of Sjogren's Syndrome. *Clin. Exp. Immunol.* 128, 562–568. doi:10.1046/j.1365-2249.2002.01869.x

Mountford, S. J., Anderson, B. M., Xu, B., Tay, E. S. V., Szabo, M., Hoang, M. L., et al. (2020). Application of a Sulfoxonium Ylide Electrophile to Generate Cathepsin X-Selective Activity-Based Probes. *ACS Chem. Biol.* 15, 718–727. doi:10.1021/acschembio.9b00961

Muller, W. A. (2011). Mechanisms of Leukocyte Transendothelial Migration. *Annu. Rev. Pathol.* 6, 323–344. doi:10.1146/annurev-pathol-011110-130224

Nadeau, R., Byvsheva, A., and Lavallée-Adam, M. (2021). PIGNON: a Protein-Protein Interaction-Guided Functional Enrichment Analysis for Quantitative Proteomics. *BMC Bioinformatics* 22, 302. doi:10.1186/s12859-021-04042-6

Nakayasu, E. S., Gritsenko, M., Piehowski, P. D., Gao, Y., Orton, D. J., Schepmoes, A. A., et al. (2021). Tutorial: Best Practices and Considerations for Mass-Spectrometry-Based Protein Biomarker Discovery and Validation. *Nat. Protoc.* 16, 3737–3760. doi:10.1038/s41596-021-00566-6

Park, D. S. J., Regmi, S. C., Svystonyuk, D. A., Teng, G., Belke, D., Turnbull, J., et al. (2018). Human Pericardial Proteoglycan 4 (Lubricin): Implications for Postcardiotomy Intrathoracic Adhesion Formation. *J. Thorac. Cardiovasc. Surg.* 156, 1598–1608.e1. doi:10.1016/j.jtcvs.2018.03.170

Perl, A. (2017). Review: Metabolic Control of Immune System Activation in Rheumatic Diseases. *Arthritis Rheumatol.* 69, 2259–2270. doi:10.1002/art.40223

Pertovaara, M., Lehtimäki, T., Rontu, R., Antonen, J., Pasternack, A., and Hurme, M. (2004). Presence of Apolipoprotein E Epsilon4 Allele Predisposes to Early Onset of Primary Sjogren's Syndrome. *Rheumatology (Oxford)* 43, 1484–1487. doi:10.1093/rheumatology/keh383

Pinto-Fraga, J., Enríquez-de-Salamanca, A., Calonge, M., González-García, M. J., López-Miguel, A., López-de la Rosa, A., et al. (2018). Severity, Therapeutic, and Activity Tear Biomarkers in Dry Eye Disease: An Analysis from a Phase III Clinical Trial. *Ocul. Surf.* 16, 368–376. doi:10.1016/j.jtos.2018.05.001

R Development Core Team (2011). *R: A Language and Environment for Statistical Computing. R Foundation for Statistical Computing*. Viennna. http://www.R-project.org.

Rabiah, N. I., Sato, Y., Kannan, A., Kress, W., Straube, F., and Fuller, G. G. (2020). Understanding the Adsorption and Potential Tear Film Stability Properties of Recombinant Human Lubricin and Bovine Submaxillary Mucins in an *In Vitro* Tear Film Model. *Colloids Surf. B Biointerfaces* 195, 111257. doi:10.1016/j.colsurfb.2020.111257

Ramos-Casals, M., Brito-Zerón, P., Sisó, A., Vargas, A., Ros, E., Bove, A., et al. (2007). High Prevalence of Serum Metabolic Alterations in Primary Sjögren's Syndrome: Influence on Clinical and Immunological Expression. *J. Rheumatol.* 34, 754–761.

Ramos-Casals, M., Brito-Zerón, P., Sisó-Almirall, A., and Bosch, X. (2012). Primary Sjogren Syndrome. *BMJ* 344, e3821–7. doi:10.1136/bmj.e3821

Regmi, S. C., Samsom, M. L., Heynen, M. L., Jay, G. D., Sullivan, B. D., Srinivasan, S., et al. (2017). Degradation of Proteoglycan 4/lubricin by Cathepsin S: Potential Mechanism for Diminished Ocular Surface Lubrication in Sjögren's Syndrome. *Exp. Eye Res.* 161, 1–9. doi:10.1016/j.exer.2017.05.006

Richards, A., Mutlu, S., Scully, C., and Maddison, P. (1992). Complications Associated with Labial Salivary Gland Biopsy in the Investigation of Connective Tissue Disorders. *Ann. Rheum. Dis.* 51, 996–997. doi:10.1136/ard.51.8.996

Rifai, N., Gillette, M. A., and Carr, S. A. (2006). Protein Biomarker Discovery and Validation: the Long and Uncertain Path to Clinical Utility. *Nat. Biotechnol.* 24, 971–983. doi:10.1038/nbt1235

Rischmueller, M., Tieu, J., and Lester, S. (2016). Primary Sjögren's Syndrome. *Best Pract. Res. Clin. Rheumatol.* 30, 189–220. doi:10.1016/j.berh.2016.04.003

Ryu, O. H., Atkinson, J. C., Hoehn, G. T., Illei, G. G., and Hart, T. C. (2006). Identification of Parotid Salivary Biomarkers in Sjogren's Syndrome by Surface-Enhanced Laser Desorption/ionization Time-Of-Flight Mass Spectrometry and Two-Dimensional Difference Gel Electrophoresis. *Rheumatology (Oxford)* 45, 1077–1086. doi:10.1093/rheumatology/kei212

Samsom, M., Chan, A., Iwabuchi, Y., Subbaraman, L., Jones, L., and Schmidt, T. A. (2015). *In Vitro* friction Testing of Contact Lenses and Human Ocular Tissues: Effect of Proteoglycan 4 (PRG4). *Tribology Int.* 89, 27–33. doi:10.1016/j.triboint.2014.11.022

Schmidt, T. A., Sullivan, D. A., Knop, E., Richards, S. M., Knop, N., Liu, S., et al. (2013). Transcription, Translation, and Function of Lubricin, a Boundary Lubricant, at the Ocular Surface. *JAMA Ophthalmol.* 131, 766–776. doi:10.1001/jamaophthalmol.2013.2385

Schmidt, T. A., Srinivasan, S., Heynen, M., Jay, G., Sullivan, B. D., Subbaraman, L., et al. (2018). Quantification of Proteoglycan 4 (PRG4)/Lubricin in normal and Sjögren Syndrome Human Tears. *Invest. Ophthalmol. Vis. Sci.* 59, 3827.

Seror, R., Nocturne, G., and Mariette, X. (2021). Current and Future Therapies for Primary Sjögren Syndrome. *Nat. Rev. Rheumatol.* 17, 475–486. doi:10.1038/s41584-021-00634-x

Shang, M. M., Talukdar, H. A., Hofmann, J. J., Niaudet, C., Asl, H. F., Jain, R. K., et al. (2014). Lim Domain Binding 2: A Key Driver of Transendothelial Migration of Leukocytes and Atherosclerosis. *Arterioscler. Thromb. Vasc. Biol.* 34, 2068–2077. doi:10.1161/ATVBAHA.113.302709

Shiboski, S. C., Shiboski, C. H., Criswell, L., Baer, A., Challacombe, S., Lanfranchi, H., et al. (2012). American College of Rheumatology Classification Criteria for Sjögren's Syndrome: a Data-Driven, Expert Consensus Approach in the Sjögren's International Collaborative Clinical Alliance Cohort. *Arthritis Care Res. (Hoboken)* 64, 475–487. doi:10.1002/acr.21591

Sohar, N., Sohar, I., and Hammer, H. (2005). Lysosomal Enzyme Activities: New Potential Markers for Sjögren's Syndrome. *Clin. Biochem.* 38, 1120–1126. doi:10.1016/j.clinbiochem.2005.09.003

Spitzer, M., Wildenhain, J., Rappsilber, J., and Tyers, M. (2014). BoxPlotR: a Web Tool for Generation of Box Plots. *Nat. Methods* 11, 121–122. doi:10.1038/nmeth.2811

Stump, K. L., Lu, L. D., Dobrzanski, P., Serdikoff, C., Gingrich, D. E., Dugan, B. J., et al. (2011). A Highly Selective, Orally Active Inhibitor of Janus Kinase 2, CEP-33779, Ablates Disease in Two Mouse Models of Rheumatoid Arthritis. *Arthritis Res. Ther.* 13, R68. doi:10.1186/ar3329

Supek, F., Bošnjak, M., Škunca, N., and Šmuc, T. (2011). REVIGO Summarizes and Visualizes Long Lists of Gene Ontology Terms. *PLoS One* 6, e21800. doi:10.1371/journal.pone.0021800

Szklarczyk, D., Gable, A. L., Lyon, D., Junge, A., Wyder, S., Huerta-Cepas, J., et al. (2019). STRING V11: Protein-Protein Association Networks with Increased Coverage, Supporting Functional Discovery in Genome-wide Experimental Datasets. *Nucleic Acids Res.* 47, D607–D613. doi:10.1093/nar/gky1131

Tu, N. H., Jensen, D. D., Anderson, B. M., Chen, E., Jimenez-Vargas, N. N., Scheff, N. N., et al. (2021). Legumain Induces Oral Cancer Pain by Biased Agonism of Protease-Activated Receptor-2. *J. Neurosci.* 41, 193–210. doi:10.1523/JNEUROSCI.1211-20.2020

van der Reijden, W. A., van der Kwaak, J. S., Veerman, E. C., and Nieuw Amerongen, A. V. (1996). Analysis of the Concentration and Output of Whole Salivary Constituents in Patients with Sjögren's Syndrome. *Eur. J. Oral Sci.* 104, 335–340. doi:10.1111/j.1600-0722.1996.tb00088.x

Verstappen, G. M., Meiners, P. M., Corneth, O. B. J., Visser, A., Arends, S., Abdulahad, W. H., et al. (2017). Attenuation of Follicular Helper T Cell-Dependent B Cell Hyperactivity by Abatacept Treatment in Primary Sjögren's Syndrome. *Arthritis Rheumatol.* 69, 1850–1861. doi:10.1002/art.40165

Vitali, C., Bombardieri, S., Jonsson, R., Moutsopoulos, H. M., Alexander, E. L., Carsons, S. E., et al. (2002). Classification Criteria for Sjögren's Syndrome: a Revised Version of the European Criteria Proposed by the American-European Consensus Group. *Ann. Rheum. Dis.* 61, 554–558. doi:10.1136/ard.61.6.554

Virdee, S., Greenan-Barrett, J., and Ciurtin, C. (2017). A Systematic Review of Primary Sjögren's Syndrome in Male and Paediatric Populations. *Clin. Rheumatol.* 36 (10), 2225–2236. doi:10.1007/s10067-017-3745-z

Vivino, F. B. (2017). Sjogren's Syndrome: Clinical Aspects. *Clin. Immunol.* 182, 48–54. doi:10.1016/j.clim.2017.04.005

Wang, H., Yin, Y. X., Gong, D. M., Hong, L. J., Wu, G., Jiang, Q., et al. (2019). Cathepsin B Inhibition Ameliorates Leukocyte-Endothelial Adhesion in the BTBR Mouse Model of Autism. *CNS Neurosci. Ther.* 25, 476–485. doi:10.1111/cns.13074

Wang, L., Main, K., Wang, H., Julien, O., and Dufour, A. (2021). Biochemical Tools for Tracking Proteolysis. *J. Proteome Res.* doi:10.1021/acs.jproteome.1c00289

Wei, J., Zheng, M., Liang, P., Wei, Y., Yin, X., Tang, Y., et al. (2013). Apolipoprotein E and its Mimetic Peptide Suppress Th1 and Th17 Responses in Experimental Autoimmune Encephalomyelitis. *Neurobiol. Dis.* 56, 59–65. doi:10.1016/j.nbd.2013.04.009

Wei, L., Wenjia, Z., Yuanhao, W., Yue, J., Lei, Z., Bin, L., et al. (2018). AB0020 Differentially Expressed Genes in Sjgren's Syndrome Microarray. *Ann. Rheum. Dis.* 77, 1213.1–1213. doi:10.1136/annrheumdis-2018-eular.6931

Zhou, L., Beuerman, R. W., Chan, C. M., Zhao, S. Z., Li, X. R., Yang, H., et al. (2009). Identification of Tear Fluid Biomarkers in Dry Eye Syndrome Using iTRAQ Quantitative Proteomics. *J. Proteome Res.* 8, 4889–4905. doi:10.1021/pr900686s

Zhou, Y., Zhou, B., Pache, L., Chang, M., Khodabakhshi, A. H., Tanaseichuk, O., et al. (2019). Metascape Provides a Biologist-Oriented Resource for the Analysis of Systems-Level Datasets. *Nat. Commun.* 10, 1523. doi:10.1038/s41467-019-09234-6

Conflict of Interest: The authors declare that the research was conducted in the absence of any commercial or financial relationships that could be construed as a potential conflict of interest.

Publisher's Note: All claims expressed in this article are solely those of the authors and do not necessarily represent those of their affiliated organizations, or those of the publisher, the editors, and the reviewers. Any product that may be evaluated in this article, or claim that may be made by its manufacturer, is not guaranteed or endorsed by the publisher.

frontiers in Pharmacology

ORIGINAL RESEARCH
published: 17 December 2021
doi: 10.3389/fphar.2021.778470

Soluble Epoxide Hydrolase Deletion Limits High-Fat Diet-Induced Inflammation

*Karen M. Wagner, Jun Yang, Christophe Morisseau and Bruce D. Hammock**

Department of Entomology and Nematology, UC Davis Comprehensive Cancer Center, University of California Davis, Davis, CA, United States

The soluble epoxide hydrolase (sEH) enzyme is a major regulator of bioactive lipids. The enzyme is highly expressed in liver and kidney and modulates levels of endogenous epoxy-fatty acids, which have pleiotropic biological effects including limiting inflammation, neuroinflammation, and hypertension. It has been hypothesized that inhibiting sEH has beneficial effects on limiting obesity and metabolic disease as well. There is a body of literature published on these effects, but typically only male subjects have been included. Here, we investigate the role of sEH in both male and female mice and use a global sEH knockout mouse model to compare the effects of diet and diet-induced obesity. The results demonstrate that sEH activity in the liver is modulated by high-fat diets more in male than in female mice. In addition, we characterized the sEH activity in high fat content tissues and demonstrated the influence of diet on levels of bioactive epoxy-fatty acids. The sEH KO animals had generally increased epoxy-fatty acids compared to wild-type mice but gained less body weight on higher-fat diets. Generally, proinflammatory prostaglandins and triglycerides were also lower in livers of sEH KO mice fed HFD. Thus, sEH activity, prostaglandins, and triglycerides increase in male mice on high-fat diet but are all limited by sEH ablation. Additionally, these changes also occur in female mice though at a different magnitude and are also improved by knockout of the sEH enzyme.

Keywords: soluble epoxide hydrolase, epoxy-fatty acids (EpFA), omega-3, brown adipose tissue, eicosanoids

OPEN ACCESS

Edited by:
Pallavi R. Devchand, University of Calgary, Canada

Reviewed by:
Soon Yew Tang, University of Pennsylvania, United States
Nicolas Flamand, Laval University, Canada

****Correspondence:***
Bruce D. Hammock
bdhammock@ucdavis.edu

Specialty section:
This article was submitted to Inflammation Pharmacology, a section of the journal Frontiers in Pharmacology

Received: *16 September 2021*
Accepted: *08 November 2021*
Published: *17 December 2021*

Citation:
Wagner KM, Yang J, Morisseau C and Hammock BD (2021) Soluble Epoxide Hydrolase Deletion Limits High-Fat Diet-Induced Inflammation. Front. Pharmacol. 12:778470. doi: 10.3389/fphar.2021.778470

1 INTRODUCTION

The soluble epoxide hydrolase (sEH) enzyme plays a role in physiology and pathophysiology by regulating several classes of bioactive lipids, particularly epoxy-fatty acids (EpFA), which are rapidly hydrolyzed by the sEH. There have been several indications that this enzyme has a role in metabolic disease and obesity (Anandan et al., 2011; Luria et al., 2011; Overby et al., 2020). A high-fat diet (HFD) is known to alter the microbiome and GI tract cancers where sEH plays a role (Zhang et al., 2013b; Wang et al., 2017) and substitutions with omega 3 fatty acids can also have significant effects (Zhang et al., 2013a). The sEH has been observed to increase in inflammatory conditions (Ren et al., 2016), and HFD induces inflammation (Duan et al., 2018) and is also hypothesized to induce central nervous system (CNS) inflammation (Guillemot-Legris et al., 2016). Inhibiting the sEH with small-molecule inhibitors (sEHI) has been found to promote brown adipogenesis and reduce triglycerides in preclinical obesity (Overby et al., 2020). Here, we employ sEH ablation with the global gene knockout (sEH KO) to explore the role of sEH in different dietary conditions with both female and male mice. There is a demonstrated sexual dimorphism in sEH activity and expression (Gill and

Hammock, 1980) (Pinot et al., 1995), and this may have biological consequences (Dewey et al., 2013; Vanella et al., 2015). Therefore, we investigated the role of sEH activity as it relates not only to differences in diet but also sex in preclinical species.

The sEH is the principal degradation path of epoxy-fatty acids (EpFA) formed from long chain polyunsaturated fatty acids (LC-PUFA) *via* cytochrome P450 activity. It has been previously determined that EpFA metabolites are the most dramatically altered lipid metabolites in adipose tissue from male mice (Wang et al., 2017). The epoxides of several classes of long chain fatty acids including linoleic acid (LA), arachidonic acid (ARA), docosahexaenoic acid (DHA), and alpha-linoleic acid (α-LA) were significantly altered in inguinal, gonadal adipose, and interscapular tissue in HFD male mice (Wang et al., 2017). Among the several studies of sEH in adipose tissue, the nomenclature is variable, and a clarification may be useful. Male rodents have been the most common sex used for experiments and therefore the gonadal white adipose tissue (WAT) is often described as the epididymal WAT. Because we include females in our studies, we identify these as gonadal WAT, which appears in some studies using males as well. Additionally, the inguinal white adipose tissue is subcutaneous rather than intraperitoneal fat and therefore takes either name. In our study, we chose to focus on the gonadal fat pad compared to other types of fat tissue and did not analyze inguinal WAT and therefore refer to the gonadal WAT by only the WAT acronym. Intrascapular fat is typically brown adipose tissue (BAT). There is on some occasion beige to white fat present, but in our samples, only the BAT was sampled. Thus, in our studies, we assessed WAT, BAT, brain, and liver, and these correspond to gonadal (epididymal) WAT and intrascapular adipose or iBAT in other studies.

Early investigations in male C57/B6 mice indicated that sEH expression in liver, kidney, and gonadal adipose as well as enzyme-specific activity did not alter between standard fat diet (SFD) and HFD fed animals (De Taeye et al., 2010). However, an increase in total activity (which may include other enzyme activity) from the gonadal WAT was observed in obese HFD mice. Another study demonstrated increased sEH activity in gonadal WAT of LDL receptor null mice fed an atherogenic diet (21% fat and 0.15% cholesterol) for 14 weeks measured using a fluorescent substrate assay (Shen et al., 2015). A caution is that the fluorescent assay used is sensitive to esterase activity and several other enzymes in addition to sEH (Jones et al., 2005). Unless the esterases are purified out or inhibited and glutathione depleted, other activities in tissues with this substrate are over 10-fold the sEH activity (Shihadih et al., 2020), leading to high risk of artifactual measurements. More recently, the lack of change in sEH expression in gonadal adipose in wild-type (WT) mice on HFD was corroborated (Wang et al., 2017). Additionally, a range of omega-3 ratio enriched diets (n3FD) maintaining fat content equal to standard chow did not alter sEH activity in murine liver from standard chow fed mice (Harris et al., 2016). The omega-3 enrichment has been proposed as an intervention for several disease-related pathologies including Alzheimer's disease as well as cardiovascular disease (Shinto et al., 2014; Hu et al., 2019). It has been hypothesized that either lowering the omega-6 content in diet or enriching the omega-3 could have beneficial effects in these pathological conditions (Simopoulos, 2008). Moreover, a combination of approaches, both inhibiting sEH and omega-3 diet enrichment, is most likely to significantly reduce inflammation by decreasing inflammatory prostanoids and increasing inflammation resolving epoxides of omega-3 lipids such as EPA and DHA. Thus, while there was no previous report of sEH expression alteration in WT mice fed HFD up to 20 weeks of diet consumption, there have been notable changes in body weight, adipose fat pads, and oxylipins and therefore we investigated enzyme activity by the more sensitive and selective radiometric assay (Borhan et al., 1995) in several target tissues.

2 MATERIALS AND METHODS

2.1 Animals

Experiments were conducted in accordance with the protocols approved by the Institutional Animal Care and Use Committee of the University of California. The soluble epoxide hydrolase KO mice on a C57/B6 background and the C57/B6 were maintained separately but housed in the same vivarium under identical conditions during the same time frame. Both soluble epoxide hydrolase KO mice and C57/B6 WT female and male mice (8 weeks old) were allowed to acclimate and then administered one of the following diets for 8 weeks: HFD (60 kcal% fat, purchased from Research Diet Inc., catalog number D12492), control diet (10 kcal% fat, D12450J from Research Diet Inc.) (http://www.researchdiets.com/opensourcediets/stock-diets/dio-series-diets), Omega-3 DHA enriched diet [Diet formulated by Research Diets, 15 kcal% fat, 6.25% of Solutex0365 (by weight)], or standard chow (Teklad Global 18% Protein Rodent Diet, 18 kcal % fat). The DHA diet was produced from Solutex oils with added t-BHQ and was vacuum packed under nitrogen and stored at −20°C. Female and male WT mice and sEH KO mice fed with all four diets were assessed; weight gain and chow consumption (per cage) were measured over the course of the study (**Supplementary Figure S1**). Tissues were sampled and immediately flash frozen at −80°C and later assessed for sEH activity liver triglycerides and oxylipin metabolites.

2.2 sEH Enzyme Activity

The enzymatic activity of sEH was measured using [^{3}H]-*trans*-diphenylpropene oxide (*t*DPPO) as a substrate following published methods (Borhan et al., 1995).

2.3 Triglyceride and Total Cholesterol

Tissue total triglyceride and total cholesterol were measured at the National Mouse Metabolic Phenotyping Center (MMPC) at UC Davis per their published protocols found at (https://www.mmpc.org/shared/protocols.aspx).

2.4 LC-MS/MS Lipid Analysis

Tissue homogenates were extracted and analyzed for a focused metabolite profile per previously published methods (Yang et al., 2009; Yang et al., 2019). Briefly for the extraction, 10 µl of

deuterated internal standard solution was added to the specified tissue samples and then 400 µl of cold methanol with 0.1% of acetic acid and 0.1% of butylate hydroxytoluene (BHT) was added to these tissue samples and stored at −80°C for 30 min. After freezing, samples were homogenized ball mills at 30 Hz for 10 min and then kept at −80°C overnight. The homogenates were centrifuged at 16,000 *g* for 10 min, the supernatants collected, and remaining pellets were washed with 100 µl of ice-cold methanol with 0.1% of acetic acid and 0.1% of BHT and centrifuged at 16,000 *g* for 10 min. The supernatants of each sample were combined and diluted with 2 ml of H_2O and loaded onto Waters Oasis HLB 3cc (Waters, Milford, MA) solid phase extraction (SPE) cartridges. The final concentrations of internal standards are 100 nM, which were obtained by spiking 10 µl of 500 nM solutions before extraction.

The samples were measured on a 1200 SL ultra-high performance liquid chromatography (UHPLC) (Agilent, Santa Clara, CA) interfaced with a 4,000 QTRAP mass spectrometer (Sciex, Redwood City, CA). The separation conditions for the LC were optimized to separate critical pairs of lipid mediators, which share the same multiple reaction monitor (MRM) transitions. In brief, separation was achieved on an Agilent Eclipse Plus C18 150 × 2.1 mm 1.8 µm column with mobile phases of water with 0.1% of acetic acid as mobile phase A and acetonitrile/methanol (84/16) with 0.1% of acetic acid as mobile phase B. All the parameters on the mass spectrometer were optimized with pure standards (purchased from Cayman Chemical, Ann Arbor, MI) under negative mode. The schedule MRM scan mode was employed to increase the sensitivity of the measurement.

2.5 Data Analysis

Data were analyzed using SigmaPlot software (San Jose, CA). All data are expressed as the mean ± standard error of the mean (SEM). When data were normally distributed, statistical significance was determined using ANOVA; otherwise, significance was determined by Mann–Whitney *U* test. *p*-values less than 0.05 are reported as statistically significant.

3 RESULTS

The expression and activity of sEH previously compared among select murine tissues demonstrates that activity follows a ratio of liver > kidney > WAT (epididymal) (De Taeye et al., 2010). We similarly observed relative ratios of high activity in the liver compared to adipose tissue. In these experiments, we also investigated BAT and observed a higher overall sEH activity level in BAT compared to WAT across diet groups present in both females and males.

3.1 sEH Activity

The sEH activity appeared to correlate with the different diet treatments across groups in WT mice. The low-fat diet (LFD, 10%) tended to have lower measured activity, particularly in WT females. The HFD (60%) group had the highest activity levels and demonstrated a sexual dimorphism with WT males having a more substantial increase in sEH activity. The n3FD tended to show the highest amount of variability in outcomes in all WT mice female and male but also demonstrated significant effects. We tested the sEH mice for both catalytic activity and the sEH protein to ensure that the line was a clear knockout. The line was originally derived on an S129 line (Sinal et al., 2000) but has since been backcrossed well over 10 generations on a C57/B6 background. These mice were tested for any residual activity and to confirm if there were any low levels of expression in the KO mice that could potentially be induced by the HFD. Thus, any changes in oxylipin profiles are unrelated to any modulated activity of any possible residual sEH message or protein in the KO mice.

Measured with a sensitive radioactive substrate assay, the sEH activity in liver gave the most dynamic and statistically significant change (**Figures 1A–D**). Interestingly, in our experiments, the LFD significantly lowered the sEH activity in WT female liver compared to standard diet (**Figure 1A**, two-way ANOVA, Holm–Sidak post hoc, $p = 0.034$, $n = 4$/group). Note that for all these data on sEH activity, sEH activity is expressed in units of both mg/protein and mg/tissue in **Supplementary Table S1**. No activity was measurable in the sEH KO females (**Figure 1A**, two-way ANOVA, all groups male and female pairwise, $n = 3$–4/group, $p = 0.687$). There was also an increase in sEH activity in liver related to high dietary fat with the HFD in males (1B, two-way ANOVA, Holm–Sidak post hoc, $p \leq 0.001$ HFD, $p = 0.006$ n3FD, $n = 3$–4/group) but not sEH KO males (**Figure 1B**). Overall, a significant difference was noted in activity in WT males compared to females across the different diets with males demonstrating higher sEH activity (one-way ANOVA, Dunn's method post hoc, $p \leq 0.001$, male vs. female, $n = 15$–16/sex). This result relates to previous data regarding the expression of the enzyme being higher in mature males compared to females (Gill and Hammock, 1980; Meijer et al., 1987). Interestingly, the sexual dimorphism in sEH activity in liver extended across all diets investigated in these experiments (two-way ANOVA, Holm–Sidak post hoc, $p \leq 0.001$ male versus female, $n = 3$–4/group per sex).

In BAT, the HFD and n3FD increased the sEH activity in females (**Figure 1C**) (one-way ANOVA, Dunnett's post hoc compared to SFD, $p \leq 0.001$ HFD, $p = 0.029$ n3FD, $n = 4$/group). However, there was no difference in diet treatment on sEH activity in males (**Figure 1D**, one-way ANOVA, Dunnett's post hoc $p = 0.277$, $n = 3$–4/group). Like the results in liver, there was no activity in the sEH KO animals, female or male (not depicted). Although the sexual dimorphism did not result in significant changes in lower-fat diets, the HFD increased the sEH activity in WT females compared to males (two-way ANOVA, Holm–Sidak post hoc, $p \leq 0.001$ female versus male, $n = 3$–4/group per sex).

In the gonadal WAT, there was no statistical difference in activity between the diets for females or males [one-way ANOVA compared to SD, $n = 3$–4/group both sexes, $p = 0.239$ females (1C), $p = 0.071$ males (1D)]. However, the sexual dimorphism in WT she activity in WAT was significant (two-way ANOVA, Holm–Sidak post hoc, $p = 0.014$ male versus female, $n = 3$–4/group per sex).

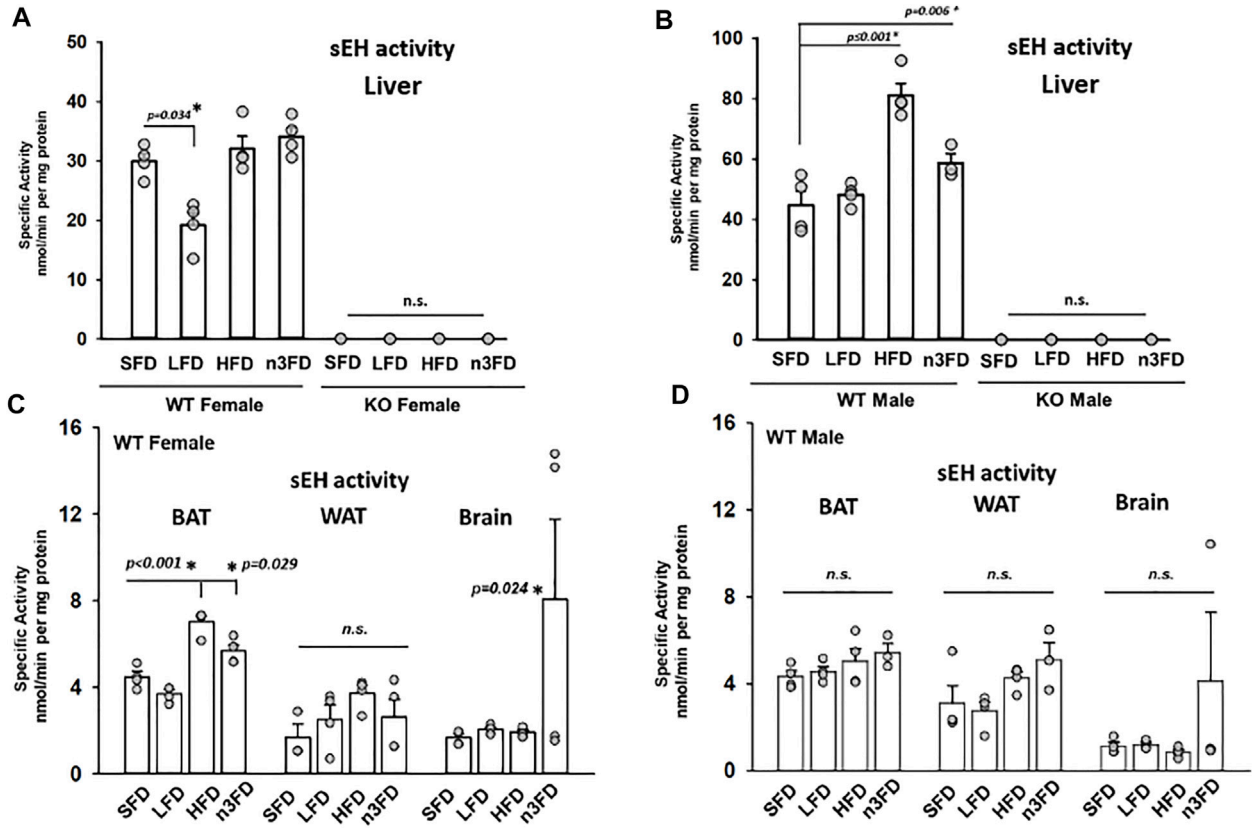

FIGURE 1 | sEH activity in liver is responsive to dietary interventions. **(A)** In WT female liver, the most significant change was a decrease in activity on the LFD (10% total fat) diet. The sEH KO females were assessed on each of the diets to confirm their status, and as predicted, there was no enzyme activity (scale adjusted for <1 nmol per mg protein). **(B)** In WT male, the sEH activity responded to 8 weeks of diet with the HFD and n3FDs inducing increased activity in liver. sEH KO males like the KO females showed no activity in the assay. In other high fat content tissues, the sEH activity modulated in response to diet. The sEH KO females and males were assayed as controls and again showed no activity and are not depicted. **(C)** The WT female mice demonstrated increased activity in scapular brown adipose tissue (BAT) on the HFD and n3FD, which have increased fat content compared to LFD and SFD. The gonadal white adipose tissue (WAT) was not significantly altered by diets; however, the n3FD diet significantly increased sEH activity in the brain despite variability within the group. **(D)** WT male mice did not have significant change induced in the sEH activity per the different diet interventions in any of the three high fat content tissues investigated. Similar to the female WT mice, there was high variation within the n3FD group and this in males resulted in no significant change.

Notably, in brain, sEH activity for both female and male WT groups showed a large population divergence on the n3FD and therefore no statistically significant changes between the sexes when compared with one-way ANOVA. This was an unanticipated amount of variability observed in the n3FD groups and speaks to the possibility of subpopulations in responding to the dietary changes that warrant further investigation. However, despite this variability, the n3FD diet did statistically increase the sEH activity in the WT female brain (**Figure 1C**, two-way ANOVA Holm–Sidak method post hoc, $p = 0.024$ n3FD vs. SD in females, $n = 3$–4/group). The sEH KO females and males showed no activity as expected (not depicted).

3.2 Body Weight

Notably, the body weights demonstrated the same change as the sEH activity in the WT female mice (**Figure 2A**). The weight of LFD WT female mice was significantly lower compared to the HFD after the 8-week treatment (two-way repeated measures ANOVA, Holm–Sidak post hoc, $p < 0.028$, $n = 4$/group). By day 45 and beyond, the HFD fed WT female mice had significantly increased body weight compared to all other diet groups (two-way repeated measures ANOVA, Holm–Sidak post hoc, $p < 0.001$, $n = 4$/group). The female sEH KO responded as well with the HFD increasing body weight significantly over the other three diet groups (**Figure 2B**, two-way repeated measures ANOVA, Holm–Sidak post hoc, $p < 0.002$–0.010 HDF vs. other diets $n = 3$/group). The body weight of WT male mice demonstrated the most significant increase on the HDF compared to the SFD treated for 8 weeks (**Figure 2C**). Despite the increased variability with the n3FD, WT males also significantly increased on n3FD compared to SFD (two-way repeated measures ANOVA, Holm–Sidak post hoc, $p < 0.001$, $n = 4$/group). Understandably, the weight of the male WT mice increased significantly compared to the WT females over time (two-way repeated measures ANOVA, Holm–Sidak post hoc, $p < 0.001$, $n = 4$/group).

The male sEH KO mice also responded to the 8 weeks of diet with the males showing significant increases in the HFD

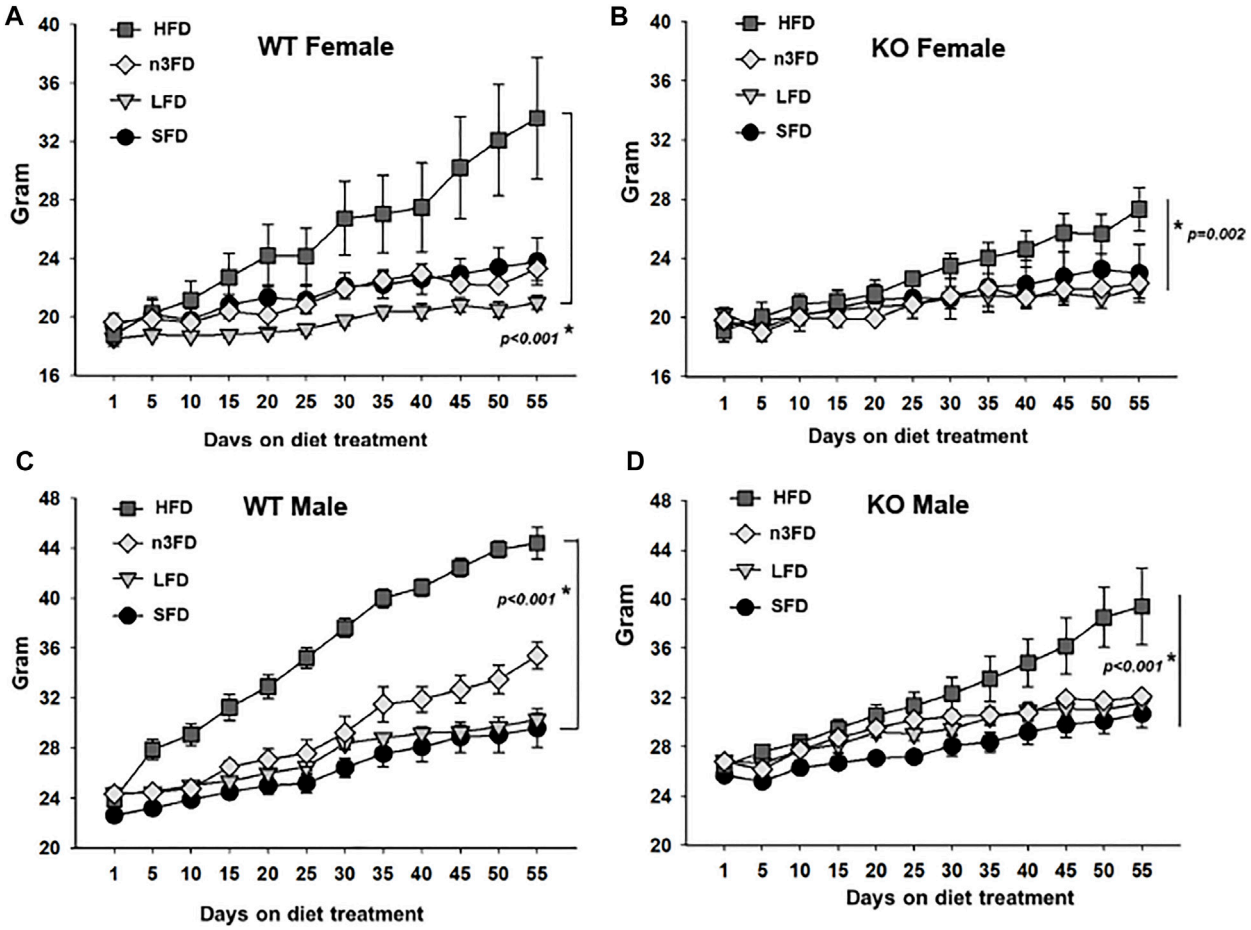

FIGURE 2 | sEH KO animals show less change than WT mice after 8 weeks of diet treatment. **(A)** WT females responded to the HFD with increased weight gain and also increased variability in weight, which was still significant to the LFD. **(B)** The sEH KO females also demonstrated a significant increase in body weight on the HFD; however, this was less than the change seen in WT mice. **(C)** WT males responded significantly to the HFD and understandably demonstrated a sexual dimorphism gaining more than WT females. They also outpaced the increase in body weight compared to sEH KO male mice. **(D)** The sEH KO males also responded to the HFD with significant body weight increases and were also increased over sEH KO females. Whole body weight for all animals is shown in grams.

compared to SFD, LFD, and n3FD diets (**Figure 2D**, two-way repeated measures ANOVA, Holm–Sidak post hoc, $p <$ 0.001–0.006 HDF 60% vs. other diets n = 3–4/group). The n3FD also increased male body weight compared to the SFD (p = 0.025). Similar to the WT mice, the male sEH KO mice increased in weight significantly compared to the females in all diets (two-way repeated measures ANOVA, Holm–Sidak post hoc, $p < 0.001$, n = 3–4/group).

When comparing the WT to sEH KO male mice, the WT males demonstrated a significant increase in body weight on the HFD [two-way repeated measures ANOVA, Holm–Sidak post hoc, $p = 0.011$ ($p < 0.001$ at Day 55), n = 3–4/group]. There were no significant differences when comparing WT female to sEH KO female mice on any diet (two-way repeated measures ANOVA, Holm–Sidak post hoc, p = 0.071–963, n = 3–4/group). Thus, the sexual dimorphism in body weight was the strongest relationship comparing all groups; however, significant increases with HFD in WT males compared to KO male mice demonstrated specifically the effect of sEH gene deletion.

3.3 Liver Triglyceride and Total Cholesterol

In the WT females, the HFD increased triglycerides (TG) significantly compared to the SFD and n3FD (**Figure 3A**, one-way ANOVA, Holm–Sidak post hoc, $p \leq 0.037$, n = 4/group). Interestingly, the diets did not induce any change in sEH KO females (3A, Kruskal–Wallis one-way ANOVA on Ranks, H = 7.777 with 3 degrees of freedom, $p = 0.051$, n = 4/group). In WT males, the liver TG increased with the HFD compared to all other diets (**Figure 3B**, one-way ANOVA, Holm Sidak post hoc, $p < 0.001$, n = 4/group). However, like the WT males, the sEH KO males responded to the HFD with significantly increased triglycerides compared to the SFD and n3FD (3B, one-way ANOVA, Holm–Sidak post hoc, $p \leq 0.038$, n = 3–4/group). Comparing the male to female TGs, WT males were significantly higher than WT females, but the sEH KO males were not significantly increased compared to the KO female groups (two-way ANOVA, Holm–Sidak post hoc, $p < 0.001$ WT, $p = 0.246$ sEH KO, n = 3–4/group). Importantly the KO males had significantly lower TG across diet groups compared to WT males (Kruskal–Wallis one-way ANOVA on Ranks, Dunn's post hoc,

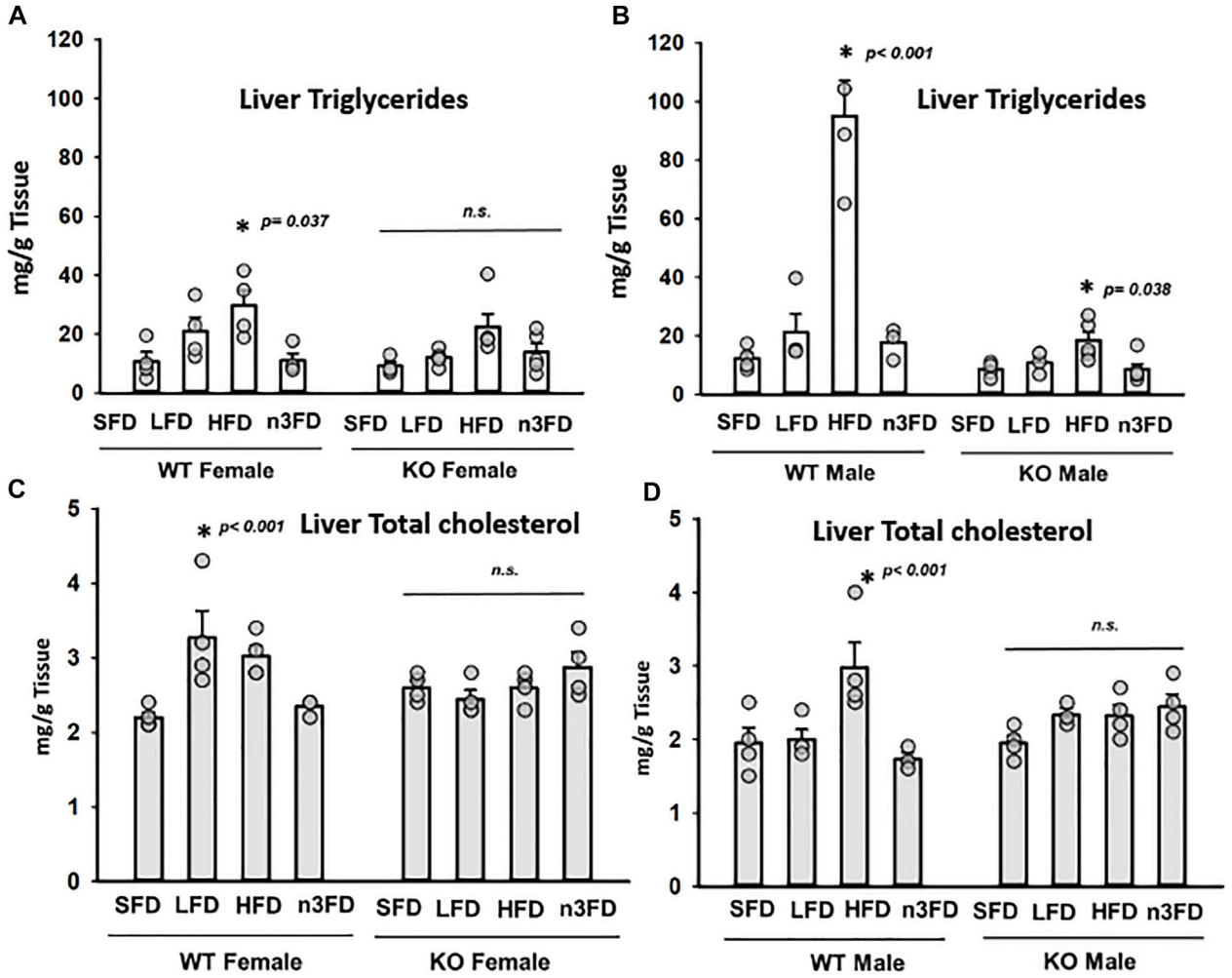

FIGURE 3 | Total triglyceride (TG) and total cholesterol (TC) levels in liver. **(A)** In WT females, the HFD significantly increased TG levels in liver. The sEH KO female mice demonstrated no significant change. In general, increased dietary fat content increased TG levels in both WT and sEH KO females; however, the n3FD-treated mice not responding despite the increased fat content compared to SFD and LFDs is noteworthy. **(B)** The WT males showed the greatest response to the HFD with increased TG levels. However, the sEH KO males also had a significant response to the HFD. Interestingly for TG levels, there was not a large sexual dimorphic difference in WT or sEH KO mice. **(C)** Total cholesterol did alter with increasing fat content in the diet in WT females although there was an increase on the LFD. The TC level appeared to increase on the n3FD in sEH KO females but did not reach statistical significance. **(D)** The WT males responded to the HFD with higher TC levels but the sEH KO males similar to the sEH KO females did not respond but tended to increase on the n3FD.

p = 0.002, n = 16–18/gene group). The female WT versus KO comparison was not significantly different with the same analysis (p = 0.380).

Total cholesterol (TC) in WT females varied from the TG results with the LFD demonstrating a significant increase compared to SFD (**Figure 3C**, Kruskal–Wallis one-way ANOVA on Ranks, p = 0.029, n = 4/group). Female KO lacked significant difference when compared across diets (3A, one-way ANOVA, Holm–Sidak post hoc, p = 0.423, n = 3–4/group). Similar to the TG results, the liver TC increased with the HFD in WT males compared to all diets (**Figure 3D**, one-way ANOVA, Holm Sidak post hoc, $p < 0.043$, n = 4/group). However, the TC levels in KO male mice lacked significant difference when compared across diets (3D, one-way ANOVA, Holm–Sidak post hoc, p = 0.054, n = 3–4/group). Comparing the TC in WT to sEH KO male mice revealed significant differences in the HFD (p = 0.005) and n3FD groups (p = 0.012) (two-way ANOVA, Holm–Sidak post hoc, n = 3–4/group). In WT females, the LFD (p = 0.006) and n3FD (p = 0.014) demonstrated significant increases in TC versus female KO (two-way ANOVA, Holm–Sidak post hoc, n = 4/group). WT females on the LFD also had higher TC than males (two-way ANOVA, Holm–Sidak post hoc, $p < 0.001$, n = 4/group). In the KO mice, the SFD and n3FD demonstrated differences in TC with males lower than females (two-way ANOVA, Holm–Sidak post hoc, p = 0.009 SFD, p = 0.007 n3FD, n = 4/group).

3.4 Oxylipins

3.4.1 EpFA

In liver (**Figure 4A**), the n3FD significantly reduced the EETs of all three regioisomers in female WT mice (two-way ANOVA,

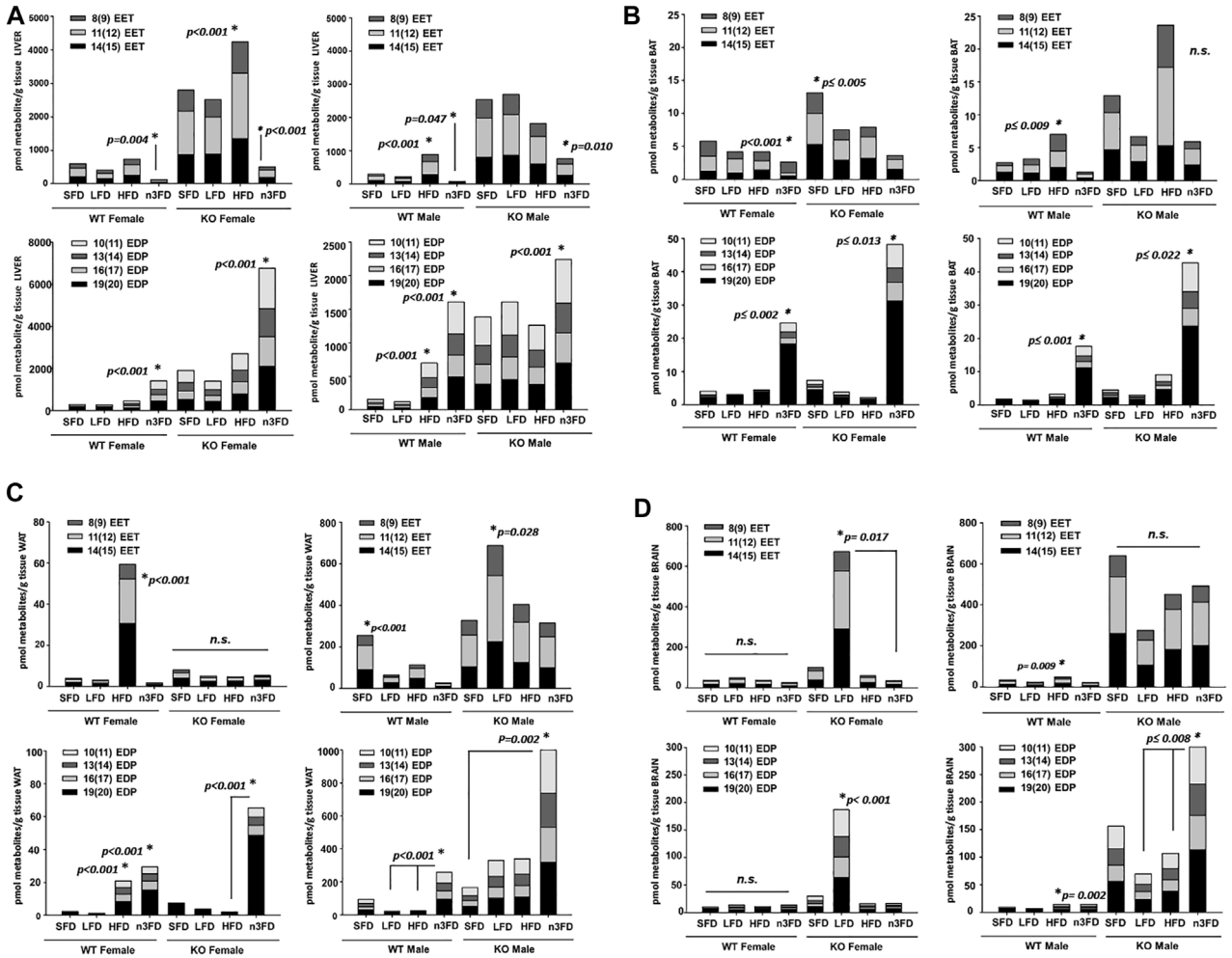

FIGURE 4 | Oxylipins respond class of fat diet and strongly to genotype. **(A)** Liver: Selected epoxy-fatty acids (EpFA) derived from arachidonic acid (EETs) and docosahexaenoic acid (EDPs) were analyzed for change due to dietary intervention and genotype. In liver, the EET levels in female WT mice were significantly decreased on the n3FD **(top left)**. This also occurred in the sEH KO females, which had decreased EETs on the n3FD but also increased EETs on the HFD. In WT males, the EETs increased on the HFD and decreased on the n3FD **(top right)**. In the sEH KO males, the n3FD decreased the EETs, therefore resulting in all groups decreasing in EETs on the n3FD. Then, assessing EDPs in liver, the n3FD significantly increased levels in WT females **(bottom left)**. This was also true for the sEH KO females where the significant increase in EDPs was several-fold increased compared to the WT. In WT male, the HFD as well as the n3FD significantly increased the EDP levels **(bottom right)**. The sEH KO males interestingly did not show an increase on the HFD but like the other groups had a significantly increased level of EDPs in the n3FD. **(B)** BAT: EETs decreased in n3FD-treated WT females in BAT **(top left)**. The sEH KO females had increased levels of EETs in BAT on the SFD compared to all other diets with the lowest level measured in the n3FD fed animals. The WT males, as with other tissues, had increased levels of EETs on the HFD and also low levels on the n3FD **(top right)**. In WT females, the EDP levels were significantly increased on the n3FD which also was the result in the sEH KO females **(bottom left)**. The WT males and sEH KO males both showed increases in EDP levels on the n3FD **(bottom right)**. It is important to note that although the amount of change within the BAT analysis in these cases was dynamic, the absolute amount of oxylipins in this tissue were comparatively low. **(C)** WAT: The WAT of WT females was impacted by the HFD with significant increases in EETs but little change in this class of oxylipin was seen on other diets **(top left)**. The sEH KO females displayed no change among diets. Notably, the absolute amount of oxylipins for all groups were low in female WAT compared to liver regardless of genotype. The WT males had increased levels of EETs on the SFD and also low levels on the n3FD **(top right)**. The sEH KO males had higher levels compared to WT males and significantly higher EETs on the LFD. The EDP metabolites were also significantly higher on the HFD in WT females, but these metabolites were also higher in mice on the n3FD **(bottom left)**. The sEH KO females demonstrated a greater amount of change in the EDPs, which were significantly increased on the n3FD. The sEH KO males were increased on the n3FD in WAT (notice scale, **bottom right**). The results of this tissue demonstrated a genotypic difference that was dependent on the sexual dimorphism resulting in higher oxylipins of both classes in male sEH KO animals. **(D)** Brain: The WT female had no significant change in brain EETs, and the sEH KO female mice demonstrated a large increase only in mice on the LFD. In the WT male the EETs increased significantly but less dramatically on the HFD **(top left)** and sEH KO males, despite the appearance in increase in SFD and HFD groups, had no significant change **(top right)**. The changes in EDP levels were not significant in WT females and sEH KO females again showed increase only on LFD **(bottom left)**. Increased EDPs were observed for male WT on HFD and for sEH KO mice on the n3FD **(bottom right)**.

Holm–Sidak post hoc, $p = 0.004$ female, $n = 4$/group). In KO females, the n3FD significantly lowered the liver concentrations of EET regioisomers and the HFD increased them (two-way ANOVA, Holm–Sidak post hoc, $p < 0.001$ n3FD and HFD, $n = 3$–4/group). WT males, like the WT females, had reduced EETs on the n3FD (two-way ANOVA, Holm–Sidak post hoc, $p = 0.047$

male, n = 4/group). KO males on the n3FD also decreased the EET regioisomers compared to the SFD and LFD (two-way ANOVA, Holm–Sidak post hoc, p = 0.010 SFD and LFD, n = 3–4/group). This is remarkable because the n3FD retains the 6.2% corn oil and has more fat content (15% total) than the LFD (10%). This is consistent with the ω-olefin of EPA and DHA being excellent substrates for cytochromes P450s that oxidize polyunsaturated lipids (Arnold et al., 2010).

The liver EDPs increased in WT females on the n3FD compared all other diets (two-way ANOVA, Holm–Sidak post hoc, $p < 0.001$, n = 3–4/group). The same increases of EDPs occurred in the sEH KO females on the n3FD (two-way ANOVA, Holm–Sidak post hoc, $p < 0.001$, n = 3–4/group). The WT males on the n3FD had higher EDP levels compared to all other diets. The HFD in WT males also increased the EDPs compared to the SFD and LFD (two-way ANOVA, Holm–Sidak post hoc, $p < 0.001$, n = 3–4/group in each case). In KO males the EDPs increased on the n3FD compared to the SFD and HFD (two-way ANOVA, Holm–Sidak post hoc, $p \leq 0.032$, n = 3–4/group). What is remarkable about the result is the difference in scale of EDPs in the liver between the female KO on the n3FD and the males. The total amount of EDPs in the female KO liver was 3-fold higher than the KO males while the WT were not significantly different between sexes (two-way ANOVA, Holm–Sidak post hoc, $p < 0.001$, n = 3–4/group). The KO females had increased EDPs on the n3FD and SFD compared to the corresponding WT of same sex and same diet (two-way ANOVA, Holm–Sidak post hoc, $p < 0.001$, n = 3–4/group). The KO males had increased EDPs on all diets different from WT males (two-way ANOVA, Holm–Sidak post hoc, $p \leq 0.048$, n = 3–4/group).

EETs in BAT (**Figure 4B**) significantly decreased on the n3FD in WT female (Kruskal–Wallis one-way ANOVA on Ranks, n3FD vs. HFD, $p < 0.001$, n = 3–4/group). KO females were higher than WT females overall and had the highest EET levels on the SFD (one-way ANOVA on Ranks, Holm–Sidak post hoc, SFD vs. LFD, HFD, n3FD, $p \leq 0.005$, n = 3–4/group). WT male demonstrated increases in EETs due to the HFD (Kruskal–Wallis one-way ANOVA on Ranks, HFD vs. SFD, n3FD, $p \leq 0.009$, n = 3–4/group). Surprisingly, the KO males showed increases in EETs but were not significant although they showed significant increases with HFD (Kruskal–Wallis one-way ANOVA on Ranks, Dunn's post hoc, p = 0.072, n = 3–4/group).

EDPs in WT females predictably increased on the n3FD (Kruskal–Wallis one-way ANOVA on Ranks, n3FD vs. SFD, HFD, n3FD, $p \leq 0.002$, n = 3–4/group) which was true for the KO female as well (Kruskal–Wallis one-way ANOVA on Ranks, Dunn's post hoc, n3FD vs. SFD, LFD, HFD, $p \leq 0.019$, n = 3–4/group). The WT male (Kruskal–Wallis one-way ANOVA on Ranks, Dunn's post hoc, n3FD vs. SFD, LFD, $p \leq 0.001$, n = 3–4/group) and sEH KO male both had higher EDPs on the n3FD as well (Kruskal–Wallis one-way ANOVA on Ranks, Dunn's post hoc, n3FD vs. LFD, $p \leq 0.022$, n = 3–4/group).

In WAT (**Figure 4C**), the EETs of all three included regioisomers increased in WT female on HFD (Kruskal–Wallis one-way ANOVA on Ranks, HFD vs. n3FD, LFD, $p \leq 0.001$, SFD, p = 0.003, n = 4/group). KO female had no significant change related to diet (p = 0.153). WT male had the highest levels on SFD (Kruskal–Wallis one-way ANOVA on Ranks, SFD vs. n3FD, LFD, $p \leq 0.031$, HFD vs. n3FD, p = 0.007, n = 4/group). The KO male EETs were higher than all other groups and had significantly higher levels on the LFD (Kruskal–Wallis one-way ANOVA on Ranks. SFD vs. LFD, p = 0.028).

The WAT EDPs were significantly higher on both the HFD and n3FD in WT female (Kruskal–Wallis one-way ANOVA on Ranks, Dunn's post hoc, n3FD vs. SFD and LFD, $p \leq 0.001$, HFD vs. SFD and LFD, $p \leq 0.001$, n = 4/group). In the KO female, the n3FD raised EDPs (Kruskal–Wallis one-way ANOVA on Ranks, Dunn's post hoc, n3FD vs. HFD, $p < 0.001$, vs. LFD and SFD, $p \leq 0.013$, n = 3–4/group). The WT male also had elevated EDPs on the n3FD (Kruskal–Wallis one-way ANOVA on Ranks, Dunn's post hoc, n3FD vs. HFD, LFD, $p \leq 0.001$, n = 4/group). However, the KO males had the largest increase in EDPs overall (Kruskal–Wallis one-way ANOVA on Ranks, Dunn's post hoc, n3FD vs. SFD, p = 0.002, n = 3–4/group).

In the brain (**Figure 4D**), EET levels in the WT females were not altered by the different diets (Kruskal–Wallis one-way ANOVA on Ranks, p = 0.104, n = 4/group). The female KO mice responded with a seemingly large increase in EETs on the LFD, which was significant compared to only the n3FD (Kruskal–Wallis one-way ANOVA on Ranks, Dunn's post hoc, n3FD vs. LFD, $p \leq 0.017$, n = 3–4/group). The WT male EETs increased on the HFD compared to both the n3FD and LFD, but overall, the levels were compared to the KO males (Kruskal–Wallis one-way ANOVA on Ranks, Dunn's post hoc, n3FD vs. LFD, $p \leq 0.009$, n = 3–4/group). The changes in male sEH KO EETs were not significant among the diet groups (p = 0.227 in same analysis) likely due to variability and the small n per group. However, these levels were nonetheless much higher than levels measured in WT animals.

The WT female EDPs did not change with the different diets (p = 0.132). The KO females, similar to the EETs results, had a large increase in EDPs on the LFD compared to other diets (two-way ANOVA, Holm–Sidak post hoc, $p < 0.001$, n = 3–4/group). The WT male EDPs increased in the HFD compared to both the n3FD and LFD (Kruskal–Wallis one-way ANOVA on Ranks, Dunn's post hoc, n3FD vs. LFD, $p \leq 0.002$, n = 3–4/group). However, again the change in EDPs for WT males was still folds lower than levels in the sEH KO males. In the sEH KO males, EDPs increased in response to the n3FD compared to both the LFD and HFD (Kruskal–Wallis one-way ANOVA on Ranks, Dunn's post hoc, n3FD vs. LFD, $p \leq 0.008$, n = 3–4/group) and the levels overall were much higher that WT animals and the KO females with the exception of the LFD effect in KO female. Numerical values for the averages ± SEM for individual regioisomers of the EpFA analyzed here are also reported in **Supplementary Table S2**.

3.4.2 Prostaglandins

The depicted prostaglandins are recognized as two of the most proinflammatory endogenous lipid metabolites. In the liver of WT mice, both female and male PGE_2 and PGD_2 increased on the HFD and decreased on the n3FD (**Figure 5A**, Kruskal–Wallis one-way ANOVA on Ranks, $p \leq 0.019$, n = 4/group female, p = 0.034, n = 4/group male). This was not the case in KO mice where

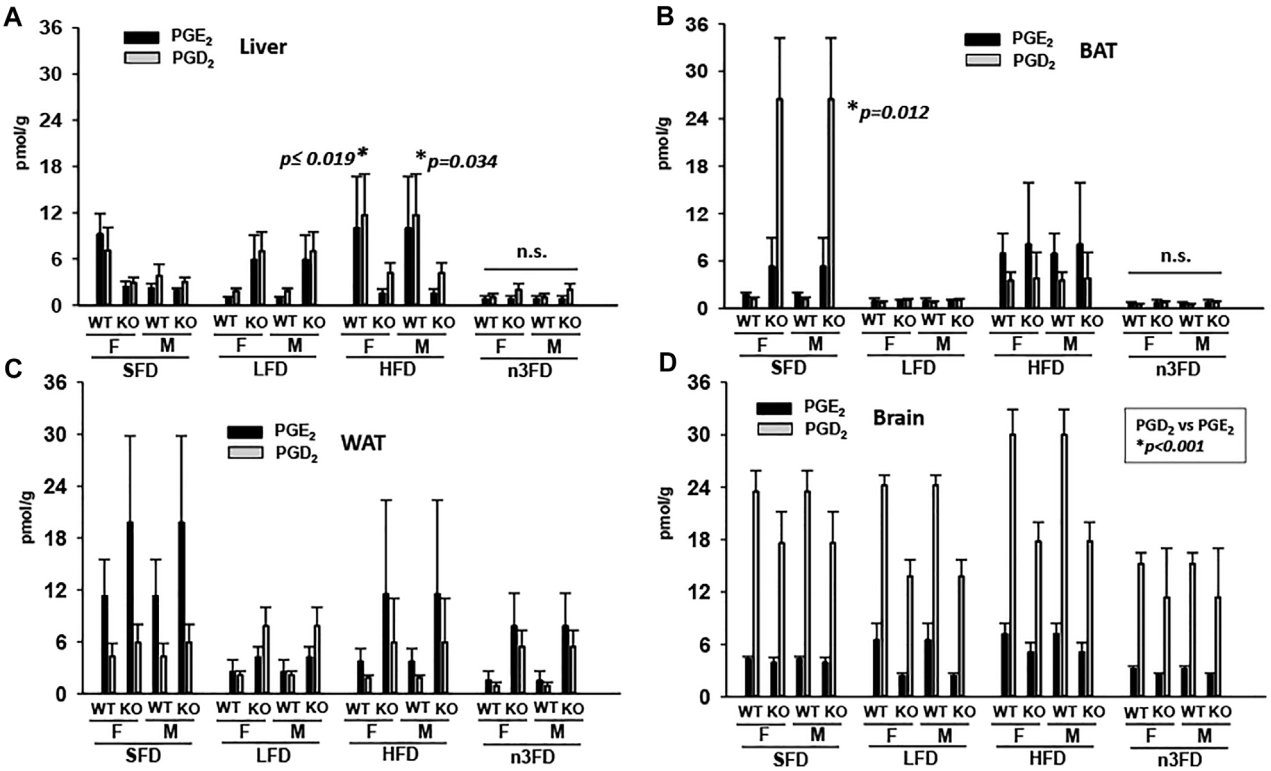

FIGURE 5 | Proinflammatory prostaglandins increase with HFD. **(A)** In liver PGE_2 and PGD_2 increase on HFD in mice of both sexes and genotype. **(B)** This is also the case in the BAT for mice with the notable difference that LFD and n3FD demonstrated decreased prostaglandins. **(C)** The WAT demonstrated the highest levels of prostaglandins, even on the SFD and these were lowered in LFD and n3FD especially in WT animals. **(D)** There was minimal change related to prostaglandins in the brain due to diet; however, large differences between the prostaglandin levels were observed.

prostaglandins in both female and male increased on the LFD compared to WT, though the KO mice also had lower levels in the n3FD. Overall, these prostaglandins were low in BAT especially on the LFD and n3FD in all mice. However, the SFD displayed increases in PGD2 levels in KO mice (**Figure 5B**, two-way ANOVA on Ranks, Holm–Sidak post hoc, $p = 0.012$, $n = 3$–4/group). The inflammatory prostaglandins increased in BAT with HFD in all mice compared to LFD and n3FD. The WAT (**Figure 5C**), showed the highest levels of the prostaglandins, which tended to be higher in sEH KO mice compared to WT mice but did not reach significance. In the brain (**Figure 5D**), there were slight decreases in PGE_2 in the sEH KO mice compared to WT on LFD and HFD. PGD_2 is known to be a more abundant prostaglandin in brain and understandably demonstrated much higher levels than PGE_2 (two-way ANOVA on Ranks, Holm–Sidak post hoc, PGD_2 vs. PGE_2 $p < 0.001$, $n = 3$–4/group). For numerical values for the averages ±SEM for these prostaglandins from cyclooxygenase metabolism, see **Supplementary Table S2**.

4 DISCUSSION

Several studies have laid the groundwork for the role of sEH in obesity. Protein expression levels of the phospholipases that liberate PUFAs from cellular membranes, the CYP enzymes that generate the EpFA substrates of sEH, sEH itself, and other enzymes in arms of the ARA cascade have been measured and correlated with inflammatory markers. These experiments have provided the information that sEH has a role in modulating the regulation of EpFA in obesity to improve health. The current study has furthered this demonstration, moving beyond the expression to the activity of sEH as a lipid-regulating enzyme in tissues with a high lipid content. An important outcome of these experiments is the demonstration of relative sEH activity in the adipose tissues compared to the brain and liver. Importantly, it also addresses the differences for female compared to male animals in all the included analyses. The liver remains the tissue with the highest sEH expression and activity, and the liver may play a role in physiopathology including in CNS diseases such as Alzheimer's disease (Estrada et al., 2019). This disease, in particular, has also demonstrated a sexual dimorphism (Fisher et al., 2018; Zhu et al., 2021) and an examination of lipid metabolism may yield information useful to determine the physiological consequences of imbalances that may coincide with or indicate susceptibility to disease states.

It is important to note when interpreting the results that few of the several studies investigating the role of sEH with dietary interventions follow identical experimental design. Some studies

have used HFD with 42–5% kcal from fat (De Taeye et al., 2010; Yang et al., 2021) compared to recent studies with HFD at 60% (Wang et al., 2017; Overby et al., 2020). Also, perhaps important for considering variability, the standard fat diets (standard chow) also vary depending on location and vendor from 12% (De Taeye et al., 2010), 13% (Lopez-Vicario et al., 2015), 14% (Yang et al., 2021), and 18% current studies. It is relevant in this scheme that the omega-3 enriched diet used here was a 15% fat diet that had equal amount of DHA and corn oil (omega-6 18:2), and thus is an enriched but at a standard fat level overall. The time interval of dietary intervention has varied from time intervals of 20 or 13 weeks (De Taeye et al., 2010) to 16 weeks (Lopez-Vicario et al., 2015) and 8 weeks (Wang et al., 2017; Overby et al., 2020). While the diet time interval has varied as widely as 5 weeks (Yang et al., 2021) to 5 months (Bettaieb et al., 2013), the studies have all been conducted in male animals. It is remarkable that none of these studies investigated female mice; thus, we have included them to elucidate changes due the difference in sex of the animals. Here, we also demonstrated the effect of diet in sEH knockout mice of both sexes.

4.1 sEH Activity

Increased sEH expression has been correlated with inflammatory pathology in the CNS (Ren et al., 2016; Hung et al., 2017) and cardiovascular system (Ai et al., 2009; Redina et al., 2017). In a previous study, significant change in sEH activity in adipose tissue was not observed. However, we note two important differences from this study compared to our current results. First, the HFD used in this study had a 42% kcal fat content compared to the 60% HFD used in several recent studies. Additionally, the lack of significant change in sEH enzyme activity in adipose tissue in male mice was observed in our current study as well; however, we did observe diet-induced change in male liver. Perhaps more impactful, we also observed significant change in sEH enzyme activity based on diet in the females.

Interestingly, the results demonstrated that LFD decreased sEH activity in the liver in WT females but showed no change on the HFD while the WT males responded to the HFD as well as n3FD with higher activity in the liver (**Figure 1**). The female WT mice appeared to be more affected by HFDs with increased sEH activity in BAT regardless of the class of fat (**Figure 1C**). Both the HFD and n3FD groups showed significantly increased activity in BAT compared to the lower fat content diets in WT females, and this was not true in the male WT mice. The fat content of the diets tended to increase activity in the WAT of both sexes but was limited and not significant likely given the variability for the small number of subjects. Remarkably, activity levels were low in both sexes compared to adipose tissues with the exception of the response to the n3FD. The n3FD significantly increased sEH activity in the WT females but not the males, though there was dynamic change for both sexes. Omega-3 fatty acids are preferentially taken up into the brain and it is possible that the sEH activity response in WT animals may correlate to subpopulations in the DHA transport system or even polymorphism in the sEH gene. There are perhaps many possible explanations for this variability, but they were not investigated with these experiments. The relationship of the n3FD diet to sEH activity in WT brain of both sexes did not result in substantially lower levels of the omega-3 metabolite EDPs in the brain of either sex. This effect was unanticipated and interesting that the variability occurred in both sexes; however, given the small number of individuals, it will need to be further explored.

The reduction in EpFA that is suggested to be due to lower expression of CYP enzymes (Wang et al., 2017) and increased she activity demonstrated here support the idea that inhibition of the sEH enzyme may be beneficial in controlling obesity. The EpFA have beneficial effects, which are limited due to their rapid degradation by sEH, which can their lower concentrations. The PUFA substrate availability to generate the EpFA, as well as the expression of both the phospholipases among other enzymes that liberate the substrates of sEH and the sEH expression itself remain unchanged (Wang et al., 2017). These observations illustrate that sEH inhibition may be the best approach for increasing the concentration of EpFA in these tissues to exert their beneficial effects. Inhibiting sEH is also beneficial by limiting diet-induced ER stress (Bettaieb et al., 2013), and decreasing diet-induced metabolic syndrome in obese rats (Iyer et al., 2012), renal injury in hypertensive obese rats (Imig et al., 2009), and endothelial disfunction in animal models (Zhang et al., 2011), among other biology.

The approach of sEH inhibition in obesity was investigated by Lopez-Vicario et al. (2015) using the fat-1 transgenic murine model. The fat-1 mice have a transgenic expression of a desaturase for omega-3 and enrich tissues with omega-3 PUFA. In this model using male mice, sEHI expanded brown adipose volume and limited ER stress as well as limiting hepatic steatosis. This suggested that sEH inhibition in combination with omega-3 enrichment is successful in countering the metabolic dysfunctions in obesity. This is supported by the data from our experiments that show that the effects of greatly increased EDP metabolites in sEH KO animals coincided with lower weight than WT animals on the same diet.

4.2 Body Weight

Overall, the body weights increased weight overtime as expected, with the greatest increased body weight on the HFD and a sexual dimorphism of males gaining more than females per genotype (**Figure 2**). As mentioned above, there was a noticeable effect of the diets between the WT and KO animals, which may indicate the role of sEH in weight gain and obesity in mice. It also supports data that showed the benefit of sEH inhibition to combat obesity. Interestingly, the WT male mice gained weight on the n3FD, which also correlated with higher sEH activity, though the diet itself has a lower percentage fat than the SFD.

Studies have suggested that sEH inhibition limits obesity and metabolic disease (Iyer et al., 2012; Xu et al., 2016) (Yang et al., 2021). In one such study, the administration of sEHI for 6 weeks did not alter male body weight once mice had been fed 8 weeks of HFD (Overby et al., 2020). Here, we demonstrate that sEH KO mice fed the diets for 8 weeks displayed less weight gain compared to WT mice of both sexes on HFD (**Figure 2**). Additionally, global knockout of the sEH enzyme was able to

limit weight gain in the HFD without any weight loss or changes to average gain over time (8 weeks) on the lower-fat diets. Thus, longer-term inhibition of sEH may hold benefits for limiting obesity. Moreover, here the male KO mice had lower TG levels compared to WT males while the TC levels were not significantly affected (**Figure 3**), which is similar to previous reported uses of sEHI (Overby et al., 2020), (Yang et al., 2021). This could be of importance as lower triglycerides have been related to improved outcomes in vascular dementia and cognitive decline (Parthasarathy et al., 2017).

4.3 Oxylipins

4.3.1 EpFA

In these experiments, we compared oxylipin levels with WT and the global sEH KO in both sexes. For the WT animals, the changes in liver oxylipins seemed to correlate with the sEH activity rather than appear as an inverse relationship. The WT females had lower sEH activity on LFD (**Figure 1**) as well as lower levels of EETs (**Figure 4A**). The WT males had higher sEH activity on HFD (**Figure 1C**) and had higher levels of EETs in liver (**Figure 4A**). EDPs also increased in liver of HFD fed WT males, which could occur due to the increased α-linolenic acid (precursor for DHA synthesis *in vivo*) in the soybean oil of this diet. This suggests that the overall dietary alteration affects more than sEH expression and the metabolism of EpFA. Interestingly, the previously investigated changes in gonadal adipose revealed changes of reduced cytochrome P450 gene expression (2J5, 2J6, and 2C44 isoforms) measured by PCR rather than a significant increase in sEH or phospholipase expression (Wang et al., 2017). Analysis of the fatty acid composition in this study demonstrated the gonadal fat pads consisted mostly of triglycerides, but the minimal levels of phospholipids present were not significantly altered by a 60% HFD. The authors concluded that the alteration of CYP expression was reduced and may have been impactful for EpFA levels, but change was due to a lack of PUFA substrates (Wang et al., 2017). Thus, the biosynthesis of EpFA may be impacted by diet as well. There are known sexual dimorphisms in both CYP450 expression, which mediates the biosynthesis of EpFA, and the expression of she, which degrades them. The results here with KO mice underscore the larger effects of sEH ablation compared to the WT sexual dimorphism in terms of EpFA levels. Other effects of diet were evident in liver with the n3FD reducing EETs in WT and sEH KO animals (**Figure 4A**) and greatly increasing EDPs in all animals (**Figure 4A**). However, more evident was the overall amount of oxylipin EpFA metabolites increasing in sEH KO mice compared to WT mice.

The scale of the differences between the WT and KO is remarkable and should be put into perspective. The global KO is of course more complete than a pharmacological intervention, but it does bring into perspective the advantages of small-molecule inhibition of sEH that balance the oxylipins in the desired manner. Overall, it was interesting to note that the most dynamic change in oxylipin concentrations was the amount of liver EDPs in female KO mice on the n3FD, which increased over all other diets in female KO, and was a greater absolute amount compared to male sEH KO and WT animals on all diets.

The BAT had overall lower levels of all depicted metabolites in both sexes and the knockout of sEH did not alter these levels as much as in other tissue types (**Figure 4B**). The change was most related to the fat type of the diet with the n3FD increasing EDPs and HFD increasing EETs levels in all mice more than genotype-related effects. In both WT females and males, the EET levels in BAT were robustly decreased on the n3FD. This compared to the effects in other adipose tissue where the fat content rather than type fat of the diet was more influential. In the WAT, the male WT EET levels were several-fold higher than WT females (note: scale differs between graphs) no matter which diet except the n3FD (**Figure 4C**). Also, there was a genotypic effect noticeable in the males with sEH KO levels higher in oxylipins compared to WT males. For the KO male compared to KO females, this was an even more striking increase in WAT EETs. The EDPs had a similar sex difference in WAT but with greater increases in EDPs on the n3FD comparatively. Interestingly, the females seemed to be influenced by the fat content of the diet with high levels of EETs for the WT female on HFD and high levels of EDPs for KO females on the n3FD.

The levels of EETs in brain were more comparable to the WAT for the WT males while the WT females had higher levels in brain than WAT (**Figure 4D**). An unexpected result was high levels of EET and EDP in the brain of LFD KO females. This seems to be an anomaly, but the methods were reviewed and in keeping with all other results. The WT males had very similar EET levels between the WAT and brain while the KO males had much lower EDP levels in brain than WAT.

The profound effect of sEH gene deletion on the EpFA is the most notable change and far exceed the changes due to sexual dimorphism within the genotype. Also remarkable are the effects of an omega-3 supplemented diet that exceeded the amount of change due to sexual dimorphism and was dynamic in lowering EET and increasing EDP metabolites in the liver in mice of both genetic backgrounds. Overall, the selected oxylipins were at the lowest levels in BAT and the BAT was the least affected by dietary change. The brain oxylipins were also not affected by dietary change but demonstrated more dynamic change based on sEH genotype with and also a sexual dimorphism among the sEH KO mice. The WAT oxylipin analysis demonstrated the largest sexual dimorphism in sEH KO mice overall. This of course indicates a mechanism that is in addition to the sexually dimorphic expression of sEH itself (Pinot et al., 1995) and should be explored in future experiments.

The relative success of inducing change in animals on HFD with sEH inhibitors has been previously described (Lopez-Vicario et al., 2015) and is not repeated here. Moreover, in support of previous data, our results demonstrate that there is increased sEH activity with higher fat content diets and that gene deletion can significantly increase EpFA metabolites. Small-molecule sEHI offer a potential to elicit similar effect as seen with gene deletion to preserve the EpFA allowing their beneficial actions. sEH inhibition has also been demonstrated to lower serum triglycerides (Overby et al., 2020), which is similar to results observed here in male mice where the sEH KO had lower TG than WT males. In our experiments, the liver triglycerides were significantly increased in HFD fed mice and liver TG levels

have the potential to be lowered by sEHI as they were with the sEH knockout.

4.3.2 Prostaglandins

Previous studies of prostaglandin (PG) oxylipins from WT male mice on HFD reported lower levels of PGE_2 in gonadal WAT and BAT (Wang et al., 2017). Our study agreed with the PGE_2 result in WAT from mice on HFD compared to SFD, but we observed an increased level of PGE_2 in the BAT of HFD fed WT and sEH KO males (**Figure 5B**). Moreover, in liver, both WT males and females responded with increased PGE_2 and PGD_2 levels on the HFD. Thus, our study supports the hypothesis that HFD is able to increase PG metabolite levels. The PG levels in liver of the sEH KO animals did not increase equally on HFD, with higher PGD_2 levels demonstrating a potential protective effect (Wang et al., 2021). The correlation of sEH ablation with lowering inflammatory metabolites relates to a recent finding using a 42% HFD where an sEHI in combination with select EpFA regioisomers limited NFKB activation in BAT in mice on HFD (Yang et al., 2021).

The same 60% HFD used here was previously administered for a longer duration (5 and 10 months) to male mice, which both increased sEH protein and induced endoplasmic reticulum stress (ER stress) in the liver and adipose tissue (Bettaieb et al., 2013). In our study, we found that the WT male mice on HFD have an increase in sEH-specific activity in liver as well. Interestingly, the WT females on HFD did not exhibit a similar increase in sEH activity. On the longer-term study, the male KO mice demonstrated attenuated hepatic ER Stress on both SFD and HFD (Bettaieb et al., 2013). Both genetic ablation and sEHI limited ER stress in the adipose tissue in the male mice (Bettaieb et al., 2013). Although the sEH enzyme activity did not increase in HFD fed WT females, it is still possible that the sEH ablation or inhibition could decrease the ER stress markers in female mice; however, this remains to be determined in future studies.

5. CONCLUSION

These experiments demonstrated the role of sEH in regulating EpFA and its response to alterations in dietary lipids. Despite the small number comprising the treatment groups and the inherent individual variability, significant changes resulted from the diet interventions in both male and female mice of both WT and sEH KO genetic backgrounds. This demonstrates the critical role of sEH in the regulation of lipid mediators and correlates with several health outcomes that have been investigated in other studies. Here, the impact of not only sEH inhibition but also diet supplementation is evident and demonstrates the potential for impacting health. It is important to consider that studies are conducted in humans and that both sexes are included, and we have demonstrated not only in absolute amount but also in changes in portions of metabolites that there are differences in the metabolism of lipid mediators between females and males not only related to the sEH enzyme.

DATA AVAILABILITY STATEMENT

The data presented in the study are deposited in the Dryad repository, and can be accessed via doi:10.5061/dryad.34tmpg4m4.

ETHICS STATEMENT

The animal study was reviewed and approved by the Institutional Animal Care and Use Committee of the University of California, Davis.

AUTHOR CONTRIBUTIONS

All in-life animal experiments, statistics, and manuscript preparation were completed by KW; the mass spectrometry analysis was completed by JY; the sEH enzyme activity assay was completed by CM; and BH and other co-authors edited the manuscript.

FUNDING

This study was supported by a RIVER grant from the National Institute of Environmental Health Sciences (NIEHS) Grant R35ES030443 and NIEHS Superfund Research Program P42 ES004699.

SUPPLEMENTARY MATERIAL

The Supplementary Material for this article can be found online at: https://www.frontiersin.org/articles/10.3389/fphar.2021.778470/full#supplementary-material

REFERENCES

Ai, D., Pang, W., Li, N., Xu, M., Jones, P. D., Yang, J., et al. (2009). Soluble Epoxide Hydrolase Plays an Essential Role in Angiotensin II-Induced Cardiac Hypertrophy. *Proc. Natl. Acad. Sci. U S A.* 106, 564–569. doi:10.1073/pnas.0811022106

Anandan, S. K., Webb, H. K., Chen, D., Wang, Y. X., Aavula, B. R., Cases, S., et al. (2011). 1-(1-Acetyl-piperidin-4-yl)-3-Adamantan-1-yl-urea (AR9281) as a Potent, Selective, and Orally Available Soluble Epoxide Hydrolase Inhibitor with Efficacy in Rodent Models of Hypertension and Dysglycemia. *Bioorg. Med. Chem. Lett.* 21, 983–988. doi:10.1016/j.bmcl.2010.12.042

Arnold, C., Markovic, M., Blossey, K., Wallukat, G., Fischer, R., Dechend, R., et al. (2010). Arachidonic Acid-Metabolizing Cytochrome P450 Enzymes Are Targets of {omega}-3 Fatty Acids. *J. Biol. Chem.* 285, 32720–32733. doi:10.1074/jbc.M110.118406

Bettaieb, A., Nagata, N., Aboubechara, D., Chahed, S., Morisseau, C., Hammock, B. D., et al. (2013). Soluble Epoxide Hydrolase Deficiency or Inhibition Attenuates

Diet-Induced Endoplasmic Reticulum Stress in Liver and Adipose Tissue. *J. Biol. Chem.* 288, 14189–14199. doi:10.1074/jbc.M113.458414

Borhan, B., Mebrahtu, T., Nazarian, S., Kurth, M. J., and Hammock, B. D. (1995). Improved Radiolabeled Substrates for Soluble Epoxide Hydrolase. *Anal. Biochem.* 231, 188–200. doi:10.1006/abio.1995.1520

De Taeye, B. M., Morisseau, C., Coyle, J., Covington, J. W., Luria, A., Yang, J., et al. (2010). Expression and Regulation of Soluble Epoxide Hydrolase in Adipose Tissue. *Obesity (Silver Spring)* 18, 489–498. doi:10.1038/oby.2009.227

Dewey, S., Lai, X., Witzmann, F. A., Sohal, M., and Gomes, A. V. (2013). Proteomic Analysis of Hearts from Akita Mice Suggests that Increases in Soluble Epoxide Hydrolase and Antioxidative Programming Are Key Changes in Early Stages of Diabetic Cardiomyopathy. *J. Proteome Res.* 12, 3920–3933. doi:10.1021/pr4004739

Duan, Y., Zeng, L., Zheng, C., Song, B., Li, F., Kong, X., et al. (2018). Inflammatory Links between High Fat Diets and Diseases. *Front. Immunol.* 9, 2649. doi:10.3389/fimmu.2018.02649

Estrada, L. D., Ahumada, P., Cabrera, D., and Arab, J. P. (2019). Liver Dysfunction as a Novel Player in Alzheimer's Progression: Looking outside the Brain. *Front. Aging Neurosci.* 11, 174. doi:10.3389/fnagi.2019.00174

Fisher, D. W., Bennett, D. A., and Dong, H. (2018). Sexual Dimorphism in Predisposition to Alzheimer's Disease. *Neurobiol. Aging* 70, 308–324. doi:10.1016/j.neurobiolaging.2018.04.004

Gill, S. S., and Hammock, B. D. (1980). Distribution and Properties of a Mammalian Soluble Epoxide Hydrase. *Biochem. Pharmacol.* 29, 389–395. doi:10.1016/0006-2952(80)90518-3

Guillemot-Legris, O., Masquelier, J., Everard, A., Cani, P. D., Alhouayek, M., and Muccioli, G. G. (2016). High-Fat Diet Feeding Differentially Affects the Development of Inflammation in the central Nervous System. *J. Neuroinflamm.* 13, 206. doi:10.1186/s12974-016-0666-8

Harris, T. R., Kodani, S., Yang, J., Imai, D. M., and Hammock, B. D. (2016). An ω-3-enriched Diet Alone Does Not Attenuate CCl4-Induced Hepatic Fibrosis. *J. Nutr. Biochem.* 38, 93–101. doi:10.1016/j.jnutbio.2016.08.010

Hu, Y., Hu, F. B., and Manson, J. E. (2019). Marine Omega-3 Supplementation and Cardiovascular Disease: An Updated Meta-Analysis of 13 Randomized Controlled Trials Involving 127 477 Participants. *J. Am. Heart Assoc.* 8, e013543. doi:10.1161/JAHA.119.013543

Hung, T. H., Shyue, S. K., Wu, C. H., Chen, C. C., Lin, C. C., Chang, C. F., et al. (2017). Deletion or Inhibition of Soluble Epoxide Hydrolase Protects against Brain Damage and Reduces Microglia-Mediated Neuroinflammation in Traumatic Brain Injury. *Oncotarget* 8, 103236–103260. doi:10.18632/oncotarget.21139

Imig, J. D., Carpenter, M. A., and Shaw, S. (2009). The Soluble Epoxide Hydrolase Inhibitor AR9281 Decreases Blood Pressure, Ameliorates Renal Injury and Improves Vascular Function in Hypertension. *Pharmaceuticals (Basel)* 2, 217–227. doi:10.3390/ph2030217

Iyer, A., Kauter, K., Alam, M. A., Hwang, S. H., Morisseau, C., Hammock, B. D., et al. (2012). Pharmacological Inhibition of Soluble Epoxide Hydrolase Ameliorates Diet-Induced Metabolic Syndrome in Rats. *Exp. Diabetes Res.* 2012, 758614. doi:10.1155/2012/758614

Jones, P. D., Wolf, N. M., Morisseau, C., Whetstone, P., Hock, B., and Hammock, B. D. (2005). Fluorescent Substrates for Soluble Epoxide Hydrolase and Application to Inhibition Studies. *Anal. Biochem.* 343, 66–75. doi:10.1016/j.ab.2005.03.041

López-Vicario, C., Alcaraz-Quiles, J., García-Alonso, V., Rius, B., Hwang, S. H., Titos, E., et al. (2015). Inhibition of Soluble Epoxide Hydrolase Modulates Inflammation and Autophagy in Obese Adipose Tissue and Liver: Role for omega-3 Epoxides. *Proc. Natl. Acad. Sci. U S A.* 112, 536–541. doi:10.1073/pnas.1422590112

Luria, A., Bettaieb, A., Xi, Y., Shieh, G. J., Liu, H. C., Inoue, H., et al. (2011). Soluble Epoxide Hydrolase Deficiency Alters Pancreatic Islet Size and Improves Glucose Homeostasis in a Model of Insulin Resistance. *Proc. Natl. Acad. Sci. U S A.* 108, 9038–9043. doi:10.1073/pnas.1103482108

Meijer, J., Lundqvist, G., and Depierre, J. W. (1987). Comparison of the Sex and Subcellular Distributions, Catalytic and Immunochemical Reactivities of Hepatic Epoxide Hydrolases in Seven Mammalian Species. *Eur. J. Biochem.* 167, 269–279. doi:10.1111/j.1432-1033.1987.tb13333.x

Overby, H., Yang, Y., Xu, X., Graham, K., Hildreth, K., Choi, S., et al. (2020). Soluble Epoxide Hydrolase Inhibition by T-TUCB Promotes Brown Adipogenesis and Reduces Serum Triglycerides in Diet-Induced Obesity. *Int. J. Mol. Sci.* 21, 7039. doi:10.3390/ijms21197039

Parthasarathy, V., Frazier, D. T., Bettcher, B. M., Jastrzab, L., Chao, L., Reed, B., et al. (2017). Triglycerides Are Negatively Correlated with Cognitive Function in Nondemented Aging Adults. *Neuropsychology* 31, 682–688. doi:10.1037/neu0000335

Pinot, F., Grant, D. F., Spearow, J. L., Parker, A. G., and Hammock, B. D. (1995). Differential Regulation of Soluble Epoxide Hydrolase by Clofibrate and Sexual Hormones in the Liver and Kidneys of Mice. *Biochem. Pharmacol.* 50, 501–508. doi:10.1016/0006-2952(95)00167-X

Redina, O. E., Abramova, T. O., Klimov, L. O., Ryazanova, M. A., Fedoseeva, L. A., Smolenskaya, S. E., et al. (2017). Soluble Epoxide Hydrolase (sEH) as a Potential Target for Arterial Hypertension Therapy. *Russ. J. Genet.* 53, 972–981. doi:10.1134/S1022795417080063

Ren, Q., Ma, M., Ishima, T., Morisseau, C., Yang, J., Wagner, K. M., et al. (2016). Gene Deficiency and Pharmacological Inhibition of Soluble Epoxide Hydrolase Confers Resilience to Repeated Social Defeat Stress. *Proc. Natl. Acad. Sci. U S A.* 113, E1944–E1952. doi:10.1073/pnas.1601532113

Shen, L., Peng, H., Peng, R., Fan, Q., Zhao, S., Xu, D., et al. (2015). Inhibition of Soluble Epoxide Hydrolase in Mice Promotes Reverse Cholesterol Transport and Regression of Atherosclerosis. *Atherosclerosis* 239, 557–565. doi:10.1016/j.atherosclerosis.2015.02.014

Shihadih, D. S., Harris, T. R., Kodani, S. D., Hwang, S. H., Lee, K. S. S., Mavangira, V., et al. (2020). Selection of Potent Inhibitors of Soluble Epoxide Hydrolase for Usage in Veterinary Medicine. *Front. Vet. Sci.* 7, 580. doi:10.3389/fvets.2020.00580

Shinto, L., Quinn, J., Montine, T., Dodge, H. H., Woodward, W., Baldauf-Wagner, S., et al. (2014). A Randomized Placebo-Controlled Pilot Trial of Omega-3 Fatty Acids and Alpha Lipoic Acid in Alzheimer's Disease. *J. Alzheimers Dis.* 38, 111–120. doi:10.3233/jad-130722

Simopoulos, A. P. (2008). The Importance of the omega-6/omega-3 Fatty Acid Ratio in Cardiovascular Disease and Other Chronic Diseases. *Exp. Biol. Med. (Maywood)* 233, 674–688. doi:10.3181/0711-mr-311

Sinal, C. J., Miyata, M., Tohkin, M., Nagata, K., Bend, J. R., and Gonzalez, F. J. (2000). Targeted Disruption of Soluble Epoxide Hydrolase Reveals a Role in Blood Pressure Regulation. *J. Biol. Chem.* 275, 40504–40510. doi:10.1074/jbc.M008106200

Vanella, L., Canestraro, M., Lee, C. R., Cao, J., Zeldin, D. C., Schwartzman, M. L., et al. (2015). Soluble Epoxide Hydrolase Null Mice Exhibit Female and Male Differences in Regulation of Vascular Homeostasis. *Prostaglandins Other Lipid Mediat.* 120, 139–147. doi:10.1016/j.prostaglandins.2015.04.004

Wang, W., Yang, J., Qi, W., Yang, H., Wang, C., Tan, B., et al. (2017). Lipidomic Profiling of High-Fat Diet-Induced Obesity in Mice: Importance of Cytochrome P450-Derived Fatty Acid Epoxides. *Obesity (Silver Spring)* 25, 132–140. doi:10.1002/oby.21692

Wang, W., Zhong, X., and Guo, J. (2021). Role of 2-Series Prostaglandins in the Pathogenesis of Type 2 Diabetes Mellitus and Non Alcoholic Fatty Liver Disease (Review). *Int. J. Mol. Med.* 47, 114. doi:10.3892/ijmm.2021.4947

Xu, X., Li, R., Chen, G., Hoopes, S. L., Zeldin, D. C., and Wang, D. W. (2016). The Role of Cytochrome P450 Epoxygenases, Soluble Epoxide Hydrolase, and Epoxyeicosatrienoic Acids in Metabolic Diseases. *Adv. Nutr.* 7, 1122–1128. doi:10.3945/an.116.012245

Yang, J., Schmelzer, K., Georgi, K., and Hammock, B. D. (2009). Quantitative Profiling Method for Oxylipin Metabolome by Liquid Chromatography Electrospray Ionization Tandem Mass Spectrometry. *Anal. Chem.* 81, 8085–8093. doi:10.1021/ac901282n

Yang, J., Bruun, D. A., Wang, C., Wan, D., Mcreynolds, C. B., Phu, K., et al. (2019). Lipidomes of Brain from Rats Acutely Intoxicated with Diisopropylfluorophosphate Identifies Potential Therapeutic Targets. *Toxicol. Appl. Pharmacol.* 382, 114749. doi:10.1016/j.taap.2019.114749

Yang, Y., Xu, X., Wu, H., Yang, J., Chen, J., Morisseau, C., et al. (2021). Differential Effects of 17,18-EEQ and 19,20-EDP Combined with Soluble Epoxide Hydrolase Inhibitor T-TUCB on Diet-Induced Obesity in Mice. *Int. J. Mol. Sci.* 22, 8267. doi:10.3390/ijms22158267

Zhang, L. N., Vincelette, J., Chen, D., Gless, R. D., Anandan, S. K., Rubanyi, G. M., et al. (2011). Inhibition of Soluble Epoxide Hydrolase Attenuates Endothelial Dysfunction in Animal Models of Diabetes, Obesity and Hypertension. *Eur. J. Pharmacol.* 654, 68–74. doi:10.1016/j.ejphar.2010.12.016

Zhang, G., Panigrahy, D., Mahakian, L. M., Yang, J., Liu, J. Y., Stephen Lee, K. S., et al. (2013a). Epoxy Metabolites of Docosahexaenoic Acid (DHA) Inhibit

Angiogenesis, Tumor Growth, and Metastasis. *Proc. Natl. Acad. Sci. U S A.* 110, 6530–6535. doi:10.1073/pnas.1304321110

Zhang, W., Liao, J., Li, H., Dong, H., Bai, H., Yang, A., et al. (2013b). Reduction of Inflammatory Bowel Disease-Induced Tumor Development in IL-10 Knockout Mice with Soluble Epoxide Hydrolase Gene Deficiency. *Mol. Carcinog.* 52, 726–738. doi:10.1002/mc.21918

Zhu, D., Montagne, A., and Zhao, Z. (2021). Alzheimer's Pathogenic Mechanisms and Underlying Sex Difference. *Cell Mol. Life Sci.* 78, 4907–4920. doi:10.1007/s00018-021-03830-w

Conflict of Interest: The authors declare that the research was conducted in the absence of any commercial or financial relationships that could be construed as a potential conflict of interest.

Publisher's Note: All claims expressed in this article are solely those of the authors and do not necessarily represent those of their affiliated organizations, or those of the publisher, the editors, and the reviewers. Any product that may be evaluated in this article, or claim that may be made by its manufacturer, is not guaranteed or endorsed by the publisher.

frontiers in Pharmacology

REVIEW
published: 22 December 2021
doi: 10.3389/fphar.2021.787541

Dysfunctional Vascular Endothelium as a Driver of Atherosclerosis: Emerging Insights Into Pathogenesis and Treatment

Steven R. Botts[1,2,3], *Jason E. Fish*[1,2,4,5] *and Kathryn L. Howe*[1,2,5,6]*

[1]Toronto General Hospital Research Institute, University Health Network, Toronto, ON, Canada, [2]Institute of Medical Science, University of Toronto, Toronto, ON, Canada, [3]Temerty Faculty of Medicine, University of Toronto, Toronto, ON, Canada, [4]Department of Laboratory Medicine and Pathobiology, University of Toronto, Toronto, ON, Canada, [5]Peter Munk Cardiac Centre, University Health Network, Toronto, ON, Canada, [6]Division of Vascular Surgery, Department of Surgery, University of Toronto, Toronto, ON, Canada

Atherosclerosis, the chronic accumulation of cholesterol-rich plaque within arteries, is associated with a broad spectrum of cardiovascular diseases including myocardial infarction, aortic aneurysm, peripheral vascular disease, and stroke. Atherosclerotic cardiovascular disease remains a leading cause of mortality in high-income countries and recent years have witnessed a notable increase in prevalence within low- and middle-income regions of the world. Considering this prominent and evolving global burden, there is a need to identify the cellular mechanisms that underlie the pathogenesis of atherosclerosis to discover novel therapeutic targets for preventing or mitigating its clinical sequelae. Despite decades of research, we still do not fully understand the complex cell-cell interactions that drive atherosclerosis, but new investigative approaches are rapidly shedding light on these essential mechanisms. The vascular endothelium resides at the interface of systemic circulation and the underlying vessel wall and plays an essential role in governing pathophysiological processes during atherogenesis. In this review, we present emerging evidence that implicates the activated endothelium as a driver of atherosclerosis by directing site-specificity of plaque formation and by promoting plaque development through intracellular processes, which regulate endothelial cell proliferation and turnover, metabolism, permeability, and plasticity. Moreover, we highlight novel mechanisms of intercellular communication by which endothelial cells modulate the activity of key vascular cell populations involved in atherogenesis, and discuss how endothelial cells contribute to resolution biology – a process that is dysregulated in advanced plaques. Finally, we describe important future directions for preclinical atherosclerosis research, including

OPEN ACCESS

Edited by:
Pallavi R. Devchand,
University of Calgary, Canada

Reviewed by:
Elisabetta Caiazzo,
University of Naples Federico II, Italy
Vaibhav B. Patel,
University of Calgary, Canada

***Correspondence:**
Kathryn L. Howe
kathryn.howe@uhn.ca

Specialty section:
This article was submitted to Inflammation Pharmacology, a section of the journal Frontiers in Pharmacology

Received: *01 October 2021*
Accepted: *06 December 2021*
Published: *22 December 2021*

Citation:
Botts SR, Fish JE and Howe KL (2021) Dysfunctional Vascular Endothelium as a Driver of Atherosclerosis: Emerging Insights Into Pathogenesis and Treatment. Front. Pharmacol. 12:787541. doi: 10.3389/fphar.2021.787541

Abbreviations: CD47, cluster of differentiation 47; CVD, cardiovascular disease; EC, endothelial cell; EndMT, endothelial-to-mesenchymal transition; eNOS, endothelial nitric oxide synthase; EV, extracellular vesicle; EZH2, enhancer of zeste homologue 2; ICAM-1, intercellular adhesion molecule-1; IL, interleukin; IL-1β, interleukin 1 beta; KLF2, Kruppel-like factor 2; LDL, low-density lipoprotein; NF-κB, nuclear factor kappa B; NLRP3, NOD like receptor family pyrin domain containing 3; oxLDL, oxidized low-density lipoprotein; RvD1, resolvin D1; SIRT1, sirtuin 1; SMC, smooth muscle cell; SPM, specialized proresolving mediator; TAZ, tafazzin; VCAM-1, vascular cell adhesion molecule 1; VE-cadherin, vascular endothelial-cadherin; YAP, yes-associated protein.

epigenetic and targeted therapies, to limit the progression of atherosclerosis in at-risk or affected patients.

Keywords: vascular endothelium, endothelial dysfunction, atherosclerosis, disturbed flow, endothelial-to-mesenchymal transition, extracellular vesicles, inflammation resolution, targeted therapy

INTRODUCTION: ATHEROSCLEROSIS AND ENDOTHELIAL DYSFUNCTION

Atherosclerosis is a chronic inflammatory process in which the accumulation of cholesterol-laden plaque restricts blood flow within the arterial vasculature. The occlusion of arteries by luminal encroachment of expanding plaque or emboli from plaque rupture underlies a spectrum of cardiovascular diseases (CVDs) including myocardial infarction, ischemic cardiomyopathy, stroke, and peripheral vascular disease. Although CVD has remained a leading cause of morbidity and mortality in high-income countries (Piepoli et al., 2016), an epidemiological shift has occurred in recent decades (Dai et al., 2020; Libby, 2021), where improvements in vaccination and treatment of infectious diseases have led to a notable increase in CVD prevalence within low- and middle-income nations. The prominent and evolving burden of atherosclerotic CVD has stimulated continued interest in the identification of cellular mechanisms that govern its pathogenesis, which may aid in the discovery of novel biomarkers and therapeutic targets for CVD prevention, detection, and treatment.

Endothelial cells (ECs) comprise the vascular endothelium, the inner lining of all blood vessels, which forms the interface between systemic circulation and underlying tissues. The quiescent or non-proliferating endothelium, once considered to be dormant outside the settings of vascular development or disease, is now understood to play an active role in maintaining vascular homeostasis by receiving and generating diverse biochemical (i.e., autocrine, paracrine, and endocrine) and mechanical signals (Cahill and Redmond, 2016; Ricard et al., 2021). The systemic functions of the endothelium are numerous, and include the provision of oxygen and nutrients to tissues, regulation of vascular tone and permeability, maintenance of hemostasis and coagulation, induction of angiogenesis, and coordination of the inflammatory response (Cahill and Redmond, 2016; Ricard et al., 2021). These essential processes are modulated by rich crosstalk between ECs and other vascular cell populations, including smooth muscle cells (SMCs), monocytes, and macrophages, which contribute to normal vascular function in physiological settings. Likewise, dysregulated communication between ECs and other vascular cell types is associated with vascular dysfunction and pathological remodeling in CVDs such as hypertension, atherosclerosis, and aneurysm (Jaipersad et al., 2014; Méndez-Barbero et al., 2021).

The pathophysiology of atherosclerosis begins with the perturbed endothelium and is mediated by a cascade of intra- and intercellular signaling events that shape the behaviour of cells within the vasculature (da Luz et al., 2018). Vascular ECs facilitate the active transport of low-density lipoprotein (LDL) to the subendothelial space through transcytosis pathways (Mundi et al., 2018), and LDL accumulation initiates a vascular inflammatory response. Early in atherosclerosis, the endothelium transitions from a quiescent to an activated state in response to proatherogenic stimuli, including oxidized LDL (oxLDL), proinflammatory cytokines, and disturbed flow (Cahill and Redmond, 2016; da Luz et al., 2018). In turn, the activated endothelium plays a critical role in the recruitment of inflammatory cells including T lymphocytes, neutrophils, and monocytes to the arterial intima, the first of which induces the adaptive immune response, and the latter of which gives rise to intimal macrophages (da Luz et al., 2018; Libby, 2021). Subsequent lipid engulfment by macrophages produces foam cells, which undergo necrosis and apoptosis to form the lipid core of the progressing atherosclerotic lesion. Vascular SMCs that comprise the medial layer of arteries migrate to the intima, form fibrous tissue through the production of collagen and elastin, and can also differentiate into macrophage-like foam cells in the developing plaque (Bennett et al., 2016). In this proatherogenic environment, communication between the endothelium and other vascular cell populations stimulates the release of proinflammatory signals, which augment local inflammation and contribute to sustained plaque progression. Intimal thickening occurs during plaque development and creates a hypoxic intraplaque environment, which stimulates angiogenesis of the vasa vasorum – adventitial blood vessels that supply larger arteries – and promotes neovascularization into the vascular wall (Jaipersad et al., 2014). Progressive thinning of the fibrous cap results from an inflammation-associated decrease in collagen synthesis and increase in degradation, which in combination with erosion of the endothelium, contributes to plaque rupture, thrombosis, and obstruction of the affected vessel (Libby, 2021). Although beyond the scope of this review, the role of endothelial dysfunction in plaque rupture (Bentzon et al., 2014; White et al., 2016), as well as the contribution to pathogenesis and the therapeutic potential of the vasa vasorum in treating atherosclerosis (Xu et al., 2015; Boyle et al., 2017; Sedding et al., 2018), has been previously discussed in detail. The pathophysiological relevance of the arterial endothelium has been similarly outlined (Cahill and Redmond, 2016; da Luz et al., 2018; Libby, 2021), however, the specific and modifiable intra- and intercellular mechanisms that mediate endothelial dysfunction and atherogenesis remain to be elucidated.

In this review, we present emerging studies that implicate the vascular endothelium as a driver of atherosclerotic CVD by directing site-specificity of plaque formation and governing plaque progression through intracellular processes. Furthermore, we highlight recent studies that describe intercellular communication between ECs and key vascular cell types involved in atherogenesis (**Figure 1**), and discuss how ECs participate in resolution biology during plaque

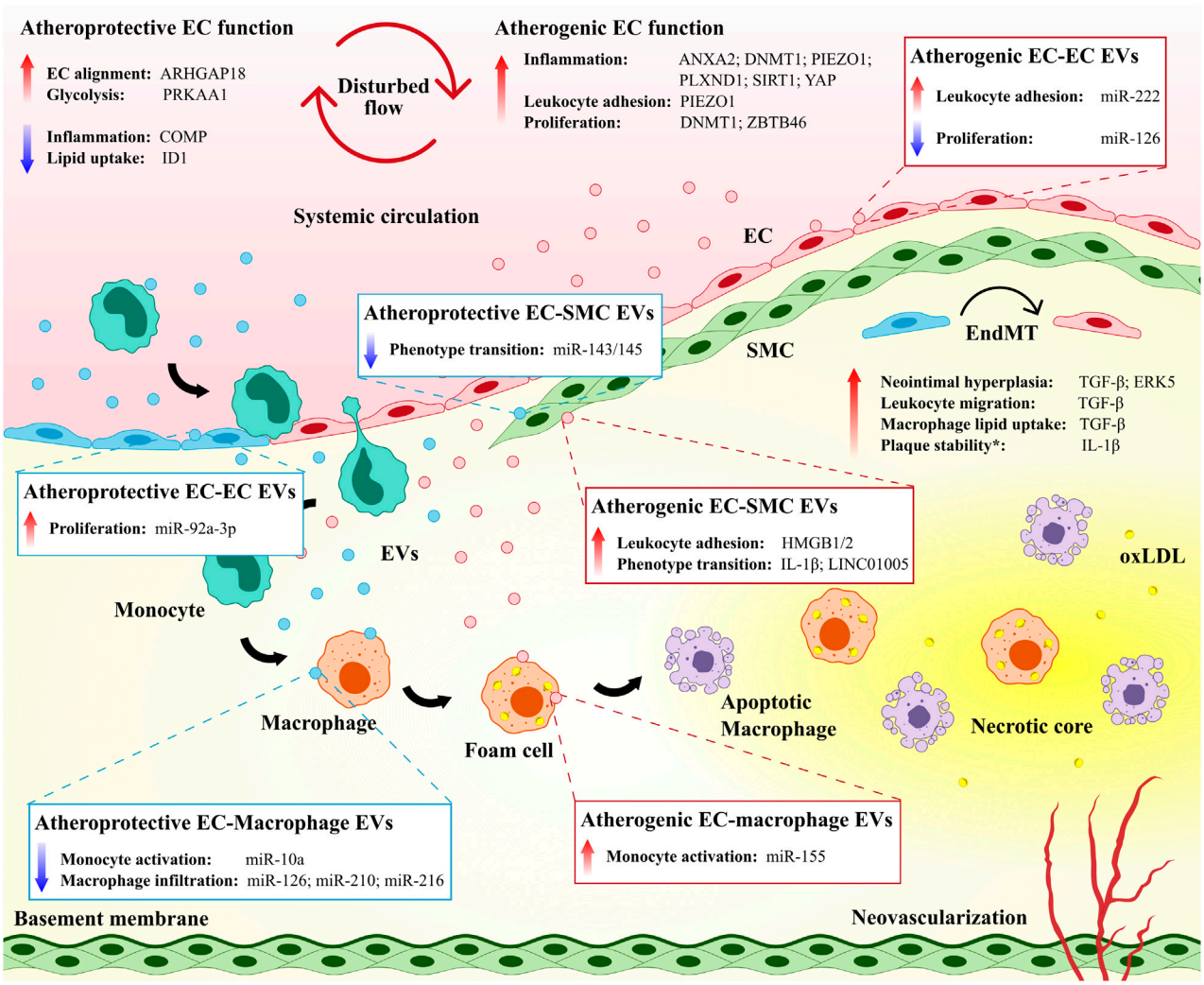

FIGURE 1 | The vascular endothelium directs site-specificity for plaque development and governs plaque progression. Both atheroprotective and atherogenic mechanisms are operative in endothelial cells (ECs) exposed to disturbed flow. EC-derived extracellular vesicles (EVs) mediate atheroprotective and atherogenic intercellular communication among ECs and between ECs and other immune and non-immune cell populations. Endothelial-to-mesenchymal transition (EndMT) contributes to the atherosclerotic disease process but may also maintain plaque stability.* ANXA2, annexin A2; ARHGAP18, Rho GTPase activating protein 18; COMP, cartilage oligomeric matrix protein; DNMT1, DNA methyltransferase 1; ERK5, extracellular signal-regulated kinase 5; HMGB1/2, high mobility group box protein 1/2; ID1, inhibitor of DNA binding 1; IL-1β, interleukin 1 beta; oxLDL, oxidized low-density lipoprotein; PLXND1, plexin D1; PRKAA1, protein kinase AMP-activated catalytic subunit alpha 1; SIRT1, sirtuin 1; SMC, smooth muscle cell; TGF-β, transforming growth factor beta; YAP, yes-associated protein; ZBTB46, zinc finger and BTB domain-containing protein 46.

development. Finally, we outline outstanding questions and future directions for atherosclerosis treatments, including epigenetic interventions and the targeted delivery of therapeutics to the activated endothelium to resolve vascular inflammation and limit atherosclerotic plaque progression.

ENDOTHELIAL CELLS GOVERN SITE-SPECIFICITY OF ATHEROGENESIS

The vascular endothelium is subjected to both tangential (i.e., shear stress) and circumferential forces (i.e., pulsatile stretch) that result from circulating blood flow. ECs at this interface convert mechanical stimuli to biochemical signals through mechanotransduction, which modulates key cellular processes in response to fluctuations in the vascular environment, including proliferation and turnover (Hahn and Schwartz, 2009; Nigro et al., 2011). The development of early atherosclerotic lesions is characteristically localized to regions of the vasculature where laminar blood flow is disturbed (e.g., arterial branch points and lesser curvatures of vessels) (Giddens et al., 1993; VanderLaan et al., 2004), which have previously been associated with decreased expression of endothelial nitric oxide synthase (eNOS) and increased nuclear

factor kappa B (NF-κB) activation (Hajra et al., 2000; Collins and Cybulsky, 2001; Won et al., 2007).

Flow Induces Atherogenic and Atheroprotective Responses in Endothelial Cells

In the setting of undisturbed laminar flow, nitric oxide (NO) is produced by elevated levels of eNOS in ECs and diffuses across cell membranes to modulate the activity of vascular cells, including SMCs and leukocytes (Pan, 2009). NO-mediated activation of soluble guanylate cyclase and S-nitrosylation has been observed to inhibit SMC proliferation (Ignarro et al., 2001), suppress EC inflammation (Matsushita et al., 2003; Kang-Decker et al., 2007), and regulate vascular tone, blood flow, and oxygen delivery to tissues (Stamler et al., 1997; Haldar and Stamler, 2013). Hydrogen sulfide, a gaseous signaling molecule and upstream regulator of NO, is similarly produced under laminar flow conditions (Huang et al., 2015) and has a critical role in reducing vascular inflammation (Zanardo et al., 2006), promoting antioxidative activity (Muzaffar et al., 2008), and limiting the formation of foam cells (Zhao et al., 2011). Laminar flow conditions have also been found to promote EC alignment (Hahn and Schwartz, 2009), and foster a reducing environment that limits oxidative stress (Berk, 2008), tumor necrosis factor α- and signal transducer and activator of transcription 3-induced inflammation (Ni et al., 2003; Yamawaki et al., 2003), and EC turnover via apoptosis (Pi et al., 2004). The transcription factor Kruppel-like factor 2 (KLF2) has emerged as a critical transcriptional mediator of vascular homeostasis that is induced under laminar shear stress and increases eNOS expression and represses adhesion proteins such as vascular cell adhesion molecule 1 (VCAM-1) and E-selectin (SenBanerjee et al., 2004; Berk, 2008), which are induced by NF-κB in regions of disturbed flow (Hajra et al., 2000; Collins and Cybulsky, 2001). In contrast to regions of laminar flow, altered hemodynamics in atheroprone regions has been associated with increased oxidative stress (Förstermann et al., 2017), reorganization of cytoskeletal and cell-cell junction proteins (Chong et al., 2013; Pfenniger et al., 2013), and enhanced senescence and turnover in ECs (Xu, 2009; Warboys et al., 2014). Curiously, hydrogen sulfide has been observed to impair dilation of coronary arteries by reducing NO production under disturbed flow (Chai et al., 2015), although hydrogen sulfide administration has also been shown to inhibit leukocyte adhesion to the endothelium in regions of shear stress by upregulating Akt/eNOS signaling (Go et al., 2012).

Recent studies continue to elucidate a plethora of EC regulatory pathways that induce a proinflammatory and proatherogenic phenotype in response to disturbed flow (Qu et al., 2020; Zhao et al., 2020; Xia et al., 2021) (**Figure 1**). The mechanosensitive cation channel Piezo1, though essential for coordinating vascular morphogenesis under physiological shear stress in embryogenesis and adulthood (Li J. et al., 2014), has been previously linked to altered flow-induced inflammation and leukocyte recruitment to the endothelium. Indeed, pathological activation of Piezo1 has been associated with induction of downstream integrin α5 and NF-κB pathways, which contributes to endothelial inflammation and the progression of murine atherosclerosis (Albarrán-Juárez et al., 2018), and elevation of intracellular calcium, which results in actin disruption and increased monocyte adhesion in cultured ECs (Swain and Liddle, 2020). Likewise, integrin α5β1-associated phosphorylation of yes-associated protein (YAP) by c-Abl kinase (Li B. et al., 2019), the coupling of integrin α5 to annexin A2 (Zhang C. et al., 2020), and the guidance receptor plexin D1, upstream of EC integrins (Mehta et al., 2020), have been identified as novel mechanisms for endothelial activation under oscillatory shear stress. In contrast, several EC processes confer *in vivo* protection against atherosclerosis under disturbed flow, including inhibition of integrin α5 by cartilage oligomeric matrix protein (Lv et al., 2021), increased glycolysis by protein kinase AMP-activated catalytic subunit alpha 1 (Yang et al., 2018), decreased lipid uptake by the transcription factor inhibitor of DNA binding 1 (Zhang K. et al., 2018), and increased EC alignment by Rho GTPase activating protein 18 (Lay et al., 2019). Many of these preclinical findings hold promise for the development of atherosclerosis treatments through pharmacological modulation of the endothelium (e.g., mitigating atherogenic responses or promoting atheroprotective functions in ECs). However, further investigation is required *in vitro* to determine the generalizability of endothelial responses between vascular cell models (e.g., shared and distinct behaviors of different EC lines under varying flow conditions) (Maurya et al., 2021), as well as *in vivo* to identify translatability in preclinical models and long-term safety and efficacy in individuals with CVD.

Flow-Mediated Transcriptional and Epigenetic Regulation Modulates Endothelial Proliferation and Turnover

Emerging evidence has also implicated disturbed blood flow in the dysregulation of EC proliferation and turnover during early atherosclerosis. Under physiological conditions, ECs that become senescent or apoptotic are replaced by the replication of neighboring cells, and more significant disruptions to the endothelium (e.g., during injury) are mitigated by circulating endothelial progenitor cells (Mannarino and Pirro, 2008). Atherosclerosis is characterized by cellular processes that promote EC turnover and induce proliferation of the activated endothelium (Xu, 2007). However, whether this proliferation is protective or detrimental has not been fully resolved. The mechanosensitive transcription factor zinc finger and BTB domain containing 46, for instance, inhibits proliferation in quiescent ECs and is downregulated by disturbed flow *in vitro* (Wang et al., 2019a). Hemodynamic signaling also impacts epigenetic pathways, and we have reviewed the impact of epigenetics on atherosclerosis elsewhere (Khyzha et al., 2017). For example, altered flow has been shown to induce DNA methyltransferase 1-mediated hypermethylation of the endothelium and its subsequent inhibition limits atherosclerosis via the cell cycle regulator cyclin A (Zhang et al., 2017). Furthermore, laminar flow-induced autophagy

and expression of the deacetylase sirtuin 1 (SIRT1) together inhibit Hippo/YAP signaling to attenuate atherosclerotic plaque formation (Yuan P. et al., 2020), and hypermethylation of eNOS promoter elements under chronic disturbed flow has been shown to contribute to repressed eNOS expression in wildtype mice (Ku et al., 2021).

Flow-sensitive microRNAs have also been identified as key modulators of endothelial proliferation and turnover in atherosclerosis (Kumar et al., 2019), including miR-126-5p, which has been shown to contribute to proliferative reserve in ECs and prevents plaque development through upregulation of Notch signaling (Schober et al., 2014). Curiously, increased expression of miR-126 has been found in atheroprone regions of the endothelium (Zhou et al., 2013). Furthermore, physiological flow conditions have also been observed to promote antiproliferative microRNA activity within the endothelium, whereby KLF2-induced miR-23b represses cyclin H to reduce activity of the cyclin-dependent kinase–activating kinase complex and limit cell cycle progression (Wang et al., 2014). The regulatory interplay of antagonistic, flow-sensitive microRNAs may serve as a mechanism for fine-tuning EC proliferation and warrants further characterization in both quiescent and activated endothelial states.

Perspectives for the Elucidation of Transcriptional and Epigenetic Regulation in Atherosclerosis

A robust characterization of the transcriptional and epigenetic regulatory elements that contribute to endothelial dysfunction has remained an important challenge for atherosclerosis research and has been recently addressed with next-generation approaches for global EC profiling. Of note, the integration of chromatin immunoprecipitation, chromatin accessibility, and RNA sequencing has enabled identification of diverse DNA regulatory elements associated with disturbed flow and proinflammatory activation (e.g., NF-κB and hypoxia inducible factor 1α, as well as ETS, zinc finger, and activator protein 1 transcription factor families) (Hogan et al., 2017; Bondareva et al., 2019; Alizada et al., 2021). Moreover, combined single-cell RNA sequencing and genome-wide chromatin accessibility assays have been used to profile the genome- and epigenome-wide changes associated with proatherogenic ECs under oscillatory shear stress (Andueza et al., 2020). Likewise, these technologies have allowed for characterization of EC heterogeneity in human atherosclerotic plaque (Depuydt et al., 2020) and identification of coronary artery disease-associated genetic variants in the open chromatin regions of activated ECs (Örd et al., 2021). The future integration of global EC profiling with functional assays will aid in the validation of putative modulators of atherogenesis, which may serve as prospective therapeutic targets for CVD treatment. Notably, real-time monitoring of the vascular endothelium has been enabled with organ-on-a-chip technologies (Sei et al., 2017), allowing for specific and quantifiable testing to elucidate the impact of environmental stimuli on endothelial function. Nevertheless, the complex cellular milieu of the atherosclerotic plaque remains difficult to fully model.

ALTERATIONS IN ENDOTHELIAL CELL METABOLISM CONTRIBUTE TO ATHEROGENESIS

Metabolic pathways prominently contribute to EC phenotypes in health and disease. Despite direct exposure to oxygen in the blood, ECs do not utilize oxidative phosphorylation as a primary means of energy production, perhaps because this might enhance oxidative stress and would hamper angiogenesis in hypoxic environments (Eelen et al., 2018). Instead, glycolysis serves as the primary method of energy delivery for ECs, in which 75–85% of ATP is generated via hexokinase 2-mediated phosphorylation of glucose to glucose-6-phosphate and conversion to lactate (Krützfeldt et al., 1990; De Bock et al., 2013; Yu et al., 2017). Fatty acid oxidation, used as a secondary source of energy by ECs, is modulated by carnitine palmitoyltransferase 1A-mediated shuttling of fatty acids to the mitochondria and ATP production via adenosine monophosphate activated protein kinase signaling (Dagher et al., 2001; Currie et al., 2013). Alternatively, fatty acids can be generated within ECs via fatty acid synthase, which has important functions for EC migration, permeability, and eNOS-mediated activity (Wei et al., 2011; Hagberg et al., 2013). Moreover, the proliferative and vasodilatory capacities of the endothelium can also be regulated by the metabolism of amino acids, in which inhibition of glutaminase-mediated conversion of glutamine to α-ketoglutarate represses angiogenesis (Kim B. et al., 2017), and the eNOS-induced conversion of arginine to NO controls vascular tone (Morris Jr, 2009).

Altered EC metabolism has been identified as both a consequence of, and a contributor to, endothelial dysfunction in atherosclerosis. In the quiescent endothelium, laminar shear stress reduces glucose uptake and glycolytic and mitochondrial activity in ECs via KLF2 (Doddaballapur et al., 2015). Conversely, in the diabetic and proatherogenic environment, elevated levels of circulating glucose induce the production of reactive oxygen species, DNA damage, and the accumulation of advanced glycation end products, which contribute to endothelial dysfunction via NF-κB signaling and increased vascular permeability (Theodorou and Boon, 2018). Disturbed flow similarly induces NF-κB and hypoxia inducible factor 1α expression, EC proliferation, and inflammation via upregulation of glycolytic enzymes (Feng et al., 2017), and can also promote EC activation and atherosclerosis through YAP/tafazzin (TAZ) signaling (Wang K.-C. et al., 2016; Wang et al., 2016 L.). Importantly, YAP/TAZ signaling has been shown to induce EC glycolysis, and glycolytic activity can in turn upregulate the YAP/TAZ pathway (Enzo et al., 2015; Bertero et al., 2016; Kim J. et al., 2017), which has been hypothesized to result in a cyclical and sustained pro-inflammatory response in the perturbed endothelium (Theodorou and Boon, 2018). Emerging preclinical studies propose altered EC metabolism as a therapeutic target for mitigating the development of atherosclerosis, including coenzyme Q10-mediated activation of the AMP-activated protein kinase-YAP-optic atrophy protein 1 pathway to promote mitochondrial function and energy metabolism (Xie et al., 2020), and inhibition of the

glycolytic regulator 6-phosphofructo-2-kinase/fructose-2,6-biphosphatase 3 to improve plaque stability in atheroprone mice (Poels et al., 2020). Although repressing glycolysis in the activated endothelium remains a promising strategy for treating patients with atherosclerotic CVD, consideration must be given to the complex interactions between genetics and environment (e.g., age, diet, diabetes, and cardiovascular fitness) that shape individual metabolic profiles to allow for patient-tailored therapies.

DISRUPTION OF ENDOTHELIAL BARRIER PROMOTES ATHEROSCLEROSIS

In its quiescent state, the vascular endothelium forms a semipermeable barrier between luminal and abluminal environments that allows for selective bidirectional movement of molecules via EC cell-cell junctions, vesicle-mediated transport within ECs, and diffusion between ECs or across endothelial gaps (Cahill and Redmond, 2016). In pioneering studies, LDL and other serum macromolecules were shown to enter the vessel wall using a paracellular route in permeable regions of the vasculature (Weinbaum et al., 1985; Lin et al., 1990). However, more recently, ECs have been implicated in the active transcytosis of LDL via caveolae, scavenger receptor B1, activin receptor-like kinase 1, LDL receptor, and high mobility group box protein 1, which contribute to the proinflammatory accumulation of LDL within the subendothelial space and promote atherogenesis (Zhang X. et al., 2018; Ghaffari et al., 2021). Loss of barrier function also potentiates atherosclerosis by facilitating leukocyte extravasation into the vessel wall through paracellular diapedesis from the vascular lumen, and may promote inflammatory infiltration through the vasa vasorum, contributing to subsequent plaque instability (Mulligan-Kehoe and Simons, 2014; Sluiter et al., 2021). Vascular insults including atherosclerosis, ischemia, and trauma are characterized by the accumulation of pathological proinflammatory mediators, which can induce acute (e.g., due to vascular injury) or chronic disruptions in endothelial permeability (e.g., due to plaque progression). Numerous mechanisms that underlie endothelial barrier disruption have been characterized, including protein kinase C-induced phosphorylation of cell junction proteins, which promotes actin reorganization and increased paracellular flux (Lum and Malik, 1996), and stimulation of myosin light chain kinase by inflammatory factors, which promotes EC retraction via actin-myosin network dynamics (Lum and Malik, 1996). Mediators including histamine, thrombin, and the proinflammatory cytokines interleukin (IL) 1 beta (IL-1β) and tumor necrosis factor α also increase permeability via modulation of tight junctions (e.g., zonula occludens 1 and occludins) and adhesion complexes (Lum and Malik, 1996). Furthermore, prolonged inflammation and oxidative stress can act to disrupt adherens junctions [e.g., vascular endothelial (VE)-cadherin] and gap junctions (e.g., connexins) via decreased NO (Komarova et al., 2017).

Emerging studies continue to uncover novel causal roles for established atherosclerosis mediators in the disruption of endothelial permeability. The mechanosensitive channel Piezo1, previously discussed as a coordinator of vascular structure and activator of integrin α5/NF-κB pathways, also promotes VE-cadherin degradation and increased vascular permeability under altered hemodynamics (Friedrich et al., 2019). Furthermore, the NOD like receptor family pyrin domain containing 3 (NLRP3) inflammasome, discussed in greater detail below as a therapeutic target for inflammation resolution in atherosclerosis, induces a loss of barrier in the diabetic vascular environment (Li X.-X. et al., 2019). Recent findings have also implicated the chemokine C–C motif ligand 8 in promoting atherosclerosis through enhanced permeability via NADPH oxidase 2 and reactive oxygen species (Xue et al., 2021), while the inhibition of insulin-like growth factor-1 signaling has been associated with disrupted endothelial barrier function *in vitro* and elevated atherosclerotic burden in mice (Higashi et al., 2020). The multifaceted roles of these atherogenic factors offer potential advantages for prospective therapies, which may simultaneously target multiple aspects of the atherosclerotic disease processes to limit plaque development (e.g., combined anti-inflammatory and pro-barrier effects of pharmacological agents that inhibit Piezo1 or NLRP3).

ENDOTHELIAL CELL PLASTICITY CONTRIBUTES TO THE ATHEROSCLEROTIC DISEASE PROCESS

The endothelium is an essential regulator of vascular homeostasis, defined as the balance of vascular injury and repair, and dynamic changes in endothelial phenotype can both potentiate and limit atherogenesis and associated complications (Bäck et al., 2019; Chen P.-Y. et al., 2020). In the setting of chronic inflammatory diseases, including atherosclerosis, ECs undergo complete or partial endothelial-to-mesenchymal transition (EndMT), during which they lose endothelial properties and gain mesenchymal cell characteristics (e.g., extracellular matrix production and contractile function) (Souilhol et al., 2018; Chen P.-Y. et al., 2020). EndMT is driven by proatherogenic stimuli including inflammation and disturbed flow (Chen et al., 2015) and early activation of transforming growth factor beta signaling (Ma et al., 2020), and has garnered interest as an important pathophysiological mechanism for atherosclerotic CVD. Indeed, previous work has linked EndMT to neointimal hyperplasia (Chen et al., 2015; Moonen et al., 2015), increased leukocyte migration (Evrard et al., 2016), lipid uptake by lesional macrophages (Chen et al., 2019), and oxidative stress (Evrard et al., 2016) in the developing plaque (**Figure 1**). Moreover, statin therapy (Li Y. et al., 2021), histone deacetylase inhibitors (Chen et al., 2021), and microRNA inhibition (Wu et al., 2021) have recently been investigated as potential strategies for limiting EndMT, the latter of which was observed to reduce plaque formation in atherosclerotic mice.

Perspectives for Future Investigation of Endothelial Plasticity

Future study is warranted to address several outstanding research areas in EndMT and atherosclerosis, including the

characterization of EndMT as a discrete versus continuous process, as well as the potential beneficial versus detrimental role of EndMT in plaque vulnerability. First, the proatherogenic endothelium has recently been shown to exist in a "metastable or partial" state of EndMT, where perturbed ECs perform both endothelial and mesenchymal functions (Helmke et al., 2019; Fledderus et al., 2021). The metastable nature of EndMT may be further elucidated with next-generation technologies that profile the atherosclerotic plaque and neighboring regions at the single-cell level, as recently used in studies of disturbed flow and endothelial reprogramming (Andueza et al., 2020) and diabetic atherogenesis (Zhao et al., 2021), as well as through the incorporation of computational models that predict endothelial activation and EndMT in various genetic and environmental conditions (Weinstein et al., 2020). Second, although augmentation of EndMT has previously been associated with increased plaque progression (Chen et al., 2015), emerging studies have highlighted a potential protective role of EndMT by maintaining plaque stability in the absence of SMC-derived myofibroblast-like cells (Evrard et al., 2016; Newman et al., 2021). Evidently, a more nuanced understanding of EndMT in the context of plaque development and rupture is required before therapeutic inhibition of EndMT is considered for the treatment of atherosclerotic CVD.

ENDOTHELIAL CELLS ARE KEY PLAYERS IN VASCULAR CELL-CELL COMMUNICATION DURING ATHEROSCLEROSIS

Vascular cell populations including ECs, monocytes, macrophages, and SMCs have well-established roles in driving atherosclerosis. ECs orchestrate the cellular interactions between these cell populations through the local expression of adhesion proteins and secretion of signaling molecules (Raines and Ferri, 2005; Liebner et al., 2006; Okamoto and Suzuki, 2017). The intercellular processes that mediate this pathophysiology have been a focus of previous studies, which have characterized EC-EC and EC-leukocyte communication via adherens junctions (e.g., VE-cadherin), tight junctions (e.g., junctional adhesion molecules), and other adhesion proteins including occludin, claudins, and platelet endothelial cell adhesion molecule (Liebner et al., 2006; Reglero-Real et al., 2016). Furthermore, a diverse group of EC-derived cytokines, chemokines, and other molecules (e.g., NO and endothelin-1) regulate vascular function by controlling proatherogenic processes such as leukocyte activation and SMC proliferation (Raines and Ferri, 2005; Gimbrone and García-Cardeña, 2016; Fledderus et al., 2021). Inflammatory cell recruitment to the activated endothelium is coordinated by the expression of EC adhesion proteins such as E-selectin, VCAM-1, and intercellular adhesion molecule-1 (ICAM-1), which facilitate leukocyte rolling and extravasation into the intimal layer, as well as the chemotactic factor monocyte chemoattractant protein-1, which attracts circulating monocytes, and the mitogen macrophage colony-stimulating factor, which stimulates monocyte proliferation and differentiation to intimal macrophages (Kleemann et al., 2008; Fledderus et al., 2021). Additionally, the proinflammatory polarization of macrophages has been associated with EndMT (Wu et al., 2017) and sprouting angiogenesis, the latter of which supports plaque progression through increased supply of oxygen and nutrients (Camaré et al., 2017; Graney et al., 2020). The developing atherosclerotic lesion is further characterized by intimal hyperplasia and neointimal formation, which are mediated by decreased production of EC-derived NO and a resultant increase in SMC proliferation, in conjunction with EndMT (Fledderus et al., 2021).

Extracellular Vesicles Mediate Paracrine Communication Between Endothelial Cells in Atheroprone and Atheroprotective Environments

In recent years, vascular cell-cell communication mediated by the secretion of extracellular vesicles (i.e., EVs; nano-sized packages of proteins, mRNAs, noncoding RNAs, and lipids) has emerged as an important research area for the pathogenesis and treatment of atherosclerosis (Charla et al., 2020; Chen Y.-T. et al., 2020; Wang H. et al., 2020). Three broad categories of EVs – exosomes (30–150 nm in diameter), microparticles (100 nm–1 μm in diameter), and apoptotic bodies (1–5 μm in diameter) – have been shown to modulate vascular function in atherogenesis via intercellular signaling among ECs, as well as between ECs and other immune and non-immune cell types (He et al., 2018; Li M. et al., 2018; Charla et al., 2020; Peng et al., 2020) (**Figure 1**). Within the vascular endothelium, EC-derived EVs with distinct microRNA content have been observed to both induce (Jansen et al., 2013; Arderiu et al., 2015) and inhibit angiogenesis (Ou et al., 2011; Liang et al., 2017, 2) via paracrine regulation of nearby ECs, whereby EVs fuse to recipient cells, and the release of EV-derived microRNAs allows for silencing of complementary mRNA targets. Moreover, the uptake of EC-secreted microparticles by neighboring ECs was shown to promote ICAM-1 expression and monocyte adhesion via miR-222 in diabetic conditions (Jansen et al., 2015), and EV-derived apoptotic bodies containing miR-126 were found to reduce macrophage content in plaque and limit atherosclerotic burden (Zernecke et al., 2009). The specific role of the proatherogenic environment in governing EV loading and function remains of interest for future study, and characterization of this environment has begun with exposure of donor ECs to proatherogenic stimuli (i.e., oxLDL and IL-6), which were observed to decrease thrombospondin 1 and increase angiogenesis in recipient ECs via EV-derived miR-92a-3p (Liu Y. et al., 2019).

Perturbed Intercellular Communication Between Endothelial Cells and Immune and Non-Immune Cells Potentiates Atherogenesis

Beyond the endothelium, EC-EVs regulate both immune and non-immune vascular cell populations involved in the

development of atherosclerosis (Li M. et al., 2018; He et al., 2018) and circulating EVs may have systemic effects at distant sites (Bär et al., 2019; Liu et al., 2021). Exosomal microRNAs mediate crosstalk between ECs and macrophages by suppressing (e.g., miR-10a) (Njock et al., 2015) or promoting monocyte activation (e.g., miR-155) (He et al., 2018), reducing macrophage infiltration, and delaying plaque progression (e.g., miR-126, miR-210, and miR-216) (Wang et al., 2019b). In turn, monocyte- and macrophage-derived EVs have been shown to induce EC apoptosis and promote murine atherosclerosis through elevated blood lipids, oxidative stress, and inflammation (Aharon et al., 2008; Li K. et al., 2021), as well as by reducing proliferation and angiogenesis in human coronary artery ECs via miR-503-5p (Wang et al., 2021). Reciprocal communication between cells of the vasculature has been similarly observed in ECs and SMCs, where EC-secreted EVs induce both atheroprone (Boyer et al., 2020; Yuan X. et al., 2020; Zhang Z. et al., 2020) and atheroprotective SMC phenotypes (Hergenreider et al., 2012; Xiang et al., 2021), while SMC-derived EVs govern endothelial migration under stimulation by platelet-derived growth factor (Heo et al., 2020) and can increase endothelial permeability and potentiate atherosclerosis via miR-155 (Zheng et al., 2017).

Perspectives for the Characterization of Circulating Extracellular Vesicles

EC-EVs that are secreted into systemic circulation may serve as biomarkers for CVD and have the potential to govern cell behaviour at distant areas of the vasculature, although definitive evidence for this regulation is lacking (Bär et al., 2019; Liu et al., 2021). Preliminary animal studies have demonstrated that microRNAs secreted by circulating blood cells, and presumably contained within EVs, can modulate SMC activity in atherogenesis (Shan et al., 2015) and have proapoptotic and antiproliferative effects on ECs (Chu et al., 2017). Further investigation is warranted to determine whether circulating EVs are present in sufficient quantities to elicit systemic effects in patients and if their regulatory functions extend to other CVDs (e.g., cardiac fibrosis and ischemic heart disease), as well as to identify the precise mechanisms by which circulating EVs promote vascular dysfunction in recipient cells. Notably, future study is also required to determine whether EVs undergo transcytosis or pass through intercellular or intracellular gaps to the subendothelial space and elicit direct effects on medial cells, or are endocytosed by ECs, which then serve as indirect mediators of altered vascular function. The continued integration of EV profiling in patients with atherosclerosis (i.e., local EVs in plaque; circulating EVs in plasma) with experimental models of EV activity will shed light on the causal role of EVs and EV-contents in the setting of atherosclerotic CVD. Such models will require the transition from *in vitro* co-culture towards *in vivo* tracking approaches to allow for a robust, physiological characterization of EV activity, which will be made possible with advances in the visualization of EV release and uptake (Durak-Kozica et al., 2018; Oesterreicher et al., 2020). With respect to the diagnostic potential of vascular EVs, the application of machine learning strategies to predict CVD from circulating EV biomarkers has garnered recent interest (Burrello et al., 2020; Castellani et al., 2020) and will likely play an important role in the development of precision cardiovascular medicine over the coming decades.

THE VASCULAR ENDOTHELIUM AS AN EMERGING THERAPEUTIC TARGET FOR ATHEROSCLEROSIS

Present therapeutic strategies to limit atherosclerosis and plaque rupture are broadly categorized as those which reduce atherosclerotic risk (e.g., lipid-lowering and antihypertensive agents) and those which prevent associated complications (e.g., antithrombotic agents) (Fledderus et al., 2021). Lipid-lowering therapies, including 3-hydroxy-3-methyl-glutaryl-coenzyme A reductase inhibitors (i.e., statins) and proprotein convertase subtilisin/kexin type 9 inhibitors, reduce circulating levels of LDL-cholesterol and thus oxLDL in the vessel wall, and decrease the incidence of severe events in CVD (Silverman et al., 2016; Mach et al., 2020), although these agents are not sufficient to prevent plaque formation (Tran-Dinh et al., 2013; Moss and Ramji, 2016). Moreover, a spectrum of anti-atherogenic effects of statins on the endothelium has been previously discussed in detail (Xu et al., 2021), and includes reduced inflammation through NF-κB blockade (Greenwood and Mason, 2007), inhibition of EC apoptosis via Janus kinase 2/signal transducer and activator of transcription 3 signaling (Wang K. et al., 2020), protection against EndMT via Kruppel-like factor 4/miR-483 (He et al., 2017), epigenetic modulation of ECs through histone modification (Mohammadzadeh et al., 2020), and increased NO production via hydrogen sulfide and eNOS (Citi et al., 2021; Xu et al., 2021). Notably, the statin-mediated mechanisms that contribute to elevated eNOS activity include increased eNOS transcription via KLF2 (Parmar et al., 2005), improved eNOS mRNA stability via polyadenylation (Kosmidou et al., 2007), and increased eNOS phosphorylation via phosphatidylinositol 3-kinase/Akt signaling (Kureishi et al., 2000). Other anti-atherogenic treatments have also been observed to mitigate endothelial dysfunction by increasing NO production, such as antihypertensive agents (e.g., angiotensin-converting enzyme inhibitors and angiotensin II receptor blockers) (Silva et al., 2019), antihyperglycemic drugs (e.g., insulin) (Muniyappa et al., 2008), and antioxidants (e.g., streptozotocin) (Varadharaj et al., 2017). In experimental settings, treatments for atherosclerosis have largely focused on antagonizing broad inflammatory pathways (e.g., IL-1β and 5-lipoxygenase) (Tardif et al., 2010; Ridker et al., 2017). Therapeutic agents that specifically target the perturbed endothelium to resolve inflammation and limit atherosclerosis, however, have not yet been fully realized in clinical studies (Fledderus et al., 2021).

Promoting Inflammation Resolution to Mitigate Atherosclerosis

The NLRP3 inflammasome is now recognized as a key player in the coordination of vascular inflammation and onset of atherogenesis (Duewell et al., 2010; Jin and Fu, 2019). NLRP3-

mediated induction of atherosclerosis has been associated with a host of causal factors including hypoxia (Folco et al., 2014), cholesterol crystals and oxLDL (Duewell et al., 2010), and disturbed flow (Xiao et al., 2013). Activation of NLRP3 subsequently leads to the maturation of proinflammatory cytokines (e.g., IL-1β and IL-18), increases the migration and lipid loading of macrophages (Li X. et al., 2014), and promotes pyroptosis, a proinflammatory form of programmed cell death that contributes to the release of additional inflammatory mediators (Bergsbaken et al., 2009). Therapeutic agents that directly inhibit the NLRP3 inflammasome, including the natural compound arglabin (Abderrazak et al., 2015), colchicine (Fernando et al., 2017), and the small molecule inhibitor MCC950 (van der Heijden et al., 2017), have been shown to ameliorate endothelial inflammation and atherosclerosis in preclinical studies. Moreover, adjunct colchicine therapy has entered clinical trials for repressing vascular inflammation in acute coronary syndrome (Bouabdallaoui et al., 2020) and coronary artery disease (Nidorf et al., 2013; Kajikawa et al., 2019; Hays et al., 2021). Previous trials have employed several outcomes related to improved cardiovascular health, including CVD endpoints, serum inflammatory markers, and proxy measures for endothelial dysfunction including flow-mediated vasodilation and exercise-induced coronary blood flow. Although the latter two of these measures remain the gold standard for clinical assessment of the perturbed endothelium (Flammer et al., 2012; Xu et al., 2021), they rely on endothelial responsiveness to vasodilatory or vasoconstrictive manipulation and do not adequately capture changes in EC phenotype during atherogenesis (e.g., permeability, metabolism, EndMT, or intercellular communication). Emerging studies have begun to address this limitation by applying machine learning techniques to predict CVD events from clinical data, CT imaging, and circulating biomarkers, including matrix metalloproteinase 9 and polymeric immunoglobulin receptor (Tamarappoo et al., 2021), very low-density lipoprotein and leucine (Coelewij et al., 2021), and serum EVs (Burrello et al., 2020; Castellani et al., 2020). Alongside functional assessment of the endothelium, robust models for CVD prediction have the potential to identify subclinical disease (Coelewij et al., 2021), aid in risk stratification, and inform treatment and prevention strategies.

Recent studies have also highlighted the potential of endogenous specialized proresolving mediators (SPMs) as anti-inflammatory therapies for limiting endothelial inflammation in CVD (Fredman and Tabas, 2017; Xu et al., 2021). Resolvin D1 (RvD1) belongs to a family of SPMs formed from metabolic processing of polyunsaturated docosahexaenoic acid and eicosapentaenoic acid, and is synthesized by ECs under proinflammatory conditions including stimulation with oxLDL (Dufour et al., 2018). Treatment of ECs with RvD1 has been observed to repress lipopolysaccharide- and cholesterol crystal-stimulated EC-monocyte interactions *in vitro* by downregulating NFκB-ICAM-1/VCAM-1 signaling (Chattopadhyay et al., 2018; Pichavaram et al., 2019), and attenuates leukocyte trafficking to the endothelium in mice fed a cholesterol rich diet (Pichavaram et al., 2019). Beyond the resolvin family, the SPMs maresin 1 and lipoxin A4 have likewise been observed to disrupt leukocyte adhesion to activated ECs (Filep et al., 1999; Chatterjee et al., 2014), suggesting that endogenous production or exogenous administration of diverse SPM metabolites may have therapeutic benefits for limiting endothelial activation in the setting of atherosclerosis.

Notably, the potential therapeutic impact of promoting inflammation resolution through efferocytosis (i.e., the clearing of apoptotic cells) is being established with preclinical studies, wherein atherosclerotic plaque progression has been attenuated by proefferocytic cluster of differentiation 47 (CD47)-blocking therapies (Kojima et al., 2016; Flores et al., 2020) or activation of the macrophage cell surface receptor MER proto-oncogene, tyrosine kinase (Thorp et al., 2008; Cai et al., 2018). While these effects appear to be mediated by lesional macrophages, ECs could facilitate the transport of inflammation resolving agents to cells within the developing plaque. Indeed, a proefferocytic and anti-atherosclerotic nanoparticle therapy has been previously hypothesized to function by uptake within circulating monocytes or delivery to macrophages within the intima (Flores et al., 2020), the latter of which would require the monocyte-independent transport of nanoparticles across the endothelium. In this role, ECs may contribute to therapeutic delivery by modulating vascular permeability and trafficking nanoparticles to macrophages via EC-secreted EVs. Clinically, the promise of inflammation resolving strategies has been highlighted in a subset of patients enrolled in a phase 1b-2 trial of the proefferocytic anti-CD47 antibody magrolimab for treating B-cell non-Hodgkin's lymphoma, where vascular inflammation was significantly reduced in the carotid arteries of patients with CVD after 9 weeks of treatment (Jarr et al., 2021).

Epigenetic Interventions to Limit Atherosclerotic Plaque Progression

Epigenetic interventions allow for broad targeting of the diverse mechanisms underlying endothelial dysfunction and have shown recent promise as anti-atherosclerotic therapies (Fledderus et al., 2021). The methyltransferase enhancer of zeste homologue 2 (EZH2) and histone deacetylase SIRT1 respectively induce and limit endothelial dysfunction in murine models of CVD (Zhou et al., 2011; Lv et al., 2016) and represent novel avenues for epigenetic treatment. EZH2 antagonism and SIRT1 agonism similarly increase NO production (Gracia-Sancho et al., 2010; Kumar et al., 2013) and decrease EC activation (Zhou et al., 2011; Wang J. et al., 2020) and EndMT (Maleszewska et al., 2016; Liu Z.-H. et al., 2019) in experimental models of CVD (**Figure 2**). More recently, natural antioxidants including epigallocatechin and naringenin have been shown to reduce oxidative damage in ECs via SIRT1 (Li H. et al., 2021; Pai et al., 2021), and an intermittent fasting regimen was found to ameliorate vascular dysfunction in a murine model of diabetes by activating the SIRT1 pathway (Hammer et al., 2021). Small molecule agents that target EZH2 and SIRT1 are currently available or under clinical study in several disease areas (e.g., oncology, dermatology, and nephrology) (Ganesan

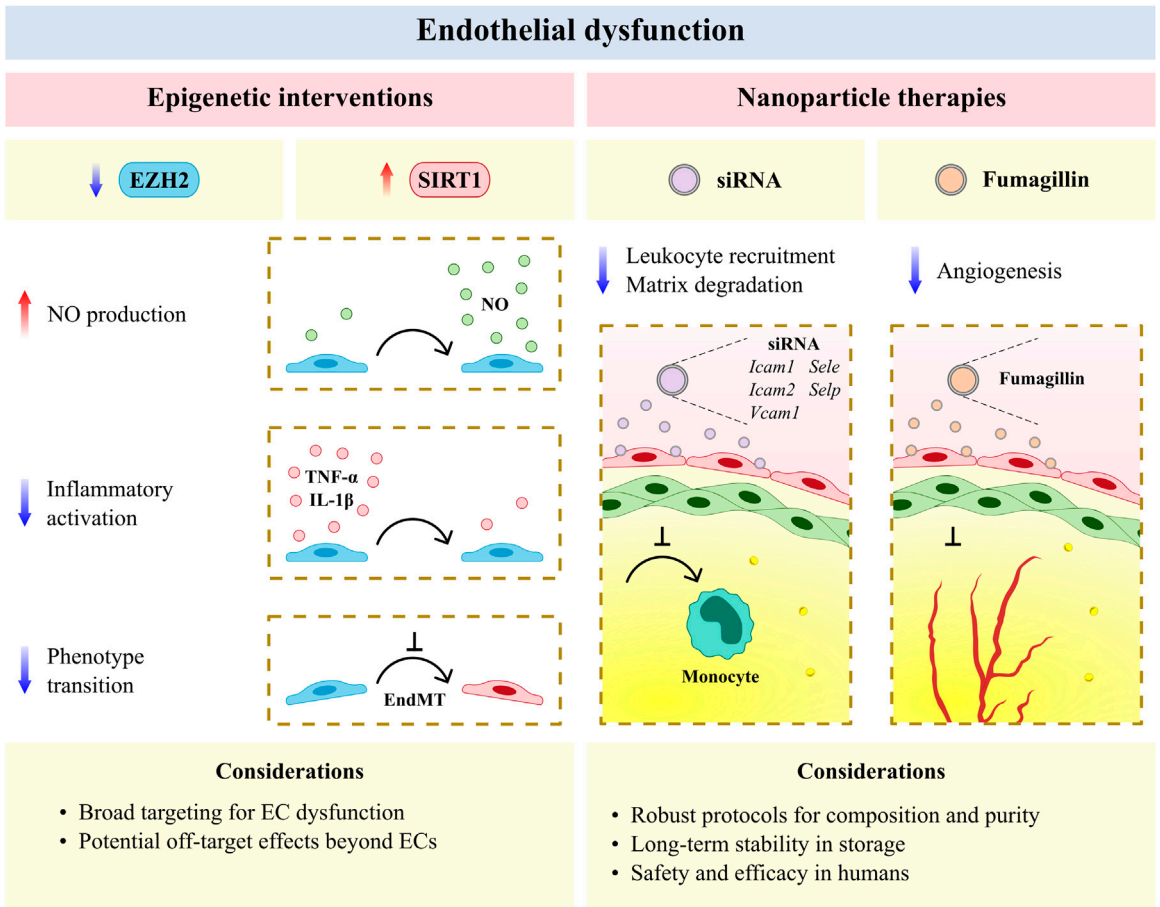

FIGURE 2 | The vascular endothelium is an emerging therapeutic target for atherosclerotic cardiovascular disease. Epigenic interventions including enhancer of zeste homologue 2 (EZH2) antagonism and sirtuin 1 (SIRT1) agonism allow for broad targeting of endothelial cell (EC) dysfunction but may have undesirable effects in other cell types and tissues. Anti-inflammatory and anti-angiogenic nanotherapies have reduced off-target effects and increased efficacy per dose, but require rigorous protocols for assessing composition and purity, as well as the development of long-term stability in storage and safety and efficacy in humans with cardiovascular disease. EndMT, endothelial-to-mesenchymal transition; Icam1, intercellular adhesion molecule 1; Icam2, intercellular adhesion molecule 2; IL-1β, interleukin 1 beta; NO, nitric oxide; Sele, selectin E; Selp, selectin P; siRNA, small interfering RNA; TNF-α, tumor necrosis factor alpha; Vcam1, vascular cell adhesion molecule 1.

et al., 2019; Fledderus et al., 2021), and may be investigated as potential anti-atherosclerotic agents by incorporating CVD endpoints into ongoing clinical trials. Beyond their desired therapeutic potential, the unintended effects of genome-wide modification via epigenetic agents also warrant consideration. Future studies may improve upon the specificity of these agents by making use of targeted CRISPR/Cas9 epigenome-editing techniques for epigenetic modifications associated with CVD risk loci (Cano-Rodriguez et al., 2016; Cano-Rodriguez and Rots, 2016; Xu et al., 2018). Alternatively, targeted EC therapies, as discussed below, may be considered for the resolution of vascular inflammation at the site of the activated endothelium in atherosclerosis. Prospective agents for targeted resolution include ICAM-1- or VCAM-1-targeted nanocarriers, which have previously been employed to limit neurovascular (Lutton et al., 2017; Marcos-Contreras et al., 2020) and pulmonary inflammation (Li S. et al., 2018; Park et al., 2021) in experimental models of disease.

Nanoparticle Therapies for the Targeted Resolution of Endothelial Dysfunction in Atherosclerosis

Advances in the development of nanoparticles (on a scale of <0.1 μm) have likewise afforded new opportunities for anti-atherosclerotic therapies that resolve endothelial dysfunction (Flores et al., 2019; Marchio et al., 2019; Chen L. et al., 2020). Vascular nanotherapies have been broadly classified as those which resolve inflammation and dysfunction in efferocytosis, limit plaque neovascularization and neointimal growth, modulate lipid metabolism, and decrease thrombosis (Flores et al., 2019). Several of these therapies have been shown to target the perturbed endothelium in experimental models of CVD, including the encapsulation of five cell adhesion molecule small interfering RNA, which reduced leukocyte migration to plaque and suppressed post-myocardial infarction inflammation in murine models (Sager et al., 2016). Integrin-targeted nanoparticles containing the antiangiogenic compound

fumagillin have likewise been shown to limit neovascularization in mice and demonstrate prolonged activity when combined with statin treatment (Winter et al., 2006; Winter et al., 2008) (**Figure 2**). More recently, engineered endothelial adrenoreceptor- (Ul Ain et al., 2017), VCAM-1- (Distasio et al., 2021), and P-selectin-targeted nanoparticles (Mocanu et al., 2021), which respectively carried the genes eNOS and IL-10 and receptor for advanced glycation end products-silencing RNA, have been found to localize to ECs and resolve inflammation within the murine atherosclerotic plaque. Nano-selenium particles have also been observed to improve endothelial dysfunction in murine atherosclerosis via Na^+/H^+ exchanger 1 inhibition (Zhu et al., 2019). Despite the therapeutic advantages offered by nanoparticles (e.g., reduced off-target effects and increased efficacy per dose), several methodological and biological challenges remain for clinical translation (Flores et al., 2019). Importantly, robust protocols are required to determine the composition and purity of nanoparticles derived using various formulations (e.g., lipid or polymeric). Furthermore, the long-term stability of nanoparticles, as well as their safety and selectivity for the activated endothelium in patients with atherosclerosis, must be assessed before these agents are clinically adopted. Nevertheless, vascular nanotherapies remain a promising avenue for the targeted resolution of endothelial dysfunction and reduction of plaque progression in atherosclerotic CVD, with encouraging evidence being generated for the systemic administration of nanoparticle-enveloped small interfering RNA in nonhuman primates to inhibit EC gene expression in multiple organs (Khan et al., 2018).

CONCLUSION AND FUTURE PERSPECTIVES

An emerging body of literature has implicated the vascular endothelium as an essential driver of atherosclerosis, a disease process that contributes to substantial mortality and healthcare burden among aging populations. These discoveries shed light on diverse cellular mechanisms that underlie endothelial activation, dysfunctional cell-cell communication, and perturbed vascular homeostasis in atherogenesis. Moreover, they highlight novel therapeutic targets and delivery methods with significant potential to prevent or limit plaque development in patients with atherosclerotic CVD. Although a broad spectrum of intra- and intercellular processes has been implicated in preclinical models of endothelial dysfunction and atherosclerosis, several methodological challenges remain to effectively translate this research to clinical practice. First, the generalizability of findings between diverse *in vitro* and *in vivo* models of endothelial activation and atherosclerosis remains an important consideration to identify strategies that hold significant therapeutic potential for distinct plaque locations and diverse patient groups. Additionally, the safety, efficacy, timing, and sustained response of candidate treatments must be considered, as the atherosclerotic disease process develops over decades and necessitates long-term intervention. A robust integration of experimental techniques (e.g., high-throughput EC profiling with functional validation), data sources (e.g., human samples with experimental models), and cutting-edge computational methods (e.g., machine learning) will be required for the creation of next-generation biomarkers and therapies that effectively mitigate atherosclerotic CVD in vulnerable patients.

AUTHOR CONTRIBUTIONS

SB synthesized literature and drafted the review. JF and KH participated in manuscript editing and supervision. All authors have read and approve the published version of the manuscript.

FUNDING

SB is supported by a University of Toronto MD/PhD Studentship and a Canadian Institutes of Health Research (CIHR) Canada Graduate Scholarship – Doctoral (CGS D). Research in the laboratory of JF is supported by CIHR Project Grants (PJT148487, PJT173489, and PJT175301) and Medicine by Design, which received funding from the Canada First Research Excellence Fund. JF is supported by a Tier 2 Canada Research Chair in Vascular Cell and Molecular Biology from CIHR. KH is supported by a CIHR Project Grant (PJT178006) and the Wylie Scholar Award (Vascular Cures), Blair Early Career Professorship in Vascular Surgery (University of Toronto), Peter Munk Cardiac Centre, and University Health Network.

ACKNOWLEDGMENTS

BioRender.com was used in the creation of figures for this review.

REFERENCES

Abderrazak, A., Couchie, D., Mahmood, D. F., Elhage, R., Vindis, C., and Laffargue, M. (2015). Anti-Inflammatory and Antiatherogenic Effects of the NLRP3 Inflammasome Inhibitor Arglabin in ApoE2.Ki Mice Fed a High-Fat Diet. *Circulation* 131, 1061–1070. doi:10.1161/CIRCULATIONAHA.114.013730

Aharon, A., Tamari, T., and Brenner, B. (2008). Monocyte-derived Microparticles and Exosomes Induce Procoagulant and Apoptotic Effects on Endothelial Cells. *Thromb. Haemost.* 100, 878–885. doi:10.1160/th07-11-0691

Albarrán-Juárez, J., Iring, A., Wang, S., Joseph, S., Grimm, M., Strilic, B., et al. (2018). Piezo1 and Gq/G11 Promote Endothelial Inflammation Depending on Flow Pattern and Integrin Activation. *J. Exp. Med.* 215, 2655–2672. doi:10.1084/jem.20180483

Alizada, A., Khyzha, N., Wang, L., Antounians, L., Chen, X., Khor, M., et al. (2021). Conserved Regulatory Logic at Accessible and Inaccessible Chromatin During the Acute Inflammatory Response in Mammals. *Nat. Commun.* 12, 567. doi:10.1038/s41467-020-20765-1

Andueza, A., Kumar, S., Kim, J., Kang, D.-W., Mumme, H. L., Perez, J. I., et al. (2020). Endothelial Reprogramming by Disturbed Flow Revealed by Single-Cell RNA and Chromatin Accessibility Study. *Cell Rep.* 33, 108491. doi:10.1016/j.celrep.2020.108491

Arderiu, G., Peña, E., and Badimon, L. (2015). Angiogenic Microvascular Endothelial Cells Release Microparticles Rich in Tissue Factor that

Promotes Postischemic Collateral Vessel Formation. *Arterioscler. Thromb. Vasc. Biol.* 35, 348–357. doi:10.1161/ATVBAHA.114.303927

Bäck, M., Yurdagul, A., Tabas, I., Öörni, K., and Kovanen, P. T. (2019). Inflammation and its Resolution in Atherosclerosis: Mediators and Therapeutic Opportunities. *Nat. Rev. Cardiol.* 16, 389–406. doi:10.1038/s41569-019-0169-2

Bär, C., Thum, T., and de Gonzalo-Calvo, D. (2019). Circulating miRNAs as Mediators in Cell-To-Cell Communication. *Epigenomics* 11, 111–113. doi:10.2217/epi-2018-0183

Bennett, M. R., Sinha, S., and Owens, G. K. (2016). Vascular Smooth Muscle Cells in Atherosclerosis. *Circ. Res.* 118, 692–702. doi:10.1161/CIRCRESAHA.115.306361

Bentzon, J. F., Otsuka, F., Virmani, R., and Falk, E. (2014). Mechanisms of Plaque Formation and Rupture. *Circ. Res.* 114, 1852–1866. doi:10.1161/CIRCRESAHA.114.302721

Bergsbaken, T., Fink, S. L., and Cookson, B. T. (2009). Pyroptosis: Host Cell Death and Inflammation. *Nat. Rev. Microbiol.* 7, 99–109. doi:10.1038/nrmicro2070

Berk, B. C. (2008). Atheroprotective Signaling Mechanisms Activated by Steady Laminar Flow in Endothelial Cells. *Circulation* 117, 1082–1089. doi:10.1161/CIRCULATIONAHA.107.720730

Bertero, T., Oldham, W. M., Cottrill, K. A., Pisano, S., Vanderpool, R. R., Yu, Q., et al. (2016). Vascular Stiffness Mechanoactivates YAP/TAZ-dependent Glutaminolysis to Drive Pulmonary Hypertension. *J. Clin. Invest.* 126, 3313–3335. doi:10.1172/JCI86387

Bondareva, O., Tsaryk, R., Bojovic, V., Odenthal-Schnittler, M., Siekmann, A. F., and Schnittler, H.-J. (2019). Identification of Atheroprone Shear Stress Responsive Regulatory Elements in Endothelial Cells. *Cardiovasc. Res.* 115, 1487–1499. doi:10.1093/cvr/cvz027

Bouabdallaoui, N., Tardif, J.-C., Waters, D. D., Pinto, F. J., Maggioni, A. P., Diaz, R., et al. (2020). Time-to-treatment Initiation of Colchicine and Cardiovascular Outcomes after Myocardial Infarction in the Colchicine Cardiovascular Outcomes Trial (COLCOT). *Eur. Heart J.* 41, 4092–4099. doi:10.1093/eurheartj/ehaa659

Boyer, M. J., Kimura, Y., Akiyama, T., Baggett, A. Y., Preston, K. J., Scalia, R., et al. (2020). Endothelial Cell-Derived Extracellular Vesicles Alter Vascular Smooth Muscle Cell Phenotype through High-Mobility Group Box Proteins. *J. Extracell. Vesicles* 9, 1781427. doi:10.1080/20013078.2020.1781427

Boyle, E. C., Sedding, D. G., and Haverich, A. (2017). Targeting Vasa Vasorum Dysfunction to Prevent Atherosclerosis. *Vascul. Pharmacol.* 96–98, 5–10. doi:10.1016/j.vph.2017.08.003

Burrello, J., Biemmi, V., Dei Cas, M., Amongero, M., Bolis, S., Lazzarini, E., et al. (2020). Sphingolipid Composition of Circulating Extracellular Vesicles after Myocardial Ischemia. *Sci. Rep.* 10, 16182. doi:10.1038/s41598-020-73411-7

Cahill, P. A., and Redmond, E. M. (2016). Vascular Endothelium – Gatekeeper of Vessel Health. *Atherosclerosis* 248, 97–109. doi:10.1016/j.atherosclerosis.2016.03.007

Cai, B., Kasikara, C., Doran, A. C., Ramakrishnan, R., Birge, R. B., and Tabas, I. (2018). MerTK Signaling in Macrophages Promotes the Synthesis of Inflammation Resolution Mediators by Suppressing CaMKII Activity. *Sci. Signal.* 11, eaar3721. doi:10.1126/scisignal.aar3721

Camaré, C., Pucelle, M., Nègre-Salvayre, A., and Salvayre, R. (2017). Angiogenesis in the Atherosclerotic Plaque. *Redox Biol.* 12, 18–34. doi:10.1016/j.redox.2017.01.007

Cano-Rodriguez, D., Gjaltema, R. A. F., Jilderda, L. J., Jellema, P., Dokter-Fokkens, J., Ruiters, M. H. J., et al. (2016). Writing of H3K4Me3 Overcomes Epigenetic Silencing in a Sustained but Context-dependent Manner. *Nat. Commun.* 7, 12284. doi:10.1038/ncomms12284

Cano-Rodriguez, D., and Rots, M. G. (2016). Epigenetic Editing: On the Verge of Reprogramming Gene Expression at Will. *Curr. Genet. Med. Rep.* 4, 170–179. doi:10.1007/s40142-016-0104-3

Castellani, C., Burrello, J., Fedrigo, M., Burrello, A., Bolis, S., Di Silvestre, D., et al. (2020). Circulating Extracellular Vesicles as Non-invasive Biomarker of Rejection in Heart Transplant. *J. Heart Lung Transpl.* 39, 1136–1148. doi:10.1016/j.healun.2020.06.011

Chai, Q., Lu, T., Wang, X.-L., and Lee, H.-C. (2015). Hydrogen Sulfide Impairs Shear Stress-Induced Vasodilation in Mouse Coronary Arteries. *Pflüg. Arch. - Eur. J. Physiol.* 467, 329–340. doi:10.1007/s00424-014-1526-y

Charla, E., Mercer, J., Maffia, P., and Nicklin, S. A. (2020). Extracellular Vesicle Signalling in Atherosclerosis. *Cell. Signal.* 75, 109751. doi:10.1016/j.cellsig.2020.109751

Chatterjee, A., Sharma, A., Chen, M., Toy, R., Mottola, G., and Conte, M. S. (2014). The Pro-resolving Lipid Mediator Maresin 1 (MaR1) Attenuates Inflammatory Signaling Pathways in Vascular Smooth Muscle and Endothelial Cells. *PLOS ONE* 9, e113480. doi:10.1371/journal.pone.0113480

Chattopadhyay, R., Mani, A. M., Singh, N. K., and Rao, G. N. (2018). Resolvin D1 Blocks H2O2-Mediated Inhibitory Crosstalk between SHP2 and PP2A and Suppresses Endothelial-Monocyte Interactions. *Free Radic. Biol. Med.* 117, 119–131. doi:10.1016/j.freeradbiomed.2018.01.034

Chen, L., Jiang, Z., Akakuru, O. U., Yang, L., Li, J., Ma, S., et al. (2020a). Recent Progress in the Detection and Treatment of Atherosclerosis by Nanoparticles. *Mater. Today Chem.* 17, 100280. doi:10.1016/j.mtchem.2020.100280

Chen, L., Shang, C., Wang, B., Wang, G., Jin, Z., Yao, F., et al. (2021). HDAC3 Inhibitor Suppresses Endothelial-To-Mesenchymal Transition via Modulating Inflammatory Response in Atherosclerosis. *Biochem. Pharmacol.* 192, 114716. doi:10.1016/j.bcp.2021.114716

Chen, P.-Y., Qin, L., Baeyens, N., Li, G., Afolabi, T., Budatha, M., et al. (2015). Endothelial-to-mesenchymal Transition Drives Atherosclerosis Progression. *J. Clin. Invest.* 125, 4514–4528. doi:10.1172/JCI82719

Chen, P.-Y., Qin, L., Li, G., Wang, Z., Dahlman, J. E., Malagon-Lopez, J., et al. (2019). Endothelial TGF-β Signalling Drives Vascular Inflammation and Atherosclerosis. *Nat. Metab.* 1, 912–926. doi:10.1038/s42255-019-0102-3

Chen, P.-Y., Schwartz, M. A., and Simons, M. (2020b). Endothelial-to-Mesenchymal Transition, Vascular Inflammation, and Atherosclerosis. *Front. Cardiovasc. Med.* 7, 53. doi:10.3389/fcvm.2020.00053

Chen, Y.-T., Yuan, H.-X., Ou, Z.-J., and Ou, J.-S. (2020c). Microparticles (Exosomes) and Atherosclerosis. *Curr. Atheroscler. Rep.* 22, 23. doi:10.1007/s11883-020-00841-z

Chong, W., Baker, B. M., Chen, C. S., and Schwartz, M. A. (2013). Endothelial Cell Sensing of Flow Direction. *Arterioscler. Thromb. Vasc. Biol.* 33, 2130–2136. doi:10.1161/ATVBAHA.113.301826

Chu, M., Wu, R., Qin, S., Hua, W., Shan, Z., Xing, R., et al. (2017). Bone Marrow–Derived MicroRNA-223 Works as an Endocrine Genetic Signal in Vascular Endothelial Cells and Participates in Vascular Injury from Kawasaki Disease. *J. Am. Heart Assoc.* 6, e004878. doi:10.1161/JAHA.116.004878

Citi, V., Martelli, A., Gorica, E., Brogi, S., Testai, L., and Calderone, V. (2021). Role of Hydrogen Sulfide in Endothelial Dysfunction: Pathophysiology and Therapeutic Approaches. *J. Adv. Res.* 27, 99–113. doi:10.1016/j.jare.2020.05.015

Coelewij, L., Waddington, K. E., Robinson, G. A., Chocano, E., McDonnell, T., Farinha, F., et al. (2021). Serum Metabolomic Signatures Can Predict Subclinical Atherosclerosis in Patients with Systemic Lupus Erythematosus. *Arterioscler. Thromb. Vasc. Biol.* 41, 1446–1458. doi:10.1161/ATVBAHA.120.315321

Collins, T., and Cybulsky, M. I. (2001). NF-κB: Pivotal Mediator or Innocent Bystander in Atherogenesis? *J. Clin. Invest.* 107, 255–264. doi:10.1172/JCI10373

Currie, E., Schulze, A., Zechner, R., Walther, T. C., and Farese, R. V. (2013). Cellular Fatty Acid Metabolism and Cancer. *Cell Metab.* 18, 153–161. doi:10.1016/j.cmet.2013.05.017

da Luz, P. L., Chagas, A. C. P., Dourado, P. M. M., and Laurindo, F. R. M. (2018). "Chapter 33 - Endothelium in Atherosclerosis: Plaque Formation and its Complications," in *Endothelium And Cardiovascular Diseases*. Editors P. L. Da Luz, P. Libby, A. C. P. Chagas, and F. R. M. Laurindo (Academic Press), 493–512. doi:10.1016/b978-0-12-812348-5.00033-7

Dagher, Z., Ruderman, N., Tornheim, K., and Ido, Y. (2001). Acute Regulation of Fatty Acid Oxidation and AMP-Activated Protein Kinase in Human Umbilical Vein Endothelial Cells. *Circ. Res.* 88, 1276–1282. doi:10.1161/hh1201.092998

Dai, H., Much, A. A., Maor, E., Asher, E., Younis, A., Xu, Y., et al. (2020). Global, Regional, and National burden of Ischaemic Heart Disease and its Attributable Risk Factors, 1990–2017: Results from the Global Burden of Disease Study 2017. *Eur. Heart J. - Qual. Care Clin. Outcomes*, qcaa076. doi:10.1093/ehjqcco/qcaa076

De Bock, K., Georgiadou, M., Schoors, S., Kuchnio, A., Wong, B. W., Cantelmo, A. R., et al. (2013). Role of PFKFB3-Driven Glycolysis in Vessel Sprouting. *Cell* 154, 651–663. doi:10.1016/j.cell.2013.06.037

Depuydt, M. A. C., Prange, K. H. M., Slenders, L., Örd, T., Elbersen, D., Boltjes, A., et al. (2020). Microanatomy of the Human Atherosclerotic Plaque by Single-

Cell Transcriptomics. *Circ. Res.* 127, 1437–1455. doi:10.1161/CIRCRESAHA.120.316770

Distasio, N., Salmon, H., Dierick, F., Ebrahimian, T., Tabrizian, M., and Lehoux, S. (2021). VCAM-1-Targeted Gene Delivery Nanoparticles Localize to Inflamed Endothelial Cells and Atherosclerotic Plaques. *Adv. Ther.* 4, 2000196. doi:10.1002/adtp.202000196

Doddaballapur, A., Michalik, K. M., Manavski, Y., Lucas, T., Houtkooper, R. H., You, X., et al. (2015). Laminar Shear Stress Inhibits Endothelial Cell Metabolism via KLF2-Mediated Repression of PFKFB3. *Arterioscler. Thromb. Vasc. Biol.* 35, 137–145. doi:10.1161/ATVBAHA.114.304277

Duewell, P., Kono, H., Rayner, K. J., Sirois, C. M., Vladimer, G., Bauernfeind, F. G., et al. (2010). NLRP3 Inflammasomes Are Required for Atherogenesis and Activated by Cholesterol Crystals. *Nature* 464, 1357–1361. doi:10.1038/nature08938

Dufour, D., Khalil, A., Nuyens, V., Rousseau, A., Delporte, C., Noyon, C., et al. (2018). Native and Myeloperoxidase-Oxidized Low-Density Lipoproteins Act in Synergy to Induce Release of Resolvin-D1 from Endothelial Cells. *Atherosclerosis* 272, 108–117. doi:10.1016/j.atherosclerosis.2018.03.012

Durak-Kozica, M., Baster, Z., Kubat, K., and Stępień, E. (2018). 3D Visualization of Extracellular Vesicle Uptake by Endothelial Cells. *Cell. Mol. Biol. Lett.* 23, 57. doi:10.1186/s11658-018-0123-z

Eelen, G., de Zeeuw, P., Treps, L., Harjes, U., Wong, B. W., and Carmeliet, P. (2018). Endothelial Cell Metabolism. *Physiol. Rev.* 98, 3–58. doi:10.1152/physrev.00001.2017

Enzo, E., Santinon, G., Pocaterra, A., Aragona, M., Bresolin, S., Forcato, M., et al. (2015). Aerobic Glycolysis Tunes YAP/TAZ Transcriptional Activity. *EMBO J.* 34, 1349–1370. doi:10.15252/embj.201490379

Evrard, S. M., Lecce, L., Michelis, K. C., Nomura-Kitabayashi, A., Pandey, G., Purushothaman, K.-R., et al. (2016). Endothelial to Mesenchymal Transition Is Common in Atherosclerotic Lesions and Is Associated with Plaque Instability. *Nat. Commun.* 7, 1–16. doi:10.1038/ncomms11853

Feng, S., Bowden, N., Fragiadaki, M., Souilhol, C., Hsiao, S., Mahmoud, M., et al. (2017). Mechanical Activation of Hypoxia-Inducible Factor 1α Drives Endothelial Dysfunction at Atheroprone Sites. *Arterioscler. Thromb. Vasc. Biol.* 37, 2087–2101. doi:10.1161/ATVBAHA.117.309249

Fernando, S., Schwarz, N., Williamson, A., Toledo, D., Zareh, J., Bartolo, B. D., et al. (2017). Anti-Inflammatory Effects of Colchicine on Oxidised Low-Density Lipoproteins and Cholesterol Crystal-Induced Macrophage Activation *In Vitro*. *Heart Lung Circ.* 26, S69–S70. doi:10.1016/j.hlc.2017.06.060

Filep, J. G., Zouki, C., Petasis, N. A., Hachicha, M., and Serhan, C. N. (1999). Anti-Inflammatory Actions of Lipoxin A4 Stable Analogs Are Demonstrable in Human Whole Blood: Modulation of Leukocyte Adhesion Molecules and Inhibition of Neutrophil-Endothelial Interactions. *Blood* 94, 4132–4142. doi:10.1182/blood.V94.12.4132

Flammer, A. J., Anderson, T., Celermajer, D. S., Creager, M. A., Deanfield, J., Ganz, P., et al. (2012). The Assessment of Endothelial Function. *Circulation* 126, 753–767. doi:10.1161/CIRCULATIONAHA.112.093245

Fledderus, J., Vanchin, B., Rots, M. G., and Krenning, G. (2021). The Endothelium as a Target for Anti-atherogenic Therapy: A Focus on the Epigenetic Enzymes EZH2 and SIRT1. *J. Pers. Med.* 11, 103. doi:10.3390/jpm11020103

Flores, A. M., Hosseini-Nassab, N., Jarr, K.-U., Ye, J., Zhu, X., Wirka, R., et al. (2020). Pro-efferocytic Nanoparticles Are Specifically Taken up by Lesional Macrophages and Prevent Atherosclerosis. *Nat. Nanotechnol.* 15, 154–161. doi:10.1038/s41565-019-0619-3

Flores, A. M., Ye, J., Kai-Uwe, J., Niloufar, H. N., Smith Bryan, R., and Leeper Nicholas, J. (2019). Nanoparticle Therapy for Vascular Diseases. *Arterioscler. Thromb. Vasc. Biol.* 39, 635–646. doi:10.1161/ATVBAHA.118.311569

Folco, E. J., Sukhova, G. K., Quillard, T., and Libby, P. (2014). Moderate Hypoxia Potentiates Interleukin-1β Production in Activated Human Macrophages. *Circ. Res.* 115, 875–883. doi:10.1161/CIRCRESAHA.115.304437

Förstermann, U., Xia, N., and Li, H. (2017). Roles of Vascular Oxidative Stress and Nitric Oxide in the Pathogenesis of Atherosclerosis. *Circ. Res.* 120, 713–735. doi:10.1161/CIRCRESAHA.116.309326

Fredman, G., and Tabas, I. (2017). Boosting Inflammation Resolution in Atherosclerosis: The Next Frontier for Therapy. *Am. J. Pathol.* 187, 1211–1221. doi:10.1016/j.ajpath.2017.01.018

Friedrich, E. E., Hong, Z., Xiong, S., Zhong, M., Di, A., Rehman, J., et al. (2019). Endothelial Cell Piezo1 Mediates Pressure-Induced Lung Vascular Hyperpermeability via Disruption of Adherens Junctions. *Proc. Natl. Acad. Sci.* 116, 12980–12985. doi:10.1073/pnas.1902165116

Ganesan, A., Arimondo, P. B., Rots, M. G., Jeronimo, C., and Berdasco, M. (2019). The Timeline of Epigenetic Drug Discovery: from Reality to Dreams. *Clin. Epigenetics* 11, 174. doi:10.1186/s13148-019-0776-0

Ghaffari, S., Jang, E., Naderinabi, F., Sanwal, R., Khosraviani, N., Wang, C., et al. (2021). Endothelial HMGB1 Is a Critical Regulator of LDL Transcytosis via an SREBP2-SR-BI Axis. *Arterioscler. Thromb. Vasc. Biol.* 41, 200–216. doi:10.1161/ATVBAHA.120.314557

Giddens, D. P., Zarins, C. K., and Glagov, S. (1993). The Role of Fluid Mechanics in the Localization and Detection of Atherosclerosis. *J. Biomech. Eng.* 115, 588–594. doi:10.1115/1.2895545

Gimbrone, M. A., and García-Cardeña, G. (2016). Endothelial Cell Dysfunction and the Pathobiology of Atherosclerosis. *Circ. Res.* 118, 620–636. doi:10.1161/CIRCRESAHA.115.306301

Go, Y.-M., Lee, H.-R., and Park, H. (2012). H2S Inhibits Oscillatory Shear Stress-Induced Monocyte Binding to Endothelial Cells via Nitric Oxide Production. *Mol. Cell* 34, 449–455. doi:10.1007/s10059-012-0200-5

Gracia-Sancho, J., Villarreal, G., Jr., Zhang, Y., and García-Cardeña, G. (2010). Activation of SIRT1 by Resveratrol Induces KLF2 Expression Conferring an Endothelial Vasoprotective Phenotype. *Cardiovasc. Res.* 85, 514–519. doi:10.1093/cvr/cvp337

Graney, P. L., Ben-Shaul, S., Landau, S., Bajpai, A., Singh, B., Eager, J., et al. (2020). Macrophages of Diverse Phenotypes Drive Vascularization of Engineered Tissues. *Sci. Adv.* 6, eaay6391. doi:10.1126/sciadv.aay6391

Greenwood, J., and Mason, J. C. (2007). Statins and the Vascular Endothelial Inflammatory Response. *Trends Immunol.* 28, 88–98. doi:10.1016/j.it.2006.12.003

Hagberg, C., Mehlem, A., Falkevall, A., Muhl, L., and Eriksson, U. (2013). Endothelial Fatty Acid Transport: Role of Vascular Endothelial Growth Factor B. *Physiology* 28, 125–134. doi:10.1152/physiol.00042.2012

Hahn, C., and Schwartz, M. A. (2009). Mechanotransduction in Vascular Physiology and Atherogenesis. *Nat. Rev. Mol. Cell Biol.* 10, 53–62. doi:10.1038/nrm2596

Hajra, L., Evans, A. I., Chen, M., Hyduk, S. J., Collins, T., and Cybulsky, M. I. (2000). The NF-κB Signal Transduction Pathway in Aortic Endothelial Cells Is Primed for Activation in Regions Predisposed to Atherosclerotic Lesion Formation. *Proc. Natl. Acad. Sci.* 97, 9052–9057. doi:10.1073/pnas.97.16.9052

Haldar, S. M., and Stamler, J. S. (2013). *S*-nitrosylation: Integrator of Cardiovascular Performance and Oxygen Delivery. *J. Clin. Invest.* 123, 101–110. doi:10.1172/JCI62854

Hammer, S. S., Vieira, C. P., McFarland, D., Sandler, M., Levitsky, Y., Dorweiler, T. F., et al. (2021). Fasting and Fasting-Mimicking Treatment Activate SIRT1/LXRα and Alleviate Diabetes-Induced Systemic and Microvascular Dysfunction. *Diabetologia* 64, 1674–1689. doi:10.1007/s00125-021-05431-5

Hays, A. G., Schär, M., Barditch-Crovo, P., Bagchi, S., Bonanno, G., Meyer, J., et al. (2021). A Randomized, Placebo-Controlled, Double-Blinded Clinical Trial of Colchicine to Improve Vascular Health in People Living with HIV. *AIDS Lond. Engl.* 35, 1041–1050. doi:10.1097/QAD.0000000000002845

He, M., Chen, Z., Martin, M., Zhang, J., Sangwung, P., Woo, B., et al. (2017). miR-483 Targeting of CTGF Suppresses Endothelial-To-Mesenchymal Transition. *Circ. Res.* 120, 354–365. doi:10.1161/CIRCRESAHA.116.310233

He, S., Wu, C., Xiao, J., Li, D., Sun, Z., and Li, M. (2018). Endothelial Extracellular Vesicles Modulate the Macrophage Phenotype: Potential Implications in Atherosclerosis. *Scand. J. Immunol.* 87, e12648. doi:10.1111/sji.12648

Helmke, A., Casper, J., Nordlohne, J., David, S., Haller, H., Zeisberg, E. M., et al. (2019). Endothelial-to-mesenchymal Transition Shapes the Atherosclerotic Plaque and Modulates Macrophage Function. *FASEB J.* 33, 2278–2289. doi:10.1096/fj.201801238R

Heo, J., Yang, H. C., Rhee, W. J., and Kang, H. (2020). Vascular Smooth Muscle Cell-Derived Exosomal MicroRNAs Regulate Endothelial Cell Migration under PDGF Stimulation. *Cells* 9, 639. doi:10.3390/cells9030639

Hergenreider, E., Heydt, S., Tréguer, K., Boettger, T., Horrevoets, A. J. G., Zeiher, A. M., et al. (2012). Atheroprotective Communication between Endothelial Cells and Smooth Muscle Cells through miRNAs. *Nat. Cell Biol.* 14, 249–256. doi:10.1038/ncb2441

Higashi, Y., Sukhanov, S., Shai, S.-Y., Danchuk, S., Snarski, P., Li, Z., et al. (2020). Endothelial Deficiency of Insulin-like Growth Factor-1 Receptor Reduces

Endothelial Barrier Function and Promotes Atherosclerosis in Apoe-Deficient Mice. *Am. J. Physiol.-Heart Circ. Physiol.* 319, H730–H743. doi:10.1152/ajpheart.00064.2020

Hogan, N. T., Whalen, M. B., Stolze, L. K., Hadeli, N. K., Lam, M. T., Springstead, J. R., et al. (2017). Transcriptional Networks Specifying Homeostatic and Inflammatory Programs of Gene Expression in Human Aortic Endothelial Cells. *eLife* 6, e22536. doi:10.7554/eLife.22536

Huang, B., Chen, C.-T., Chen, C.-S., Wang, Y.-M., Hsieh, H.-J., and Wang, D. L. (2015). Laminar Shear Flow Increases Hydrogen Sulfide and Activates a Nitric Oxide Producing Signaling cascade in Endothelial Cells. *Biochem. Biophys. Res. Commun.* 464, 1254–1259. doi:10.1016/j.bbrc.2015.07.115

Ignarro, L. J., Buga, G. M., Wei, L. H., Bauer, P. M., Wu, G., and del Soldato, P. (2001). Role of the Arginine-Nitric Oxide Pathway in the Regulation of Vascular Smooth Muscle Cell Proliferation. *Proc. Natl. Acad. Sci.* 98, 4202–4208. doi:10.1073/pnas.071054698

Jaipersad, A. S., Lip, G. Y. H., Silverman, S., and Shantsila, E. (2014). The Role of Monocytes in Angiogenesis and Atherosclerosis. *J. Am. Coll. Cardiol.* 63, 1–11. doi:10.1016/j.jacc.2013.09.019

Jansen, F., Yang, X., Baumann, K., Przybilla, D., Schmitz, T., Flender, A., et al. (2015). Endothelial Microparticles Reduce ICAM-1 Expression in a microRNA-222-dependent Mechanism. *J. Cell. Mol. Med.* 19, 2202–2214. doi:10.1111/jcmm.12607

Jansen, F., Yang, X., Hoelscher, M., Cattelan, A., Schmitz, T., Proebsting, S., et al. (2013). Endothelial Microparticle–Mediated Transfer of MicroRNA-126 Promotes Vascular Endothelial Cell Repair via SPRED1 and Is Abrogated in Glucose-Damaged Endothelial Microparticles. *Circulation* 128, 2026–2038. doi:10.1161/CIRCULATIONAHA.113.001720

Jarr, K.-U., Nakamoto, R., Doan, B. H., Kojima, Y., Weissman, I. L., Advani, R. H., et al. (2021). Effect of CD47 Blockade on Vascular Inflammation. *N. Engl. J. Med.* 384, 382–383. doi:10.1056/NEJMc2029834

Jin, Y., and Fu, J. (2019). Novel Insights into the NLRP3 Inflammasome in Atherosclerosis. *J. Am. Heart Assoc.* 8, e012219. doi:10.1161/JAHA.119.012219

Kajikawa, M., Higashi, Y., Tomiyama, H., Maruhashi, T., Kurisu, S., Kihara, Y., et al. (2019). Effect of Short-Term Colchicine Treatment on Endothelial Function in Patients with Coronary Artery Disease. *Int. J. Cardiol.* 281, 35–39. doi:10.1016/j.ijcard.2019.01.054

Kang-Decker, N., Cao, S., Chatterjee, S., Yao, J., Egan, L. J., Semela, D., et al. (2007). Nitric Oxide Promotes Endothelial Cell Survival Signaling through S-Nitrosylation and Activation of Dynamin-2. *J. Cell Sci.* 120, 492–501. doi:10.1242/jcs.03361

Khan, O. F., Kowalski, P. S., Doloff, J. C., Tsosie, J. K., Bakthavatchalu, V., Winn, C. B., et al. (2018). Endothelial siRNA Delivery in Nonhuman Primates Using Ionizable Low–Molecular Weight Polymeric Nanoparticles. *Sci. Adv.* 4, eaar8409. doi:10.1126/sciadv.aar8409

Khyzha, N., Alizada, A., Wilson, M. D., and Fish, J. E. (2017). Epigenetics of Atherosclerosis: Emerging Mechanisms and Methods. *Trends Mol. Med.* 23, 332–347. doi:10.1016/j.molmed.2017.02.004

Kim, B., Li, J., Jang, C., and Arany, Z. (2017a). Glutamine Fuels Proliferation but Not Migration of Endothelial Cells. *EMBO J.* 36, 2321–2333. doi:10.15252/embj.201796436

Kim, J., Kim, Y. H., Kim, J., Park, D. Y., Bae, H., Lee, D.-H., et al. (2017b). YAP/TAZ Regulates Sprouting Angiogenesis and Vascular Barrier Maturation. *J. Clin. Invest.* 127, 3441–3461. doi:10.1172/JCI93825

Kleemann, R., Zadelaar, S., and Kooistra, T. (2008). Cytokines and Atherosclerosis: a Comprehensive Review of Studies in Mice. *Cardiovasc. Res.* 79, 360–376. doi:10.1093/cvr/cvn120

Kojima, Y., Volkmer, J.-P., McKenna, K., Civelek, M., Lusis, A. J., Miller, C. L., et al. (2016). CD47-blocking Antibodies Restore Phagocytosis and Prevent Atherosclerosis. *Nature* 536, 86–90. doi:10.1038/nature18935

Komarova, Y. A., Kruse, K., Mehta, D., and Malik, A. B. (2017). Protein Interactions at Endothelial Junctions and Signaling Mechanisms Regulating Endothelial Permeability. *Circ. Res.* 120, 179–206. doi:10.1161/CIRCRESAHA.116.306534

Kosmidou, I., Moore, J. P., Weber, M., and Searles, C. D. (2007). Statin Treatment and 3′ Polyadenylation of eNOS mRNA. *Arterioscler. Thromb. Vasc. Biol.* 27, 2642–2649. doi:10.1161/ATVBAHA.107.154492

Krützfeldt, A., Spahr, R., Mertens, S., Siegmund, B., and Piper, H. M. (1990). Metabolism of Exogenous Substrates by Coronary Endothelial Cells in Culture. *J. Mol. Cell. Cardiol.* 22, 1393–1404. doi:10.1016/0022-2828(90)90984-A

Ku, K. H., Dubinsky, M. K., Sukumar, A. N., Subramaniam, N., Feasson, M. Y. M., Nair, R., et al. (2021). *In Vivo* Function of Flow-Responsive Cis-DNA Elements of eNOS Gene: A Role for Chromatin-Based Mechanisms. *Circulation* 144, 365–381. doi:10.1161/CIRCULATIONAHA.120.051078

Kumar, A., Kumar, S., Vikram, A., Hoffman, T. A., Naqvi, A., Lewarchik, C. M., et al. (2013). Histone and DNA Methylation–Mediated Epigenetic Downregulation of Endothelial Kruppel-like Factor 2 by Low-Density Lipoprotein Cholesterol. *Arterioscler. Thromb. Vasc. Biol.* 33, 1936–1942. doi:10.1161/ATVBAHA.113.301765

Kumar, S., Williams, D., Sur, S., Wang, J.-Y., and Jo, H. (2019). Role of Flow-Sensitive microRNAs and Long Noncoding RNAs in Vascular Dysfunction and Atherosclerosis. *Vascul. Pharmacol.* 114, 76–92. doi:10.1016/j.vph.2018.10.001

Kureishi, Y., Luo, Z., Shiojima, I., Bialik, A., Fulton, D., Lefer, D. J., et al. (2000). The HMG-CoA Reductase Inhibitor Simvastatin Activates the Protein Kinase Akt and Promotes Angiogenesis in Normocholesterolemic Animals. *Nat. Med.* 6, 1004–1010. doi:10.1038/79510

Lay, A. J., Coleman, P. R., Formaz-Preston, A., Ting, K. K., Roediger, B., Weninger, W., et al. (2019). ARHGAP18: A Flow-Responsive Gene that Regulates Endothelial Cell Alignment and Protects against Atherosclerosis. *J. Am. Heart Assoc.* 8, e010057. doi:10.1161/JAHA.118.010057

Li, B., He, J., Lv, H., Liu, Y., Lv, X., Zhang, C., et al. (2019a). c-Abl Regulates YAP^{Y357} Phosphorylation to Activate Endothelial Atherogenic Responses to Disturbed Flow. *J. Clin. Invest.* 129, 1167–1179. doi:10.1172/JCI122440

Li, H., Liu, L., Cao, Z., Li, W., Liu, R., Chen, Y., et al. (2021a). Naringenin Ameliorates Homocysteine Induced Endothelial Damage via the AMPKα/Sirt1 Pathway. *J. Adv. Res.* 34, 137–147. doi:10.1016/j.jare.2021.01.009

Li, J., Hou, B., Tumova, S., Muraki, K., Bruns, A., Ludlow, M. J., et al. (2014a). Piezo1 Integration of Vascular Architecture with Physiological Force. *Nature* 515, 279–282. doi:10.1038/nature13701

Li, K., Cui, M., Zhang, K., Wang, G., and Zhai, S. (2021b). M1 Macrophages-Derived Extracellular Vesicles Elevate microRNA-185-3p to Aggravate the Development of Atherosclerosis in ApoE-/- Mice by Inhibiting Small Mothers against Decapentaplegic 7. *Int. Immunopharmacol.* 90, 107138. doi:10.1016/j.intimp.2020.107138

Li, M., Qian, M., Kyler, K., and Xu, J. (2018a). Endothelial–Vascular Smooth Muscle Cells Interactions in Atherosclerosis. *Front. Cardiovasc. Med.* 5, 151. doi:10.3389/fcvm.2018.00151

Li, S., Chen, L., Wang, G., Xu, L., Hou, S., Chen, Z., et al. (2018b). Anti-ICAM-1 Antibody-Modified Nanostructured Lipid Carriers: a Pulmonary Vascular Endothelium-Targeted Device for Acute Lung Injury Therapy. *J. Nanobiotechnology* 16, 105. doi:10.1186/s12951-018-0431-5

Li, X.-X., Ling, S.-K., Hu, M.-Y., Ma, Y., Li, Y., and Huang, P.-L. (2019b). Protective Effects of Acarbose against Vascular Endothelial Dysfunction through Inhibiting Nox4/NLRP3 Inflammasome Pathway in Diabetic Rats. *Free Radic. Biol. Med.* 145, 175–186. doi:10.1016/j.freeradbiomed.2019.09.015

Li, X., Zhang, Y., Xia, M., Gulbins, E., Boini, K. M., and Li, P.-L. (2014b). Activation of Nlrp3 Inflammasomes Enhances Macrophage Lipid-Deposition and Migration: Implication of a Novel Role of Inflammasome in Atherogenesis. *PLOS ONE* 9, e87552. doi:10.1371/journal.pone.0087552

Li, Y., Zhang, Y.-X., Ning, D.-S., Chen, J., Li, S.-X., Mo, Z.-W., et al. (2021c). Simvastatin Inhibits POVPC-Mediated Induction of Endothelial-To-Mesenchymal Cell Transition. *J. Lipid Res.* 62, 100066. doi:10.1016/j.jlr.2021.100066

Liang, H., Li, S., and Chen, H. (2017). GW28-e0938 Endothelial Microparticles-Mediated Transfer of microRNA-19b,a Novel Messenger in Cell-Cell Communication, Plays a Key Role in Endothelial Migration and Angiogenesis. *J. Am. Coll. Cardiol.* 70, C34. doi:10.1016/j.jacc.2017.07.118

Libby, P. (2021). The Changing Landscape of Atherosclerosis. *Nature* 592, 524–533. doi:10.1038/s41586-021-03392-8

Liebner, S., Cavallaro, U., and Dejana, E. (2006). The Multiple Languages of Endothelial Cell-To-Cell Communication. *Arterioscler. Thromb. Vasc. Biol.* 26, 1431–1438. doi:10.1161/01.ATV.0000218510.04541.5e

Lin, S. J., Jan, K. M., and Chien, S. (1990). Role of Dying Endothelial Cells in Transendothelial Macromolecular Transport. *Arteriosclerosis* 10, 703–709. doi:10.1161/01.atv.10.5.703

Liu, Q., Piao, H., Wang, Y., Zheng, D., and Wang, W. (2021). Circulating Exosomes in Cardiovascular Disease: Novel Carriers of Biological Information. *Biomed. Pharmacother.* 135, 111148. doi:10.1016/j.biopha.2020.111148

Liu, Y., Li, Q., Hosen, M. R., Zietzer, A., Flender, A., Levermann, P., et al. (2019a). Atherosclerotic Conditions Promote the Packaging of Functional MicroRNA-92a-3p into Endothelial Microvesicles. *Circ. Res.* 124, 575–587. doi:10.1161/CIRCRESAHA.118.314010

Liu, Z.-H., Zhang, Y., Wang, X., Fan, X.-F., Zhang, Y., Li, X., et al. (2019b). SIRT1 Activation Attenuates Cardiac Fibrosis by Endothelial-To-Mesenchymal Transition. *Biomed. Pharmacother.* 118, 109227. doi:10.1016/j.biopha.2019.109227

Lum, H., and Malik, A. B. (1996). Mechanisms of Increased Endothelial Permeability. *Can. J. Physiol. Pharmacol.* 74, 787–800. doi:10.1139/y96-081

Lutton, E. M., Razmpour, R., Andrews, A. M., Cannella, L. A., Son, Y.-J., Shuvaev, V. V., et al. (2017). Acute Administration of Catalase Targeted to ICAM-1 Attenuates Neuropathology in Experimental Traumatic Brain Injury. *Sci. Rep.* 7, 3846. doi:10.1038/s41598-017-03309-4

Lv, H., Wang, H., Quan, M., Zhang, C., Fu, Y., Zhang, L., et al. (2021). Cartilage Oligomeric Matrix Protein fine-tunes Disturbed Flow-Induced Endothelial Activation and Atherogenesis. *Matrix Biol.* 95, 32–51. doi:10.1016/j.matbio.2020.10.003

Lv, Y.-C., Tang, Y.-Y., Zhang, P., Wan, W., Yao, F., He, P.-P., et al. (2016). Histone Methyltransferase Enhancer of Zeste Homolog 2-Mediated ABCA1 Promoter DNA Methylation Contributes to the Progression of Atherosclerosis. *PLOS ONE* 11, e0157265. doi:10.1371/journal.pone.0157265

Ma, J., Sanchez-Duffhues, G., Goumans, M.-J., and ten Dijke, P. (2020). TGF-β-Induced Endothelial to Mesenchymal Transition in Disease and Tissue Engineering. *Front. Cell Dev. Biol.* 8, 260. doi:10.3389/fcell.2020.00260

Mach, F., Baigent, C., Catapano, A. L., Koskinas, K. C., Casula, M., Badimon, L., et al. (2020). 2019 ESC/EAS Guidelines for the Management of Dyslipidaemias: Lipid Modification to Reduce Cardiovascular Risk: The Task Force for the Management of Dyslipidaemias of the European Society of Cardiology (ESC) and European Atherosclerosis Society (EAS). *Eur. Heart J.* 41, 111–188. doi:10.1093/eurheartj/ehz455

Maleszewska, M., Vanchin, B., Harmsen, M. C., and Krenning, G. (2016). The Decrease in Histone Methyltransferase EZH2 in Response to Fluid Shear Stress Alters Endothelial Gene Expression and Promotes Quiescence. *Angiogenesis* 19, 9–24. doi:10.1007/s10456-015-9485-2

Mannarino, E., and Pirro, M. (2008). Endothelial Injury and Repair: A Novel Theory for Atherosclerosis. *Angiology* 59, 69S–72S. doi:10.1177/0003319708320761

Marchio, P., Guerra-Ojeda, S., Vila, J. M., Aldasoro, M., Victor, V. M., and Mauricio, M. D. (2019). Targeting Early Atherosclerosis: A Focus on Oxidative Stress and Inflammation. *Oxid. Med. Cell. Longev.* 2019, e8563845. doi:10.1155/2019/8563845

Marcos-Contreras, O. A., Greineder, C. F., Kiseleva, R. Y., Parhiz, H., Walsh, L. R., Zuluaga-Ramirez, V., et al. (2020). Selective Targeting of Nanomedicine to Inflamed Cerebral Vasculature to Enhance the Blood–Brain Barrier. *Proc. Natl. Acad. Sci.* 117, 3405–3414. doi:10.1073/pnas.1912012117

Matsushita, K., Morrell, C. N., Cambien, B., Yang, S.-X., Yamakuchi, M., Bao, C., et al. (2003). Nitric Oxide Regulates Exocytosis by S-Nitrosylation of N-Ethylmaleimide-Sensitive Factor. *Cell* 115, 139–150. doi:10.1016/S0092-8674(03)00803-1

Maurya, M. R., Gupta, S., Li, J. Y.-S., Ajami, N. E., Chen, Z. B., Shyy, J. Y.-J., et al. (2021). Longitudinal Shear Stress Response in Human Endothelial Cells to Atheroprone and Atheroprotective Conditions. *Proc. Natl. Acad. Sci.* 118, e2023236118. doi:10.1073/pnas.2023236118

Mehta, V., Pang, K.-L., Rozbesky, D., Nather, K., Keen, A., Lachowski, D., et al. (2020). The Guidance Receptor Plexin D1 Is a Mechanosensor in Endothelial Cells. *Nature* 578, 290–295. doi:10.1038/s41586-020-1979-4

Méndez-Barbero, N., Gutiérrez-Muñoz, C., and Blanco-Colio, L. M. (2021). Cellular Crosstalk between Endothelial and Smooth Muscle Cells in Vascular Wall Remodeling. *Int. J. Mol. Sci.* 22, 7284. doi:10.3390/ijms22147284

Mocanu, C. A., Fuior, E. V., Voicu, G., Rebleanu, D., Safciuc, F., Deleanu, M., et al. (2021). P-selectin Targeted RAGE-shRNA Lipoplexes Alleviate Atherosclerosis-Associated Inflammation. *J. Controlled Release* 338, 754–772. doi:10.1016/j.jconrel.2021.09.012

Mohammadzadeh, N., Montecucco, F., Carbone, F., Xu, S., Al-Rasadi, K., and Sahebkar, A. (2020). Statins: Epidrugs with Effects on Endothelial Health? *Eur. J. Clin. Invest.* 50, e13388. doi:10.1111/eci.13388

Moonen, J.-R. A. J., Lee, E. S., Schmidt, M., Maleszewska, M., Koerts, J. A., Brouwer, L. A., et al. (2015). Endothelial-to-mesenchymal Transition Contributes to Fibro-Proliferative Vascular Disease and Is Modulated by Fluid Shear Stress. *Cardiovasc. Res.* 108, 377–386. doi:10.1093/cvr/cvv175

Morris, S. M., Jr (2009). Recent Advances in Arginine Metabolism: Roles and Regulation of the Arginases. *Br. J. Pharmacol.* 157, 922–930. doi:10.1111/j.1476-5381.2009.00278.x

Moss, J. W. E., and Ramji, D. P. (2016). Nutraceutical Therapies for Atherosclerosis. *Nat. Rev. Cardiol.* 13, 513–532. doi:10.1038/nrcardio.2016.103

Mulligan-Kehoe, M. J., and Simons, M. (2014). Vasa Vasorum in normal and Diseased Arteries. *Circulation* 129, 2557–2566. doi:10.1161/CIRCULATIONAHA.113.007189

Mundi, S., Massaro, M., Scoditti, E., Carluccio, M. A., van Hinsbergh, V. W. M., Iruela-Arispe, M. L., et al. (2018). Endothelial Permeability, LDL Deposition, and Cardiovascular Risk Factors—A Review. *Cardiovasc. Res.* 114, 35–52. doi:10.1093/cvr/cvx226

Muniyappa, R., Iantorno, M., and Quon, M. J. (2008). An Integrated View of Insulin Resistance and Endothelial Dysfunction. *Endocrinol. Metab. Clin. North. Am.* 37, 685–711. doi:10.1016/j.ecl.2008.06.001

Muzaffar, S., Shukla, N., Bond, M., Newby, A. C., Angelini, G. D., Sparatore, A., et al. (2008). Exogenous Hydrogen Sulfide Inhibits Superoxide Formation, NOX-1 Expression and Rac1 Activity in Human Vascular Smooth Muscle Cells. *J. Vasc. Res.* 45, 521–528. doi:10.1159/000129686

Newman, A. A. C., Serbulea, V., Baylis, R. A., Shankman, L. S., Bradley, X., Alencar, G. F., et al. (2021). Multiple Cell Types Contribute to the Atherosclerotic Lesion Fibrous Cap by PDGFRβ and Bioenergetic Mechanisms. *Nat. Metab.* 3, 166–181. doi:10.1038/s42255-020-00338-8

Ni, C.-W., Hsieh, H.-J., Chao, Y.-J., and Wang, D. L. (2003). Shear Flow Attenuates Serum-Induced STAT3 Activation in Endothelial Cells. *J. Biol. Chem.* 278, 19702–19708. doi:10.1074/jbc.M300893200

Nidorf, S. M., Eikelboom, J. W., Budgeon, C. A., and Thompson, P. L. (2013). Low-dose Colchicine for Secondary Prevention of Cardiovascular Disease. *J. Am. Coll. Cardiol.* 61, 404–410. doi:10.1016/j.jacc.2012.10.027

Nigro, P., Abe, J.-I., and Berk, B. C. (2011). Flow Shear Stress and Atherosclerosis: a Matter of Site Specificity. *Antioxid. Redox Signal.* 15, 1405–1414. doi:10.1089/ars.2010.3679

Njock, M.-S., Cheng, H. S., Dang, L. T., Nazari-Jahantigh, M., Lau, A. C., Boudreau, E., et al. (2015). Endothelial Cells Suppress Monocyte Activation through Secretion of Extracellular Vesicles Containing Antiinflammatory microRNAs. *Blood* 125, 3202–3212. doi:10.1182/blood-2014-11-611046

Oesterreicher, J., Pultar, M., Schneider, J., Mühleder, S., Zipperle, J., Grillari, J., et al. (2020). Fluorescence-Based Nanoparticle Tracking Analysis and Flow Cytometry for Characterization of Endothelial Extracellular Vesicle Release. *Int. J. Mol. Sci.* 21, 9278. doi:10.3390/ijms21239278

Okamoto, T., and Suzuki, K. (2017). The Role of Gap Junction-Mediated Endothelial Cell–Cell Interaction in the Crosstalk between Inflammation and Blood Coagulation. *Int. J. Mol. Sci.* 18, 2254. doi:10.3390/ijms18112254

Örd, T., Õunap, K., Stolze, L. K., Aherrahrou, R., Nurminen, V., Toropainen, A., et al. (2021). Single-Cell Epigenomics and Functional Fine-Mapping of Atherosclerosis GWAS Loci. *Circ. Res.* 129, 240–258. doi:10.1161/CIRCRESAHA.121.318971

Ou, Z.-J., Chang, F.-J., Luo, D., Liao, X.-L., Wang, Z.-P., Zhang, X., et al. (2011). Endothelium-derived Microparticles Inhibit Angiogenesis in the Heart and Enhance the Inhibitory Effects of Hypercholesterolemia on Angiogenesis. *Am. J. Physiol.-Endocrinol. Metab.* 300, E661–E668. doi:10.1152/ajpendo.00611.2010

Pai, P.-Y., Chou, W.-C., Chan, S.-H., Wu, S.-Y., Chen, H.-I., Li, C.-W., et al. (2021). Epigallocatechin Gallate Reduces Homocysteine-Caused Oxidative Damages through Modulation SIRT1/AMPK Pathway in Endothelial Cells. *Am. J. Chin. Med.* 49, 113–129. doi:10.1142/S0192415X21500063

Pan, S. (2009). Molecular Mechanisms Responsible for the Atheroprotective Effects of Laminar Shear Stress. *Antioxid. Redox Signal.* 11, 1669–1682. doi:10.1089/ars.2009.2487

Park, J. H., Jiang, Y., Zhou, J., Gong, H., Mohapatra, A., Heo, J., et al. (2021). Genetically Engineered Cell Membrane–Coated Nanoparticles for Targeted Delivery of Dexamethasone to Inflamed Lungs. *Sci. Adv.* 7, eabf7820. doi:10.1126/sciadv.abf7820

Parmar, K. M., Nambudiri, V., Dai, G., Larman, H. B., Gimbrone, M. A., and García-Cardeña, G. (2005). Statins Exert Endothelial Atheroprotective Effects via the KLF2 Transcription Factor. *J. Biol. Chem.* 280, 26714–26719. doi:10.1074/jbc.C500144200

Peng, M., Liu, X., and Xu, G. (2020). Extracellular Vesicles as Messengers in Atherosclerosis. *J. Cardiovasc. Transl. Res.* 13, 121–130. doi:10.1007/s12265-019-09923-z

Pfenniger, A., Chanson, M., and Kwak, B. R. (2013). Connexins in Atherosclerosis. *Biochim. Biophys. Acta BBA - Biomembr.* 1828, 157–166. doi:10.1016/j.bbamem.2012.05.011

Pi, X., Yan, C., and Berk, B. C. (2004). Big Mitogen-Activated Protein Kinase (BMK1)/ERK5 Protects Endothelial Cells from Apoptosis. *Circ. Res.* 94, 362–369. doi:10.1161/01.RES.0000112406.27800.6F

Pichavaram, P., Mani, A. M., Singh, N. K., and Rao, G. N. (2019). Cholesterol Crystals Promote Endothelial Cell and Monocyte Interactions via H2O2-Mediated PP2A Inhibition, NFκB Activation and ICAM1 and VCAM1 Expression. *Redox Biol.* 24, 101180. doi:10.1016/j.redox.2019.101180

Piepoli, M. F., Hoes, A. W., Agewall, S., Albus, C., Brotons, C., Catapano, A. L., et al. (2016). 2016 European Guidelines on Cardiovascular Disease Prevention in Clinical Practice. *Eur. Heart J.* 37, 2315–2381. doi:10.1093/eurheartj/ehw106

Poels, K., Schnitzler, J. G., Waissi, F., Levels, J. H. M., Stroes, E. S. G., Daemen, M. J. A. P., et al. (2020). Inhibition of PFKFB3 Hampers the Progression of Atherosclerosis and Promotes Plaque Stability. *Front. Cell Dev. Biol.* 8, 581641. doi:10.3389/fcell.2020.581641

Qu, D., Wang, L., Huo, M., Song, W., Lau, C.-W., Xu, J., et al. (2020). Focal TLR4 Activation Mediates Disturbed Flow-Induced Endothelial Inflammation. *Cardiovasc. Res.* 116, 226–236. doi:10.1093/cvr/cvz046

Raines, E. W., and Ferri, N. (2005). Thematic Review Series: The Immune System and Atherogenesis. Cytokines Affecting Endothelial and Smooth Muscle Cells in Vascular Disease. *J. Lipid Res.* 46, 1081–1092. doi:10.1194/jlr.R500004-JLR200

Reglero-Real, N., Colom, B., Bodkin, J. V., and Nourshargh, S. (2016). Endothelial Cell Junctional Adhesion Molecules. *Arterioscler. Thromb. Vasc. Biol.* 36, 2048–2057. doi:10.1161/ATVBAHA.116.307610

Ricard, N., Bailly, S., Guignabert, C., and Simons, M. (2021). The Quiescent Endothelium: Signalling Pathways Regulating Organ-specific Endothelial Normalcy. *Nat. Rev. Cardiol.* 18, 565–580. doi:10.1038/s41569-021-00517-4

Ridker, P. M., Everett, B. M., Thuren, T., MacFadyen, J. G., Chang, W. H., Ballantyne, C., et al. (2017). Antiinflammatory Therapy with Canakinumab for Atherosclerotic Disease. *N. Engl. J. Med.* 377, 1119–1131. doi:10.1056/NEJMoa1707914

Sager, H. B., Dutta, P., Dahlman, J. E., Hulsmans, M., Courties, G., Sun, Y., et al. (2016). RNAi Targeting Multiple Cell Adhesion Molecules Reduces Immune Cell Recruitment and Vascular Inflammation after Myocardial Infarction. *Sci. Transl. Med.* 8, 342ra80. doi:10.1126/scitranslmed.aaf1435

Schober, A., Nazari-Jahantigh, M., Wei, Y., Bidzhekov, K., Gremse, F., Grommes, J., et al. (2014). MicroRNA-126-5p Promotes Endothelial Proliferation and Limits Atherosclerosis by Suppressing Dlk1. *Nat. Med.* 20, 368–376. doi:10.1038/nm.3487

Sedding, D. G., Boyle, E. C., Demandt, J. A. F., Sluimer, J. C., Dutzmann, J., Haverich, A., et al. (2018). Vasa Vasorum Angiogenesis: Key Player in the Initiation and Progression of Atherosclerosis and Potential Target for the Treatment of Cardiovascular Disease. *Front. Immunol.* 9, 706. doi:10.3389/fimmu.2018.00706

Sei, Y. J., Ahn, S. I., Virtue, T., Kim, T., and Kim, Y. (2017). Detection of Frequency-dependent Endothelial Response to Oscillatory Shear Stress Using a Microfluidic Transcellular Monitor. *Sci. Rep.* 7, 10019. doi:10.1038/s41598-017-10636-z

SenBanerjee, S., Lin, Z., Atkins, G. B., Greif, D. M., Rao, R. M., Kumar, A., et al. (2004). KLF2 Is a Novel Transcriptional Regulator of Endothelial Proinflammatory Activation. *J. Exp. Med.* 199, 1305–1315. doi:10.1084/jem.20031132

Shan, Z., Qin, S., Li, W., Wu, W., Yang, J., Chu, M., et al. (2015). An Endocrine Genetic Signal between Blood Cells and Vascular Smooth Muscle Cells. *J. Am. Coll. Cardiol.* 65, 2526–2537. doi:10.1016/j.jacc.2015.03.570

Silva, I. V. G., de Figueiredo, R. C., and Rios, D. R. A. (2019). Effect of Different Classes of Antihypertensive Drugs on Endothelial Function and Inflammation. *Int. J. Mol. Sci.* 20, 3458. doi:10.3390/ijms20143458

Silverman, M. G., Ference, B. A., Im, K., Wiviott, S. D., Giugliano, R. P., Grundy, S. M., et al. (2016). Association between Lowering LDL-C and Cardiovascular Risk Reduction Among Different Therapeutic Interventions: A Systematic Review and Meta-Analysis. *JAMA* 316, 1289–1297. doi:10.1001/jama.2016.13985

Sluiter, T. J., van Buul, J. D., Huveneers, S., Quax, P. H. A., and de Vries, M. R. (2021). Endothelial Barrier Function and Leukocyte Transmigration in Atherosclerosis. *Biomedicines* 9, 328. doi:10.3390/biomedicines9040328

Souilhol, C., Harmsen, M. C., Evans, P. C., and Krenning, G. (2018). Endothelial–mesenchymal Transition in Atherosclerosis. *Cardiovasc. Res.* 114, 565–577. doi:10.1093/cvr/cvx253

Stamler, J. S., Jia, L., Eu, J. P., McMahon, T. J., Demchenko, I. T., Bonaventura, J., et al. (1997). Blood Flow Regulation by S-Nitrosohemoglobin in the Physiological Oxygen Gradient. *Science* 276, 2034–2037. doi:10.1126/science.276.5321.2034

Swain, S. M., and Liddle, R. A. (2020). Piezo1 Acts Upstream of TRPV4 to Induce Pathological Changes in Endothelial Cells Due to Shear Stress. *J. Biol. Chem.* 296, 100171. doi:10.1074/jbc.RA120.015059

Tamarappoo, B. K., Lin, A., Commandeur, F., McElhinney, P. A., Cadet, S., Goeller, M., et al. (2021). Machine Learning Integration of Circulating and Imaging Biomarkers for Explainable Patient-specific Prediction of Cardiac Events: A Prospective Study. *Atherosclerosis* 318, 76–82. doi:10.1016/j.atherosclerosis.2020.11.008

Tardif, J.-C., L'Allier, P. L., Ibrahim, R., Grégoire, J. C., Nozza, A., Cossette, M., et al. (2010). Treatment with 5-Lipoxygenase Inhibitor VIA-2291 (Atreleuton) in Patients with Recent Acute Coronary Syndrome. *Circ. Cardiovasc. Imaging* 3, 298–307. doi:10.1161/CIRCIMAGING.110.937169

Theodorou, K., and Boon, R. A. (2018). Endothelial Cell Metabolism in Atherosclerosis. *Front. Cell Dev. Biol.* 6, 82. doi:10.3389/fcell.2018.00082

Thorp, E., Cui, D., Schrijvers, D. M., Kuriakose, G., and Tabas, I. (2008). Mertk Receptor Mutation Reduces Efferocytosis Efficiency and Promotes Apoptotic Cell Accumulation and Plaque Necrosis in Atherosclerotic Lesions of Apoe-/- Mice. *Arterioscler. Thromb. Vasc. Biol.* 28, 1421–1428. doi:10.1161/ATVBAHA.108.167197

Tran-Dinh, A., Diallo, D., Delbosc, S., Varela-Perez, L. M., Dang, Q. B., Lapergue, B., et al. (2013). HDL and Endothelial protection. *Br. J. Pharmacol.* 169, 493–511. doi:10.1111/bph.12174

Ul Ain, Q., Chung, H., Chung, J. Y., Choi, J.-H., and Kim, Y.-H. (2017). Amelioration of Atherosclerotic Inflammation and Plaques via Endothelial Adrenoceptor-Targeted eNOS Gene Delivery Using Redox-Sensitive Polymer Bearing L-Arginine. *J. Controlled Release* 262, 72–86. doi:10.1016/j.jconrel.2017.07.019

van der Heijden, T., Kritikou, E., Venema, W., van Duijn, J., van Santbrink, P. J., Slütter, B., et al. (2017). NLRP3 Inflammasome Inhibition by MCC950 Reduces Atherosclerotic Lesion Development in Apolipoprotein E–Deficient Mice—Brief Report. *Arterioscler. Thromb. Vasc. Biol.* 37, 1457–1461. doi:10.1161/ATVBAHA.117.309575

VanderLaan, P. A., Reardon, C. A., and Getz, G. S. (2004). Site Specificity of Atherosclerosis. *Arterioscler. Thromb. Vasc. Biol.* 24, 12–22. doi:10.1161/01.ATV.0000105054.43931.f0

Varadharaj, S., Kelly, O. J., Khayat, R. N., Kumar, P. S., Ahmed, N., and Zweier, J. L. (2017). Role of Dietary Antioxidants in the Preservation of Vascular Function and the Modulation of Health and Disease. *Front. Cardiovasc. Med.* 4, 64. doi:10.3389/fcvm.2017.00064

Wang, H., Xie, Y., Salvador, A. M., Zhang, Z., Chen, K., Li, G., et al. (2020a). Exosomes: Multifaceted Messengers in Atherosclerosis. *Curr. Atheroscler. Rep.* 22, 57. doi:10.1007/s11883-020-00871-7

Wang, J., Li, P., Xu, X., Zhang, B., and Zhang, J. (2020b). MicroRNA-200a Inhibits Inflammation and Atherosclerotic Lesion Formation by Disrupting EZH2-Mediated Methylation of STAT3. *Front. Immunol.* 11, 907. doi:10.3389/fimmu.2020.00907

Wang, K.-C., Nguyen, P., Weiss, A., Yeh, Y.-T., Chien, H. S., Lee, A., et al. (2014). MicroRNA-23b Regulates Cyclin-dependent Kinase–Activating Kinase Complex through Cyclin H Repression to Modulate Endothelial Transcription and Growth under Flow. *Arterioscler. Thromb. Vasc. Biol.* 34, 1437–1445. doi:10.1161/ATVBAHA.114.303473

Wang, K.-C., Yeh, Y.-T., Nguyen, P., Limqueco, E., Lopez, J., Thorossian, S., et al. (2016a). Flow-dependent YAP/TAZ Activities Regulate Endothelial

Phenotypes and Atherosclerosis. *Proc. Natl. Acad. Sci.* 113, 11525–11530. doi:10.1073/pnas.1613121113

Wang, K., Li, B., Xie, Y., Xia, N., Li, M., and Gao, G. (2020c). Statin Rosuvastatin Inhibits Apoptosis of Human Coronary Artery Endothelial Cells through Upregulation of the JAK2/STAT3 Signaling Pathway. *Mol. Med. Rep.* 22, 2052–2062. doi:10.3892/mmr.2020.11266

Wang, L., Luo, J.-Y., Li, B., Tian, X. Y., Chen, L.-J., Huang, Y., et al. (2016b). Integrin-YAP/TAZ-JNK cascade Mediates Atheroprotective Effect of Unidirectional Shear Flow. *Nature* 540, 579–582. doi:10.1038/nature20602

Wang, Y., Sun, H.-Y., Kumar, S., Puertadel, M. M., Jo, H., and Rezvan, A. (2019a). ZBTB46 Is a Shear-Sensitive Transcription Factor Inhibiting Endothelial Cell Proliferation via Gene Expression Regulation of Cell Cycle Proteins. *Lab. Invest.* 99, 305–318. doi:10.1038/s41374-018-0060-5

Wang, Y., Xie, Y., Zhang, A., Wang, M., Fang, Z., and Zhang, J. (2019b). Exosomes: An Emerging Factor in Atherosclerosis. *Biomed. Pharmacother.* 115, 108951. doi:10.1016/j.biopha.2019.108951

Wang, Y., Xu, Z., Wang, X., Zheng, J., Peng, L., Zhou, Y., et al. (2021). Extracellular-vesicle Containing miRNA-503-5p Released by Macrophages Contributes to Atherosclerosis. *Aging* 13, 12239–12257. doi:10.18632/aging.103855

Warboys, C. M., de Luca, A., Amini, N., Luong, L., Duckles, H., Hsiao, S., et al. (2014). Disturbed Flow Promotes Endothelial Senescence via a P53-dependent Pathway. *Arterioscler. Thromb. Vasc. Biol.* 34, 985–995. doi:10.1161/ATVBAHA.114.303415

Wei, X., Schneider, J. G., Shenouda, S. M., Lee, A., Towler, D. A., Chakravarthy, M. V., et al. (2011). De Novo Lipogenesis Maintains Vascular Homeostasis through Endothelial Nitric-Oxide Synthase (eNOS) Palmitoylation. *J. Biol. Chem.* 286, 2933–2945. doi:10.1074/jbc.M110.193037

Weinbaum, S., Tzeghai, G., Ganatos, P., Pfeffer, R., and Chien, S. (1985). Effect of Cell Turnover and Leaky Junctions on Arterial Macromolecular Transport. *Am. J. Physiol.* 248, H945–H960. doi:10.1152/ajpheart.1985.248.6.H945

Weinstein, N., Mendoza, L., and Álvarez-Buylla, E. R. (2020). A Computational Model of the Endothelial to Mesenchymal Transition. *Front. Genet.* 11, 40. doi:10.3389/fgene.2020.00040

White, S. J., Newby, A. C., and Johnson, T. W. (2016). Endothelial Erosion of Plaques as a Substrate for Coronary Thrombosis. *Thromb. Haemost.* 115, 509–519. doi:10.1160/TH15-09-0765

Winter, P. M., Caruthers, S. D., Zhang, H., Williams, T. A., Wickline, S. A., and Lanza, G. M. (2008). Antiangiogenic Synergism of Integrin-Targeted Fumagillin Nanoparticles and Atorvastatin in Atherosclerosis. *JACC Cardiovasc. Imaging* 1, 624–634. doi:10.1016/j.jcmg.2008.06.003

Winter, P. M., Neubauer, A. M., Caruthers, S. D., Harris, T. D., Robertson, J. D., Williams, T. A., et al. (2006). Endothelial αvβ3 Integrin–Targeted Fumagillin Nanoparticles Inhibit Angiogenesis in Atherosclerosis. *Arterioscler. Thromb. Vasc. Biol.* 26, 2103–2109. doi:10.1161/01.ATV.0000235724.11299.76

Won, D., Zhu, S.-N., Chen, M., Teichert, A.-M., Fish, J. E., Matouk, C. C., et al. (2007). Relative Reduction of Endothelial Nitric-Oxide Synthase Expression and Transcription in Atherosclerosis-Prone Regions of the Mouse Aorta and in an *In Vitro* Model of Disturbed Flow. *Am. J. Pathol.* 171, 1691–1704. doi:10.2353/ajpath.2007.060860

Wu, K. Q., Muratore, C. S., So, E.-Y., Sun, C., Dubielecka, P. M., Reginato, A. M., et al. (2017). M1 Macrophage–Induced Endothelial-To-Mesenchymal Transition Promotes Infantile Hemangioma Regression. *Am. J. Pathol.* 187, 2102–2111. doi:10.1016/j.ajpath.2017.05.014

Wu, X., Du, X., Yang, Y., Liu, X., Liu, X., Zhang, N., et al. (2021). Inhibition of miR-122 Reduced Atherosclerotic Lesion Formation by Regulating NPAS3-Mediated Endothelial to Mesenchymal Transition. *Life Sci.* 265, 118816. doi:10.1016/j.lfs.2020.118816

Xia, L., Zhang, B., Sun, Y., Chen, B., and Yu, Z. (2021). Analysis of Syk/PECAM-1 Signaling Pathway in Low Shear Stress Induced Atherosclerosis Based on Ultrasound Imaging. *Comput. Methods Programs Biomed.* 201, 105953. doi:10.1016/j.cmpb.2021.105953

Xiang, D., Li, Y., Cao, Y., Huang, Y., Zhou, L., Lin, X., et al. (2021). Different Effects of Endothelial Extracellular Vesicles and LPS-Induced Endothelial Extracellular Vesicles on Vascular Smooth Muscle Cells: Role of Curcumin and its Derivatives. *Front. Cardiovasc. Med.* 8, 649352. doi:10.3389/fcvm.2021.649352

Xiao, H., Lu, M., Lin, T. Y., Chen, Z., Chen, G., Wang, W.-C., et al. (2013). Sterol Regulatory Element Binding Protein 2 Activation of NLRP3 Inflammasome in Endothelium Mediates Hemodynamic-Induced Atherosclerosis Susceptibility. *Circulation* 128, 632–642. doi:10.1161/CIRCULATIONAHA.113.002714

Xie, T., Wang, C., Jin, Y., Meng, Q., Liu, Q., Wu, J., et al. (2020). CoenzymeQ10-Induced Activation of AMPK-YAP-OPA1 Pathway Alleviates Atherosclerosis by Improving Mitochondrial Function, Inhibiting Oxidative Stress and Promoting Energy Metabolism. *Front. Pharmacol.* 11, 1034. doi:10.3389/fphar.2020.01034

Xu, J., Lu, X., and Shi, G.-P. (2015). Vasa Vasorum in Atherosclerosis and Clinical Significance. *Int. J. Mol. Sci.* 16, 11574–11608. doi:10.3390/ijms160511574

Xu, Q. (2009). Disturbed Flow-Enhanced Endothelial Turnover in Atherosclerosis. *Trends Cardiovasc. Med.* 19, 191–195. doi:10.1016/j.tcm.2009.12.002

Xu, Q. (2007). Progenitor Cells in Vascular Repair. *Curr. Opin. Lipidol.* 18, 534–539. doi:10.1097/MOL.0b013e3282a66082

Xu, S., Ilyas, I., Little, P. J., Li, H., Kamato, D., Zheng, X., et al. (2021). Endothelial Dysfunction in Atherosclerotic Cardiovascular Diseases and beyond: From Mechanism to Pharmacotherapies. *Pharmacol. Rev.* 73, 924–967. doi:10.1124/pharmrev.120.000096

Xu, X., Tan, X., Tampe, B., Wilhelmi, T., Hulshoff, M. S., Saito, S., et al. (2018). High-fidelity CRISPR/Cas9- Based Gene-specific Hydroxymethylation Rescues Gene Expression and Attenuates Renal Fibrosis. *Nat. Commun.* 9, 3509. doi:10.1038/s41467-018-05766-5

Xue, S., Tang, H., Zhao, G., Fang, C., Shen, Y., Yan, D., et al. (2021). C–C Motif Ligand 8 Promotes Atherosclerosis via NADPH Oxidase 2/reactive Oxygen Species-Induced Endothelial Permeability Increase. *Free Radic. Biol. Med.* 167, 181–192. doi:10.1016/j.freeradbiomed.2021.02.022

Yamawaki, H., Lehoux, S., and Berk, B. C. (2003). Chronic Physiological Shear Stress Inhibits Tumor Necrosis Factor–Induced Proinflammatory Responses in Rabbit Aorta Perfused *Ex Vivo*. *Circulation* 108, 1619–1625. doi:10.1161/01.CIR.0000089373.49941.C4

Yang, Q., Xu, J., Ma, Q., Liu, Z., Sudhahar, V., Cao, Y., et al. (2018). PRKAA1/AMPKα1-driven Glycolysis in Endothelial Cells Exposed to Disturbed Flow Protects against Atherosclerosis. *Nat. Commun.* 9, 4667. doi:10.1038/s41467-018-07132-x

Yu, P., Wilhelm, K., Dubrac, A., Tung, J. K., Alves, T. C., Fang, J. S., et al. (2017). FGF-dependent Metabolic Control of Vascular Development. *Nature* 545, 224–228. doi:10.1038/nature22322

Yuan, P., Hu, Q., He, X., Long, Y., Song, X., Wu, F., et al. (2020a). Laminar Flow Inhibits the Hippo/YAP Pathway via Autophagy and SIRT1-Mediated Deacetylation against Atherosclerosis. *Cell Death Dis.* 11, 141. doi:10.1038/s41419-020-2343-1

Yuan, X., Bhat, O. M., Samidurai, A., Das, A., Zhang, Y., and Li, P.-L. (2020b). Reversal of Endothelial Extracellular Vesicle-Induced Smooth Muscle Phenotype Transition by Hypercholesterolemia Stimulation: Role of NLRP3 Inflammasome Activation. *Front. Cell Dev. Biol.* 8, 597423. doi:10.3389/fcell.2020.597423

Zanardo, R. C. O., Brancaleone, V., Distrutti, E., Fiorucci, S., Cirino, G., and Wallace, J. L. (2006). Hydrogen Sulfide Is an Endogenous Modulator of Leukocyte-Mediated Inflammation. *FASEB J. Off. Publ. Fed. Am. Soc. Exp. Biol.* 20, 2118–2120. doi:10.1096/fj.06-6270fje

Zernecke, A., Bidzhekov, K., Noels, H., Shagdarsuren, E., Gan, L., Denecke, B., et al. (2009). Delivery of MicroRNA-126 by Apoptotic Bodies Induces CXCL12-dependent Vascular Protection. *Sci. Signal.* 2, ra81. doi:10.1126/scisignal.2000610

Zhang, C., Zhou, T., Chen, Z., Yan, M., Li, B., Lv, H., et al. (2020a). Coupling of Integrin α5 to Annexin A2 by Flow Drives Endothelial Activation. *Circ. Res.* 127, 1074–1090. doi:10.1161/CIRCRESAHA.120.316857

Zhang, K., Chen, Y., Zhang, T., Huang, L., Wang, Y., Yin, T., et al. (2018a). A Novel Role of Id1 in Regulating Oscillatory Shear Stress-Mediated Lipid Uptake in Endothelial Cells. *Ann. Biomed. Eng.* 46, 849–863. doi:10.1007/s10439-018-2000-3

Zhang, X., Sessa, W. C., and Fernández-Hernando, C. (2018b). Endothelial Transcytosis of Lipoproteins in Atherosclerosis. *Front. Cardiovasc. Med.* 5, 130. doi:10.3389/fcvm.2018.00130

Zhang, Y.-P., Huang, Y.-T., Huang, T.-S., Pang, W., Zhu, J.-J., Liu, Y.-F., et al. (2017). The Mammalian Target of Rapamycin and DNA Methyltransferase 1 axis Mediates Vascular Endothelial Dysfunction in Response to Disturbed Flow. *Sci. Rep.* 7, 14996. doi:10.1038/s41598-017-15387-5

Zhang, Z., Yi, D., Zhou, J., Zheng, Y., Gao, Z., Hu, X., et al. (2020b). Exosomal LINC01005 Derived from Oxidized Low-Density Lipoprotein-Treated Endothelial Cells Regulates Vascular Smooth Muscle Cell Phenotypic Switch. *BioFactors* 46, 743–753. doi:10.1002/biof.1665

Zhao, G., Lu, H., Liu, Y., Zhao, Y., Zhu, T., Garcia-Barrio, M. T., et al. (2021). Single-Cell Transcriptomics Reveals Endothelial Plasticity during Diabetic Atherogenesis. *Front. Cell Dev. Biol.* 9, 689469. doi:10.3389/fcell.2021.689469

Zhao, Y., Ren, P., Li, Q., Umar, S. A., Yang, T., Dong, Y., et al. (2020). Low Shear Stress Upregulates CX3CR1 Expression by Inducing VCAM-1 via the NF-κB Pathway in Vascular Endothelial Cells. *Cell Biochem. Biophys.* 78, 383–389. doi:10.1007/s12013-020-00931-4

Zhao, Z.-Z., Wang, Z., Li, G.-H., Wang, R., Tan, J.-M., Cao, X., et al. (2011). Hydrogen Sulfide Inhibits Macrophage-Derived Foam Cell Formation. *Exp. Biol. Med.* 236, 169–176. doi:10.1258/ebm.2010.010308

Zheng, B., Yin, W., Suzuki, T., Zhang, X., Zhang, Y., Song, L., et al. (2017). Exosome-Mediated miR-155 Transfer from Smooth Muscle Cells to Endothelial Cells Induces Endothelial Injury and Promotes Atherosclerosis. *Mol. Ther.* 25, 1279–1294. doi:10.1016/j.ymthe.2017.03.031

Zhou, J., Li, Y.-S., Nguyen, P., Wang, K.-C., Weiss, A., Kuo, Y.-C., et al. (2013). Regulation of Vascular Smooth Muscle Cell Turnover by Endothelial Cell–Secreted MicroRNA-126. *Circ. Res.* 113, 40–51. doi:10.1161/CIRCRESAHA.113.280883

Zhou, S., Chen, H.-Z., Wan, Y., Zhang, Q.-J., Wei, Y.-S., Huang, S., et al. (2011). Repression of P66Shc Expression by SIRT1 Contributes to the Prevention of Hyperglycemia-Induced Endothelial Dysfunction. *Circ. Res.* 109, 639–648. doi:10.1161/CIRCRESAHA.111.243592

Zhu, M.-L., Wang, G., Wang, H., Guo, Y.-M., Song, P., Xu, J., et al. (2019). Amorphous Nano-Selenium Quantum Dots Improve Endothelial Dysfunction in Rats and Prevent Atherosclerosis in Mice through Na+/H+ Exchanger 1 Inhibition. *Vascul. Pharmacol.* 115, 26–32. doi:10.1016/j.vph.2019.01.005

Conflict of Interest: The authors declare that the research was conducted in the absence of any commercial or financial relationships that could be construed as a potential conflict of interest.

Publisher's Note: All claims expressed in this article are solely those of the authors and do not necessarily represent those of their affiliated organizations, or those of the publisher, the editors and the reviewers. Any product that may be evaluated in this article, or claim that may be made by its manufacturer, is not guaranteed or endorsed by the publisher.

frontiers in Pharmacology

ORIGINAL RESEARCH
published: 13 January 2022
doi: 10.3389/fphar.2021.785193

Sex-Specific Differences in Resolution of Airway Inflammation in *Fat-1* Transgenic Mice Following Repetitive Agricultural Dust Exposure

*Arzu Ulu[1], Jalene V. Velazquez[1], Abigail Burr[1], Stefanie N. Sveiven[1], Jun Yang[2], Carissa Bravo[1], Bruce D. Hammock[2] and Tara M. Nordgren[1,3]**

[1]*Division of Biomedical Sciences, School of Medicine, University of California, Riverside, Riverside, CA, United States,* [2]*Department of Entomology and Nematology, University of California Davis Comprehensive Cancer Center, University of California, Davis, Davis, CA, United States,* [3]*Department of Environmental and Radiological Health Sciences, Colorado State University, Fort Collins, CO, United States*

In agriculture industries, workers are at increased risk for developing pulmonary diseases due to inhalation of agricultural dusts, particularly when working in enclosed confinement facilities. Agricultural dusts inhalation leads to unresolved airway inflammation that precedes the development and progression of lung disease. We have previously shown beneficial effects of the omega-3 polyunsaturated fatty acid (ω-3 PUFA) DHA in protecting against the negative inflammatory effects of repetitive dust exposure in the lung. Dietary manipulation of pulmonary disease risk is an attractive and timely approach given the contribution of an increased ω-6 to ω-3 PUFA ratio to low grade inflammation and chronic disease in the Western diet. To prevent any confounding factors that comes with dietary supplementation of ω-3 PUFA (different sources, purity, dose, and duration), we employed a *Fat-1* transgenic mouse model that convert ω-6 PUFA to ω-3 PUFA, leading to a tissue ω-6 to ω-3 PUFA ratio of approximately 1:1. Building on our initial findings, we hypothesized that attaining elevated tissue levels of ω-3 PUFA would attenuate agricultural dust-induced lung inflammation and its resolution. To test this hypothesis, we compared wild-type (WT) and *Fat-1* transgenic mice in their response to aqueous extracts of agricultural dust (DE). We also used a soluble epoxide hydrolase inhibitor (sEH) to potentiate the effects of ω-3 PUFA, since sEH inhibitors have been shown to stabilize the anti-inflammatory P450 metabolites derived from both ω-3 and ω-6 PUFA and promote generation of specialized pro-resolving lipid mediators from ω-3 PUFA. Over a three-week period, mice were exposed to a total of 15 intranasal instillations of DE obtained from swine confinement buildings in the Midwest. We observed genotype and sex-specific differences between the WT vs. *Fat-1* transgenic mice in response to repetitive dust exposure, where three-way ANOVA revealed significant main effects of treatment, genotype, and sex. Also, *Fat-1* transgenic mice displayed reduced lymphoid aggregates in the lung following DE exposure as compared to WT animals exposed to DE, suggesting improved resilience to the DE-induced inflammatory effects. Overall, our data implicate a protective role of ω-3 FA in the lung following repetitive dust exposure.

Keywords: *fat-1* transgenic mice, omega-3 fatty acids, agricultural dust, resolution of inflammation, sex

OPEN ACCESS

Edited by:
Pallavi R. Devchand, University of Calgary, Canada

Reviewed by:
Gerard Bannenberg, Global Organization for EPA and DHA Omega-3s (GOED), United States
Hong Yong Peh, Brigham and Women's Hospital and Harvard Medical School, United States

****Correspondence:***
Tara M. Nordgren
tmnordgren@gmail.com

Specialty section:
This article was submitted to Inflammation Pharmacology, a section of the journal Frontiers in Pharmacology

Received: *28 September 2021*
Accepted: *23 December 2021*
Published: *13 January 2022*

Citation:
Ulu A, Velazquez JV, Burr A, Sveiven SN, Yang J, Bravo C, Hammock BD and Nordgren TM (2022) Sex-Specific Differences in Resolution of Airway Inflammation in Fat-1 *Transgenic Mice Following Repetitive Agricultural Dust Exposure. Front. Pharmacol. 12:785193. doi: 10.3389/fphar.2021.785193*

1 INTRODUCTION

Agricultural workers are at increased risk for developing various respiratory diseases including chronic bronchitis, asthma, and COPD, due in part to exposure to respirable organic dusts associated with these environments (Von Essen and Romberger, 2003; Nordgren and Charavaryamath, 2018; Sigsgaard et al., 2020). Individuals that work in concentrated animal feeding operations, such as those housing swine, have appreciably increased risk for negative lung health outcomes (Iversen and Dahl, 2000; Kirkhorn and Garry, 2000; Pedersen et al., 2000; May et al., 2012; Pavilonis et al., 2013; Guillien et al., 2016; Nordgren and Bailey, 2016; Nordgren and Charavaryamath, 2018). Therapeutic options for affected individuals are limited, with no current treatments to reverse lung function decline associated with these ailments (American Thoracic, 1998; Kirkhorn and Garry, 2000; Kachan et al., 2012; Hoppin et al., 2014). Thus, novel treatment strategies that harness and/or promote reparative processes in the lung are necessary.

It is increasingly appreciated that inflammation resolution is an active process and regulated by a variety of pathways and mediators, some of which involve omega-3 (ω-3) and omega-6 (ω-6) polyunsaturated fatty acids (PUFA) (Levy and Serhan, 2014; Serhan et al., 2014; Hammock et al., 2020). As ω-3 PUFA are essential fatty acids that cannot be synthesized *de novo* by humans, dietary consumption of ω-3 PUFA dictates the tissue availability for these fatty acids and mediators derived from them. In a typical Western diet, ω-3 PUFA intakes are below recommended guidelines, while ω-6 PUFA intakes are high (Thompson et al., 2019). Conversely to ω-3 PUFA, ω-6 PUFA are metabolized into lipid mediators (e.g., leukotrienes, thromboxane, prostaglandins) that are largely involved in the induction of inflammatory processes (Calder et al., 2020). Thus, individuals consuming a diet with a high ω-6: ω-3 PUFA ratio may be at increased risk for inadequate control of inflammatory processes, with increased substrate to produce pro-inflammatory lipid mediators and a dearth of substrate for the production of specialized pro-resolving mediators (SPM).

We have recently assessed the efficacy of dietary supplementation with the ω-3 PUFA docosahexaenoic acid (DHA) on altering the lung inflammatory response and recovery following acute and repetitive organic dust exposure (Nordgren et al., 2014; Dominguez et al., 2020; Ulu et al., 2021a). Mice were fed a mouse chow supplemented with DHA for four consecutive weeks prior to challenge with a single DE exposure (acute model) or DE challenge over 3 weeks (repetitive model). In these investigations, we identified impacts of a high DHA diet on lung inflammation, including alterations in macrophage activation, that were overall protective against the deleterious impacts of DE exposure. However, these studies were limited in that they only assessed the impacts of one ω-3 PUFA, DHA, on male sex and on a limited dietary regimen of 4–7 weeks (Dominguez et al., 2020; Ulu et al., 2021a). Sex-specific differences in respiratory symptoms are observed among the asthmatic individuals and agricultural workers with asthma being more common in women than men and respiratory symptoms being more prevalent in men than women among the farmers (CDC, 2019; Fix et al., 2020). To better assess the impacts of a high ω-3 PUFA diet on the lung inflammatory response to DE and achieve a total tissue ω-6: ω-3 PUFA ratio of ~1:1 that is considered ideal, we have now utilized the *Fat-1* mouse transgenic model (Kang et al., 2004; Bilal et al., 2011) to better assess the sex-specific impacts of ω-3 PUFA on DE-induced inflammation. These mice express the *Caenorhabditis elegans (C. elegans)* fatty acid desaturase gene that converts ω-6 PUFA to ω-3 PUFA, thus yielding an overall tissue ratio of ~1:1. We hypothesized that use of this model would enhance the protective effects identified in initial studies utilizing only DHA supplementation, while also overcoming study limitations that plague fatty acid supplementation investigations, including ambiguous outcomes due to different fatty acid sources, purity, doses, and duration of supplementation (Bradberry and Hilleman, 2013). In addition, we have also tested a strategy to further enhance the efficacy of ω-3 PUFAs through the use of a therapeutic inhibitor of soluble epoxide hydrolase (sEH) an enzyme that metabolizes lipid mediators such as SPM into inactive or less active forms (Ulu et al., 2013; Ulu et al., 2014; Ulu et al., 2016; Dileepan et al., 2019).

Through these investigations, we have clarified a role for ω-3 PUFA in regulating the initiation of lung inflammation following DE inhalation and identified differentially regulated genes in repair and recovery following these exposures. These studies warrant consideration of ω-3 PUFA supplementation as a complementary therapeutic strategy for protecting against the deleterious lung diseases associated with environmental dust exposures, such as those experienced by agriculture workers.

2 MATERIALS AND METHODS

2.1 Preparation of Aqueous Dust Extracts

Settled dusts in closed swine confinement facilities (Nebraska) were collected one foot above the ground and kept at −20°C. Dust extracts were prepared as previously described (Romberger et al., 19852002). Briefly, 5 g dust was mixed with 50 ml Hank's Balanced Salt Solution at room temperature for 1 h. The mixture was then centrifuged at 2,500 rpm for 20 min at 4°C, supernatant was centrifuged one more time and resultant supernatant was sterile filtered using a 0.22 μm filter. Extracts were aliquoted, labeled as 100% dust extract (DE) and kept frozen at −20°C. A 12.5% DE solution was prepared for use in mouse intranasal instillations by diluting the 100% extract with sterile saline. Detailed analyses of the DE have been performed previously (Poole et al., 2010; Boissy et al., 2014; Romberger et al., 2015). A previous study compared immune response to the agricultural dust administered *via* intranasal instillation and 100 μg LPS challenge in mice (Poole et al., 2011), which has been estimated to be approximately 250× more than the LPS in 12.5% DE. In this same study, the mean endotoxin levels have been reported to be 0.384 μg/ml. Given this finding, when we administer 50 μL DE *via* intranasal route, this would correspond to approximately 20 ng LPS. In addition, other studies report respirable LPS levels to be between 14–129 EU/mL (one EU is approximately 0.1–0.2 ng/ml) (Demanche et al., 2009).

2.2 Animals and Dust Exposure Studies

All animal protocols were approved by the Institutional Animal Care and Use Committee of the University of California, Riverside. Male and female 10–12-week-old C57BL/6 WT (WT) and *Fat-1* transgenic mice [C57BL/6-Tg (CAG-*Fat-1*)1Jxk/J] were purchased from Jackson Laboratories and used to obtain a mouse colony. Breeding pairs were set as *WT x Fat-1* or *Fat-1 x Fat-1* to obtain both the WT and *Fat-1* genotypes. Mice had *ad libitum* access to food and water. Male and female mice were housed in separate cages with five mice/cage. Male and female pups reaching the age of 6–8 weeks were administered the sEH inhibitor TPPU [1-trifluoromethoxyphenyl-3-(1-propionylpiperidin-4-yl) urea] in their drinking water at 1 mg/kg dose for 1 week before intranasal dust exposure commences. For the repetitive dust exposure model, mice were instilled *via* the intranasal route with 50 μL of 12.5% DE for three-weeks (a total of 15 instillations, 5 days/week) as published before (Poole et al., 2009; Nordgren et al., 2015; Nordgren et al., 2019). Instillations were performed under light anesthesia using isoflurane.

2.3 Assessment of Airway Inflammation

2.3.1 Enumeration of Infiltrating Immune Cells Into the Lung

At the end of the three-week period, mice were euthanized, and trachea were cannulated to obtain bronchoalveolar lavage fluid (BALF) from each mouse. Collection of BALF included three times washing with 1 ml PBS each time. All washes were centrifuged at 1,200 rpm for 5 min. While the first wash was kept separate, the second and third washes were combined before centrifugation. The supernatant from the first wash was aliquoted and stored in −80°C for cytokine profiling. The pelleted cells obtained from all the washes were combined and counted. Cytospin slides were prepared using 100,000 cells, stained with Diff-Quik kit (Siemens, Newark, DE) and differential cell counts were obtained as described before (Nordgren et al., 2015).

2.3.2 Lung Histopathology

For histopathological assessments, lungs were inflated with 10% buffered formalin at 15 cm pressure. The same mouse lungs that were lavaged with PBS to obtain BALF was used for histology. Fixed lungs were transferred into 70% ethanol and then shipped to UC Irvine Pathology Research Services Core for paraffin embedding, sectioning, and Hematoxylin and Eosin (H and E) staining. The observer was blinded to the identity of each slide. A lymphoid aggregate was defined as close aggregation of ≥20 lymphocytes. Alveolar cellularity was evaluated by the number of cells in the alveolar spaces in the lung parenchyma in a total of five images obtained throughout the whole lung using 40× objective with 150% optical zoom. The resulting five values were averaged per tissue section. Each histopathological evaluation was represented as percentiles and a score between 0-to-4 was assigned for each percentile.

2.4 Lung NanoString Gene Expression Analysis

A mouse NanoString Immunology panel (NanoString Technologies, Seattle, WA, United States) was purchased for direct counting of 561 RNA transcripts using a nCounter Sprint Profiler. Each mouse lung was immediately put into 1 ml of RNA Later, kept at 4°C overnight, then stored in RNA Later at −80°C until RNA extraction. A total of three male mouse lungs per group obtained from three independent studies were thawed for RNA extraction. After lung samples were rinsed in sterile PBS, they were homogenized in 1 ml of Trizol using a 7 cm polypropylene pellet pestle in a microtube, then the extraction was performed as per manufacturer's instructions using a PureLink RNA mini kit (Invitrogen, Carlsbad, California, United States). RNA integrity number was obtained for each sample (ranged from 7–9 on a scale of 1–10) at the UC Riverside Institute for Integrative Genome Biology Core Facility using an Agilent Bioanalyzer 2,100 (Agilent Technologies, Santa Clara, California, United States). Samples were prepared by a 16-h hybridization step of 50 ng RNA with the codeset probe provided in the Immunology panel. At the end of the hybridization, samples were diluted with nuclease-free water to 35 μL, and 32 μL of each sample was loaded onto a nCounter Sprint Cartridge. Given each cartridge can hold up to 12 samples, a total of 24 samples were run on two cartridges. All samples passed the QC test without any QC flags. The data resulting from each run were combined and analyzed together using nSolver 4.0 and NanoString Advanced analysis. On the nSolver software, gene expression data were normalized using ten housekeeping genes that showed strong correlation with each other, these included *Rpl19, Alas1, Ppia, Oaz1, Sdha, Eef1g, Gusb, Gapdh, Hprt and Tbp.* Heatmaps were generated using the agglomerative clustering analysis in nSolver software (nSolver 4.0, NanoString Technologies, Seattle, WA, United States, User Manual). For the advanced analysis, at least three housekeeping genes whose expression correlated well with each other (*Alas1, Ppia, Tbp and Tubb5*), and thus ideal for normalization of the data were used to normalize the raw data (NanoString, MAN-C0011-04 Gene Expression Data Analysis Guidelines), and a 77 transcript counts were taken as "count threshold", which is two times the highest background-to-noise ratio (average of negative controls/sample + 2*standard deviation of negative controls/sample). Advanced analysis produced differential expression analysis, gene set analysis, and pathway scores. Differential expression outcomes identified the top 20 most upregulated genes among all the treatments, while gene set analysis displayed which pathways those most upregulated genes are related to.

To further explore the protein-protein interactions among differentially regulated proteins, we used the STRING database (https://string-db.org) of genes that were statistically significant based on the unadjusted p-values (Szklarczyk et al., 2021). Genes with low counts (counts < 79) were not included in any of the analyses. Raw and normalized NanoString data are deposited to https://www.ncbi.nlm.nih.gov/geo/info/spreadsheet.html.

2.5 Statistical Analyses

GraphPad Prism software (Prism 9) was utilized to perform two-way ANOVA tests and version eight was used to perform three-

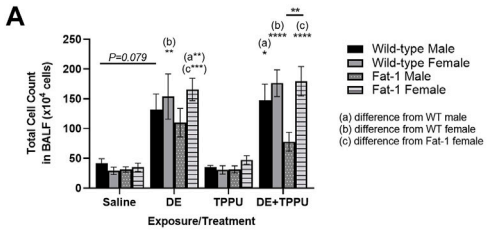

Significant Main Effects	Significance, *P* value
Exposure/ treatment (Dust/ TPPU)	**** $P < 0.0001$
Sex	** $P = 0.0096$
Exposure/ treatment x sex	$P = 0.052$
Genotype x sex	$P = 0.072$

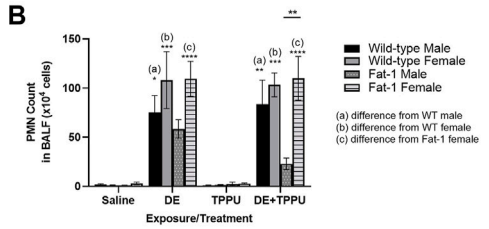

Significant Main Effects	Significance, *P* value
Exposure/ treatment (Dust/ TPPU)	**** $P < 0.0001$
Sex	** $P = 0.0011$
Exposure/ treatment x sex	* $P = 0.013$
Genotype x sex	P=0.12

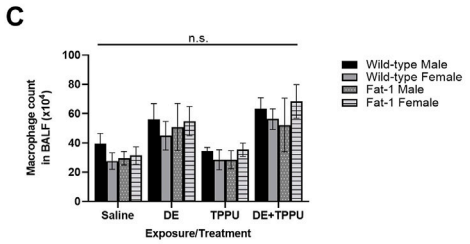

Significant Main Effects	Significance, P value
Exposure/ treatment (Dust/ TPPU)	**** $P < 0.0001$
Genotype x sex	$P = 0.092$

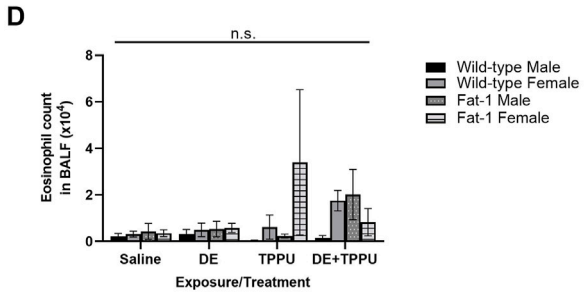

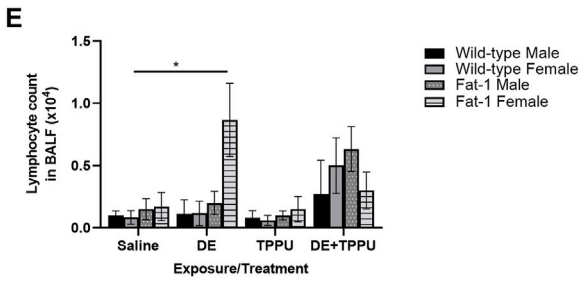

Significant Main Effects	Significance, *P* value
Exposure/ treatment (Dust/ TPPU)	** $P = 0.0076$
Genotype	* $P = 0.046$
Treatment x genotype x sex	* $P = 0.045$

FIGURE 1 | Genotype and sex-specific changes in infiltrating immune cells in the bronchoalveolar lavage fluid after a three-weeks repetitive dust exposure with or without TPPU treatment. **(A)** Total infiltrating cell counts, **(B)** neutrophil count, **(C)** macrophage count, **(D)** eosinophil count, **(E)** lymphocyte count; n = 6–8 mice WT male (except for WT TPPU n = 5), n = 6–8 WT female, n = 6 *Fat-1* male, n = 6–7 *Fat-1* female. Significant main effects of three-way ANOVA are shown. Statistical significance is shown with letters: **(a)** significantly different from WT male, **(b)** significantly different from WT female, **(c)** significantly different from *Fat-1* male, **(d)** significantly different from *Fat-1* female. Data are mean ± SEM. *p < 0.05, **p < 0.01, ***p < 0.001, ****p < 0.0001.

way ANOVA on data to determine the main effects of exposure and treatments, and post-hoc comparisons were performed to reveal significant differences among all the groups. Differences between groups were considered significant if the p value ≤ 0.05. Data are represented with mean ± standard error of the mean on all figures.

3 RESULTS

3.1 Effects of Elevated Tissue Levels of ω-3 Fatty Acids on Dust-Induced Airway Inflammation

3.1.1 Infiltrating Immune Cells and Pro-Inflammatory Cytokines

To test the hypothesis that elevated tissue levels of ω-3 fatty acids are protective against agricultural dust induced lung inflammation and improve inflammation resolution, we compared WT and *Fat-1* transgenic mice for their response to three-weeks repetitive dust exposure. As expected, mice exposed to aqueous dust extracts for the duration of three-weeks (5 instillations/week) had 2-3-fold increase in total BALF cell counts as compared to their corresponding saline controls. First, we examined the main effects of exposure, genotype, sex and TPPU treatment on the total infiltrating immune cell counts (**Figure 1A**). We found statistically significant differences among the groups that are driven by DE exposure, TPPU treatment ($F = 51.2$, $p < 0.0001$) and sex ($F = 3.028$, $p = 0.0096$). Further statistical analysis of the total cell counts also revealed that both sex and genotype plays a role in response to DE exposure and TPPU treatment (interaction between exposure/treatment x sex, $F = 3.463$, $p = 0.052$; genotype x sex, $F = 1.417$, $p = 0.073$). We observed similarly significant results for the infiltrating neutrophils but not for macrophages (**Figures 1B,C**). This increase in neutrophil numbers is consistent with the cellular signature of repetitive DE exposure (Nordgren et al., 2014; Nordgren et al., 2013; Ulu et al., 2021b; Warren et al., 2017). With regards to eosinophils, we did not detect any differences among the groups (**Figure 1D**). Lymphocyte counts showed a statistically significant increase only in *Fat-1* females that were exposed to dust. These counts were lower in the presence of TPPU; however, this difference did not reach significance (**Figure 1E**). All the significant main effects and relevant multiple comparisons are shown in each figure. When administered alone, TPPU did not affect any immune cell infiltration into the lung, which is consistent with previously reported homeostatic effects of sEH inhibition (Morisseau and Hammock, 2013; Vanella et al., 2015; Kuo et al., 2019). At the dose we administered (1 mg/kg), TPPU reaches plasma concentrations of >50-fold of the mouse IC_{50} of 2.8 nM, suggesting good target engagement (**Supplementary Figure S1**). Among the DE-exposed mice, TPPU was most effective in reducing the number of infiltrating cells in *Fat-1* male mice (**Figures 1A,B**). While this decrease with TPPU was not significant for total infiltrating neutrophils ($p = 0.9$, *Fat-1*+DE male mice vs. *Fat-1* DE + TPPU), we observed a striking difference between the *Fat-1* male versus *Fat-1* female mice receiving the TPPU treatment during dust-exposure ($p = 0.032$ for total infiltrating cells and $p = 0.0029$ for neutrophils between *Fat-1* male + DE + TPPU vs. *Fat-1* female + DE + TPPU). Since TPPU can stabilize the P450 metabolites derived from the ω-3 fatty acids, EPA (eicosapentaenoic acid) and DHA and also promote generation of SPMs, these data suggest that elevated ω-3 fatty acids could be stabilized with a sEH inhibitor to contribute to the decrease in pro-inflammatory cell influx into the lung in male sex.

Similarly, pro-inflammatory cytokines in BALF decreased in *Fat-1* transgenic mice receiving TPPU among the other *Fat-1* mice exposed to dust (**Figure 2**). The three-way ANOVA analysis showed significant main effects of dust exposure/TPPU ($F = 13.87$, $p = 0.0024$) and a trend for the main effect of sex ($F = 3.02$, $p = 0.068$) on BALF IL-6 levels (**Figure 2A**). Regarding the BALF levels of TNF-α, we observed significant main effects of dust exposure or TPPU ($F = 9.48$, $p = 0.037$). For the neutrophil chemoattractant CXCL-1, we observed a statistically significant main effect of exposure/treatment ($F = 29.8$, $p < 0.0001$) and a statistical trend for interaction between dust exposure/TPPU x genotype ($F = 5.4$, $p = 0.064$). Since sex did not have a significant effect on CXCL-1 BALF levels, we also examined the data after combining both sexes. Similarly, we found a significant main effect of treatment ($F = 30.36$, $p < 0.0001$). When we investigated the specific differences among the groups, we found significant differences between WT + DE vs. WT + DE + TPPU as well as WT + DE vs. *Fat-1* + DE + TPPU groups (**Figure 2C**, inset). Similarly, dust-exposed *Fat-1* transgenic mice exhibited lower levels of CXCL-1 as compared to WT mice; however, this difference did not reach significance ($p = 0.1$).

3.1.2 Effect of Dust Exposure on Lung Histopathology in *Fat-1* Transgenic Mice

Lung histopathology was evaluated in H&E-stained paraffin-embedded tissue sections mounted on slides to evaluate dust-induced lung inflammation (**Figure 3**). We have previously shown that total number of lymphoid aggregates (defined as at least 20 closely aggregating cells) and alveolar inflammation evaluated as the number of macrophages in alveolar spaces increase with repetitive exposure to agricultural dust (Ulu et al., 2021b). The 2-3-fold increase in the number of BALF leukocytes following repetitive exposure to DE was reflected in approximately two fold increase in histopathological scores.

As expected, the number of macrophages in alveolar spaces increased approximately two-fold with three-weeks repetitive exposure to DE in both WT and *Fat-1* transgenic mice with a significant main effect of dust exposure and/or TPPU ($F = 29.97$, $p < 0.0001$) (**Figures 3A,C**). We also observed significant interaction between sex and genotype ($F = 5.11$, $p = 0.018$), which was reflected in a statistically significant difference in alveolar inflammation score in *Fat-1* males and WT females that were receiving the three-weeks DE exposure as compared to their saline control counterparts.

Similarly, we observed a significant main effect of DE and/or TPPU ($F = 32.15$, $p < 0.0001$) and their interaction with genotype ($F = 16.95$, $p < 0.0001$) on lymphoid aggregate formation (**Figures 3B,D**). In WT mice receiving the three-weeks DE exposure, the number of lymphoid aggregates significantly increased as compared to WT saline controls ($p < 0.0001$). Among the mice exposed to DE, *Fat-1* mice exhibited less lymphoid aggregates than the WT mice but only in the male sex ($p = 0.0002$). In addition, we observed a sex-dependent difference in TPPU treatment, which significantly reduced lymphoid aggregate formation in male mice receiving the three-weeks DE exposure regardless of the genotype ($p = 0.0019$, WT + DE male vs. WT +

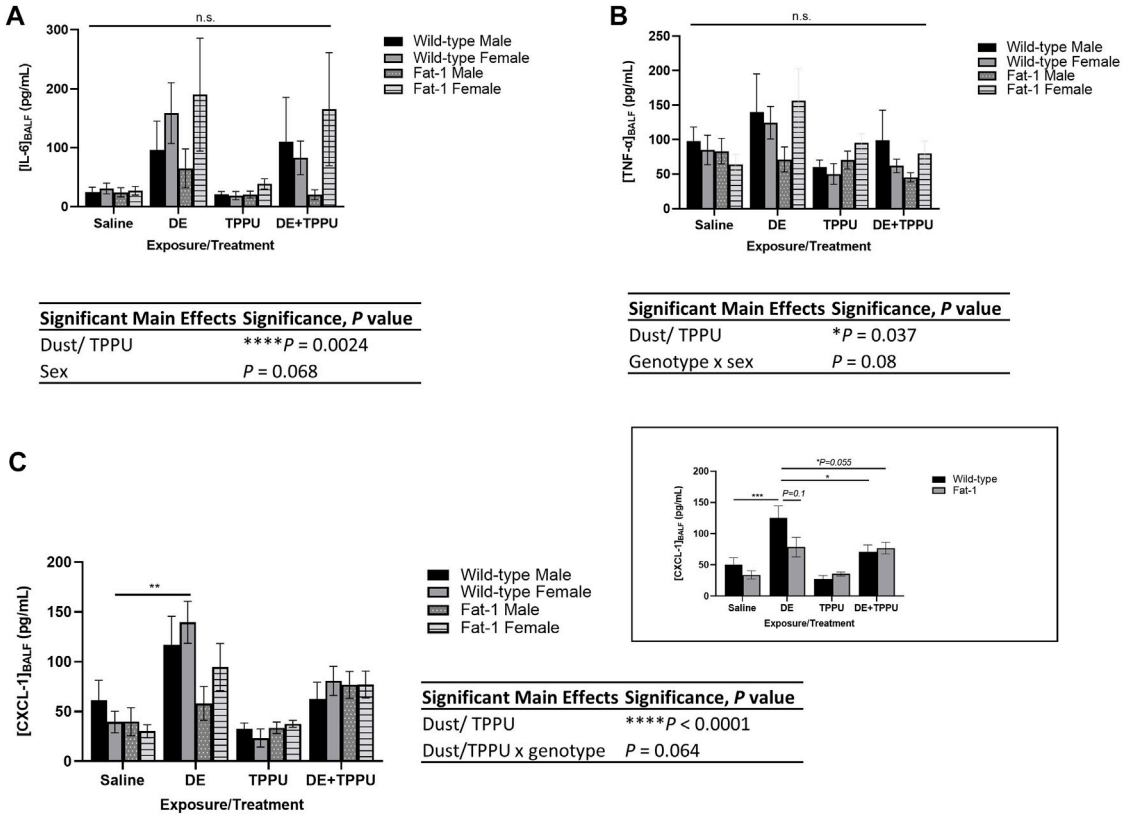

FIGURE 2 | Effects of three-weeks repetitive dust exposure on pro-inflammatory cytokine levels in the bronchoalveolar lavage fluid with or without TPPU treatment. **(A)** IL-6, n = 5–7 mice WT male, n = 6–8 WT female, n = 5–7 *Fat-1* male, n = 6–7 *Fat-1* female; **(B)** CXCL-1, n = 5–8 mice WT male, n = 5–6 WT female, n = 4–6 *Fat-1* male, n = 5–7 *Fat-1* female; **(C)** TNF-α, n = 5–8 mice WT male, n = 5–7 WT female, n = 5-6 *Fat-1* male, n = 5–7 *Fat-1* female. The inset shows data from both female and male sexes, n = 11–13 for WT and n = 9–12 for *Fat-1* mice. Data are mean ± SEM. Significant main effects of three-way ANOVA are shown. Statistical significance is shown with letters: **(a)** significantly different from WT male, **(b)** significantly different from WT female, **(c)** significantly different from *Fat-1* male, **(d)** significantly different from *Fat-1* female. $^{**}p < 0.01$, $^{***}p < 0.001$.

DE + TPPU male and $p = 0.014$, WT DE male vs. *Fat-1* + DE + TPPU male).

3.2 Changes in Expression of Genes Related to Immune Response in WT and *Fat-1* Transgenic Mice Following Repetitive Dust Exposure

ω-3 fatty acids are known to regulate gene expression (Ulven and Holven, 2020). To elucidate differences in lung gene expression between the WT and *Fat-1* transgenic mice following repetitive dust exposure, we used a NanoString Mouse Immunology Panel as described in the Methods. We used only male sex for the gene expression study since we saw the most significant changes in the male sex as compared to the females. Following data acquisition, an automated QC test (quality control) was performed on nSolver software which showed that all samples passed this test with no warning flags. Then, samples were normalized to housekeeping genes and principal component analysis (PCA) of the data were performed. The most significantly altered genes after the three-weeks dust exposure are shown for both WT and *Fat-1* mice in volcano plots on **Figures 4A,B** as compared to WT saline controls. The overall significant changes among all the groups are summarized with the heatmap in **Supplementary Figure S2**. Among these genes, several gene sets included in the Immunology panel showed high PC1 scores and a clear clustering of the saline vs. DE-exposed groups regardless of genotype or treatment with TPPU, suggesting that DE exposure is the main driver of the observed changes (**Figure 4**). Some of the gene sets with high PC1 scores include innate immune system, cell proliferation, transport, wound healing, and collagen. (**Figures 4C–G**, and **Supplementary Figure S3**).

To assess the effects of genotype and TPPU treatment on gene expression, we performed additional analyses that allowed us to make direct comparisons between the groups. These included advanced analyses of the raw NanoString data by selecting WT + DE, *Fat-1* + DE, WT + DE + TPPU groups as reference instead of the WT saline group as selected in the initial analysis. When WT + DE group served as reference, nSolver software was able to directly compare WT + DE with *Fat-1* + DE group. The most significantly altered gene between the two genotypes was NFκBIA, which acts a NFκB inhibitor by binding and confining it to the cytoplasm (**Figure 4H**). We found a

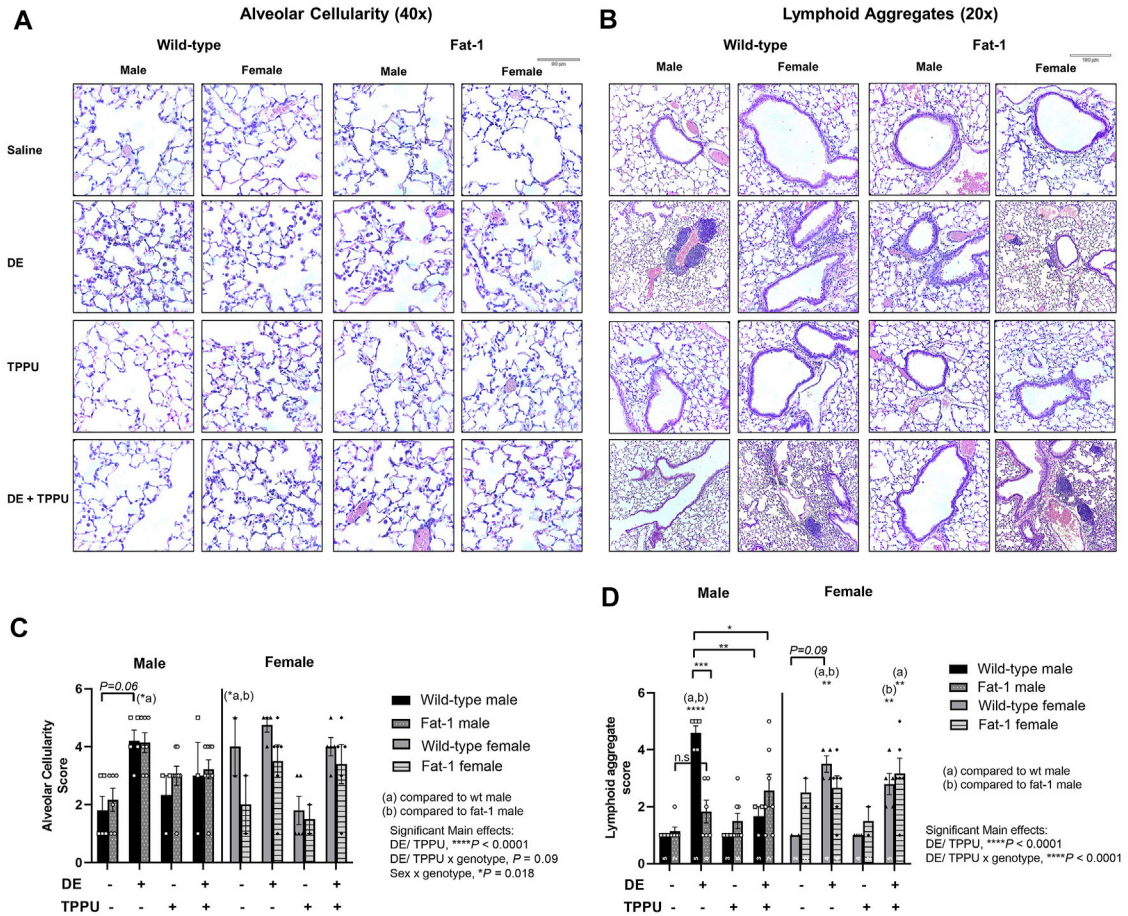

FIGURE 3 | Representative images and scoring of lung histopathology in WT and *Fat-1* transgenic mice following 3 weeks exposure. **(A)** Alveolar cellularity, $n = 3–5$ mice WT male, $n = 2–5$ WT female, $n = 5–9$ *Fat-1* male, $n = 2–6$ *Fat-1* female; **(B)** lymphoid aggregate formation, $n = 5–8$ mice WT male, $n = 5–6$ WT female, $n = 4–6$ *Fat-1* male, $n = 5–7$ *Fat-1* female; **(C)** quantification and pathological scoring of the alveolar cellularity and **(D)** lymphoid aggregate formation. Sample sizes for each group were shown on each graph. **(a)** significantly different from WT male, **(b)** significantly different from WT female. Data are mean ± SEM. $^{*}p < 0.05$, $^{**}p < 0.01$, $^{***}p < 0.001$, $^{****}p < 0.0001$.

significant interaction between the exposure/treatment and genotype (F = 39.56, $p = 0.0068$) and close to statistical significance with DE exposure and TPPU treatment (F = 19.86, $p = 0.065$). The *Fat-1* transgenic mice had significantly higher log2 counts of NFκBIA as compared to *Fat-1* saline controls ($p = 0.0061$) and to that of WT mice receiving the repetitive DE exposure ($p = 0.025$). When looking at the significant unadjusted p values, among the top 20 differentially regulated genes, we found *Cd83, Tnfaip3, Il33, Xbp-1, Il4ra, S100a9, S100a8, Cebpb, Csf1, Il1rn, Ptpn2, Il10rb, Jak2, Il13ra1, Tmem173, Fcgr2b, and Ccrl2 to be upregulated in Fat-1 + DE, and Ahr and Cd2* to be down-regulated in *Fat-1* + DE as compared to WT + DE groups. With this analysis, we also examined the differentially regulated genes between the WT + DE *versus* WT + DE + TPPU groups, and we observed only the *LCP2 (Lymphocyte cytosolic protein 2)* gene to be upregulated based on the significant unadjusted p values. Next, we repeated the analysis selecting *Fat-1* + DE group as the reference which allowed us to compare gene expression in *Fat-1* + DE group to *Fat-1* + DE + TPPU. Based on the unadjusted p values, the top 20 upregulated genes in *Fat-1* + DE + TPPU included *Cxcr1, Cd2, Prkcd, H2-Dma, Itgb2, Fn1, H2-Eb1, Itgax, Csf1r, C1qb, Itga4, Lcp2, Ly86, Xbp-1, Irf8, Cd48, Npc1, Tlr8, C1qa, and Cd79b*. After identifying differentially regulated genes for the hypotheses we wanted to test, we entered these genes into the STRING Database to identify any possible interactions and biological pathways that these cluster of genes would be related to. Results from these analyses are shown on **Table 1**. As expected, DE exposure was consistent with pathways related to immune cell activation, cell proliferation, neutrophil aggregation, and antigen presentation regardless of mouse genotype. To our surprise, this analysis revealed a role for DE exposure in positively regulating hematopoietic stem cell migration as well as negative regulation of hippocampal neuron apoptotic processes. Interestingly, the main differences between the WT and *Fat-1* genotype were associated with response to macrophage colony stimulating factor, immune clearance, and neutrophil aggregation. Upon examining the different gene sets, we found that genes in the protein autophosphorylation pathway show a

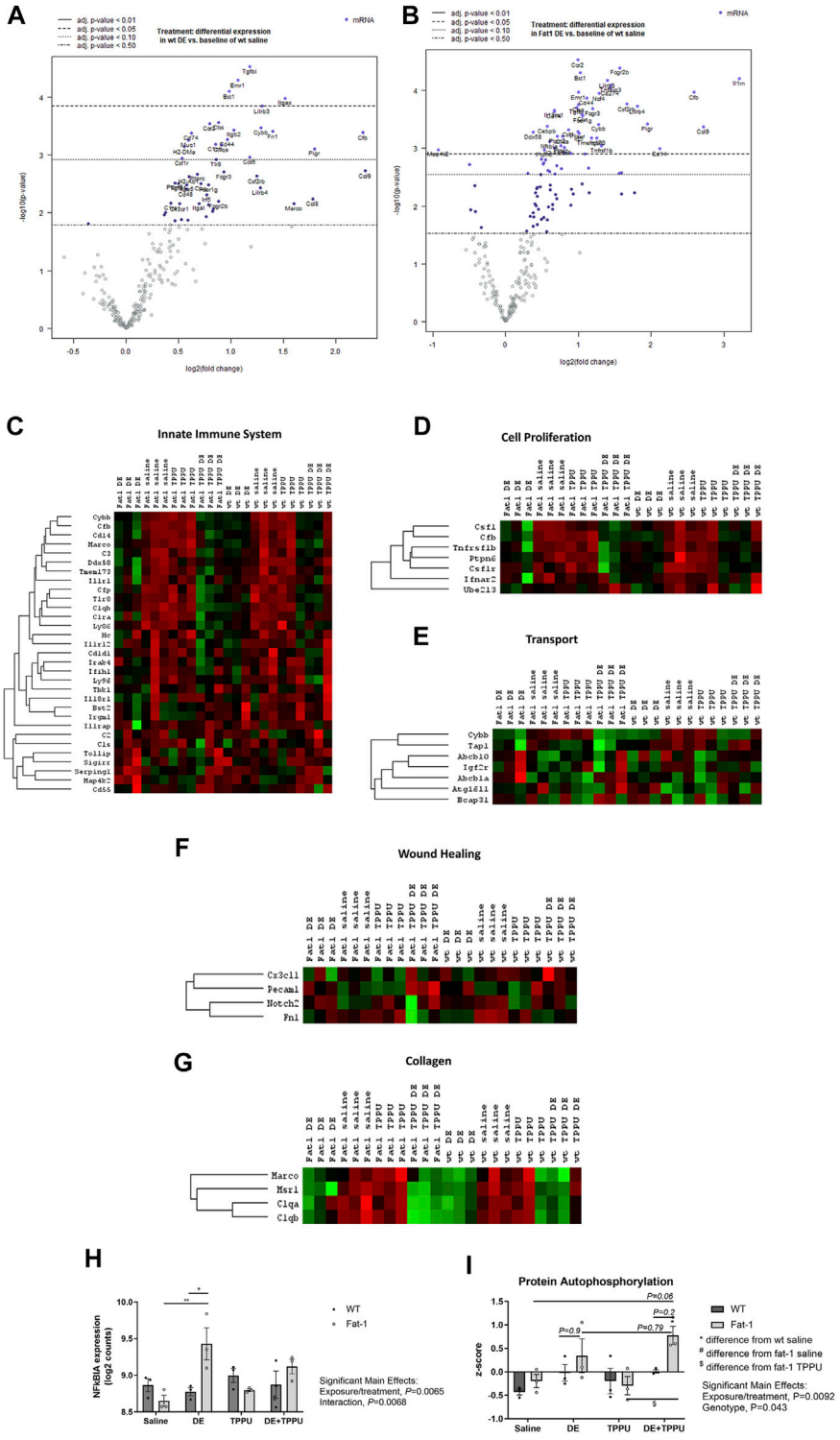

FIGURE 4 | Changes in gene expression and related pathways altered after three-weeks repetitive dust exposure. Volcano plots showing differential expression of genes in **(A)** WT and **(B)** *Fat-1* transgenic mice as compared to WT saline controls. Heatmaps were generated for each sample for genes involved in **(C)** innate immune system, **(D)** cell proliferation, **(E)** transport, **(F)** wound healing and **(G)** collagen. **(H)** The top up-regulated gene, NFκBIA in *Fat-1* mice as compared to WT mice receiving the repetitive DE exposure. **(I)** Expression of genes coding for proteins involved in autophosphorylation. n = 3 male mice/group.

TABLE 1 | STRING Database analysis of the differentially regulated genes and their association with biological pathways.

	Upregulated genes	STRING database biological process	P	Downregulated genes	STRING database biological process	P
WT DE vs. WT saline	74	Pos reg hematopoietic stem cell migration Neg reg hippocampal neuron apoptotic process Immune cell clearance	<1.0e-16	2	n/a	n/a
Fat-1 DE vs. WT saline	99	Pos reg cellular response to macrophage colony stimulating factor Pos reg hematopoietic stem cell migration Pos reg growth factor dependent skeletal muscle proliferation Neutrophil aggregation Antigen processing and presentation of exogenous peptide *via* MHC Class I	<1.0e-16	13	Protein localization to bicellular tight junction Regulation of macrophage cytokine production Regulation of ECM disassembly	2.11e-06
Fat-1 DE vs. Fat-1 saline	80	Pos reg cellular response to macrophage colony stimulating factor Pos reg hematopoietic stem cell migration Neutrophil aggregation	<1.0e-16	24	B-1 B cell homeostasis IL-17 production Protein localization to bicellular tight junction	7.86e-08
Fat-1 DE vs. WT DE	25	Immune complex clearance Neutrophil aggregation	<1.0e-16	8	Neutrophil aggregation Immune complex clearance	n.s.
WT DE vs. WT DE + TPPU	1 (*LCP2*)	Positive regulation of T-cell differentiation	n/a	0	n/a	n/a
Fat-1 DE + TPPU vs. Fat-1 DE	31	Positive regulation of PMN activation Synapse pruning	<1.0e-16	9	IL-33 mediated signaling pathway Pos regulation of IgG, IL-5, IL-13 and IL-6 secretion	0.000471
Fat-1 DE + TPPU vs. WT DE + TPPU	43	Pos reg hematopoietic stem cell migration Neg reg hippocampal neuron apoptotic process Antigen processing and presentation of exogenous peptide *via* MHC Class I Macrophage colony-stimulating factor signaling pathway	<1.0e-16	4	Cell autonomous role of endothelial GTP cyclohydrolase1 and tetrahydrobiopterin in blood pressure regulation	0.109

significant main effect of genotype (**Figure 4I**). The genes involved in this gene set include *Jak 1/2, Irak 1/2, Mapk14, Csf1r, Ptk2, Fyn, Prkcd, and Src.* With TPPU treatment, main differences appeared to be in positive regulation of T-cell differentiation in WT mice and positive regulation of PMN activation in *Fat-1* mice. Consistent with these changes in upregulated genes, downregulated genes also showed a similar pattern. A list of upregulated and downregulated genes is provided separately in the **Supplementary Table S1**.

4 DISCUSSION

The lungs are continually exposed to harmful stimuli found in the air, including environmental dusts, diesel exhaust particles, and smoke exposures. The ability of the airways to respond to these stimuli and repair damage caused by the exposures is vital to respiratory health, because unrepaired damage can lead to debilitating airway diseases (Ehrlich, 1980; Kirkhorn and Garry, 2000; Smit et al., 2014; Franklin et al., 2015; Nordgren and Bailey, 2016; Watkins et al., 2017). Long-term particulate matter exposures have been consistently linked to negative cardiovascular and lung health outcomes and increased mortality (Franklin et al., 2015; Watkins et al., 2017). Disease susceptibility caused by chronic inhalation of particulates is clearly evidenced by occupational exposures such as those seen in agriculture workers; exposures to livestock farming operations are consistently linked to increased respiratory symptoms and inflammatory lung disease in not only workers, but in individuals living in the surrounding communities, including children and adults (Radon et al., 2007; Pavilonis et al., 2013; Nordgren and Bailey, 2016; van Dijk et al., 2016; Baliatsas et al., 2017; Borlee et al., 2017; Rasmussen et al., 2017; Burkes et al., 2018). Approximately two-thirds of agriculture workers report respiratory disease; 50% of agriculture industry workers experience asthma-like symptoms (American Thoracic, 1998),

25–35% of individuals working in concentrated animal feeding operations experience chronic bronchitis (American Thoracic, 1998), and the prevalence of chronic obstructive pulmonary disease (COPD) among agriculture workers is doubled compared to nonfarming working control subjects (Guillien et al., 2016). Curative options are not available for these workers, with current therapeutic options aimed primarily at symptom management and the prevention of lung disease.

To improve treatment options for this population, studies investigating therapeutic mechanisms to stimulate endogenous lung tissue repair mechanisms are warranted. To this end, we have assessed the impacts of a low (~1:1) ω-6: ω-3 PUFA total body tissue ratio on lung inflammation following repetitive exposure to inhaled environmental dusts, using a well-described mouse model of DE inhalation. In addition, we have explored the therapeutic utility of an sEH inhibitor, TPPU, in enhancing the impacts of high ω-3 PUFA tissue levels, including exploring its effects in regulating SPM levels during inflammation resolution. Taken together, our results indicate sex-dependent protective effects associated with elevated tissue levels of ω-3 fatty acids in reducing the number of infiltrating immune cells (i.e., neutrophils) into the lung, lower pro-inflammatory cytokine levels and reduced overall histopathology of the lung.

The results identified herein model a long-term dietary intake of high ω-3 PUFA and reduced intake of ω-6 PUFA that achieves an ideal ω-6:ω-3 PUFA ratio throughout the body as reviewed before (Lands et al., 2018). This was achieved through the use of the *Fat-1* transgenic mouse model; these mice express the *Fat-1* gene from *C. elegans* encoding an ω-3 FA desaturase, converting ω-6 PUFA to ω-3 PUFA, leading to tissue ω-6:ω-3 PUFA ratios of ~1:1 (Kang et al., 2004). This model is advantageous because it overcomes several issues that limit diet- and supplementation-based experimental strategies; current clinical and preclinical studies have no standardization in terms of dose, duration, or source and quality of ω-3 PUFA, and each of these factors has implications on outcomes (e.g., due to differences in tissue incorporation, lipid peroxide or aldehyde formation) (Yang et al., 2019). These inconsistencies are considered leading factors for discrepancies in ω-3 PUFA study outcomes (von Schacky, 2014; Calder, 2010; Deckelbaum and Torrejon, 2012). The *Fat-1* mouse thus provides a preclinical model for assessing how elevated tissue levels of ω-3 PUFA and reduced ω-6 PUFA can influence health outcomes by minimizing variation based on supplementation, intake and absorption and distribution of ω-3 rich fatty acids. Using this model, we have found genotype and sex-specific differences in infiltrating cells (**Figure 1**), pro-inflammatory cytokines (**Figure 2**) and lung histopathology (**Figure 3**). The decreases in infiltrating PMNs and cytokines were consistent with each other within the *Fat-1* male sex. Among the swine farm workers, sex-specific differences in lung function and *TLR* gene polymorphisms, which is a toll like receptor activated by swine farm dust, have been reported before (Senthilselvan et al., 2009; Gao et al., 2018). Gao et al. found that lung function is worse in males with the *TLR9* gene polymorphism (rs187084) as compared to those males without the polymorphism, and females with the *TLR2* gene polymorphism (rs4696480) exhibit better functioning lungs as compared to those females without the polymorphism in swine farm full-time workers (Gao et al., 2018). Another study by Senthilselvan et al. found increased plasma levels of TNF-α in males without any *TLR4* gene polymorphisms (*TLR4 299/399* polymorphism), and in females with the *TLR4* gene polymorphism following 5 hours of swine farm exposure in naïve healthy subjects (Senthilselvan et al., 2009). We are not the first ones to report sex-specific differences in *Fat-1* mice; a recent study investigating the role of elevated tissue levels of ω-3 fatty acids in obesity-associated post-traumatic osteoarthritis also reported sex-specific differences in *Fat-1* transgenic mice (Kimmerling et al., 2020). It appears that such sex-dependent differences are disease model-specific where one sex in the *Fat-1* transgenic background exhibits a greater response than the other sex. Another study reported on sex-and age-specific differences of Resolvin D1 (RvD1, an SPM derived from DHA) levels in the retina. This study found sex-dependent differences in retinal levels of RvD1 in aged mice (24-months) as compared to young mice (three-months old), with aged male mice showing a larger decrease in RvD1 levels (Trotta et al., 2021). Sex-dependent changes in the expression of genes involved in fatty acid synthesis, steroids and drug metabolizing enzymes have been identified before (Waxman and Holloway, 2009). Some of those genes encode for enzymes involved in the metabolism of ω-3 and ω-6 PUFA, thus identifying sex-dependent differences can inform pharmacokinetics, bioavailability and treatment options related to ω-3 and ω-6 PUFA-derived lipid mediators. The sEH inhibitor TPPU was used in this study as an indicator that to the inflammation resolving epoxide metabolites of ω-3 lipids might be a partial explanation for their beneficial effect. It is attractive to consider sEH inhibitors or mimics of ω-3 fatty acid epoxides as a prophylactic or therapeutic agent (Falck et al., 2011; Adebesin et al., 2019). Such mimics and sEH inhibitors are in clinical development by several companies but none are available on the market (Lazaar et al., 2016; Hammock et al., 2021). However, there are a number of sEH inhibitors from natural sources that are commercially available such as Maca (also known as Peruvian ginseng, *Lepidium meyenii*) (Kitamura et al., 2017; Singh et al., 2020).

One of the sex-dependent observations in our study was related to lymphoid aggregate formation in the lung. Male sex in the *Fat-1* transgenic mouse had lesser number of aggregates as compared to their corresponding WT controls, which was further reduced in the presence of TPPU (**Figures 3B,D**). While we observed a similar trend for the female mice these differences did not reach significance. Lymphoid aggregates, which can be composed of T cells, B cells and dendritic cells (van der Strate et al., 2006) play different roles in different disease models such as COPD and *tuberculosis*. For example, in a chronic cigarette smoke-induced murine COPD model, lymphoid aggregates are associated with adverse outcomes and thus pathological, whereas in a *tuberculosis* model induced by the *Mycobacterium tuberculosis*, it is found to be a host defense mechanism (Hertz et al., 2020; Tam et al., 2020). To our knowledge sex-differences in lymphoid aggregate formation in the lung has not been fully explored. A recent study found that females are more susceptible to lymphoid aggregate formation as compared to males, and this

was further confirmed by ovariectomy in a smoke-induced COPD model (Tam et al., 2020). This is consistent with the previous reports indicating that women are more susceptible to develop COPD than men (Martinez et al., 2007; de Torres et al., 2009; Perez et al., 2020). Overall, our results are consistent with the previously published literature on the effects of agricultural dust in males; and the improved histopathological effects seen in the male sex are novel.

We observed an elevated alveolar cellularity (approximately two-fold), in wild-type female mice as compared to male mice. A study investigated the differences in alveolar macrophage proteome between males and females, and found several proteins associated with inflammation and interact with estrogen receptor to be expressed higher in females than males (Phelps et al., 2012). Another study looking at sex-related differences in lung inflammation showed a higher baseline for lung histology score and number of infiltrating cells into the lungs in females compared to males in sham-operated controls (Vegeto et al., 2010). Both studies are consistent with the histological finding we observed in female wild-type mouse lungs. Because males responded TPPU treatment better, this might be related to differences in fatty acid metabolism between males and females given fatty acid epoxides regulate alveolar cell influx, as shown in a study demonstrating that pharmacological modulation of fatty acid epoxides affect inflammatory cell influx to the lungs (Yang et al., 2015). In addition, SPMs also modulate macrophage chemotaxis, trans-endothelial migration and cytokine release from macrophages as reviewed by Haworth and Levy (2007). More studies are needed to dissect differences in fatty acid metabolism between males and females.

It is well accepted that sex-specific differences that result in different biological responses between males and females stem from sex hormones. These differences affect storage and distribution of lipids thereby affect free fatty acid availability between sexes. Stable isotope studies report that ARA and DHA contribute more to blood lipids in women than in men and that there are differences in the conversion rate of fatty acids, for example conversion of ALA to omega-3 fatty acids is higher in women than in men (Decsi and Kennedy, 2011). Also, preclinical studies show that reproductive hormones affect the enzymes involved in the biosynthesis of fatty acids. Another study found that sex-related differences in COPD might be related in part to the increased production of leukotoxin-diol (linoleic acid derived diol) by goblet cell P450 and sEH activities (Balgoma et al., 2016). Overall, our results suggest a mechanism that 1) availability of free fatty acids from the elevated tissue levels of ω-3 acids in *Fat-1* mice are sex-dependent and 2) females have different conversion rates of fatty acids as compared to males and this might lead to changes in gene expression of chemokines and cytokines, thereby affecting alveolar macrophage recruitment into the lung and thus creating sex-dependent host defense mechanism within the *Fat-1* genotype.

In addition to dietary strategies aimed at promoting the healthful benefits of ω-3 PUFA, therapeutic strategies leveraging the endogenous repair SPM pathways to promote inflammation resolution and repair hold great clinical promise. For example, many investigations have identified positive outcomes in ameliorating lung inflammation/disease *via* therapeutic administration of SPM (Croasdell et al., 19502016; Seki et al., 19502010; Aoki et al., 2008; Haworth et al., 2011; Hsiao et al., 2013; Miyata and Arita, 2015; Kim et al., 2016), including our own previous studies identifying beneficial effects of the DHA-derived SPM maresin-1 in reducing the lung inflammatory effects of acute and repetitive organic dust exposure (Nordgren et al., 2013; Nordgren et al., 2015). While SPM can potently inhibit inflammation while promoting tissue repair, these bioactive metabolites are quickly deactivated by subsequent metabolism (Lopez-Vicario et al., 2015; Basil and Levy, 2016). Thus, another therapeutic strategy to leverage these endogenous inflammation resolution pathways is to combine ω-3 PUFA supplementation with pharmacologic inhibition of enzymes responsible for the deactivation of SPM. One such strategy has been the use of inhibitors of the sEH enzyme to prevent the deactivation of the cytochrome P450 family of SPM, thereby potentiating their protective effects (Guedes et al., 2013; Ulu et al., 2013; Ulu et al., 2014; Yang et al., 2015; Ulu et al., 2016; Zhou et al., 2016; Goswami et al., 2017; Zhou et al., 2017; Yang et al., 2020; Zhang et al., 2020). Previous studies have found enhanced protective effects of ω-3 PUFA when used in combination with inhibitors of sEH such as TPPU (Wang et al., 2012; Lopez-Vicario et al., 2015; Yang et al., 2015; Zhou et al., 2016; Zhou et al., 2017). This enzyme deactivates the epoxide SPM (e.g., 19, 20-EDP; produced through CYP450 metabolism) into less active diol forms (e.g., 19 (20)-DiHDPA). A recent study in a model of metabolic disease identified that a sEH inhibitor enhanced the protective effects identified in *Fat-1* mice vs. WT mice (Lopez-Vicario et al., 2015), while previous studies also identify beneficial effects of sEH inhibition in murine models of acute lung injury (Zhou et al., 2017), pulmonary fibrosis (Zhou et al., 2016), asthma (Yang et al., 2015), and COPD (Wang et al., 2012). Corroborating these previous reports, when we utilized TPPU in the experiments described herein, we found that addition of TPPU lowered all outcomes examined in the DE-exposed animals, suggesting that TPPU not only enhanced the effects of ω-3 fatty acids as in *Fat-1* + DE + TPPU animals, but also showed efficacy independent of the *Fat-1* genotype. In addition, we observed a better response in the *Fat-1* male sex receiving the TPPU treatment and three-weeks DE exposure. Consistent with our results sex-specific differences have been reported in sEH null mice and sEH activity in other mouse disease models (Vanella et al., 2015; Wagner et al., 2017; Jamieson et al., 2020).

While our results support a beneficial effect of maintaining a low omega6:omega3 ratio in response to agricultural dust, omega-6 PUFAs and their metabolites also modulate inflammation and participate in inflammation resolution and tissue homeostasis. The SPMs derived from arachidonic acid, such as LXA4 and metabolites generated by the P450 pathway (i.e., EETs or epoxyeicosatrienoic acids) have been repeatedly shown to have anti-inflammatory effects (Levy and Serhan, 2003; Morisseau and Hammock, 2013). Most surprisingly, the ARA metabolites generated by the COX-2 pathway, such as PGE2 have protective effects in the lung despite their infamous proinflammatory notion, as shown in asthma and allergic

airway inflammation (Vancheri et al., 2004; Herrerias et al., 2009). Airway epithelial cells are the major source of PGE2 production in the lung, and PGE2 protects against airway hyperresponsiveness to allergens by inhibiting leukotriene and thromboxane synthesis that cause bronchoconstriction and by reducing eosinophil recruitment, both of which are anti-inflammatory effects of PGE2. Similarly, in asthma, it has been shown that the homeostatic balance between the COX and LOX pathways metabolizing ARA are altered due to damaged epithelium in asthmatic airways. Given this, it has been proposed that the dysregulation of these pathways leads to an imbalance between PGE2 and PGD2/LT which is in part responsible for increased bronchoconstriction. Other roles attributed to PGE2 in the lung include inflammatory cell recruitment, eosinophil degranulation, bronchodilation, T-cell recruitment and differentiation and adhesion molecule expression as reviewed before (Vancheri et al., 2004).

With regards to sex-related differences in response to environmental stimuli, a study examined changes in gene expression in the lung associated with inflammation and immunity after ozone exposure (Cabello et al., 2015). This study found increased lung histological scores and increased infiltrating PMN in the female sex as compared to males after ozone exposure. Among control mice exposed to filtered air alone, females displayed about 5% difference in gene expression of genes related to chemokines and cytokines as compared to males. These genes included *Cxcl2* and *Ccl19* (involved in activation of macrophages), *Myd88* (involved in TLR activation), and *C4b* (associated with IL-6 response), all of which were associated with immune cell adhesion and recruitment. Considering the sex- and genotype-dependent differences in our model, we examined changes in gene expression as well. Since the most significant changes we observed in our model was in the male sex (as in *Fat-1* mice with TPPU), we focused our gene expression studies to male sex. NanoString gene expression analysis identified differentially regulated pathways consistent with our previous results (Dominguez et al., 2020; Ulu et al., 2021b) indicating that immune cell activation, cell proliferation, wound healing and transport pathways were altered following 3-weeks DE exposure. In an In-depth analysis both using STRING database protein-protein interaction and NanoString advanced analyses, we also identified changes in NFκBIA, response to macrophage colony stimulating factor, immune clearance, and neutrophil aggregation between the two genotypes (**Figure 4**). In addition, TPPU treatment affected distinct cellular processes such as T-cell differentiation in WT mice and regulation of neutrophil activation in the *Fat-1* genotype. This observed effect of TPPU is consistent with a previous report showing modulation of the Th1/Th17 response while elevating regulatory T-cells by TPPU in an arthritis model (Trindade-da-Silva et al., 2020). Evaluation of both upregulated and downregulated genes among the experimental groups were in the direction of inflammation resolution. For example, in the *Fat-1* genotype the observed differences in the downregulated genes were associated with cytokine production in macrophages, regulation of tight junctions and ECM disassembly, suggesting a move towards resolution of inflammation in tissue (**Table 1**). Cytokine production and tight junctions contribute significantly to the maintenance of epithelial cell integrity and mucosal immunity of the lung in response to environmental insults as well as pathogens (Kyd et al., 2001; Brune et al., 2015). Similarly, changes in ECM are important for recruitment of immune cells into and within the lung (Wight et al., 2017). Altogether, changes in these processes promoted by elevated levels of ω-3 fatty acids as in *Fat-1* transgenic mice might affect how the lung responds to DE exposure. Particularly with TPPU, we identified downregulation of genes involved in IL-33 mediated signaling, as well as IL-5, IL-13, and IL-6 secretion. Overall, these data identified differences in immune clearance between the two genotypes and TPPU appeared to contribute to T-cell differentiation and regulation of PMN activation in part by downregulating the IL-33-mediated signaling pathway. IL-33 has previously been reported as an important regulator of Th-2 immune response in allergic inflammation (Chan et al., 2019).

The studies described herein do have numerous limitations. As with all transgenic animal models, the use of the *Fat-1* mice to increase total body tissue levels of ω-3 PUFA and achieve an ideal ~1:1 ratio of ω-6:ω-3 PUFA does not fully recapitulate the human condition. For example, differences in PUFA intakes are seen not only between individuals, but temporal fluctuations in diet tendencies for each individual also undoubtedly alter daily to monthly PUFA levels, and the impacts of this will vary across different tissues based on PUFA uptake kinetics (Katan et al., 1997; Raphael and Sordillo, 2013; Gurzell et al., 2014). As PUFA substrate utilized during inflammatory events likely comes from both tissue sources as well as circulating blood and associated inflammatory cell infiltration, the impacts of recent dietary intake versus long-term dietary patterns on PUFA substrate availability are difficult to ascertain. Also, there are numerous recognized health benefits of diets high in ω-3 PUFA, due at least partly to their role in the endogenous production of SPM that regulate inflammation resolution and repair activities (Titos et al., 19502011; Schwab et al., 2007; Serhan et al., 2009; Levy, 2010; Serhan, 2014). SPM are produced temporally during an inflammatory response; their levels increase within hours to days following an inflammatory insult, and their production is critical to inflammation catabasis, including promoting neutrophil clearance, reducing inflammatory cytokine production, activating M2-like pro-resolution macrophages, promoting regulatory T cell recruitment, and activating tissue repair (Widgerow, 2012; Basil and Levy, 2016). Deficiencies in SPM generation pathways have been identified in asthma, and SPM are decreased in lavage, sputum, and/or exhaled breath condensates of COPD and asthma patients compared to individuals without lung disease (Levy et al., 2007; Bhavsar et al., 2010; Croasdell et al., 2015). Therefore, an in-depth analysis of both ω -3 and ω -6 PUFA derived SPMs is necessary, and lipid metabolomics analyses of our data are currently underway in our laboratory.

Another limitation is that we have used a model of organic dust exposure that utilizes a sterile-filtered aqueous extract of environmental dusts that is intranasally instilled to mice in a saline solution. This model will not fully recapitulate the inhalant

injury that is experienced by an individual working in a swine confinement facility, as it does not consider certain components, including live pathogens or gaseous components that have recognized respiratory impacts in these workers (Von Essen and Donham, 1999; Kirkhorn and Garry, 2000; Charavaryamath et al., 2005; Charavaryamath et al., 2008; Langley, 2011; May et al., 2012; Madsen et al., 2015; Nordgren and Bailey, 2016; Schneberger et al., 2017; Nordgren and Charavaryamath, 2018; Schneberger et al., 2021). It has been reported that airway inflammation in swine confinement workers differ from naïve subjects even after repetitive exposures, one displaying neutrophilic airway inflammation and the other neutrophilic and eosinophilic inflammation, respectively (Larsson et al., 1994; Von Essen and Romberger, 2003). We have characterized a number of components that are likely to be involved in neutrophilic inflammation. Proteases are one of the components of agricultural dust that has been shown to be in part responsible for this type of inflammation (Von Essen and Romberger, 2003; Romberger et al., 2015). Our results are consistent with neutrophilic inflammation observed in people.

In addition, since we delivered agricultural dust extract under light isoflurane anesthesia, the previously reported sex-related differences of isoflurane might confound some of the sex-related effects we observed in our study; however, given all the mice in each group underwent this light anesthesia the significant differences between the groups would still stand.

Compelling data indicate the importance of having a balanced ω-6:ω-3 PUFA ratio for optimal health (~1:1 is considered ideal), yet the typical Western diet has a ratio of ~10–20:1 (Simopoulos, 2008; Patterson et al., 2012). This imbalance is considered a driving or compounding factor in chronic inflammatory diseases, with many pro-inflammatory lipids formed from the ω-6 PUFA arachidonic acid, such as leukotrienes, thromboxanes and prostaglandins (Calder, 2006; Calder, 2010; Patterson et al., 2012; Calder, 2013; Barden et al., 2016). It was recently reported that Veterans with COPD and an occupational history that include agricultural work had an ω-6:ω-3 PUFA ratio of ~50:1 (Hanson et al., 2017), underscoring the potential vulnerability of this population. Supplementation with ω-3 PUFA has demonstrated health benefits in clinical studies of cystic fibrosis, COPD, and other lung diseases (Strasser et al., 1985; Pontes-Arruda et al., 2008; Giudetti and Cagnazzo, 2012; Oliver and Watson, 2013). Thus, increasing ω-3 FA intake, possibly in combination with a reduced intake of ω-6 PUFA, could be an accessible and effective means of preventing and ameliorating airway disease in patients with inflammatory lung diseases such as those caused by agricultural dust exposures. Taken together, our investigations utilizing the *Fat-1* mouse model in conjunction with sEH inhibition highlight the potentials of targeting repair/resolution pathways therapeutically to promote lung protection from environmental dust exposures, and also highlight differences based on sex in the protectiveness offered by these interventions. In the case of agriculture workers who are chronically inhaling inflammatory dusts, these outcomes hold promise for improving lung health outcomes *via* both limiting lung inflammation but also promoting repair following injury in this vulnerable population.

DATA AVAILABILITY STATEMENT

The original contributions presented in the study are included in the article/**Supplementary Material**, further inquiries can be directed to the corresponding author.

ETHICS STATEMENT

The animal study was reviewed and approved by the Institutional Animal Care and Use Committee of the University of California, Riverside.

AUTHOR CONTRIBUTIONS

TN, AU, and BH conceptually contributed and designed experiments; AU, JV, AB, SS, JY, and CB collected samples, acquired, and analyzed data; AU and TN drafted the manuscript; AU, JV, AB, SS, JY, CB, BH, and TN reviewed and edited the manuscript.

FUNDING

This work was supported in part by the National Institute of Environmental Health Sciences (R00ES025819 to TN), the National Heart, Lung, and Blood Institute (R01HL158926 to TN), and with partial support from NIH/NIEHS (RIVER Award, R35 ES030443-01 to BH) and NIH/NIEHS (Superfund Award, P42 ES004699 to BH).

ACKNOWLEDGMENTS

Authors gratefully acknowledge Debra Romberger at the University of Nebraska Medical Center for the kind gift of the swine confinement facility dusts used for these investigations.

SUPPLEMENTARY MATERIAL

The Supplementary Material for this article can be found online at: https://www.frontiersin.org/articles/10.3389/fphar.2021.785193/full#supplementary-material

REFERENCES

Adebesin, A. M., Wesser, T., Vijaykumar, J., Konkel, A., Paudyal, M. P., Lossie, J., et al. (2019). Development of Robust 17. *J. Med. Chem.* 62 (22), 10124–10143. doi:10.1021/acs.jmedchem.9b00952

American Thoracic, S. (1998). Respiratory Health Hazards in Agriculture. *Am. J. Respir. Crit. Care Med.* 158 (5 Pt 2), S1–S76. doi:10.1164/ajrccm.158.supplement_1.rccm1585s1

Aoki, H., Hisada, T., Ishizuka, T., Utsugi, M., Kawata, T., Shimizu, Y., et al. (2008). Resolvin E1 Dampens Airway Inflammation and Hyperresponsiveness in a Murine Model of Asthma. *Biochem. biophysical Res. Commun.* 367 (2), 509–515. doi:10.1016/j.bbrc.2008.01.012

Balgoma, D., Yang, M., Sjödin, M., Snowden, S., Karimi, R., Levänen, B., et al. (2016). Linoleic Acid-Derived Lipid Mediators Increase in a Female-Dominated Subphenotype of COPD. *Eur. Respir. J.* 47 (6), 1645–1656. doi:10.1183/13993003.01080-2015

Baliatsas, C., Borlee, F., van Dijk, C. E., van der Star, B., Zock, J. P., Smit, L. A. M., et al. (2017). Comorbidity and Coexisting Symptoms and Infections Presented in General Practice by COPD Patients: Does Livestock Density in the Residential Environment Play a Role? *Int. J. Hyg. Environ. Health* 220 (4), 704–710. doi:10.1016/j.ijheh.2017.02.005

Barden, A. E., Mas, E., and Mori, T. A. (2016). n-3 Fatty Acid Supplementation and Proresolving Mediators of Inflammation. *Curr. Opin. Lipidol.* 27 (1), 26–32. doi:10.1097/MOL.0000000000000262

Basil, M. C., and Levy, B. D. (2016). Specialized Pro-resolving Mediators: Endogenous Regulators of Infection and Inflammation. *Nat. reviewsImmunology* 16 (1), 51–67. doi:10.1038/nri.2015.4

Bhavsar, P. K., Levy, B. D., Hew, M. J., Pfeffer, M. A., Kazani, S., Israel, E., et al. (2010). Corticosteroid Suppression of Lipoxin A4 and Leukotriene B4from Alveolar Macrophages in Severe Asthma. *Respir. Res.* 11, 71. doi:10.1186/1465-9921-11-71

Bilal, S., Haworth, O., Wu, L., Weylandt, K. H., Levy, B. D., and Kang, J. X. (2011). Fat-1 Transgenic Mice with Elevated omega-3 Fatty Acids Are Protected from Allergic Airway Responses. *Biochim. Biophys. Acta* 1812 (9), 1164–1169. doi:10.1016/j.bbadis.2011.05.002

Boissy, R. J., Romberger, D. J., Roughead, W. A., Weissenburger-Moser, L., Poole, J. A., and LeVan, T. D. (2014). Shotgun Pyrosequencing Metagenomic Analyses of Dusts from Swine Confinement and Grain Facilities. *PLoS One* 9 (4), e95578. doi:10.1371/journal.pone.0095578

Borlee, F., Yzermans, C. J., Aalders, B., Rooijackers, J., Krop, E., Maassen, C. B. M., et al. (2017). Air Pollution from Livestock Farms Is Associated with Airway Obstruction in Neighboring Residents. *Am. J. Respir. Crit. Care Med.* 196 (9), 1152–1161. doi:10.1164/rccm.201701-0021OC

Bradberry, J. C., and Hilleman, D. E. (2013). Overview of omega-3 Fatty Acid Therapies. *P T* 38 (11), 681–691.

Brune, K., Frank, J., Schwingshackl, A., Finigan, J., and Sidhaye, V. K. (2015). Pulmonary Epithelial Barrier Function: Some New Players and Mechanisms. *Am. J. Physiol. Lung Cel Mol Physiol* 308 (8), L731–L745. doi:10.1152/ajplung.00309.2014

Burkes, R. M., Gassett, A. J., Ceppe, A. S., Anderson, W., O'Neal, W. K., Woodruff, P. G., et al. (2018). Rural Residence and COPD Exacerbations: Analysis of the SPIROMICS Cohort. *Ann. Am. Thorac. Soc.* 15, 808–816. doi:10.1513/AnnalsATS.201710-837OC

Cabello, N., Mishra, V., Sinha, U., DiAngelo, S. L., Chroneos, Z. C., Ekpa, N. A., et al. (2015). Sex Differences in the Expression of Lung Inflammatory Mediators in Response to Ozone. *Am. J. Physiol. Lung Cel Mol Physiol* 309 (10), L1150–L1163. doi:10.1152/ajplung.00018.2015

Calder, P. C. (2013). N-3 Fatty Acids, Inflammation and Immunity: New Mechanisms to Explain Old Actions. *Proc. Nutr. Soc.* 72 (3), 326–336. doi:10.1017/S0029665113001031

Calder, P. C. (2006). N-3 Polyunsaturated Fatty Acids, Inflammation, and Inflammatory Diseases. *Am. J. Clin. Nutr.* 83 (6 Suppl. l), 1505S–19S. doi:10.1093/ajcn/83.6.1505S

Calder, P. C. (2010). Omega-3 Fatty Acids and Inflammatory Processes. *Nutrients* 2 (3), 355–374. doi:10.3390/nu2030355

Calder, P. C., Waitzberg, D. L., Klek, S., and Martindale, R. G. (2020). Lipids in Parenteral Nutrition: Biological Aspects. *JPEN J. Parenter. Enteral Nutr.* 44 (Suppl. 1), S21–S7. doi:10.1002/jpen.1756

Cdc (2019). CDC - Asthma - Most Recent Asthma Data. Available at: https://www.cdc.gov/asthma/most_recent_national_asthma_data.htm2018.

Chan, B. C. L., Lam, C. W. K., Tam, L. S., and Wong, C. K. (2019). IL33: Roles in Allergic Inflammation and Therapeutic Perspectives. *Front. Immunol.* 10, 364. doi:10.3389/fimmu.2019.00364

Charavaryamath, C., Janardhan, K. S., Townsend, H. G., Willson, P., and Singh, B. (2005). Multiple Exposures to Swine Barn Air Induce Lung Inflammation and Airway Hyper-Responsiveness. *Respir. Res.* 6, 50. doi:10.1186/1465-9921-6-50

Charavaryamath, C., Juneau, V., Suri, S. S., Janardhan, K. S., Townsend, H., and Singh, B. (2008). Role of Toll-like Receptor 4 in Lung Inflammation Following Exposure to Swine Barn Air. *Exp. Lung Res.* 34 (1), 19–35. doi:10.1080/01902140701807779

Croasdell, A., Lacy, S. H., Thatcher, T. H., Sime, P. J., and Phipps, R. P. (19502016). Resolvin D1 Dampens Pulmonary Inflammation and Promotes Clearance of Nontypeable Haemophilus Influenzae. *J. Immunol. (Baltimore, Md* 196 (6), 2742–2752. doi:10.4049/jimmunol.1502331

Croasdell, A., Thatcher, T. H., Kottmann, R. M., Colas, R. A., Dalli, J., Serhan, C. N., et al. (2015). Resolvins Attenuate Inflammation and Promote Resolution in Cigarette Smoke-Exposed Human Macrophages. *Am. J. physiologyLung Cell. Mol. Physiol.* 309 (8), L888–L901. doi:10.1152/ajplung.00125.2015

de Torres, J. P., Cote, C. G., López, M. V., Casanova, C., Díaz, O., Marin, J. M., et al. (2009). Sex Differences in Mortality in Patients with COPD. *Eur. Respir. J.* 33 (3), 528–535. doi:10.1183/09031936.00096108

Deckelbaum, R. J., and Torrejon, C. (2012). The omega-3 Fatty Acid Nutritional Landscape: Health Benefits and Sources. *J. Nutr.* 142 (3), 587S–91S. doi:10.3945/jn.111.148080

Decsi, T., and Kennedy, K. (2011). Sex-specific Differences in Essential Fatty Acid Metabolism. *Am. J. Clin. Nutr.* 94 (6 Suppl. l), 1914S–9S. doi:10.3945/ajcn.110.000893

Demanche, A., Bonlokke, J., Beaulieu, M. J., Assayag, E., and Cormier, Y. (2009). Swine Confinement Buildings: Effects of Airborne Particles and Settled Dust on Airway Smooth Muscles. *Ann. Agric. Environ. Med.* 16 (2), 233–238.

Dileepan, M., Rastle-Simpson, S., Greenberg, Y., Wijesinghe, D. S., Kumar, N. G., Yang, J., et al. (2019). Effect of Dual sEH/COX-2 Inhibition on Allergen-Induced Airway Inflammation. *Front. Pharmacol.* 10, 1118. doi:10.3389/fphar.2019.01118

Dominguez, E. C., Heires, A. J., Pavlik, J., Larsen, T. D., Guardado, S., Sisson, J. H., et al. (2020). A High Docosahexaenoic Acid Diet Alters the Lung Inflammatory Response to Acute Dust Exposure. *Nutrients* 12 (8). doi:10.3390/nu12082334

Ehrlich, R. (1980). Interaction between Environmental Pollutants and Respiratory Infections. *Environ. Health Perspect.* 35, 89–99. doi:10.1289/ehp.803589

Falck, J. R., Wallukat, G., Puli, N., Goli, M., Arnold, C., Konkel, A., et al. (2011). 17(R),18(S)-epoxyeicosatetraenoic Acid, a Potent Eicosapentaenoic Acid (EPA) Derived Regulator of Cardiomyocyte Contraction: Structure-Activity Relationships and Stable Analogues. *J. Med. Chem.* 54 (12), 4109–4118. doi:10.1021/jm200132q

Fix, J., Annesi-Maesano, I., Baldi, I., Boulanger, M., Cheng, S., Cortes, S., et al. (2020). Gender Differences in Respiratory Health Outcomes Among Farming Cohorts Around the globe: Findings from the AGRICOH Consortium. *J. Agromedicine* 26, 97–108. doi:10.1080/1059924X.2020.1713274

Franklin, B. A., Brook, R., and Arden Pope, C., 3rd (2015). Air Pollution and Cardiovascular Disease. *Curr. Probl. Cardiol.* 40 (5), 207–238. doi:10.1016/j.cpcardiol.2015.01.003

Gao, Z., Dosman, J. A., Rennie, D. C., Schwartz, D. A., Yang, I. V., Beach, J., et al. (2018). Gender-specific Associations between Polymorphisms in the Toll-like Receptor (TLR) Genes and Lung Function Among Workers in Swine Operations. *J. Toxicol. Environ. Health A.* 81 (22), 1186–1198. doi:10.1080/15287394.2018.1544523

Giudetti, A. M., and Cagnazzo, R. (2012). Beneficial Effects of N-3 PUFA on Chronic Airway Inflammatory Diseases. *Prostaglandins & other lipid mediators* 99 (3-4), 57–67. doi:10.1016/j.prostaglandins.2012.09.006

Goswami, S. K., Rand, A. A., Wan, D., Yang, J., Inceoglu, B., Thomas, M., et al. (2017). Pharmacological Inhibition of Soluble Epoxide Hydrolase or Genetic Deletion Reduces Diclofenac-Induced Gastric Ulcers. *Life Sci.* 180, 114–122. doi:10.1016/j.lfs.2017.05.018

Guedes, A. G., Morisseau, C., Sole, A., Soares, J. H., Ulu, A., Dong, H., et al. (2013). Use of a Soluble Epoxide Hydrolase Inhibitor as an Adjunctive Analgesic in a Horse with Laminitis. *Vet. Anaesth. Analg* 40 (4), 440–448. doi:10.1111/vaa.12030

Guillien, A., Puyraveau, M., Soumagne, T., Guillot, S., Rannou, F., Marquette, D., et al. (2016). Prevalence and Risk Factors for COPD in Farmers: a Cross-Sectional Controlled Study. *Eur. Respir. J.* 47 (1), 95–103. doi:10.1183/13993003.00153-2015

Gurzell, E. A., Wiesinger, J. A., Morkam, C., Hemmrich, S., Harris, W. S., and Fenton, J. I. (2014). Is the omega-3 index a Valid Marker of Intestinal Membrane Phospholipid EPA+DHA Content? Prostaglandins, Leukotrienes, and Essential Fatty Acids. *Prostaglandins Leukot. Essent. Fatty Acids* 91 (3), 87–96. doi:10.1016/j.plefa.2014.04.001

Hammock, B. D., McReynolds, C. B., Wagner, K., Buckpitt, A., Cortes-Puch, I., Croston, G., et al. (2021). Movement to the Clinic of Soluble Epoxide Hydrolase Inhibitor EC5026 as an Analgesic for Neuropathic Pain and for Use as a Nonaddictive Opioid Alternative. *J. Med. Chem.* 64 (4), 1856–1872. doi:10.1021/acs.jmedchem.0c01886

Hammock, B. D., Wang, W., Gilligan, M. M., and Panigrahy, D. (2020). Eicosanoids: The Overlooked Storm in Coronavirus Disease 2019 (COVID-19)? *Am. J. Pathol.* 190, 1782–1788. doi:10.1016/j.ajpath.2020.06.010

Hanson, C., Lyden, E., Weissenburger-Moser, L., Furtado, J., Hinds, J., and LeVan, T. (2017). Serum Level of Nutritional Antioxidants Are Decreased in Veteran Smokers with COPD. *Mil. Veterans Health* 25, 9.

Haworth, O., Cernadas, M., and Levy, B. D. (2011). NK Cells Are Effectors for Resolvin E1 in the Timely Resolution of Allergic Airway Inflammation. *J. Immunol. (Baltimore, Md: 1950)* 186 (11), 6129–6135. doi:10.4049/jimmunol.1004007

Haworth, O., and Levy, B. D. (2007). Endogenous Lipid Mediators in the Resolution of Airway Inflammation. *Eur. Respir. J.* 30 (5), 980–992. doi:10.1183/09031936.00005807

Herrerias, A., Torres, R., Serra, M., Marco, A., Pujols, L., Picado, C., et al. (2009). Activity of the Cyclooxygenase 2-Prostaglandin-E Prostanoid Receptor Pathway in Mice Exposed to House Dust Mite Aeroallergens, and Impact of Exogenous Prostaglandin E2. *J. Inflamm. (Lond).* 6, 30. doi:10.1186/1476-9255-6-30

Hertz, D., Dibbern, J., Eggers, L., von Borstel, L., and Schneider, B. E. (2020). Increased Male Susceptibility to *Mycobacterium tuberculosis* Infection Is Associated with Smaller B Cell Follicles in the Lungs. *Sci. Rep.* 10 (1), 5142. doi:10.1038/s41598-020-61503-3

Hoppin, J. A., Umbach, D. M., Long, S., Rinsky, J. L., Henneberger, P. K., Salo, P. M., et al. (2014). Respiratory Disease in United States Farmers. *Occup. Environ. Med.* 71 (7), 484–491. doi:10.1136/oemed-2013-101983

Hsiao, H. M., Sapinoro, R. E., Thatcher, T. H., Croasdell, A., Levy, E. P., Fulton, R. A., et al. (2013). A Novel Anti-inflammatory and Pro-resolving Role for Resolvin D1 in Acute Cigarette Smoke-Induced Lung Inflammation. *PloS one* 8 (3), e58258. doi:10.1371/journal.pone.0058258

Iversen, M., and Dahl, R. (2000). Working in Swine-Confinement Buildings Causes an Accelerated Decline in FEV1: a 7-yr Follow-Up of Danish Farmers. *Eur. Respir. J. : official J. Eur. Soc. Clin. Respir. Physiol.* 16 (3), 404–408. doi:10.1034/j.1399-3003.2000.016003404.x

Jamieson, K. L., Keshavarz-Bahaghighat, H., Darwesh, A. M., Sosnowski, D. K., and Seubert, J. M. (2020). Age and Sex Differences in Hearts of Soluble Epoxide Hydrolase Null Mice. *Front. Physiol.* 11, 48. doi:10.3389/fphys.2020.00048

Kachan, D., Fleming, L. E., LeBlanc, W. G., Goodman, E., Arheart, K. L., Caban-Martinez, A. J., et al. (2012). Worker Populations at Risk for Work-Related Injuries across the Life Course. *Am. J. Ind. Med.* 55 (4), 361–366. doi:10.1002/ajim.21994

Kang, J. X., Wang, J., Wu, L., and Kang, Z. B. (2004). Transgenic Mice: Fat-1 Mice Convert N-6 to N-3 Fatty Acids. *Nature* 427 (6974), 504. doi:10.1038/427504a

Katan, M. B., Deslypere, J. P., van Birgelen, A. P., Penders, M., and Zegwaard, M. (1997). Kinetics of the Incorporation of Dietary Fatty Acids into Serum Cholesteryl Esters, Erythrocyte Membranes, and Adipose Tissue: an 18-month Controlled Study. *J. lipid Res.* 38 (10), 2012–2022. doi:10.1016/s0022-2275(20)37132-7

Kim, K. H., Park, T. S., Kim, Y. S., Lee, J. S., Oh, Y. M., Lee, S. D., et al. (2016). Resolvin D1 Prevents Smoking-Induced Emphysema and Promotes Lung Tissue Regeneration. *Int. J. Chron. Obstruct Pulmon Dis.* 11, 1119–1128. doi:10.2147/COPD.S100198

Kimmerling, K. A., Oswald, S. J., Huebner, J. L., Little, D., Kraus, V. B., Kang, J. X., et al. (2020). Transgenic Conversion of ω-6 to ω-3 Polyunsaturated Fatty Acids via Fat-1 Reduces the Severity of post-traumatic Osteoarthritis. *Arthritis Res. Ther.* 22 (1), 83. doi:10.1186/s13075-020-02170-7

Kirkhorn, S. R., and Garry, V. F. (2000). Agricultural Lung Diseases. *Environ. Health Perspect.* 108 (Suppl. 4), 705–712. doi:10.1289/ehp.00108s4705

Kitamura, S., Morisseau, C., Harris, T. R., Inceoglu, B., and Hammock, B. D. (2017). Occurrence of Urea-Based Soluble Epoxide Hydrolase Inhibitors from the Plants in the Order Brassicales. *PLoS One* 12 (5), e0176571. doi:10.1371/journal.pone.0176571

Kuo, Y. M., Hsu, P. C., Hung, C. C., Hu, Y. Y., Huang, Y. J., Gan, Y. L., et al. (2019). Soluble Epoxide Hydrolase Inhibition Attenuates Excitotoxicity Involving 14,15-Epoxyeicosatrienoic Acid-Mediated Astrocytic Survival and Plasticity to Preserve Glutamate Homeostasis. *Mol. Neurobiol.* 56 (12), 8451–8474. doi:10.1007/s12035-019-01669-8

Kyd, J. M., Foxwell, A. R., and Cripps, A. W. (2001). Mucosal Immunity in the Lung and Upper Airway. *Vaccine* 19 (17-19), 2527–2533. doi:10.1016/s0264-410x(00)00484-9

Lands, B., Bibus, D., and Stark, K. D. (2018). Dynamic Interactions of N-3 and N-6 Fatty Acid Nutrients. *Prostaglandins Leukot. Essent. Fatty Acids* 136, 15–21. doi:10.1016/j.plefa.2017.01.012

Langley, R. L. (2011). Consequences of Respiratory Exposures in the Farm Environment. *North Carolina Med. J.* 72 (6), 477–480. doi:10.18043/ncm.72.6.477

Larsson, K. A., Eklund, A. G., Hansson, L. O., Isaksson, B. M., and Malmberg, P. O. (1994). Swine Dust Causes Intense Airways Inflammation in Healthy Subjects. *Am. J. Respir. Crit. Care Med.* 150 (4), 973–977. doi:10.1164/ajrccm.150.4.7921472

Lazaar, A. L., Yang, L., Boardley, R. L., Goyal, N. S., Robertson, J., Baldwin, S. J., et al. (2016). Pharmacokinetics, Pharmacodynamics and Adverse Event Profile of GSK2256294, a Novel Soluble Epoxide Hydrolase Inhibitor. *Br. J. Clin. Pharmacol.* 81 (5), 971–979. doi:10.1111/bcp.12855

Levy, B. D., Kohli, P., Gotlinger, K., Haworth, O., Hong, S., Kazani, S., et al. (2007). Protectin D1 Is Generated in Asthma and Dampens Airway Inflammation and Hyperresponsiveness. *J. Immunol.* 178 (1), 496–502. doi:10.4049/jimmunol.178.1.496

Levy, B. D. (2010). Resolvins and Protectins: Natural Pharmacophores for Resolution Biology. *Prostaglandins, Leukot. Essent. fatty Acids* 82 (4-6), 327–332. doi:10.1016/j.plefa.2010.02.003

Levy, B. D., and Serhan, C. N. (2003). Exploring New Approaches to the Treatment of Asthma: Potential Roles for Lipoxins and Aspirin-Triggered Lipid Mediators. *Drugs Today (Barc)* 39 (5), 373–384. doi:10.1358/dot.2003.39.5.740217

Levy, B. D., and Serhan, C. N. (2014). Resolution of Acute Inflammation in the Lung. *Annu. Rev. Physiol.* 76, 467–492. doi:10.1146/annurev-physiol-021113-170408

Lopez-Vicario, C., Alcaraz-Quiles, J., Garcia-Alonso, V., Rius, B., Hwang, S. H., Titos, E., et al. (2015). Inhibition of Soluble Epoxide Hydrolase Modulates Inflammation and Autophagy in Obese Adipose Tissue and Liver: Role for omega-3 Epoxides. *Proc. Natl. Acad. Sci. U S A.* 112 (2), 536–541. doi:10.1073/pnas.1422590112

Madsen, A. M., Zervas, A., Tendal, K., and Nielsen, J. L. (2015). Microbial Diversity in Bioaerosol Samples Causing ODTS Compared to Reference Bioaerosol Samples as Measured Using Illumina Sequencing and MALDI-TOF. *Environ. Res.* 140, 255–267. doi:10.1016/j.envres.2015.03.027

Martinez, F. J., Curtis, J. L., Sciurba, F., Mumford, J., Giardino, N. D., Weinmann, G., et al. (2007). Sex Differences in Severe Pulmonary Emphysema. *Am. J. Respir. Crit. Care Med.* 176 (3), 243–252. doi:10.1164/rccm.200606-828OC

May, S., Romberger, D. J., and Poole, J. A. (2012). Respiratory Health Effects of Large Animal Farming Environments. *J. Toxicol. Environ. healthPart B, Crit. Rev.* 15 (8), 524–541. doi:10.1080/10937404.2012.744288

Miyata, J., and Arita, M. (2015). Role of omega-3 Fatty Acids and Their Metabolites in Asthma and Allergic Diseases. *Allergol. Int. : official J. Jpn. Soc. Allergol.* 64 (1), 27–34. doi:10.1016/j.alit.2014.08.003

Morisseau, C., and Hammock, B. D. (2013). Impact of Soluble Epoxide Hydrolase and Epoxyeicosanoids on Human Health. *Annu. Rev. Pharmacol. Toxicol.* 53, 37–58. doi:10.1146/annurev-pharmtox-011112-140244

Nordgren, T. M., and Bailey, K. L. (2016). Pulmonary Health Effects of Agriculture. *Curr. Opin. Pulm. Med.* 22 (2), 144–149. doi:10.1097/MCP.0000000000000247

Nordgren, T. M., Bauer, C. D., Heires, A. J., Poole, J. A., Wyatt, T. A., West, W. W., et al. (2015). Maresin-1 Reduces Airway Inflammation Associated with Acute and Repetitive Exposures to Organic Dust. *Transl Res.* 166 (1), 57–69. doi:10.1016/j.trsl.2015.01.001

Nordgren, T. M., and Charavaryamath, C. (2018). Agriculture Occupational Exposures and Factors Affecting Health Effects. *Curr. Allergy Asthma Rep.* 18 (12), 65. doi:10.1007/s11882-018-0820-8

Nordgren, T. M., Friemel, T. D., Heires, A. J., Poole, J. A., Wyatt, T. A., and Romberger, D. J. (2014). The omega-3 Fatty Acid Docosahexaenoic Acid Attenuates Organic Dust-Induced Airway Inflammation. *Nutrients* 6 (12), 5434–5452. doi:10.3390/nu6125434

Nordgren, T. M., Heires, A. J., Wyatt, T. A., Poole, J. A., LeVan, T. D., Cerutis, D. R., et al. (2013). Maresin-1 Reduces the Pro-inflammatory Response of Bronchial Epithelial Cells to Organic Dust. *Respir. Res.* 14, 51. doi:10.1186/1465-9921-14-51

Nordgren, T. M., Heires, A. J., Zempleni, J., Swanson, B. J., Wichman, C., and Romberger, D. J. (2019). Bovine Milk-Derived Extracellular Vesicles Enhance Inflammation and Promote M1 Polarization Following Agricultural Dust Exposure in Mice. *J. Nutr. Biochem.* 64, 110–120. doi:10.1016/j.jnutbio.2018.10.017

Oliver, C., and Watson, H. (2013). Omega-3 Fatty Acids for Cystic Fibrosis. *Cochrane database Syst. Rev.* 11, CD002201. doi:10.1002/14651858.CD002201.pub4

Palmberg, L., Larssson, B. M., Malmberg, P., and Larsson, K. (2002). Airway Responses of Healthy Farmers and Nonfarmers to Exposure in a Swine Confinement Building. *Scand. J. work, Environ. Health* 28 (4), 256–263. doi:10.5271/sjweh.673

Patterson, E., Wall, R., Fitzgerald, G. F., Ross, R. P., and Stanton, C. (2012). Health Implications of High Dietary Omega-6 Polyunsaturated Fatty Acids. *J. Nutr. Metab.* 2012. doi:10.1155/2012/539426

Pavilonis, B. T., Sanderson, W. T., and Merchant, J. A. (2013). Relative Exposure to Swine Animal Feeding Operations and Childhood Asthma Prevalence in an Agricultural Cohort. *Environ. Res.* 122, 74–80. doi:10.1016/j.envres.2012.12.008

Pedersen, S., Nonnenmann, M., Rautiainen, R., Demmers, T. G., Banhazi, T., and Lyngbye, M. (2000). Dust in Pig Buildings. *J. Agric. Saf. Health* 6 (4), 261–274. doi:10.13031/2013.1909

Perez, T. A., Castillo, E. G., Ancochea, J., Pastor Sanz, M. T., Almagro, P., Martínez-Camblor, P., et al. (2020). Sex Differences between Women and Men with COPD: A New Analysis of the 3CIA Study. *Respir. Med.* 171, 106105. doi:10.1016/j.rmed.2020.106105

Phelps, D. S., Umstead, T. M., and Floros, J. (2012). Sex Differences in the Response of the Alveolar Macrophage Proteome to Treatment with Exogenous Surfactant Protein-A. *Proteome Sci.* 10 (1), 44. doi:10.1186/1477-5956-10-44

Pontes-Arruda, A., Demichele, S., Seth, A., and Singer, P. (2008). The Use of an Inflammation-Modulating Diet in Patients with Acute Lung Injury or Acute Respiratory Distress Syndrome: a Meta-Analysis of Outcome Data. *JPENJournal Parenter. enteral Nutr.* 32 (6), 596–605. doi:10.1177/0148607108324203

Poole, J. A., Dooley, G. P., Saito, R., Burrell, A. M., Bailey, K. L., Romberger, D. J., et al. (2010). Muramic Acid, Endotoxin, 3-hydroxy Fatty Acids, and Ergosterol Content Explain Monocyte and Epithelial Cell Inflammatory Responses to Agricultural Dusts. *J. Toxicol. Environ. Health A.* 73 (10), 684–700. doi:10.1080/15287390903578539

Poole, J. A., Wyatt, T. A., Kielian, T., Oldenburg, P., Gleason, A. M., Bauer, A., et al. (2011). Toll-like Receptor 2 Regulates Organic Dust-Induced Airway Inflammation. *Am. J. Respir. Cel Mol Biol* 45 (4), 711–719. doi:10.1165/rcmb.2010-0427OC

Poole, J. A., Wyatt, T. A., Oldenburg, P. J., Elliott, M. K., West, W. W., Sisson, J. H., et al. (2009). Intranasal Organic Dust Exposure-Induced Airway Adaptation Response Marked by Persistent Lung Inflammation and Pathology in Mice. *Am. J. Physiol. Lung Cel Mol Physiol* 296 (6), L1085–L1095. doi:10.1152/ajplung.90622.2008

Radon, K., Schulze, A., Ehrenstein, V., van Strien, R. T., Praml, G., and Nowak, D. (2007). Environmental Exposure to Confined Animal Feeding Operations and Respiratory Health of Neighboring Residents. *Epidemiology (Cambridge, Mass)* 18 (3), 300–308. doi:10.1097/01.ede.0000259966.62137.84

Raphael, W., and Sordillo, L. M. (2013). Dietary Polyunsaturated Fatty Acids and Inflammation: the Role of Phospholipid Biosynthesis. *Int. J. Mol. Sci.* 14 (10), 21167–21188. doi:10.3390/ijms141021167

Rasmussen, S. G., Casey, J. A., Bandeen-Roche, K., and Schwartz, B. S. (2017). Proximity to Industrial Food Animal Production and Asthma Exacerbations in Pennsylvania, 2005-2012. *Int. J. Environ. Res. Public Health* 14 (4). doi:10.3390/ijerph14040362

Romberger, D. J., Bodlak, V., Von Essen, S. G., Mathisen, T., and Wyatt, T. A. (19852002). Hog Barn Dust Extract Stimulates IL-8 and IL-6 Release in Human Bronchial Epithelial Cells via PKC Activation. *J. Appl. Physiol.* 93 (1), 289–296. doi:10.1152/japplphysiol.00815.2001

Romberger, D. J., Heires, A. J., Nordgren, T. M., Souder, C. P., West, W., Liu, X. D., et al. (2015). Proteases in Agricultural Dust Induce Lung Inflammation through PAR-1 and PAR-2 Activation. *Am. J. Physiol. Lung Cel Mol Physiol* 309 (4), L388–L399. doi:10.1152/ajplung.00025.2015

Schneberger, D., DeVasure, J., Bailey, K., Romberger, D., and Wyatt, T. (2017). Effect of Low-Level CO 2 on Innate Inflammatory Protein Response to Organic Dust from Swine Confinement Barns. *J. Occup. Med. Toxicol. (London, England)* 12 (9). doi:10.1186/s12995-017-0155-8

Schneberger, D., Pandher, U., Thompson, B., and Kirychuk, S. (2021). Effects of Elevated CO 2 Levels on Lung Immune Response to Organic Dust and Lipopolysaccharide. *Respir. Res.* 22 (1), 104. doi:10.1186/s12931-021-01700-4

Schwab, J. M., Chiang, N., Arita, M., and Serhan, C. N. (2007). Resolvin E1 and Protectin D1 Activate Inflammation-Resolution Programmes. *Nature* 447 (7146), 869–874. doi:10.1038/nature05877

Seki, H., Fukunaga, K., Arita, M., Arai, H., Nakanishi, H., Taguchi, R., et al. (19502010). The Anti-inflammatory and Proresolving Mediator Resolvin E1 Protects Mice from Bacterial Pneumonia and Acute Lung Injury. *J. Immunol. (Baltimore, Md* 184 (2), 836–843. doi:10.4049/jimmunol.0901809

Senthilselvan, A., Chénard, L., Kirychuk, S., Predicala, B., Schwartz, D. A., Burch, L. H., et al. (2009). Gender-related Tumor Necrosis Factor-Alpha Responses in Naïve Volunteers with Toll-like Receptor 4 Polymorphisms Exposed in a Swine Confinement Facility. *J. Interferon Cytokine Res.* 29 (12), 781–790. doi:10.1089/jir.2009.0002

Serhan, C. N., Chiang, N., Dalli, J., and Levy, B. D. (2014). Lipid Mediators in the Resolution of Inflammation. *Cold Spring Harb Perspect. Biol.* 7 (2), a016311. doi:10.1101/cshperspect.a016311

Serhan, C. N. (2014). Pro-resolving Lipid Mediators Are Leads for Resolution Physiology. *Nature* 510 (7503), 92–101. doi:10.1038/nature13479

Serhan, C. N., Yang, R., Martinod, K., Kasuga, K., Pillai, P. S., Porter, T. F., et al. (2009). Maresins: Novel Macrophage Mediators with Potent Antiinflammatory and Proresolving Actions. *J. Exp. Med.* 206 (1), 15–23. doi:10.1084/jem.20081880

Sigsgaard, T., Basinas, I., Doekes, G., de Blay, F., Folletti, I., Heederik, D., et al. (2020). Respiratory Diseases and Allergy in Farmers Working with Livestock: a EAACI Position Paper. *Clin. Transl Allergy* 10, 29. doi:10.1186/s13601-020-00334-x

Simopoulos, A. P. (2008). The Importance of the omega-6/omega-3 Fatty Acid Ratio in Cardiovascular Disease and Other Chronic Diseases. *Exp. Biol. Med. (Maywood).* 233 (6), 674–688. doi:10.3181/0711-MR-311

Singh, N., Barnych, B., Morisseau, C., Wagner, K. M., Wan, D., Takeshita, A., et al. (2020). -Benzyl-linoleamide, a Constituent of. *J. Nat. Prod.* 83 (12), 3689–3697. doi:10.1021/acs.jnatprod.0c00938

Smit, L. A., Hooiveld, M., van der Sman-de Beer, F., Opstal-van Winden, A. W., Beekhuizen, J., Wouters, I. M., et al. (2014). Air Pollution from Livestock Farms, and Asthma, Allergic Rhinitis and COPD Among Neighbouring Residents. *Occup. Environ. Med.* 71 (2), 134–140. doi:10.1136/oemed-2013-101485

Strasser, T., Fischer, S., and Weber, P. C. (1985). Leukotriene B5 Is Formed in Human Neutrophils after Dietary Supplementation with Icosapentaenoic Acid. *Proc. Natl. Acad. Sci. United States America* 82 (5), 1540–1543. doi:10.1073/pnas.82.5.1540

Szklarczyk, D., Gable, A. L., Nastou, K. C., Lyon, D., Kirsch, R., Pyysalo, S., et al. (2021). The STRING Database in 2021: Customizable Protein-Protein Networks, and Functional Characterization of User-Uploaded Gene/measurement Sets. *Nucleic Acids Res.* 49 (D1), D605–D12. doi:10.1093/nar/gkaa1074

Tam, A., Tanabe, N., Churg, A., Wright, J. L., Hogg, J. C., and Sin, D. D. (2020). Sex Differences in Lymphoid Follicles in COPD Airways. *Respir. Res.* 21 (1), 46. doi:10.1186/s12931-020-1311-8

Thompson, M., Hein, N., Hanson, C., Smith, L. M., Anderson-Berry, A., Richter, C. K., et al. (2019). Omega-3 Fatty Acid Intake by Age, Gender, and Pregnancy Status in the United States: National Health and Nutrition Examination Survey 2003(-)2014. *Nutrients* 11 (1). doi:10.3390/nu11010177

Titos, E., Rius, B., Gonzalez-Periz, A., Lopez-Vicario, C., Moran-Salvador, E., Martinez-Clemente, M., et al. (19502011). Resolvin D1 and its Precursor Docosahexaenoic Acid Promote Resolution of Adipose Tissue Inflammation by Eliciting Macrophage Polarization toward an M2-like Phenotype. *J. Immunol. (Baltimore, Md* 187 (10), 5408–5418. doi:10.4049/jimmunol.1100225

Trindade-da-Silva, C. A., Clemente-Napimoga, J. T., Abdalla, H. B., Rosa, S. M., Ueira-Vieira, C., Morisseau, C., et al. (2020). Soluble Epoxide Hydrolase Inhibitor, TPPU, Increases Regulatory T Cells Pathway in an Arthritis Model. *FASEB J.* 34, 9074–9086. doi:10.1096/fj.202000415R

Trotta, M. C., Gharbia, S., Herman, H., Mladin, B., Hermenean, A., Balta, C., et al. (2021). Sex and Age-Related Differences in Neuroinflammation and Apoptosis in. *Int. J. Mol. Sci.* 22 (12). doi:10.3390/ijms22126280

Ulu, A., Burr, A., Heires, A., Pavlik, J., Larsen, T., Perez, P., et al. (2021). A High Docosahexaenoic Acid Diet Alters Lung Inflammation and Recovery Following Repetitive Exposure to Aqueous Organic Dust Extracts: Role of DHA in Repetitive Organic Dust Exposure. *J. Nutr. Biochem.* 97, 108797. doi:10.1016/j.jnutbio.2021.108797

Ulu, A., Burr, A., Heires, A. J., Pavlik, J., Larsen, T., Perez, P. A., et al. (2021). A High Docosahexaenoic Acid Diet Alters Lung Inflammation and Recovery Following Repetitive Exposure to Aqueous Organic Dust Extracts. *J. Nutr. Biochem.* 97, 108797. doi:10.1016/j.jnutbio.2021.108797

Ulu, A., Harris, T. R., Morisseau, C., Miyabe, C., Inoue, H., Schuster, G., et al. (2013). Anti-inflammatory Effects of omega-3 Polyunsaturated Fatty Acids and Soluble Epoxide Hydrolase Inhibitors in Angiotensin-II-dependent Hypertension. *J. Cardiovasc. Pharmacol.* 62 (3), 285–297. doi:10.1097/FJC.0b013e318298e460

Ulu, A., Inceoglu, B., Yang, J., Singh, V., Vito, S., Wulff, H., et al. (2016). Inhibition of Soluble Epoxide Hydrolase as a Novel Approach to High Dose Diazepam Induced Hypotension. *J. Clin. Toxicol.* 6 (3). doi:10.4172/2161-0495.1000300

Ulu, A., Stephen Lee, K. S., Miyabe, C., Yang, J., Hammock, B. G., Dong, H., et al. (2014). An omega-3 Epoxide of Docosahexaenoic Acid Lowers Blood Pressure in Angiotensin-II-dependent Hypertension. *J. Cardiovasc. Pharmacol.* 64 (1), 87–99. doi:10.1097/FJC.0000000000000094

Ulven, S. M., and Holven, K. B. (2020). Metabolomic and Gene Expression Analysis to Study the Effects of Dietary Saturated and Polyunsaturated Fats. *Curr. Opin. Lipidol.* 31 (1), 15–19. doi:10.1097/MOL.0000000000000651

van der Strate, B. W., Postma, D. S., Brandsma, C. A., Melgert, B. N., Luinge, M. A., Geerlings, M., et al. (2006). Cigarette Smoke-Induced Emphysema: A Role for the B Cell? *Am. J. Respir. Crit. Care Med.* 173 (7), 751–758. doi:10.1164/rccm.200504-594OC

van Dijk, C. E., Garcia-Aymerich, J., Carsin, A. E., Smit, L. A., Borlee, F., Heederik, D. J., et al. (2016). Risk of Exacerbations in COPD and Asthma Patients Living in the Neighbourhood of Livestock Farms: Observational Study Using Longitudinal Data. *Int. J. Hyg. Environ. Health* 219 (3), 278–287. doi:10.1016/j.ijheh.2016.01.002

Vancheri, C., Mastruzzo, C., Sortino, M. A., and Crimi, N. (2004). The Lung as a Privileged Site for the Beneficial Actions of PGE2. *Trends Immunol.* 25 (1), 40–46. doi:10.1016/j.it.2003.11.001

Vanella, L., Canestraro, M., Lee, C. R., Cao, J., Zeldin, D. C., Schwartzman, M. L., et al. (2015). Soluble Epoxide Hydrolase Null Mice Exhibit Female and Male Differences in Regulation of Vascular Homeostasis. *Prostaglandins Other Lipid Mediat* 120, 139–147. doi:10.1016/j.prostaglandins.2015.04.004

Vegeto, E., Cuzzocrea, S., Crisafulli, C., Mazzon, E., Sala, A., Krust, A., et al. (2010). Estrogen Receptor-Alpha as a Drug Target Candidate for Preventing Lung Inflammation. *Endocrinology* 151 (1), 174–184. doi:10.1210/en.2009-0876

Von Essen, S., and Donham, K. (1999). Illness and Injury in Animal Confinement Workers. *Occup. Med. (Philadelphia, Pa)* 14 (2), 337–350.

Von Essen, S., and Romberger, D. (2003). The Respiratory Inflammatory Response to the Swine Confinement Building Environment: the Adaptation to Respiratory Exposures in the Chronically Exposed Worker. *J. Agric. Saf. Health* 9 (3), 185–196. doi:10.13031/2013.13684

von Schacky, C. (2014). Omega-3 index and Cardiovascular Health. *Nutrients* 6 (2), 799–814. doi:10.3390/nu6020799

Wagner, K., Gilda, J., Yang, J., Wan, D., Morisseau, C., Gomes, A. V., et al. (2017). Soluble Epoxide Hydrolase Inhibition Alleviates Neuropathy in Akita (Ins2 Akita) Mice. *Behav. Brain Res.* 326, 69–76. doi:10.1016/j.bbr.2017.02.048

Wang, L., Yang, J., Guo, L., Uyeminami, D., Dong, H., Hammock, B. D., et al. (2012). Use of a Soluble Epoxide Hydrolase Inhibitor in Smoke-Induced Chronic Obstructive Pulmonary Disease. *Am. J. Respir. Cel Mol Biol* 46 (5), 614–622. doi:10.1165/rcmb.2011-0359OC

Warren, K. J., Wyatt, T. A., Romberger, D. J., Ailts, I., West, W. W., Nelson, A. J., et al. (2017). Post-injury and Resolution Response to Repetitive Inhalation Exposure to Agricultural Organic Dust in Mice. *Safety (Basel)* 3 (1). doi:10.3390/safety3010010

Watkins, D. A., Dabestani, N., Mock, C. N., Cullen, M. R., Smith, K. R., and Nugent, R. (2017). "Trends in Morbidity and Mortality Attributable to Injuries and Selected Environmental Hazards," in *Injury Prevention and Environmental Health*. Editors C. N. rdMock, R. Nugent, O. Kobusingye, and K. R. Smith (Washington (DC): The International Bank for Reconstruction and Development /The World Bank(c).). doi:10.1596/978-1-4648-0522-6_ch2

Waxman, D. J., and Holloway, M. G. (2009). Sex Differences in the Expression of Hepatic Drug Metabolizing Enzymes. *Mol. Pharmacol.* 76 (2), 215–228. doi:10.1124/mol.109.056705

Widgerow, A. D. (2012). Cellular Resolution of Inflammation-Ccatabasis. Wound Repair and Regeneration : Official Publication of the Wound Healing Society [and] the European Tissue Repair Society. *Wound Repair Regen.* 20 (1), 2–7. doi:10.1111/j.1524-475X.2011.00754.x

Wight, T. N., Frevert, C. W., Debley, J. S., Reeves, S. R., Parks, W. C., and Ziegler, S. F. (2017). Interplay of Extracellular Matrix and Leukocytes in Lung Inflammation. *Cell Immunol* 312, 1–14. doi:10.1016/j.cellimm.2016.12.003

Yang, B., Fritsche, K. L., Beversdorf, D. Q., Gu, Z., Lee, J. C., Folk, W. R., et al. (2019). Yin-Yang Mechanisms Regulating Lipid Peroxidation of Docosahexaenoic Acid and Arachidonic Acid in the Central Nervous System. *Front. Neurol.* 10, 642. doi:10.3389/fneur.2019.00642

Yang, H. H., Duan, J. X., Liu, S. K., Xiong, J. B., Guan, X. X., Zhong, W. J., et al. (2020). A COX-2/sEH Dual Inhibitor PTUPB Alleviates Lipopolysaccharide-Induced Acute Lung Injury in Mice by Inhibiting NLRP3 Inflammasome Activation. *Theranostics* 10 (11), 4749–4761. doi:10.7150/thno.43108

Yang, J., Bratt, J., Franzi, L., Liu, J. Y., Zhang, G., Zeki, A. A., et al. (2015). Soluble Epoxide Hydrolase Inhibitor Attenuates Inflammation and Airway Hyperresponsiveness in Mice. *Am. J. Respir. Cel Mol Biol* 52 (1), 46–55. doi:10.1165/rcmb.2013-0440OC

Zhang, Y. F., Sun, C. C., Duan, J. X., Yang, H. H., Zhang, C. Y., Xiong, J. B., et al. (2020). A COX-2/sEH Dual Inhibitor PTUPB Ameliorates Cecal Ligation and Puncture-Induced Sepsis in Mice via Anti-inflammation and Anti-oxidative Stress. *Biomed. Pharmacother.* 126, 109907. doi:10.1016/j.biopha.2020.109907

Zhou, Y., Liu, T., Duan, J. X., Li, P., Sun, G. Y., Liu, Y. P., et al. (2017). Soluble Epoxide Hydrolase Inhibitor Attenuates Lipopolysaccharide-Induced Acute Lung Injury and Improves Survival in Mice. *Shock* 47 (5), 638–645. doi:10.1097/SHK.0000000000000767

Zhou, Y., Yang, J., Sun, G. Y., Liu, T., Duan, J. X., Zhou, H. F., et al. (2016). Soluble Epoxide Hydrolase Inhibitor 1-trifluoromethoxyphenyl-3- (1-Propionylpiperidin-4-Yl) Urea Attenuates Bleomycin-Induced Pulmonary Fibrosis in Mice. *Cell Tissue Res* 363 (2), 399–409. doi:10.1007/s00441-016-2379-9

Conflict of Interest: The authors declare that the research was conducted in the absence of any commercial or financial relationships that could be construed as a potential conflict of interest.

Publisher's Note: All claims expressed in this article are solely those of the authors and do not necessarily represent those of their affiliated organizations, or those of the publisher, the editors and the reviewers. Any product that may be evaluated in this article, or claim that may be made by its manufacturer, is not guaranteed or endorsed by the publisher.

frontiers in Pharmacology

ORIGINAL RESEARCH
published: 28 January 2022
doi: 10.3389/fphar.2021.781282

Dermal Fibroblast Migration and Proliferation Upon Wounding or Lipopolysaccharide Exposure is Mediated by Stathmin

Ruiyan Cen, Liqun Wang, Yongqing He, Chenda Yue, Yang Tan, Lingfei Li and Xia Lei**

Department of Dermatology, Daping Hospital, The Army Medical University, Chongqing, China

The dermal fibroblast is a crucial executor involved in wound healing, and lipopolysaccharide is a key factor in initiating the migration and proliferation of the dermal fibroblasts, followed by wound healing. However, the underlying molecular mechanism is still unknown. In this study, we demonstrated that stathmin increased concomitantly with p38/MAPK pathway activation by lipopolysaccharide stimulation of the human dermal fibroblast (HDF), which induced microtubule (MT) depolymerization followed by increased HDF migration and proliferation. In contrast, the application of taxol, the small interfering RNA transfection of stathmin, or the application of the p38/MAPK inhibitor SB203580 suppressed MT depolymerization and HDF migration and proliferation. Additionally, the overexpression of a MKK6(Glu) mutant, which constitutively activated p38/MAPK, resulted in MT depolymerization and, subsequently, promoted HDF migration and proliferation. Our data reveal a crucial role of stathmin in HDF migration and proliferation. These findings will provide new targets and strategies for clinical interventions in wound healing.

Keywords: stathmin, microtubule, migration, proliferation, lipopolysaccharide

OPEN ACCESS

Edited by:
Pallavi R. Devchand, University of Calgary, Canada

Reviewed by:
David Dolivo, Northwestern University, United States
Junhui Zhang, Army Medical University, China
Gerard Bannenberg, Global Organization for EPA and DHA Omega-3s (GOED), United States

****Correspondence:***
Lingfei Li
lingfeili@126.com
Xia Lei
xialeidpyy@163.com.

Specialty section:
This article was submitted to Inflammation Pharmacology, a section of the journal Frontiers in Pharmacology

Received: *22 September 2021*
Accepted: *28 December 2021*
Published: *28 January 2022*

Citation:
Cen R, Wang L, He Y, Yue C, Tan Y, Li L and Lei X (2022) Dermal Fibroblast Migration and Proliferation Upon Wounding or Lipopolysaccharide Exposure is Mediated by Stathmin. Front. Pharmacol. 12:781282. doi: 10.3389/fphar.2021.781282

INTRODUCTION

Wound healing is an interactive and dynamic biological process involving an inflammation phase, a proliferation phase, and a tissue remodeling phase (Kaplani et al., 2018; Canedo-Dorantes and Canedo-Ayala, 2019). The dermal fibroblast is a critical executor during wound healing, and its migration and proliferation are essential and rate-limiting steps to repair wounds due to its central role in the formation of granulation tissue. If granulation tissue formation is dysfunction, wound healing may be delayed or wounds may not heal at all. Upon wounding, various cell types are activated by exogenous or endogenous stimuli to create conditions for wound healing (Singampalli et al., 2020; Shi et al., 2021). Although the lipopolysaccharide (LPS) exposure has been proven to be a key initial factor in wound healing and the dermal fibroblasts play an essential role in this process, the correlation between LPS exposure and the dermal fibroblast and their potential regulatory mechanisms remain largely unclear. Therefore, a comprehensive understanding of the biological processes of the dermal fibroblasts during wound healing is required.

The microtubule (MT), a crucial component of the cytoskeleton, is composed of α- and β-tubulin heterodimers (Kim and Matthew, 2007). The transition between the depolymerization and polymerization of tubulin is recognized as MT dynamics, which are regulated by destabilizing proteins (e.g., stathmin family) and stabilizing proteins (e.g., microtubule-associated protein family)

(Walczak, 2000; Hu et al., 2010). MT dynamics determine the biological behavior of cells. Previous studies have indicated that MT depolymerization leads to increased epidermal or tumor cell migration and proliferation, whereas MT polymerization abolishes migration and proliferation (Garcin and Straube, 2019; Zhang et al., 2019; Seetharaman and Etienne-Manneville, 2020). However, MT stabilization also promotes carcinoma invasion (Yoon et al., 2005). Thus, a further mechanistic exploration of MT dynamics is needed to understand its role in cell migration and proliferation (Zhang et al., 2013; Yan et al., 2019).

Stathmin is a widely expressed and highly conserved cytosolic protein that belongs to the stathmin family (Sobel, 1991). Stathmin destabilizes MTs by both binding tubulin dimers as well as directly binding MTs and promoting depolymerization (Cassimeris, 2002; Al-Bassam and Chang, 2011). Cell proliferation involves the progression from interphase to mitotic phase. Cytoplasmic MT regulatory proteins, such as the stathmin family, play a significant role in cell cycle regulation (Rubin and Atweh, 2004). Recent studies indicated that stathmin expression levels were closely correlated with cell proliferation and migration, with enhanced stathmin expression observed in highly proliferating neuroblastoma cells or gastric cancer cells (Hasegawa et al., 2007; Shu et al., 2019). In addition, the involvement of signal transduction in regulating stathmin expression includes mitogen-activated protein kinases (MAPKs), microtubule affinity-regulating kinases, and protein kinase A (Feng et al., 2017; Esnault et al., 2020). Previous studies indicated that p38/MAPK activation regulated stathmin in cardiomyocytes (Hu et al., 2010) and that p38/MAPK activation affected gallbladder carcinoma cell and inflammatory cell proliferation and migration by regulating stathmin (Wang et al., 2016; Esnault et al., 2020). However, the effect and mechanism of stathmin in LPS-induced the dermal fibroblast migration and proliferation during wound healing are still poorly understood.

In this study, we aimed to explore the role of stathmin in the human dermal fibroblast (HDF) migration and proliferation during wound healing. We found that stathmin promotes HDF migration and proliferation under LPS stimulation, and the p38/MAPK pathway is a potential upstream kinase of stathmin-dependent MT depolymerization in response to LPS stimulation. Collectively, these findings provide a novel role for stathmin in promoting HDF migration and proliferation, indicating its therapeutic potential in the treatment of wound healing.

MATERIALS AND METHODS

Ethics Statement

The Laboratory Animal Welfare and Ethics Committee of The Army Medical University reviewed and approved the animal study (approval number: AMUWEC2019509).

In vivo Wound Model

For the animal experiment, 8- to 12-week-old male wild-type C57BL/6 J mice (n = 5) were anesthetized with intraperitoneal injection of sodium pentobarbital, and full-thickness skin wounds were constructed on the mid-dorsal skin with 5-mm disposable biopsy punches.

Cell Culture

HDF was bought from American Type Culture Collection (Cat# PCS-201-012, cell type: fibroblast, origin: human skin) and cultured in Dulbecco's modified Eagle's medium (DMEM) supplemented with 10% fatal bovine serum at 37°C, 5% CO_2 atmosphere (Gusarov et al., 2021). Lipopolysaccharide (Cat# L4391, *e. coli*. 0111: B4, Merck, Germany) was used to stimulate HDF *in vitro*. Taxol (1 μM, Cat# S1150, Selleck, United States) or SB203580 (5 μM, Cat# S1076, Selleck, United States) was used to the culture and pretreated at 37°C for 1 h before LPS stimulation.

Cell Proliferation Assay

The Cell Counting Kit-8 (CCK-8; Cat# C0042, Beyotime, China) assay is based on WST-8 and was used to assess cell proliferation (Liu et al., 2020). The plate was preincubated for 24 h. After the CCK-8 solution was added to the 96 well plate, the plate was incubated for an additional 4 h. The absorbance was measured at 450 nm using a microplate reader (ELX800, BioTek). In addition, cell proliferation was assessed using a Edu-488 kit (Cat# C0071S, Beyotime, China), which is based on the incorporation of thymidine analogue Edu (5-ethynyl-2'-deoxyuridine) in the process of DNA synthesis, and Edu is labeled by Alexa Fluor 488 through subsequent click reaction to detect proliferation. After being subjected to the different treatments, cell proliferation was assessed by Edu staining and analyzed by a fluorescence microscope (IX75, Olympus, Japan). Edu staining (green) in cultured cells is shown in the representative images. Nuclei were stained with Hoechst 33342, which could stain DNA (blue).

Scratch Wound Healing Assay

The monolayers of HDFs were incubated at 37°C for 2 h with mitomycin-C (5 μg/ml, Cat# S8146, Selleck, United States) to inhibit cell proliferation before wounded with a 1-ml plastic pipette tip and then washed with phosphate-buffered saline (PBS) to remove redundant cell debris. The wound healing course was observed with a light microscope (IX75, Olympus, Japan). Cell migration was defined as the wound healing rate (wound healing rate = the wound distance (0 h) (inches)—the wound distance (24 h) (inches)/the wound distance (0 h) (inches)), which was analyzed with NIH ImageJ software.

Immunohistochemistry

The mouse skin tissues were cut at wound edges and fixed in 4% paraformaldehyde (Cat# P0099, Beyotime, China), embedded in paraffin, and sectioned. Sectioned wound tissues were deparaffinized and rehydrated. Antigen retrieval was performed by heating the sections in citrate buffer (pH 6.0) in a microwave at 600 W for 8 min. To perform immunohistochemistry staining for stathmin, wound tissues were incubated with stathmin rabbit mAb (1:100, Cat# 13655S, Cell Signaling Technology, United States) as the primary antibody at 4°C overnight. The tissues were then rinsed and incubated with a biotinylated secondary antibody (1:500, Cat# GB23303, Servicebio, China) and streptavidin-HRP (Cat#SP-9001, ZSGB-BIO, China). The color was developed using DAB peroxidase substrate (Cat# ZLI-9018, ZSGB-BIO, China) until an optimal color was observed.

Recombinant Adenovirus Construction and Transduction

The adenovirus that activates MAPK kinase 6 (MKK6(Glu)), which precisely and stably activates p38/MAPK signaling, was produced by Shanghai Gene Chem Co., Ltd. (China) (Hu et al., 2010). CMV-null adenovirus was used as the negative control. The multiplicity of infection is thirty. After transfection of the HDF with adenoviruses for 48 h, the cells were used for experiments.

Small Interfering RNA (siRNA) Transfection

For RNA interference, cells were transfected with siRNA targeted for stathmin (siSTMN) (sense (5'-3') GCACGAGAAAGAAGUGCU UTT, antisense (3'-5') AAGCACUUCUUUCUCGUGCTT) or the corresponding scramble siRNA (siNC) (sense (5'-3') UUCUCCGAA CGUGUCACGUTT, antisense (3'-5') ACGUGACACGUUCGG AGAATT) with GP-transfect Mate according to the manual (https://www.genepharma.com/public/upload/1554367091.pdf). The siRNAs and GP-transfect-Mate were ordered from Shanghai Gene Pharma Company (China).

Western Blot Analysis

The mouse skin tissues and whole-cell extracts were prepared in RIPA lysis buffer for Western blotting (Cat# P0013, Beyotime, China) and centrifuged at 13700 × g for 15 min at 4°C. After obtained the supernatants, protein concentrations were detected using a Bradford Protein Quantification Kit (Cat# P0010, Beyotime, China). The protein samples were loaded and separated by SDS–PAGE (Cat# 1610183, Bio–Rad, United States) and then transferred to PVDF membranes (Cat# FFP26, Beyotime, China). Membranes were incubated overnight at 4°C with specific primary antibodies. Sequentially, membranes were incubated with secondary antibodies and visualized using a ChemiDoc XRS System (ChemiDoc, Bio–Rad, United States). Primary antibodies used for Western blotting were as follows: stathmin (Cat# 11157-1-AP, Proteintech, United States), PCNA (Cat# 13110S, Cell Signaling Technology, United States), p38 (Cat# 8690, Cell Signaling Technology, United States), phosphorylated p38 (p-P38, Cat# 9211S, Cell Signaling Technology, United States), and β-actin (Cat# 2148S, Cell Signaling Technology, United States).

Immunofluorescence Staining of Microtubules

HDFs were cultured in 15-mm diameter confocal petri dishes (NEST, China) overnight. After treatments, cells were fixed with 4% paraformaldehyde for 20 min. Then the cells were washed twice with PBS before blocking in immunostaining blocking buffer (Cat# P0102, Beyotime, China) for 1 h. After incubation with rat anti-tubulin antibody (Cat# ab6160, Abcam, United Kingdom) diluted in 1% bovine serum albumin (BSA) in PBS overnight at 4°C, the dishes were washed with PBS for three times and then stained with Alexa Fluor 488 fluorescent secondary antibody (Cat# A32731, Invitrogen, United States) at 37°C for 1 h in the dark. Nuclei were counterstained with 4',6-diamidino-2-phenylindole (DAPI) (Cat# C1005, Beyotime, China), and the plates were sealed with anti-fluorescence quenching solution (Cat# P0126, Beyotime, China) before imaging. The pictures were acquired using a Leica confocal microscope (Leica Microsystems, Wetzlar, Germany).

Statistical Analysis

Statistical analysis was handled with GraphPad Prism 8 (GraphPad Software, California, United States). All results are shown as the mean ± SEM. Comparisons between two groups were analyzed using a two-tailed unpaired *t*-test. Statistical significance among three or more groups was determined by one-way analysis of variance (ANOVA) and followed by Tukey's multiple comparison test. $p < 0.05$ was considered to be significant.

RESULTS

Lipopolysaccharide Promotes the Migration and Proliferation of Human Dermal Fibroblast and Microtubule Depolymerization

The migration and proliferation of HDF are critical processes for wound repair. We used LPS to stimulate HDF *in vitro*. First, HDF was treated with six concentrations of LPS for 24 h to observe cell migration, which was determined using a scratch wound healing assay (**Figures 1A,B**). LPS in 500 ng/ml showed the most significant effect on the scratch wound healing assay. Therefore, we selected LPS (500 ng/ml) to examine HDF proliferation at 3 time points, as represented by CCK-8 kit testing. The results revealed that only at 24 h is LPS promoting proliferation compared to the control group (**Figure 1C**). According to the above results, LPS (500 ng/ml for 24 h) was used in the following experiments. The results showed that HDF proliferation was significantly increased about 18% by exposure to LPS, as shown by Edu staining (**Figures 1D,E**). PCNA, a cell proliferation marker, was also robustly increased (**Figures 1F,G**). In the morphological studies, the HDF subjected to LPS showed a less regular organization of MT network and some tubulin breakages that changed the MT appearance, whereas the control group revealed a uniformly distributed lattice network, as indicated by the tubulin immunofluorescence staining (**Figure 1H**).

Involvement of Microtubule Depolymerization in Lipopolysaccharide-Induced Human Dermal Fibroblast Migration and Proliferation

In **Figure 1H**, it is shown that LPS induced MT depolymerization. To determine whether the observed HDF migration and proliferation are correlated with MT structural changes, taxol was used to stabilize the MTs and prevent them from depolymerizing. Our results showed that LPS stimulation promoted HDF migration and proliferation (**Figures 2A–D,F–H**); in contrast, taxol pretreatment significantly abrogated LPS-induced HDF migration, as

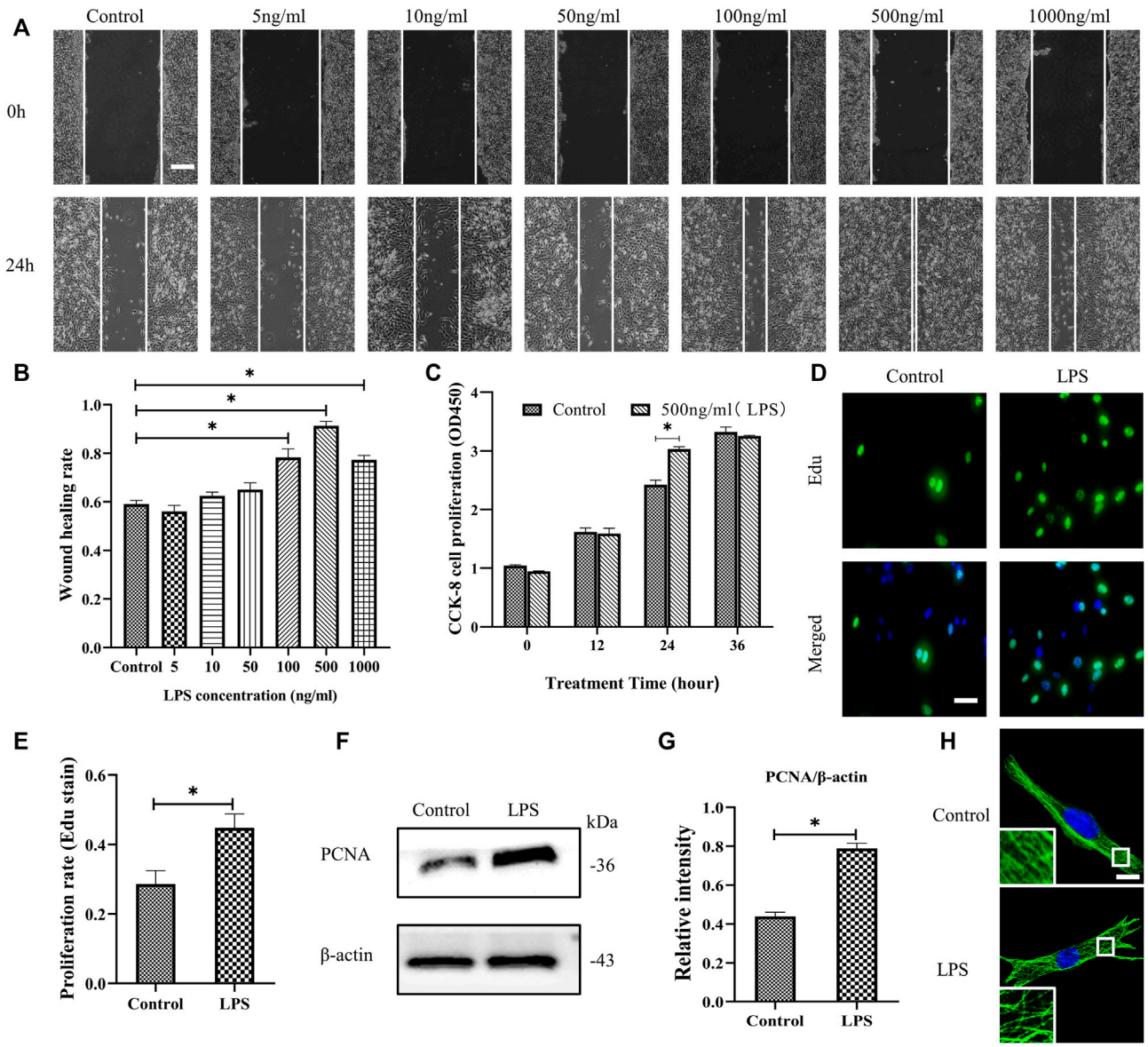

FIGURE 1 | LPS promotes the migration and proliferation of HDF and MT depolymerization. **(A)** Scratch wound healing assays were performed to examine HDF migration with or without LPS (5, 10, 50, 100, 500 and 1,000 ng/ml) for 24 h. Representative pictures of the scratch wound are shown. Bar, 200 μm, and **(B)** the images were quantitatively analyzed (n = 5). **(C)** HDF was subjected to LPS (500 ng/ml) for 12, 24 and 36 h to detect cell proliferation using the CCK-8 assay (n = 6). **(D)** HDF proliferation was detected after 24 h with or without LPS by Edu staining and **(E)** quantitative analysis (n = 5). Nuclei were stained with Hoechst 33342. The merged image is to show the proportion of proliferating cells (green) to total cells (blue). Bar, 20 μm. **(F)** Western blotting was performed to detect PCNA with or without LPS (500 ng/ml) treatment and **(G)** quantitative analysis (n = 5). **(H)** Representative confocal tubulin immunofluorescence images showing the MT structure with or without LPS (500 ng/ml) for 24 h. The inserts show high-magnification images of the MT network. Bar, 10 μm. LPS, lipopolysaccharide; PCNA, proliferating cell nuclear antigen. The results are shown as means ± SEM. *p < 0.05 was considered to be significant.

reflected by the scratch wound healing assay (**Figures 2A,B**) and cell proliferation, as indicated by Edu staining (**Figures 2C,D**) and CCK-8 assay (**Figure 2F**). Moreover, the expression of the proliferation marker PCNA was also elevated after LPS challenge (**Figures 2G,H**). In contrast, taxol pretreatment suppressed this effect, while taxol group showed a change comparable to that of the control group (**Figures 2G,H**). Then, we assessed the role of an MT stabilizer in mediating LPS-induced MT depolymerization. The results showed that LPS induced MT depolymerization, whereas taxol pretreatment promoted the preservation of the MT network and led to an increased density of MT fragments near the plasma cell membrane after LPS challenge (**Figure 2E**). These findings suggested a crucial role of MTs in regulating LPS-promoted HDF migration and proliferation.

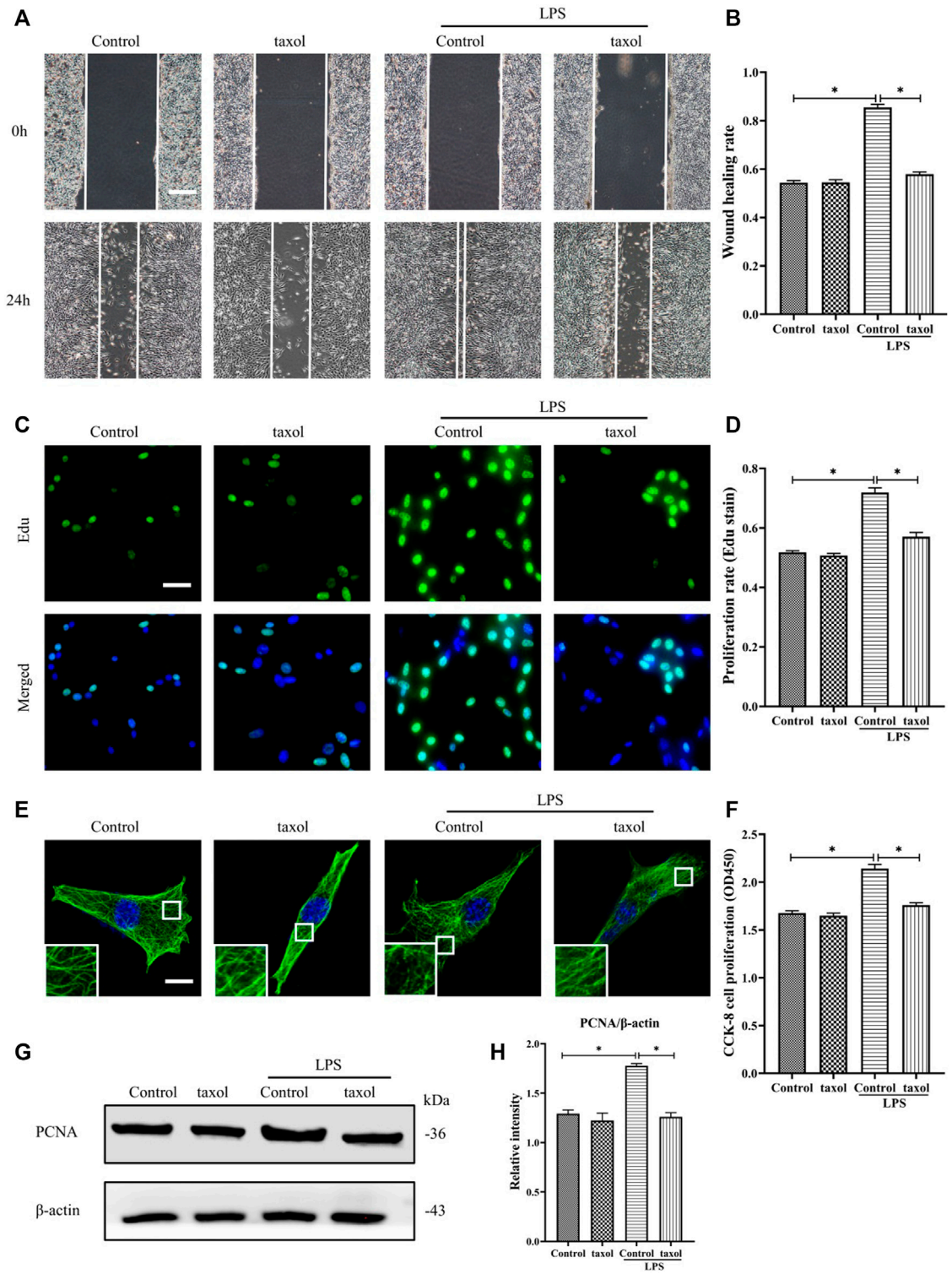

FIGURE 2 | Involvement of MT depolymerization in LPS-induced HDF migration and proliferation. **(A)** Scratch wound healing assays were performed to detect HDF migration treated with LPS with or without taxol (1 μm) pretreatment, Bar, 200 μm, and **(B)** quantitative analysis (n = 5). **(C)** HDF proliferation was detected after LPS treatment with or without taxol pretreatment by Edu staining and **(D)** quantitative analysis (n = 5). Nuclei were stained with Hoechst 33342. The merged image is to show the proportion of proliferating cells (green) to total cells (blue). Bar, 20 μm. **(E)** For the tubulin immunofluorescence images of MTs, cells were pretreated with taxol before LPS stimulation. These inserts show high-magnification images of the peripheral MT network. Bar, 10 μm. **(F)** HDF was subjected to LPS with or without taxol pretreatment to detect cell proliferation using the CCK-8 assay (n = 10). **(G)** Western blotting was performed to detect PCNA after LPS treatment with or without taxol, and **(H)** the results were quantitatively analyzed (n = 5). The data are represented as the mean ± SEM. *p < 0.05 was considered to be significant.

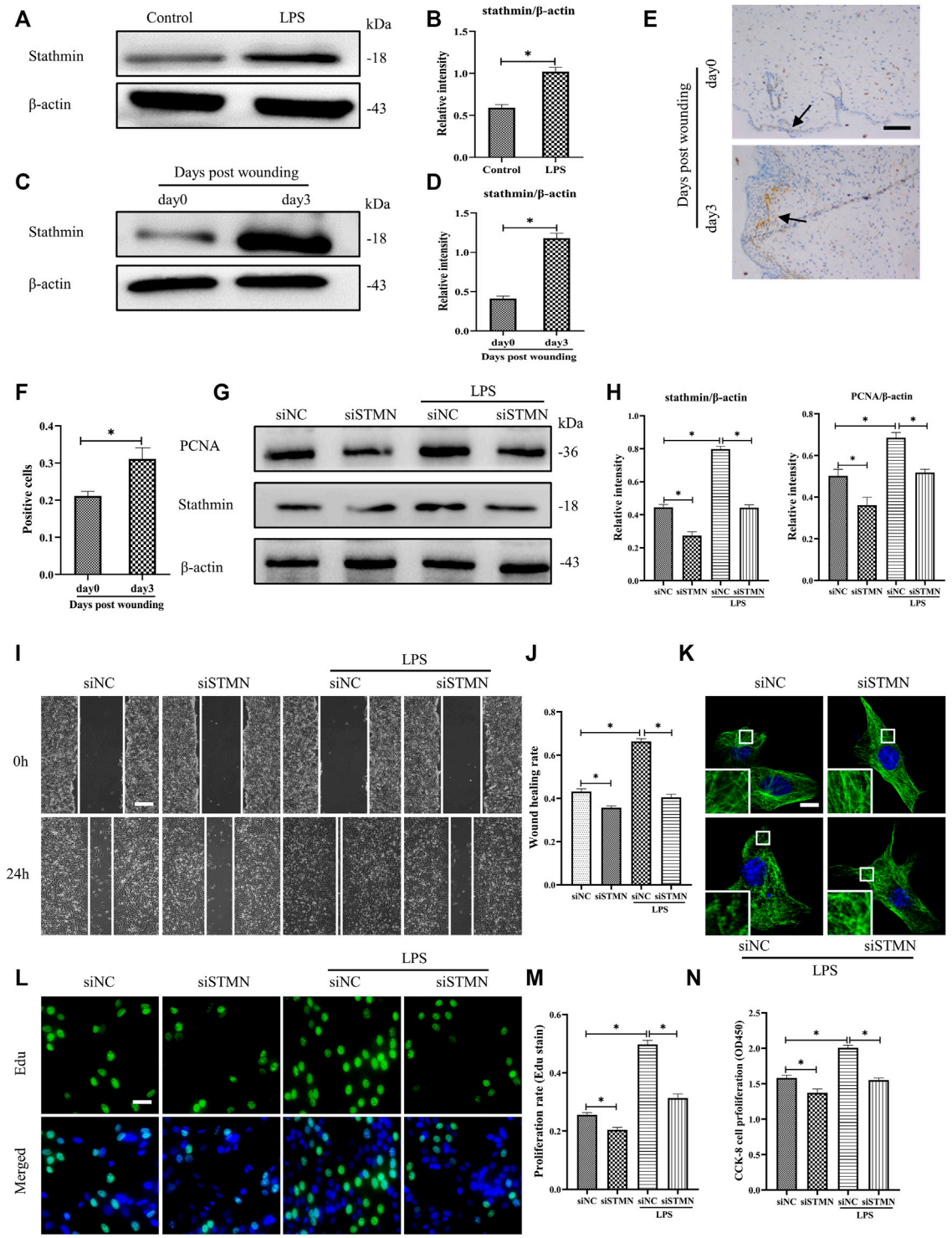

FIGURE 3 | LPS-induced stathmin expression and its effects on HDF migration and proliferation and MT depolymerization. **(A)** Western blotting was performed to detect stathmin expression with or without LPS, and **(B)** the results were quantitatively analyzed (n = 5). **(C)** Western blotting was performed to detect stathmin expression in wound edge tissue post wounding, and **(D)** the results were quantitatively analyzed (n = 5). **(E)** Stathmin expression at the wound edge of mice post wounding was detected by immunohistochemical staining. Bar, 100 μm, the arrow points to the positive cells, and **(F)** the results were quantitatively analyzed (n = 5). **(G)** Cells were transfected with siSTMN or siNC before treatment with or without LPS stimulation. Western blotting was performed to detect stathmin and PCNA expression, and **(H)** the results were quantitatively analyzed (n = 5). **(I)** Scratch wound healing assays were performed to detect HDF migration treated with LPS after siSTMN or siNC transfection., Bar, 200 μm, and **(J)** the results were quantitatively analyzed (n = 5). **(K)** For the tubulin immunofluorescence images of MTs, cells were

(*Continued*)

FIGURE 3 | transfected with siNC or siSTMN before LPS treatment. The inserts show high-magnification images of the peripheral MT network. Bar, 10 μm. **(L)** The cells were transfected with siSTMN or siNC before LPS stimulation and detected by Edu staining, and **(M)** the results were quantitatively analyzed (n = 5). Nuclei were stained with Hoechst 33342. The merged image is to show the proportion of proliferating cells (green) to total cells (blue). Bar, 20 μm. **(N)** HDF proliferation was tested using the CCK-8 assay (n = 10). siSTMN, small interfering RNA for stathmin; siNC, small interfering RNA for negative control. The results are shown as means ± SEM. *p < 0.05 was considered to be significant.

Lipopolysaccharide-Induced Stathmin Expression and its Effects on Human Dermal Fibroblast Migration and Proliferation and Microtubule

To determine whether the above-noted MT depolymerization was attributed to stathmin expression changes, we first detected stathmin expression with LPS stimulation or in a vivo wound healing model (**Figures 3A–F**). Stathmin was found to show weak basal levels in cultured HDF, and expression of stathmin significantly increased after LPS stimulation (**Figures 3A,B**). In an *in vivo* model, a higher stathmin level at 3 days post wounding was noted compared to the control group, as represented by western blotting assay and immunohistochemistry staining (**Figures 3C–F**).

We then considered the possibility that stathmin was essential in mediating HDF migration and proliferation and MT depolymerization after LPS challenge. After transfection with siSTMN, the expression of stathmin decreased. We found that stathmin and PCNA expression levels were robustly elevated after LPS stimulation; however, after transfection with siSTMN, the expression levels of stathmin and PCNA were significantly decreased with or without LPS stimulation compared to their corresponding control groups (**Figures 3G,H**). A reduction in cell migration was observed after siSTMN transfection with or without LPS stimulation, as indicated by the scratch wound healing assay (**Figures 3I,J**). The siSTMN transfection abrogated cell proliferation with or without LPS stimulation (**Figures 3L–N**). A preserved MT network and an increased density of MT fragments were observed after siSTMN transfection with or without LPS stimulation (**Figure 3K**). Collectively, these data suggested that stathmin is a crucial regulator of HDF migration and proliferation and MT depolymerization during wound healing both in the absence and presence of LPS.

P38/MAPK Activation Mediates Stathmin Expression in Lipopolysaccharide-Induced Human Dermal Fibroblast Migration and Proliferation

Previous studies have shown that p38/MAPK is critically important in fibroblasts (Molkentin et al., 2017). Besides, some other studies demonstrated that both p38 and ERK coordinate the dynamics of wound healing: while growth factor-stimulated p38 induced epithelial migration, and ERK1/2 activation induced cell proliferation (Sharma et al., 2003; Li et al., 2019). In our current study, to investigate whether p38/MAPK was involved in LPS-induced stathmin expression, MT depolymerization and HDF migration and proliferation, we first detected p38/MAPK activation. The results suggested that p38/MAPK was activated after LPS compared to the control group (**Figures 4A,B**). In addition, activated p38/MAPK was also observed at 3 days post wounding in animal studies compared to the control group (**Figures 4C,D**). We then tested whether the p38/MAPK signaling pathway was essential for stathmin regulation in LPS-induced HDF migration and proliferation. A p38/MAPK inhibitor, SB203580, was used in an *in vitro* study. We found that stathmin expression increased concomitantly with p38/MAPK activation by LPS stimulation of HDF, while SB203580 pretreatment showed comparable phosphorylated p38 and stathmin expression to the corresponding control group (**Figures 4E,F**). Conversely, pretreatment with the p38/MAPK inhibitor SB203580 significantly suppressed p38/MAPK activation and stathmin expression compared to the LPS group (**Figures 4E,F**). Thus, these results suggested that the p38/MAPK signaling pathway was responsible for stathmin regulation in LPS-induced HDF migration and proliferation.

Role of p38/MAPK Activation in Lipopolysaccharide-Induced Human Dermal Fibroblast Migration and Proliferation and Microtubule Depolymerization

We explored the role of p38/MAPK in the regulation of HDF migration and proliferation and MT depolymerization. The results reveal that LPS promoted HDF migration, as indicated by the scratch wound healing assay, whereas the application of the p38/MAPK inhibitor SB203580 largely abolished this effect (**Figures 5A,B**). Additionally, HDF proliferation was elevated after LPS challenge compared to the control group (**Figures 5C,D,F–H**). In contrast, SB203580 pretreatment suppressed the increased cell proliferation with LPS challenge and revealed a comparable change to the control group (**Figures 5C,D,F–H**). Concomitant with the suppression of HDF migration and proliferation, SB203580 preserved the MT network in the LPS-induced HDF and showed a similar MT structure compared to the control group (**Figure 5E**).

Then, we assessed the critical role of stathmin in mediating the p38/MAPK regulation of MT depolymerization and HDF migration and proliferation (**Figure 6**). A constitutively activated p38/MAPK activator, MKK6(Glu), was constructed and transfected into HDF to activate the p38/MAPK pathway (**Figures 6A,B**). MKK6 (Glu) overexpression promoted HDF proliferation, as represented by an increase in the proliferation marker PCNA (**Figures 6C,D**). In addition, elevated HDF proliferation was detected by Edu staining (**Figures 6G,H**) and CCK-8 kit testing (**Figure 6J**) after MKK6 (Glu) transfection. Conversely, transfection with siSTMN suppressed HDF proliferation with or without MKK6(Glu) compared to their corresponding control treatments (**Figures 6C,D,G,H,J**). In addition, MKK6(Glu) overexpression promoted HDF migration, as shown by a scratch wound healing assay, compared with the control

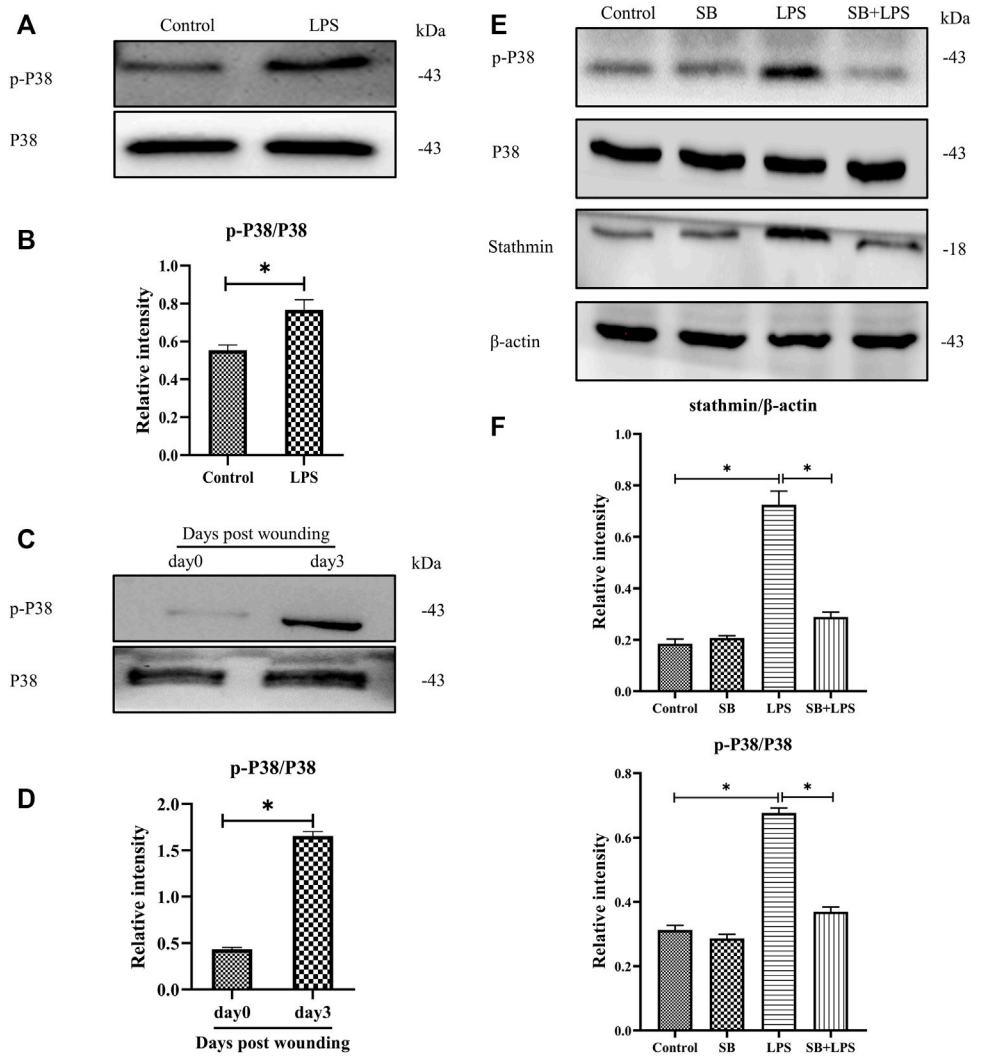

FIGURE 4 | P38/MAPK activation mediates stathmin expression in LPS-induced HDF migration and proliferation. **(A)** Western blotting was performed to detect p38/MAPK activation with or without LPS, and **(B)** the results were quantitatively analyzed ($n = 5$). **(C)** Western blotting was performed to detect p38/MAPK activation in wound edge tissue post wounding, and **(D)** the results were quantitatively analyzed ($n = 5$). **(E)** Western blotting was performed to detect stathmin expression and p38/MAPK activation after LPS treatment with or without the p38/MAPK inhibitor SB, and **(F)** the results were quantitatively analyzed ($n = 5$). SB, SB203580. These data are represented as the mean ± SEM. *$p < 0.05$ was considered to be significant.

group; in contrast, siSTMN transfection abrogated this effect with or without MKK6(Glu) overexpression (**Figures 6E,F**). Moreover, the HDF transfected with siSTMN were much more resistant than the control group to MT depolymerization in response to MKK6(Glu) transfection, as indicated by MT staining (**Figure 6I**). These findings are consistent with our concept of an essential role for stathmin in LPS-stimulated p38/MAPK-mediated MT depolymerization and HDF migration and proliferation.

DISCUSSION

The salient findings from our current study indicated that stathmin, a classical cytosolic MT-destabilizing protein, promoted HDF migration and proliferation, followed by wound healing. This notion was proved in both cell and animal models. Our data revealed that stathmin is elevated following wounding *in vivo*, as well as LPS exposure *in vitro* during a short time period, and is an important factor for wound healing. Stathmin increased concomitantly with p38/MAPK signaling activation by LPS stimulation of HDF, which led to MT depolymerization, accelerated HDF migration and proliferation, and the onset and progression of wound healing (**Figure 7**).

Wound healing is a complex and precisely regulated biological processes. Upon wounding, a large number of genes, including cytokines, chemokines, and antimicrobial peptides, are activated or expressed to initiate wound repair (Canedo-Dorantes and Canedo-Ayala, 2019; Rodrigues et al., 2019; Singampalli et al., 2020). Although the LPS exposure has been considered to be a

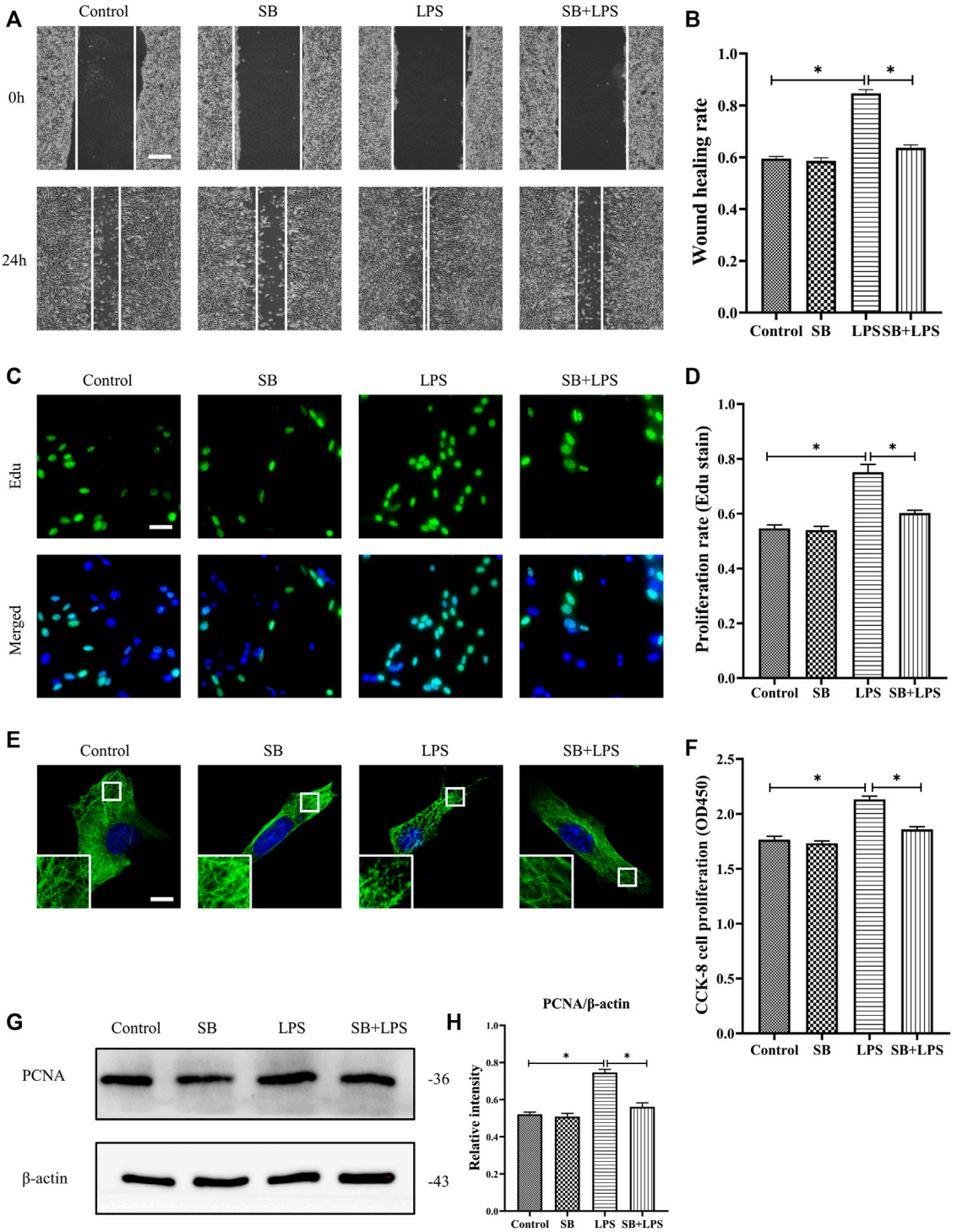

FIGURE 5 | Role of p38/MAPK activation in LPS-induced HDF migration and proliferation and MT depolymerization. **(A)** Scratch wound healing assays were performed to detect HDF migration treated with LPS with or without SB (5 μm) pretreatment. Bar, 200 μm, and **(B)** the results were quantitatively analyzed ($n = 5$). **(C)** HDF proliferation was detected after LPS treatment with or without SB pretreatment by Edu staining, and **(D)** the results were quantitatively analyzed ($n = 5$). Nuclei were stained with Hoechst 33342. The merged image is to show the proportion of proliferating cells (green) to total cells (blue). Bar, 20 μm. **(E)** For the tubulin immunofluorescence images of MTs, cells were pretreated with SB before LPS treatment. These inserts show high-magnification images of the peripheral MT network. Bar, 10 μm. **(F)** HDF was subjected to LPS treatment with or without SB pretreatment to detect cell proliferation using the CCK-8 assay ($n = 10$). **(G)** Western blotting was performed to detect PCNA expression after LPS treatment with or without SB, and **(H)** the results were quantitatively analyzed ($n = 5$). The data are represented as the mean ± SEM. *$p < 0.05$ was considered to be significant.

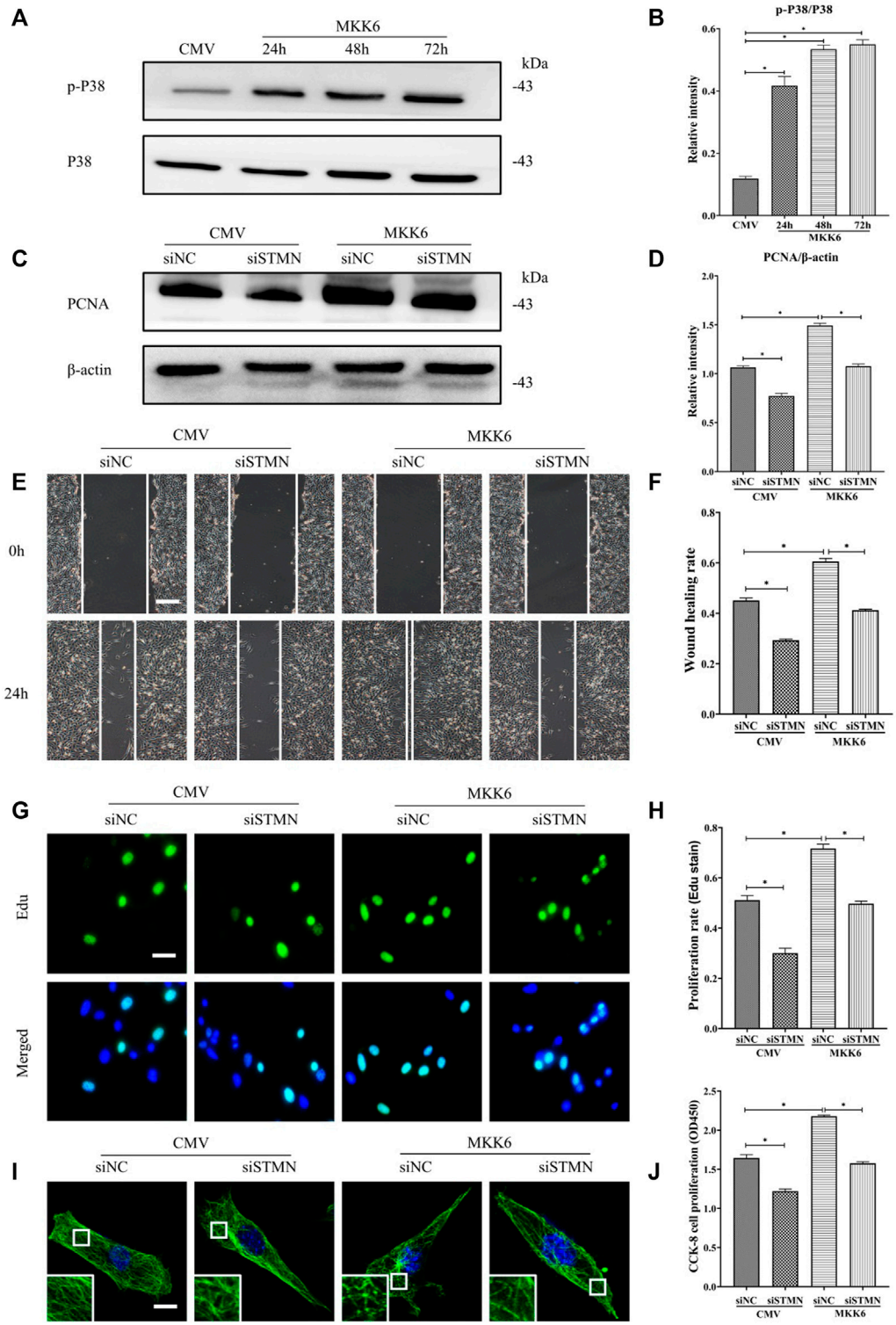

FIGURE 6 | P38/MAPK induced HDF migration and proliferation *via* stathmin-dependent MT depolymerization. **(A)** Western blotting was performed to analyze the effects of MKK6(Glu) transfection for the indicated times, and **(B)** the results were quantitatively analyzed (n = 3). **(C)** Western blotting was performed to detect PCNA expression after the cells were transfected or cotransfected with siSTMN or MKK6(Glu), and **(D)** the results were quantitatively analyzed (n = 5). **(E)** Scratch wound healing assays were performed to detect HDF migration after cells were transfected or cotransfected with siSTMN or MKK6(Glu). Bar, 200 μm, and **(F)** the results were quantitatively analyzed (n = 5). **(G)** HDF proliferation was detected after the cells were transfected or cotransfected with siSTMN or MKK6(Glu) by EdU staining, and **(H)** the results were quantitatively analyzed (n = 5). Nuclei were stained with Hoechst 33342. The merged image is to show the proportion of proliferating cells (green) to

(*Continued*)

FIGURE 6 | total cells (blue). Bar, 20 μm. **(I)** For the tubulin immunofluorescence images of MTs, cells were transfected or cotransfected with siSTMN or MKK6(Glu). These inserts show high-magnification images of the peripheral MT network. Bar, 10 μm. **(J)** Cell proliferation was detected after the HDF was transfected or cotransfected with siSTMN or MKK6(Glu) using the CCK-8 assay (n = 10). The results are shown as the means ± SEM. *p < 0.05 was considered to be significant.

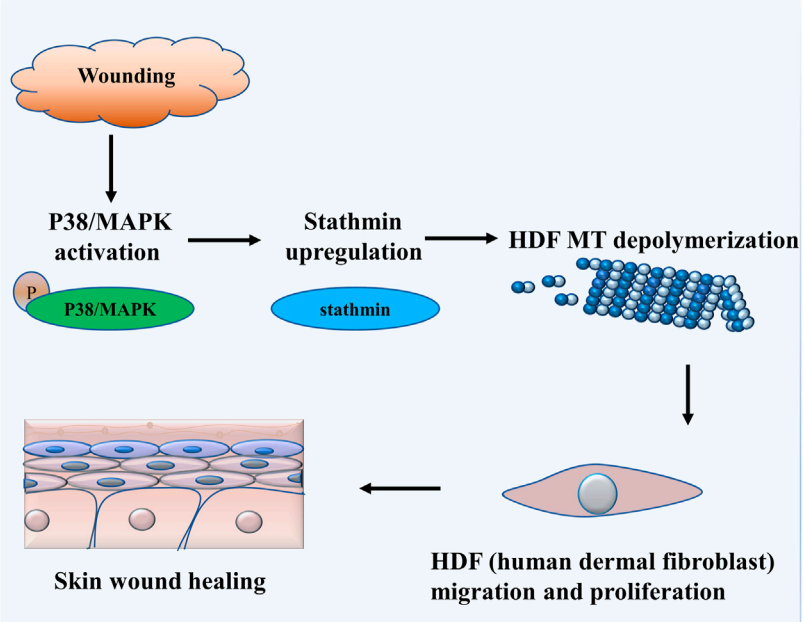

FIGURE 7 | Schematic illustrating that stathmin promotes HDF migration and proliferation during wound healing. The LPS stimulates p38/MAPK activation and subsequently induces increased stathmin expression. Increased stathmin leads to MT depolymerization, which is required for HDF migration and proliferation, followed by skin wound healing.

crucial initial factor in wound healing (Ninan et al., 2015; Visan, 2019) and fibroblasts are deemed to play an essential role in this process (Desjardins-Park et al., 2018; Visan, 2019), the relationship and mechanisms between fibroblasts and LPS exposure remain less well defined. In our present study, we used LPS (500 ng/ml, 24 h) to mimic inflammatory stimulation *in vitro* during wound healing with a superimposed infection, because appropriate LPS stimulation could activate inflammatory response and start wound healing (Landén et al., 2016; Li et al., 2017), whereas inappropriate dose or treatment time of LPS may not promote wound healing, or even delay wound healing due to excessive oxidative stress or severe infection (Ning et al., 2021). We found that LPS induced elevated stathmin expression and promoted HDF migration and proliferation. Additionally, stathmin is robustly increased in wound edge tissue in animal models. Stathmin belongs to the stathmin family, which includes stathmin, SCG-10, SCLIP and RB3, and is ubiquitously expressed in various cell types (Cassimeris, 2002). It is a classical MT-depolymerization protein and involves a wide range of physiological and cellular functions (e.g., cell cycle, proliferation and migration) (Shu et al., 2019). However, whether stathmin is involved in LPS-induced HDF migration and proliferation is still unknown. Our results showed that stathmin was involved in LPS-mediated HDF migration and proliferation during wound healing.

The MT is a vital component of the cytoskeleton and involves a series of cellular functions, including organelle transport, cell cycle regulation, and maintenance of cellular morphology (Kapitein and Hoogenraad, 2015). Accumulating evidence has indicated that microfilament, another cytoskeleton component, is crucial in regulating cell migration, but whether MT is also involved in cell migration and even in cell proliferation should be further elucidated. The balance between MT depolymerization and polymerization reflects MT dynamics, which is affected by the factors that stabilize MTs, including MAPs, and the opposing effect that destabilizes MTs, such as the stathmin family (Mizumura et al., 2006). Previous studies suggested that stathmin is involved in tumor cell proliferation and invasion (Wang et al., 2016; Shu et al., 2019). However, whether stathmin is involved in HDF migration and proliferation during wound healing is uncertain. In our present study, we demonstrated that stathmin promoted HDF migration and proliferation upon wounding or LPS exposure. In addition, altered stathmin expression promoted MT dynamics changes, affecting the cell cycle, followed by cell proliferation (Rubin and Atweh, 2004),

and MT depolymerization accelerated the assembly of focal adhesions and increased cell migration (Seetharaman and Etienne-Manneville, 2020), which supported our current findings. Thus, these data provide evidence of MT depolymerization in stathmin-mediated wound healing.

Our earlier studies suggested that stathmin-mediated MT depolymerization is involved in HDF migration and proliferation; however, the precise mechanism by which stathmin regulates MT dynamics deserves further elucidation. Accordingly, we demonstrated that p38/MAPK was activated concomitantly with elevated stathmin expression and MT depolymerization, meanwhile, phosphorylated p38/MAPK was elevated in wound edge tissue in animal models. In addition, growing evidence has revealed that p38/MAPK is a classical signaling pathway involved in wound healing and is recognized as a crucial pathway in regulating MT dynamics (Fabris et al., 2015; Esnault et al., 2020). Moreover, several studies have reported that the MAPK, MARK and PKA pathways are involved in the regulation of stathmin (Yip et al., 2014; Feng et al., 2017). We suppressed p38/MAPK under LPS stimulation. Decreased stathmin expression and MT depolymerization were observed, followed by reduced HDF migration and proliferation. In contrast, the transfection of MKK6 (Glu), an activator of p38/MAPK, could promote stathmin expression, MT depolymerization, and HDF migration and proliferation. Moreover, the application of siSTMN in HDF significantly abrogated the effect caused by MKK6 (Glu) transfection. Collectively, these data indicated that the p38/MAPK signaling pathway is an upstream kinase of stathmin, and is crucial for LPS-induced HDF migration and proliferation *via* stathmin-mediated MT depolymerization. In spite of this, it should be noted that several reports (Henklova et al., 2008; Muniyappa and Das, 2008) found that SB203580 could also activate ERK and JNK, both of which showed a certain role in migration and proliferation. Thus, we cannot completely exclude the role of ERK and JNK in our study, and further experiment would be shown to demonstrate the unique role of p38/MAPK in HDF migration and proliferation. Pathologic tissue repair usually refers to two types of wound healing: excessive healing and deficient healing. The excessive healing, such as keloids and hypertrophic scars, and the deficient healing, including diabetic foot ulcers and venous leg ulcers, are characterized by excessive and suppressed fibroblast proliferation respectively (Zou et al., 2021). In addition, p38/MAPK activation is deemed important in keloids (Song et al., 2012) and p38/MAPK inactivation is correlated with diabetic foot ulcers (Singh et al., 2015), indicating that p38/MAPK-mediated fibroblast proliferation is crucial in skin wound healing. In addition to its role in healing of skin wounds, stathmin and p38/MAPK are involved in tumor cells migration and proliferation (Yurong et al., 2017). Moreover, fibroblast overexpressing p38/MAPK induced interstitial and perivascular fibrosis in the heart, lung, and kidney (Molkentin et al., 2017). Considering a possible role for the interaction of p38/MAPK and stathmin in the current and previous studies, this interaction may be important in various hyper- and dysproliferative disorders. New studies are needed to address this possibility.

Taken together, the findings of our present study reveal a novel role of stathmin in HDF migration and proliferation during wound healing, while p38/MAPK serves as the upstream kinase of stathmin-mediated MT depolymerization, followed by HDF migration and proliferation. Furthermore, our results point to stathmin regulation as a potential target for the development of therapeutic interventions for wound healing.

DATA AVAILABILITY STATEMENT

The original contributions presented in the study are included in the article/Supplementary Material, further inquiries can be directed to the corresponding authors.

ETHICS STATEMENT

The animal study was reviewed and approved by The Laboratory Animal Welfare and Ethics Committee of The Army Medical University.

AUTHOR CONTRIBUTIONS

XL and LL supervised the work. RC and LL designed the experiments with help from XL. RC performed the experiments with help from LW and YH. RC analyzed the data with the help from CY and YT. RC wrote the manuscript with help from LL. All authors discussed the results and commented on the manuscript.

FUNDING

This work was supported by the National Natural Science Foundation of China (82003323), the National Natural Science Foundation of China (81773348), the Military Medical Innovation Program in Daping Hospital (2019CXJSC014).

REFERENCES

Al-Bassam, J., and Chang, F. (2011). Regulation of Microtubule Dynamics by TOG-Domain Proteins XMAP215/Dis1 and CLASP. *Trends Cel Biol* 21 (10), 604–614. doi:10.1016/j.tcb.2011.06.007

Cañedo-Dorantes, L., and Cañedo-Ayala, M. (2019). Skin Acute Wound Healing: A Comprehensive Review. *Int. J. Inflam* 2019, 3706315. doi:10.1155/2019/3706315

Cassimeris, L. (2002). The Oncoprotein 18/Stathmin Family of Microtubule Destabilizers. *Curr. Opin. Cel Biol.* 14, 18–24. doi:10.1016/s0955-0674(01)00289-7

Desjardins-Park, H. E., Foster, D. S., and Longaker, M. T. (2018). Fibroblasts and Wound Healing: An Update. *Regen. Med.* 13 (5), 491–495. doi:10.2217/rme-2018-0073

Esnault, S., Leet, J. P., Johansson, M. W., Barretto, K. T., Fichtinger, P. S., Fogerty, F. J., et al. (2020). Eosinophil Cytolysis on Immunoglobulin G Is Associated with Microtubule Formation and Suppression of Rho-Associated Protein Kinase Signalling. *Clin. Exp. Allergy* 50 (2), 198–212. doi:10.1111/cea.13538

Fabris, L., Berton, S., Pellizzari, I., Segatto, I., D'Andrea, S., Armenia, J., et al. (2015). p27kip1 Controls H-Ras/MAPK Activation and Cell Cycle Entry *via* Modulation of MT Stability. *Proc. Natl. Acad. Sci. U S A.* 112 (45), 13916–13921. doi:10.1073/pnas.1508514112

Feng, T., Xu, J., He, P., Chen, Y., Fang, R., and Shao, X. (2017). Decrease in Stathmin Expression by Arsenic Trioxide Inhibits the Proliferation and Invasion of Osteosarcoma Cells *via* the MAPK Signal Pathway. *Oncol. Lett.* 14 (2), 1333–1340. doi:10.3892/ol.2017.6347

Garcin, C., and Straube, A. (2019). Microtubules in Cell Migration. *Essays Biochem.* 63 (5), 509–520. doi:10.1042/EBC20190016

Gusarov, I., Shamovsky, I., Pani, B., Gautier, L., Eremina, S., Katkova-Zhukotskaya, O., et al. (2021). Dietary Thiols Accelerate Aging of *C. E. Nat. Commun.* 12 (1), 4336. doi:10.1038/s41467-021-24634-3

Hasegawa, A., Hisatomi, O., Yamamoto, S., Ono, E., and Tokunaga, F. (2007). Stathmin Expression during Newt Retina Regeneration. *Exp. Eye Res.* 85 (4), 518–527. doi:10.1016/j.exer.2007.07.003

Henklova, P., Vrzal, R., Papouskova, B., Bednar, P., Jancova, P., Anzenbacherova, E., et al. (2008). SB203580, a Pharmacological Inhibitor of P38 MAP Kinase Transduction Pathway Activates ERK and JNK MAP Kinases in Primary Cultures of Human Hepatocytes. *Eur. J. Pharmacol.* 593 (1-3), 16–23. doi:10.1016/j.ejphar.2008.07.007

Hu, J. Y., Chu, Z. G., Han, J., Dang, Y. M., Yan, H., Zhang, Q., et al. (2010). The P38/MAPK Pathway Regulates Microtubule Polymerization through Phosphorylation of MAP4 and Op18 in Hypoxic Cells. *Cell. Mol. Life Sci.* 67 (2), 321–333. doi:10.1007/s00018-009-0187-z

Kapitein, L. C., and Hoogenraad, C. C. (2015). Building the Neuronal Microtubule Cytoskeleton. *Neuron* 87 (3), 492–506. doi:10.1016/j.neuron.2015.05.046

Kaplani, K., Koutsi, S., Armenis, V., Skondra, F. G., Karantzelis, N., Champeris Tsaniras, S., et al. (2018). Wound Healing Related Agents: Ongoing Research and Perspectives. *Adv. Drug Deliv. Rev.* 129, 242–253. doi:10.1016/j.addr.2018.02.007

Kim, A., and Matthew, P. W. (2007). Microtubule Regulation of Corneal Fibroblast Morphology and Mechanical Activity in 3-D Culture. *Exp. Eye Res.* 85 (4), 546–556. doi:10.1016/j.exer.2007.07.008

Landén, N. X., Li, D., and Ståhle, M. (2016). Transition from Inflammation to Proliferation: a Critical Step during Wound Healing. *Cel. Mol. Life Sci.* 73 (20), 3861–3885. doi:10.1007/s00018-016-2268-0

Li, Y., Zhu, H., Wei, X., Li, H., Yu, Z., Zhang, H., et al. (2017). LPS Induces HUVEC Angiogenesis *In Vitro* through miR-146a-Mediated TGF-β1 Inhibition. *Am. J. Transl. Res.* 9 (2), 591–600.

Li, L., Zhang, J., Zhang, Q., Zhang, D., Xiang, F., Jia, J., et al. (2019). High Glucose Suppresses Keratinocyte Migration through the Inhibition of P38 MAPK/Autophagy Pathway. *Front. Physiol.* 10, 24. doi:10.3389/fphys.2019.00024

Liu, Y., Chen, Q., Zhang, N., Zhang, K., Dou, T., Cao, Y., et al. (2020). Proteomic Profiling and Genome-Wide Mapping of O-GlcNAc Chromatin-Associated Proteins Reveal an O-GlcNAc-Regulated Genotoxic Stress Response. *Nat. Commun.* 11 (1), 5898. doi:10.1038/s41467-020-19579-y

Mizumura, K., Takeda, K., Hashimoto, S., Horie, T., and Ichijo, H. (2006). Identification of Op18/stathmin as a Potential Target of ASK1-P38 MAP Kinase cascade. *J. Cel. Physiol.* 206 (2), 363–370. doi:10.1002/jcp.20465

Molkentin, J. D., Bugg, D., Ghearing, N., Dorn, L. E., Kim, P., Sargent, M. A., et al. (2017). Fibroblast-Specific Genetic Manipulation of P38 Mitogen-Activated Protein Kinase *In Vivo* Reveals its central Regulatory Role in Fibrosis. *Circulation* 136 (6), 549–561. doi:10.1161/CIRCULATIONAHA.116.026238

Muniyappa, H., and Das, K. C. (2008). Activation of C-Jun N-Terminal Kinase (JNK) by Widely Used Specific P38 MAPK Inhibitors SB202190 and SB203580: A MLK-3-MKK7-Dependent Mechanism. *Cell. Signal.* 20 (4), 675–683. doi:10.1016/j.cellsig.2007.12.003

Ninan, N., Thomas, S., and Grohens, Y. (2015). Wound Healing in Urology. *Adv. Drug Deliv. Rev.* 82-83, 93–105. doi:10.1016/j.addr.2014.12.002

Ning, M., Li, Y., Chen, Z., Han, P., Tang, X., Zhang, Y., et al. (2021). Role of Haematopoietic Cell-Specific Protein 1-Associated Protein X-1 Gene in Lipopolysaccharide-induced Apoptosis of Human Dermal Fibroblasts. *Wound Rep. Reg* 30 (1), 34–44. doi:10.1111/wrr.12985

Rodrigues, M., Kosaric, N., Bonham, C. A., and Gurtner, G. C. (2019). Wound Healing: A Cellular Perspective. *Physiol. Rev.* 99 (1), 665–706. doi:10.1152/physrev.00067.2017

Rubin, C. I., and Atweh, G. F. (2004). The Role of Stathmin in the Regulation of the Cell Cycle. *J. Cel. Biochem.* 93 (2), 242–250. doi:10.1002/jcb.20187

Seetharaman, S., and Etienne-Manneville, S. (2020). Cytoskeletal Crosstalk in Cell Migration. *Trends Cel Biol* 30 (9), 720–735. doi:10.1016/j.tcb.2020.06.004

Sharma, G. D., He, J., and Bazan, H. E. (2003). p38 and ERK1/2 Coordinate Cellular Migration and Proliferation in Epithelial Wound Healing: Evidence of Cross-Talk Activation between MAP Kinase Cascades. *J. Biol. Chem.* 278 (24), 21989–21997. doi:10.1074/jbc.M302650200

Shi, J., Shi, S., Xie, W., Zhao, M., Li, Y., Zhang, J., et al. (2021). IL-10 Alleviates Lipopolysaccharide-Induced Skin Scarring *via* IL-10R/STAT3 axis Regulating TLR4/NF-Kb Pathway in Dermal Fibroblasts. *J. Cel. Mol. Med.* 25 (3), 1554–1567. doi:10.1111/jcmm.16250

Shu, F., Zou, X., Tuo, H., She, S., Huang, J., Ren, H., et al. (2019). Stathmin Gene Silencing Suppresses Proliferation, Migration and Invasion of Gastric Cancer Cells *via* AKT/sCLU and STAT3 Signaling. *Int. J. Oncol.* 54 (3), 1086–1098. doi:10.3892/ijo.2019.4674

Singampalli, K. L., Balaji, S., Wang, X., Parikh, U. M., Kaul, A., Gilley, J., et al. (2020). The Role of an IL-10/Hyaluronan Axis in Dermal Wound Healing. *Front Cel Dev Biol* 8, 636. doi:10.3389/fcell.2020.00636

Singh, K., Agrawal, N. K., Gupta, S. K., Mohan, G., Chaturvedi, S., and Singh, K. (2015). Decreased Expression of Heat Shock Proteins May lead to Compromised Wound Healing in Type 2 Diabetes Mellitus Patients. *J. Diabetes Complications* 29 (4), 578–588. doi:10.1016/j.jdiacomp.2015.01.007

Sobel, A. (1991). Stathmin: A Relay Phosphoprotein for Multiple Signal Transduction? *Trends Biochem. Sci.* 16 (8), 301–305. doi:10.1016/0968-0004(91)90123-d

Song, J., Xu, H., Lu, Q., Xu, Z., Bian, D., Xia, Y., et al. (2012). Madecassoside Suppresses Migration of Fibroblasts from Keloids: Involvement of P38 Kinase and PI3K Signaling Pathways. *Burns* 38 (5), 677–684. doi:10.1016/j.burns.2011.12.017

Visan, I. (2019). Wound Healing. *Nat. Immunol.* 20 (9), 1089. doi:10.1038/s41590-019-0484-0

Walczak, C. E. (2000). Microtubule Dynamics and Tubulin Interacting Proteins. *Curr. Opin. Cel Biol.* 12 (1), 52–56. doi:10.1016/s0955-0674(99)00056-3

Wang, J., Yao, Y., Ming, Y., Shen, S., Wu, N., Liu, J., et al. (2016). Downregulation of Stathmin 1 in Human Gallbladder Carcinoma Inhibits Tumor Growth *In Vitro* and *In Vivo*. *Sci. Rep.* 6, 28833. doi:10.1038/srep28833

Yan, T., Jiang, X., Lin, G., Tang, D., Zhang, J., Guo, X., et al. (2019). Autophagy Is Required for the Directed Motility of Keratinocytes Driven by Electric Fields. *FASEB J.* 33 (3), 3922–3935. doi:10.1096/fj.201801294R

Yip, Y. Y., Yeap, Y. Y., Bogoyevitch, M. A., and Ng, D. C. (2014). cAMP-Dependent Protein Kinase and C-Jun N-Terminal Kinase Mediate Stathmin Phosphorylation for the Maintenance of Interphase Microtubules during Osmotic Stress. *J. Biol. Chem.* 289 (4), 2157–2169. doi:10.1074/jbc.M113.470682

Yoon, S. O., Shin, S., and Mercurio, A. M. (2005). Hypoxia Stimulates Carcinoma Invasion by Stabilizing Microtubules and Promoting the Rab11 Trafficking of the Alpha6beta4 Integrin. *Cancer Res.* 65 (7), 2761–2769. doi:10.1158/0008-5472.CAN-04-4122

Yurong, L., Biaoxue, R., Wei, L., Zongjuan, M., Hongyang, S., Ping, F., et al. (2017). Stathmin Overexpression Is Associated with Growth, Invasion and Metastasis of Lung Adenocarcinoma. *Oncotarget* 8 (16), 26000–26012. doi:10.18632/oncotarget.11006

Zhang, L., Shao, H., Zhu, T., Xia, P., Wang, Z., Liu, L., et al. (2013). DDA3 Associates with Microtubule Plus Ends and Orchestrates Microtubule Dynamics and Directional Cell Migration. *Sci. Rep.* 3, 1681. doi:10.1038/srep01681

Zhang, J., Li, L., Zhang, Q., Wang, W., Zhang, D., Jia, J., et al. (2019). Microtubule-Associated Protein 4 Phosphorylation Regulates Epidermal Keratinocyte Migration and Proliferation. *Int. J. Biol. Sci.* 15 (9), 1962–1976. doi:10.7150/ijbs.35440

Zou, M. L., Teng, Y. Y., Wu, J. J., Liu, S. Y., Tang, X. Y., Jia, Y., et al. (2021). Fibroblasts: Heterogeneous Cells with Potential in Regenerative Therapy for Scarless Wound Healing. *Front. Cel Dev Biol* 9, 713605. doi:10.3389/fcell.2021.713605

Conflict of Interest: The authors declare that the research was conducted in the absence of any commercial or financial relationships that could be construed as a potential conflict of interest.

The reviewer (JZ) declared a shared affiliation with the authors to the handling editor at time of review.

Publisher's Note: All claims expressed in this article are solely those of the authors and do not necessarily represent those of their affiliated organizations, or those of the publisher, the editors and the reviewers. Any product that may be evaluated in this article, or claim that may be made by its manufacturer, is not guaranteed or endorsed by the publisher.

frontiers in Pharmacology

REVIEW
published: 03 March 2022
doi: 10.3389/fphar.2022.838079

Inflammation and Cancer: From the Development of Personalized Indicators to Novel Therapeutic Strategies

Patrizia Ballerini[1,2], *Annalisa Contursi*[1,3], *Annalisa Bruno*[1,3], *Matteo Mucci*[1,3], *Stefania Tacconelli*[1,3] *and Paola Patrignani*[1,3]*

[1]*Center for Advanced Studies and Technology (CAST), Chieti, Italy,* [2]*Department of Innovative Technologies in Medicine and Dentistry, Chieti, Italy,* [3]*Department of Neuroscience, Imaging and Clinical Science, G. d'Annunzio University, Chieti, Italy*

Colorectal (CRC) and hepatocellular carcinoma (HCC) are associated with chronic inflammation, which plays a role in tumor development and malignant progression. An unmet medical need in these settings is the availability of sensitive and specific noninvasive biomarkers. Their use will allow surveillance of high-risk populations, early detection, and monitoring of disease progression. Moreover, the characterization of specific fingerprints of patients with nonalcoholic fatty liver disease (NAFLD) without or with nonalcoholic steatohepatitis (NASH) at the early stages of liver fibrosis is necessary. Some lines of evidence show the contribution of platelets to intestinal and liver inflammation. Thus, low-dose Aspirin, an antiplatelet agent, reduces CRC and liver cancer incidence and mortality. Aspirin also produces antifibrotic effects in NAFLD. Activated platelets can trigger chronic inflammation and tissue fibrosis via the release of soluble mediators, such as thromboxane (TX) A_2 and tumor growth factor (TGF)-β, and vesicles containing genetic material (including microRNA). These platelet-derived products contribute to cyclooxygenase (COX)-2 expression and prostaglandin (PG)E_2 biosynthesis by tumor microenvironment cells, such as immune and endothelial cells and fibroblasts, alongside cancer cells. Enhanced COX-2-dependent PGE_2 plays a crucial role in chronic inflammation and promotes tumor progression, angiogenesis, and metastasis. Antiplatelet agents can indirectly prevent the induction of COX-2 in target cells by inhibiting platelet activation. Differently, selective COX-2 inhibitors (coxibs) block the activity of COX-2 expressed in the tumor microenvironment and cancer cells. However, coxib chemopreventive effects are hampered by the interference with cardiovascular homeostasis via the coincident inhibition of vascular COX-2-dependent prostacyclin biosynthesis, resulting in enhanced risk of atherothrombosis. A strategy to improve anti-inflammatory agents' use in cancer prevention could be to develop tissue-specific drug delivery systems. Platelet ability to interact with tumor cells and transfer their molecular cargo can be employed to design platelet-mediated drug delivery systems to enhance the efficacy and reduce toxicity associated with anti-inflammatory agents in these settings. Another peculiarity of platelets is their capability to uptake proteins and transcripts from the circulation. Thus, cancer patient platelets show specific proteomic and transcriptomic expression profiles that could be used as biomarkers for early cancer detection and disease monitoring.

OPEN ACCESS

Edited by:
Pallavi R. Devchand, University of Calgary, Canada

Reviewed by:
Aneta Radziwon-Balicka, Nordsjællands Hospital, Denmark
Emanuela Marcantoni, New York University, United States

***Correspondence:**
Paola Patrignani
ppatrignani@unich.it

Specialty section:
This article was submitted to Inflammation Pharmacology, a section of the journal Frontiers in Pharmacology

Received: *17 December 2021*
Accepted: *09 February 2022*
Published: *03 March 2022*

Citation:
Ballerini P, Contursi A, Bruno A, Mucci M, Tacconelli S and Patrignani P (2022) Inflammation and Cancer: From the Development of Personalized Indicators to Novel Therapeutic Strategies. Front. Pharmacol. 13:838079. doi: 10.3389/fphar.2022.838079

Keywords: colorectal cancer, HCC, aspirin, COX-2, platelets, inflammation, NSAIDs, drug delivery

INTRODUCTION

Inflammation is a physiological protective response to various harmful stimuli, such as pathogens, damaged cells, and toxic compounds, that involves innate and adaptive immune systems. Acute inflammation is a self-limiting process that can develop into chronic inflammation, whether it is persistently unresolved (Furman et al., 2019). Chronic inflammation promotes many pathological conditions, including atherothrombosis (Libby et al., 2009; Ridker 2019), tissue fibrosis (Wynn and Ramalingam 2012), aberrant angiogenesis (Jackson et al., 1997), and neoplasia (Coussens and Werb, 2002; Grivennikov et al., 2010; Hanahan and Weinberg 2011).

Gawatz et al. (2005) have highlighted the molecular machinery and inflammatory pathways that platelets use to initiate and accelerate atherothrombosis. The pioneering intuition of Rudolf Virchow, who, in 1863, formulated the hypothesis of a link between microinflammation and subsequent cancer development, has been confirmed by numerous clinical and experimental data (Coussens and Werb, 2002; Grivennikov et al., 2010; Hanahan and Weinberg, 2011). Recently, the role of platelets in driving chronic intestinal inflammation and fibrosis has been elegantly demonstrated by Sacco et al. (2019) by generating a mouse with the specific deletion of cyclooxygenase (COX)-1 in megakaryocytes/platelets (platelet COX-1 cKO mouse) treated with dextran sodium sulfate

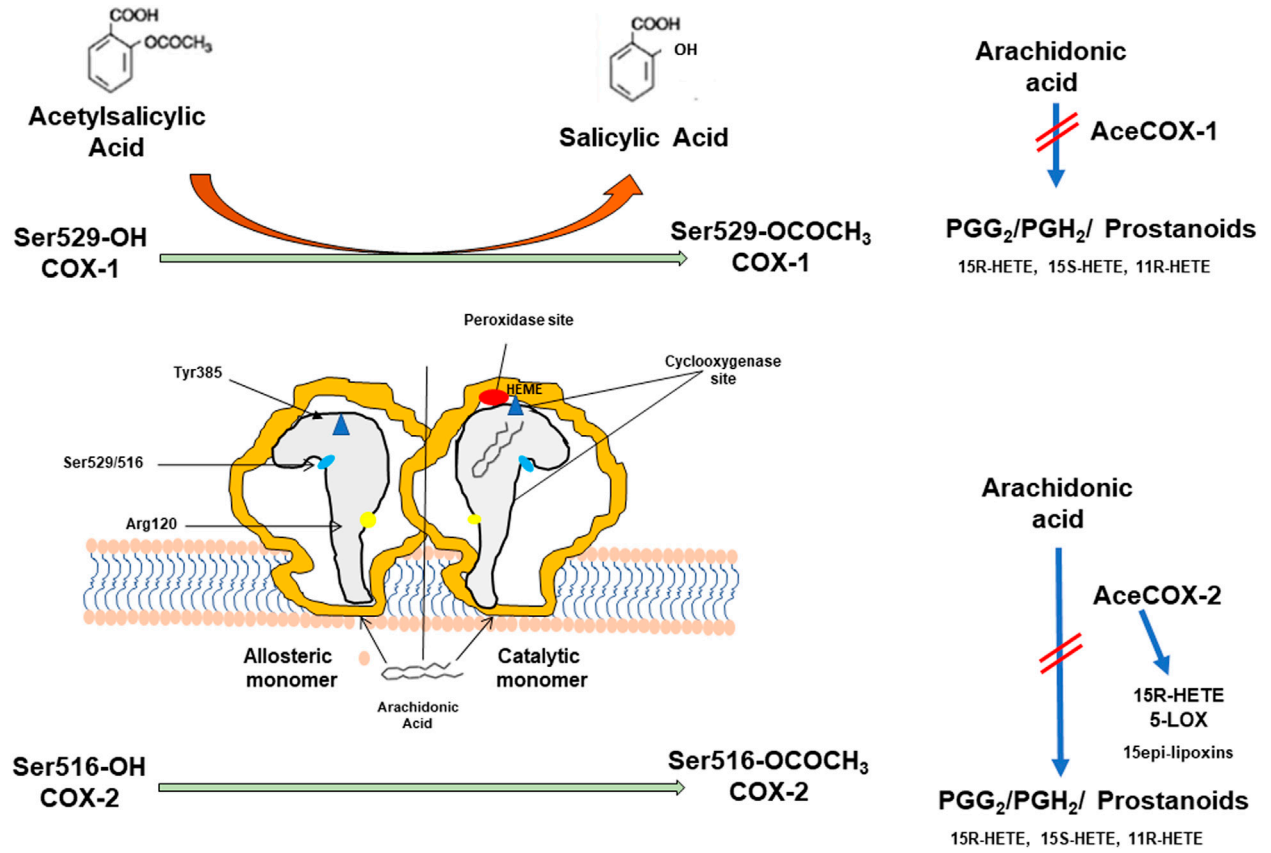

FIGURE 1 | Aspirin (acetylsalicylic acid, ASA) acts by irreversibly acetylating cyclooxygenase (COX)-1 and COX-2. Prostaglandin H synthase (PGHS)-1 and -2 (also known as COX-1 and COX-2) are microsomal homodimeric heme glycoproteins that catalyze two key reactions in the biosynthesis of prostanoids: the bis-dioxygenation of arachidonic acid to form PGG_2 (by the cyclooxygenase activity) and the reduction of PGG_2 to PGH_2 (by the peroxidase activity). In addition to PGH_2, the monohydroxy acids 11(R)-hydroxyeicosatetraenoic acid 11(R)-hydroxyeicosatetraenoic acid 11R-(HETE), 15S-HETE, and 15R-HETE are generated as minor products of the cyclooxygenase reaction. COX-isozymes function as conformational heterodimers comprised of a regulatory allosteric monomer and a catalytic monomer. The catalytic monomer has a bound heme, whereas the allosteric monomer does not. The cyclooxygenase active site is a hydrophobic channel (reported in grey), and Arg-120 is located near its mouth. Arg-120 forms an ionic bond with the carboxylate group of arachidonate, and this interaction is an important contributor to the overall strength of arachidonate binding to COX-1 more than COX-2. Arg-120 is also the binding site for Aspirin. At the top of the channel is located Tyr-385, which is the critical catalytic amino acid for the cyclooxygenase reaction. Ser-529 and Ser-516 are the aminoacids acetylated by Aspirin. The acetylation of COX-isozymes is associated with the formation of salicylic acid, a weak COX inhibitor. The acetylation of only one monomer of COX dimer is sufficient for causing profound inhibition of cyclooxygenase activity. The acetylation of COX-1 at Ser-516 inhibits the catalytic activity of cyclooxygenase and prevents the generation of PGG_2. In contrast, acetylated COX-2 at Ser-516 gains a novel catalytic activity and forms 15 R-HETE. 15R-HETE could be transformed to 15(R)epi-lipoxin $(LX)A_4$ and 15epi-LXB_4 in cells expressing the 5-lipoxygenase (5-LOX), the enzyme also responsible for leukotriene biosynthesis.

(DSS) to induced colitis. The platelet COX-1 cKO mouse has a phenotype resembling that induced by the antiplatelet agent low-dose Aspirin in humans. The drug causes complete and persistent inhibition of platelet COX-1 with a limited inhibitory effect on vascular COX-2-dependent prostacyclin [prostaglandin (PG)I_2] (Patrignani et al., 1982; Capone et al., 2004).

Aspirin inhibits platelet function by causing an irreversible inactivation of COX-1 through the acetylation of a serine residue at position 529 of the COX active site (**Figure 1**). Once acetylated, COX-1 is inhibited for the lifetime of the anucleate platelets since they have a limited capacity to generate new protein. Thus, low-dose Aspirin causes a virtually complete inhibition of platelet thromboxane (TX) A_2 biosynthesis, a primary agonist of platelet aggregation, throughout dosing intervals (24 h), even if the drug has a short half-life (Pedersen and FitzGerald 1984). Aspirin also acetylates COX-2 at serine 516, and the enzyme gains a new catalytic activity with the formation of 15R-hydroxyeicosatetraenoic acid (HETE) from arachidonic acid (AA) (Lecomte et al., 1994) (**Figure 1**). However, we have recently shown that in the human colon cancer cell line, HCA-7, stimulated with 0.5 μM of AA *in vitro*, Aspirin causes concentration-dependent acetylation of COX-2 at serine 516 and inhibition of PGE_2 production with comparable EC_{50} values (concentration causing 50% of maximal effect: 19.84 and 19.58 μM, respectively) while 15R-HETE is undetectable (Tacconelli et al., 2020). PGE_2 plays a crucial role in chronic inflammation and promotes tumor progression, angiogenesis, and metastasis (Wang and Dubois 2018). Aspirin affects COX-2-dependent PGE_2 with comparable potency to platelet COX-1 *in vitro* (Patrignani et al., 2017). However, when administered at low doses once a day, the drug targets mainly platelet COX-1 due to rapid *de novo* synthesis of COX-2 in nucleated cells (Patrignani et al., 2017). The development of direct biomarkers of aspirin action (i.e., the evaluation of the extent of acetylation of COX-1 at serine 529) (Li et al., 2014; Patrignani et al., 2014) has confirmed that low-dose Aspirin acts through a major effect on the platelet with a minor direct impact on the colorectal mucosa (Patrignani et al., 2017). Aspirin has been reported to cause anticancer effects by affecting different COX-independent molecular pathways (Alfonso et al., 2014; Ricciotti et al., 2021). However, these effects have been mainly found *in vitro* at supratherapeutic concentrations (millimolar concentrations).

The analysis of randomized clinical trials (RCTs) with Aspirin for cardiovascular (CV) prevention has shown that low doses are associated with a maximal efficacy to reduce incidence and mortality from colorectal cancer (CRC) over long-term follow-up (reviewed in Patrignani and Patrono 2016; Patrignani and Patrono 2018). This is like that found for Aspirin's secondary prevention of atherothrombotic vascular events (Patrono et al., 2017). Thus, the pharmacodynamics features of low-dose Aspirin and the clinical data suggest that the inhibition of COX-1-dependent platelet function is a central mechanism for CV and intestinal tumorigenesis prevention (Patrignani and Patrono 2016; Patrignani and Patrono 2018).

Platelets can contribute to tumorigenesis and metastasis via the release of many soluble factors (including prostanoids, cytokines, growth, and angiogenic proteins and transcripts) and extracellular vesicles (EVs), which promote the change of the phenotype of stromal (such as fibroblasts and immune cells), endothelial, epithelial cells and cancer cells (Gay and Felding-Habermann 2011; Burnouf et al., 2014; Contursi et al., 2017; Dovizio et al., 2018). We have shown that platelets induce COX-2 expression and enhance PGE_2 biosynthesis in colon cancer cells *in vitro* associated with epithelial-mesenchymal transition (EMT), increased migration, and metastatic potential when injected in mice (Dovizio et al., 2013; Guillem-Llobat et al., 2016). The overexpression of COX-2 is an important event for the development and progression of CRC (Wang and Dubois 2018). Importantly, COX-2-dependent PGE_2 causes immunosuppression and tumor immune escape (Zelenay et al., 2015; Wang and Dubois 2018). Low-dose Aspirin cannot directly inhibit COX-2 activity but can restrain COX-2 induction in stromal cells and intestinal epithelial cells by inhibiting platelet activation (Patrignani and Patrono 2016; Dovizio et al., 2017; Patrignani and Patrono 2018).

Selective COX-2 inhibitors (coxibs) have antitumor effects (reviewed by Patrignani and Patrono, 2016), and they might be effective adjuvants for immune-based therapies in cancer patients (Zelenay et al., 2015; Wang and Dubois 2018). However, the chronic use of coxibs interferes with CV homeostasis due to the inhibition of vascular COX-2-dependent PGI_2 biosynthesis and the resulting increased risk of atherothrombosis (Grosser et al., 2006). Platelet ability to transfer their contents to cancer cells might be used to develop platelet-based drug delivery systems (Lu et al., 2019), thus improving the efficacy of anti-inflammatory drugs and reducing their toxicity.

A peculiarity of platelets is that they can uptake many soluble components (proteins, transcripts, including microRNAs) from plasma, and this phenotypically distinct population is termed tumor-educated blood platelets (TEPs). TEPs originate as a systemic and local response to tumor growth, and their assessment has diagnostic potential (Roweth and Battinelli, 2021), indicating the individual's clinical condition.

CRC and primary liver cancer are leading causes of cancer-related deaths worldwide (Bray et al., 2018). Therefore, their prevention and appropriate treatments represent an unmet medical need and a global health challenge. This review aims to put together evidence on the possible role of platelets in the development and perpetuation of chronic inflammation associated with CRC and hepatocellular carcinoma (HCC) and opening the way to therapeutic strategies involving antiplatelet agents and platelet-mediated drug delivery systems to enhance the efficacy and reduce the toxicity of anti-inflammatory agents. Finally, the evidence on the possible use of proteomics and transcriptomics expression profiles of TEPs as biomarkers for early cancer detection and disease monitoring is discussed.

COLORECTAL CANCER

Inflammation, Platelets, and CRC

CRC ranks third among the most diagnosed cancers accounting for 10% of the cancer burden (Bray et al., 2018). Two chronic relapsing inflammatory disorders of the gastrointestinal tract,

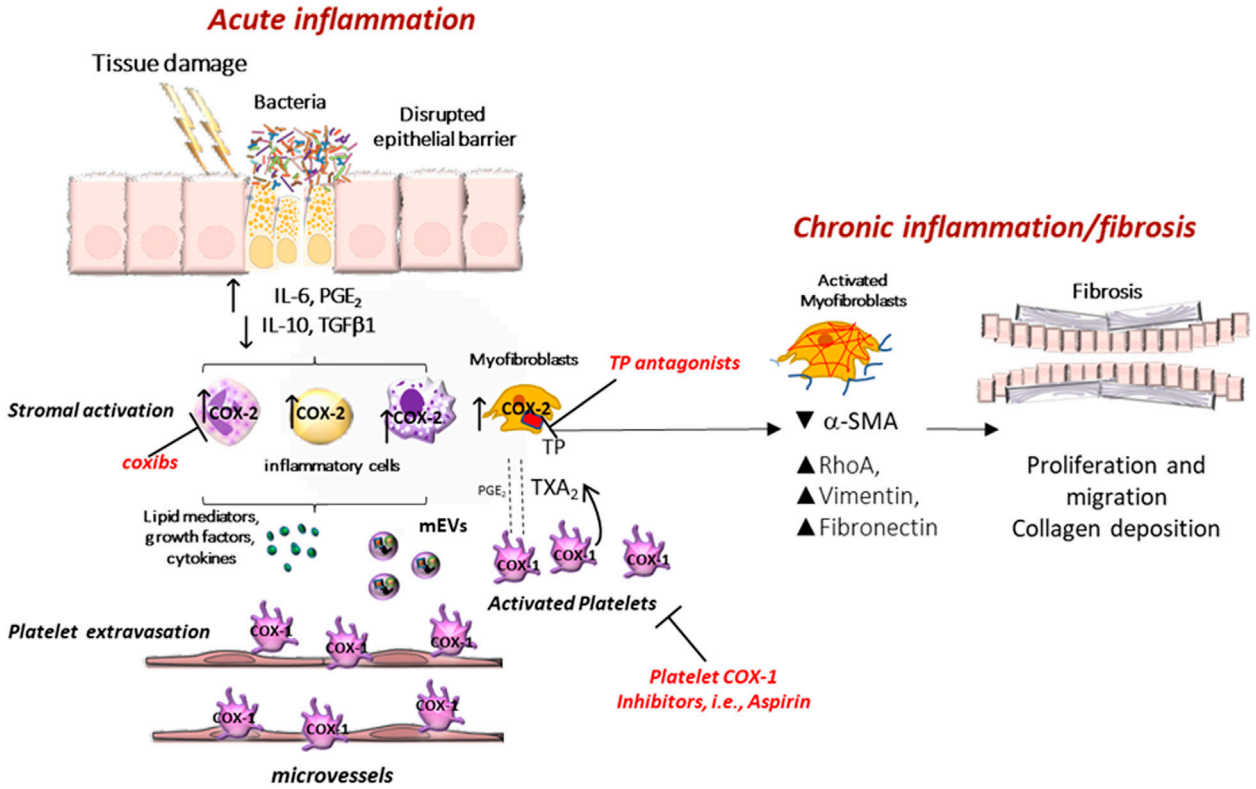

FIGURE 2 | Clinical implications of eicosanoid inhibition in intestinal tumorigenesis. Activated platelets release soluble mediators, including thromboxane A_2 (TXA_2), prostaglandin E_2 (PGE_2), 12S-hydroxyeicosatetraenoic acid (12S-HETE), growth factors, cytokines, and platelet-derived medium-sized extracellular vesicles (mEVs) containing microRNAs, which contribute to the phenotypic changes of the cells in the stromal microenvironment. Interactions between epithelial cells and stromal cells undergo an alteration that induces the development of intestinal neoplasia. A crucial event is the enhanced biosynthesis of PGE_2 in the intestinal mucosa, occurring in the early stages of tumor development via the cyclooxygenase (COX)-1 activity, in association with the suppression of the prostaglandin-degrading enzyme 15-prostaglandin dehydrogenase (15-PGDH). Later, the overexpression of COX-2 contributes to the generation of aberrant levels of PGE_2 in the stromal compartment and epithelial cells. PGE_2 plays multifaceted roles in cancer promotion, including proliferation, migration, epithelial-mesenchymal transition (EMT), and immune escape. Tumor cells that undergo this phenomenon acquire a migratory capacity that facilitates metastatic colonization. By inhibiting platelet activation, antiplatelet agents can indirectly restrain the induction of COX-2 in target cells. Differently, selective COX-2 inhibitors (coxibs) affect COX-2 activity already expressed in the tumor microenvironment and cancer cells. 12S-HETE generated by 12-lipoxygenase (LOX) may have protumorigenic effects, and selective 12-LOX inhibitors are in clinical development.

Crohn's disease (CD) and ulcerative colitis (UC), which represent the main subtypes of inflammatory bowel diseases (IBD), are associated with CRC development. For these patients, the relative risk for CRC is about two to three times greater than that of the general population (Carter et al., 2004) and correlates with the disease duration, increasing by 0.5–1% yearly, 8–10 years after diagnosis (Herszenyi et al., 2007). This indicates that chronic intestinal inflammation contributes to tumor formation. Indeed, differently from the wound healing process that resolves following proper immune cell recruitment and epithelial cell proliferation, growing tumors enter into a feed-forward loop of inflammation-induced signaling and inflammatory cell recruitment (Dovizio et al., 2017).

Platelets can extravasate and infiltrate the mucosa of the inflamed intestine, thus interacting with stromal cells, such as myofibroblasts (Sacco et al., 2019). This contributes to developing a chronic inflammatory state of the colorectum. Thus, in an animal model of intestinal colitis, the specific deletion of COX-1 in megakaryocytes/platelets, associated with the inhibition of platelet TXA_2, promotes the resolution of chronic inflammation and ameliorates the colitis symptoms and fibrosis (Sacco et al., 2019) (**Figure 2**). The results of a recent study showed that tumor-platelet infiltration (TIPs) was associated with decreased postsurgical survival in CRC patients and that the combination of TIPs and the Classification of Malignant Tumours TNM staging (T category describes the primary tumor site and size; N category describes the regional lymph node involvement; M category describes the presence of distant metastatic spread) establish a nomogram with better prognostic ability than TNM alone (Miao et al., 2022). When CRC is diagnosed early and localized, the 5-year survival rate can reach about 90%. Unfortunately, according to the American Cancer Society, only four out of 10 CRC patients are detected in the early stages (https://www.cancer.org/cancer/colon-rectal-cancer/detection-diagnosis-staging/detection.html); the 5-years survival rate drops to 10% for CRC patients with distant

metastasis (Haggar and Boushey, 2009). Colonoscopy is still the gold standard for CRC screening, for both early detection and primary prevention, thanks to the possibility of performing biopsies and removing precancerous lesions. However, this procedure has several limitations: 1) it is invasive with bleeding and intestinal perforation occurring in 0.001–0.687% and 0.005–0.085%, respectively; 2) it is uncomfortable and 3) it must be managed by qualified health personnel (Kim et al., 2019). The fecal occult blood test and the fecal immunochemical tests help identify CRC patients, but their sensitivity is low; these tests can detect only 27% of advanced neoplasms and 66% of invasive cancer (Morikawa et al., 2005). These data show an urgent need to have noninvasive and highly sensitive screening tools to detect CRC at the early stage accurately.

Aspirin in the Prevention of CRC

The first evidence of the apparent chemopreventive effect of Aspirin against CRC derives from epidemiological studies. In case-control and cohort studies, daily use of Aspirin, with a regular drug consumption for at least a decade, has been associated with a reduction of about 50% in the incidence and mortality of CRC (Giovannucci et al., 1995; Thun et al., 2002; Cuzick et al., 2009).

The meta-analyses of CV RCTs with Aspirin versus placebo have shown that the drug, when chronically administered for at least 5 years, reduces the risk of cancer at the gastrointestinal (GI) tract (i.e., esophagus, stomach, and colon) by ~20% (Rothwell et al., 2010; Rothwell et al., 2011). However, protection against other cancers, such as breast, lung, and prostate, has been detected with a lower reduction in risk (Rothwell et al., 2011). Death due to CRC on long-term follow-up after RCTs of Aspirin versus placebo showed that the protective effect was saturable at low doses (Rothwell et al., 2010). Within the limitations of post hoc analyses of cancer events that were not pre-specified endpoints, the results of the Thrombosis Prevention Trial (TPT) (Meade, 1998) are of interest since the anticancer effect of Aspirin was apparent in men at high CV risk treated with a 75-mg controlled-release aspirin formulation associated with tiny concentrations measured in the systemic circulation. This Aspirin formulation was developed to maximize cumulative inhibition of platelet COX-1 in the pre-hepatic circulation and minimize inhibition of COX-2 in the systemic compartment (Charman et al., 1993). Moreover, a reduced risk for CRC (a pre-specified secondary endpoint) was detected in the long-term observational follow-up of the Women's Health Study where Aspirin was administered in alternate-day 100-mg Aspirin versus placebo (Cook et al., 2005). Altogether these findings suggest that the chemopreventive effect of Aspirin has features comparable to its antiplatelet effect, i.e., a long-lasting duration and, most importantly, its saturability at low doses (Patrignani et al., 1982; Patrignani et al., 2014).

In individuals with sporadic colorectal adenomas, placebo-controlled RCTs have shown a significant risk reduction of reoccurrence after treatment with Aspirin (81–325 mg daily) (Baron et al., 2003; Benamouzig et al., 2003; Sandler et al., 2003; Benamouzig et al., 2012). However, a comparable benefit was detected in the placebo-controlled RCTs with the selective COX-2 inhibitors celecoxib and rofecoxib in individuals with a history of colorectal adenomas (Bresalier et al., 2005; Bertagnolli et al., 2006). The comparable benefit of low-dose Aspirin (which targets platelet COX-1) and coxibs (which target COX-2 in extraplatelet cellular sources) has led to hypothesize that platelets contribute to adenoma development via the induction of COX-2 expression in stromal cells of colorectal mucosa and then in epithelial cells (Patrono et al., 2001; Patrignani and Patrono, 2016; Dovizio et al., 2017; Patrignani and Patrono, 2018).

Familial adenomatous polyposis (FAP) represents an accelerated clinical manifestation of the adenoma to carcinoma sequence that characterizes the development of most CRCs; the studies in FAP patients contribute to enhancing knowledge in the interaction of genetic and molecular events occurring in the development of sporadic colorectal neoplasia (Fearon and Vogelstein, 1990). The chemopreventive effect of Aspirin in FAP patients is not completely clarified yet. Colorectal Adenoma/Carcinoma Prevention Program 1 (CAPP1) is a multicenter, randomized, placebo-controlled trial performed in FAP patients (10–21 years old of both sexes) treated with 600 mg/day (two tablets/day) and/or resistant starch 30 g/d (30 g as two sachets/day) (Burn et al., 2011). The duration of intervention was from one to a potential maximum of 12 years, with a scheduled annual clinical examination including endoscopy. Among 133 evaluable patients, Aspirin treatment resulted in a nonsignificant reduction in polyp number (RR = 0.77; 95% CI, 0.54–1.10) compared with nonaspirin, and a significant decrease in the diameter of the largest polyps (principal secondary endpoint) among patients treated with Aspirin for more than 1 year. No serious adverse effects were recorded.

Recently, Ishikawa et al. (2021) performed a double-blind, placebo-controlled, multicenter trial in 104 patients (age: 16–70 years) with FAP for the effects of low-dose Aspirin (100 mg/day) and mesalazine (2 g/day) on the recurrence of colorectal polyps (J-FAPP Study IV). The primary endpoint was the incidence of colorectal polyps of at least 5 mm; treatment continued until 1 week before an 8-month colonoscopy. Polyp recurrence was significantly reduced in patients who received Aspirin versus mesalazine [OR values: 0.37 (95% CI, 0.16–0.86) for Aspirin and 0.87 (95% CI, 0.38–2) for mesalazine)]. The most common adverse events recorded were low-grade upper GI symptoms. This trial has some limitations (Lynch, 2021), including the fact that the emergence of adenomas greater than 5.0 mm is not an accurate measure of clinical benefit. Like all other chemoprevention trials for FAP, achieving reproducible endoscopic examinations from baseline to post-intervention is a challenge; thus, advanced endoscopic image capture of all the available adenoma evaluated by independent audit should be used in further trials. In J-FAPP Study IV, the average age of patients at entry was over 30 years suggesting that many patients had attenuated FAP.

Dovizio et al. (2012) have reported that enhanced systemic biosynthesis of TXA_2 occurs *in vivo* in FAP, possibly from activated platelets; in fact, it was not affected by celecoxib. Activated platelets can induce several signaling pathways, including those related to TXA_2, in stromal and tumor cells,

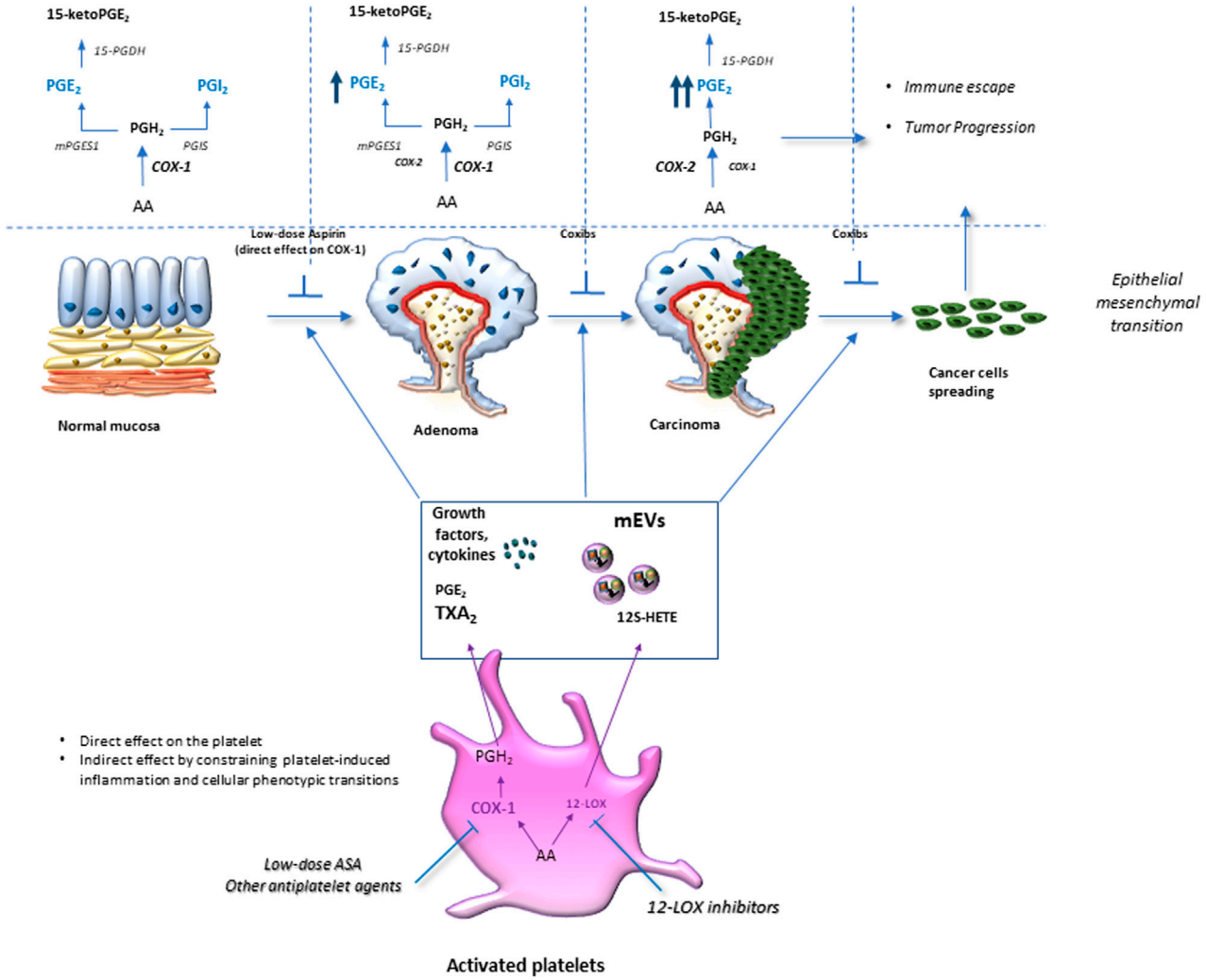

FIGURE 3 | Platelet activation in response to intestinal damage is crucial in chronic inflammation/fibrosis. Platelet activation in response to intestinal epithelial damage contributes to acute inflammation by promoting leukocyte recruitment to restore normal tissue function. However, exaggerated platelet activation is associated with an elevated release of thromboxane (TX) A_2 and prostaglandin (PG)E_2, growth factors, angiogenic factors, cytokines, and chemokines, as well as medium-sized extracellular vesicles (mEVs) rich in genetic material (mRNAs and microRNAs). These factors activate stromal cells (such as myofibroblasts and immune cells), thus increasing the production and release of growth factors and inflammatory mediators, including PGE_2, due to cyclooxygenase (COX)-2 induction. Platelet-derived TXA_2 induces phenotypic and functional changes in myofibroblasts, such as the reduction of α-Alpha Smooth Muscle Actin (SMA) and the increase of vimentin fibronectin RhoA expression; these events lead to an enhanced capacity to proliferate and migrate, thus, contributing to chronic intestinal inflammation and fibrosis. The inhibition of platelet COX-1 activity (by low-dose Aspirin) or blocking the TXA_2 receptor (TP) can mitigate chronic intestinal inflammation and fibrosis.

thus contributing to inflammatory and carcinogenic responses mediated, at least in part, by enhanced biosynthesis of COX-2-dependent PGE_2 (Patrignani and Patrono, 2016; Patrignani and Patrono, 2018) (**Figure 3**). Thus, low-dose Aspirin can mitigate these effects indirectly by inhibiting platelet function. It is noteworthy to consider that high doses of Aspirin used in the CAPP1 trial could have reduced the chemopreventive effect of Aspirin due to the coincident depression of vascular PGI_2, which exerts anticarcinogenic effects (Dovizio et al., 2012).

In Lynch Syndrome (LS) carriers, formerly known as hereditary nonpolyposis colon cancer, which results from pathogenic variants in one of the DNA mismatch repair genes (Li et al., 2021), Aspirin 600 mg/day (2 tablets/day) for 2 years resulted in 60% reduction in the incidence of CRC- and other LS-associated tumors. The protection persisted for over a decade but did not become apparent until about 5 years from the beginning. In this relatively young group of individuals, serious adverse events did not differ significantly in the Aspirin group versus the placebo group (Burn et al., 2020). These positive results support the use of Aspirin as a cancer prevention measure in individuals with LS. However, the optimal dose has still not been determined and is the objective of the ongoing CAPP3 study that compares daily Aspirin at 600, 300, and 100 mg for cancer prevention versus adverse events (http://www.capp3.org).

Overall, numerous lines of evidence support the role of the antiplatelet agent low-dose Aspirin in preventing

atherothrombosis and CRC. However, its use cannot be recommended for the primary prevention of these diseases due to the possible enhanced risk of hemorrhage via inhibition of TXA_2-dependent platelet function, an important component of primary hemostasis. The bleeding risk is smaller in young people and substantially higher in elderly individuals and those with a history of ulcer bleeding. The publication in 2018 of three placebo-controlled RCTs, i.e., ARRIVE, ASCEND, and ASPREE (ASCEND Study Collaborative Group et al., 2018; Gaziano et al., 2018; McNeil et al., 2018), in three populations at increased risk of myocardial infarction or ischaemic stroke in the absence of established CV disease show that low-dose Aspirin conferred little or no cardiovascular benefit and a small risk for major hemorrhage. In October 2021, United States Preventive ServicesTask Force (USPSTF) stated that "the decision to initiate low-dose aspirin use for the primary prevention of CV disease in adults ages 40–59 years who have a 10% or greater 10-year CV risk should be an individual one. Persons who are not at increased risk for bleeding and are willing to take low-dose Aspirin daily are more likely to benefit." Aspirin use is best reserved for individuals with specific molecularly driven cancer risks, such as those with LS, with a low risk of bleeding due to young age.

These findings convincingly show that it is necessary to develop novel antiplatelet agents with an improved safety profile (Majithia and Bhatt, 2019) and novel technologies involved in transporting a pharmaceutical compound to its target site to achieve a desired therapeutic outcome, thus reducing systemic off-target effects (targeted drug delivery systems) (Dovizio et al., 2020). Moreover, an important field of research is the development of biomarkers predictive for the response to a drug on an individual basis (precision medicine). The ongoing ADD-Aspirin trial will contribute to realizing this objective (Coyle et al., 2016). The trial includes four phase III RCTs evaluating the effect of two doses of daily Aspirin, i.e., 100 and 300 mg/day, on recurrence and survival after radical cancer therapy in patients with four non-metastatic common solid tumors (colorectal, gastroesophageal, breast, and prostate cancer). In addition to the clinical outcomes, samples are collected to identify mechanistic biomarkers of aspirin responses.

Experimental Evidence on the Role of Platelets in CRC

Platelets are rapidly activated to repair tissue injury/dysfunction (Gawaz et al., 2005; Dovizio et al., 2017; Tourdot and Holinstat, 2017) (**Figure 2**). Several functions of platelets are involved: the adhesion to extracellular matrix (ECM) proteins exposed by the tissue damage (Bergmeier and Hynes, 2012), the aggregation leading to the amplification of platelet activation (Davì and Patrono, 2007), the release of many factors such as the eicosanoids (TXA_2 and PGE_2 and 12S-HETE), proteins (growth and angiogenic factors) and Extracellular visicles (EVs) (Dovizio et al., 2020). EVs are of various sizes and play an important role in the delivery of platelet cargo (including proteins and transcripts, including microRNAs) to other cell types even far from the site of the tissue damage (Burnouf et al., 2014; Dovizio et al., 2020; Dovizio et al., 2018; Puhm et al., 2021). The crosstalk with EVs contributes to chronic inflammation and fibrosis by activating immune cells, fibroblasts, and endothelial cells (**Figure 2**). Chronic inflammation contributes to several diseases, including atherothrombosis (Soehnlein and Libby, 2021) and cancer (Hanahan and Weinberg, 2011). Lifestyle habits, such as low physical activity, excessive consumption of red, processed meats, alcohol, low dietary fiber content, and smoking can alter intestinal homeostasis, which requires the appropriate integration of various cell signaling pathways and balanced crosstalk between different cell types composing the organ (Grazioso et al., 2019). Dysregulation of this balance can impair the mucosal barrier allowing the gut bacteria to invade the mucosa inducing platelet activation and an excessive immune response (**Figure 2**). In an animal model of colitis, the inhibition of platelet function by selective deletion of COX-1 in platelets (which recapitulated the human pharmacodynamics of low-dose Aspirin, i.e., suppression of platelet TXA_2 production associated with substantial sparing of the systemic prostanoid biosynthesis) ameliorates colitis symptoms, chronic intestinal inflammation, and fibrosis (Sacco et al., 2019) (**Figure 2**). These findings suggest that platelet activation is an upstream event in the development of chronic intestinal inflammation. Platelet-derived TXA_2 enhances the ability of myofibroblasts to proliferate and migrate *in vitro*, and these effects were prevented by platelet COX-1 inhibition (Aspirin) or antagonism of the TXA_2 receptor (Sacco et al., 2019). Interestingly, platelet-derived TXA_2 enhanced the expression of mesenchymal markers, such as vimentin and fibronectin, and these effects were abrogated by incubating the myofibroblasts with platelets preexposed to Aspirin (Sacco et al., 2019) (**Figure 2**).

Platelets can also promote a mesenchymal phenotype in cancer cells *in vitro* (Labelle et al., 2011; Guillem-Llobat et al., 2016); mesenchymal-like cancer cells are characterized by the enhanced capacity of cell mobility *in vitro* and a prothrombotic and prometastatic potential when injected into mice (Guillem-Llobat et al., 2016). In cocultures of platelets and colorectal HT29 cancer cells, platelet-derived PGE_2 upregulated TWIST1 via the activation of the EP4 receptor (one of the four PGE_2 receptors) (Guillem-Llobat et al., 2016). TWIST1 encodes a basic helix-loop-helix transcription factor that contributes to EMT, a key process in the metastases formation of cancer (Yang et al., 2004; Kalluri and Weinberg, 2009). This effect was associated with the downregulation of E-cadherin, a typical marker of the epithelial phenotype (van Roy and Berx, 2008), and the upregulation of Rac1 (a small G-protein of the Rho family) involved in modulation of migration (Yang et al., 2012). Different antiplatelet agents prevented these changes, Aspirin (an inhibitor of COX-1), DG-041 (an antagonist of the PGE_2 EP3 receptor subtype), and Ticagrelor (a P2Y12 receptor antagonist), which all reduced the release of PGE_2 from platelets, thus preventing the activation of EP4 on HT29 cells by platelet-derived PGE_2 (Guillem-Llobat et al., 2016). Therefore, platelets prime colon cancer cells for metastasis, and antiplatelet agents can restrain it. Contursi et al. (2021) have recently found that platelets can promote EMT in cancer cells via the transfer of platelet-type 12-lipoxygenase (LOX) contained in platelet-derived medium-sized EVs (mEVs). The cancer cells now generate 12S-HETE, considered a key modulator of cancer metastasis (Dilly et al.,

2013). Interestingly, 12-HETE was mainly esterified in plasmalogen phospholipids. Modifying cancer cell phospholipids by 12S-HETE may functionally impact cancer cell biology and represent a novel target for anticancer agent development. Selective inhibitors of 12-LOX, which are in clinical development, such as ML-355 (Tourdot and Holinstat, 2017), and macropinocytosis inhibitors (Lin et al., 2018), which prevent the internalization of mEVs (Contursi et al., 2021), are potential anticancer tools.

Role of Intestinal COX-Isozymes in CRC

In the course of inflammation, many protumorigenic signalings are activated, including the induction of COX-2 and aberrant generation of PGE_2 (Wang and DuBois, 2018). However, in the early events of intestinal tumorigenesis, the suppression of the expression of the enzyme 15-prostaglandin dehydrogenase (15-PGDH), a prostaglandin-degrading enzyme, allows enhanced biosynthesis of PGE_2 via COX-1, before the overexpression of COX-2 (Myung et al., 2006) (**Figure 3**).

PGE_2 can phosphorylate ribosomal protein S6 (p-S6) via protein kinase A (PKA) (Moore et al., 2009). S6 regulates the 40S ribosome biogenesis transcriptional program, and its phosphorylated form is related to cell growth and tumor progression (Ruvinsky et al., 2005). Patrignani et al. (2017) have shown that the human rectal mucosal levels of p-S6/S6 significantly correlated with PGE_2. In individuals undergoing CRC screening, low-dose Aspirin reduced the levels of p-S6/S6 in apparently healthy colorectal mucosa in association with the acetylation of COX-1 at serine 529 and an approximately 50% reduction of PGE_2 biosynthesis (Patrignani et al., 2017).

During intestinal tumor progression, aberrant generation of PGE_2 occurs for the coordinated overexpression of COX-2 and microsomal PGE_2 synthase-1 (mPGES-1) (Sasaki et al., 2012). PGE_2 activates target cells by binding to four subtypes of G protein-coupled receptors (EP1, EP2, EP3, and EP4) expressed on the plasma membrane and/or nuclear envelope (Ricciotti and FitzGerald, 2011). This prostanoid promotes intestinal tumorigenesis via EP2 and EP4, but not EP3 (Wang and DuBois, 2018). The role of EP1 in CRC remains unclear. PGE_2 promotes tumor epithelial cell proliferation, survival, migration/invasion, and epigenetic changes and contributes to the metastatic spread by inhibiting immunosurveillance and inducing angiogenesis (Wang and DuBois, 2018 Zelenay et al., 2015) (**Figure 3**). Thus, coxibs' inhibition of COX-2-dependent PGE_2 reduces the risk of sporadic colorectal adenoma recurrence (Bresalier et al., 2005; Bertagnolli et al., 2006). However, as reported above, coxibs' use is hampered by their interference with CV homeostasis for the coincident inhibition of vascular COX-2-dependent PGI_2 biosynthesis, resulting in enhanced risk of atherothrombosis (Grosser et al., 2006; Patrignani and Patrono, 2015).

HEPATOCELLULAR CARCINOMA

Inflammation, Platelets, and HCC

Hepatocellular carcinoma (HCC) is the most common form of liver cancer and accounts for 75–85% of cases (Bray et al., 2018). Hepatitis B virus (HBV) and hepatitis C virus (HCV) infections are responsible for about 50% of liver cancer mortality followed by alcohol consumption (~30%) and by other causes (~15%) (Akinyemiju et al., 2017).

HBV is a non-cytopathic, hepatotropic DNA virus that integrates into the host genome (Wang et al., 1990). A direct oncogenic activity has been described for the truncated and mutated HBV proteins, mainly HBx or preS2/S. These proteins contribute to hepatocarcinogenesis by affecting different signal transduction pathways, including inflammatory responses (Hai et al., 2014). HBx has been shown to induce COX-2 expression and PGE_2 biosynthesis when transfected in Hep3B hepatocellular carcinoma cells, characterized by low levels of COX-2 (Cheng et al., 2004). More recently, it has been reported that HBV activates the expression of COX-2 and PGE_2 biosynthesis in HepG2 cells and Huh7 human hepatoma cells co-transfected with plasmid pHBV-1.2 (to produce mature HBV virions) and with the reporter plasmids pGL3-COX-2-Luc (Yu et al., 2011).

HCV is an RNA virus. It is a hepatotropic, principally non-cytopathic virus with a high mutation rate; it is one of the most important risk factors for HCC. The viral protein NS5A has been reported to induce COX-2 promoter activity in a concentration-dependent manner in Huh7 human hepatoma cells (Chen et al., 2019).

Although infection by HBV and HCV remain the main risk factors for HCC development, nonalcoholic fatty liver disease (NAFLD), a pathological liver condition associated with obesity, insulin resistance, or metabolic syndrome, is becoming a more frequent risk factor in the western countries characterized by a high socio-demographic index (Pennisi et al., 2019). NAFLD includes a spectrum of pathological conditions ranging from simple steatosis (NAFL) to steatohepatitis (NASH), which can lead to cirrhosis in approximately 9–20% of patients during 5–10 years and eventually in HCC (Bessone et al., 2019). In this scenario, it is worth mentioning that NASH and older age are expected to cause the most marked increase of primary liver cancer cases in 2030 (Liu et al., 2021).

NAFLD progression results from a complex integrated combination of different not yet fully elucidated pathogenic molecular events (Tilg and Moschen, 2010; Yilmaz, 2012). Inflammation in NASH is driven by liver cells and non-hepatic tissues, such as adipose tissue, which produce several pro-inflammatory cytokines (e.g., TGF-α, IL-1β, IL-6, IL-8) and chemokines (e.g., MCP-1). Inflammation has been associated with the development of liver fibrosis found in a high percentage of NASH patients (from 37 up to 84%) and is a negative prognostic factor. As for viral hepatitis, in NASH, resident hematopoietic stem cells (HSCs) are the primary effector cells responsible for ECM protein production, mainly of type I and type II collagen. Also, extrahepatic cells may play a role in modulating HSC-mediated pro-fibrotic effects, including sinusoidal endothelial cells and platelets. Indeed, platelet-derived growth factor (PDGF) is one of the most potent factors reported to: 1) stimulate HSC proliferation, differentiation, and migration; 2) promote HSC-mediated collagen production and deposition; 3) favor HSC transformation into myofibroblasts (Kocabayoglu et al., 2015). A significant increase in platelet number and

aggregates was found in livers of C57Bl/6 mice fed with a choline-deficient, high-fat diet compared with standard chow diet-fed animals (Malehmir et al., 2019). A similar result was described in NASH patients who displayed an increased number of platelets in the liver samples compared to healthy controls (Malehmir et al., 2019).

In the chronically injured liver, unresolved inflammation plays a predominant role in liver fibrosis by activating HSCs, which acquire the ability to migrate and accumulate at sites of tissue repair (Bataller and Brenner, 2005). Liver fibrosis is the excessive accumulation of extracellular matrix proteins, including collagen, occurring in most types of chronic liver disease. Advanced liver fibrosis results in cirrhosis, liver failure, and portal hypertension and often requires liver transplantation. Cirrhosis represents the higher risk factor for HCC (Marrero et al., 2018). In cirrhotic patients, HCC is the leading cause of death, with a reported annual incidence in the range of 1–6% (Trinchet et al., 2015).

Developing reliable noninvasive biomarkers for early detection of liver fibrosis and its eventual progression towards cirrhosis is an important goal to realize in this setting. Most importantly, the efficacy of antifibrotic drugs known to attenuate experimental liver fibrosis should be tested in humans (Bataller and Brenner, 2005).

Most patients with HCC are diagnosed at a late stage of the disease with a median survival of less than 1 year, whereas when detected at early-stage, patients can reach a survival rate of 70%, thanks to liver resection or transplant (Singal et al., 2014). During the last years, the incidence of NAFLD, the primary cause of chronic liver disease, has increased in association with the rise in the prevalence of other metabolic disorders and has reached a global prevalence of 25% (Younossi et al., 2016). About 10–20% of NAFLD patients progress towards NASH, leading to cirrhosis and liver-related mortality. HCC increases up to 5.29 per 1,000 person-years after NAFLD-to-NASH transition (Younossi et al., 2016).

Currently, liver biopsy represents the only accepted method to differentiate NASH from simple steatosis. However, liver biopsy can be considered neither an acceptable first-line investigation nor an acceptable method to monitor disease progression and/or drug response. It is associated with several risks, including potentially fatal bleeding and tumor seeding. On the other hand, proposed noninvasive steatosis biomarkers such as fatty liver index have shown limited clinical utility since they cannot quantify the presence of steatosis with the same accuracy as histological analysis (Haggar and Boushey, 2009).

A better understanding of the pathogenesis of NAFLD and the mechanisms underlying NALFD-to-NASH transition and related fibrosis is crucial for developing reliable, noninvasive biomarkers that allow early diagnosis and prognosis and monitor the progression of this complex pathological condition towards HCC.

Aspirin in the Prevention of HCC

Several epidemiological studies performed in the general population or selected patients have shown that Aspirin (at different doses) was associated with a significantly lower risk of HCC and liver-related mortality than no Aspirin use (Sahasrabuddhe et al., 2012; Petrick et al., 2015; Hwang et al., 2018; Simon et al., 2018; Lee et al., 2019; Simon et al., 2020).

Pooled analysis of two prospective United States cohort studies (the Nurses' Health Study and thistle Health Professionals Follow-up Study) (Colditz et al., 1986; Chasan-Taber et al., 1996) reported that regular Aspirin use [defined as consumption of two or more standard-dose (325-mg) Aspirin tablets per week] was associated with reduced HCC risk (adjusted HR, 0.51; 95% CI, 0.34–0.77) (Simon et al., 2018). This reduction of risk was dose-dependent [> 1.5 to 5 tablets per week (p = 0.006)] and time-dependent (becoming apparent when Aspirin was given for five or more years, $p = 0.03$). The protective effect of Aspirin was reported for individuals with or without cirrhosis. More recently, Simon et al. (2020) examined the impact of low-dose Aspirin (75 or 160 mg/day) on two primary outcomes, i.e., the incident HCC and liver-related mortality, in the Cancer and Cause of Death registries in Swedish adults with confirmed chronic hepatitis B or hepatitis C infection. A reduction of the estimated cumulative incidence of HCC was 31% at 7.9 years of follow-up versus nonusers. Liver-related mortality was also reduced by 27% in aspirin users versus nonusers. Lower risk of HCC was detected after 3–5 years of use. Aspirin benefits were not associated with a higher incidence of gastrointestinal bleeding (Simon et al., 2020).

In a retrospective Taiwan nationwide cohort study, HBV patients taking Aspirin (mainly 100 mg/day) showed a significant ($p < 0.001$) lower 5-year cumulative incidence of HCC versus the untreated group ($p < 0.001$) (Lee et al., 2019). The multivariable regression analysis showed that low-dose Aspirin represented an independent factor associated with a risk reduction of HCC development. However, older age, male sex, and liver cirrhosis were associated with a higher HCC risk. The use of antiviral medicines, such as nucleos(t)ide analog (NA) or statins, was associated with a lower HCC risk. The beneficial chemopreventive effect of Aspirin was evident after 2 years of aspirin therapy. In addition, the multivariable stratified analysis for aspirin therapy showed that statistical significance was not reached in several patient subgroups, including those with underlying cirrhosis, NA, and statin users. Some systematic reviews of published observational studies were recently performed to evaluate the association between the use of Aspirin and the incidence of HCC (Memel et al., 2020; Wang et al., 2020). It was confirmed that aspirin use significantly reduces the risk of HCC versus nonusers. The association between aspirin use and HCC risk was modestly or nonattenuated in populations with liver disease.

While several preclinical data suggest that Aspirin may protect against liver fibrosis (Yoshida et al., 2014; Li et al., 2017), clinical evidence of aspirin efficacy on fibrosis in patients with NAFLD remains scarce. Two cross-sectional studies were performed in NAFLD treated with Aspirin (Jiang et al., 2016; Devaki and McCullough, 2017). In Devaki's study, Aspirin administration was inversely associated with steatosis, defined by abdominal ultrasound. In Jiang's study, Aspirin treatment was associated with lower serum markers of hepatic fibrosis. However, these studies presented important limitations, such as the cross-sectional design and lack of hepatic histology at the severity

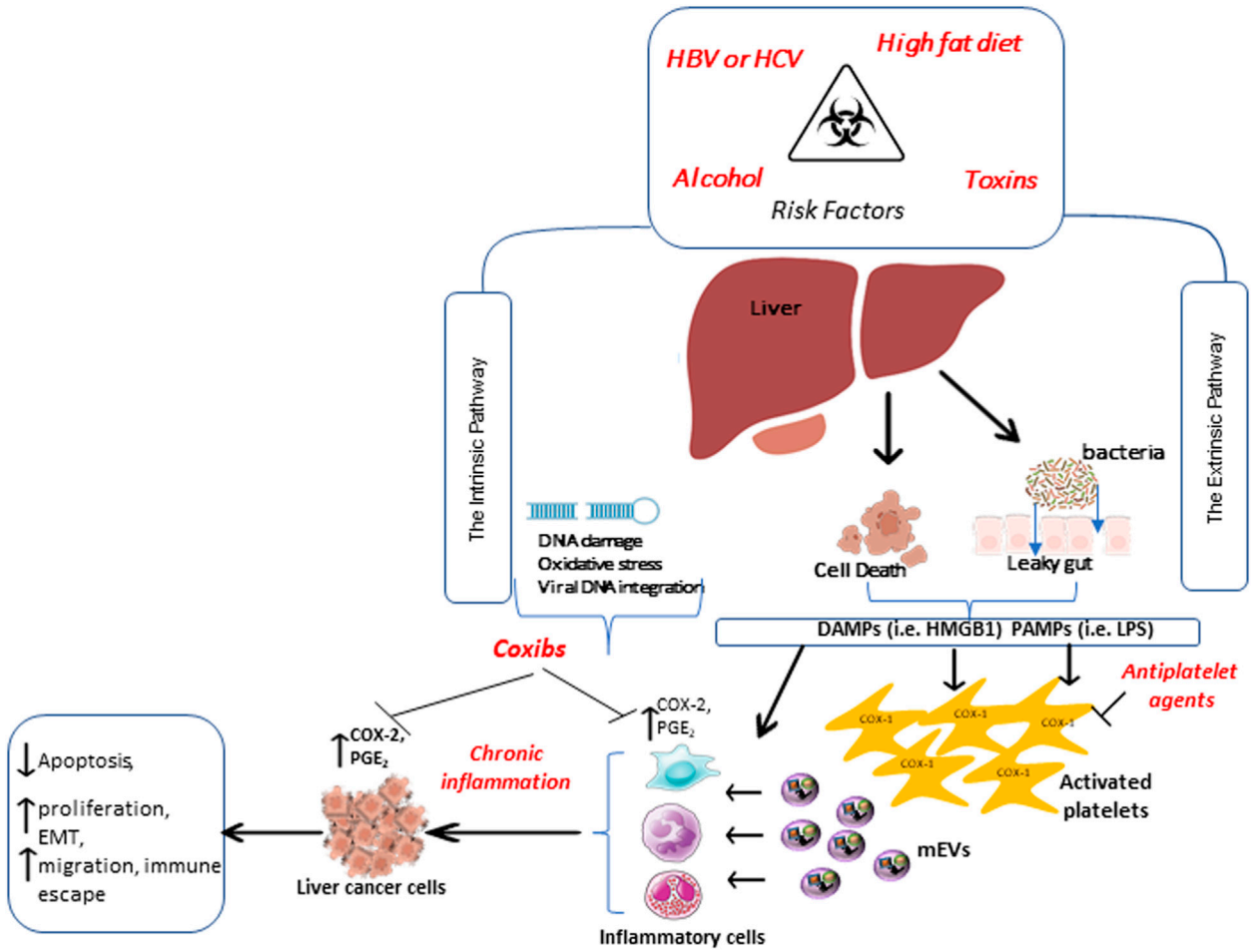

FIGURE 4 | Extrinsic and intrinsic pathways promote chronic inflammation involved in developing hepatocellular carcinoma. Two distinct pathways are involved in chronic inflammation during hepatocarcinogenesis. The extrinsic pathway is triggered by exogenous factors, such as pathogen-associated molecular patterns (PAMPs) or damage-associated molecular patterns (DAMPs) from dying cells. These, in turn, are recognized by specific receptors expressed in inflammatory cells and platelets. PAMPs and DAMPs activate platelets, which release medium-sized extracellular vesicles (mEVs) able to exit the vasculature, reach tissues, and sustain inflammation, thus increasing cancer risk. The intrinsic pathway, induced by alteration in cancer-associated genetic factors, activates the expression of inflammation-related programs, thus contributing to the generation and perpetuation of an inflammatory milieu. All these events further contribute to the overexpression of COX-2 and enhanced PGE_2 biosynthesis, promoting the transformation of normal epithelial cells to cancer. Antiplatelet drugs, such as low-dose Aspirin, can affect the early step of tumor development by inhibiting platelet function. In contrast, selective COX-2 inhibitors (coxibs) may exert an antitumor effect by inhibiting the synthesis of PGE_2 in leukocytes and tumor cells.

stage of NAFLD. Simon et al. (2019) performed a prospective cohort study of 361 adults with biopsy-confirmed NAFLD. They demonstrated that daily Aspirin administration was associated with less severe histologic features of NAFLD and NASH and a reduced risk for the progression to advanced fibrosis. These results were consistent in women and men, and the inverse relationship was duration-dependent. Similar associations were not found with nonaspirin NSAIDs users, i.e., anyone reporting nonaspirin NSAID use at least twice weekly or who received an NSAID prescription (i.e., ibuprofen, naproxen, ketoprofen, diclofenac, indomethacin) at least twice weekly.

In summary, the majority of the evidence linking aspirin use in the protection against NAFLD, NASH, or HCC arises from observational studies (Ricciotti et al., 2021). These studies often miss some critical information necessary to make mechanistic interpretations on aspirin effects, such as the dose and the duration of aspirin therapy, the safety, alcohol consumption, smoking habit, fibrosis stage, cancer stage, use of other potential chemopreventive drugs.

Experimental Evidence on the Role of Platelets in HCC

HCC represents a classic paradigm of inflammation-linked cancer, as more than 90% of HCCs arise in the context of hepatic injury and inflammation (El-Serag and Rudolph, 2007). Two distinct pathways can develop chronic inflammation during hepatocarcinogenesis (Yu et al., 2018) (**Figure 4**). The extrinsic pathway is driven by exogenous factors (e.g., the PAMPs from pathogens or DAMPs from

dead cells), triggering a persistent inflammatory response by engaging the receptors expressed in the inflammatory cells and establishing an inflammatory condition that increases cancer risk. Platelets possess receptors that respond to PAMPs and DAMPs; their activation triggers hemostatic and inflammatory responses against bacterial and viral infections (Jenne, 2014). Activated platelets produce mEVs during bacterial (Ogura et al., 2001) and viral infection (Mayne et al., 2012) that can exit the vasculature and enter tissues to activate immune and stromal cells to drive the inflammatory response further. For example, platelet mEVs enhance the expression of cell adhesion molecules such as leukocyte αMβ2 (Mac-1, CD11b/CD18) for monocyte adhesion (Barry et al., 1998). Levi et al. (2017) reported that platelet mEVs were significantly elevated in the blood of patients with HCC. Importantly, platelet-derived mEVs can induce the expression of marker genes of EMT in cancer cells and endothelial mesenchymal transition (EndMT) in human microvascular endothelial cells (Grande et al., 2019).

Altogether this knowledge sustains a central role of platelet activation in HCC. Numerous studies have been performed in mouse models to verify the impact of antiplatelet agents. In chronic HBV immune-mediated HCC, platelet activation contributed to the accumulation of virus-specific $CD8^+$ T cells and virus-nonspecific inflammatory cells in the liver. In this model, the administration of Aspirin and/or Clopidogrel [an antagonist of the platelet P2Y12 receptor for ADP (Ballerini et al., 2018)] reduced inflammation and immune cell infiltration (Sitia et al., 2012). The two drugs reduced liver fibrosis, HCC progression, and survival when co-administered. These effects were not associated with increased bleeding (Sitia et al., 2012). The antitumor effect of Aspirin and Clopidogrel was also confirmed in a recent study, where this combination prevented nonalcoholic steatohepatitis and subsequent HCC development in different dietary and genetic mouse models (Ribas et al., 2021). This study also found that another P2Y12 inhibitor, Ticagrelor, had a similar effect. Differently, nonaspirin NSAIDs did not affect the development of nonalcoholic steatohepatitis and HCC in this setting. The findings that the two antiplatelet agents (Aspirin and Clopidogrel) reduced liver fibrosis and HCC progression suggest that the inhibition of platelet activation was the central mechanism involved in their beneficial effects.

However, other studies performed *in vitro* and *in vivo* at supratherapeutic concentrations of Aspirin evidenced the capacity of the drug to cause extraplatelet effects (Ricciotti et al., 2021). Li et al. (2013) showed that 1 mM of Aspirin enhanced the anti-proliferative and pro-apoptotic action induced by IFN through the phosphorylation of STAT-1. In a xenograft model in nude mice, Aspirin (15 mg kg/day) reduced both tumor growth and the number of STAT1-expressing apoptotic cells present in the tumor (Li et al., 2013). Whether the dose of Aspirin administered to mice was selective for the platelets or caused systemic effects was not explored. In another study, Aspirin reduced the expression of collagen prolyl 4-hydroxylase α2 (P4HA2), the essential enzyme during collagen formation, in HCC cells (Wang et al., 2019). Also, in this study, the *in vitro* effects were studied at millimolar concentrations of Aspirin, which are supratherapeutic. In xenograft mice, Aspirin used at a high dose (75 mg/kg/day) affected P4HA2 to decrease collagen deposition, inhibiting liver tumor growth. In contrast, mice overexpressing P4HA2 had increased collagen deposition in the liver and larger tumor size than wild-type xenograft mice (Wang et al., 2019).

To summarize, the efficacy demonstrated by different antiplatelet agents convincingly supports the platelets' hypothesis in the development of HCC. In contrast, some studies performed *in vitro* in cell cultures or *in vivo* in animal models with Aspirin used very high concentrations/doses, which are not reached even after administering anti-inflammatory doses of Aspirin. Although these studies are not appropriate to clarify the mechanism of the apparent anticancer effect of Aspirin detected in clinical studies, their results have evidenced possible new targets for developing novel therapies to prevent and treat HCC.

The other pathway contributing to developing chronic inflammation during hepatocarcinogenesis is the intrinsic one (Yu et al., 2018) induced by alterations in cancer-associated genetic factors (e.g., mutation of either oncogenes or tumor suppressor genes), which activate the expression of inflammation-related programs (**Figure 4**). In this scenario, the upregulation of COX-2 is noteworthy. COX-2 expression is increased in injured livers and human HCC (Shiota et al., 1999; Cheng et al., 2004) and is associated with reduced overall survival in HCC (Chen et al., 2016). *In vitro* and *in vivo*, COX-2 inhibition constrains cell growth of liver cancer cells due to the inflammation reduction and apoptosis induction (Foderà et al., 2004; Fredriksson et al., 2011; Chu et al., 2018). Thus, the coxibs could be effective in HCC prevention and progression, but the possible increased cardiovascular risk associated with their use limit this therapeutic strategy. The development of drug target therapies with anti-inflammatory agents could be an exciting approach to develop safer and more effective treatments.

LIQUID BIOPSY AND DRUG DELIVERY SYSTEM DEVELOPMENT: THE CONTRIBUTION OF PLATELETS

In oncology, although highly informative, the canonical analysis of tumor tissue provides a static and partial image of a pathological condition in continuous transformation, and it does not consider the evolution and time in which the disease has developed. A reliable and comprehensive characterization of tumor cell genetic profile may guide the choice of drug treatments based on the individual patient characteristics toward a more effective and safer personalized therapy approach. However, the development of noninvasive biomarkers of early disease detection is not completely realized.

In the last few years, the suitability of liquid biopsy has opened the way to novel strategies to provide valuable information about tumor biology (Pantel and Speicher, 2016). Liquid biopsy is minimally invasive allows for longitudinal monitoring of disease progression and assessment of therapy failure/resistance even before clinical or radiographic progression is

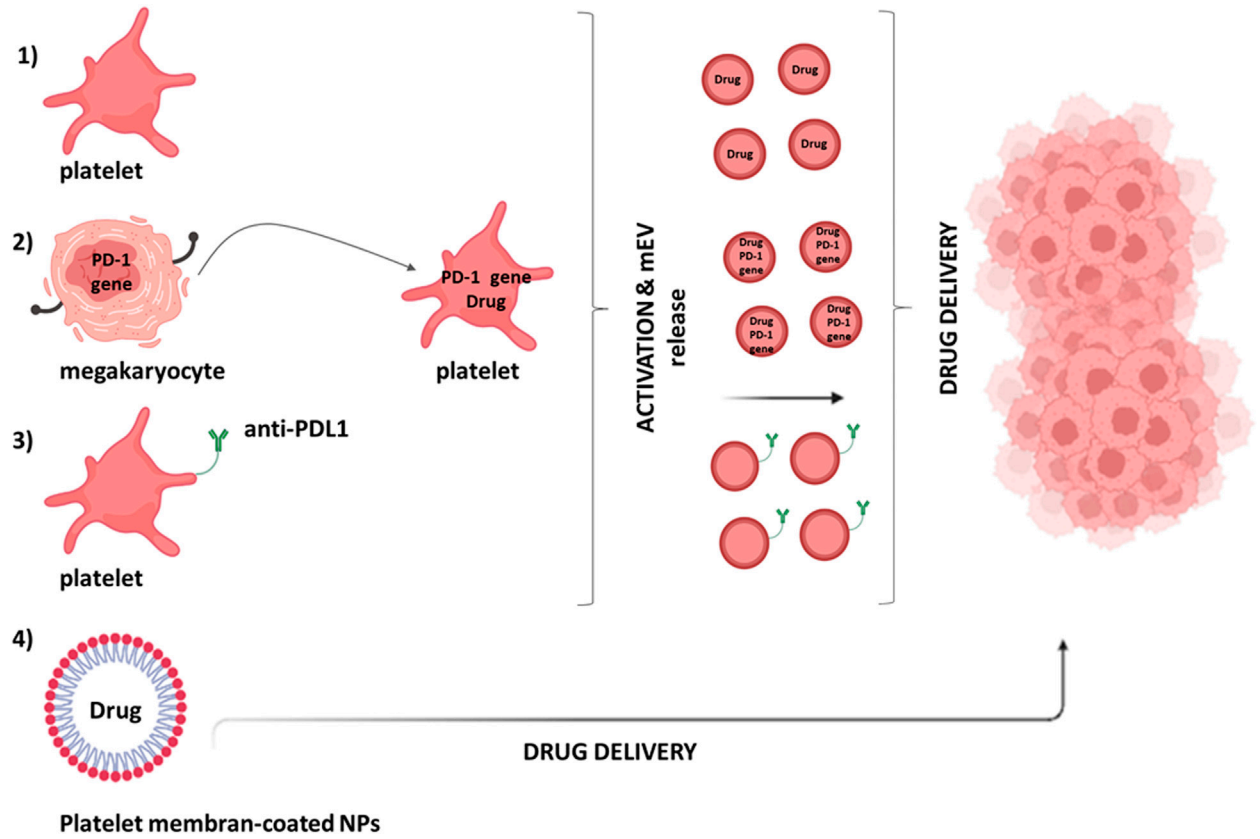

FIGURE 5 | Platelet's contribution in drug delivery systems. Different approaches can be used to deliver drugs to the tumor microenvironment by platelets: (1) platelets can be loaded with the anticancer drug via the open canalicular system; (2) genetically modified megakaryocytes (MKs) can give rise to mature platelets expressing programmed death-1 (PD-1) [involved in the immune checkpoint PD-1/programmed death-ligand 1 (PDL-1)] that can also be loaded with the anticancer drug; (3) monoclonal antibodies against PDL-1 (aPDL1) can be covalently bound to resting platelets; (4) melanin nanoparticles (MNPs) can be coated with platelet membranes.

evident; its use can improve cancer patients survival chances (Roschewski et al., 2016). Primary sources of liquid biopsy for biomarker detection include circulating free DNA (cfDNA) or circulating tumor DNA (ctDNA), circulating tumor cells (CTCs), extracellular vesicles, and recently platelets (Aravanis et al., 2017; Babayan and Pantel, 2018; Best et al., 2018; Heitzer et al., 2019).

Best et al. (2015) explored the possible analysis of TEPs to acquire information about the clinical condition of individuals. TEP RNA assessment can serve as a biomarker trove to detect and classify cancer via self-learning support vector machine (SVM)-based algorithms (Best et al., 2015); this highly multiplexed biomarker signature detection platform is called thromboSeq. They also investigated the potential and origin of spliced RNA profiles from TEPs for the noninvasive detection of early- and late-stage non-small-cell lung cancer (NSCLC) (Best et al., 2017). Biomarker panels to discriminate patients with NSCLC from healthy individuals and patients with various noncancerous inflammatory conditions were identified using particle-swarm optimization (PSO) driven algorithms (Best et al., 2017). The biological mechanisms responsible for TEP RNA signatures remain to be identified. However, it can be involved: 1) altered megakaryocytic RNA expression, 2) enrichment of reticulated platelets in patients with NSCLC, 3) induction of splicing, possibly partially mediated by RNA-binding protein (RBP) activity and upstream regulatory kinases such as CLK, 4) sequestration of RNAs and 5) alternative splicing events (Best et al., 2017).

A study by Clancy et al. proposed the existence of an RNA profile that discriminates platelets over their half-life (Clancy et al., 2017), distinguishing old platelets from the young ones based on their size. Notably, cancer patients show larger platelets than healthy subjects, and these platelets exhibit an abundance of genes that regulate homeostasis. These changes could explain the increased thrombotic potential in cancer (Clancy et al., 2017).

Platelets are active players in tumor progression (Patrignani and Patrono, 2016; Patrignani and Patrono, 2018). Among the numerous mechanisms described, the ability of platelets to extravasate into the tumor microenvironment is notable (Morrell et al., 2014). Once there, platelets interact with tumor cells and promote the metastatic process by many mechanisms, including EMT and COX-2 induction (Kalluri and Weinberg, 2009; Dovizio et al., 2013; Guillem-Llobat et al., 2016).

Due to their propensity to interact with cancer cells, platelets have aroused great interest in developing cell-based strategies for

drug delivery (Dovizio et al., 2020). Platelet-based approaches to drug delivery depend on: 1) low invasiveness during platelet collection from patients; 2) possibility of *in vitro* manipulation and reintroduction in the patient; 3) relatively long half-life (8–10 days), which could improve the pharmacokinetics of some drugs (Ziegler et al., 2017). Platelets can act as carriers of potent anticancer drugs such as Doxorubicin, which inhibits topoisomerase II (Sarkar et al., 2013) (**Figure 5**). The doxorubicin-loaded platelet delivery system effectively treated lymphoma by reducing tumor size in a mouse model obtained after injection of Burkitt lymphoma cells (Xu et al., 2017).

The application of genetic engineering to modify platelets for drug delivery applications is limited because platelets are anucleated and fully differentiated. However, their progenitor or precursor cells can be manipulated to obtain modified platelets for well-defined applications (Sim et al., 2017). Genetically modified megakaryocytes (MKs) have been created that can give rise to mature platelets expressing programmed death-1 (PD-1) and loaded with cyclophosphamide, an inhibitor of regulatory T cells (Treg) (Scurr et al., 2018) (**Figure 5**). In a mouse model transplanted with B16F10 melanoma tumor cells, these platelets, expressing PD1, blocked PDL-1, thus inhibiting the activity of immunosuppressive Tregs and were able to promote the anticancer activity of $CD8^+$ T lymphocytes (Scurr et al., 2018).

On the other hand, platelets have numerous binding sites on their plasma membrane and can also be non-engineered to act as drug carriers (**Figure 5**). One example is monoclonal antibodies against programmed death-ligand 1 (aPDL1) covalently bound to resting platelets (Wang et al., 2017) released via the formation of mEVs. The administration of platelet-bound anti-PDL1 significantly reduced tumor recurrence and increased survival in experimental metastasis models (Wang et al., 2017).

To further improve their targetability, the surface of platelets was embellished with HSCs (Hu et al., 2018). These modifications induced a lack of platelet-HSC aggregation, enhancing the immune response and inhibiting leukemia progression.

Recently, nanoparticles coated with platelet membranes have been considered for drug delivery (**Figure 5**). Thus, melanin nanoparticles (MNPs) and Doxorubicin (DOX) were encapsulating inside platelet-derived vesicles coupled with the RGD peptide on the surface (Jing et al., 2018). They effectively suppressed tumor growth in a model where MDA-MB-231/ADR cells (adriamycin-resistant breast cancer cells) were subcutaneously implanted in BALB/c nude mice (Jing et al., 2018). Platelet membrane-coated nanoparticles have also been used in radiotherapy to improve the treatment of solid tumors; their use in a mouse model of breast cancer leads to a significant reduction in the mass and volume of the tumor itself (Chen et al., 2019).

CONCLUSION AND PERSPECTIVES

Considerable experimental and clinical evidence sustains chronic inflammation as an essential cancer driver. However, developing an anti-inflammatory therapy is particularly challenging in oncology (Nathan and Ding, 2010). Potent inhibitors of inflammation can lead to the possibility of increasing the risk of infections. Coxibs' use can be associated with an enhanced risk of thrombotic events (Grosser et al., 2006). In the CANTOS trial (Canakinumab Anti-inflammatory Thrombosis Outcomes Study) (Ridker et al., 2017), Canakinumab, an IL-1β-neutralizing antibody, significantly diminished cardiovascular event rates, and the retrospective analysis showed a marked reduction (50%) in lung cancer incidence, particularly at the high-dose. However, the use of Canakinumab as a first-, second-, or third-line treatment with chemotherapy in NSCLC did not confirm the benefit (CANOPY-1 and CANOPY-2 trials) (https://bit.ly/3l0IISp). However, subgroup analysis showed a potential anticancer effect on individuals with circulating inflammation biomarkers.

The development of noninvasive biomarkers predictive of disease susceptibility or drug response is still an unmet clinical need. A range of cancer biomarkers can be found in TEPs, but their utility warrants further prospective validation (Antunes-Ferreira et al., 2021). In particular, it remains to define and validate specific and reproducible transcriptomic profiles associated with cancer that distinguish from noncancerous processes and therapeutics (such as antiplatelet agents and anticoagulants) (Antunes-Ferreira et al., 2021).

A crucial clinical need is the development of drug delivery technologies for anti-inflammatory and chemotherapeutic agents to improve safety and efficacy by enhancing the delivery of a therapeutic to its target site, minimizing off-target accumulation, and facilitating patient compliance (Vargason et al., 2021). An interesting approach can be via platelet-mediated drug delivery systems by exploiting the platelet's ability to interact with tumor cells and transfer their molecular cargo (Dovizio et al., 2020).

Novel disease mechanisms have been proposed in CRC and HCC, enlightening the contribution of platelets in the triggering and maintaining an unresolved state of inflammation (i.e., chronic inflammation) (Patrignani and Patrono, 2016; Dovizio et al., 2017; Patrignani and Patrono, 2018). This knowledge opens the way to novel therapeutic strategies with antiplatelet agents and compounds interfering with the platelet-derived mEV uptake and cargo delivery to recipient cells. Developing personalized therapies with low-dose Aspirin and other antiplatelet agents is necessary to improve anticancer efficacy and reduce the major bleeding associated with their use.

Future clinical studies should be performed incorporating clinical and biomarker endpoints analyzed with a systems biology approach which will allow identifying dynamic systems modeling of candidate pathways involved in the antineoplastic effect of chemotherapeutic agents. This strategy will also identify susceptibility profiles for efficacy and toxicity of drug treatments in cancer.

AUTHOR CONTRIBUTIONS

The conception of work: PB, PP; design of work: PB and PP; Writing-original draft preparation: PB, AC, AB, ST, PP; writing-review and editing: PB, MM, ST, PP; funding

acquisition: PP, PB; final approval of work: all authors have read and agreed to the published version of the manuscript.

FUNDING

This review was funded by Associazione Italiana per la Ricerca sul Cancro (AIRC) (IG 2017-ID. 20365 Project; Principal Investigator PP). In addition, this review was conducted on Behalf of the Aspirin for Cancer Prevention Group (AsCaP), Wolfson Institute of Preventive Medicine, Queen Mary School of Medicine and Dentistry, University of London, United Kingdom. This study was funded by Ministero dell'Istruzione, dell'Università e della Ricerca (MIUR) (Fondi per la Ricerca Scientifica di Ateneo, (ex 60%)) to PB.

REFERENCES

Akinyemiju, T., Akinyemiju, T., Abera, S., Ahmed, M., Alam, N., Alemayohu, M. A., et al. (2017). The Burden of Primary Liver Cancer and Underlying Etiologies from 1990 to 2015 at the Global, Regional, and National Level: Results from the Global Burden of Disease Study 2015. *JAMA Oncol.* 3, 1683–1691. doi:10.1001/jamaoncol.2017.3055

Alfonso, L., Ai, G., Spitale, R. C., and Bhat, G. J. (2014). Molecular Targets of Aspirin and Cancer Prevention. *Br. J. Cancer* 111, 61–67. doi:10.1038/bjc.2014.271

Antunes-Ferreira, M., Koppers-Lalic, D., and Würdinger, T. (2021). Circulating Platelets as Liquid Biopsy Sources for Cancer Detection. *Mol. Oncol.* 15, 1727–1743. doi:10.1002/1878-0261.12859

Aravanis, A. M., Lee, M., and Klausner, R. D. (2017). Next-Generation Sequencing of Circulating Tumor DNA for Early Cancer Detection. *Cell* 168, 571–574. doi:10.1016/j.cell.2017.01.030

Babayan, A., and Pantel, K. (2018). Advances in Liquid Biopsy Approaches for Early Detection and Monitoring of Cancer. *Genome Med.* 10, 21. doi:10.1186/s13073-018-0533-6

Ballerini, P., Dovizio, M., Bruno, A., Tacconelli, S., and Patrignani, P. (2018). P2Y12 Receptors in Tumorigenesis and Metastasis. *Front. Pharmacol.* 9, 66. doi:10.3389/fphar.2018.00066

Baron, J. A., Cole, B. F., Sandler, R. S., Haile, R. W., Ahnen, D., Bresalier, R., et al. (2003). A Randomized Trial of Aspirin to Prevent Colorectal Adenomas. *N. Engl. J. Med.* 348, 891–899. doi:10.1056/NEJMoa021735

Barry, O. P., Praticò, D., Savani, R. C., and FitzGerald, G. A. (1998). Modulation of Monocyte-Endothelial Cell Interactions by Platelet Microparticles. *J. Clin. Invest.* 102, 136–144. doi:10.1172/JCI2592

Bataller, R., and Brenner, D. A. (2005). Liver Fibrosis. *J. Clin. Invest.* 115, 209–218. doi:10.1172/JCI24282

Benamouzig, R., Deyra, J., Martin, A., Girard, B., Jullian, E., Piednoir, B., et al. (2003). Daily Soluble Aspirin and Prevention of Colorectal Adenoma Recurrence: One-Year Results of the APACC Trial. *Gastroenterology* 125, 328–336. doi:10.1016/s0016-5085(03)00887-4

Benamouzig, R., Uzzan, B., Deyra, J., Martin, A., Girard, B., Little, J., et al. (2012). Prevention by Daily Soluble Aspirin of Colorectal Adenoma Recurrence: 4-year Results of the APACC Randomised Trial. *Gut* 61, 255–261. doi:10.1136/gutjnl-2011-300113

Bergmeier, W., and Hynes, R. O. (2012). Extracellular Matrix Proteins in Hemostasis and Thrombosis. *Cold Spring Harb Perspect. Biol.* 4, a005132. doi:10.1101/cshperspect.a005132

Bertagnolli, M. M., Eagle, C. J., Zauber, A. G., Redston, M., Solomon, S. D., Kim, K., et al. (2006). Celecoxib for the Prevention of Sporadic Colorectal Adenomas. *N. Engl. J. Med.* 355, 873–884. doi:10.1056/NEJMoa061355

Bessone, F., Razori, M. V., and Roma, M. G. (2019). Molecular Pathways of Nonalcoholic Fatty Liver Disease Development and Progression. *Cell Mol Life Sci* 76, 99–128. doi:10.1007/s00018-018-2947-0

Best, M. G., Sol, N., In 't Veld, S. G. J. G., Vancura, A., Muller, M., Niemeijer, A. N., et al. (2017). Swarm Intelligence-Enhanced Detection of Non-small-cell Lung Cancer Using Tumor-Educated Platelets. *Cancer Cell* 32, 238–e9. doi:10.1016/j.ccell.2017.07.004

Best, M. G., Sol, N., Kooi, I., Tannous, J., Westerman, B. A., Rustenburg, F., et al. (2015). RNA-seq of Tumor-Educated Platelets Enables Blood-Based Pan-Cancer, Multiclass, and Molecular Pathway Cancer Diagnostics. *Cancer Cell* 28, 666–676. doi:10.1016/j.ccell.2015.09.018

Best, M. G., Wesseling, P., and Wurdinger, T. (2018). Tumor-Educated Platelets as a Noninvasive Biomarker Source for Cancer Detection and Progression Monitoring. *Cancer Res.* 78, 3407–3412. doi:10.1158/0008-5472.CAN-18-0887

ASCEND Study Collaborative GroupBowman, L., Bowman, L., Mafham, M., Wallendszus, K., Stevens, W., Buck, G., et al. (2018). Effects of Aspirin for Primary Prevention in Persons with Diabetes Mellitus. *N. Engl. J. Med.* 379, 1529–1539. doi:10.1056/NEJMoa1804988

Bray, F., Ferlay, J., Ervik, M., Lam, F., Colombet, M., Mery, L., et al. (2018). *GLOBOCAN 2018, Global and Regional Estimates of the Incidence and Mortality for 36 Cancers Global Cancer Observatory: Cancer Today*. Lyon: International Agency for Research on Cancer.

Bresalier, R. S., Sandler, R. S., Quan, H., Bolognese, J. A., Oxenius, B., Horgan, K., et al. (2005). Cardiovascular Events Associated with Rofecoxib in a Colorectal Adenoma Chemoprevention Trial. *N. Engl. J. Med.* 352, 1092–1102. doi:10.1056/NEJMoa050493

Burn, J., Bishop, D. T., Chapman, P. D., Elliott, F., Bertario, L., Dunlop, M. G., et al. (2011). A Randomized Placebo-Controlled Prevention Trial of Aspirin And/or Resistant Starch in Young People with Familial Adenomatous Polyposis. *Cancer Prev. Res. (Phila)* 4, 655–665. doi:10.1158/1940-620710.1158/1940-6207.CAPR-11-0106

Burn, J., Sheth, H., Elliott, F., Reed, L., Macrae, F., Mecklin, J. P., et al. (2020). Cancer Prevention with Aspirin in Hereditary Colorectal Cancer (Lynch Syndrome), 10-year Follow-Up and Registry-Based 20-year Data in the CAPP2 Study: a Double-Blind, Randomised, Placebo-Controlled Trial. *Lancet* 395, 1855–1863. doi:10.1016/S0140-6736(20)30366-4

Burnouf, T., Goubran, H. A., Chou, M. L., Devos, D., and Radosevic, M. (2014). Platelet Microparticles: Detection and Assessment of Their Paradoxical Functional Roles in Disease and Regenerative Medicine. *Blood Rev.* 28, 155–166. doi:10.1016/j.blre.2014.04.002

Capone, M. L., Tacconelli, S., Sciulli, M. G., Grana, M., Ricciotti, E., Minuz, P., et al. (2004). Clinical Pharmacology of Platelet, Monocyte, and Vascular Cyclooxygenase Inhibition by Naproxen and Low-Dose Aspirin in Healthy Subjects. *Circulation* 109, 1468–1471. doi:10.1161/01.CIR.0000124715.27937.78

Carter, M. J., Lobo, A. J., and Travis, S. P.IBD Section, British Society of Gastroenterology (2004). Guidelines for the Management of Inflammatory Bowel Disease in Adults. *Gut* 53 Suppl 5, V1–V16. doi:10.1136/gut.2004.043372

Charman, W. N., Charman, S. A., Monkhouse, D. C., Frisbee, S. E., Lockhart, E. A., Weisman, S., et al. (1993). Biopharmaceutical Characterisation of a Low-Dose (75 Mg) Controlled-Release Aspirin Formulation. *Br. J. Clin. Pharmacol.* 36, 470–473. doi:10.1111/j.1365-2125.1993.tb00399.x

Chasan-Taber, S., Rimm, E. B., Stampfer, M. J., Spiegelman, D., Colditz, G. A., Giovannucci, E., et al. (1996). Reproducibility and Validity of a Self-Administered Physical Activity Questionnaire for Male Health Professionals. *Epidemiology* 7, 81–86. doi:10.1097/00001648-199601000-00014

Chen, G., Li, X., Yang, J., Li, J., Wang, X., He, J., et al. (2016). Prognostic Significance of Cyclooxygenase-2 Expression in Patients with Hepatocellular Carcinoma: a Meta-Analysis. *Arch. Med. Sci.* 12, 1110–1117. doi:10.5114/aoms.2016.61916

Chen, Y., Zhao, G., Wang, S., He, Y., Han, S., Du, C., et al. (2019). Platelet-membrane-camouflaged Bismuth Sulfide Nanorods for Synergistic Radio-Photothermal Therapy against Cancer. *Biomater. Sci.* 7, 3450–3459. doi:10.1039/c9bm00599d

Cheng, A. S., Chan, H. L., Leung, W. K., To, K. F., Go, M. Y., Chan, J. Y., et al. (2004). Expression of HBx and COX-2 in Chronic Hepatitis B, Cirrhosis and Hepatocellular Carcinoma: Implication of HBx in Upregulation of COX-2. *Mod. Pathol.* 17, 1169–1179. doi:10.1038/modpathol.3800196

Chu, T. H., Chan, H. H., Hu, T. H., Wang, E. M., Ma, Y. L., Huang, S. C., et al. (2018). Celecoxib Enhances the Therapeutic Efficacy of Epirubicin for Novikoff Hepatoma in Rats. *Cancer Med.* 7, 2567–2580. doi:10.1002/cam4.1487

Clancy, L., Beaulieu, L. M., Tanriverdi, K., and Freedman, J. E. (2017). The Role of RNA Uptake in Platelet Heterogeneity. *Thromb. Haemost.* 117, 948–961. doi:10.1160/TH16-11-0873

Colditz, G. A., Martin, P., Stampfer, M. J., Willett, W. C., Sampson, L., Rosner, B., et al. (1986). Validation of Questionnaire Information on Risk Factors and Disease Outcomes in a Prospective Cohort Study of Women. *Am. J. Epidemiol.* 123, 894–900. doi:10.1093/oxfordjournals.aje.a114319

Contursi, A., Sacco, A., Grande, R., Dovizio, M., and Patrignani, P. (2017). Platelets as Crucial Partners for Tumor Metastasis: from Mechanistic Aspects to Pharmacological Targeting. *Cell Mol Life Sci* 74, 3491–3507. doi:10.1007/s00018-017-2536-7

Contursi, A., Schiavone, S., Dovizio, M., Hinz, C., Fullone, R., Tacconelli, S., et al. (2021). Platelets Induce Free and Phospholipid-Esterified 12-hydroxyeicosatetraenoic Acid Generation in colon Cancer Cells by Delivering 12-lipoxygenase. *J. Lipid Res.* 62, 100109. doi:10.1016/j.jlr.2021.100109

Cook, N. R., Lee, I. M., Gaziano, J. M., Gordon, D., Ridker, P. M., Manson, J. E., et al. (2005). Low-dose Aspirin in the Primary Prevention of Cancer: the Women's Health Study: a Randomized Controlled Trial. *JAMA* 294, 47–55. doi:10.1001/jama.294.1.47

Coussens, L. M., and Werb, Z. (2002). Inflammation and Cancer. *Nature* 420, 860–867. doi:10.1038/nature01322

Coyle, C., Cafferty, F. H., Rowley, S., MacKenzie, M., Berkman, L., Gupta, S., et al. (2016). ADD-ASPIRIN: A Phase III, Double-Blind, Placebo Controlled, Randomised Trial Assessing the Effects of Aspirin on Disease Recurrence and Survival after Primary Therapy in Common Non-metastatic Solid Tumours. *Contemp. Clin. Trials* 51, 56–64. doi:10.1016/j.cct.2016.10.004

Cuzick, J., Otto, F., Baron, J. A., Brown, P. H., Burn, J., Greenwald, P., et al. (2009). Aspirin and Non-steroidal Anti-inflammatory Drugs for Cancer Prevention: an International Consensus Statement. *Lancet Oncol.* 10, 501–507. doi:10.1016/S1470-2045(09)70035-X

Davì, G., and Patrono, C. (2007). Platelet Activation and Atherothrombosis. *N. Engl. J. Med.* 357, 2482–2494. doi:10.1056/NEJMra071014

Devaki, P., and McCullough, A. (2017). Association between Aspirin and Statin Use and the Prevalence of Non-alcoholic Fatty Liver Disease: A Cross Sectional Study from National Health and Nutrition Examination Survey (1999-2012). *Gastroenterology* 152, S1202–S1203. doi:10.1016/s0016-5085(17)34005-2

Dilly, A. K., Ekambaram, P., Guo, Y., Cai, Y., Tucker, S. C., Fridman, R., et al. (2013). Platelet-type 12-lipoxygenase Induces MMP9 Expression and Cellular Invasion via Activation of PI3K/Akt/NF-Kb. *Int. J. Cancer* 133, 1784–1791. doi:10.1002/ijc.28165

Dovizio, M., Bruno, A., Contursi, A., Grande, R., and Patrignani, P. (2018). Platelets and Extracellular Vesicles in Cancer: Diagnostic and Therapeutic Implications. *Cancer Metastasis Rev.* 37, 455–467. doi:10.1007/s10555-018-9730-4

Dovizio, M., Maier, T. J., Alberti, S., Di Francesco, L., Marcantoni, E., Münch, G., et al. (2013). Pharmacological Inhibition of Platelet-Tumor Cell Cross-Talk Prevents Platelet-Induced Overexpression of Cyclooxygenase-2 in HT29 Human colon Carcinoma Cells. *Mol. Pharmacol.* 84, 25–40. doi:10.1124/mol.113.084988

Dovizio, M., Sacco, A., and Patrignani, P. (2017). Curbing Tumorigenesis and Malignant Progression through the Pharmacological Control of the Wound Healing Process. *Vascul Pharmacol.* 89, 1–11. doi:10.1016/j.vph.2017.01.003

Dovizio, M., Tacconelli, S., Ricciotti, E., Bruno, A., Maier, T. J., Anzellotti, P., et al. (2012). Effects of Celecoxib on Prostanoid Biosynthesis and Circulating Angiogenesis Proteins in Familial Adenomatous Polyposis. *J. Pharmacol. Exp. Ther.* 341, 242–250. doi:10.1124/jpet.111.190785

Dovizio, M., Ballerini, P., Fullone, R., Tacconelli, S., Contursi, A., and Patrignani, P. (2020). Multifaceted Functions of Platelets in Cancer: From Tumorigenesis to Liquid Biopsy Tool and Drug Delivery System. *Ijms* 21, 9585. doi:10.3390/ijms21249585

El-Serag, H. B., and Rudolph, K. L. (2007). Hepatocellular Carcinoma: Epidemiology and Molecular Carcinogenesis. *Gastroenterology* 132, 2557–2576. doi:10.1053/j.gastro.2007.04.061

Fearon, E. R., and Vogelstein, B. (1990). A Genetic Model for Colorectal Tumorigenesis. *Cell* 61, 759–767. doi:10.1016/0092-8674(90)90186-i

Foderà, D., D'Alessandro, N., Cusimano, A., Poma, P., Notarbartolo, M., Lampiasi, N., et al. (2004). Induction of Apoptosis and Inhibition of Cell Growth in Human Hepatocellular Carcinoma Cells by COX-2 Inhibitors. *Ann. N. Y Acad. Sci.* 1028, 440–449. doi:10.1196/annals.1322.052

Fredriksson, L., Herpers, B., Benedetti, G., Matadin, Q., Puigvert, J. C., de Bont, H., et al. (2011). Diclofenac Inhibits Tumor Necrosis Factor-α-Induced Nuclear Factor-Kb Activation Causing Synergistic Hepatocyte Apoptosis. *Hepatology* 53, 2027–2041. doi:10.1002/hep.24314

Furman, D., Campisi, J., Verdin, E., Carrera-Bastos, P., Targ, S., Franceschi, C., et al. (2019). Chronic Inflammation in the Etiology of Disease across the Life Span. *Nat. Med.* 25, 1822–1832. doi:10.1038/s41591-019-0675-0

Gawaz, M., Langer, H., and May, A. E. (2005). Platelets in Inflammation and Atherogenesis. *J. Clin. Invest.* 115, 3378–3384. doi:10.1172/JCI27196

Gay, L. J., and Felding-Habermann, B. (2011). Contribution of Platelets to Tumour Metastasis. *Nat. Rev. Cancer* 11, 123–134. doi:10.1038/nrc3004

Gaziano, J. M., Brotons, C., Coppolecchia, R., Cricelli, C., Darius, H., Gorelick, P. B., et al. (2018). Use of Aspirin to Reduce Risk of Initial Vascular Events in Patients at Moderate Risk of Cardiovascular Disease (ARRIVE): a Randomised, Double-Blind, Placebo-Controlled Trial. *Lancet* 392, 1036–1046. doi:10.1016/S0140-6736(18)31924-X

Giovannucci, E., Egan, K. M., Hunter, D. J., Stampfer, M. J., Colditz, G. A., Willett, W. C., et al. (1995). Aspirin and the Risk of Colorectal Cancer in Women. *N. Engl. J. Med.* 333, 609–614. doi:10.1056/NEJM199509073331001

Grande, R., Dovizio, M., Marcone, S., Szklanna, P. B., Bruno, A., Ebhardt, H. A., et al. (2019). Platelet-Derived Microparticles from Obese Individuals: Characterization of Number, Size, Proteomics, and Crosstalk with Cancer and Endothelial Cells. *Front. Pharmacol.* 10, 7. doi:10.3389/fphar.2019.00007

Grazioso, T. P., Brandt, M., and Djouder, N. (2019). Diet, Microbiota, and Colorectal Cancer. *iScience* 21, 168–187. doi:10.1016/j.isci.2019.10.011

Grivennikov, S. I., Greten, F. R., and Karin, M. (2010). Immunity, Inflammation, and Cancer. *Cell* 140, 883–899. doi:10.1016/j.cell.2010.01.025

Grosser, T., Fries, S., and FitzGerald, G. A. (2006). Biological Basis for the Cardiovascular Consequences of COX-2 Inhibition: Therapeutic Challenges and Opportunities. *J. Clin. Invest.* 116, 4–15. doi:10.1172/JCI27291

Guillem-Llobat, P., Dovizio, M., Bruno, A., Ricciotti, E., Cufino, V., Sacco, A., et al. (2016). Aspirin Prevents Colorectal Cancer Metastasis in Mice by Splitting the Crosstalk between Platelets and Tumor Cells. *Oncotarget* 7, 32462–32477. doi:10.18632/oncotarget.8655

Haggar, F. A., and Boushey, R. P. (2009). Colorectal Cancer Epidemiology: Incidence, Mortality, Survival, and Risk Factors. *Clin. Colon Rectal Surg.* 22, 191–197. doi:10.1055/s-0029-1242458

Hai, H., Tamori, A., and Kawada, N. (2014). Role of Hepatitis B Virus DNA Integration in Human Hepatocarcinogenesis. *World J. Gastroenterol.* 20, 6236–6243. doi:10.3748/wjg.v20.i20.6236

Hanahan, D., and Weinberg, R. A. (2011). Hallmarks of Cancer: the Next Generation. *Cell* 144, 646–674. doi:10.1016/j.cell.2011.02.013

Heitzer, E., Haque, I. S., Roberts, C. E. S., and Speicher, M. R. (2019). Current and Future Perspectives of Liquid Biopsies in Genomics-Driven Oncology. *Nat. Rev. Genet.* 20, 71–88. doi:10.1038/s41576-018-0071-5

Herszenyi, L., Miheller, P., and Tulassay, Z. (2007). Carcinogenesis in Inflammatory Bowel Disease. *Dig. Dis.* 25, 267–269. doi:10.1159/000103898

Hu, Q., Sun, W., Wang, J., Ruan, H., Zhang, X., Ye, Y., et al. (2018). Conjugation of Haematopoietic Stem Cells and Platelets Decorated with Anti-PD-1 Antibodies Augments Anti-leukaemia Efficacy. *Nat. Biomed. Eng.* 2, 831–840. doi:10.1038/s41551-018-0310-2

Hwang, I. C., Chang, J., Kim, K., and Park, S. M. (2018). Aspirin Use and Risk of Hepatocellular Carcinoma in a National Cohort Study of Korean Adults. *Sci. Rep.* 8, 4968. doi:10.1038/s41598-018-23343-0

Ishikawa, H., Mutoh, M., Sato, Y., Doyama, H., Tajika, M., Tanaka, S., et al. (2021). Chemoprevention with Low-Dose Aspirin, Mesalazine, or Both in Patients with Familial Adenomatous Polyposis without Previous Colectomy (J-FAPP Study IV): a Multicentre, Double-Blind, Randomised, Two-By-Two Factorial Design Trial. *Lancet Gastroenterol. Hepatol.* 6, 474–481. doi:10.1016/S2468-1253(21)00018-2

Jackson, J. R., Seed, M. P., Kircher, C. H., Willoughby, D. A., and Winkler, J. D. (1997). The Codependence of Angiogenesis and Chronic Inflammation. *FASEB J.* 11, 457–465. doi:10.1096/fasebj.11.6.9194526

Jenne, C. N. (2014). Platelets: Crossroads of Immunity and Hemostasis. *Blood* 124, 671–672. doi:10.1182/blood-2014-05-572875

Jiang, Z. G., Feldbrügge, L., Tapper, E. B., Popov, Y., Ghaziani, T., Afdhal, N., et al. (2016). Aspirin Use Is Associated with Lower Indices of Liver Fibrosis Among Adults in the United States. *Aliment. Pharmacol. Ther.* 43, 734–743. doi:10.1111/apt.13515

Jing, L., Qu, H., Wu, D., Zhu, C., Yang, Y., Jin, X., et al. (2018). Platelet-camouflaged Nanococktail: Simultaneous Inhibition of Drug-Resistant Tumor Growth and Metastasis via a Cancer Cells and Tumor Vasculature Dual-Targeting Strategy. *Theranostics* 8, 2683–2695. doi:10.7150/thno.23654

Kalluri, R., and Weinberg, R. A. (2009). The Basics of Epithelial-Mesenchymal Transition. *J. Clin. Invest.* 119, 1420–1428. doi:10.1172/JCI39104

Kim, S. Y., Kim, H. S., and Park, H. J. (2019). Adverse Events Related to Colonoscopy: Global Trends and Future Challenges. *World J. Gastroenterol.* 25, 190–204. doi:10.3748/wjg.v25.i2.190

Kocabayoglu, P., Lade, A., Lee, Y. A., Dragomir, A. C., Sun, X., Fiel, M. I., et al. (2015). β-PDGF Receptor Expressed by Hepatic Stellate Cells Regulates Fibrosis in Murine Liver Injury, but Not Carcinogenesis. *J. Hepatol.* 63, 141–147. doi:10.1016/j.jhep.2015.01.036

Labelle, M., Begum, S., and Hynes, R. O. (2011). Direct Signaling between Platelets and Cancer Cells Induces an Epithelial-mesenchymal-like Transition and Promotes Metastasis. *Cancer Cell* 20, 576–590. doi:10.1016/j.ccr.2011.09.009

Lecomte, M., Laneuville, O., Ji, C., DeWitt, D. L., and Smith, W. L. (1994). Acetylation of Human Prostaglandin Endoperoxide Synthase-2 (Cyclooxygenase-2) by Aspirin. *J. Biol. Chem.* 269, 13207–13215. doi:10.1016/s0021-9258(17)36820-5

Lee, T. Y., Hsu, Y. C., Tseng, H. C., Yu, S. H., Lin, J. T., Wu, M. S., et al. (2019). Association of Daily Aspirin Therapy with Risk of Hepatocellular Carcinoma in Patients with Chronic Hepatitis B. *JAMA Intern. Med.* 179, 633–640. doi:10.1001/jamainternmed.2018.8342

Levi, C., Payance, A., Bissonnette, J., Tanguy, M., Roux, O., Bouattour, M., et al. (2017). Plasma Microvesicles Levels Can Predict the Development of Hepatocellular Carcinoma in Patients with Cirrhosis. *J. Hepatol.* 66, S221. doi:10.1016/S0168-8278(17)30740-7

Li, C. J., Yang, Z. H., Shi, X. L., and Liu, D. L. (2017). Effects of Aspirin and Enoxaparin in a Rat Model of Liver Fibrosis. *World J. Gastroenterol.* 23, 6412–6419. doi:10.3748/wjg.v23.i35.6412

Li, T., Dong, Z. R., Guo, Z. Y., Wang, C. H., Tang, Z. Y., Qu, S. F., et al. (2013). Aspirin Enhances IFN-α-Induced Growth Inhibition and Apoptosis of Hepatocellular Carcinoma via JAK1/STAT1 Pathway. *Cancer Gene Ther.* 20, 366–374. doi:10.1038/cgt.2013.29

Li, X., Fries, S., Li, R., Lawson, J. A., Propert, K. J., Diamond, S. L., et al. (2014). Differential Impairment of Aspirin-dependent Platelet Cyclooxygenase Acetylation by Nonsteroidal Antiinflammatory Drugs. *Proc. Natl. Acad. Sci. U S A.* 111, 16830–16835. doi:10.1073/pnas.1406997111

Li, X., Liu, G., and Wu, W. (2021). Recent Advances in Lynch Syndrome. *Exp. Hematol. Oncol.* 10, 37. doi:10.1186/s40164-021-00231-4

Libby, P., Ridker, P. M., and Hansson, G. K. (2009). Inflammation in Atherosclerosis: from Pathophysiology to Practice. *J. Am. Coll. Cardiol.* 54, 2129–2138. doi:10.1016/j.jacc.2009.09.009

Lin, H. P., Singla, B., Ghoshal, P., Faulkner, J. L., Cherian-Shaw, M., O'Connor, P. M., et al. (2018). Identification of Novel Macropinocytosis Inhibitors Using a Rational Screen of Food and Drug Administration-Approved Drugs. *Br. J. Pharmacol.* 175, 3640–3655. doi:10.1111/bph.14429

Liu, Z., Xu, K., Jiang, Y., Cai, N., Fan, J., Mao, X., et al. (2021). Global Trend of Aetiology-Based Primary Liver Cancer Incidence from 1990 to 2030: a Modelling Study. *Int. J. Epidemiol.* 50, 128–142. doi:10.1093/ije/dyaa196

Lu, Y., Hu, Q., Jiang, C., and Gu, Z. (2019). Platelet for Drug Delivery. *Curr. Opin. Biotechnol.* 58, 81–91. doi:10.1016/j.copbio.2018.11.010

Lynch, P. M. (2021). Low-dose Aspirin and Mesalazine for Patients with Familial Adenomatous Polyposis. *Lancet Gastroenterol. Hepatol.* 6, 418–419. doi:10.1016/S2468-1253(21)00102-3

Majithia, A., and Bhatt, D. L. (2019). Novel Antiplatelet Therapies for Atherothrombotic Diseases. *Arterioscler Thromb. Vasc. Biol.* 39, 546–557. doi:10.1161/ATVBAHA.118.310955

Malehmir, M., Pfister, D., Gallage, S., Szydlowska, M., Inverso, D., Kotsiliti, E., et al. (2019). Platelet GPIbα Is a Mediator and Potential Interventional Target for NASH and Subsequent Liver Cancer. *Nat. Med.* 25, 641–655. doi:10.1038/s41591-019-0379-5

Marrero, J. A., Kulik, L. M., Sirlin, C. B., Zhu, A. X., Finn, R. S., Abecassis, M. M., et al. (2018). Diagnosis, Staging, and Management of Hepatocellular Carcinoma: 2018 Practice Guidance by the American Association for the Study of Liver Diseases. *Hepatology* 68, 723–750. doi:10.1002/hep.29913

Mayne, E., Funderburg, N. T., Sieg, S. F., Asaad, R., Kalinowska, M., Rodriguez, B., et al. (2012). Increased Platelet and Microparticle Activation in HIV Infection: Upregulation of P-Selectin and Tissue Factor Expression. *J. Acquir Immune Defic Syndr.* 59, 340–346. doi:10.1097/QAI.0b013e3182439355

McNeil, J. J., Nelson, M. R., Woods, R. L., Lockery, J. E., Wolfe, R., Reid, C. M., et al. (2018). Effect of Aspirin on All-Cause Mortality in the Healthy Elderly. *N. Engl. J. Med.* 379, 1519–1528. doi:10.1056/NEJMoa1803955

Meade, T. W. (1998). Thrombosis Prevention Trial: Randomised Trial of Low-Intensity Oral Anticoagulation with Warfarin and Low-Dose Aspirin in the Primary Prevention of Ischaemic Heart Disease in Men at Increased Risk. The Medical Research Council's General Practice Research Framework. *Lancet* 351, 233–241. doi:10.1016/s0140-6736(05)79156-x

Memel, Z. N., Arvind, A., Moninuola, O., Philpotts, L., Chung, R. T., Corey, K. E., et al. (2021). Aspirin Use Is Associated with a Reduced Incidence of Hepatocellular Carcinoma: A Systematic Review and Meta-Analysis. *Hepatol. Commun.* 5, 133–143. doi:10.1002/hep4.1640

Miao, Y., Xu, Z., Feng, W., Zheng, M., Xu, Z., Gao, H., et al. (2022). Platelet Infiltration Predicts Survival in Postsurgical Colorectal Cancer Patients. *Int. J. Cancer*. 150, 509–520. doi: doi: doi:10.1002/ijc.33816

Moore, C. E., Xie, J., Gomez, E., and Herbert, T. P. (2009). Identification of cAMP-dependent Kinase as a Third *In Vivo* Ribosomal Protein S6 Kinase in Pancreatic Beta-Cells. *J. Mol. Biol.* 389, 480–494. doi:10.1016/j.jmb.2009.04.020

Morikawa, T., Kato, J., Yamaji, Y., Wada, R., Mitsushima, T., and Shiratori, Y. (2005). A Comparison of the Immunochemical Fecal Occult Blood Test and Total Colonoscopy in the Asymptomatic Population. *Gastroenterology* 129, 422–428. doi:10.1016/j.gastro.2005.05.056

Morrell, C. N., Aggrey, A. A., Chapman, L. M., and Modjeski, K. L. (2014). Emerging Roles for Platelets as Immune and Inflammatory Cells. *Blood* 123, 2759–2767. doi:10.1182/blood-2013-11-462432

Myung, S. J., Rerko, R. M., Yan, M., Platzer, P., Guda, K., Dotson, A., et al. (2006). 15-Hydroxyprostaglandin Dehydrogenase Is an *In Vivo* Suppressor of colon Tumorigenesis. *Proc. Natl. Acad. Sci. U S A.* 103, 12098–12102. doi:10.1073/pnas.0603235103

Nathan, C., and Ding, A. (2010). Nonresolving Inflammation. *Cell* 140, 871–882. doi:10.1016/j.cell.2010.02.029

Ogura, H., Kawasaki, T., Tanaka, H., Koh, T., Tanaka, R., Ozeki, Y., et al. (2001). Activated Platelets Enhance Microparticle Formation and Platelet-Leukocyte Interaction in Severe Trauma and Sepsis. *J. Trauma* 50, 801–809. doi:10.1097/00005373-200105000-00005

Pantel, K., and Speicher, M. R. (2016). The Biology of Circulating Tumor Cells. *Oncogene* 35, 1216–1224. doi:10.1038/onc.2015.192

Patrignani, P., Filabozzi, P., and Patrono, C. (1982). Selective Cumulative Inhibition of Platelet Thromboxane Production by Low-Dose Aspirin in Healthy Subjects. *J. Clin. Invest.* 69, 1366–1372. doi:10.1172/jci110576

Patrignani, P., and Patrono, C. (2016). Aspirin and Cancer. *J. Am. Coll. Cardiol.* 68, 967–976. doi:10.1016/j.jacc.2016.05.083

Patrignani, P., and Patrono, C. (2018). Aspirin, Platelet Inhibition and Cancer Prevention. *Platelets* 29, 779–785. doi:10.1080/09537104.2018.1492105

Patrignani, P., and Patrono, C. (2015). Cyclooxygenase Inhibitors: From Pharmacology to Clinical Read-Outs. *Biochim. Biophys. Acta* 1851, 422–432. doi:10.1016/j.bbalip.2014.09.016

Patrignani, P., Sacco, A., Sostres, C., Bruno, A., Dovizio, M., Piazuelo, E., et al. (2017). Low-Dose Aspirin Acetylates Cyclooxygenase-1 in Human Colorectal Mucosa: Implications for the Chemoprevention of Colorectal Cancer. *Clin. Pharmacol. Ther.* 102, 52–61. doi:10.1002/cpt.639

Patrignani, P., Tacconelli, S., Piazuelo, E., Di Francesco, L., Dovizio, M., Sostres, C., et al. (2014). Reappraisal of the Clinical Pharmacology of Low-Dose Aspirin by Comparing Novel Direct and Traditional Indirect Biomarkers of Drug Action. *J. Thromb. Haemost.* 12, 1320–1330. doi:10.1111/jth.12637

Patrono, C., Morais, J., Baigent, C., Collet, J. P., Fitzgerald, D., Halvorsen, S., et al. (2017). Antiplatelet Agents for the Treatment and Prevention of Coronary

Atherothrombosis. *J. Am. Coll. Cardiol.* 70, 1760–1776. doi:10.1016/j.jacc.2017.08.037

Patrono, C., Patrignani, P., and García Rodríguez, L. A. (2001). Cyclooxygenase-selective Inhibition of Prostanoid Formation: Transducing Biochemical Selectivity into Clinical Read-Outs. *J. Clin. Invest.* 108, 7–13. doi:10.1172/JCI13418

Pedersen, A. K., and FitzGerald, G. A. (1984). Dose-related Kinetics of Aspirin. Presystemic Acetylation of Platelet Cyclooxygenase. *N. Engl. J. Med.* 311, 1206–1211. doi:10.1056/NEJM198411083111902

Pennisi, G., Celsa, C., Giammanco, A., Spatola, F., and Petta, S. (2019). The Burden of Hepatocellular Carcinoma in Non-alcoholic Fatty Liver Disease: Screening Issue and Future Perspectives. *Int. J. Mol. Sci.* 20, 5613. doi:10.3390/ijms20225613

Petrick, J. L., Sahasrabuddhe, V. V., Chan, A. T., Alavanja, M. C., Beane-Freeman, L. E., Buring, J. E., et al. (2015). NSAID Use and Risk of Hepatocellular Carcinoma and Intrahepatic Cholangiocarcinoma: The Liver Cancer Pooling Project. *Cancer Prev. Res. (Phila)* 8, 1156–1162. doi:10.1158/1940-6207.CAPR-15-0126

Puhm, F., Boilard, E., and Machlus, K. R. (2021). Platelet Extracellular Vesicles: Beyond the Blood. *Arterioscler Thromb. Vasc. Biol.* 41, 87–96. doi:10.1161/ATVBAHA.120.314644

Ribas, V., de la Rosa, L. C., Robles, D., Núñez, S., Segalés, P., Insausti-Urkia, N., et al. (2021). Dietary and Genetic Cholesterol Loading rather Than Steatosis Promotes Liver Tumorigenesis and NASH-Driven HCC. *Cancers (Basel)* 13, 4091. doi:10.3390/cancers13164091

Ricciotti, E., and FitzGerald, G. A. (2011). Prostaglandins and Inflammation. *Arterioscler Thromb. Vasc. Biol.* 31, 986–1000. doi:10.1161/ATVBAHA.110.207449

Ricciotti, E., Wangensteen, K. J., and FitzGerald, G. A. (2021). Aspirin in Hepatocellular Carcinoma. *Cancer Res.* 81, 3751–3761. doi:10.1158/0008-5472.CAN-21-0758

Ridker, P. M. (2019). Anticytokine Agents: Targeting Interleukin Signaling Pathways for the Treatment of Atherothrombosis. *Circ. Res.* 124, 437–450. doi:10.1161/CIRCRESAHA.118.313129

Ridker, P. M., Everett, B. M., Thuren, T., MacFadyen, J. G., Chang, W. H., Ballantyne, C., et al. (2017). CANTOS Trial GroupAntiinflammatory Therapy with Canakinumab for Atherosclerotic Disease. *N. Engl. J. Med.* 377, 1119–1131. doi:10.1056/NEJMoa1707914

Roschewski, M., Staudt, L. M., and Wilson, W. H. (2016). Dynamic Monitoring of Circulating Tumor DNA in Non-hodgkin Lymphoma. *Blood* 127, 3127–3132. doi:10.1182/blood-2016-03-635219

Rothwell, P. M., Fowkes, F. G., Belch, J. F., Ogawa, H., Warlow, C. P., and Meade, T. W. (2011). Effect of Daily Aspirin on Long-Term Risk of Death Due to Cancer: Analysis of Individual Patient Data from Randomised Trials. *Lancet* 377, 31–41. doi:10.1016/S0140-6736(10)62110-1

Rothwell, P. M., Wilson, M., Elwin, C. E., Norrving, B., Algra, A., Warlow, C. P., et al. (2010). Long-term Effect of Aspirin on Colorectal Cancer Incidence and Mortality: 20-year Follow-Up of Five Randomised Trials. *Lancet* 376, 1741–1750. doi:10.1016/S0140-6736(10)61543-7

Roweth, H. G., and Battinelli, E. M. (2021). Lessons to Learn from Tumor-Educated Platelets. *Blood* 137, 3174–3180. doi:10.1182/blood.2019003976

Ruvinsky, I., Sharon, N., Lerer, T., Cohen, H., Stolovich-Rain, M., Nir, T., et al. (2005). Ribosomal Protein S6 Phosphorylation Is a Determinant of Cell Size and Glucose Homeostasis. *Genes Dev.* 19, 2199–2211. doi:10.1101/gad.351605

Sacco, A., Bruno, A., Contursi, A., Dovizio, M., Tacconelli, S., Ricciotti, E., et al. (2019). Platelet-Specific Deletion of Cyclooxygenase-1 Ameliorates Dextran Sulfate Sodium-Induced Colitis in Mice. *J. Pharmacol. Exp. Ther.* 370, 416–426. doi:10.1124/jpet.119.259382

Sahasrabuddhe, V. V., Gunja, M. Z., Graubard, B. I., Trabert, B., Schwartz, L. M., Park, Y., et al. (2012). Nonsteroidal Anti-inflammatory Drug Use, Chronic Liver Disease, and Hepatocellular Carcinoma. *J. Natl. Cancer Inst.* 104, 1808–1814. doi:10.1093/jnci/djs452

Sandler, R. S., Halabi, S., Baron, J. A., Budinger, S., Paskett, E., Keresztes, R., et al. (2003). A Randomized Trial of Aspirin to Prevent Colorectal Adenomas in Patients with Previous Colorectal Cancer. *N. Engl. J. Med.* 348, 883–890. doi:10.1056/NEJMoa021633

Sarkar, S., Alam, M. A., Shaw, J., and Dasgupta, A. K. (2013). Drug Delivery Using Platelet Cancer Cell Interaction. *Pharm. Res.* 30, 2785–2794. doi:10.1007/s11095-013-1097-1

Sasaki, Y., Kamei, D., Ishikawa, Y., Ishii, T., Uematsu, S., Akira, S., et al. (2012). Microsomal Prostaglandin E Synthase-1 Is Involved in Multiple Steps of colon Carcinogenesis. *Oncogene* 31, 2943–2952. doi:10.1038/onc.2011.472

Scurr, M., Pembroke, T., Bloom, A., Roberts, D., Thomson, A., Smart, K., et al. (2018). Low-Dose Cyclophosphamide Induces Antitumor T-Cell Responses, Which Associate with Survival in Metastatic Colorectal Cancer. *Clin. Cancer Res.* 23, 6771–6780. doi:10.1158/1078-0432.CCR-17-0895

Shiota, G., Okubo, M., Noumi, T., Noguchi, N., Oyama, K., Takano, Y., et al. (1999). Cyclooxygenase-2 Expression in Hepatocellular Carcinoma. *Hepatogastroenterology* 46, 407–412.

Sim, X., Jarocha, D., Hayes, V., Hanby, H. A., Marks, M. S., Camire, R. M., et al. (2017). Identifying and Enriching Platelet-Producing Human Stem Cell-Derived Megakaryocytes Using Factor V Uptake. *Blood* 130, 192–204. doi:10.1182/blood-2017-01-761049

Simon, T. G., Duberg, A. S., Aleman, S., Chung, R. T., Chan, A. T., and Ludvigsson, J. F. (2020). Association of Aspirin with Hepatocellular Carcinoma and Liver-Related Mortality. *N. Engl. J. Med.* 382, 1018–1028. doi:10.1056/NEJMoa1912035

Simon, T. G., Henson, J., Osganian, S., Masia, R., Chan, A. T., Chung, R. T., et al. (2019). Daily Aspirin Use Associated with Reduced Risk for Fibrosis Progression in Patients with Nonalcoholic Fatty Liver Disease. *Clin. Gastroenterol. Hepatol.* 17, 2776–e4. e4. doi:10.1016/j.cgh.2019.04.061

Simon, T. G., Ma, Y., Ludvigsson, J. F., Chong, D. Q., Giovannucci, E. L., Fuchs, C. S., et al. (2018). Association between Aspirin Use and Risk of Hepatocellular Carcinoma. *JAMA Oncol.* 4, 1683–1690. doi:10.1001/jamaoncol.2018.4154

Singal, A. G., Pillai, A., and Tiro, J. (2014). Early Detection, Curative Treatment, and Survival Rates for Hepatocellular Carcinoma Surveillance in Patients with Cirrhosis: a Meta-Analysis. *PLoS Med.* 11, e1001624. doi:10.1371/journal.pmed.1001624

Sitia, G., Aiolfi, R., Di Lucia, P., Mainetti, M., Fiocchi, A., Mingozzi, F., et al. (2012). Antiplatelet Therapy Prevents Hepatocellular Carcinoma and Improves Survival in a Mouse Model of Chronic Hepatitis B. *Proc. Natl. Acad. Sci. U S A.* 109, E2165–E2172. doi:10.1073/pnas.1209182109

Soehnlein, O., and Libby, P. (2021). Targeting Inflammation in Atherosclerosis - from Experimental Insights to the Clinic. *Nat. Rev. Drug Discov.* 20, 589–610. doi:10.1038/s41573-021-00198-1

Tacconelli, S., Contursi, A., Falcone, L., Mucci, M., D'Agostino, I., Fullone, R., et al. (2020). Characterization of Cyclooxygenase-2 Acetylation and Prostanoid Inhibition by Aspirin in Cellular Systems. *Biochem. Pharmacol.* 178, 114094. doi:10.1016/j.bcp.2020.114094

Thun, M. J., Henley, S. J., and Patrono, C. (2002). Nonsteroidal Anti-inflammatory Drugs as Anticancer Agents: Mechanistic, Pharmacologic, and Clinical Issues. *J. Natl. Cancer Inst.* 94, 252–266. doi:10.1093/jnci/94.4.252

Tilg, H., and Moschen, A. R. (2010). Evolution of Inflammation in Nonalcoholic Fatty Liver Disease: the Multiple Parallel Hits Hypothesis. *Hepatology* 52, 1836–1846. doi:10.1002/hep.24001

Tourdot, B. E., and Holinstat, M. (2017). Targeting 12-Lipoxygenase as a Potential Novel Antiplatelet Therapy. *Trends Pharmacol. Sci.* 38, 1006–1015. doi:10.1016/j.tips.2017.08.001

Trinchet, J. C., Bourcier, V., Chaffaut, C., Ait Ahmed, M., Allam, S., Marcellin, P., et al. (2015). Complications and Competing Risks of Death in Compensated Viral Cirrhosis (ANRS CO12 CirVir Prospective Cohort). *Hepatology* 62, 737–750. doi:10.1002/hep.27743

van Roy, F., and Berx, G. (2008). The Cell-Cell Adhesion Molecule E-Cadherin. *Cell Mol Life Sci* 65, 3756–3788. doi:10.1007/s00018-008-8281-1

Vargason, A. M., Anselmo, A. C., and Mitragotri, S. (2021). The Evolution of Commercial Drug Delivery Technologies. *Nat. Biomed. Eng.* 5, 951–967. doi:10.1038/s41551-021-00698-w

Wang, C., Sun, W., Ye, Y., Hu, Q., Bomba, H. N., and Gu, Z. (2017). *In Situ* activation of Platelets with Checkpoint Inhibitors for post-surgical Cancer Immunotherapy. *Nat. Biomed. Eng.* 1, 0011. doi:10.1038/s41551-016-0011

Wang, D., and DuBois, R. N. (2018). Role of Prostanoids in Gastrointestinal Cancer. *J. Clin. Invest.* 128, 2732–2742. doi:10.1172/JCI97953

Wang, J., Chenivesse, X., Henglein, B., and Bréchot, C. (1990). Hepatitis B Virus Integration in a Cyclin A Gene in a Hepatocellular Carcinoma. *Nature* 343, 555–557. doi:10.1038/343555a0

Wang, S., Yu, Y., Ryan, P. M., Dang, M., Clark, C., Kontogiannis, V., et al. (2020). Association of Aspirin Therapy with Risk of Hepatocellular Carcinoma: A Systematic Review and Dose-Response Analysis of Cohort Studies with 2.5 Million Participants. *Pharmacol. Res.* 151, 104585. doi:10.1016/j.phrs.2019.104585

Wang, T., Fu, X., Jin, T., Zhang, L., Liu, B., Wu, Y., et al. (2019). Aspirin Targets P4HA2 through Inhibiting NF-Kb and LMCD1-AS1/let-7g to Inhibit Tumour Growth and Collagen Deposition in Hepatocellular Carcinoma. *EBioMedicine* 45, 168–180. doi:10.1016/j.ebiom.2019.06.048

Wynn, T. A., and Ramalingam, T. R. (2012). Mechanisms of Fibrosis: Therapeutic Translation for Fibrotic Disease. *Nat. Med.* 18, 1028–1040. doi:10.1038/nm.2807

Xu, P., Zuo, H., Chen, B., Wang, R., Ahmed, A., Hu, Y., et al. (2017). Doxorubicin-loaded Platelets as a Smart Drug Delivery System: An Improved Therapy for Lymphoma. *Sci. Rep.* 7, 42632. doi:10.1038/srep42632

Yang, J., Mani, S. A., Donaher, J. L., Ramaswamy, S., Itzykson, R. A., Come, C., et al. (2004). Twist, a Master Regulator of Morphogenesis, Plays an Essential Role in Tumor Metastasis. *Cell* 117, 927–939. doi:10.1016/j.cell.2004.06.006

Yang, W. H., Lan, H. Y., Huang, C. H., Tai, S. K., Tzeng, C. H., Kao, S. Y., et al. (2012). RAC1 Activation Mediates Twist1-Induced Cancer Cell Migration. *Nat. Cell Biol* 14, 366–374. doi:10.1038/ncb2455

Yilmaz, Y. (2012). Review Article: Is Non-alcoholic Fatty Liver Disease a Spectrum, or Are Steatosis and Non-alcoholic Steatohepatitis Distinct Conditions? *Aliment. Pharmacol. Ther.* 36, 815–823. doi:10.1111/apt.12046

Yoshida, S., Ikenaga, N., Liu, S. B., Peng, Z. W., Chung, J., Sverdlov, D. Y., et al. (2014). Extrahepatic Platelet-Derived Growth Factor-β, Delivered by Platelets, Promotes Activation of Hepatic Stellate Cells and Biliary Fibrosis in Mice. *Gastroenterology* 147, 1378–1392. doi:10.1053/j.gastro.2014.08.038

Younossi, Z. M., Blissett, D., Blissett, R., Henry, L., Stepanova, M., Younossi, Y., et al. (2016). The Economic and Clinical burden of Nonalcoholic Fatty Liver Disease in the United States and Europe. *Hepatology* 64, 1577–1586. doi:10.1002/hep.28785

Yu, L. X., Ling, Y., and Wang, H. Y. (2018). Role of Nonresolving Inflammation in Hepatocellular Carcinoma Development and Progression. *NPJ Precis Oncol.* 2, 6. doi:10.1038/s41698-018-0048-z

Yu, Y., Gong, R., Mu, Y., Chen, Y., Zhu, C., Sun, Z., et al. (2011). Hepatitis B Virus Induces a Novel Inflammation Network Involving Three Inflammatory Factors, IL-29, IL-8, and Cyclooxygenase-2. *J. Immunol.* 187, 4844–4860. doi:10.4049/jimmunol.1100998

Zelenay, S., van der Veen, A. G., Böttcher, J. P., Snelgrove, K. J., Rogers, N., Acton, S. E., et al. (2015). Cyclooxygenase-Dependent Tumor Growth through Evasion of Immunity. *Cell* 162, 1257–1270. doi:10.1016/j.cell.2015.08.015

Ziegler, M., Wang, X., Lim, B., Leitner, E., Klingberg, F., Ching, V., et al. (2017). Platelet-Targeted Delivery of Peripheral Blood Mononuclear Cells to the Ischemic Heart Restores Cardiac Function after Ischemia-Reperfusion Injury. *Theranostics* 7, 3192–3206. doi:10.7150/thno.19698

Conflict of Interest: The authors declare that the research was conducted in the absence of any commercial or financial relationships that could be construed as a potential conflict of interest.

Publisher's Note: All claims expressed in this article are solely those of the authors and do not necessarily represent those of their affiliated organizations, or those of the publisher, the editors and the reviewers. Any product that may be evaluated in this article, or claim that may be made by its manufacturer, is not guaranteed or endorsed by the publisher.

frontiers in Pharmacology

BRIEF RESEARCH REPORT
published: 22 March 2022
doi: 10.3389/fphar.2022.806240

The IRE1α Inhibitor KIRA6 Blocks Leukotriene Biosynthesis in Human Phagocytes

Xiao Tang, Tarvi Teder, Bengt Samuelsson and Jesper Z. Haeggström**

Division of Physiological Chemistry II, Department of Medical Biochemistry and Biophysics, Karolinska Institutet, Stockholm, Sweden

The ER stress and Unfolded Protein Response (UPR) component inositol-requiring enzyme 1α (IRE1α) has been linked to inflammation and lipid mediator production. Here we report that the potent IRE1α inhibitor, KIRA6, blocks leukotriene biosynthesis in human phagocytes activated with lipopolysaccharide (LPS) plus N-formyl-methionyl-leucyl-phenylalanine (fMLP) or thapsigargin (Tg). The inhibition affects both leukotriene B_4 (LTB_4) and cysteinyl leukotriene (cys-LTs) production at submicromolar concentration. Macrophages made deficient of IRE1α were still sensitive to KIRA6 thus demonstrating that the compound's effect on leukotriene production is IRE1α-independent. KIRA6 did not exhibit any direct inhibitory effect on key enzymes in the leukotriene pathway, as assessed by phospholipase A_2 (PLA_2), 5-lipoxygenase (5-LOX), LTA_4 hydrolase (LTA4H), and LTC_4 synthase (LTC4S) enzyme activity measurements in cell lysates. However, we find that KIRA6 dose-dependently blocks phosphorylation of p38 and ERK, mitogen-activated protein kinases (MAPKs) that have established roles in activating cytosolic PLA_2α ($cPLA_2$α) and 5-LOX. The reduction of p38 and ERK phosphorylation is associated with a decrease in $cPLA_2$α phosphorylation and attenuated leukotriene production. Furthermore, KIRA6 inhibits p38 activity, and molecular modelling indicates that it can directly interact with the ATP-binding pocket of p38. This potent and unexpected, non-canonical effect of KIRA6 on p38 and ERK MAPKs and leukotriene biosynthesis may account for some of the immune-modulating properties of this widely used IRE1α inhibitor.

Keywords: leukotrienes, KIRA6, inflammation, IRE1α, MAPKs

OPEN ACCESS

Edited by:
Pallavi R. Devchand, Other, United States

Reviewed by:
Kyle L. Flannigan, University of Calgary, Canada
Nicolas Flamand, Laval University, Canada

****Correspondence:***
Xiao Tang
xiao.tang@ki.se
Jesper Z. Haeggström
jesper.haeggstrom@ki.se

Specialty section:
This article was submitted to Inflammation Pharmacology, a section of the journal Frontiers in Pharmacology

Received: *31 October 2021*
Accepted: *03 March 2022*
Published: *22 March 2022*

Citation:
Tang X, Teder T, Samuelsson B and Haeggström JZ (2022) The IRE1α Inhibitor KIRA6 Blocks Leukotriene Biosynthesis in Human Phagocytes. Front. Pharmacol. 13:806240. doi: 10.3389/fphar.2022.806240

INTRODUCTION

Leukotrienes (LTs) are a class of lipid mediators derived from arachidonic acid (AA), predominantly produced in myeloid cells (granulocytes, monocytes/macrophages and mast cells). There are two types of leukotrienes-leukotriene B_4 (LTB_4), a potent chemoattractant and pro-inflammatory mediator, and cysteinyl leukotrienes (cys-LTs, which comprise LTC_4, D_4, and E_4), referred to as slow-reacting substance of anaphylaxis (SRS-A) (Samuelsson, 1983). These mediators act in an autocrine or paracrine manner, exerting their functions through their cognate G-protein coupled receptors (GPCRs) on the target cells (Haeggström and Funk, 2011). The biosynthesis of leukotrienes requires several enzymatic steps. First, phospholipase A_2 (PLA_2), especially cytosolic PLA_2α ($cPLA_2$α), catalyzes the release of free AA from membrane phospholipids, which is believed to be the rate-limiting step for the cellular output of leukotrienes and prostaglandins (PGs) (Funk, 2001). In a second step, the key enzyme 5-lipoxygenase (5-LOX) converts free AA to the transient

epoxide intermediate LTA_4 which, depending on the availability of downstream enzymes, is rapidly converted to LTB_4 by LTA_4 hydrolase (LTA4H), or to LTC_4 by LTC_4 synthase (LTC4S). Together with the accessory proteins in the pathway, these enzymes form the leukotriene biosynthetic complex and control cellular production of leukotrienes (Haeggström, 2018).

In phagocytes, the activities of $cPLA_2\alpha$ and 5-LOX are regulated by cytosolic calcium and protein phosphorylation (Gijón et al., 2000; Rådmark et al., 2007). In resting cells, $cPLA_2\alpha$ and 5-LOX are located in the cytosol, or in some cell types, in a nuclear soluble compartment associated with chromatin (Rådmark et al., 2007). Classical leukotriene stimuli (e.g., PAF, fMLP, thapsigargin, and A23187) cause calcium mobilization to the cytosol and binding to the C2 or C2-like domain of $cPLA_2\alpha$ and 5-LOX, respectively. Simultaneously, $cPLA_2\alpha$ and 5-LOX are phosphorylated by certain mitogen-activated protein kinases (e.g., p38 and ERK), which also modulates the activity of the two enzymes (Werz, 2002).

At the center of the most conventional arm of unfolded protein response (UPR), inositol-requiring enzyme 1α (IRE1α) plays an important role in sensing misfolded proteins and maintaining homeostasis of the endoplasmic reticulum (ER) (Hetz, 2012). Exposure of misfolded proteins leads to autophosphorylation of IRE1α at its kinase domain and oligomerization, which in turn causes activation of its RNase domain, resulting in splicing and activation of the transcription factor XBP1 (Korovesis et al., 2020). However, hyperactive IRE1α degrades ER-localized RNA and cause cell death (Ghosh et al., 2014). In addition, IRE1α has also been strongly implicated in macrophage polarization, cytokine secretion and prostaglandin production, in several immunological and metabolic disorders (Shan et al., 2017; Smith, 2018; Chopra et al., 2019; Batista et al., 2020; Hull-Ryde et al., 2021).

Small molecules known as kinase-inhibiting RNase-attenuators (KIRA) s have been designed to allosterically inhibit the RNase activity of IRE1α by stabilizing the ATP-binding kinase domain and preventing oligomerization (Ghosh et al., 2014). As an optimized KIRA, KIRA6 has been widely used experimentally to target IRE1α. It has been shown that KIRA6 effectively blocks PGE_2-mediated pain with a comparable efficacy as celecoxib (Chopra et al., 2019), whereas the effect of KIRA6 and IRE1α activation in leukotriene production remains to be assessed.

METHODS

Reagents

KIRA6 was from Cayman Chemicals (Ann Arbor, MI, United States). Monoclonal antibodies (mAb) against phosphorylated $cPLA_2\alpha$ (p-$cPLA_2\alpha$) (Ser-505), p-p38 (Thr180/Tyr182), p-ERK (Thr202/Tyr204), and p-5-LOX (Ser271 and Ser663) were from Cell Signaling Technology (Danvers, MA, United States). LPS, Thapsigargin, fMLP 4μ8C, RPMI-1640 cell culture medium, HEPES solution, 1,25-dihydroxy vitamin D3, horseradish peroxidase (HRP)-linked mAb against β-actin were from Sigma-Aldrich (St. Louis, MO, United States). TGF-β1 and M-CSF were from Thermofisher Scientific (Waltham, MA, United States). SB203580 was from Tocris Bioscience (Bristol, UK).

Cell Culture

Human monocyte-derived macrophages (hMDMs) and neutrophils were isolated as previously described (Wan et al., 2007; Wan et al., 2018). Briefly, peripheral blood monocytes and neutrophils were isolated by dextran sedimentation and gradient centrifugation with Ficoll-paque Premium (GE Healthcare, Little Chalfont, United Kingdom) from freshly prepared buffy coats (Karolinska Blood Bank). Isolated monocytes were further cultured in RPMI-1640 medium supplemented with 10% heat-inactivated fetal bovine serum (FBS) and M-CSF (50 ng/ml) for 6 days to obtain mature macrophages. The human monocytic cell line Mono Mac 6 (MM6) were cultured in RPMI-1640 supplemented with 10% FBS, and differentiated into macrophages with 1,25-dihydroxy vitamin D3 (50 nM) and TGF-β1 (2 ng/ml) for 4 days.

Generation of Inositol-Requiring Enzyme 1α Knockdown Cells

MM6 cells were transfected with lentiviral shRNA against IRE1α (NM_001433) and non-target shRNA to generate IRE1α knockdown (KD) and control MM6 cells. The knockdown efficiency was evaluated by qPCR analysis of the mRNA expression of IRE1α.

ELISA

LTB_4, cys-LTs, and PGE_2 in cell supernatants were measured with ELISA kits (Cayman chemicals) according to the manufacturer's instructions. The absorbance at 405 nm was recorded by a TECAN Infinite M200 plate reader.

Western Blot

Cells were lysed with RIPA buffer supplemented with protease inhibitor and phosphatase inhibitor cocktails (Roche Diagnostics, Mannheim, Germany). SDS-PAGE and western blot transfer were carried out with NuPAGE Novex 4–12% Bis-Tris gels and iBlot2 blotting system (Thermofisher). Afterwards, the membranes were incubated with 3% non-fat milk for 1 h and further incubated with HRP-linked β-actin antibody (Sigma-Aldrich) for 1 h, or desired primary antibodies overnight at 4°C followed by HRP-linked anti-rabbit antibody (GE Healthcare). The enhanced chemiluminescence substrate was then added to the membranes to visualize the immunoreactive protein bands.

Kinase Activity Assay

The p38 and ERK kinase assays were performed according to the manufacturer's protocol (Promega) with optimized conditions. The p38 assay was carried out with 10 ng of the p38 enzyme, 150 μM ATP and 0.2 μg/μL p38 peptide as substrates, and 0–10 μM of KIRA6, 4 μ8C or SB203580 as the positive control. The ERK kinase assay was performed with 3 ng of ERK1 or ERK2, 50 μM ATP and 0.5 μg MAP kinase substrate (MBP), together

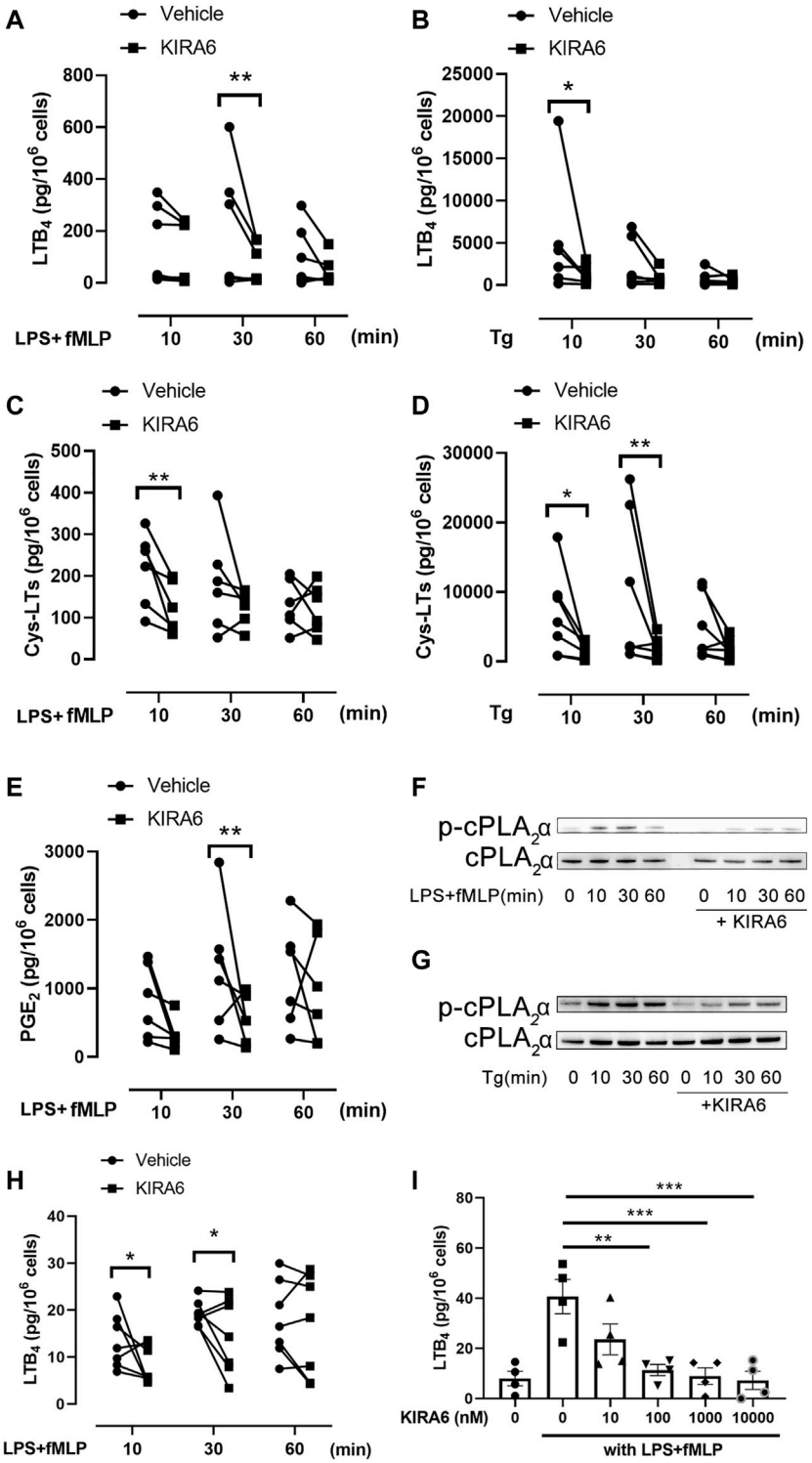

FIGURE 1 | KIRA6 inhibits leukotriene production from hMDMs and neutrophils. **(A–E)** hMDMs were pretreated with 1 μM KIRA6 or vehicle (0.1% DMSO) for 30 min. Afterwards, cells were treated with 100 ng/ml LPS for 10 min, followed by fMLP (1 μM) stimulation for 10, 30 or 60 min **(A,C,E)**, or stimulated with 1 μM thapsigargin (Tg) for the same time **(B,D)**. LTB4, cys-LTs or PGE2 in the cell supernatants were analyzed by ELISA. **(A)**: $n = 5$, **(B–E)**: $n = 6$. **(F,G)** Phosphorylated cPLA$_2$α (p-cPLA$_2$α) and cPLA$_2$α protein were analyzed by western blot (representative of three independent experiments). **(H,I)** Neutrophils were treated with vehicle (0.1% DMSO) or 1 μM KIRA6, followed by LPS (100 ng/ml) and fMLP (1 μM) stimulation for 10, 30 or 60 min **(H)** ($n = 7$). Alternatively, neutrophils were treated with vehicle (0.1% DMSO) or different concentrations of KIRA6 for 30 min, followed by LPS (100 ng/ml, 10 min), and fMLP (1 μM, 30 min) stinulation **(I)** ($n = 4$). LTB$_4$ production in cell supernatants was analyzed by ELISA. $^{*}p < 0.05$, $^{**}p < 0.01$, $^{***}p < 0.001$, $^{****}p < 0.0001$.

with 0–100 μM of KIRA6 or K252a as the positive control. Produced ADP was converted to ATP by ADP-Glo Assay (Promega) and the luminescence recorded using the TECAN Infinite M200 plate reader. Fluorescence values were normalized to vehicle group and the dose response curve was created using non-linear regression from which IC_{50} values were determined with the GraphPad Prism program.

Molecular Docking

The crystal structure of p38 in complex with SB203580 (PDB ID: 1A9U) was used as a template to perform docking simulations with KIRA6. KIRA6 as the ligand was prepared using the Grade Web Server (https://www.globalphasing.com). Prior to the docking, SB203580 was removed from the X-ray structure. Docking simulations with KIRA6 was carried out with the AutoDock Vina tool (Trott and Olson, 2010). In parallel, docking with SB203580 was performed to determine the binding score. The binding conformation with the best score was visualized with the Chimera 1.15 software. The 2D map for the protein-ligand interactions were generated using BIOVIA Discovery Studio Visualizer (Dassault Systems) and reproduced using ChemDraw 19.0.

Statistics

Data were presented as Mean ± SEM unless otherwise specified. Differences among groups were evaluated by Student's t-test, One-way or Two-way ANOVA. A value of $p < 0.05$ was considered statistically significant.

RESULTS

KIRA6 Blocks Leukotriene Production From Macrophages and Neutrophils

To assess the effect of KIRA6 on leukotriene biosynthesis, monocytes were isolated from human peripheral blood and further differentiated into macrophages with M-CSF. KIRA6 was added to the cells before stimulation with LPS plus fMLP or thapsigargin, an inducer of ER stress. In both conditions, LTB_4 and cys-LT production were triggered and peaked at 10 or 30 min 1 μM KIRA6 significantly inhibited the peak production of LTB_4 and cys-LTs (**Figure 1A–D**). The inhibition was not limited to leukotrienes and also affected synthesis of prostaglandins (**Figure 1E**), suggesting an inhibition of AA release. Since $cPLA_2\alpha$ is the key enzyme for AA release in macrophages, and $cPLA_2\alpha$ activity is dependent on phosphorylation at Ser-505 (Gijón et al., 2000), we measured $cPLA_2\alpha$ phosphorylation in KIRA6 treated cells and observed a reduction in phosphorylated $cPLA_2\alpha$ protein level (**Figure 1F,G**). We further asked if the inhibition of leukotriene production is a cell-specific effect and performed similar experiments with neutrophils isolated from peripheral blood. In neutrophils, KIRA6 inhibited LTB4 production at 10 and 30 min stimulation by LPS/fMLP (**Figure 1H**). The inhibitory effect of KIRA6 was dose-dependent and started to be statistically significant from 100 nM (**Figure 1I**).

Phosphorylation of p38 and ERK Are Diminished in KIRA6 Treated Cells, Association With Decreased Leukotriene Production and Cytosolic $PLA_2\alpha$ Phosphorylation

To further investigate the mechanisms by which KIRA6 inhibits leukotriene biosynthesis, we measured its effect on enzymatic activity of PLA_2, 5-LOX, LTA4H, and LTC4S enzyme activity in homogenates of isolated neutrophils and differentiated MM6 cells. KIRA6 failed to attenuate any of these key enzymes in the leukotriene pathway at the concentrations indicated in **Supplementary Figure S1**. We also tested the effect of KIRA6 on mobilization of cytosolic calcium in hMDMs and found that 1 μM KIRA6 had no significant effect on calcium, also in presence of 2 mM EGTA (**Supplementary Figure S2**). As $cPLA_2\alpha$ phosphorylation was inhibited by KIRA6 (**Figures 1E,F**), we asked whether KIRA6 may target the upstream kinases p38 and ERK. To test this, MM6 cells were used and a similar inhibitory effect of KIRA6 on cys-LT production was observed with IC_{50} values of 89 and 112 nM for the two stimuli, LPS/fMLP and thapsigargin, respectively (**Figure 2A,B**). KIRA6 dose-dependently inhibited p38 and ERK phosphorylation in MM6 cells, which is associated with attenuation of $cPLA_2\alpha$ phosphorylation and cys-LT production (**Figure 2C,D**). KIRA6 inhibited p38 phosphorylation already at 100 nM while a higher concentration (1 μM) was required to inhibit ERK phosphorylation. To further assess if the two kinases are involved in the regulation of cys-LTs by KIRA6, we used the p38 kinase inhibitor SB203580 and U0126- a kinase inhibitor that blocks ERK phosphorylation. As expected, both inhibitors attenuated cys-LTs production from LPS/fMLP stimulated cells. However, they had no apparent inhibitory effects in KIRA6 pre-treated cells, suggesting 1 μM KIRA6 is sufficient to block p38 and ERK pathways to reduce leukotriene production (**Figure 2E**).

KIRA6 Inhibits Leukotriene Production Independent of Inositol-Requiring Enzyme 1α

Inasmuch as KIRA6 is a potent IRE1α inhibitor, it was expected that this protein would be involved in the inhibition of leukotriene production. To specifically target IRE1α, we silenced this enzyme in MM6 cells (**Supplementary Figure S3**) and analyzed the effect of KIRA6. Interestingly, KIRA6 showed significant inhibitory effect on leukotriene production by IRE1α deficient cells, in a similar manner as in control MM6 cells (**Figures 3A, B**). Furthermore, when control MM6 cells were treated with another potent IRE1α inhibitor, 4 μ8C, the leukotriene production and the phosphorylation of p38 and ERK were not significantly influenced (**Figures 3C, D**), suggesting the effects of KIRA6 (**Figure 2A,B**) are IRE1α-independent.

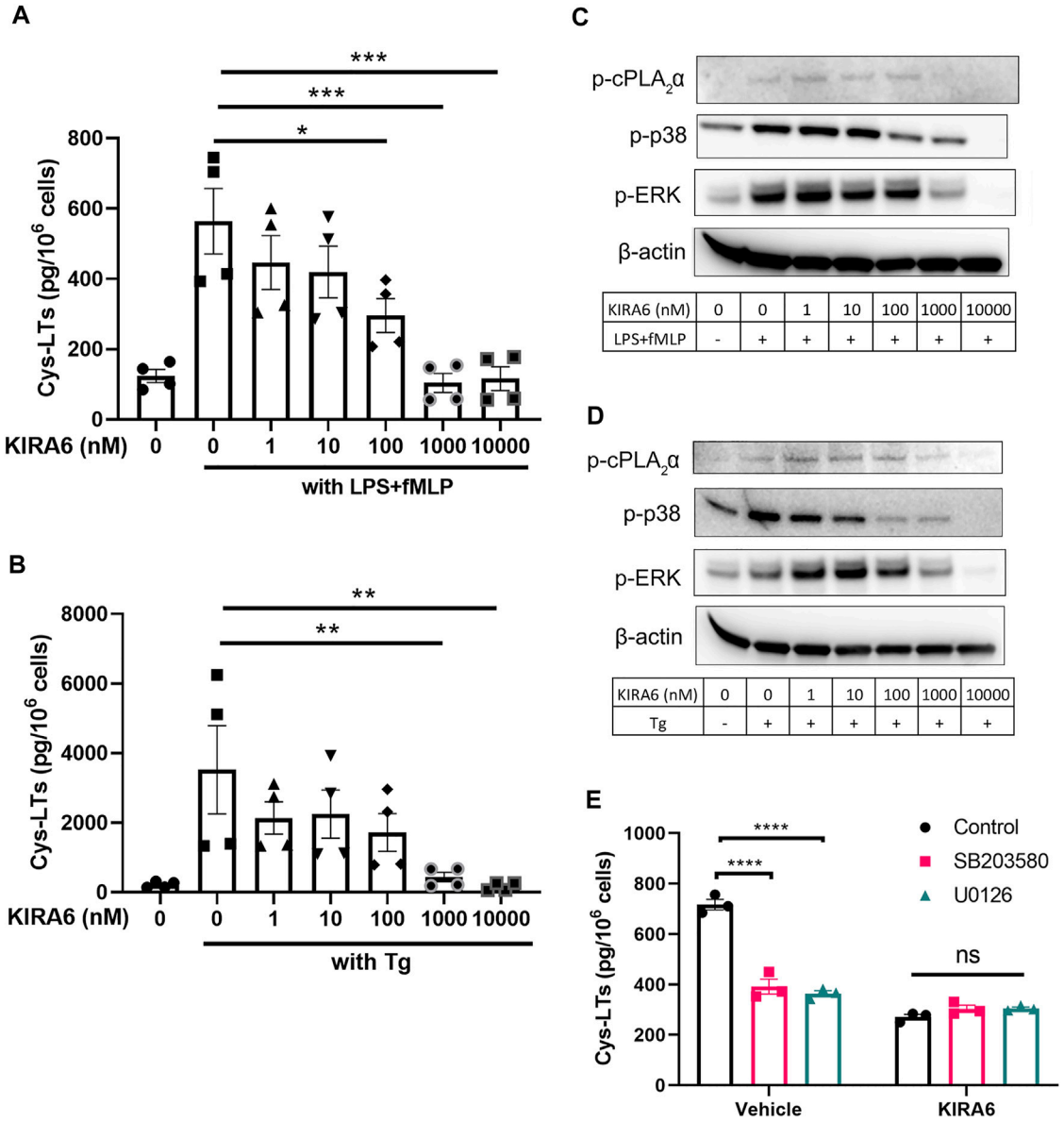

FIGURE 2 | Phosphorylation of p38 and cPLA$_2$α is reduced in KIRA6 treated cells **(A,B)**. MM6 cells were pretreated with vehicle (0.1% DMSO) or different concentrations of KIRA6 for 30 min, followed by challenge with LPS (100 ng/ml, 10 min), and fMLP (5 μM, 30 min), or Tg alone (1 μM, 30 min). Cys-LTs in cell supernatants were analyzed by ELISA (n = 4). **(C,D)** Phosphorylated cPLA$_2$α, p38, and ERK (p-cPLA$_2$α, p-p38, and p-ERK) were analyzed by western blot (representative of three independent experiments). **(E)** MM6 cells were pre-treated with vehicle (0.1% DMSO) or KIRA6 (1 μM) followed by incubation of SB203580 (10 μM) or U0126 (10 μM) for 30 min. The cells were further stimulated with LPS (100 ng/ml, 10 min) and fMLP (5 μM, 30 min). Cys-LTs in cell supernatants were analyzed by ELISA (n = 3). *p < 0.05, **p < 0.01, ***p < 0.001, ****p < 0.0001, ns: no significance.

KIRA6 Is a Potent p38 Inhibitor With Potential Affinity to the ATP-Binding Pocket

We also tested if KIRA6 has direct effects on the activity of p38 and/or ERK. The potent p38 inhibitor SB203580, used as positive control, inhibited p38 kinase activity with an IC_{50} value of 130 nM. Though somewhat less potent than SB203580, KIRA6 also attenuated p38 activity, with an IC_{50} value of about 1 μM (**Figure 4A**). In contrast, 4 μ8C, another inhibitor of IRE1α, did not affect the kinase activity of p38. On the other hand, KIRA6 did not exhibit any apparent direct effect on the kinase activity of ERK1/2, in contrast to the ERK inhibitor K252a (**Figure 4B,C**). Furthermore, molecular docking indicates that KIRA6 binds to the active site of p38 (**Figure 4D–F**). Thus, the docking scores with Autodock Vina for KIRA6 and the potent p38 inhibitor, SB203580, were similar. In addition, KIRA6 and SB203580 were both interacting with key residues of the ATP binding cavity of p38 (**Supplementary Figure S4**). These results indicate that KIRA6, which belongs to a group of type II kinase inhibitors (Ghosh et al., 2014), potently interacts with p38.

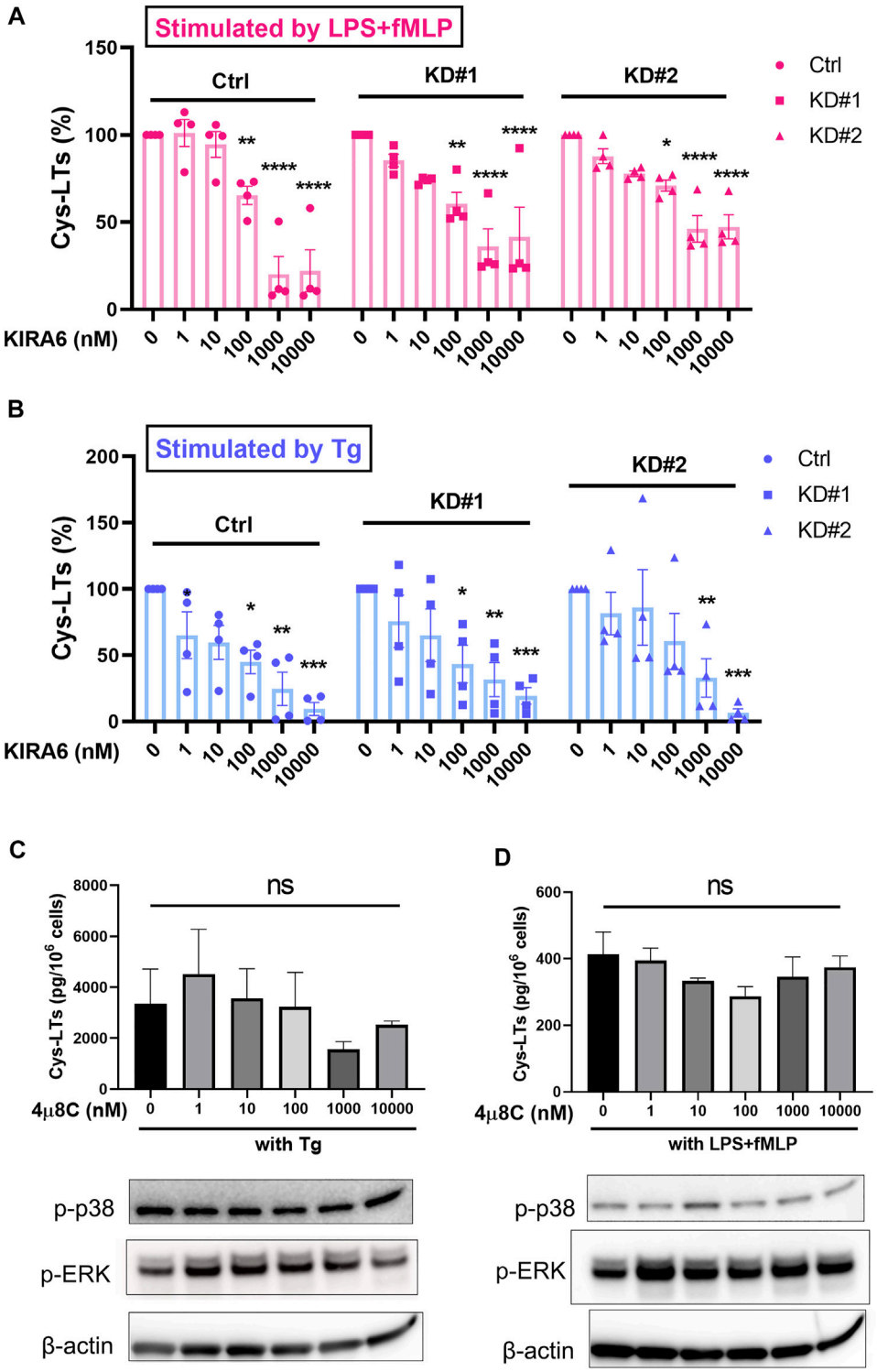

FIGURE 3 | KIRA6 inhibits leukotriene biosynthesis by a mechanism independent of IRE1α. **(A,B)** MM6 cells transfected with shRNA against non-target shRNA (Control) and IRE1α (KD#1 and KD#2) were treated with different concentrations of KIRA6, followed by challenge with LPS (100 ng/ml, 10 min) and fMLP (5 μM, 30 min), or Tg alone (1 μM, 30 min). Cys-LTs production in cell supernatants were analyzed by ELISA (n = 4). **(C,D)** MM6 cells were pretreated with vehicle (0.1% DMSO) or different concentrations of 4 μ8C for 30 min, followed by challenge with LPS (100 ng/ml, 10 min) and fMLP (5 μM, 30 min), or Tg alone (1 μM, 30 min). Phosphorylated p38 (p-p38) and p-ERK were analyzed by western blot (representative of three independent experiments). Cys-LT production in cell supernatants were analyzed by ELISA (n = 4). $^{*}p < 0.05$, $^{**}p < 0.01$, $^{***}p < 0.001$, $^{****}p < 0.0001$, ns: no significance.

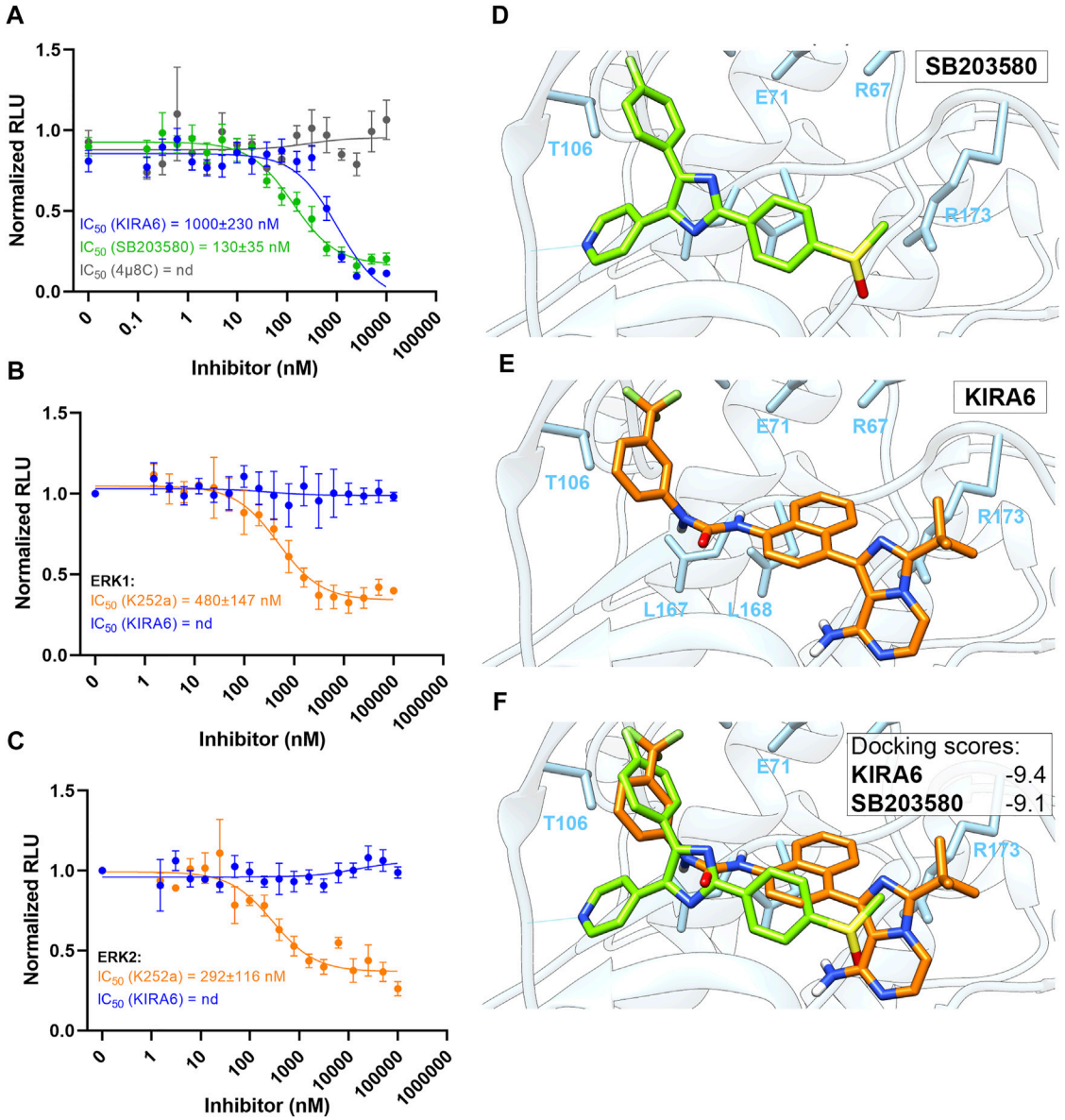

FIGURE 4 | Molecular docking of KIRA6 into the active site of p38. **(A)** Dose response curves of p38 kinase activity inhibition by KIRA6 (blue trace; *n* = 10), SB203580 (green trace; *n* = 4) and 4 μ8C (grey trace; *n* = 4). **(B,C)** Dose response curves of ERK1 **(B)** and ERK2 **(C)** kinase activity inhibition by KIRA6 (blue trace) and K252a (orange trace) (*n* = 4). **(D–F)** Binding conformations of KIRA6 (orange) and SB203580 (green) in the active site of p38 and the respective docking scores.

DISCUSSION

Leukotrienes are pro-inflammatory and immune-modulating lipid mediators that play divergent roles in various pathological conditions and represent important targets for drug development (Haeggström, 2018). The current study presents an unexpected and potent inhibitory effect of KIRA6 on leukotriene biosynthesis in human phagocytes, *viz.* macrophages and neutrophils. The cellular LTB_4 and cys-LTs production in macrophages was stimulated by two distinct means, i.e., the microbial components LPS and fMLP, or the stress molecule thapsigargin (**Figure 1**). In both cases, leukotriene production was successfully stimulated, but with large variability from donor to donor, which has been broadly observed in the eicosanoid field and may be due to various factors such as gender and intake of non-steroidal anti-inflammatory drugs.

Inasmuch as KIRA6 blocked leukotriene biosynthesis with equal, or even better potency compared to its action against IRE1α, we initially hypothesized that this arm of the UPR was closely linked to the leukotriene cascade, in analogy with what has been reported for prostaglandin synthesis (Chopra et al., 2019). However, we could not observe any significant effects of KIRA6 on calcium mobilization or key enzymes of the leukotriene cascade, and macrophages made deficient of IRE1α still responded to KIRA6 (**Figure 3A,B**). Instead, we followed the observation that KIRA6 reduced phosphorylation of

cPLA$_2$α, which releases AA for leukotriene and prostaglandin biosynthesis. It turned out that in intact cells, the suppression of leukotriene production was associated with reduction of phosphorylated p38 and ERK (**Figure 2A–D**), established kinases for 5-LOX and cPLA$_2$α (Surette et al., 1998; Gijón et al., 2000; Rådmark et al., 2007; Ghosh et al., 2014), and 1 μM KIRA6 was sufficient to mask the inhibitory effects SB203580 and U0126 in leukotriene production (**Figure 2E**). This suggests that KIRA6 is able to block the p38 and ERK pathways presumably *via* inhibition of mitogen-activated protein kinase kinases (MKKs), for instance MKK3/6 and MKK1/2, respectively, which would in turn reduce p38 and ERK phosphorylation and thereby leukotriene biosynthesis. Moreover, the important decreases of p38 and ERK phosphorylation also predict a reduction of 5-LOX phosphorylation at Ser271 and Ser663, which could contribute to the decreased leukotriene production. However, we were not able to detect endogenous 5-LOX phosphorylation with commercially available antibodies (data not shown), suggesting that 5-LOX phosphorylation, or its inhibition, is not involved in this model.

Besides reducing p38 and ERK phosphorylation, KIRA6 was also found to directly interact with p38 and inhibit its kinase activity. Through molecular docking, KIRA6 was assigned binding affinity to p38 and a potential to enter its ATP-binding domain. Moreover, the inhibitory potency of KIRA6 against p38 kinase activity (IC_{50} = 1 μM, **Figure 4A**) is close to that reported for the IRE1α-XBP1 UPR activity [IC_{50} = 0.6 μM, (Ghosh et al., 2014)]. It is noteworthy that KIRA6 also exerts inhibitory effects on prostaglandin production by macrophages stimulated with LPS/fMLP, presumably mediated by inhibition of cPLA$_2$α (**Figure 1E**). This provides a second mechanism for KIRA6 in targeting prostaglandin synthesis, apart from the recently described IRE1α-dependent transcriptional regulation of cyclooxygenase-2 and microsomal prostaglandin E synthase-1 (Chopra et al., 2019).

As a potent allosteric inhibitor of IRE1α, KIRA6 has been developed to inhibit IRE1α-mediated cell death, and has been demonstrated to promote cell survival and prevent ER stress-induced cell degeneration *in vivo* (Ghosh et al., 2014). Of note, recent studies have indicated that KIRA6 possesses anti-inflammatory and immune-modulating properties (Chen et al., 2019; Hull-Ryde et al., 2021; Rufo et al., 2022). In light of our results, it is possible that inhibition of the p38/ERK- cPLA$_2$α axis of leukotriene synthesis may account for some of these drug effects. Moreover, p38 and ERK participate in a variety of cellular processes by integrating different stress, metabolic, and inflammatory signals suggesting that KIRA6 may interfere with other fundamental cellular processes, yet to be characterized.

In summary, we have uncovered a novel potent action of KIRA6, in which this small molecule interferes with p38 and ERK signaling pathways, leading to inhibition of leukotriene production. While KIRA6 is a promising lead for pharmacological intervention in the IRE1α-XBP1 pathway, further work is required to detail the full pharmacological repertoire of this drug.

DATA AVAILABILITY STATEMENT

The raw data supporting the conclusions of this article will be made available by the authors, without undue reservation.

AUTHOR CONTRIBUTIONS

JH and BS provided the conception of the study. JH and XT designed the study. XT and TT performed the experiments and data analysis. XT, TT, and JH wrote the manuscript. All the authors contributed to the revision and approved the submitted manuscript.

FUNDING

This study was supported by the Swedish Research Council (Grant 2018-02818), immunometabolism grants (NNF15CC0018346 and 0064142) and Karolinska Institutet. XT was supported by the Konsul Th C Berghs Foundation (Grant 2356). TT was supported by the Estonian Research Council (Grant PUTJD1046).

ACKNOWLEDGMENTS

The authors are grateful to Prof. Per Uhlén for valuable input on calcium signaling.

SUPPLEMENTARY MATERIAL

The Supplementary Material for this article can be found online at: https://www.frontiersin.org/articles/10.3389/fphar.2022.806240/full#supplementary-material

REFERENCES

Batista, A., Rodvold, J. J., Xian, S., Searles, S. C., Lew, A., Iwawaki, T., et al. (2020). IRE1α Regulates Macrophage Polarization, PD-L1 Expression, and Tumor Survival. *Plos Biol.* 18 (6), e3000687. doi:10.1371/journal.pbio.3000687

Chen, G., Ribeiro, C. M. P., Sun, L., Okuda, K., Kato, T., Gilmore, R. C., et al. (2019). XBP1S Regulates MUC5B in a Promoter Variant-Dependent Pathway in Idiopathic Pulmonary Fibrosis Airway Epithelia. *Am. J. Respir. Crit. Care Med.* 200 (2), 220–234. doi:10.1164/rccm.201810-1972OC

Chopra, S., Giovanelli, P., Alvarado-Vazquez, P. A., Alonso, S., Song, M., Sandoval, T. A., et al. (2019). IRE1α-XBP1 Signaling in Leukocytes Controls Prostaglandin Biosynthesis and Pain. *Science* 365 (6450), eaau6499. doi:10.1126/science.aau6499

Funk, C. D. (2001). Prostaglandins and Leukotrienes: Advances in Eicosanoid Biology. *Science* 294 (5548), 1871–1875. doi:10.1126/science.294.5548.1871

Ghosh, R., Wang, L., Wang, E. S., Perera, B. G., Igbaria, A., Morita, S., et al. (2014). Allosteric Inhibition of the IRE1α RNase Preserves Cell Viability and Function during Endoplasmic Reticulum Stress. *Cell* 158 (3), 534–548. doi:10.1016/j.cell.2014.07.002

Gijón, M. A., Spencer, D. M., Siddiqi, A. R., Bonventre, J. V., and Leslie, C. C. (2000). Cytosolic Phospholipase A2 Is Required for Macrophage Arachidonic Acid Release by Agonists that Do and Do Not Mobilize Calcium. Novel Role of Mitogen-Activated Protein Kinase Pathways in Cytosolic Phospholipase A2 Regulation. *J. Biol. Chem.* 275 (26), 20146–20156. doi:10.1074/jbc.M908941199

Haeggström, J. Z., and Funk, C. D. (2011). Lipoxygenase and Leukotriene Pathways: Biochemistry, Biology, and Roles in Disease. *Chem. Rev.* 111 (10), 5866–5898. doi:10.1021/cr200246d

Haeggström, J. Z. (2018). Leukotriene Biosynthetic Enzymes as Therapeutic Targets. *J. Clin. Invest.* 128 (7), 2680–2690. doi:10.1172/JCI97945

Hetz, C. (2012). The Unfolded Protein Response: Controlling Cell Fate Decisions under ER Stress and beyond. *Nat. Rev. Mol. Cel. Biol.* 13 (2), 89–102. doi:10.1038/nrm3270

Hull-Ryde, E. A., Minges, J. T., Martino, M. E. B., Kato, T., Norris-Drouin, J. L., and Ribeiro, C. M. P. (2021). IRE1α Is a Therapeutic Target for Cystic Fibrosis Airway Inflammation. *Int. J. Mol. Sci.* 22 (6), 3063. doi:10.3390/ijms22063063

Korovesis, D., Rufo, N., Derua, R., Agostinis, P., and Verhelst, S. H. L. (2020). Kinase Photoaffinity Labeling Reveals Low Selectivity Profile of the IRE1 Targeting Imidazopyrazine-Based KIRA6 Inhibitor. *ACS Chem. Biol.* 15 (12), 3106–3111. doi:10.1021/acschembio.0c00802

Rådmark, O., Werz, O., Steinhilber, D., and Samuelsson, B. (2007). 5-Lipoxygenase: Regulation of Expression and Enzyme Activity. *Trends Biochem. Sci.* 32 (7), 332–341. doi:10.1016/j.tibs.2007.06.002

Rufo, N., Korovesis, D., Van Eygen, S., Derua, R., Garg, A. D., Finotello, F., et al. (2022). Stress-Induced Inflammation Evoked by Immunogenic Cell Death Is Blunted by the IRE1alpha Kinase Inhibitor KIRA6 through HSP60 Targeting. *Cell Death Differ* 29 (1), 230–245. doi:10.1038/s41418-021-00853-5

Samuelsson, B. (1983). Leukotrienes: Mediators of Immediate Hypersensitivity Reactions and Inflammation. *Science* 220 (4597), 568–575. doi:10.1126/science.6301011

Shan, B., Wang, X., Wu, Y., Xu, C., Xia, Z., Dai, J., et al. (2017). The Metabolic ER Stress Sensor IRE1α Suppresses Alternative Activation of Macrophages and Impairs Energy Expenditure in Obesity. *Nat. Immunol.* 18 (5), 519–529. doi:10.1038/ni.3709

Smith, J. A. (2018). Regulation of Cytokine Production by the Unfolded Protein Response; Implications for Infection and Autoimmunity. *Front. Immunol.* 9, 422. doi:10.3389/fimmu.2018.00422

Surette, M. E., Dallaire, N., Jean, N., Picard, S., and Borgeat, P. (1998). Mechanisms of the Priming Effect of Lipopolysaccharides on the Biosynthesis of Leukotriene B4 in Chemotactic Peptide-Stimulated Human Neutrophils. *FASEB J.* 12 (14), 1521–1531. doi:10.1096/fasebj.12.14.1521

Trott, O., and Olson, A. J. (2010). AutoDock Vina: Improving the Speed and Accuracy of Docking with a New Scoring Function, Efficient Optimization, and Multithreading. *J. Comput. Chem.* 31 (2), 455–461. doi:10.1002/jcc.21334

Wan, M., Sabirsh, A., Wetterholm, A., Agerberth, B., and Haeggström, J. Z. (2007). Leukotriene B4 Triggers Release of the Cathelicidin LL-37 from Human Neutrophils: Novel Lipid-Peptide Interactions in Innate Immune Responses. *FASEB J.* 21 (11), 2897–2905. doi:10.1096/fj.06-7974com

Wan, M., Tang, X., Rekha, R. S., Muvva, S. S. V. J. R., Brighenti, S., Agerberth, B., et al. (2018). Prostaglandin E2 Suppresses hCAP18/LL-37 Expression in Human Macrophages *via* EP2/EP4: Implications for Treatment of *Mycobacterium tuberculosis* Infection. *FASEB J.* 32 (5), 2827–2840. doi:10.1096/fj.201701308

Werz, O. (2002). 5-Lipoxygenase: Cellular Biology and Molecular Pharmacology. *Curr. Drug Targets Inflamm. Allergy* 1 (1), 23–44. doi:10.2174/1568010023344959

Conflict of Interest: The authors declare that the research was conducted in the absence of any commercial or financial relationships that could be construed as a potential conflict of interest.

Publisher's Note: All claims expressed in this article are solely those of the authors and do not necessarily represent those of their affiliated organizations, or those of the publisher, the editors and the reviewers. Any product that may be evaluated in this article, or claim that may be made by its manufacturer, is not guaranteed or endorsed by the publisher.

frontiers | Frontiers in Pharmacology

MINI REVIEW
published: 17 May 2022
doi: 10.3389/fphar.2022.867431

Single Cell Biology: Exploring Somatic Cell Behaviors, Competition and Selection in Chronic Disease

*Wandi Zhu, Rahul C. Deo and Calum A. MacRae**

Cardiovascular Medicine Division and Department of Medicine, Brigham and Women's Hospital, Harvard Medical School, Boston, MA, United States

The full range of cell functions is under-determined in most human diseases. The evidence that somatic cell competition and clonal imbalance play a role in non-neoplastic chronic disease reveal a need for a dedicated effort to explore single cell function if we are to understand the mechanisms by which cell population behaviors influence disease. It will be vital to document not only the prevalent pathologic behaviors but also those beneficial functions eliminated or suppressed by competition. An improved mechanistic understanding of the role of somatic cell biology will help to stratify chronic disease, define more precisely at an individual level the role of environmental factors and establish principles for prevention and potential intervention throughout the life course and across the trajectory from wellness to disease.

Keywords: clonal hematopoeisis, cell competition, chronic inflammation, single cell physiology, therapeutics

OPEN ACCESS

Edited by:
Pallavi R. Devchand, University of Calgary, Canada

Reviewed by:
Jason E. Fish, University Health Network (UHN), Canada
Walter Wahli, University of Lausanne, Switzerland

****Correspondence:***
Calum A. MacRae
cmacrae@bwh.harvard.edu

Specialty section:
This article was submitted to Inflammation Pharmacology, a section of the journal Frontiers in Pharmacology

Received: *01 February 2022*
Accepted: *29 March 2022*
Published: *17 May 2022*

Citation:
Zhu W, Deo RC and MacRae CA (2022) Single Cell Biology: Exploring Somatic Cell Behaviors, Competition and Selection in Chronic Disease. Front. Pharmacol. 13:867431. doi: 10.3389/fphar.2022.867431

INTRODUCTION

Infectious disease is perhaps the most obvious and acute form of cell "competition" in human experience, with innate and adaptive immune responses collaborating to eliminate exogenous cells which themselves are participants in the competition. Related biology also drives the clearance of aberrant native cells, such as damaged or neoplastic cells. These processes require activation and consumption of the immune system, generally described as the inflammatory response (Baldridge et al., 2010; King and Goodell 2011). A substantial component of the variation in inflammatory responses between individuals is thought to reflect inherited differences in immune reactivity or the overt effects of chronic comorbidities (Initiative 2021). The discrete outcomes from identical insults among superficially similar individuals are a manifestation of our limited ability to detect meaningful intrinsic differences in many biological processes with current tools. Looking at orthogonal outputs of these same immune or inflammatory pathways may be useful as these cellular functions also play central roles in defining hierarchies in distinctive cell non-autonomous processes including synaptogenesis, metabolism, and aging (Lee et al., 2014; Sekar et al., 2016).

Accumulating evidence shows that individual variation in inflammatory responses may also be influenced by lifelong competition between different somatic cell populations, some of which arise as they acquire cell behaviors with differential advantages in various tissues. Such competitions among somatic cell populations represent potentially modifiable components of many chronic diseases (Thorpe et al., 2020). In this model, the emerging dominance of particular cellular populations may result from active selection at many levels including specific functional attributes which create advantage, differential rates of proliferation in dividing cells or simple survival in terminally differentiated cells (Nagata and Igaki 2018; Lawlor et al., 2020).

The preponderance of genetic selection in evolution antedates multicellularity, so that cell competition is a useful framework for understanding emerging mechanisms of somatic selection and for understanding the net outputs of competing cell behaviors (Maruyama and Fujita 2021; Swiatczak 2021). In this short perspective, we will summarize existing evidence of contributions from distinctive somatic cell populations to chronic disease, highlight those few mechanisms that have been established, outline the constraints which limit detection of somatic selection, and illustrate the potential of scalable single cell biology to explore the dynamics of cell competition throughout the course of many common diseases. We will focus on inflammatory biology, but the mechanisms and investigative approaches we discuss are likely pertinent in many other areas.

MECHANISMS OF CELL COMPETITION

The specification of cell behaviors during development, the general patterning of the body plan, tissue architecture, and even long-term features of cell states, are dependent on stereotypic cellular events prespecified by transcriptional programs and interactive cues from neighboring or remote cells (Bruce and Zernicka-Goetz 2010; Zhu and Zernicka-Goetz 2020; Maruyama and Fujita 2021). These cues operate in pathways that share overlapping mechanisms with single cell organisms, and have been conceptually aggregated under the framework of cell competition. The outcomes of cellular competition are dependent on the baseline fitness or dynamic responses of participating cells and the prevailing conditions under which competition takes place. Together, the combination of innate cell behaviors, acquired functional properties, and the extrinsic selection forces determine the discrete outcomes of cell competition.

The spectrum of pathways implicated in cell competition includes those with obvious mechanisms, as well as others where the distinctive cellular advantages conferred may be more obscure (Baker 2020). Clearly, the efficiency of cell division varies among cells and those capable of more rapid cell division or improved use of metabolic resources fare better throughout development (Lawlor et al., 2020). The ribosome is a complex molecular machine that is responsible for protein synthesis. The biogenesis of ribosome is one of the most energy demanding cellular processes and it is strongly associated with cell survival and proliferative capacity. In cell or organismal screens, gene variation affecting ribosomal biogenesis has consistently been found to be among the most important differences between successful and vanquished cells. Not surprisingly, strong selection bias is also observed with mutants in genes encoding core drivers of cell division itself, such as the tumor suppressors *Myc* and T*p53* (Madan et al., 2018; Nagata and Igaki 2018). Why tumor suppressors more generally do not exhibit effects on developmental cell competition is not obvious from extant experimental data. It is possible there may be strong evolutionary advantages to carefully balanced competition in most tissues, particularly in epithelia. Indeed, intercellular coupling in epithelia is related to cellular competition in a complex manner. Coupling can average differences across multiple cells, for example in the concentrations of intracellular metabolites or second messengers (Kiselyov et al., 2003). This effect can synchronize cell signaling across entire cellular compartments, but also can be a direct sensor of gradients of competitiveness particularly with metabolic substrates or toxins. These aspects may be reflected in the apicobasal cell polarity genes identified in cell competition screens (Nagata and Igaki 2018). Selection based on fitness or stochastic processes is also a key component of the formation of discrete cellular networks from neuronal circuits to antigen processing (Willis et al., 2006; Costa-Rodrigues et al., 2021). The ultimate fate of the 'losers' in such cellular population competitions is not often studied, though it may include different forms of programmed cell death, new local cell fates, or escapes to new futures. Indeed, the extrusion of less competitive cells is one means by which cell competition has been identified (Maruyama and Fujita 2021). Some extruded cells undergo apoptotic cell death, while others may initiate epithelial-mesenchymal transitions (EMTs) or revert to stem cell-like fates (Ohsawa et al., 2018). The same pathways are exploited in normal development and throughout adult life where travelling cellular offspring may leave progenitor compartments for new environments.

Cell competition signals are also central to cellular maturation and adaptation in multiple contexts from early development to aging (Alvarez-Dominguez and Melton 2022). In chronic disease, it has recently become evident that cellular competition and the balance between germline or somatic variation and the environment is playing out at many levels, potentially explaining significant components of the interindividual variation in the progression, responses to therapy and outcomes of highly prevalent disorders.

INSIGHTS FROM CLONAL HEMATOPOIETIC ABNORMALITIES

Early insights into the role of cell competition in chronic disease emerged from the study of human genomics, where spontaneous somatic mutation with proliferative advantage became detectable as genotyping technologies enabled deeper characterization of variation from germline in DNA samples collected from peripheral blood. Accessible cells in the periphery are dominated by representatives from the hematopoietic compartment which includes the majority of cells that govern inflammation (King and Goodell 2011). Hematopoiesis provides a distinctive setting to investigate cell competition during adulthood, as the system generates hundreds of billions of cells across multiple lineages every day throughout life. To maintain this output, the hematopoietic system has adopted a hierarchical differentiation scheme that allows enormous amplification from a few hematopoietic stem cell (HSC) clones (Orkin and Zon 2008). As part of the inflammatory response, HSCs are exposed to cues that signal specific adaptations and the production of new immune cells (Medzhitov 2008; King and

Goodell 2011), which may accelerate the acquisition of somatic mutations. The emergence of dominant HSC clones is partly due to the effects of mutations on fitness advantages for proliferation or survival in the bone marrow environment (Watson et al., 2020). However, studies also suggest HSCs possessing mutations remain small clones in the bone marrow for many years and are present in healthy individuals (Mendez-Ferrer et al., 2020). It is plausible that a shift in bone marrow microenvironment, the accumulation of additional mutations or a change in the effective selection pressures is necessary to initiate clonal expansion. For example, a recent study showed that the expansion of mutant HSCs is driven by their resistance to inflammatory signals, driven by their mature cell progeny (Avagyan et al., 2021). Besides the hematopoietic lineages, DNA isolated from peripheral blood may also contain nucleic acids from other sources including endothelial cell "progenitors," neoplastic cells from multiple tissues, chimaeric fetal cells, subcellular exosomes and cell-free nucleic acids (Szilagyi et al., 2020; Avramovic et al., 2021). The complexity of these DNA sources also impacts our interpretation of the mechanisms of cell competition in chronic disease (Avramovic et al., 2021).

Seminal work from Ebert's group first identified the presence of age-related clonal hematopoietic abnormalities in peripheral blood, distinct from the myelodysplastic syndrome but associated with increased risk of adverse outcomes including hematologic cancer, incident stroke, coronary heart disease and all-cause mortality (Jaiswal et al., 2014). The detected clones shared a series of underlying mutations in a small number of genes that are recurrently mutated in hematological neoplasia, including *DNMT3A*, *TET2* and *ASXL1*. Subsequent work has defined a growing number of associations between this phenomenon, known as clonal hematopoiesis of indeterminate potential (ChiP), and a wide range of other chronic disease outcomes including heart failure, atrial fibrillation, chronic obstructive lung disease, osteoporosis, transplant outcomes, and severe COVID-19 (Jaiswal et al., 2017; Dorsheimer et al., 2019; Dawoud et al., 2021; Feusier et al., 2021).

The underlying mechanisms for such associations are not yet evident and are likely to differ among clones and among chronic diseases. In at least some of these settings it appears that CHiP may be an index of prior exposures, presumably driving mutagenesis or selection (Coombs et al., 2017; Dawoud et al., 2020). There is evidence that some forms of CHiP are a reflection of a shared upstream susceptibility to a range of disorders mediated by different hematopoietic lineages (Bick et al., 2020). It is quite consistent with existing data that in many situations CHiP represents a sophisticated index of environmental genotoxicity or of inflammatory risk *per se* but is not necessarily a mechanistic driver. Only mechanistically targeted interventional studies will directly address these uncertainties.

Mouse models have demonstrated the potential importance of clonal hematopoietic behaviors in non-neoplastic phenomena including lesion formation in atherosclerosis. TET2 null progenitor clones expand in a chimeric transplant and also drive substantial increases in lesion size in the LDLR homozygous null model of atherosclerosis (Fuster et al., 2017). JAK2-mutant clones are associated with the highest levels of risk for atherosclerotic events among human CHiP cohorts. In murine models of these same JAK2 mutations (V617F), expressed selectively in macrophage lineages, increased proliferation of macrophages and prominent formation of necrotic cores in atherosclerotic lesions was observed. These changes can be suppressed by loss of function alleles in inflammasome components or by deletion of gasdermin D or AIM2 (Fidler et al., 2021). These experiments reinforce existing concepts of atherosclerosis progression and support a role for CHiP in the exacerbation of endovascular inflammation. Nevertheless, it remains difficult to fully recapitulate the likely decades-long effects of interactions between clones where only the victors ultimately manifest in the genomic analyses. Until there are comprehensive models of the lifelong competition between clones and the variable influences of other intrinsic or environmental factors on various stages of disease progression, it will prove difficult to define the relative contributions of different cellular mechanisms to the final outcomes. Once again, understanding the role of the losers may be at least as important as characterizing the winners in clonal competitions.

One tantalizing insight into the potential determinants of the final outcomes in complex and dynamic cellular competitions is the observation that the presence of CHiP was related to the observed effects of IL1β inhibition (with the monoclonal antibody canukinumab) on incident coronary events and on incident lung cancer in the rigorous CANTOS trial (Ridker et al., 2017; Svensson et al., 2022). This response to therapy may be a consequence of the particular features of the inflammatory response in these individuals, but also suggests there may be much broader roles for CHiP as an index or driver of potential outcomes in a wide range of disease-relevant and therapy-relevant cellular competitions.

As sequencing depth increases, evidence is accumulating from genotyping of peripheral blood and tissue samples from broader populations that somatic variation is a universal phenomenon. The initial identification of CHiP mainly focused on genes that have been previously implicated in causing hematologic malignancy. It has become clear that those genes may only underlie a limited portion of clonal selection (Zink et al., 2017). Examples are emerging of somatic mutations in single genes or even at single residues underlying very specific clinical syndromes. For example, somatic mutations in the X-chromosomal ubiquitinylation enzyme, UBA-1, have been shown to cause an adult onset autoinflammatory disorder in males through activation of the innate immune system as the underlying clone becomes dominant (Beck et al., 2020).

Unassayed somatic variation and underlying clonal competition must be considered as potential contributors in all genotype-phenotype associations (Avramovic et al., 2021). It will require serial genotyping and/or single cell analysis of genotypes to deconvolute fully the contributions of clonal competition to the large number of established genetic associations, and at present genotyping depth is the rate-limiting step in the detection of clonal imbalance. In addition, evidence is now emerging that dynamic non-genetic selection with sustained effects on cell behavior is

contributing to the progression of chronic disease and may also be more widespread than previously imagined.

FUNCTIONAL SELECTION

The existence of cellular competition between clones with a definable genomic basis for winning or losing, also implies a need for single cell genomic and functional analyses to understand those clonal attributes selected or lost in the competition. In addition genomics (even single cell genomics) may offer insufficient resolution to detect cell population shifts in the setting of epigenetic differences due to prior exposures or in the context of small or isogenic clones. There is now emerging definitive evidence of the existence of active cellular competition and selection based on functional attributes resulting not from genetic variation between clones, but rather from acquired 'fitness' under specific environmental constraints. In the absence of genetic mechanisms and consequent effects on allelic distributions, such selection may only be detected using single cell analyses. Together these observations suggest that single cell genotypic and phenotypic characterization of somatic cellular populations will be an important step in improving our understanding of the relationship between genotype and phenotype as well as the discrete and dynamic contributions of cell competition to the trajectories of common diseases.

Functional selection may operate through multiple mechanisms and is also likely to be more readily modifiable than intrinsic genotype-based clonal imbalance. All the factors that influence clonal behaviors can bias cellular, tissue or organ physiology in the absence of any changes in the genotypes, numbers, or capabilities of the underlying cell populations. For example, a period of exposure to low oxygen tension (PaO_2) may result in an erythrocyte cohort with dysregulated expression of erythropoietin (EPO) and hypoxia inducible factors (HIFs), with potential consequences for numerous disease states through the life cycle of these specific erythrocytes. Systematically classifying, across multiple phenotypic dimensions, single cell responses to disease, drug and other "environmental" exposures will enable the development of mechanistic insights into clonal and non-clonal behaviors underpinning individual variation in disease biology.

EVIDENCE OF ENVIRONMENTAL SELECTION

There is extensive evidence that environmental factors including stress, pollution and determinants of health all influence both acute and chronic inflammation, though in most instances the molecular mechanisms are not known or are incompletely understood. With the increasing accessibility of single cell biology (Gradeci et al., 2020), in particular in immunophenotyping, there is accumulating evidence of the direct effects of even modest changes in acquired or environmental factors on integrated cellular responses.

Salt and Autoimmunity

Work in mouse has elegantly defined the effects of modest increases in salt intake on the architecture of T-cell responses. The TH17 phenotype of helper T cells was known to be stabilized and reinforced by IL-23 signaling. Transcriptomic studies of the development and differentiation of the TH17 subset revealed a dependence on the salt inducible serum glucocorticoid kinase 1 (SGK1) (Wu et al., 2013). Genetic studies in mouse revealed a requirement for SGK1 as a mediator of the effects of high salt concentrations on TH17 production and on consequent inflammation. Increased dietary salt intake was also shown to lead to a more severe phenotype in murine autoimmunity models through the induction of a population of pathogenic and highly stable TH17 cells (Kleinewietfeld et al., 2013). These studies demonstrate regulation of T cell clonal selection process by dietary salt intake that ultimately impacts the autoimmune response and promotes tissue inflammation.

Smoking and Clonal Hematopoiesis

Smoking triggers immunological responses and alters inflammatory markers, such as C-reactive protein (CRP), fibrinogen, and leukocyte count, due to its direct effects on macrophage, neutrophil, and dendritic cell activity, as well as activation of subsequential immune responses due to epithelial and endothelial cell damage caused by reactive oxygen species. Analyses of human whole genome and whole exome sequencing data established a strong association between smoking and the occurrence of clonal hematopoiesis. The proinflammatory environment caused by smoking promotes the outgrowth of ASXL1-mutant hematopoietic stem cell clones (Dawoud et al., 2020). Moreover, smoking is linked to hematopoietic clonal expansion in absence of mutations in the traditionally defined driver genes, such as *TET2*, *DNMT3A*, *ASXL1*, and *PPM1D* (Zink et al., 2017), suggesting that environmental factors may drive cell competition without basal predisposition to somatic mutation.

Hyperglycemia, Thrombosis and Piezo1

Mechanical cues from the local environment or neighboring cells regulate cell behaviors and competitive interactions. Ion channels in the cell membrane, including the mechanosensory ion channel Piezo1, transduce mechanical cues into rapid electrical signals that control and amplify many downstream cellular functions. While the roles of ion channels are well-defined in excitable cell types, such as cardiomyocytes and neurons, their functions in non-excitable cells remain poorly understood. Recent studies reveal that ion channels are expressed abundantly on the cell membranes of peripheral blood cells and regulate processes including adaptive and innate immune responses, platelet activation, and red blood cell homeostasis (Cahalan et al., 2015; Feske et al., 2015; Ma et al., 2018). Besides somatic genetic alterations, ion channel expression and function may also be modulated by the environment or by chronic disease.

Thrombosis is the leading complication of common human disorders including diabetes, coronary heart disease, cancer, and infection. In a focused screen for single cell ion channel phenotypes associated with disease, it was possible to demonstrate a direct role for the mechanosensory ion

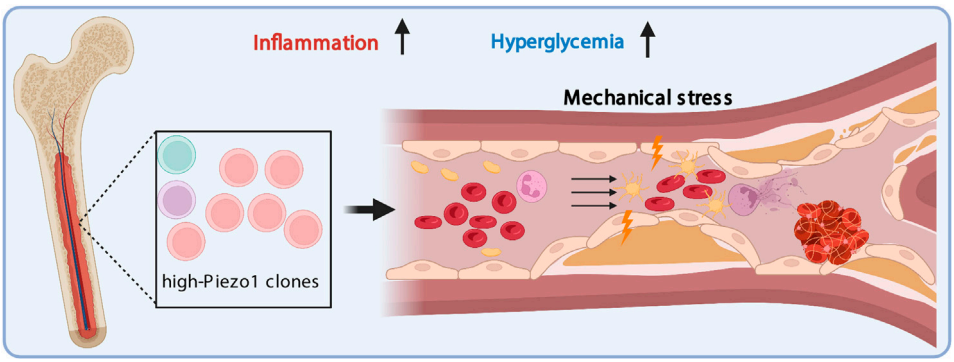

FIGURE 1 | Cell competition related to PIEZO1 during hematopoiesis. PIEZO1 expression levels lead to selection at several levels. High PIEZO1 expressing cells have proliferative advantage at baseline which is accentuated by hyperglycemia at key stages of hematopoiesis. This advantage may be determined by genetics, epigenetics or even stochastic variation. Subsequent selection may include survival advantages in multiple other settings each of which may apply only to specific cell types, but the net outcome is an associated increase in the susceptibility to thrombosis in a significant proportion of diabetic patients. Detecting such variation requires single cell phenotyping at scale.

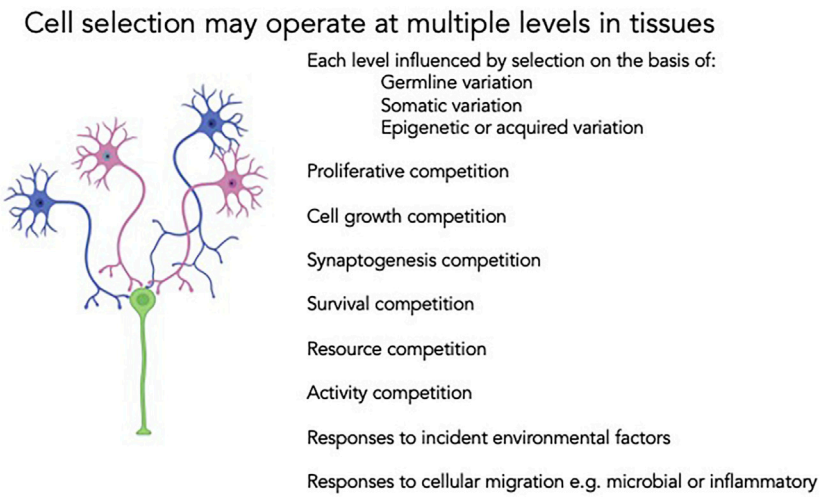

FIGURE 2 | Cell competition is also feasible in terminally differentiated cell lineages. Neurons may undergo selective pressures at multiple stages of their life cycle. Proliferative advantages for individual clones may be reinforced or counteracted in subsequent competition for synaptogenesis with other cells in neuronal circuits, activity-based functional inputs or differential susceptibility to ischemia, inflammation or other external pressures. The net output of the system, and the penetrance and expressivity of germline genotype, is a reflection of each of these levels of selection. A more rigorous appraisal of the discrete steps and the operant selection pressures will enable improved diagnosis, prognostication and therapy.

channel Piezo1 in clot formation in subjects with type 2 diabetes (T2DM) that is triggered by disordered blood flow (Zhu et al., 2022). Piezo1 function and expression are exquisitely controlled by the glycemic environment and in T2DM Piezo1 was upregulated in multiple blood lineages. In both *ex vivo* HSC differentiation and *in vivo* zebrafish whole kidney marrow transplantation, there was evidence that exposure to an elevated glucose concentration enriched high-PIEZO1-expressing HSCs and enhanced HSC differentiation towards pro-inflammatory monocytes and dendritic cells. The net effects of this modulation of mechanosensory channel expression and function in T2DM were a distinctive prothrombotic state which could be suppressed by specific inhibition of the Piezo1 channel. Subsequent studies in human samples confirmed a Piezo1-dependent prothrombotic state in a significant proportion of patients with T2DM. Findings from this study implicate the hyperglycemic environment in HSC clonal expansion and differentiation based on underlying variation in mechanosensitivity, which substantially contributes to elevated thrombotic risk (**Figure 1**). This modulation may be further impacted by changes in mechanical properties of the bone marrow microenvironment due to aging and chronic diseases.

Together these examples suggest that general environmental exposures or acquired microenvironmental features of chronic diseases exert selection pressure during hematopoiesis and lead to distinctive pathophysiologic courses. The detection and modulation of such effects in chronic diseases may open new therapeutic strategies, while the exploration of such single cell biology in simple blood samples highlights the possibility for scalable translational studies to define the dynamic effects of acquired factors on cellular physiology (Gradeci et al., 2020).

SYSTEMATIC CHARACTERIZATION OF HUMAN CELL POPULATION FUNCTION

Cell biology offers critical insights into the dynamic interactions between genes and environment but has long been relatively inaccessible in clinical and translational investigation. Human cell biology has been studied in only a few clinical settings; excised neoplastic tissue, liquid tumors and immunophenotyping, all typically at modest scale. Even in these contexts, the collection of single cell functional data is limited, though interest in circulating tumor cells and the falling costs of flow cytometry are slowly impacting the field. Unbiased approaches to even simple cellular data can predict clinically useful disease outcomes (Patel et al., 2015), and the association of CHiP and somatic genetic variation with discrete risk for a wide range of pathologies further highlights the need for deeper mechanistic insight. To understand fully the diversity of cellular mechanisms at play in somatic cell behavior, and their contributions to human responses to the environment, to drugs or to acquired components of chronic disease, there is a need for much broader exploration of single cell function and single cell genomics in clinical cohorts. In addition, to understand the dynamic responses even in terminally differentiated cells it will be important to assess biology under baseline and perturbed conditions (See **Figure 2**).

EMERGING TECHNOLOGIES AND FUTURE DIRECTIONS

How can cell biology be implemented at a scale similar to that of population genomics? The use of simple accessible technologies in large clinical populations would enable efficient expansion of the collection of clinically annotated cell biological data. An initial focus on widely available tools including morphometry, microscopy and vital dyes could identify disease areas where deeper exploration of cell function might be of utility. Using cellular data, computational approaches, including deep learning, can facilitate the extraction of relevant functional response signatures and identify discrete and previously unobserved cell populations or behaviors. Microfluidic systems, single cell capture methodologies and a range of cellular resolution phenotypes will enable much more granular exploration of the basic functional abnormalities in disease states. Expanding the capabilities of such tools to include exosomes and other circulating cell-derived particles with their contents will open a window into non-circulating cells in health and disease. Combining these assays to discern the features associating with specific cellular states will offer novel insights into the inflammation and other chronic disease mechanisms.

Ultimately, it will be important to characterize the full range of cell states and behaviors in health and disease. Exploring cell biology and its effects on cell population dynamics will likely offer mechanistic insights which are pertinent far beyond the specific cell types that are assayed. For instance, a combination of single cell transcriptional profiling, spatial, and temporal tracking has been applied to reveal dynamic and complex immune cell populational behaviors at the site of inflammation. There are now numerous examples of peripheral cellular phenotypes revealing biology of impact in remote and inaccessible cell types such as podocytes, adipocytes or even cardiomyocytes (Genovese et al., 2010; Asimaki et al., 2016). Scalable approaches to single cell function are available and will complement the genomic tools developed over the last 2 decades. Indeed, without additional phenotyping granularity, it will be difficult to realize mechanistic insights at the level of the individual patient, a prerequisite for the full potential of precision medicine. Cellular studies will also offer direct insight at a personal level into environmental or acquired factors.

The full range of cell functions is one of the most underdetermined aspects of disease biology. The evidence that somatic clonal imbalance and cell competition play a role in non-neoplastic chronic disease reveals the need for a dedicated effort to explore single cell function to understand disease mechanisms. It will be vital to document not only the prevalent pathologic behaviors but also those beneficial functions eliminated or suppressed by competition. Phenotype expansion in this way to define the roles of somatic cell biology will help to stratify chronic disease, annotate the human genome in regular clinical encounters, and define quantitative contributions from genes and environment across the lifecourse.

AUTHOR CONTRIBUTIONS

WZ and CAM conceptualized and wrote the manuscript. RCD edited the manuscript. All authors listed have made a substantial, direct, and intellectual contribution to the work and approved it for publication.

FUNDING

This work was supported by the One Brave Idea Award to CAM from the American Heart Association, Verily Life Sciences, and AstraZeneca with pillar support from Quest Diagnostics, and National Institutes of Health 1R24OD017870. WZ was supported by a Mower Fellowship Award.

REFERENCES

Alvarez-Dominguez, J. R., and Melton, D. A. (2022). Cell Maturation: Hallmarks, Triggers, and Manipulation. *Cell* 185 (2), 235–249. doi:10.1016/j.cell.2021.12.012

Asimaki, A., Protonotarios, A., James, C. A., Chelko, S. P., Tichnell, C., Murray, B., et al. (2016). Characterizing the Molecular Pathology of Arrhythmogenic Cardiomyopathy in Patient Buccal Mucosa Cells. *Circ. Arrhythm Electrophysiol.* 9 (2), e003688. doi:10.1161/CIRCEP.115.003688

Avagyan, S., Henninger, J. E., Mannherz, W. P., Mistry, M., Yoon, J., Yang, S., et al. (2021). Resistance to Inflammation Underlies Enhanced Fitness in Clonal Hematopoiesis. *Science* 374 (6568), 768–772. doi:10.1126/science.aba9304

Avramovic, V., Frederiksen, S. D., Brkic, M., and Tarailo-Graovac, M. (2021). Driving Mosaicism: Somatic Variants in Reference Population Databases and Effect on Variant Interpretation in Rare Genetic Disease. *Hum. Genomics* 15 (1), 71. doi:10.1186/s40246-021-00371-y

Baker, N. E. (2020). Emerging Mechanisms of Cell Competition. *Nat. Rev. Genet.* 21 (11), 683–697. doi:10.1038/s41576-020-0262-8

Baldridge, M. T., King, K. Y., Boles, N. C., Weksberg, D. C., and Goodell, M. A. (2010). Quiescent Haematopoietic Stem Cells Are Activated by IFN-Gamma in Response to Chronic Infection. *Nature* 465 (7299), 793–797. doi:10.1038/nature09135

Beck, D. B., Ferrada, M. A., Sikora, K. A., Ombrello, A. K., Collins, J. C., Pei, W., et al. (2020). Somatic Mutations in UBA1 and Severe Adult-Onset Autoinflammatory Disease. *N. Engl. J. Med.* 383, 2628. doi:10.1056/nejmoa2026834

Bick, A. G., Weinstock, J. S., Nandakumar, S. K., Fulco, C. P., Bao, E. L., Zekavat, S. M., et al. (2020). Inherited Causes of Clonal Haematopoiesis in 97,691 Whole Genomes. *Nature* 586 (7831), 763–768. doi:10.1038/s41586-020-2819-2

Bruce, A. W., and Zernicka-Goetz, M. (2010). Developmental Control of the Early Mammalian Embryo: Competition Among Heterogeneous Cells that Biases Cell Fate. *Curr. Opin. Genet. Dev.* 20 (5), 485–491. doi:10.1016/j.gde.2010.05.006

Cahalan, S. M., Lukacs, V., Ranade, S. S., Chien, S., Bandell, M., and Patapoutian, A. (2015). Piezo1 Links Mechanical Forces to Red Blood Cell Volume. *Elife* 4, 7370. doi:10.7554/eLife.07370

Coombs, C. C., Zehir, A., Devlin, S. M., Kishtagari, A., Syed, A., Jonsson, P., et al. (2017). Therapy-Related Clonal Hematopoiesis in Patients with Non-hematologic Cancers Is Common and Associated with Adverse Clinical Outcomes. *Cell Stem Cell* 21 (3), 374–e4. doi:10.1016/j.stem.2017.07.010

Costa-Rodrigues, C., Couceiro, J., and Moreno, E. (2021). Cell Competition from Development to Neurodegeneration. *Dis. Model. Mech.* 14 (7), 48926. doi:10.1242/dmm.048926

Dawoud, A. A. Z., Tapper, W. J., and Cross, N. C. P. (2020). Clonal Myelopoiesis in the UK Biobank Cohort: ASXL1 Mutations Are Strongly Associated with Smoking. *Leukemia* 34 (10), 2660–2672. doi:10.1038/s41375-020-0896-8

Dawoud, A. A. Z., Gilbert, R. D., Tapper, W. J., and Cross, N. C. P. (2021). Clonal Myelopoiesis Promotes Adverse Outcomes in Chronic Kidney Disease. *Leukemia* 36, 507. doi:10.1038/s41375-021-01382-3

Dorsheimer, L., Assmus, B., Rasper, T., Ortmann, C. A., Abou-El-Ardat, K., Kiefer, K. C., et al. (2019). Hematopoietic Alterations in Chronic Heart Failure Patients by Somatic Mutations Leading to Clonal Hematopoiesis. *Haematologica* 105, e328–e332. doi:10.3324/haematol.2019.224402

Feske, S., Wulff, H., and Skolnik, E. Y. (2015). Ion Channels in Innate and Adaptive Immunity. *Annu. Rev. Immunol.* 33, 291–353. doi:10.1146/annurev-immunol-032414-112212

Feusier, J. E., Arunachalam, S., Tashi, T., Baker, M. J., VanSant-Webb, C., Ferdig, A., et al. (2021). Large-Scale Identification of Clonal Hematopoiesis and Mutations Recurrent in Blood Cancers. *Blood Cancer Discov.* 2 (3), 226–237. doi:10.1158/2643-3230.BCD-20-0094

Fidler, T. P., Xue, C., Yalcinkaya, M., Hardaway, B., Abramowicz, S., Xiao, T., et al. (2021). The AIM2 Inflammasome Exacerbates Atherosclerosis in Clonal Haematopoiesis. *Nature* 592 (7853), 296–301. doi:10.1038/s41586-021-03341-5

Fuster, J. J., MacLauchlan, S., Zuriaga, M. A., Polackal, M. N., Ostriker, A. C., Chakraborty, R., et al. (2017). Clonal Hematopoiesis Associated with TET2 Deficiency Accelerates Atherosclerosis Development in Mice. *Science* 355 (6327), 842–847. doi:10.1126/science.aag1381

Genovese, G., Friedman, D. J., Ross, M. D., Lecordier, L., Uzureau, P., Freedman, B. I., et al. (2010). Association of Trypanolytic ApoL1 Variants with Kidney Disease in African Americans. *Science* 329 (5993), 841–845. doi:10.1126/science.1193032

Gradeci, D., Bove, A., Charras, G., Lowe, A. R., and Banerjee, S. (2020). Single-cell Approaches to Cell Competition: High-Throughput Imaging, Machine Learning and Simulations. *Semin. Cancer Biol.* 63, 60–68. doi:10.1016/j.semcancer.2019.05.007

Initiative, C.-H. G. (2021). Mapping the Human Genetic Architecture of COVID-19. *Nature* 600 (7889), 472–477. doi:10.1038/s41586-021-03767-x

Jaiswal, S., Fontanillas, P., Flannick, J., Manning, A., Grauman, P. V., Mar, B. G., et al. (2014). Age-related Clonal Hematopoiesis Associated with Adverse Outcomes. *N. Engl. J. Med.* 371 (26), 2488–2498. doi:10.1056/NEJMoa1408617

Jaiswal, S., Natarajan, P., Silver, A. J., Gibson, C. J., Bick, A. G., Shvartz, E., et al. (2017). Clonal Hematopoiesis and Risk of Atherosclerotic Cardiovascular Disease. *N. Engl. J. Med.* 377 (2), 111–121. doi:10.1056/NEJMoa1701719

King, K. Y., and Goodell, M. A. (2011). Inflammatory Modulation of HSCs: Viewing the HSC as a Foundation for the Immune Response. *Nat. Rev. Immunol.* 11 (10), 685–692. doi:10.1038/nri3062

Kiselyov, K., Shin, D. M., and Muallem, S. (2003). Signalling Specificity in GPCR-dependent Ca2+ Signalling. *Cell Signal* 15 (3), 243–253. doi:10.1016/s0898-6568(02)00074-8

Kleinewietfeld, M., Manzel, A., Titze, J., Kvakan, H., Yosef, N., Linker, R. A., et al. (2013). Sodium Chloride Drives Autoimmune Disease by the Induction of Pathogenic TH17 Cells. *Nature* 496 (7446), 518–522. doi:10.1038/nature11868

Lawlor, K., Pérez-Montero, S., Lima, A., and Rodríguez, T. A. (2020). Transcriptional versus Metabolic Control of Cell Fitness during Cell Competition. *Semin. Cancer Biol.* 63, 36–43. doi:10.1016/j.semcancer.2019.05.010

Lee, H., Brott, B. K., Kirkby, L. A., Adelson, J. D., Cheng, S., Feller, M. B., et al. (2014). Synapse Elimination and Learning Rules Co-regulated by MHC Class I H2-Db. *Nature* 509 (7499), 195–200. doi:10.1038/nature13154

Ma, S., Cahalan, S., LaMonte, G., Grubaugh, N. D., Zeng, W., Murthy, S. E., et al. (2018). Common PIEZO1 Allele in African Populations Causes RBC Dehydration and Attenuates Plasmodium Infection. *Cell* 173 (2), 443–e12. e412. doi:10.1016/j.cell.2018.02.047

Madan, E., Gogna, R., and Moreno, E. (2018). Cell Competition in Development: Information from Flies and Vertebrates. *Curr. Opin. Cel Biol* 55, 150–157. doi:10.1016/j.ceb.2018.08.002

Maruyama, T., and Fujita, Y. (2022). Cell Competition in Vertebrates - a Key Machinery for Tissue Homeostasis. *Curr. Opin. Genet. Dev.* 72, 15–21. doi:10.1016/j.gde.2021.09.006

Medzhitov, R. (2008). Origin and Physiological Roles of Inflammation. *Nature* 454 (7203), 428–435. doi:10.1038/nature07201

Méndez-Ferrer, S., Bonnet, D., Steensma, D. P., Hasserjian, R. P., Ghobrial, I. M., Gribben, J. G., et al. (2020). Bone Marrow Niches in Haematological Malignancies. *Nat. Rev. Cancer* 20 (5), 285–298. doi:10.1038/s41568-020-0245-2

Nagata, R., and Igaki, T. (2018). Cell Competition: Emerging Mechanisms to Eliminate Neighbors. *Dev. Growth Differ.* 60 (9), 522–530. doi:10.1111/dgd.12575

Ohsawa, S., Vaughen, J., and Igaki, T. (2018). Cell Extrusion: A Stress-Responsive Force for Good or Evil in Epithelial Homeostasis. *Dev. Cel* 44 (3), 532–296. doi:10.1016/j.devcel.2018.02.007

Orkin, S. H., and Zon, L. I. (2008). Hematopoiesis: an Evolving Paradigm for Stem Cell Biology. *Cell* 132 (4), 631–644. doi:10.1016/j.cell.2008.01.025

Patel, H. H., Patel, H. R., and Higgins, J. M. (2015). Modulation of Red Blood Cell Population Dynamics Is a Fundamental Homeostatic Response to Disease. *Am. J. Hematol.* 90 (5), 422–428. doi:10.1002/ajh.23982

Ridker, P. M., Everett, B. M., Thuren, T., MacFadyen, J. G., Chang, W. H., Ballantyne, C., et al. (2017). Antiinflammatory Therapy with Canakinumab for Atherosclerotic Disease. *N. Engl. J. Med.* 377 (12), 1119–1131. doi:10.1056/NEJMoa1707914

Sekar, A., Bialas, A. R., de Rivera, H., Davis, A., Hammond, T. R., Kamitaki, N., et al. (2016). Schizophrenia Risk from Complex Variation of Complement Component 4. *Nature* 530 (7589), 177–183. doi:10.1038/nature16549

Svensson, E. C., Madar, A., Campbell, C. D., He, Y., Sultan, M., Healey, M. L., et al. (2022). TET2-Driven Clonal Hematopoiesis and Response to Canakinumab: An Exploratory Analysis of the CANTOS Randomized Clinical Trial. *JAMA Cardiol.* doi:10.1001/jamacardio.2022.0386

Swiatczak, B. (2021). Struggle within: Evolution and Ecology of Somatic Cell Populations. *Cell Mol Life Sci* 78 (21-22), 6797–6806. doi:10.1007/s00018-021-03931-6

Szilágyi, M., Pös, O., Márton, É., Buglyó, G., Soltész, B., Keserű, J., et al. (2020). Circulating Cell-free Nucleic Acids: Main Characteristics and Clinical Application. *Int. J. Mol. Sci.* 21 (18), 6827. doi:10.3390/ijms21186827

Thorpe, J., Osei-Owusu, I. A., Avigdor, B. E., Tupler, R., and Pevsner, J. (2020). Mosaicism in Human Health and Disease. *Annu. Rev. Genet.* 54, 487–510. doi:10.1146/annurev-genet-041720-093403

Watson, C. J., Papula, A. L., Poon, G. Y. P., Wong, W. H., Young, A. L., Druley, T. E., et al. (2020). The Evolutionary Dynamics and Fitness Landscape of Clonal Hematopoiesis. *Science* 367 (6485), 1449–1454. doi:10.1126/science.aay9333

Willis, R. A., Kappler, J. W., and Marrack, P. C. (2006). CD8 T Cell Competition for Dendritic Cells *In Vivo* Is an Early Event in Activation. *Proc. Natl. Acad. Sci. U S A.* 103 (32), 12063–12068. doi:10.1073/pnas.0605130103

Wu, C., Yosef, N., Thalhamer, T., Zhu, C., Xiao, S., Kishi, Y., et al. (2013). Induction of Pathogenic TH17 Cells by Inducible Salt-Sensing Kinase SGK1. *Nature* 496 (7446), 513–517. doi:10.1038/nature11984

Zhu, M., and Zernicka-Goetz, M. (2020). Principles of Self-Organization of the Mammalian Embryo. *Cell* 183 (6), 1467–1478. doi:10.1016/j.cell.2020.11.003

Zhu, W., Guo, S., Homilius, M., Nsubuga, C., Wright, S. H., Quan, D., et al. (2022). PIEZO1 Mediates a Mechanothrombotic Pathway in Diabetes. *Sci. Transl Med.* 14 (626), eabk1707. doi:10.1126/scitranslmed.abk1707

Zink, F., Stacey, S. N., Norddahl, G. L., Frigge, M. L., Magnusson, O. T., Jonsdottir, I., et al. (2017). Clonal Hematopoiesis, with and without Candidate Driver Mutations, Is Common in the Elderly. *Blood* 130 (6), 742–752. doi:10.1182/blood-2017-02-769869

Conflict of Interest: The authors declare that the research was conducted in the absence of any commercial or financial relationships that could be construed as a potential conflict of interest.

Publisher's Note: All claims expressed in this article are solely those of the authors and do not necessarily represent those of their affiliated organizations or those of the publisher, the editors, and the reviewers. Any product that may be evaluated in this article, or claim that may be made by its manufacturer, is not guaranteed or endorsed by the publisher.

Advantages of publishing in Frontiers

OPEN ACCESS
Articles are free to read for greatest visibility and readership

FAST PUBLICATION
Around 90 days from submission to decision

HIGH QUALITY PEER-REVIEW
Rigorous, collaborative, and constructive peer-review

TRANSPARENT PEER-REVIEW
Editors and reviewers acknowledged by name on published articles

Frontiers
Avenue du Tribunal-Fédéral 34
1005 Lausanne | Switzerland

Visit us: www.frontiersin.org
Contact us: frontiersin.org/about/contact

REPRODUCIBILITY OF RESEARCH
Support open data and methods to enhance research reproducibility

DIGITAL PUBLISHING
Articles designed for optimal readership across devices

FOLLOW US
@frontiersin

IMPACT METRICS
Advanced article metrics track visibility across digital media

EXTENSIVE PROMOTION
Marketing and promotion of impactful research

LOOP RESEARCH NETWORK
Our network increases your article's readership